ORGANOZIRCONOCENE NUCLEOPHILES IN CU-CATALYSED ASYMMETRIC TRANSFORMATIONS: METHODOLOGIES, APPLICATIONS TO TOTAL SYNTHESIS AND NMR MECHANISTIC STUDIES

EMELINE RIDEAU



Doctor of Philosophy

University of Oxford

Department of Chemistry
Lincoln College

July 2016

DECLARATION

The work presented in this thesis was conducted at the Chemistry Research Laboratory, University of Oxford, between October 2008 and March 2012 under the supervision of Prof Stephen P. Fletcher. This thesis is the result of my own work, except when otherwise stated, and has not been submitted for any other degree at this or any other university.

Emeline Rideau

July 2016

ABSTRACT

Organozirconocene Nucleophiles in Cu-Catalysed Asymmetric Transformations: Methodologies, Applications to Total Synthesis and NMR Mechanistic Studies.

The development of powerful and adaptable methods to form new C-C bond enantioselectively is highly desirable. Many methodologies emerged in recent years using a wide array of nucleophilic organometallics and catalytic metals[1,2]. In this work, a general introduction on the current development of Cu-catalysed asymmetric additions is primarily described (Chapter 1). We particularly focus on the applications of such methodologies, the study of their mechanisms and the transition from using common organometallics in favour of milder and functional group tolerant nucleophiles such as organozirconocenes.

We then present the development of new methods for asymmetric conjugate addition towards its application to the synthesis of prostaglandins (Part I). For example, we describe the use of alkenylzirconocene nucleophiles (Chapter 2) and conjugate additions of alkylzirconocenes to 5-membered rings[3] (Chapter 3). We then investigated the application of these methodologies towards the total synthesis of a prostaglandin analogue, Latanoprost (Xalatan®) (Chapter 4).

Then we carried out mechanistic studies by NMR (Part II). The mechanism of asymmetric allylic alkylation of alkylzirconocene to allylchlorides[4] (Chapter 5) and allylphosphates (Chapter 6) is discussed in detail. We also developed and investigated the heterocyclic asymmetric allylic alkylation of alkylzirconocene[5] (Chapter 7). Finally we describe the NMR mechanistic studies of asymmetric conjugate addition of alkylzirconocenes (Chapter 8).

ACKNOWLEDGEMENTS

I would like to express my gratitude to all the people without which my DPhil would have not been possible, namely:

My supervisor, Prof. Stephen Fletcher, for his guidance, help and advice which made the advancement of this thesis possible.

The members of the Fletcher groups past and present for many helpful recommendations, support, assistance in the laboratory and discussions.

The Oxford chemistry department staff and technical services such as the people running the NMR, MS and the X-ray crystallography facilities. Special thanks to Prof. Tim Claridge and Dr Barbara Odell for guidance with NMR techniques.

My friends and family for being so positive, cheering me up, hanging out, playing board games, cooking and eating (too much) nice food, drinking posh tea, making 2 am soufflé (…), more Limoncello-than-ice-cream ice-cream, Settembrini, scuba-diving, visiting the San Francisco area, listening to my complaining throughout this thesis, keeping me going and getting me through tough times, more specifically Karo, Laura, Silvainou and Catherine, Jérôme, Anna and Matthew, the 'mostly not-German Germans' Gustav, Wendy and Michael and of course a very special mention to Lukas who is always there for me.

And finally but not least to my parents for being so supportive and loving, for holidays and weekends in Italy and around the Côte d'Azur, cultural and Nordic walking trips, nice restaurants, baking and cooking, and for always sending those delicious Easter chocolate eggs and Aix-en-Provence Calissons for moral support (if only the Sun and the Mediterranean climate could be posted to the UK…).

TABLE OF CONTENT

Declaration i
Abstract ii
Acknowledgements iii
Table of Content iv
Abbreviations vii

CHAPTER 1 - INTRODUCTION 1
Asymmetric synthesis 3
Asymmetric Carbon-Carbon Bond Formation 4
Cu-catalysed Asymmetric Addition Reactions 5
Asymmetric Conjugate Addition (ACA) and Allylic Alkylation (AAA) 6
Organometallics 7
Cu source 10
Ligands 10
Total synthesis applications 12
Hydrometallation of Alkenes 15
Reaction Mechanism and Catalytic Complexes Structures 17

PART I - METHODOLOGIES TOWARDS THE SYNTHESIS OF PROSTAGLANDINS 23
Introduction 25
Aims 31

CHAPTER 2 - HYDROMETALLATION AND CATALYTIC ASYMMETRIC CONJUGATE ADDITION OF ALKYNES 33
Introduction 33
Results and Discussion 35
Conclusion 46

CHAPTER 3 - ASYMMETRIC CONJUGATE ADDITION OF ALKYLZIRCONOCENES TO CYCLOPENTENONE-3,5-DIONE MONOACETALS 47
Introduction 47
Results and Discussion 54
Conclusion 63

CHAPTER 4 - TOWARDS THE TOTAL SYNTHESIS OF LATANOPROST 65
Introduction 65
Results and Discussion 68
Conclusion 87

PART II - MECHANISTIC NMR STUDIES OF CU-CATALYSED METHODOLOGY 89
Introduction 91
Aims 94

CHAPTER 5 - NMR MECHANISTIC STUDIES OF CU-CATALYSED ASYMMETRIC ALLYLIC ALKYLATION USING ALLYLCHLORIDE 97
Introduction 97
Results and discussion 104
Conclusion and proposed mechanism 146

CHAPTER 6 - NMR MECHANISTIC STUDIES OF CU-CATALYSED ASYMMETRIC ALLYLIC ALKYLATION USING ALLYLPHOSPHATE 149
Introduction 149
Results and discussion 150
Conclusion and proposed mechanism 182

CHAPTER 7 - CU-CATALYSED ASYMMETRIC ALLYLIC ADDITION OF ALKYLZIRCONOCENES TO RACEMIC 3,6-DIHYDRO-2*H*-PYRANS 185
Introduction 185
Results and Discussion 186
Conclusion 197

CHAPTER 8 - MECHANISTIC NMR STUDIES OF AN ASYMMETRIC CONJUGATE ADDITION BY CU-PHOSPHORAMIDITE COMPLEXES USING ORGANOZIRCONOCENES AS NUCLEOPHILES 199
Introduction 199
Results and Discussion 203
Conclusion and proposed mechanism 227

CHAPTER 9 - CONCLUSION AND FUTURE WORKS 231
Conclusions 233
Future Works 236

EXPERIMENTAL DATA AND ANALYSIS 239
I. General Information 241
II. Chemicals 243
III. NMR experiments 244
IV. Experimentals Chapter 2 245
V. Experimentals Chapter 3 261
VI. Experimentals Chapter 4 299
VII. Experimentals Chapter 5 339
VIII. Experimentals Chapter 6 409
IX. Experimentals Chapter 7 448
X. Experimentals Chapter 8 498

REFERENCES 541

$[\alpha]_D^{25}$	Specific rotation (D= 589.3 nm wavelength, 25 °C)
1D	1-dimensional
3D	3-dimentional
Å	Ångstroms
AAA	Asymmetric allylic alkylation
Ab initio	(Latin) from the beginning
Ac	Acetate
ACA	Asymmetric Conjugate Addition
anti	Opposite (Greek)
App.	Apparent (NMR)
aq.	Aqueous
Ar	Aryl
Ar-C	Aromatic Carbon
Ar-H	Aromatic proton
atm	Atmospheric pressure
BARF	Tetrakis[3,5-bis(trifluoromethyl)phenyl]boron
BINAP	2,2'-bis(diphenylphosphino)-1,1'-binaphthyl
Binaphthol	1,1′-Binaphthalene-2,2′-diol
BINPO	BINAP monophosphine oxide
Bn	Benzyl
BOM	Benzyloxymethyl acetal
Br.	Broad (NMR)
Bu	Butyl
c	Concentration (optical rotation)
Calcd	Calculated
cap	Caprolactamate (Tetrakis[μ-(hexahydro-2*H*-azepin-2-onato-κ*N*1,κ*O*2)])
cat.	Catalytic/Catalyst
Cf	*Confer* (Latin) bring together
Cl	Chloride anion
cm^{-1}	Wavenumber
COSY	Correlation Spectroscopy
COX	Cyclooxygenase
Cp	Cyclopentadienyl
Cq	Quaternary Carbon
Cu-AAA	Cu-catalysed Asymmetric Allylic Alkylation
Cu-ACA	Cu-catalysed Asymmetric Conjugate Addition
D	Deuterium
d	Doublet (NMR)
DCM	Dichloromethane
dd	Doublet of doublet (NMR)
ddd	Doublet of double of doublet (NMR)
dddt	Doublet of doublet of doublet of triplet (NMR)
ddq	Doublet of doublet of quartet (NMR)
ddt	Doublet of doublet of triplet (NMR)
DET	Direct enantioconvergent transformation

T	Density functional theory
DKR	Dynamic kinetic resolution
DMAP	4-Dimethylaminopyridine
DMF	Dimethylformamide
DMP	Dess–Martin periodinane
DMS	Dimethyl sulfide
DoE	Design of experiments
DOSY	Diffusion Ordered Spectroscopy
dq	Doublet of quartet (NMR)
dquint	Doublet of quintet (NMR)
dr	*Diastereomeric ratio*
dt	Doublet of triplet (NMR)
dt	Doublet of triplet (NMR)
DTBM	3,5-Di-*tert*-butyl-4-methoxyphenyl
DYKAT	Dynamic kinetic asymmetric transformation
DYKAT	Dynamic kinetic asymmetric transformation
e.g.	*Exempli gratia* (Latin) for example
ee	Enantiomeric excess
EI	Electron impact ionisation
eq	Equivalent
ESI	Electron spray ionisation
Et	Ethyl
et al.	*Et alia* (Latin) and others
etc.	*Et cetera* (Latin) and other things
EXSY	Exchange Spectroscopy
FI	Field Ionisation
FTIR	Fourier transform infrared spectroscopy
g	Gradient (NMR)
GC	Gas chromatography
HMBC	Heteronuclear Multiple-Bond Correlation Spectroscopy
HMDS	Bis(trimethylsilyl)amide (HexaMethylDiSilazide)
HPLC	High Performance Liquid Chromatography
HRMS	High resolution mass spectrometry
HSQC	Heteronuclear Single-Quantum Correlation Spectroscopy
HWE	Horner-Wadsworth-Emmons
i.e.	*Id est* (Latin) in other words
***i*Bu**	Isobutyl
in situ	(Latin) on site
IPA	Isopropyl alcohol
***i*Pr**	Isopropyl
IR	Infrared
J	Coupling constant (NMR)
Jacobsen Co^{II} catalyst	(S,S)-N,N'-Bis(3,5-di-tert-butylsali-cylidene)-1,2-cyclohexanediamino-cobalt(II)
Josiphos	(1-(Dialkylphosphino)-2-1-(dialkylphosphino)ethyl]ferrocene
k	Reaction rate coefficient

L	Ligand
L*	Chiral ligand
LDA	Lithium diisopropylamide
LG	Leaving group
LRMS	Low resolution mass spectrometry
M	Molar (mol.L^{-1}), Mega (NMR), Mass (MS)
m	Multiplet (NMR)
m/z	Mass-to-charge ratio
M_0	Initial z-magnetisation
***m*CPBA**	*meta*-Chloroperoxybenzoic acid
Me	Methyl
meso	Middle (Greek)
Me-THF	2-Methyltetrahydrofuran
Mp	Melting point
MS	Mass Spectrometry
M_t	z-magnetisation
n	Generic integer
***n*Bu**	Normal (primary) butyl
NHC	N-Heterocyclic Carbene
NMR	Nuclear magnetic resonance
NOE	Nuclear Overhauser effect
NOESY	Nuclear Overhauser Effect Spectroscopy
Nu	Nucleophile
o	Ortho
o.n.	Overnight
PG	Protecting group/Prostaglandin
Ph	Phenyl
pH	Potential Hydrogen
pK_a	Logarithmic acid dissociation constant
ppm	Parts per million
Pr	Propyl
psi	Pound-force per square inch
PTFE	Polytetrafluoroethylene
pts	Points
q	Quartet (NMR)
Quinox	2-(4,5-dihydro-2-oxazolyl)quinoline
quint.	Quintet (NMR)
R	Alkyl
R1	Spin-lattice relaxation rate (NMR)
R^2	Coefficient of determination
RT	Room temperature
s	Singlet (NMR)
sat.	Saturated
Segphos	5,5′-Bis(diphenylphosphino)-4,4′-bi-1,3-benzodioxole
sep.	Septet (NMR)
SiPhos-PE	*N*-Di[(*R*)-1-phenylethyl]-[(*R*)-1,1′-spirobiindane-7,7′-diyl]-phosphoramidite
SM	Starting Material
S_N2	Bimolecular nucleophilic substitution

S_N2'	Bimolecular nucleophilic substitution with allylic rearrangement
sp^2	Orbital hybridisation:33% s and 67% p character
sp^3	Orbital hybridisation: 25% s and 75% p character
SST	Spin saturation transfer
SSTD	Spin saturation transfer difference
Syn	Together (Greek)
t	Triplet (NMR)
T1	Spin-lattice relaxation time (NMR)
TADDOL	α,α,α,α-Tetra aryl-1,3-dioxolane-4,5- dimethanol
Taniaphos	1-[(Dimethylamino)[2-(dialkylphosphino)phenyl]methyl]-2-(dialkylphosphino)ferrocene
TBAF	Tetra-*n*-butylammonium fluoride
TBAI	Tetra-*n*-butylammonium iodide
TBME	*tert*-Butyl methyl ether
TBS	*tert*-Butyldimethylsilyl
***t*Bu**	Tertiary butyl
TC	Thiophene-2-carboxylate
TEMPO	(2,2,6,6-Tetramethylpiperidin-1-yl)oxyl or (2,2,6,6-tetramethylpiperidin-1-yl)oxidanyl
Tf	Trifluoromethanesulfonyl
THF	Tetrahydrofuran
TIPS	Triisopropylsilyl
t_{mix}	Mixing time (NMR)
TMS	Trimethylsilyl
TOCSY	Total Correlation Spectroscopy
t_R	Retention time
Triflate	Trifluoromethanesulfonate
Triflimide	Bis(trifluoromethanesulfonyl)imide
tt	Triplet of triplet (NMR)
UV	Ultraviolet
w/w	Mass fraction
WHO	World Health Organisation
X	Halogen
δ	Chemical shift (NMR) or diffusion gradient length (DOSY)
λ	Wavelength (HPLC)
ν	Wavenumber
Δ	Diffusion delay (DOSY)

CHAPTER 1

INTRODUCTION

ASYMMETRIC SYNTHESIS

Chirality is a fundamental part of nature as life developed asymmetrically by some yet unknown processes[6]. Cells generally only recognise L-amino acids and from these homochiral building blocks manufacture specifically handed proteins. In turn, the chiral proteins and enzymes discriminate between enantiomers of small molecules for binding, perpetuating the requirement of chirality. Thus the majority of natural products and biologically active molecules are chiral.

It is therefore not surprising that there is a high demand for enantioenriched products in a vast array of domains (e.g. agrochemicals, pharmaceuticals, liquid crystals, polymers etc.)[7]. Clinical drugs often manifest different biological activities for enantiomers and even unwanted enantiomers can exhibit high toxicity, underlying the importance of enantioselective synthesis[8,9]. However, the pharmaceutical industry has often avoided the synthesis of chiral centres, as industrially applicable methods were scarce[10]. And as aforementioned, the cellular chiral information suggests that chiral molecules should be more efficient drugs[11].

In order to engineer enantioenriched molecules, some chiral information needs to be present in the reaction. Early works relied on stoichiometric or sub-stoichiometric amount of chiral components (chiral auxiliaries[12-17], chiral starting materials[18-22] or chiral reagents[12,23,24]). The obvious drawbacks of such methodologies are the amount of chiral reagents used due to their cost and value, lengthy synthesis and disposal. Modern chemistry has successfully reduced the chiral reagent quantity to catalytic amount in processes known as asymmetric

catalysis, whether with transition metal catalysis[25-27] or organocatalysis[28-30]. The catalyst is generally the exclusive source of chirality and is only added in small quantities, greatly improving the cost efficiency of asymmetric synthesis. Asymmetric catalysis has revolutionised synthetic chemistry providing chemists with affordable and diverse tools to synthesise complex enantioenriched molecules.

ASYMMETRIC CARBON-CARBON BOND FORMATION

Natural products and complex biomolecules (proteins, nucleic acids, carbohydrates, fatty acids, phospholipids etc.) almost always contain an extended carbon backbone with many chiral centres on carbons. Thus enantioselective C-C bond forming reactions are amongst the most strategically important reactions in synthetic chemistry[31]. The vast majority of the C-C bond syntheses in industry are Pd cross-coupling reactions (Suzuki, Stille, Heck, Negishi etc.)[32]. Those reactions are undoubtedly practical and effective but they are not asymmetric processes. In academia, a variety of transition metals have been used in catalytic asymmetric processes where nucleophiles are added to an electrophile. These involve the use of Mg, Zn, B and Al nucleophiles catalysed by chiral Pd, Rh, Cu, Ir, Ru and Ni complexes[33-35].

However, despite these incredible advances in asymmetric catalysis, there are still on-going challenges. Optimising enantioselective processes is time-consuming and the required starting materials and reagents can be expensive (e.g. chiral non-racemic compounds, rare metals) or lengthy synthesis (e.g.

ligands) and these reactions are often developed with simple bench-mark substrates and they can be difficult to apply to more complex structures. Therefore there is still a demand for simpler, non-toxic, mild, tolerant and adaptable processes[36].

Cu-catalysed Asymmetric Addition Reactions

Cu is a metal of choice in organometallic chemistry: it is abundant, cheap and versatile. Notably it has five oxidation states and high electronegativity enabling diverse chemical reactivity and it has proved particularly important in C-C bond formation[1,2,7]. The depletion of rare metal elements has reiterated the interest in using Cu as a metal in synthesis[37].

At first, Cu was commonly used in stoichiometric amount in organocopper or cuprates. Nowadays it is extensively used in catalytic amounts in combination with a stoichiometric amount of an unstabilised organometallic nucleophile such as Grignards, organozinc or organoaluminium[1,2,7,37]. Organolithium and Grignard reagents were the dominant sources of carbanions for many decades. Then a myriad of new, mildly reactive nucleophiles (Zn, Ti, Zr, Al) became popular in 1980s and their utility has been amply demonstrated[37].

Cu is particularly useful in the enantioselective formation of new C-C bonds by conjugate addition or allylic alkylation[2,7]. Many methods have been developed using a variety of alkyl[38], aryl[38,39] and alkenyl[38,40] nucleophiles to form both tertiary and quaternary centres and are used in a variety of applications[1,2,7,33,39].

ASYMMETRIC CONJUGATE ADDITION (ACA) AND ALLYLIC ALKYLATION (AAA)

Conjugate addition and allylic alkylation have emerged as powerful and versatile methodologies for the synthesis of new C-C bonds enantioselectively (Scheme 1.1)[1,2,7].

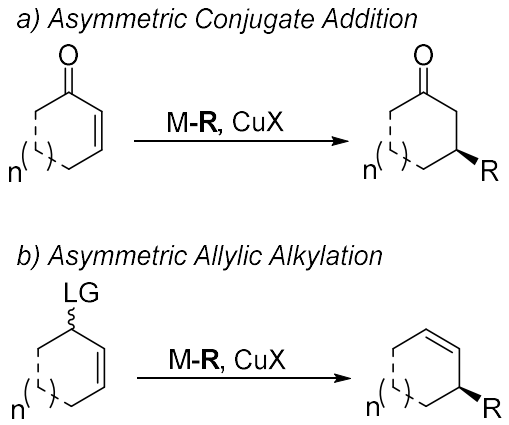

Scheme 1.1. General asymmetric conjugate addition and allylic alkylation reactions.

Asymmetric conjugate addition (ACA) is a powerful reaction. It uses the α,β-unsaturated ketones extended π-system to form an enolate. The final product is obtained upon quenching the enolate. ACA is also highly versatile as the intermediate enolate can be trapped by an electrophile, promoting multi-components systems. This reaction is highly developed and a large variety of donors and acceptors are available for a broad scope of methodologies and products[2,7,12].

On the other hand, interest in asymmetric allylic alkylation (AAA) has been increasingly rising in the last decades[1,41-45]. Not only does this transformation facilitate the formation of new C-C bond enantioselectively, the product provides a non-functionalised alkene that can be easily elaborated further, achieving complex scaffolds in a few steps. AAA is indeed commonly combined with ring

closing metathesis[46-48]. Although various metals are able to provide this reaction, Cu remains one of the cheapest and most efficient metals when associated with hard organometallics[2].

Many parallels can be drawn between conjugate addition and allylic alkylation. Notably both processes require the development of a suitable catalyst that is not only enantioselective, but also highly regioselective in order to avoid 1,2-addition or S_N2-addition, which competes with the desired 1,4-addition or S_N2'-addition (Scheme 1.2)[1].

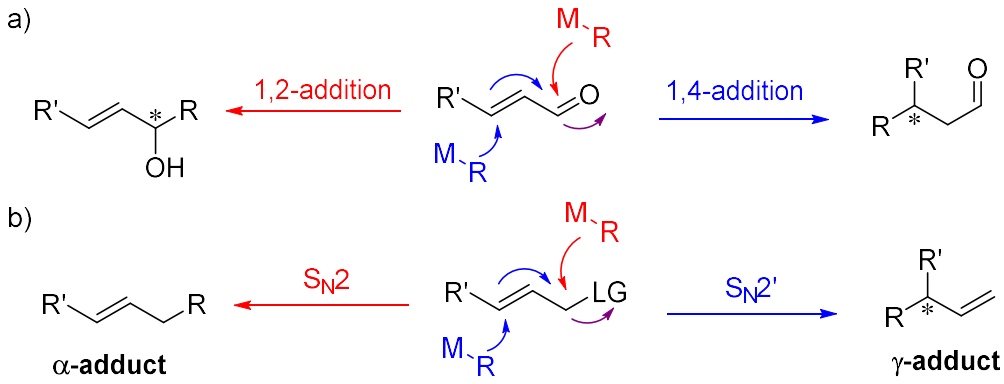

Scheme 1.2. Regioselective complications of conjugate addition (a) and allylic alkylation (b).

ORGANOMETALLICS

In terms of organometallic nucleophiles, Gilman reagents (lithium cuprates) have traditionally been used in conjugate addition[37]. However, many other premade nucleophiles have been coupled to catalytic Cu to produce desirable methods. Grignard reagents were particularly attractive due to their high reactivity and were the first class of unstabilised nucleophiles that were employed in AAA by Bäckvall[49,50].

However, the high reactivity of Grignard makes it difficult to control regio- and enantioselectivity and limit side-reactions. For example the allylic substitution of linear allylacetates using an arenethiolatocopper(I) complex gave excellent regioselectivity (100:0) but poor ee (28-53% ee)[49,50]. Grignards have since came a long way in AAA and ACA reactions and now can achieve excellent regio- and enantioselectivity[1,2,7,33,34,51-55] (Scheme 1.3). Moreover, Grignards are commercially available with a variety of alkyl groups (Me, Et, Bu etc.).

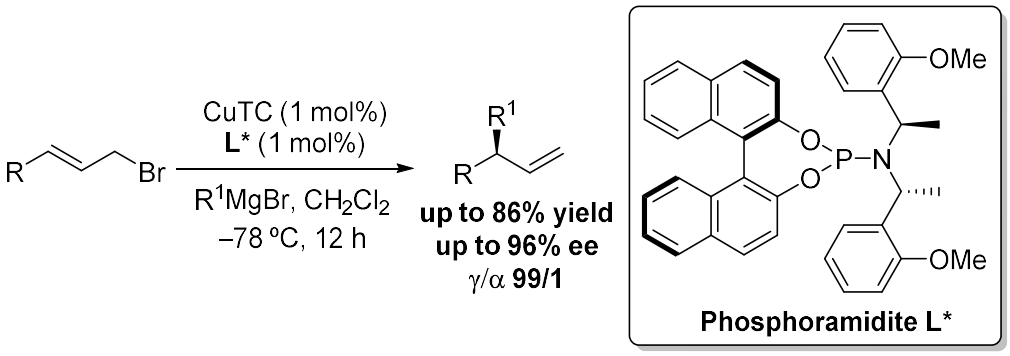

Scheme 1.3. Example of using Grignard nucleophiles in AAA[51].

Asymmetric diorganozinc additions were developed in the 1990s and somewhat replaced the use of Grignards due to their lower, more controllable, reactivity and high functional group compatibility. Their use kick-started efficient and highly enantioselective ACAs and AAAs and are very well studied[12,23,56-60] (Scheme 1.4). However, their low reactivity became a problem for poorly reactive substrates such as esters, multi-substituted substrates and those with poor leaving groups etc[2].

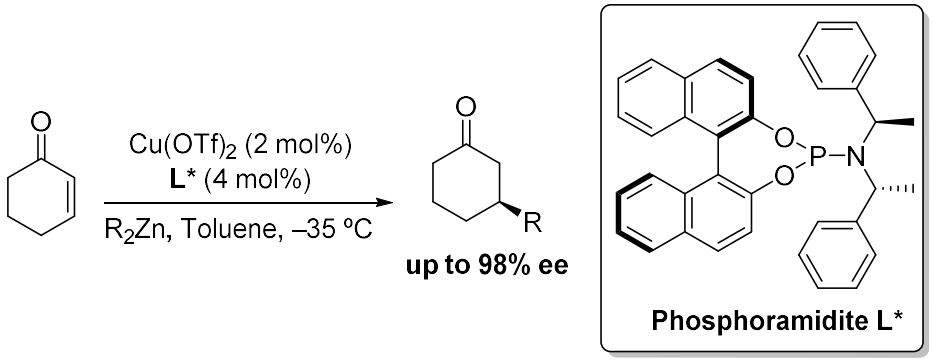

Scheme 1.4. Example of using diorganozinc in ACA[61].

Finally, a third class of commonly used nucleophiles is triorganoaluminiums. Their reactivity differs from organozinc and Grignard reagents in that they are good nucleophiles as well as powerful Lewis acids[2]. However, only a limited number of triorganoaluminium are commercially available, restricting the scope of these reactions. Alkenylaluminiums can be prepared from the hydroalumination of alkynes. Hoveyda[62-66] described a series of elaborate AAA reactions using alkynyl-, vinyl-, aryl-, heteroaryl-aluminium reagents catalysed by a new generation of sulfonate NHC ligands (Scheme 1.5).

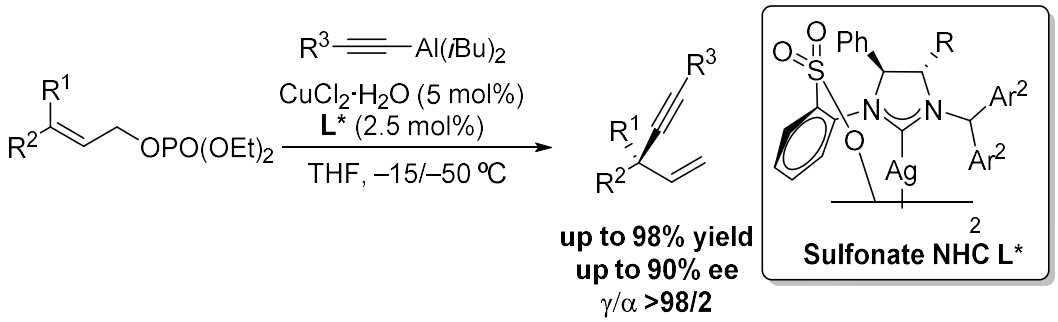

Scheme 1.5. Example of using alkynylaluminiums in AAA[66].

New types of organometallics that can be used in these reactions are still expending (for example Zr, B, Si)[2,67] and methodologies are still being published

using both older and newer organometallics depending on the desired reactivity, functional group tolerance and required complexity.

Cu source

The Cu salt is crucial to the reactivity and enantioselectivity and highly dependent on the combination of the other reaction components (solvent, nucleophiles, ligand etc.)[2]. The nature of the counterion would modify the cationic character of the Cu atom and even the aggregates and superstructures formed. Halogens are often considered stabilising counterions and these Cu-salts are therefore less reactive so more controllable, whereas triflate and triflimide are non-stabilising counterions, making the Cu atom cationic in nature and highly reactive. Also Cu salts can be found in different oxidative states (I or II) modifying their reactivity. Cu^{I} is considered the active catalyst but Cu^{II} salts are often used and *in situ* reduced to Cu^{I} as they are less hygroscopic and moisture sensitive[2] than Cu^{I} thus easier to handle.

Ligands

In asymmetric catalysis, as the ligands are generally the sole bearer of chirality (a few methodologies also use chiral counterions[68-70]), they are obviously crucial for the induction of chirality in the products. It is therefore not

surprising that a wide variety of ligand classes have been developed and within these, many analogues exists.

Chiral phosphorus based ligands have undoubtedly dominated asymmetric catalysis[1]. A class of common efficient ligands in ACA and AAA are bis-phosphines (e.g. BINAP, ferrocenes) and phosphoramidites (Feringa ligand, Alexakis ligand)[2,55]. We have already seen phosphoramidite ligands in a few previous examples[51,61] (Scheme 1.3 and 1.4) and it is the type of ligand that we used throughout this thesis. However, ferrocenyl type ligands (TaniaPhos, JosiPhos, etc.) have been extremely successful with Grignard reagents (Scheme 1.6)[71].

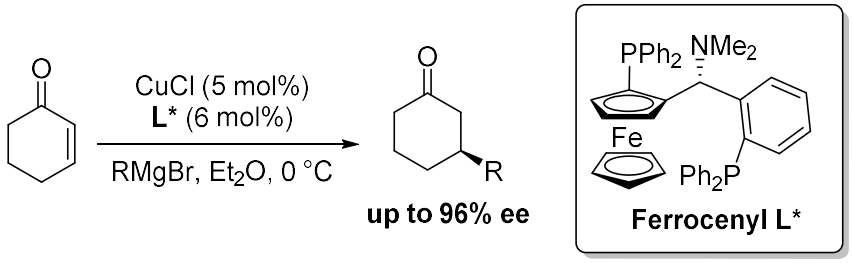

Scheme 1.6. Example of ferrocenyl-type chiral ligands (Taniaphos) in ACA[71].

Another class of ligands that were combined with Grignard reagents are NHCs and these work especially well in ACAs to form challenging quaternary centres (Scheme 1.7)[2,72]. NHCs were also successful with diorganozinc and triorganoaluminium when using preformed Ag or Cu carbene complexes (for example Scheme 1.5)[66].

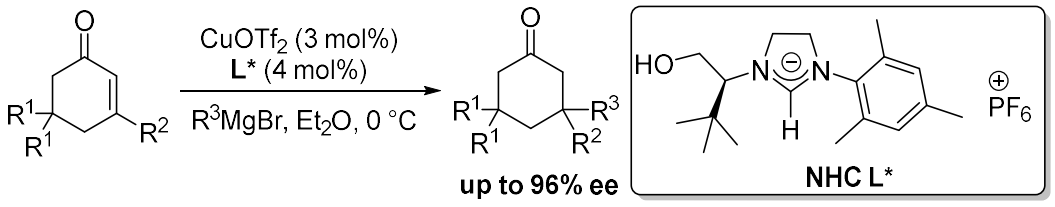

Scheme 1.7. Example of NHC chiral ligands in ACA[72].

Many more ligands exist and cannot all be discussed here. However, it is worth mentioning that Hoveyda has developed highly tuneable, but relatively uncommon, peptidic based chiral ligands that work very well with substituted allylphosphate and diorganozinc nucleophiles (Scheme 1.8)[73].

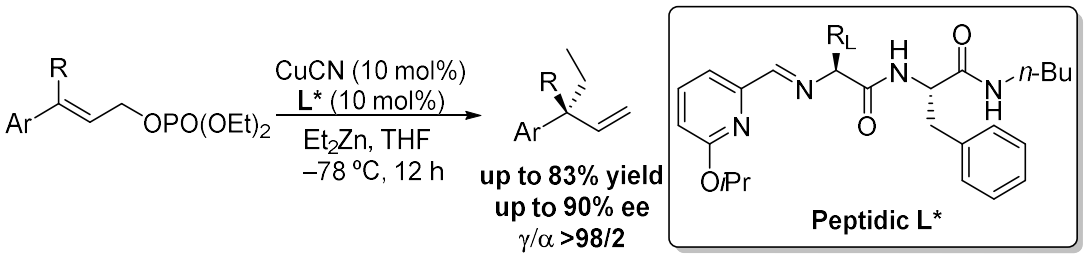

Scheme 1.8. Example of peptidic chiral ligands in AAA[73].

TOTAL SYNTHESIS APPLICATIONS

As discussed ACA and AAA are high impact reactions with great variability and scope. However, a critical aspect of methodologies is their applicability to the total syntheses of biologically active molecules. Only through such studies can the utility and the limitation of different methodologies be truly assessed.

As previously mentioned, the products of Cu-catalysed ACA and AAA can easily be transformed into multifunctional building block. Thus it is not surprising that these processes are now often used as key steps in the synthesis

of many biologically complex molecules[74-79]. A few examples of complex molecules synthesised using Cu-catalysed asymmetric transformation are emphasised in Figure 1.1.

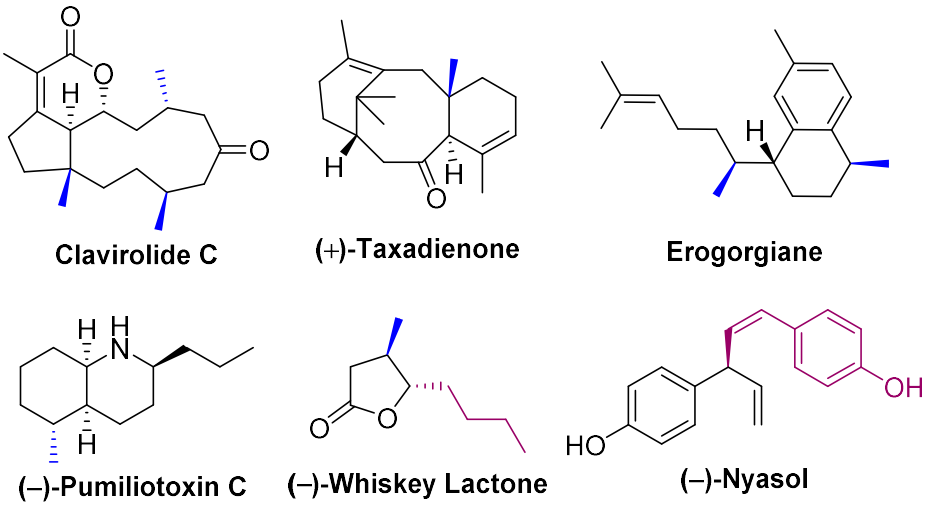

Figure 1.1. Examples of biologically complex molecules where ACA (blue) or AAA (purple) are used in their synthesis (Clavorolide C[76,77], Taxadieone[79], Erogorgiane[74], Pumiliotoxin C[75], Whiskey Lactone[78], Nyasol[63]).

The asymmetric addition of a methyl group is particularly desirable as these are highly abundant in biologically active compounds as observed in Figure 1.1. Moreover, the addition of methyl allows the use of commercially available nucleophiles such as MeMgBr, Me_2Zn and $AlMe_3$. Therefore the asymmetric addition of a methyl group is a prominent feature of asymmetric Cu-catalysis and is tremendously useful in the total synthesis of complex agents.

For example, methyl nucleophiles were used in the enantioselective synthesis of (*R*)-muscone (Scheme 1.9), the principal component of musk, a valuable compound in the perfume industry. Alexakis[80] and Rosini[81,82] described the conjugate addition of Me_2Zn to (E)-cyclopentadecenone using $Cu(OTf)_2$-**L*** complex achieving moderate ee (79% and 82% respectively). Gladiali[83] on the

other hand used $AlMe_3$, in the presence of catalytic $Cu(MeCN)_2PF_6$ and BINPO, giving 77% ee.

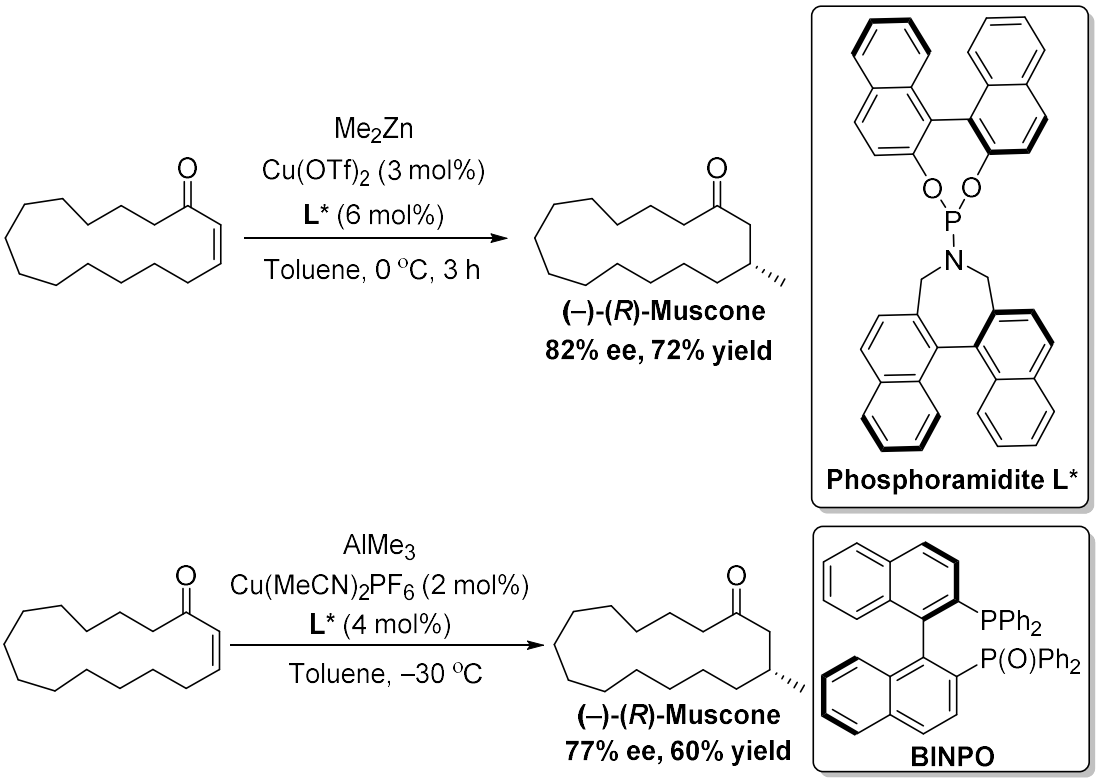

Scheme 1.9. Synthesis of (–)-(*R*)-Muscone using Cu-ACA of Me_2Zn[82] and $AlMe_3$[83].

ACA and AAA are so powerful that α,β-unsaturated ketones or allylic moieties are often purposely implemented into synthesis design strategy, so that new chiral centres can be obtained in high enantioselectivity. This is the case, for example, in the synthesis of Erogorgiane by Hoveyda[74], a marine diterpene and potential anti-tuberculosis agent (Scheme 1.10).

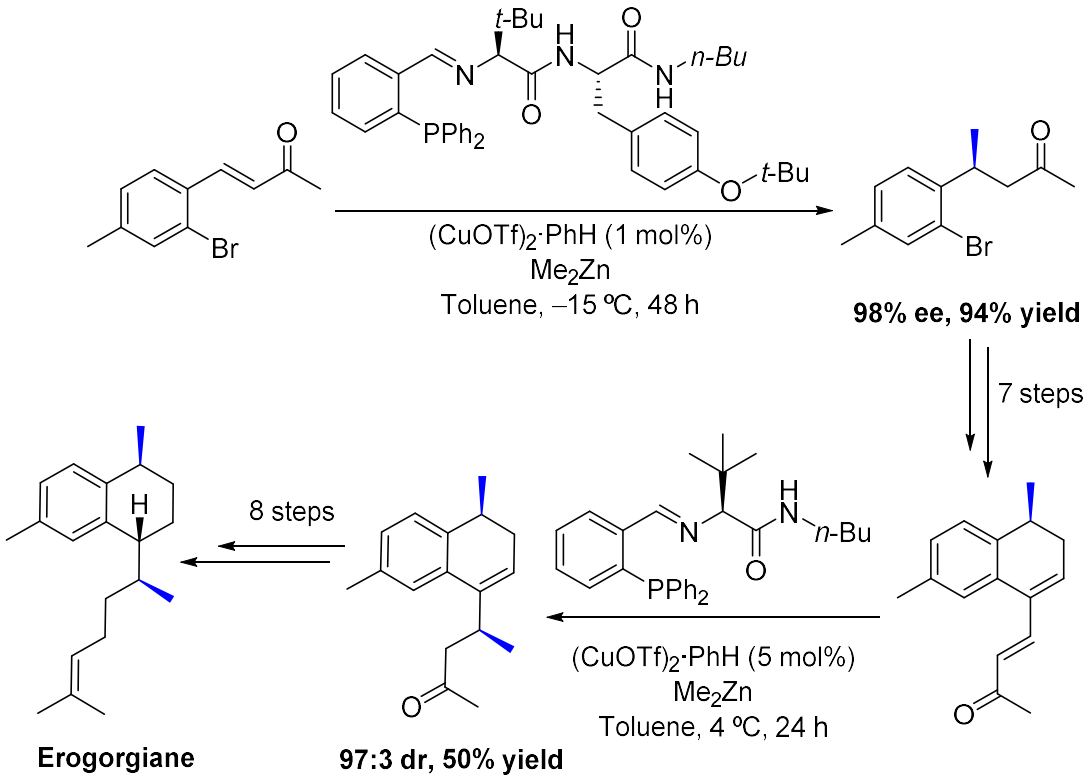

Scheme 1.10. Total synthesis of Erogorgiane using Cu-ACA for the implementation of chiral centres[74].

In this elegant application of asymmetric Cu-catalysis, highly enantioselective Cu-ACA (using $(CuOTf)_2$·PhH coupled with peptidic ligands and Me_2Zn nucleophiles) are used twice in the synthesis. In both cases, the α,β-unsaturated moieties are further transformed to achieve the desired product, exempt of any reminiscence of the conjugate addition other than the highly enantioselective carbon centres.

HYDROMETALLATION OF ALKENES

The current asymmetric methods primarily rely on the use of premade organometallic reagents[40]. Simple nucleophilic (Me, Et, Pr, Bu, vinyl, etc.) reagents can be purchased, proving easy access to premade organometallics

when developing new methodologies. However, when it comes to even mildly functionalised nucleophiles, which are often required for applications in target synthesis, premade organometallics are limited particularly at large scale. They need to be prepared in non-trivial procedures as they are pyrophoric, unstable, sensitive to moisture and air and they often lack functional group tolerance[67]. Moreover, due to their high reactivity, the driving force for the formation of a new C-C bond, organomagnesium, organoaluminium and organozinc nucleophiles use cryogenic temperatures to control the stereogenic outcome which is usually problematic for application to industry[84].

In recent years, some conjugate additions and allylic alkylations used nucleophiles generated *in situ* from the hydrometallation or carbometallation of alkynes or alkenes[67]. There are great advantages in using readily available, stable and easy to handle alkynes or alkenes in this manner. Due to the accessibility of alkenes and alkyne commercially, their use provide a great variability of potential nucleophiles. These methodologies are convenient to obtain complex organometallic nucleophiles and incorporation of a broader scope of functional groups. Common metals used in such methods are B, Si or Zr.

Previous work in our group[85] showed that alkylzirconocenes generated *in situ* from the hydrometallation of alkenes using Schwartz reagent can be used in highly enantioselective ACA when using ligand **A** (Scheme 1.11).

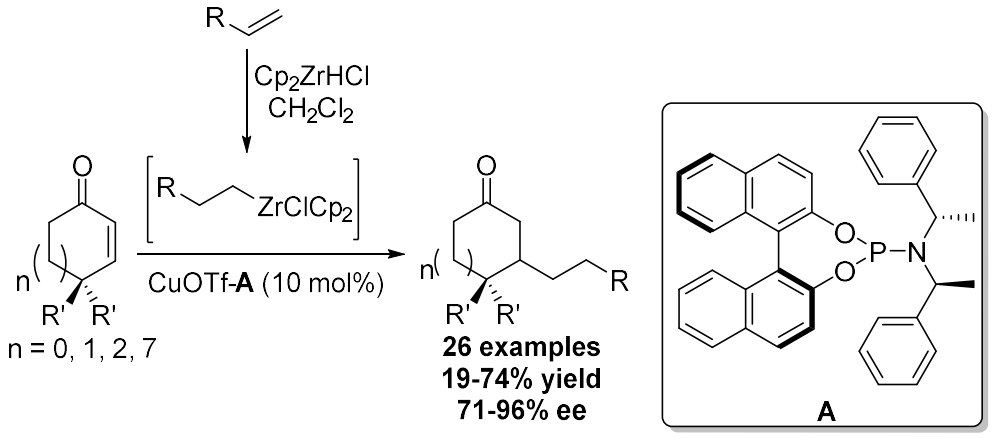

Scheme 1.11. Previous work in our group using alkylzirconocenes generated from the hydrometallation of alkenes in ACA[85].

This reaction is performed at room temperature and is robust and mild. Functional groups such as halogens, terminal alkenes and protected alcohol are all tolerated. The scope of this reaction was then extended to tri-substituted enones[86], lactones[87], linear substrates[88] and steroids[89,90]. The main restriction of such methodologies is the inability to add groups such as methyl, phenyl, *t*-butyl or branched groups. We are currently working towards toward new methodologies to circumvent these issues.

REACTION MECHANISM AND CATALYTIC COMPLEXES STRUCTURES

Intrinsic to organic chemistry is the study of reaction mechanism, to understand how components interact together and possibly tuning the reactivity to our advantage. Understanding mechanism can be highly fruitful not only for pure and simple academic knowledge but also as a powerful tool for optimisation and improvement of known methodologies. Beneficial insights into the mechanism include: minimisation of side-reactions; reducing reagent amount

and usage; improving reactivity by intelligently modify electronic and steric factors, optimising ligand design etc. Understanding mechanisms is also a means to efficiently design new reactions.

The synthetic utility of organocopper is undeniable and a myriad of recent methods have been developed with excellent results. However, these mechanisms and structures were poorly understood for a long time[37]. Although organocuprate structure and mechanism have been relatively well studied[37], much less effort has been directed to the elucidation of the mechanism of newer asymmetric methodologies using organozinc, organoaluminium or organomagnesium nucleophiles.

Very little is known about pre-catalytic complexes used despite the wide variety of ligands available and only a few X-ray structures have been described. In terms of Cu-phosphoramidite complexes, Feringa reported a CuI-monophos X-ray crystal to have a $[CuIL_3]$ structure[56] (Scheme 1.12a) and Zhou reported completely different connectivity in the CuBr-spirophosphoramidite as a $[CuBrL_2]_2$ dimer[91] (Scheme 1.12b). However, these crystal arrangements are implausible for ligand-accelerated catalysis and have been found to be inactive upon examination[91].

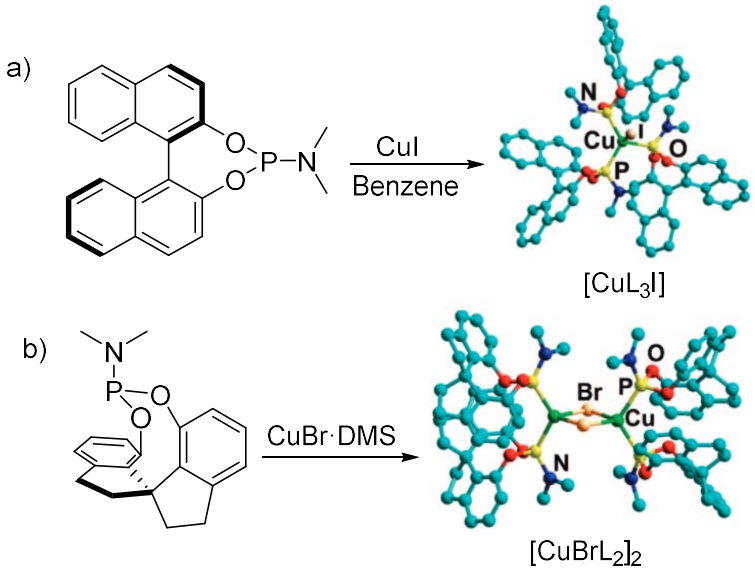

Scheme 1.12. Crystal structures of phosphoramidite-Cu complexes with a) CuI[56] and b) CuBr[92]. Adapted with permission from Ruth M. Gschwind, Chemical Reviews, "*Organocuprates and Diamagnetic Copper Complexes: Structures and NMR Spectroscopic Structure Elucidation in Solution*"[91]. Copyright 2008 American Chemical Society.

Unfortunately, the relevance and impact of solid-state structures on the reaction mechanisms are low due to the intrinsic influences of environment on the catalyst system (aggregation, solvation, chelation effects, etc.)[37]. Therefore studies of the catalytically active complexes are more pertinent in solution, the same environment as the reaction. In the 1980s, computational chemistry emerged as a powerful new tool for studying mechanisms, especially of organometallic reactions. *Ab initio* and density functional theories (DFT) calculations greatly contributed to the understanding of organocopper complexes structures and reactivity in solution[37]. However, the far most promising and accurate technique to study the mechanism of those complex Cu-catalysed additions in solution is NMR. Despite its clear advantages, mechanistic NMR studies are rare and would be thoroughly discussed in Part II of this thesis.

Regardless of a lack of experimental evidence, converging proposed mechanisms for stoichiometric and catalytic CA and AA have emerged. The

mechanisms of conjugate addition is thought to involve three key steps (Scheme 1.13): (i) transmetallation of an organometallic nucleophile to Cu^{I} to give an organocopper species followed by the rapid formation of a π-complex when interacting with the α,β-unsaturated ketone (observed for organocuprates by NMR[91,93-95]); (ii) oxidative addition to form a Cu^{III} π-complex and (iii) reductive elimination of the Cu^{III} species to release the chiral product and regenerate the pre-catalytic Cu^{I} species to complete the catalytic cycle[2,37]. Throughout the reaction, the transition metal from the nucleophile is thought to stay associated with the organocopper and act as a Lewis acid facilitating the oxidative addition step.

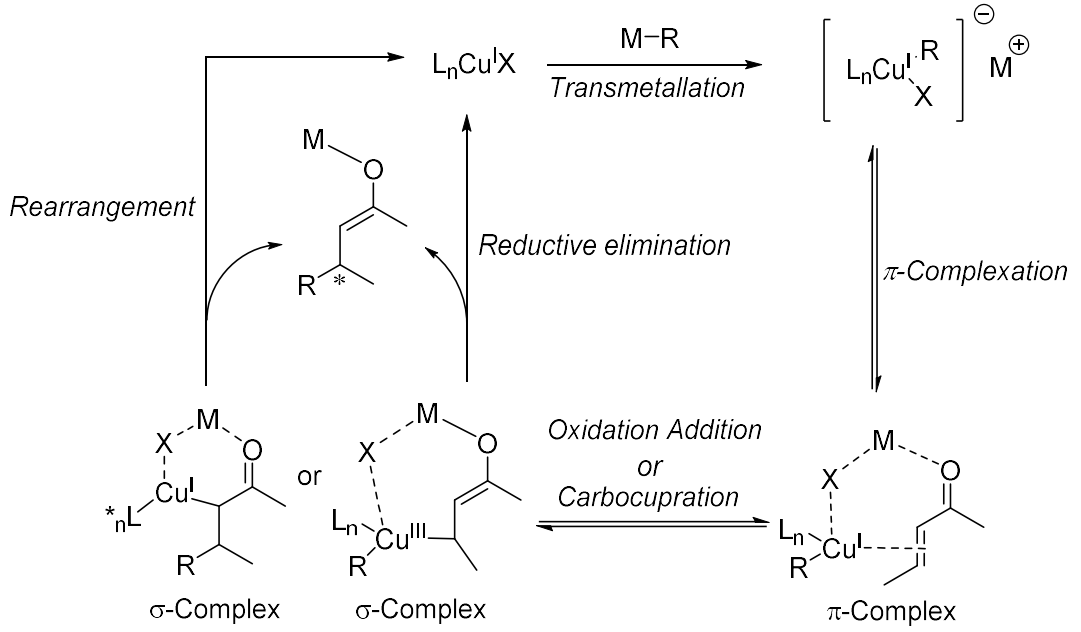

Scheme 1.13. Two proposed mechanisms for ACA[2,37].

An alternative pathway was proposed which involved a carbocupration (1,2-migratory insertion) with subsequent rearrangement to release the product instead of the oxidative addition/reductive elimination steps. However, that

pathway has been regarded as less plausible as the isomerisation of acyclic enones and DFT calculations support the oxidative addition pathway[37].

The mechanism of asymmetric allylic alkylation is similar to that of conjugate addition. It involves the same three key steps (Scheme 1.14): (i) Transmetallation, (ii) Oxidative addition, (iii) Reductive elimination. The equilibration of the π-complex and σ-complexes was observed by NMR[96]. DFT calculations suggest that reductive elimination is achieved from the π-allylcopper and that the σ-allylcopper plays a major role in the stereo-isomerisation[2]. In both ACA and AAA, the reductive elimination is thought to be the rate limiting step and/or regioselective and stereoselective determining step[37].

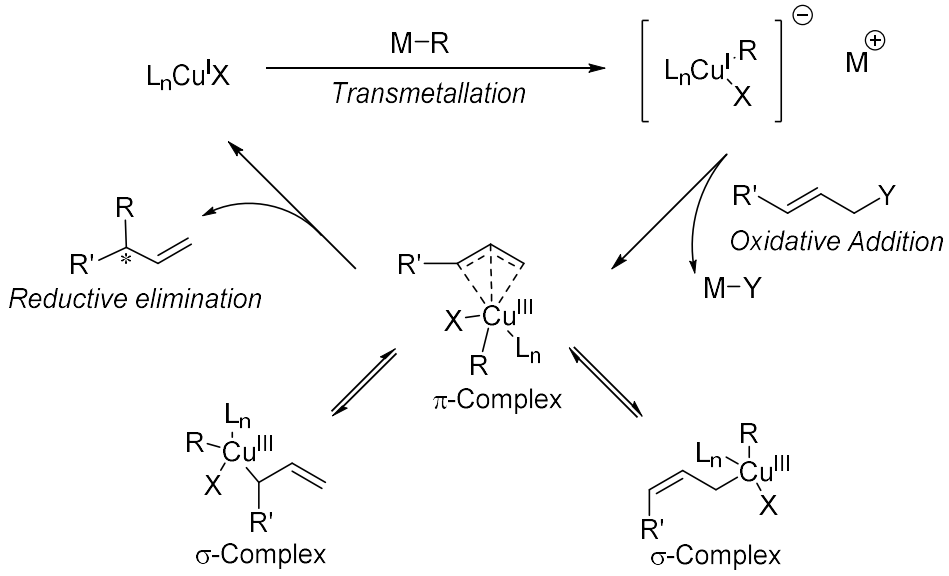

Scheme 1.14. Proposed mechanisms for AAA[2,37].

It is only in the 1990s that tri-coordinated organocopper (III) was observed at very low temperature and identified as an important intermediate in Cu^{I} mediated reactions[37]. Cu^{III} species are challenging to observe due to their kinetic

instability and the fact that they spontaneously undergo reductive elimination[37]. This high reactivity and low energy barrier to the formation of the product is thought to be the driving force of Cu^{I} processes.

Despite the popularity and importance of Cu-catalysed ACA and AAA in asymmetric catalysis, experimental evidence of mechanistic aspects is still shortcoming. Moreover, these studies are challenging and mechanistic studies need to be carefully designed in order to minimise overreaching extrapolations.

PART I

METHODOLOGIES TOWARDS THE SYNTHESIS OF PROSTAGLANDINS

INTRODUCTION

Prostaglandins are an extended family of natural hormone-like small molecules. They have a specific set nomenclature to describe their cyclic core (A, B, C, D, E, F_α, F_β and J) and degrees of unsaturation in the chain (0, 1 or 2). They have fascinated chemists due to their synthetic challenges and their vast array of biological activities, such as vascular smooth muscle control (bronchoconstriction/vasodilatation), platelet aggregation or disaggregation (coagulation), sensitisation of spinal neurons to pain, regulation of inflammation, calcium, hormones, cell growth and many other physiological pathways[97-99]. Notably recently, prostaglandins have been found to differentiate pluripotent stem cells and may serve as a means for a new generation of medicine against degenerative diseases (Parkinson's disease, Alzheimer, diabetes etc.)[100,101].

Natural prostaglandins are synthesised from arachidonic acid which itself is obtained from the catalytic cleavage of phospholipids (Scheme I.1). Arachidonic acid is then subsequently transformed to PGH_2 upon cyclisation and oxygenation. The same enzyme (PGH_2 synthases or cyclooxygenase-1 and -2 (COX-1 and COX-2)) carries out the cyclooxygenation and peroxidation. PGH_2 is the key biosynthetic intermediate for the biosynthesis of prostaglandins (PGE, PGF, PGI, PGD etc.)[98,102-104].

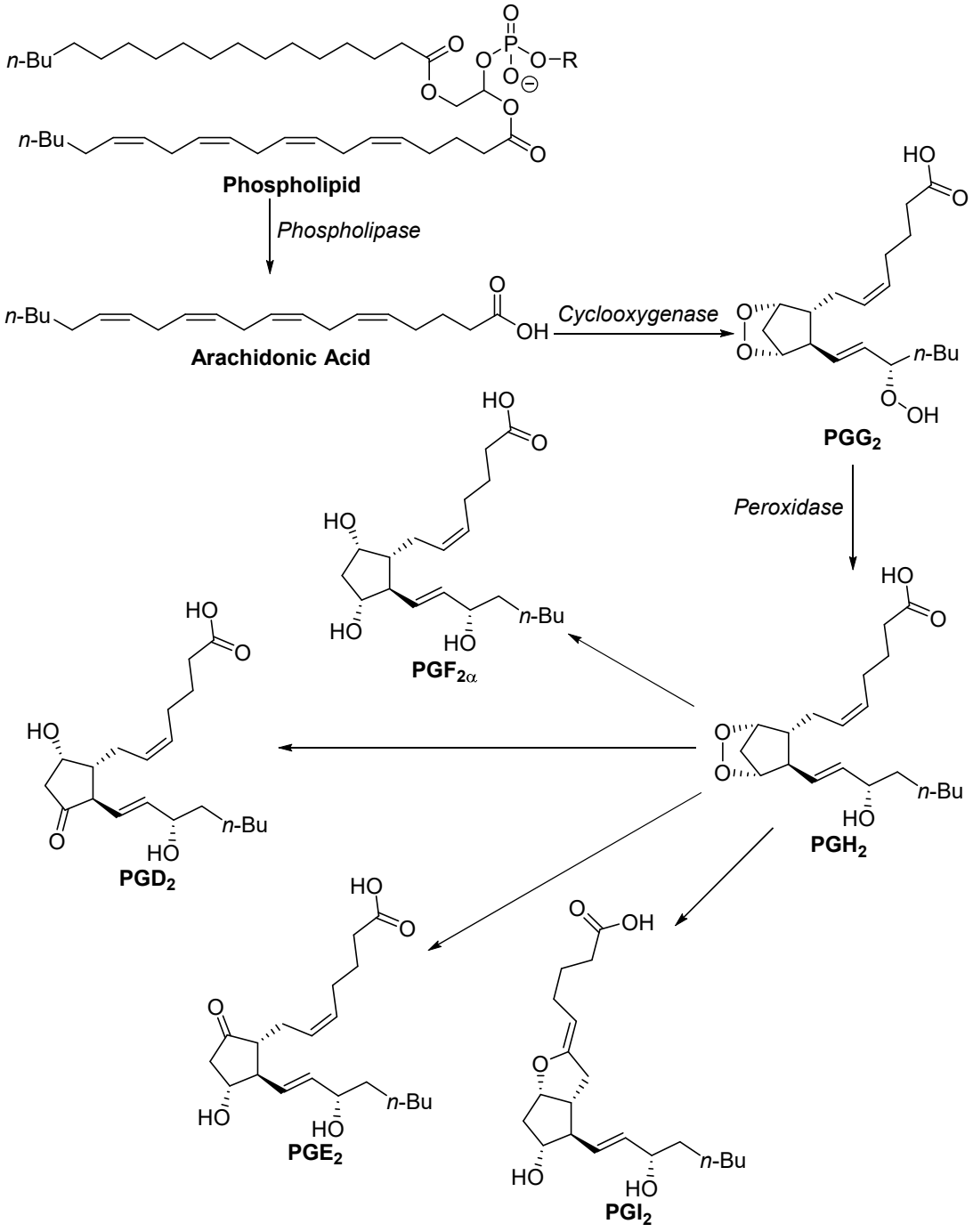

Scheme I.1. Prostaglandin biosynthesis[98,102-104].

The pharmaceutical industry has taken advantage of the prostaglandin family's biodiversity. Frequently, prostaglandin analogues bear the same cyclic core as natural prostaglandins. However, many variations on the chains have led to a vast array of clinical drugs, for example: Bimatoprost (ocular

hypertension)[105], Misoprostol (labour induction)[106], Iloprost (pulmonary arterial hypertension)[107], Lubiprostone (irritable-bowel syndrome)[108,109] (Figure I.1).

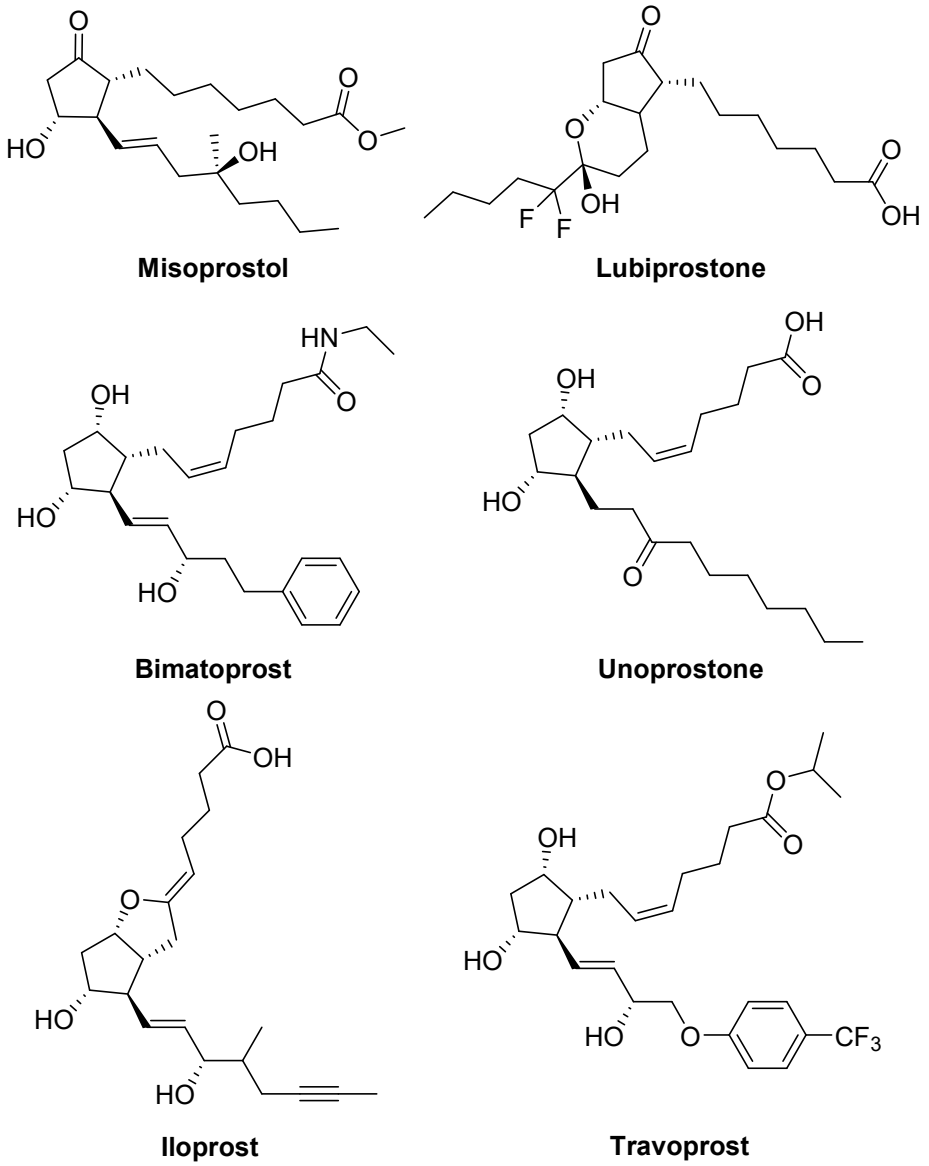

Figure I.1. Examples of synthetic prostaglandins used as clinical drugs.

Despite the discovery of prostaglandin dating back to 1930s[98,99], no synthesis of prostaglandin was successful for more than 30 years. Corey[110] pioneered the synthesis of $PGF_{2\alpha}$ and PGE_2 in 1969. The key intermediate is what is now referred as the 'Corey Lactone' (Scheme I.2). Its stereochemistry is

controlled by the Diels Alder reaction which then stereoselectively control all other chiral centres. From the Corey lactone, a Horner-Wadsworth-Emmons (HWE) and a Wittig reaction are carried out to add the two chains with E and Z double bond selectivity respectively. Nowadays this synthesis has been greatly improved with catalytic enantioselective Diels Alder[111-115] but the core synthetic steps have stayed the same and it is by far the most used route for prostaglandin synthesis in industry[99,116].

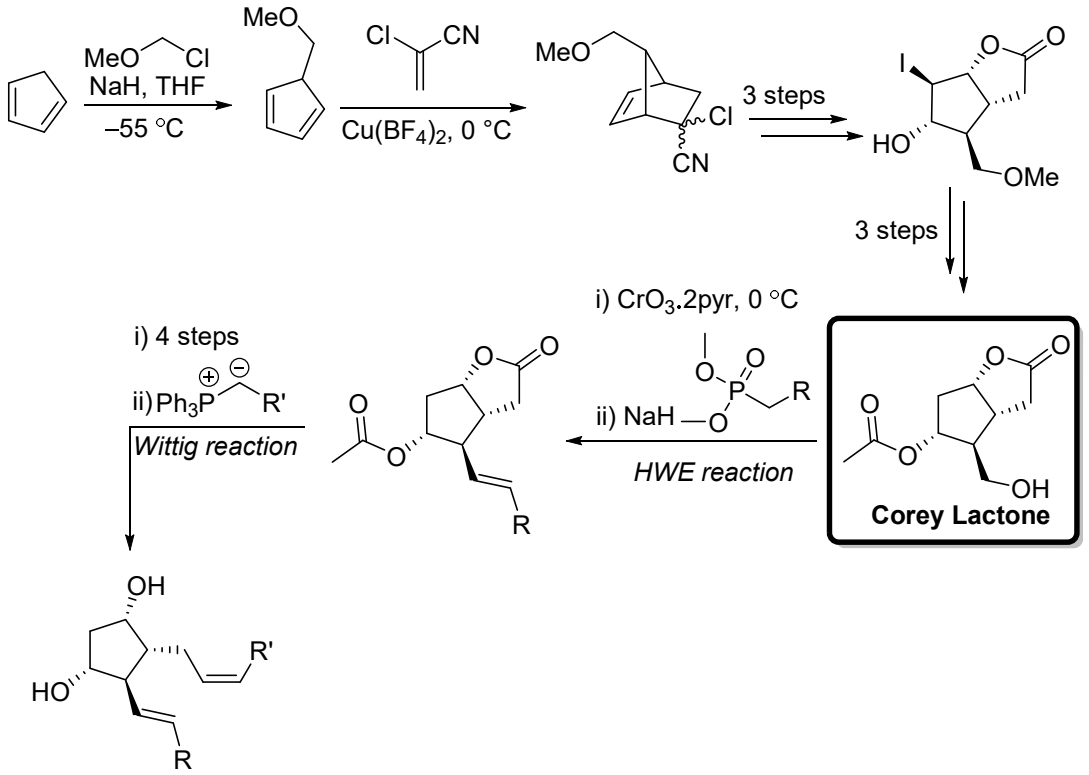

Scheme I.2. First synthesis of PGF_{2a} and PGE_2 in 1969 by Corey[110].

Another common strategy towards the synthesis of prostaglandin is catalytic and stoichiometric conjugate addition with tandem electrophilic trapping[117-123]. This synthesis, pioneered by Stork[117,118] in 1975, uses the enolate intermediate formed during the conjugate addition step to attack an electrophile and thus formally add the two chains to cyclopentenone in one step (Scheme I.3).

Noyori[119-122] also greatly contributed to the 3-component synthesis and achieved the addition of much more complex electrophiles than formaldehyde.

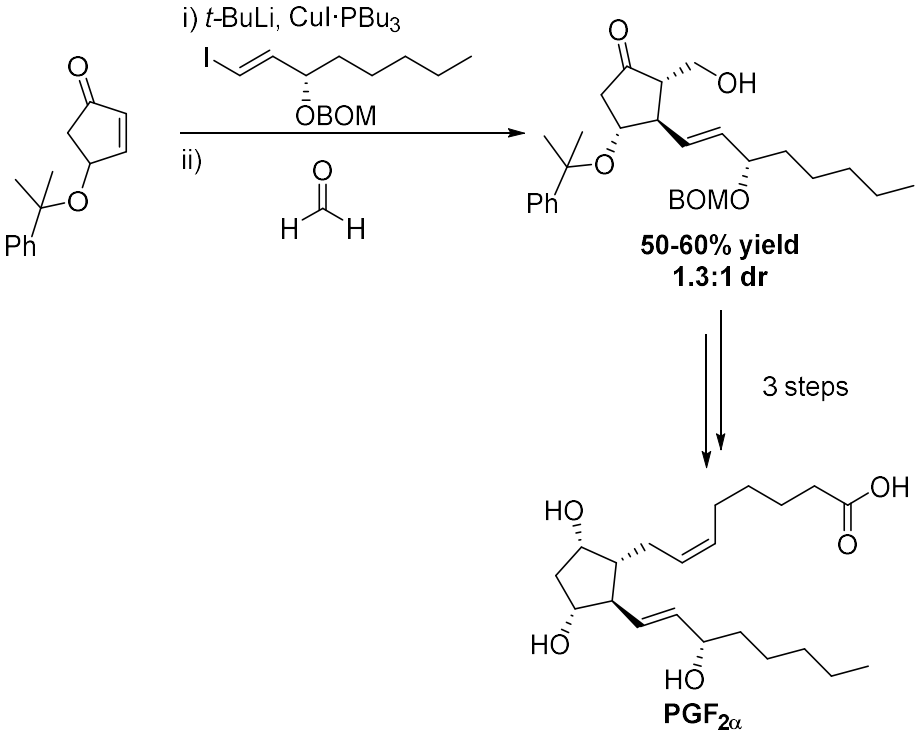

Scheme I.3. First synthesis of prostaglandins using a 3-component conjugate addition in 1975[117,118].

Many publications have described alternative 3-component conjugate additions using a variety of nucleophiles and electrophiles[123]. Historically the synthesis of prostaglandins using conjugate addition strategies relied on diastereoselective addition to chiral substrates as these were the only methods available. Their syntheses are now adapted to metal-catalysed ACA. However, the pharmaceutical industry has yet to implement 3-component conjugate addition in the synthesis of prostaglandins.

Aggarwal[99,105,124] recently described a synthesis of $PGF_{2\alpha}$ which combines both the Corey and 3-component approaches. It relies on the amino acid proline as the only source of chirality to stereoselectively control the outcome of all the

newly formed chiral centres. A complex cuprate is added to cyclopentafuran-5-carbaldehyde **1**, a Corey lactone analogue, in a 1,4-addition fashion to add the primary chain of $PGF_{2\alpha}$ (Scheme I.4). The second chain is added to the bicyclic 5-membered lactone via a Wittig reaction, in a similar fashion to the Corey synthesis.

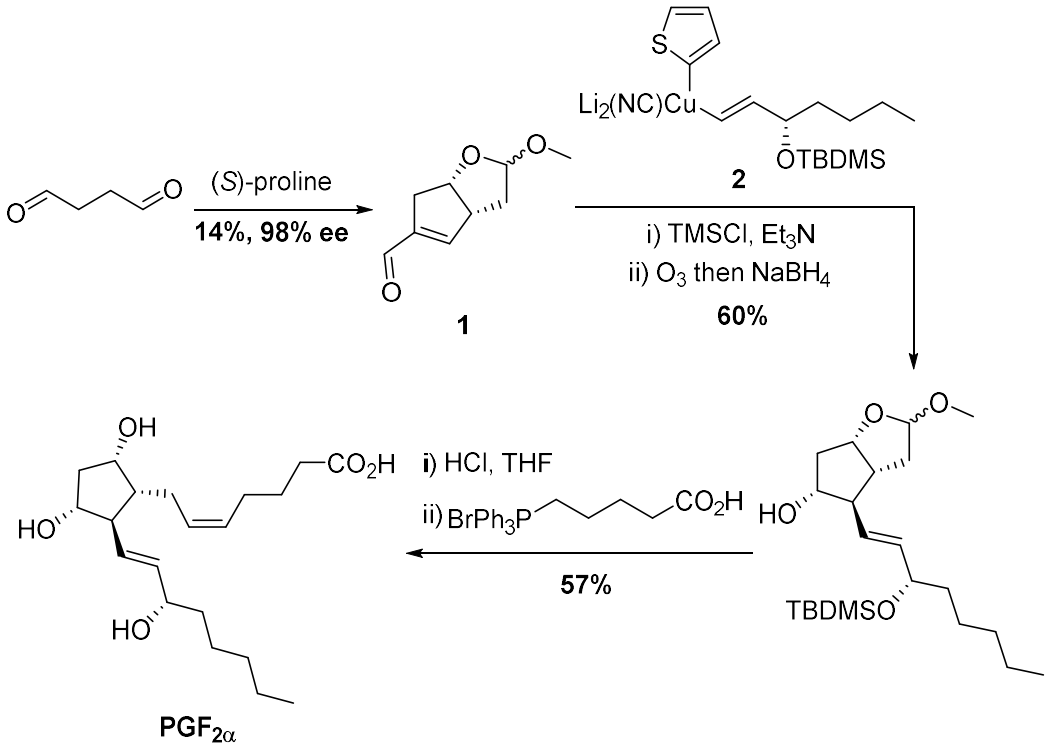

Scheme I.4. Aggarwal's synthesis of $PGF_{2\alpha}$[99,124].

This synthesis has even been implemented in industry due to the availability of the starting materials particularly (*S*)-proline as the sole source of chirality. However, the limitations of this synthesis mostly lie in the poor yield obtained to form **1** (only 14%) and the tedious synthesis of the mixed cuprate **2** (Scheme I.5).

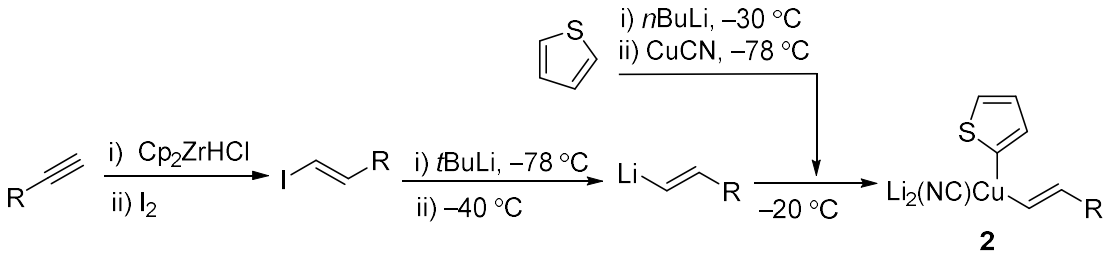

Scheme I.5. Synthesis of the mixed cuprate used in Aggarwal's conjugate addition[99,124].

AIMS

Based on the success and variability of the Fletcher's group first asymmetric conjugate addition of alkylzirconocenes (Chapter 1, Scheme 1.11), we wanted to demonstrate the use of organozirconocenes in the synthesis of prostaglandins and implement a platform for the rapid synthesis of many analogues.

CHAPTER 2

HYDROMETALLATION AND CATALYTIC ASYMMETRIC CONJUGATE ADDITION OF ALKYNES

INTRODUCTION

The Fletcher group developed the addition of alkylzirconocenes in tandem ACA (Chapter 1 Scheme 1.11)[85]. However, many prostaglandins and analogues bear a double bond directly adjacent to the cyclic core and thus synthesis using asymmetric conjugate addition requires the addition of sp^2-hybridised nucleophiles.

Traditionally, Cu-catalysed asymmetric 1,4-addition methods involving alkenyl nucleophiles primarily rely on the use of premade organometallic reagents. For example, Schmalz[40] reported the conjugate addition of sp^2-hybridised Grignard reagent to cyclic enones (Scheme 2.1).

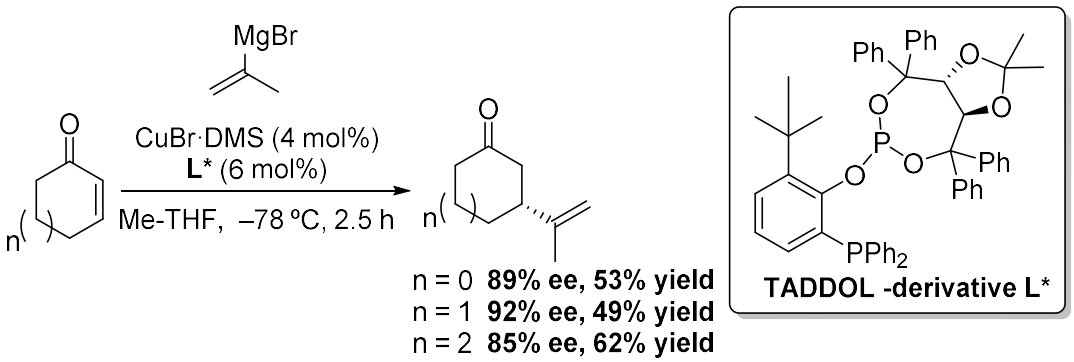

Scheme 2.1. Example of a ACA methodology using alkenyl Grignard reagent as the nucleophile[40].

Since the 1970s, the hydrozirconation of alkynes has been long studied by Schwartz[125,126] and others and would provide vinyl nucleophiles, which can be used in asymmetric addition reactions. In this perspective, Schwartz developed a racemic Ni catalysed tandem alkyne hydrozirconation-1,4-addition (Scheme 2.2)[127]. This methodology has been employed in the synthesis of prostaglandins[127] and even patented by Hoffman-La Roche in the synthesis of a Trimoprostil, an anti-ulcerative agent[128].

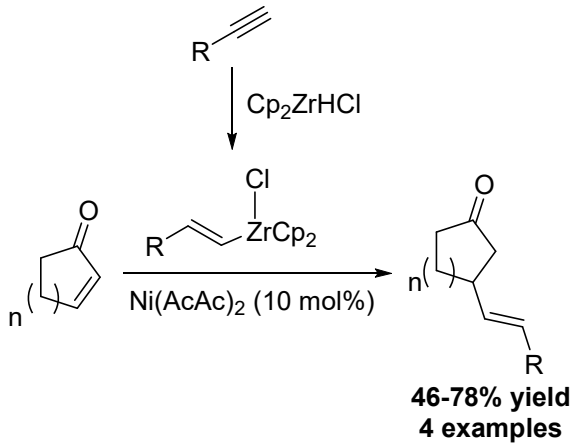

Scheme 2.2. Schwartz racemic Ni-catalysed conjugate addition of vinylzirconium reagent to cyclic enone[127].

Alkenylzirconocene nucleophiles were also used in ACA by Inoue[129] with rhodium complexes. Inoue's system provides high enantioselectivity but only simple alkyl substituents (linear all-carbon chains) on the alkenyl moiety were found to give products **3** in good yields and ee (Scheme 2.3). Indeed, phenyl nucleophiles gave good ee (90% ee) in very poor yields (20%) while the bulky *t*-butyl group was obtained in medium yield (49%) with only 79% ee. This method was subsequently used by Nicolaou[130] in a tandem asymmetric 1,4-addition–trapping sequence, a key step in the total synthesis of Vannusal A, a marine secondary metabolite.

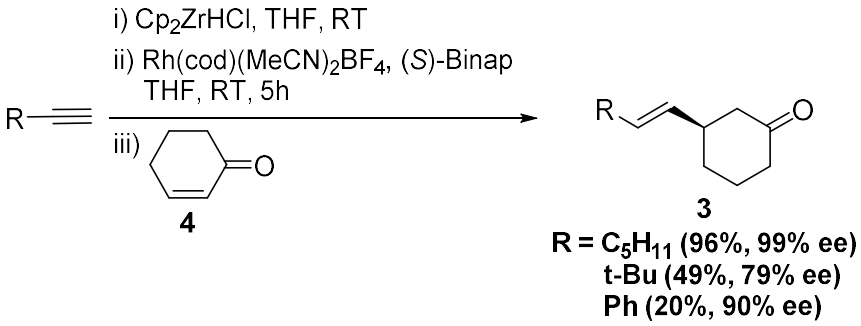

Scheme 2.3. Inoue's tandem alkyne hydrozirconation-asymmetric 1,4-addition system using Rh catalysis[129].

Therefore, based on previous uses of alkenylzirconocene nucleophiles in Ni and Rh catalysed conjugate addition and the success of our group in using alkylzirconocene in Cu-catalysed ACA, we wanted to investigate the use of alkenylzirconocenes in Cu-catalysed ACA.

RESULTS AND DISCUSSION

Initial ligand screening

Firstly, we began our studies using 2-cyclohexen-1-none **4** and 5-phenyl-1-pentyne **5** with the conditions used in the alkylzirconocene ACA screening, $(CuOTf)_2$·PhH-**A** in CH_2Cl_2[85]. Although those conditions are not the alkylzirconocene ACA optimised conditions, previous studies showed that using $(CuOTf)_2$·PhH in CH_2Cl_2 was generally better for more ligands, allowing for a wider and effective screening.

We decided to start with ligand screening and more than 30 ligands in a variety of classes were tested. We tested ferrocene ligands such as Taniaphos or Josiphos (**B**), diphosphine ligand such as Binap and derivatives (**C**) and Segphos

and derivatives (**D**) and phosphoramidite such as Feringa Ligand (**A**), SiPhos-PE (**E**) and Taddol Monophos. A few of them are shown in Scheme 2.4.

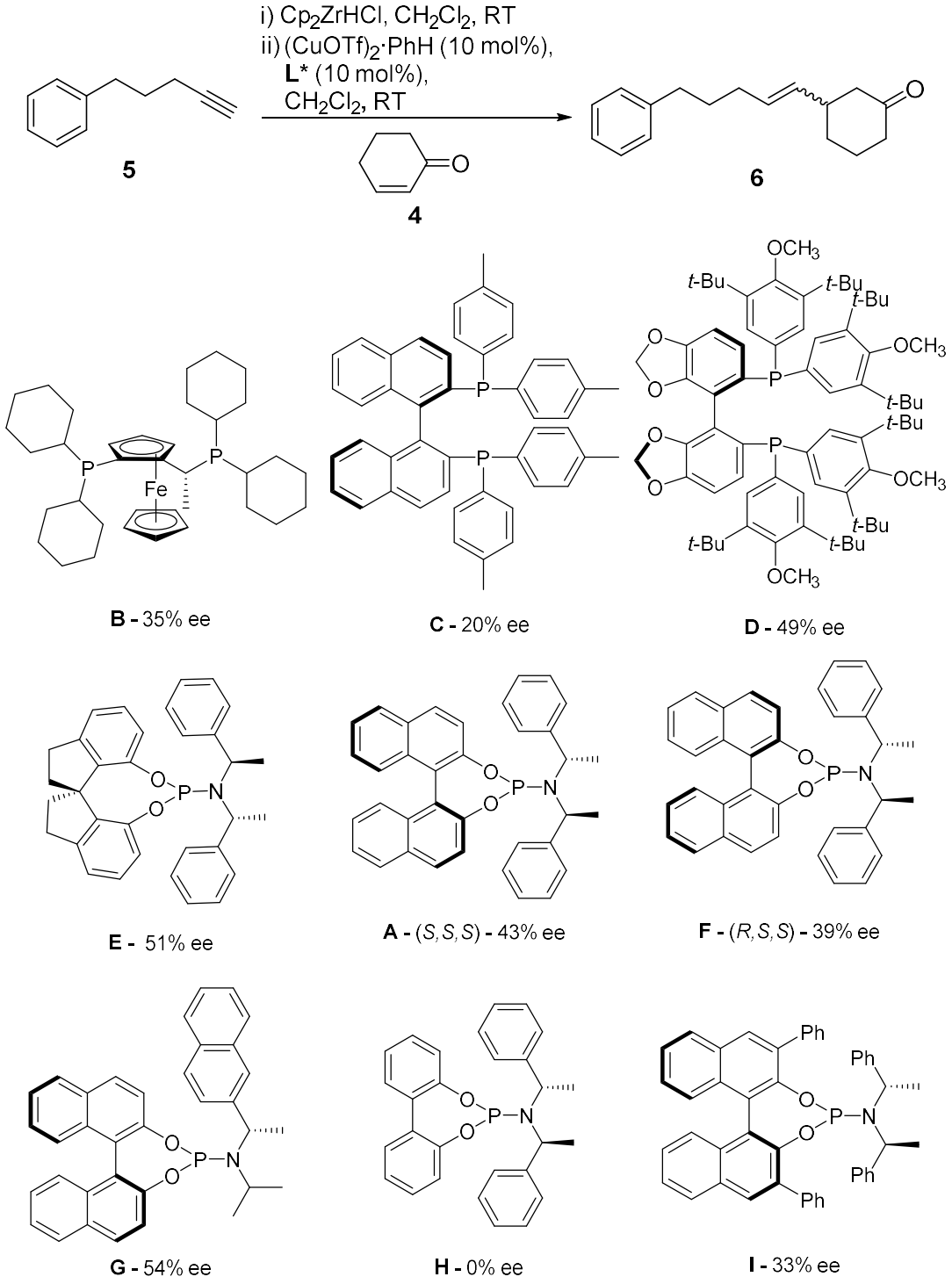

Scheme 2.4. Sample of our initial ligand screening in the Cu-catalysed ACA of alkenylzirconocenes. Conditions: 5-phenyl-1-pentyne **5** (2.5 eq), Cp_2ZrHCl (2.0 eq), CH_2Cl_2, cyclohexenone **4** (1.0 eq), $(CuOTf)_2$·PhH (5 mol%), **L*** (10 mol%) in CH_2Cl_2, room temperature. ee determined by HPLC.

Our initial screen shows that product **6** was obtained with the highest ee with phosphoramidite ligands which gave up to 54% ee for ligand **G** in CH_2Cl_2. Ferrocene based ligands such as Josiphos **B** and diphosphine ligands such as T-Binap **C** consistently gave product **6** in low ee, the best of these classes giving 35% ee for **B** and 20% ee for **C**. The very bulky diphosphine DTBM-Segphos **D** gave a moderate 49% ee, closely related to the 54% ee obtained with phosphoramidite ligand **G**. In the case of phosphoramidites, the backbone had a high impact on the ee obtained as the biphenol ligand **H** gave no enantioselectivity and the phenyl substituted binaphthol ligand **I** gave 33% ee. The more common binaphthol backbone ligand such as **A, F** and **G** were more favourable, giving product **6** in ee between 31-54%. The spiro-backbone ligand **E** was also favourable giving a high 51% ee.

In the alkylzirconocene ACA, the optimised conditions used Et_2O as a solvent and TMSCl (5.0 eq) as an additive. We wanted to test these conditions on the most promising ligands in each classes (Scheme 2.5). Results showed that in the case of ferrocene **B** and diphosphine ligands **C** and **D**, using Et_2O and TMSCl was detrimental to the ee giving no product, 6% ee and 19% ee respectively. In the case of phosphoramidite ligands, results were more mixed. For the spiro ligand **E** and binaphthol ligand **G,** the ee dropped to 45% ee and 44% ee respectively. However in the case of the commonly used Feringa ligand **A** the ee increased from 43% ee in CH_2Cl_2 to 64% ee in Et_2O with TMSCl. Thus ligand **A** was also found to be the best ligand for the alkylzirconocene nucleophiles in Et_2O with TMSCl[85]. Moreover it would seem that Et_2O and TMSCl have a special tuning effect on ligand **A**, which is not observed with any other classes of ligand or even other phosphoramidites. TMSCl is well known to accelerate Cu-catalysed

addition reactions however the mechanism behind this effect are debated[131-137]. TMSCl might act as a Lewis acid on the organocopper-enone π-complex, facilitating the reductive elimination of the intermediate Cu^{III} species. We also observed in Chapter 8 the capacity of TMSCl to directly modify the Cu-catalyst (CuOTf-**A**) itself therefore explaining the special affinity of ligand **A** for TMSCl.

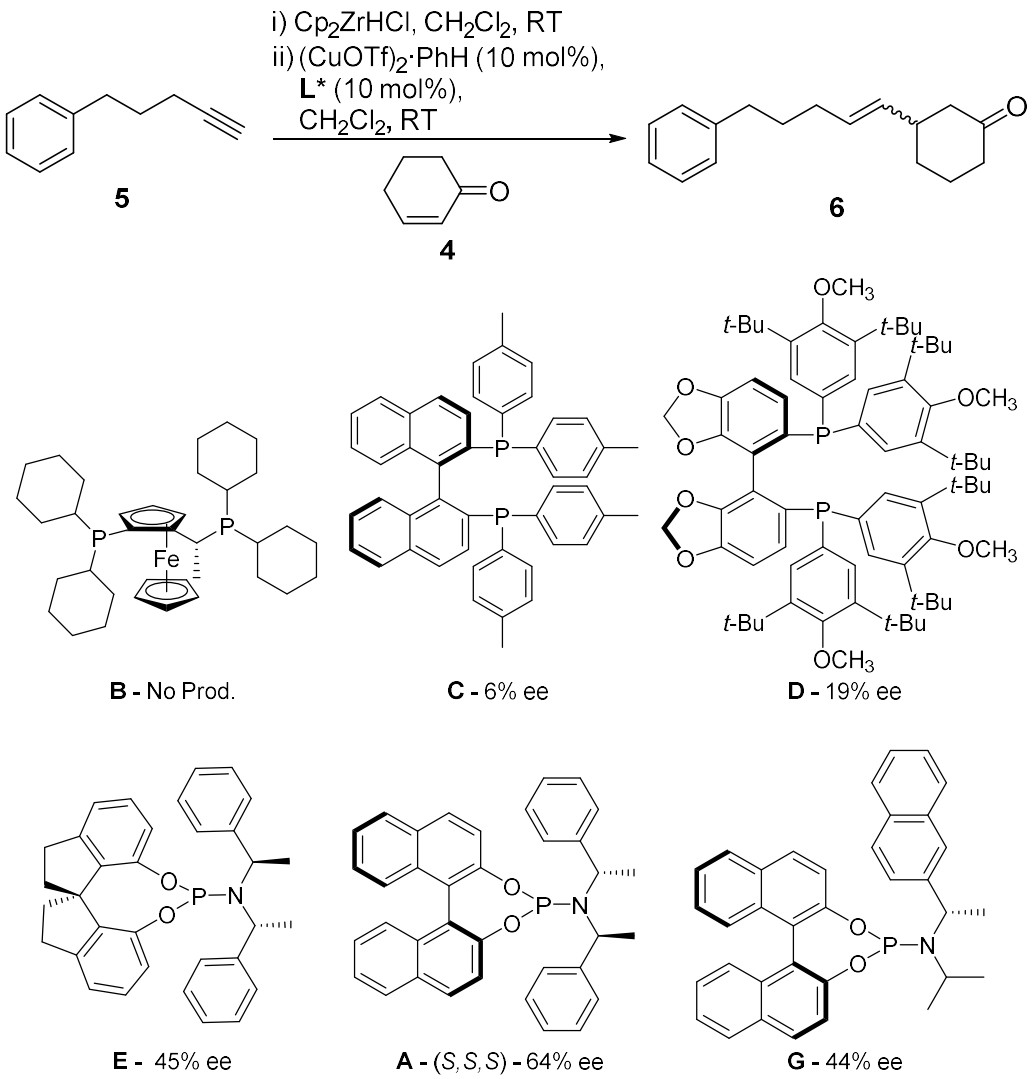

Scheme 2.5. Screening of the best ligands in each class in Et_2O with TMSCl (5.0 eq). Conditions: 5-phenyl-1-pentyne **5** (2.5 eq), Cp_2ZrHCl (2.0 eq), CH_2Cl_2, cyclohexenone **4** (1.0 eq), $(CuOTf)_2$·PhH (5 mol%), in Et_2O, TMSCl (5.0 eq), room temperature. ee determined by HPLC.

Cu source screening

Subsequently, a Cu screen was implemented using ligand **G** in CH_2Cl_2 (Table 2.1) due to the lack of improvement on the enantioselectivity for ligand **A** with any other conditions than $(CuOTf)_2 \cdot PhH$ in Et_2O with TMSCl. A variety of Cu^I salts are commercially available but some of them are not stable enough to be sold. Hence it is common practice to transmetallate a Ag counterion to CuCl, with the precipitation of AgCl as the driving force for this exchange.

Table 2.1. Cu source screening of alkenylzirconocene nucleophiles.

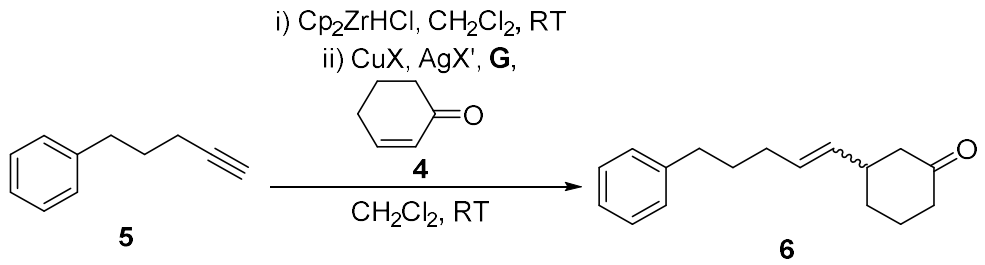

Entry	CuX	ee[§]
1	$(CuOTf)_2 \cdot PhH$	54%
2	CuI	5%
3	CuBr	10%
4	CuCl	22%
5	Cu(*t*BuCN)$_2$OTf	53%
6	Cu(MeCN)$_2$OTf	58%
7	Cu(MeCN)$_4$OTf	45%
8	Cu(OTf)$_2$	38%
9	CuCl, AgNTf$_2$	46%
10	CuCl, AgClO$_4$	44%
11	CuCl, AgPF$_6$	14%
12	CuCl, AgSbF$_6$	62%
13	CuCl, AgBF$_4$	17%
14	Cu(MeCN)$_4$BF$_4$	51%
15	CuCl, NaBARF	45%
16	CuCl, AgNO$_3$	13%
17	CuOAc	10%

Conditions: 5-phenyl-1-pentyne **5** (2.5 eq), Cp_2ZrHCl (2.0 eq), CH_2Cl_2, cyclohexenone **4** (1.0 eq), CuX (10 mol% or 5 mol% for $(CuOTf)_2 \cdot PhH$), AgX' (11 mol%), **G** (10 mol%), in CH_2Cl_2, room temperature. [§]ee determined by HPLC.

Many different Cu sources were tested. Similarly to the alkylzirconocene nucleophiles, the Cu-halide sources gave poor enantioselectivity with alkenylnucleophile (5%, 10% and 22% respectively for CuI (entry 2), CuBr (entry 3) and CuCl (entry 4)). We then decided to test various source of $Cu^{I}OTf$ and $Cu^{II}OTf$ (entry 5-8). All gave similar results (45-58% ee) with $Cu(tBuCN)_2OTf$ giving the highest ee (58% ee, entry 5). $Cu(OTf)_2$, a Cu^{II} source, only gave 38% ee, a much lower value than the 45-58% ee obtained with $Cu^{I}OTf$ sources. Many other counterions were tested such as $CuNTf_2$ which only gave 46% ee (entry 9). The counterions gave variable results, ranging from poor ee for $CuPF_6$ (14% ee, entry 11), $CuBF_4$ (17% ee, entry 13), $CuNO_3$ (13% ee, entry 16) and CuOAc (10% ee, entry 17) to moderate ee for $CuClO_4$ (44% ee, entry 10), $Cu(MeCN)_4BF_4$ (51% ee, entry 14) and CuBARF (45% ee, entry 15). There was a great difference between $CuBF_4$ (17% ee, entry 13) and $Cu(MeCN)_4BF_4$ (51% ee, entry 14) presumably due to the instability of $AgBF_4$, a highly hygroscopic species. Best results were achieved for $CuSbF_6$, giving 62% ee (entry 12). We also tested ligand **A** with these optimised conditions and only obtained 59% ee and in Et_2O with TMSCl, a poor 12% ee was observed reaffirming that no further optimisation could be obtained with ligand **A**.

Secondary ligand screening

We then examined a variety of additional phosphoramidite ligands using $CuSbF_6$. A few of them are shown in Scheme 2.6.

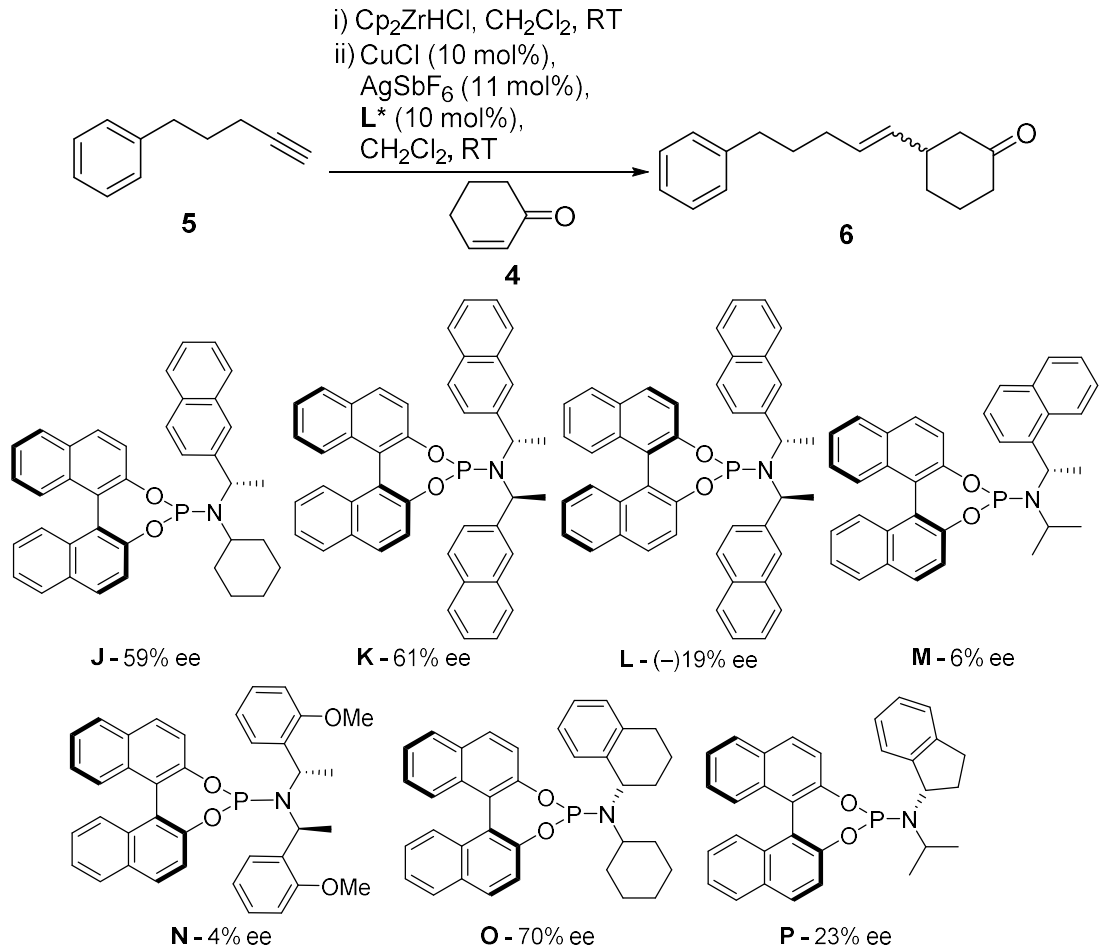

Scheme 2.6. Secondary ligand screen using phosphoramidite ligands. Conditions: 5-phenyl-1-pentyne **5** (2.5 eq), Cp_2ZrHCl (2.0 eq), CH_2Cl_2, cyclohexenone **4** (1.0 eq), CuCl (10 mol%), $AgSbF_6$ (11 mol%), **L*** (10 mol%), in CH_2Cl_2, room temperature. ee determined by HPLC.

A strong matched-mismatched effect was observed when using (*S,S,S*)-**K** (61% ee) compared to (*R,S,S*)-**L** (19% ee). All matched ligands possessing a (*S)*-2-naphthalene side-chain gave similar ee (**G** (62% ee), **J** (59% ee), **K** (61% ee)). (*S, S*)**-**1-naphthalene (**M**, 6% ee) and methoxy (**N**, 4% ee) substituents were however detrimental to the ee. Best results were obtained with (*S,S*)**-O** (70% ee) featuring a fixed side chain. A smaller homologue ((*S,S*)**-P** (23% ee)) was not as successful. These experiments demonstrated that subtle changes in sterics or electronics provided highly variable results and no straightforward trend in enantiomeric induction was deduced, clearly emphasising the difficulty of finding

a ligand inducing high enantioselectivity when lacking 3D models and conformation potentials by computational chemistry.

Reactivity challenges

Unfortunately, in all above experiments, low yields of **6** (13-15%) were consistently observed. The reaction does not reach completion, stopping after 3 h despite cyclohexenone **4** still being present and many side-products are formed. A significant amount of alkenylzirconocene was found to dimerise (23% yield) to give the aliphatic product **7** (Figure 2.1). This dimer was also observed in later studies of the asymmetric allylic alkylation of alkenylzirconocene[138]. The origin of this dimer is uncertain but must come from the oxidation of the alkenyl homocuprate that might be favoured by the electron rich nature of alkenylzirconocenes. The fast homocoupling of the nucleophile will significantly reduce the amount of nucleophile present in the reaction and thus chances of obtaining the desired ACA product. In the AAA of alkenylzirconocene, this problem was circumvented by using more reactive starting material such as allylbromide and cooling down the reaction to −40 °C in order to favour the AAA process over the fast dimerisation of the nucleophile. However, in the case of ACA, the difference in reactivity of different enones is unfortunately negligible compared to the use of potent leaving groups in AAA. Reactions carried out without excess alkyne in order to control the alkenylzirconocene homocoupling did not improve the yields (10% yield).

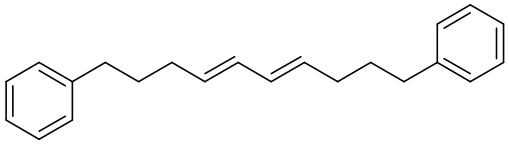

7

Figure 2.1. Homocoupling product obtained in the ACA reaction of alkenylzirconocenes.

Another side product, alcohol **8**, was also isolated (12% yield, Figure 2.2) presumably arising from the rearrangement of the 1,2-addition quaternary-alcohol product to the conjugated product **8**. A rearranged conjugated product was also observed in the AAA of alkenylzirconocenes. Therefore those observations were not isolated to the ACA system and sp^2-hybridised Zr nucleophiles tend to be more problematic than sp^3-hybridised Zr nucleophiles. Attempts to identify other side-products were unsuccessful due to their numbers and low yields.

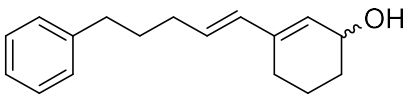

8

Figure 2.2. Secondary product obtained in the ACA reaction of alkenylzirconocenes.

Using cryogenic temperatures (–40 °C, –78 °C, –78 °C to 0 °C), heating (40 °C) and/or using freshly distilled starting materials were unsuccessful at improving the yield (<10% yield in all cases). Using a stoichiometric amount of CuOTf-**A** gave slightly improved yield (17%) but surprisingly, the ee was much lower, giving 14% ee compared to the 62% ee obtained with 10 mol% catalyst.

Inoue also reported his rhodium system[129] to give low yield (20%) when using alkynes functionalised with an aromatic ring. Consequently, we examined a

simple linear alkyne, 1-hexyne **9**, in the ACA reaction of alkenylzirconocenes. However we only obtained product **10** in 7% yield (Scheme 2.7).

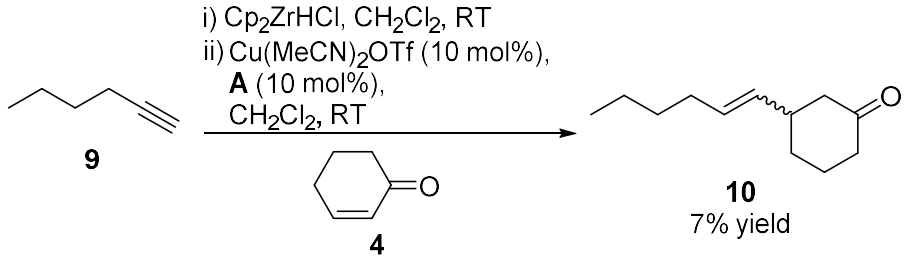

Scheme 2.7. Testing the effect of 1-hexyne 6 on the ACA reaction yield. Conditions: 1-hexyne **6** (2.5 eq), Cp_2ZrHCl (2.0 eq), CH_2Cl_2, cyclohexenone **4** (1.0 eq), $Cu(MeCN)_2OTf$ (10 mol%), **A** (10 mol%), in CH_2Cl_2, room temperature. Isolated yield.

Previous work on the ACA of alkylzirconocenes[85] showed that using 4,4-dimethylcyclohexenone **11** improve the yield from 59% to 66%. In the case of sp^2-hybridised Zr nucleophiles, enone **11** exclusively gave unselective (0% ee) 1,2-addition product **12** in 43% yield. The same selectivity for the 1,2-addition product **12** was observed in various conditions, even at –40 °C (Scheme 2.8). When using stoichiometric CuBr·DMS, we exclusively observed the formation of the 1,4-addition product **13** in 9% yield whilst the majority of starting material was recovered.

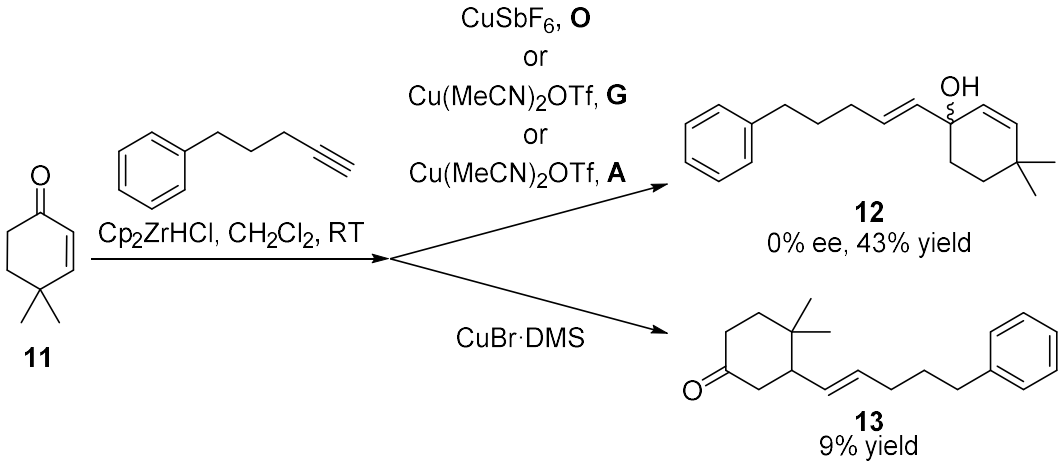

Scheme 2.8. Reactivity of enone 11 upon addition of alkenylzirconocenes. Conditions: 5-phenyl-1-pentyne **5** (2.5 eq), Cp_2ZrHCl (2.0 eq), CH_2Cl_2, cyclohexenone **11** (1.0 eq), CuX (10 mol%), **L*** (10 mol%), in CH_2Cl_2, room temperature. Stoichiometric system: 5-phenyl-1-pentyne **5** (2.5 eq), Cp_2ZrHCl (2.0 eq), CH_2Cl_2, cyclohexenone **11** (1.0 eq), CuBr·DMS (1.0 eq), in CH_2Cl_2 (0.2 M), room temperature. Isolated yields. ee determined by HPLC.

This shift in reactivity is surprising as Zr nucleophiles are thought to be mild nucleophiles, less prone to undergo 1,2-addition than Grignard reagents for example. Moreover, Cu catalysis is generally highly selective for 1,4-addition. We speculate that the combination of steric hindrance by the methyl groups at the 4 position on enone **11** and the relatively electron-rich alkenylzirconocene favours a non-catalysed 1,2-addition. This hypothesis would explain the lack of enantioselectivity (0% ee) observed. The different results (9% of **13**) obtained in the presence of stoichiometric CuBr·DMS can be rationalised by the difference in reactivity of Cu-halogen species compared to more ionic Cu sources and the already observed divergence in reactivity of this system when using stoichiometric Cu. The presence of stoichiometric CuBr·DMS might interfere with the alkenylzirconocene non-catalytic 1,2-addition pathways and favours a poorly reactive 1,4-addition.

Furthermore, the 1,2-addition product **12** obtained with enone **11** reinforced the hypothesis that the conjugated product **8** is obtained from the rearrangement of the quaternary alcohol 1,2 addition product of

alkenylzirconocenes to enone **4**. The origin of the rearrangement is unclear but is probably due to acid catalysis. Presumably, the 1,2-addition product undergoes an ionisation *in situ* or upon work up to give a stable tertiary carbocation (Scheme 2.9). Then, the carbocation is attacked by H_2O during work-up to generate the more stable product **8**.

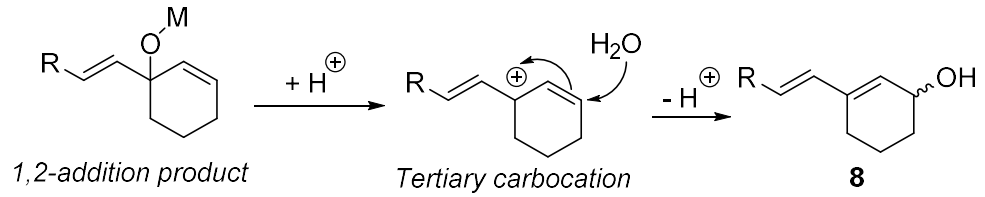

Scheme 2.9. Proposed rearrangement of 1,2-addition product driven by the extension of conjugation.

CONCLUSION

To conclude, alkenylzirconocene nucleophiles are challenging due to poor control of reaction outcomes. These sp^2-hybridised nucleophiles dimerise, consuming one of the crucial reactants independently of the alkyne used. Due to the presence of two double bonds, products have a tendency to rearrange to conjugated system such as product **8** and studies using enone **11** even showed that the 1,2-addition might be favoured over the 1,4-addition. Unfortunately those observations seem to be intrinsic to alkenylzirconocenes and we could not tune our understanding of the systems' poor reactivity to improve the yield. However, the Fletcher group has recently developed a powerful Rh-catalysed AAA of aryl and vinyl boronic acid nucleophiles[139] which have yet to be applied to the synthesis of prostaglandins.

CHAPTER 3

ASYMMETRIC CONJUGATE ADDITION OF ALKYLZIRCONOCENES TO CYCLOPENTENONE-3,5-DIONE MONOACETALS

Parts of this Chapter has been published in Synthesis[140] and highlighted in Synfact[141]. Florian Mäsing, a visiting Masters student, carried out the initial screening. Lukas Pfeifer ran the X-ray crystal structure of product ***21a****.*

INTRODUCTION

In Chapter 2, we discussed our attempts to develop a new method for the Cu-catalysed ACA of alkenylzirconocenes (sp^2-hybridised nucleophiles) but this system proved inefficient and problematic. However, in the diversity of prostaglandins, many natural and synthetic prostaglandins do not feature a double bond adjacent to the cyclic core (Figure 3.1). Thus we decided to focus on the asymmetric conjugate addition of alkylzirconocenes towards the synthesis of these prostaglandins. Even if this would reduce our scope, these are nonetheless desirable and would provide an initial platform towards the synthesis of prostaglandins.

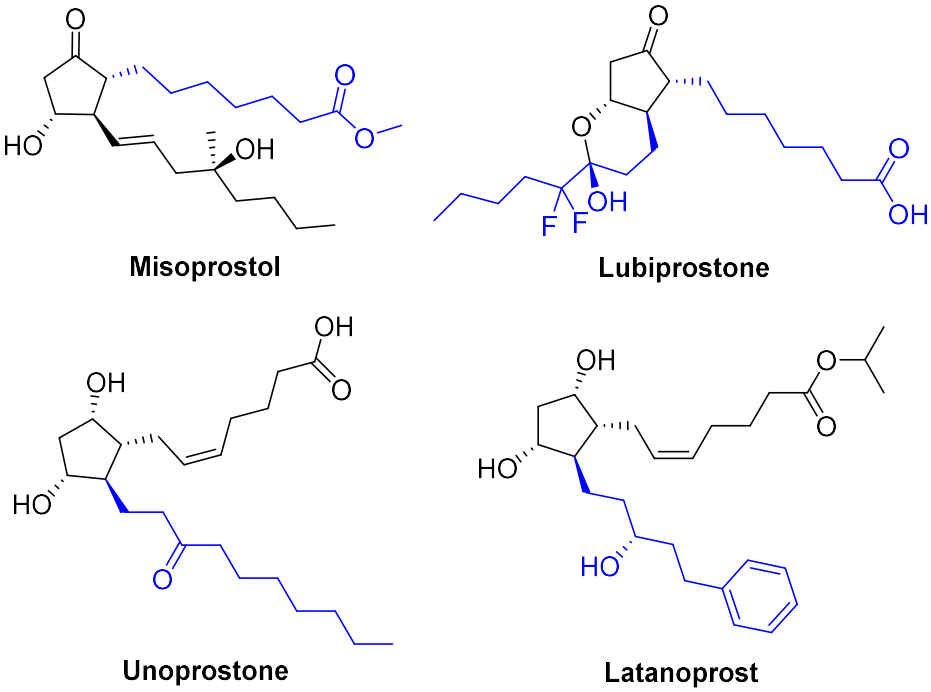

Figure 3.1. Examples of pharmaceutical prostaglandins featuring at least one sp^3-hybridised chain (blue).

The methodology for using alkylzirconium reagents as nucleophiles in asymmetric conjugate addition has already been developed by our group and has been thoroughly described earlier (Scheme 1.11)[85,142]. This system worked well for 6-membered ring or larger, giving good yield and high enantioselectivity. However, the 5-membered ring substrate, cyclopentenone **14**, was problematic and gave a low 23% yield and 75% ee in the formation of tertiary ketone **15** (Scheme 3.1). Even by lowering the temperature to 0 °C, the yield was still poor (29%) despite a reasonably high 85% ee. As prostaglandins all have a 5-membered ring core we decided to develop a new ACA methodology to add alkylzirconium nucleophiles to 5-membered rings.

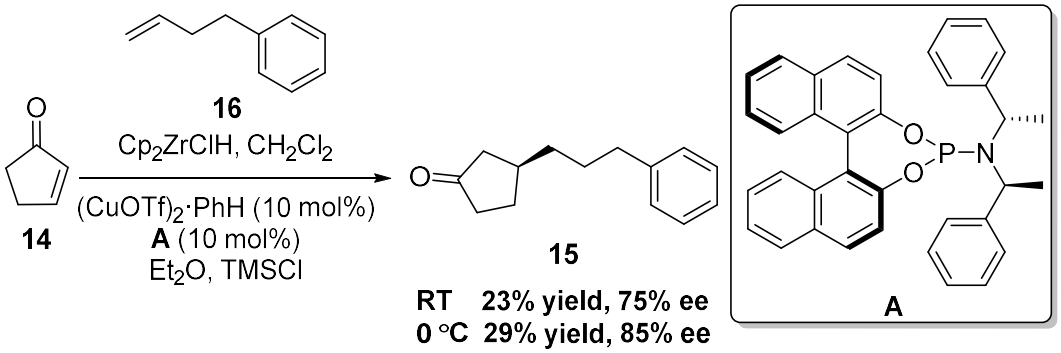

Scheme 3.1. ACA of cyclopentenone 14 by alkylzirconocene nucleophiles. Conditions: 4-phenyl-1-butene **16** (2.5 eq), Cp_2ZrHCl (2.0 eq), CH_2Cl_2, cyclopentenone **14** (1.0 eq), $(CuOTf)_2$·PhH (5 mol%), TMSCl (5.0 eq) in Et_2O, room temperature. Isolated yields, ee determined by HPLC.

Cyclopentenone is a notoriously difficult substrate and therefore often under-examined. Typically, successful methodologies on cyclohexenone, cycloheptenone and even cyclooctenone fail to give both acceptable yield and enantioselectivity with cyclopentenone **14**[57,58,143]. Scheme 3.2 shows a variety of powerful Cu-catalysed ACA methodologies using organozinc[58], organomagnesium[143] and organoaluminium[144] nucleophiles that work extremely well for 6-membered ring or larger and fail to give similar results for cyclopentenone **14**.

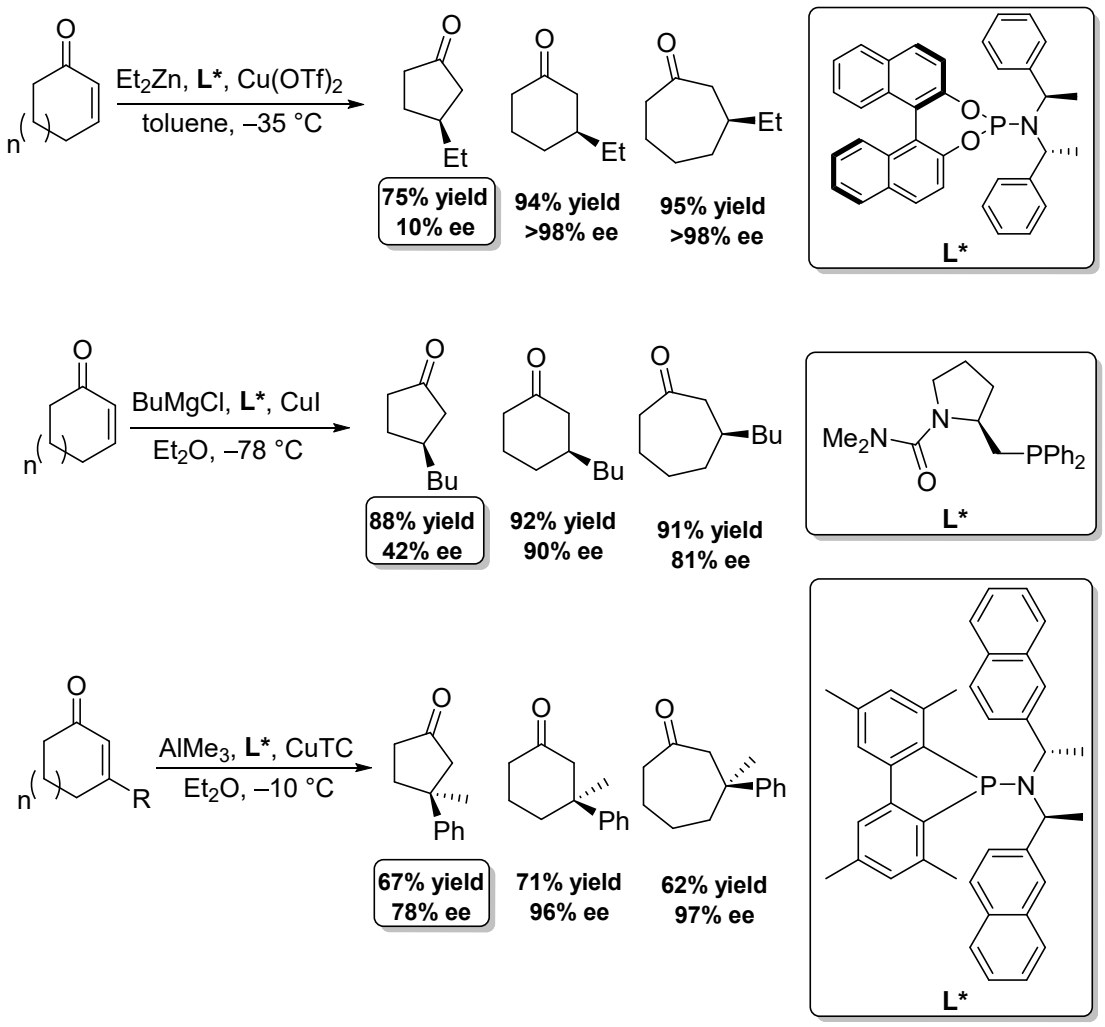

Scheme 3.2. Various examples of Cu-catalysed ACA which give high ee and yield for 6-membered ring and larger but fail for cyclopentenone **14**[57,58,143].

This consistent observation has been attributed to the flatness of cyclopentenone and its enolate higher reactivity[7,145]. The enolate product **17** formed during the ACA is more reactive than the starting enone **14**. Enolate **17** is nucleophilic enough to attack unreacted starting material **14** (Scheme 3.3). This reactivity accounts for the low yields observed when using cyclopentenone in the ACA. The low enantioselectivity of cyclopentenone is thought to be due to the relative flatness of the starting material **14**, thus reducing steric effects and enantioselective induction of the chiral ligand (Figure 3.2).

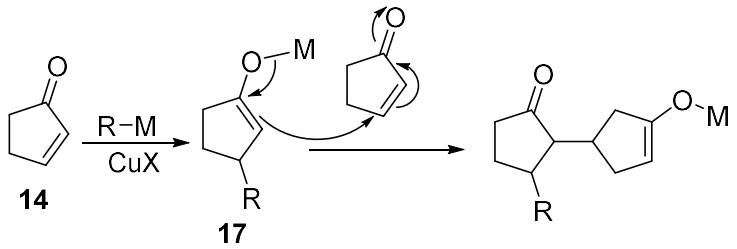

Scheme 3.3. High reactivity of cyclopentenone 14.

Figure 3.2. 3D model showing flatness of cyclopentenone 14 (Chembio3D Ultra 13.0).

Therefore cyclopentenone **14** is considered a challenging example and often gets dedicated methodologies with specifically tuned ligands and conditions[1,7]. Nonetheless, the ACA of cyclopentenones is desirable and is a key step in the synthesis of many natural products and biologically active molecules[77,146-148].

Feringa reported the use of the bulky cyclopentenone derivative, cyclopentene-3,5-dione monoacetal **18a**, in the ACA of dialkylzinc reagents with Cu-phosphoramidite catalysis (Scheme 3.4)[147,149]. Moderate 40% yield and high 90% ee were obtained in the presence of $Cu^{II}OTf$ at cryogenic temperature. The yield was significantly improved to 69% by trapping the *in situ* formed enolate with an aldehyde while keeping the ee of the 1,4-addition step high (96%) and with a good dr (83:17). This step not only eliminates the problematic enolate attack on unreacted enone **18a**, but also forms three chiral centres in one step. Due to the low diastereomeric ratio obtained at the alcohol centre, PCC was used to oxidise the intermediate to ketone **19** and remove this chiral centre.

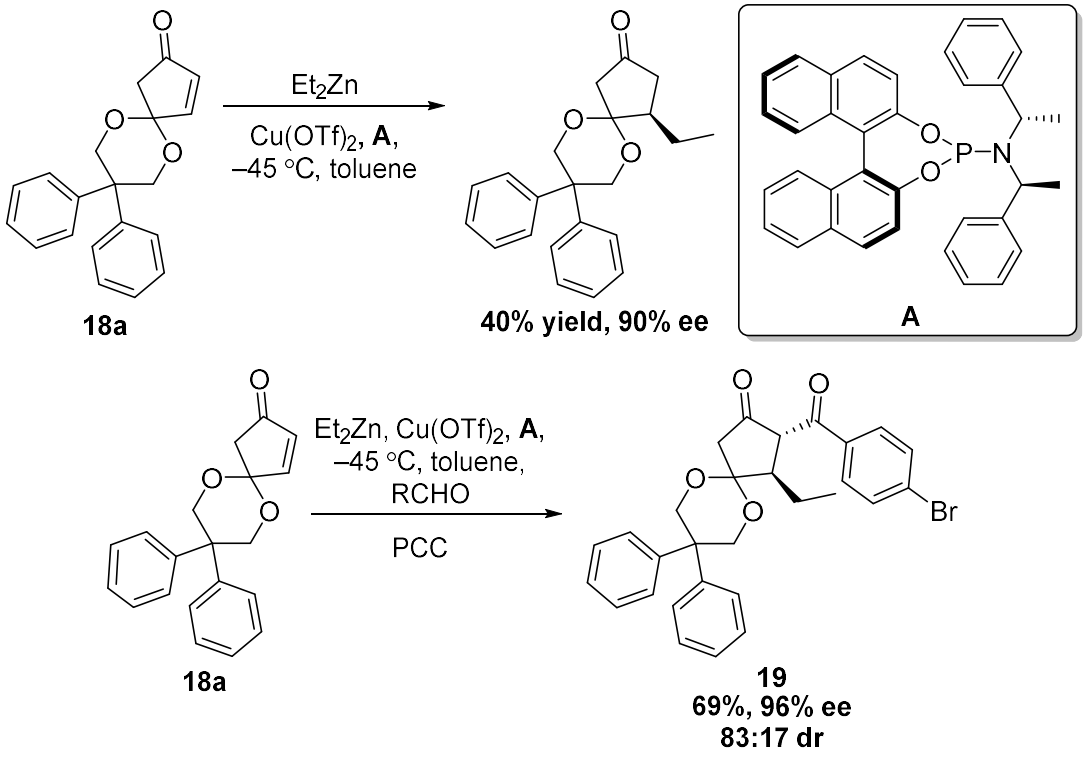

Scheme 3.4. Methodology using cyclopentene-3,5-dione monoacetal 18a in the ACA of dialkylzinc[147,149].

This cyclopentenone derivative **18a** can be easily synthesised from the acetal protection of commercially available cyclopent-4-ene-1,3-dione. Cyclopentene-3,5-dione monoacetal **18a** has the advantage of being more bulky than cyclopentenone **14**, thus potentially reducing the dimerisation of the starting material with the reactive enolate product. Also even though the cyclopentenone core is still flat, the acetal moiety is bulky and changes the electronic properties of the starting material. Furthermore, the acetal moiety can be easily derivatised to an alcohol or a ketone.

Feringa[147,149] further developed his 3-component conjugate addition of dialkylzinc towards the synthesis of PGE_1 methyl ester (Scheme 3.5). The ACA step gave a high 60% yield and good 83:17 dr. However, the use of cryogenic temperatures due to the high reactivity of the dialkylzinc makes this reaction less green and less applicable to industry[84]. Synthesising premade complex

dialkylzinc is difficult, as those nucleophiles are instable and pyrophoric[1,59]. Furthermore, the optimised conditions are highly complex and while they provide three chemical modifications in one step, do not solve the issue of simply adding a nucleophile to a cyclopentenone core in high yield and ee.

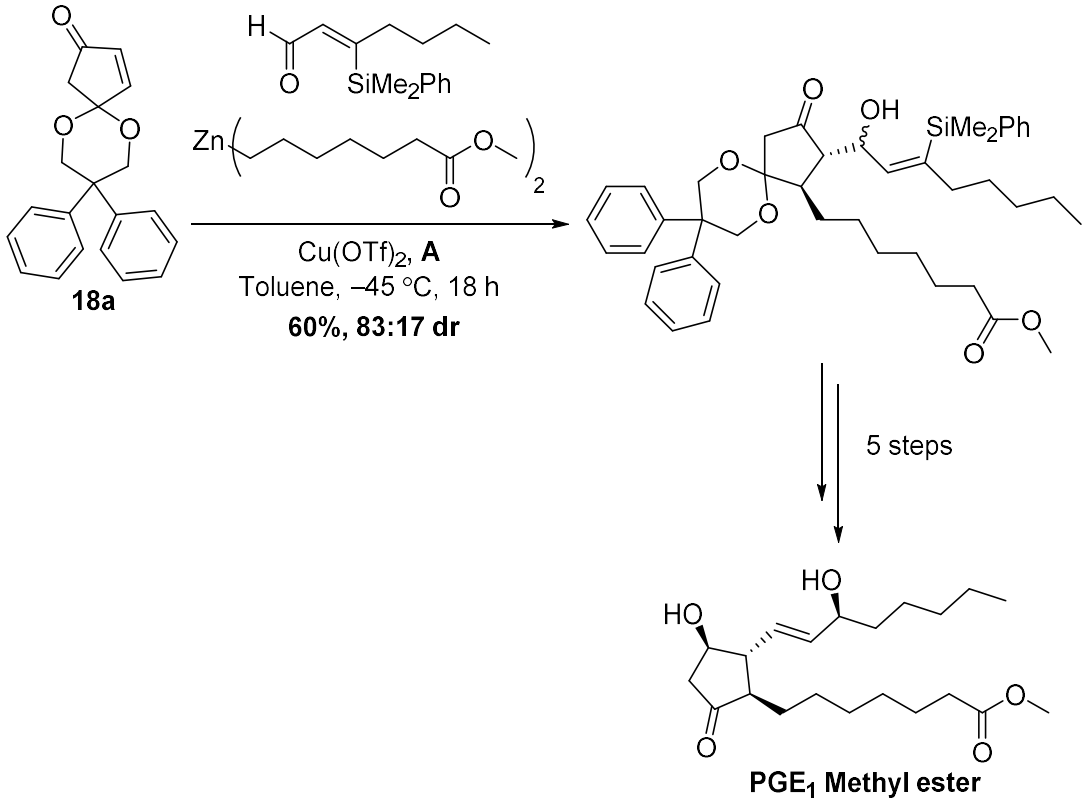

Scheme 3.5. Feringa's 3-component conjugate addition synthesis of PGE_1 methyl ester[147,149].

The Fletcher group has shown the utility and efficacy of alkylzirconocenes[4,85,142]. As it was previously observed that increasing the steric bulk on the cyclohexenone improved the yields[85], inspired by the work of Feringa[147,149], we decided to investigate the ACA of alkylzirconocenes to cyclopentene-3,5-dione monoacetal **18a**. Not only would this methodology bring us closer to a potential synthesis of prostaglandins and analogues in an innovative, mild, functional group tolerant methodology but would also broaden

the scope of ACA to a simple, reliable and accessible method using 5-membered rings.

RESULTS AND DISCUSSION

Initial Screening

We first examined the *in situ* hydrometallation/asymmetric conjugate addition of 4-phenyl-1-butene **16** to cyclopentene-3,5-dione monoacetal **18b** (Table 3.1). We arbitrarily chose to first examine **18b** as it can be synthesised in one step instead of two for **18a** and should behave similarly. An initial ligand screen was carried out with various phosphoramidite ligands. Subtle variations in the amine moiety of the phosphoramidite ligand proved important. Structural isomers **A** and **Q** gave similar results, 80% ee (entry 1) and 84% ee (entry 2a) respectively. On the other hand, ligands **M** and **R**, close relatives of **A** and **Q**, gave poorer enantioselectivity, 54% ee (entry 3) and 68% ee (entry 4) respectively. Second generation phosphoramidite ligands synthesised in our group based on ligand **Q**, such as **S** and **T** did not improve the ee giving 82% ee (entry 5) and 84% ee (entry 6) respectively. However as we obtained >80% ee for four ligands, it would seem that the reaction conditions are robust to enantioselective induction. The yields were however still moderate, 41% for ligand **A** (entry 1) and 31% for ligand **Q** (entry 2a) and required further optimisation. Even though both ligand **Q** and **T** gave 84% ee, we decided to carry out further testing on ligand **Q** rather than **T** due to its simpler synthesis. At this stage, lowering the

temperature to 0 °C gave poorer 78% ee for ligand **Q** (entry 2b) rather than 84% ee at room temperature.

Table 3.1. Initial ligand screening.

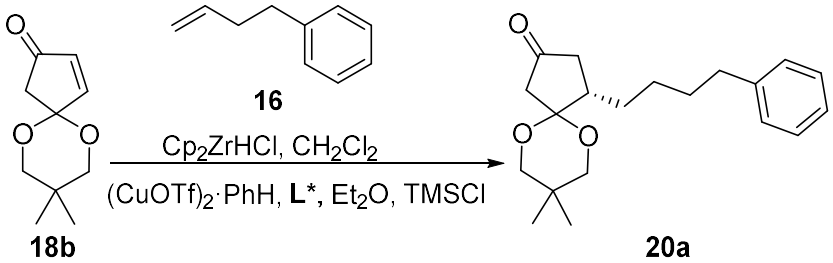

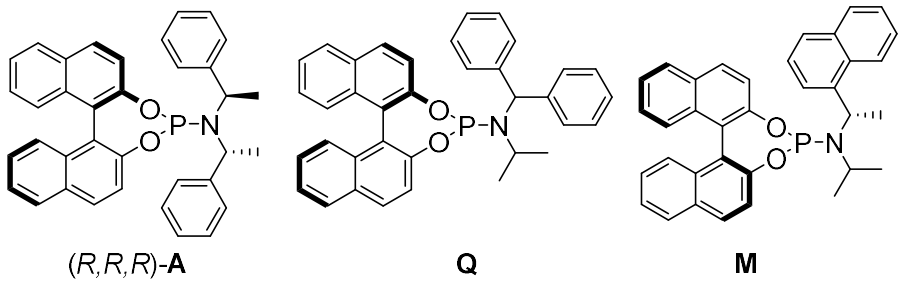

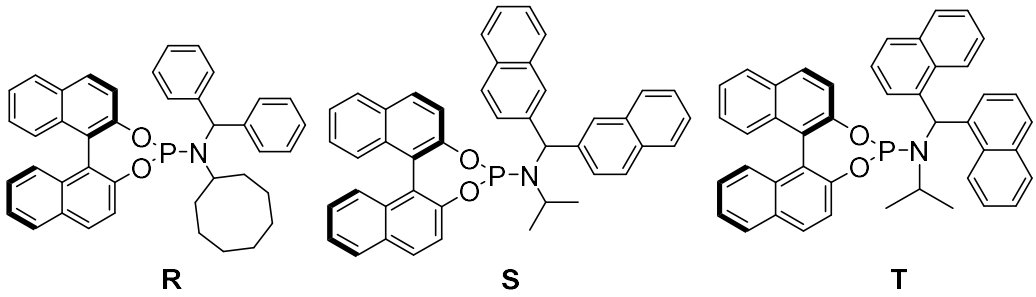

Entry	L*	Yield*	ee§
1	**A**	41%	80%
2a	**Q**	31%	84%
2b[a]		-	78%[a]
3	**M**	-	–54%
4	**R**	-	68%
5	**S**	-	82%
6	**T**	-	84%

Conditions: 4-phenyl-1-butene **16** (2.5 eq), Cp_2ZrHCl (2.0 eq) in CH_2Cl_2, cyclopentenone-3,5-dione monoacetal **18b** (1.0 eq), $(CuOTf)_2$·PhH (5 mol%), **L*** (10 mol%), TMSCl (5.0 eq), in Et_2O, room temperature unless specified. *Isolated yield. §ee determined by HPLC. [a]Reaction performed at 0 °C. *Note: These experiments were performed by FM.*

When exploring different Cu counterions (Table 3.2), it became clear that the initial Cu^{I} triflate salt (from $(CuOTf)_2$·PhH) gave the highest ee and yield. The

triflimide anion NTf_2, gave very poor 7% yield for only 65% ee (entry 1). $CuClO_4$ gave medium results, 73% ee in 28% yield (entry 2), slightly less selective than $(CuOTf)_2$·PhH (84% ee, Table 3.1 entry 2a). Despite the obvious drawbacks, we decided to increase the catalyst loading to 20 mol% which improved the ee to 87% without changing the yield (entry 3a). The beneficial effect of TMSCl are poorly understood in the ACA of Zr nucleophiles and have been found to give mixed results but we had observed in the past, a symbiotic relationship towards ligand **A** and Et_2O. When we carried out the ACA reaction without TMSCl, the ee drastically dropped 33% ee (entry 3b) without changing the yield (40%). Therefore under these conditions, TMSCl clearly has a strong beneficial effect on the enantioselective induction as discussed in Chapter 2 presumably as a Lewis acid, facilitating the stereoselective reductive elimination and/or by modifying the catalyst aggregates, reactivity and enantioselective induction.

Table 3.2. Initial Cu screening and catalyst loading.

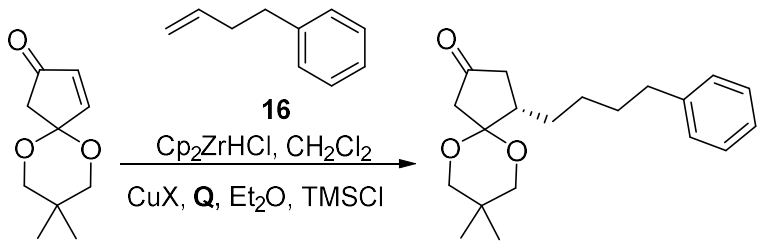

18b **20a**

Entry	Cu	Cat. load	Yield*	ee§
1	$CuNTf_2$ (Ag)	10 mol%	7%	65%
2	$CuClO_4$ (Ag)	10 mol%	28%	73%
3a	$(CuOTf)_2$·PhH	20 mol%	~40%	87%
3b[a]			~40%	33%[b]

Conditions: 4-phenyl-1-butene **16** (2.5 eq), Cp_2ZrHCl (2.0 eq) in CH_2Cl_2, cyclopentenone-3,5-dione monoacetal **18b** (1.0 eq), CuX (as specified), **Q** (as specified), TMSCl (5.0 eq), in Et_2O, room temperature unless specified. * Isolated yield. § ee determined by HPLC. [a] Reaction performed without TMSCl. *Note: These experiments were performed by FM.*

Finally, we concluded our primary screening with the screening of solvents (Table 3.3). The initial solvent (Et_2O) gave the best results (87% ee, 40% yield) and all other solvents were detrimental to the yield. Indeed, most solvents resulted in no product observed (such as THF, entry 3), or only trace amounts (in toluene, entry 4). CH_2Cl_2 and TBME gave low 20% yield (entry 1 and 2a). In terms of enantioselectivity, good ees were obtained in CH_2Cl_2 (81% ee, entry 1), TBME (85% ee, entry 2a) and toluene (94% e, entry 4). These observations reiterate the system's robustness for enantioselective induction and weakness of the system in terms of yields, as conditions strongly influence the reactivity. We also tested the ACA reaction in TBME without TMSCl, the ee moderately dropped to 70% ee without any effect to the yield (entry 2b).

Table 3.3. Initial solvent screening.

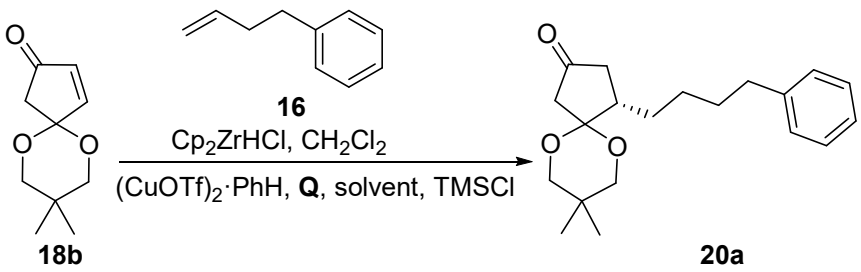

Entry	Solvent	Yield*	ee§
1	DCM	~20%	81%
2a	TBME	~20%	85%
2b[a]		~20%	70%[b]
3	THF	-	-
4	Toluene	traces	94%

Conditions: 4-phenyl-1-butene **16** (2.5 eq), Cp_2ZrHCl (2.0 eq) in CH_2Cl_2, cyclopentenone-3,5-dione monoacetal **18b** (1.0 eq), $(CuOTf)_2$·PhH (10 mol%), **Q** (20 mol%), TMSCl (5.0 eq), in specified solvent, room temperature. *Isolated yield. §ee determined by HPLC. [a]Reaction performed without TMSCl. *Note: These experiments were performed by FM.*

Secondary Screening – reaction yield optimisation

In the initial screening studies we obtained good enantioselectivity (87% ee), but the yield was still moderate (<40%). We decided to examine more subtle differences in the system that might lead to improved yields. We were pleased to observe that adding 3.0 eq of alkylzirconocene instead of 2.0 eq increased the yield from 40% to 46% without any change to the ee (87%) (Table 3.4, entry 3a).

Table 3.4. Screening different form of CuOTf.

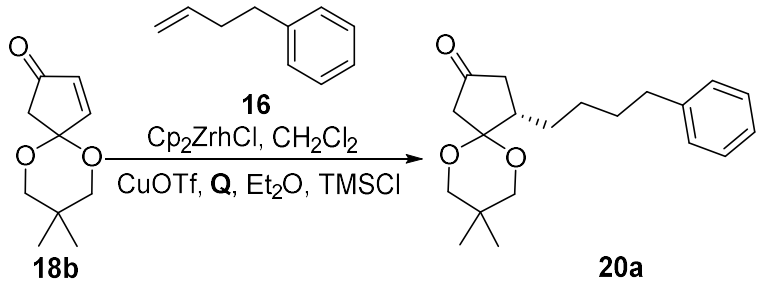

Entry	Cu	Zr. eq	Yield*	ee§
1[a]	$(CuOTf)_2$·PhH	2.0	~40%	87%
3a[a]	$(CuOTf)_2$·PhH	3.0	46%	87%
3b[b]			34%	85%
4	$Cu^{(II)}OTf_2$	3.0	25%	60%
5[a]	$Cu(MeCN)_2OTf$	3.0	53%	73%
6a[c]	CuCl, AgOTf	3.0	41%	88%
6b[c,d]			27%	86%
6c[c,e]			29%	86%

Conditions: 4-phenyl-1-butene **16** (2.5 eq or 3.5 eq), Cp_2ZrHCl (as specified), cyclopentenone-3,5-dione monoacetal **18b** (1.0 eq), 'CuOTf' (20 mol%), **Q** (20 mol%), TMSCl (5.0 eq), in Et_2O, room temperature. *Isolated yield. §ee determined by HPLC. [a]Reaction performed using a premade $(CuOTf)_2$·PhH-**Q** complex. [b]Reaction performed using $(CuOTf)_2$·PhH-**Q** prepared *in situ*. [c]Reaction performed using CuOTf-**Q** prepared *in situ* from CuCl (20 mol%), AgOTf (20 mol%), **Q** (20 mol%) and filtered. [d]Without filtration. [e]Reaction performed using CH_2Cl_2 to prepare CuOTf-**Q**, filtration, solvent removal and addition of Et_2O.

Moreover, the best Cu source screened was CuOTf, however multiple forms of this Cu salt exists (Table 3.4). Originally, we used $(CuOTf)_2$·PhH as it was the

one used in the previous ACAs[85] and gave good results up to 87% ee, 46% yield in this system (entry 2). However, $(CuOTf)_2$·PhH is highly moisture sensitive. As observed in the previous methodology, using a premade $(CuOTf)_2$·PhH-**Q** complex[87] (entry 3a) gave better results than procedures involving *in situ* mixing of the Cu and ligand **Q** (entry 3b) which lowered the yield to 34% while the ee was almost unchanged (85% ee). This finding generated questions on the effect of isolating the $(CuOTf)_2$·PhH-**Q** complex and the difficulties associated with synthesising and handling $(CuOTf)_2$·PhH in air[85]. Thus we wished to find a more stable and simple source of CuOTf.

The commercially available $Cu^{II}OTf_2$ gave poor yields (25%) and significantly reduced the ee to 60% (entry 4). $Cu(MeCN)_2OTf$ (entry 5) improved the yield (53%) but at the expense of selectivity, which dropped to 73% ee. CuOTf generated from the metathesis of commercial CuCl and AgOTf gave 88% ee in 41% yield, similar results as $(CuOTf)_2$·PhH, albeit with a slightly lower yield (entry 6a). The results obtained with AgOTf were more reproducible and operationally convenient and so further experiments were carried out using this procedure. When synthesising CuOTf in this way, the AgCl is removed by filtration. We thought this may also partially remove the catalyst complex, especially due to the catalyst poor solubility in Et_2O. However, not filtering (entry 6b) or forming CuOTf in CH_2Cl_2, filtering and then changing the solvent to Et_2O (entry 6c) dropped the yield to 27% and 29% respectively without changing the ee.

In previous methodologies using organozirconocenes, we always used 1:1 equivalent of Cu:**L*** ratio. However, many existing methodologies have an array of Cu:**L*** ratios which modify the catalytic complexes and improve the yield and

ee. We decided to test the effect of Cu:**L*** ratio in the hope to improve the yield of our system (Table 3.5). We found that using a slight excess of ligand over Cu (1.1:1) improved the yield to 48% (entry 2) with 86% ee. Further additional ligand did not lead to improvements in yields and ee (entries 3-4) as yields between 47-49% were obtained and the ee was constantly 86%.

Table 3.5. Screening ligand equivalence.

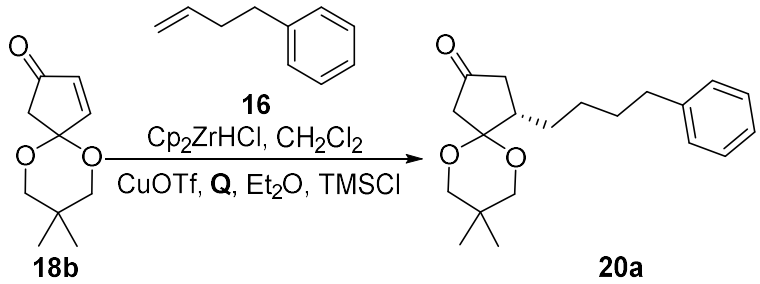

Entry	Q eq	Yield*	ee§
1	0.20	41%	88%
2	0.22	48%	86%
3	0.30	49%	86%
4	0.40	47%	86%

Conditions: 4-phenyl-1-butene **16** (3.5 eq), Cp_2ZrHCl (3.0 eq), cyclopentenone-3,5-dione monoacetal **18b** (1.0 eq), CuCl (20 mol%), AgOTf (20 mol%), **Q** (as specified), TMSCl (5.0 eq), in Et_2O, room temperature. *Isolated yield. §ee determined by HPLC.

In his methodology, Feringa used cyclopentene-3,5-dione monoacetal **18a**[147,149]. Conducting our reaction on cyclopentene-3,5-dione monoacetal **18a** slightly improved the yield to 50% and gave similar ee (87%) (Table 3.6 entry 2) Cyclopentene-3,5-dione monoacetal **18a** was therefore used in subsequent screening.

Table 3.6. Screening reaction concentration.

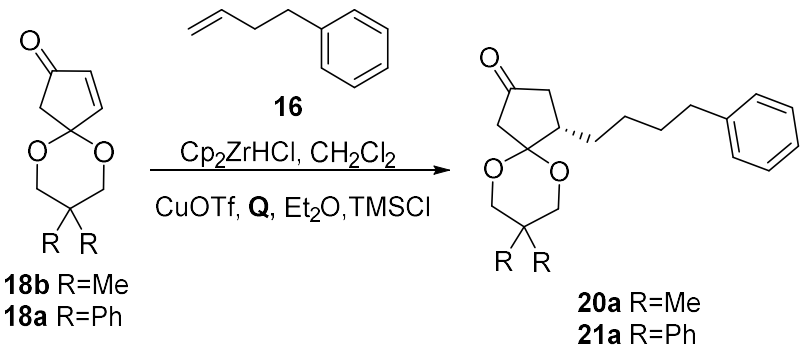

Entry	R	Concentration	Yield*	ee§
1	Me	0.2 M	48%	86%
2	Ph	0.2 M	50%	87%
3	Ph	0.4 M	37%	87%
4a	Ph	0.1 M	54%	90%
4b[a]			61%	92%

Conditions: 4-phenyl-1-butene **16** (3.5 eq), Cp_2ZrHCl (3.0 eq), cyclopentenone-3,5-dione monoacetal **18** (1.0 eq), CuCl (20 mol%), AgOTf (20 mol%), **Q** (22 mol%), TMSCl (5.0 eq), in Et_2O (as specified), room temperature otherwise specified. *Isolated yield. §ee determined by HPLC. [a]Reaction performed at 0 °C.

Concentration can have a great impact on reaction outcomes as it will affect the rate of reactivity and potential side-reactions. Therefore, we examined the effect of concentration on the yield and ee. Increasing the concentration to 0.4 M lowered the yield to 37% without any change to the ee (entry 3). Diluting the reaction mixture to 0.1 M improved the yield to 54% and increased the enantioselectivity to 90% ee (entry 4a). At this concentration lowering the temperature to 0 °C improves the results to 61% yield and 92% ee (entry 6b). The beneficial effect of the temperature in these conditions was interesting due to the previous detrimental effect of using 0 °C (Table 3.1, entry 2b) and exemplified the difficulties associated with traditional screening approach in efficiently exploring the optimum conditions. The effect of the dilution and low temperature on the yield can be rationalised by a lower risk of side-reactions.

Reaction Scope

Using the optimised conditions of Table 3.6 entry 4b, we next examined the addition of different alkylzirconocene species to cyclopentenone derivative **18a** (Figure 3.3). Non-functionalised and functionalised alkenes all gave moderate to good yields and high ee illustrating that the reaction tolerance to changes in the alkene coupling partner such as aromatics (**21a**), linear chains (**21c**), halogens (**21d**) and protected alcohol (**21f**). The use of electron rich styrene and allyltrimethylsilane in asymmetric hydrometallation–1,4-addition procedures is often challenging but product **21b** and product **21e** were formed in high ee (95% ee and 92% ee respectively) and moderate yield (36% and 39% respectively).

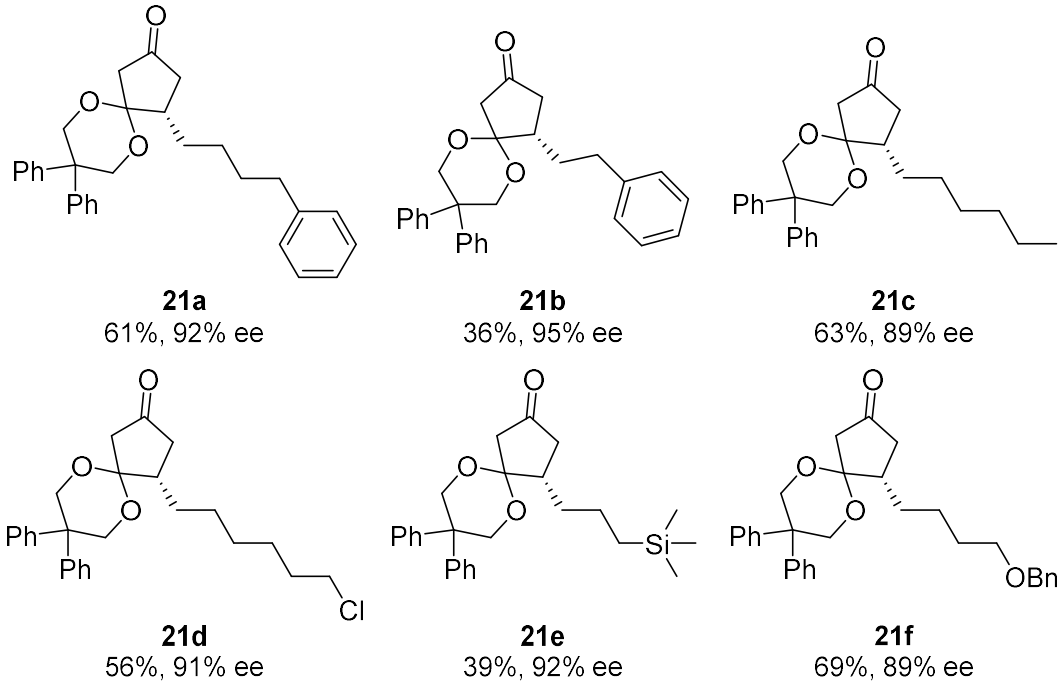

Figure 3.3. Scope of nucleophiles. Conditions: alkene (3.5 eq), Cp_2ZrHCl (3.0 eq) in CH_2Cl_2, cyclopentenone-3,5-dione monoacetal **18a** (1.0 eq), CuCl (20 mol%), AgOTf (20 mol%), (*R*)-**Q** (22 mol%), TMSCl (5.0 eq), in Et_2O (0.1 M), at 0 °C. Isolated yield. ee determined by HPLC.

We subsequently recrystallised product **21a** from CH_2Cl_2/pentane and determined the absolute configuration of the product (Figure 3.4) by X-ray crystallography.

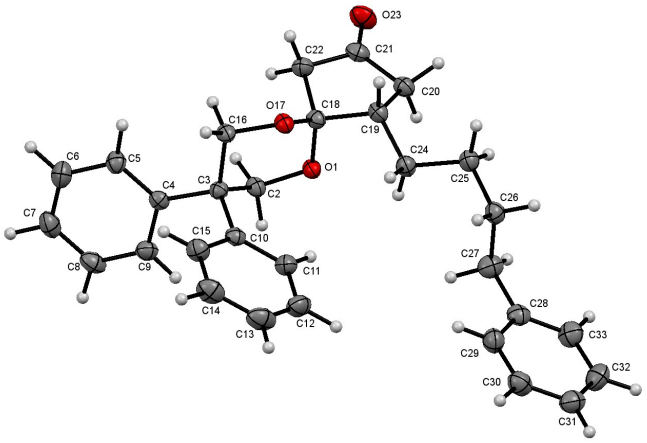

Figure 3.4. Crystal Structure of 21a used to determine the absolute configuration. *Note: the crystals structure was collected and analysed by LP.*

CONCLUSION

We have demonstrated, after extensive screening that despite some challenges, highly functionalised enantioenriched cyclopentanone derivatives can be successfully prepared by asymmetric conjugate addition with alkylzirconocene species. Good yields and high levels of enantioselectivity were achieved with high functional group tolerance. Determining the absolute configuration of the products was important in order to apply this method to the total synthesis of complex bioactive molecules such as prostaglandins.

CHAPTER 4

TOWARDS THE TOTAL SYNTHESIS OF LATANOPROST

INTRODUCTION

Latanoprost (Figure 4.1) quickly became a blockbuster drug sold by Pfizer as Xalatan® with annual sales exceeding $1.75 billion in 2010[105], before generic versions became available after the patent expired in 2011[150,151]. This unnatural prostaglandin, is an analogue of prostaglandin F and is a strongly potent molecule delivered via an eye drop to combat ocular hypertension (glaucoma), the second leading cause of blindness after cataracts[105,106]. It is widely used and is found on the World Health Organisation's List of Essential Medicines[152]. Like many other industrial synthetic prostaglandins, Latanoprost is manufactured in 19 steps using the Corey synthetic route[105,106]. More recently, many alternative, shorter syntheses of Latanoprost have surfaced using variations of the Corey lactone[105,153,154] or new methods for the addition of the aliphatic chains[155-157]

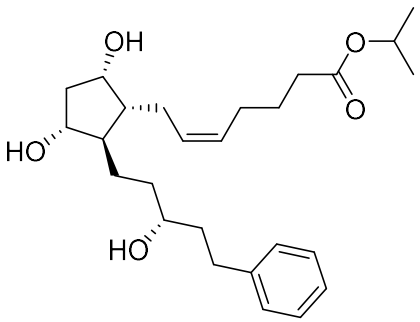

22

Figure 4.1. Structure of Latanoprost 22.

Prostaglandin E_2 (PGE_2) was found to regulate blood cell formation from stem cells[100,158] and interfering with receptors of PGE_2 stimulates the release of stem cells from the bone marrow into the circulatory system[101]. Stem cells play a key role in the maintenance and repair of many tissues and organs in the body and are anticipated to offer treatment options to a wide range of degenerative diseases. The ability to differentiate stem cells may provide ways for scientist to reliably transform pluripotent cells into a desired type of cell on demand and there is tremendous scientific interest in this area[159-162]. The understanding of the role of PGE_2 suggests it is possible to discover and optimise prostaglandin analogues as stem cell modulators.

Our aim is to establish an innovative platform, diverging from the Corey synthesis[105,106] and newer alternatives[105,153-157], for a new competitive synthetic route to Latanoprost using organozirconocene nucleophiles. We aim to develop an approach where the catalyst is the exclusive source of chirality. Thus, even though the alkylzirconocene may contain stereogenic centres, formation of the core will be done in a completely stereo-independent manner contrary to the Corey synthesis.

There are several important drugs that are closely related in structure to Latanoprost (Figure 4.2). Once a short and robust route to Latanoprost is found, we would demonstrate the versatility of our approach by synthesising these, as well as novel analogues. Ideally, due to the PGE_2 known influence on stem cells, we envision our route serving as a platform for the synthesis of prostaglandin analogues that will allow rapid access to a wide range of derivatives to facilitate structural-activity relationship studies and enable the discovery and optimisation of new stem cell modulators.

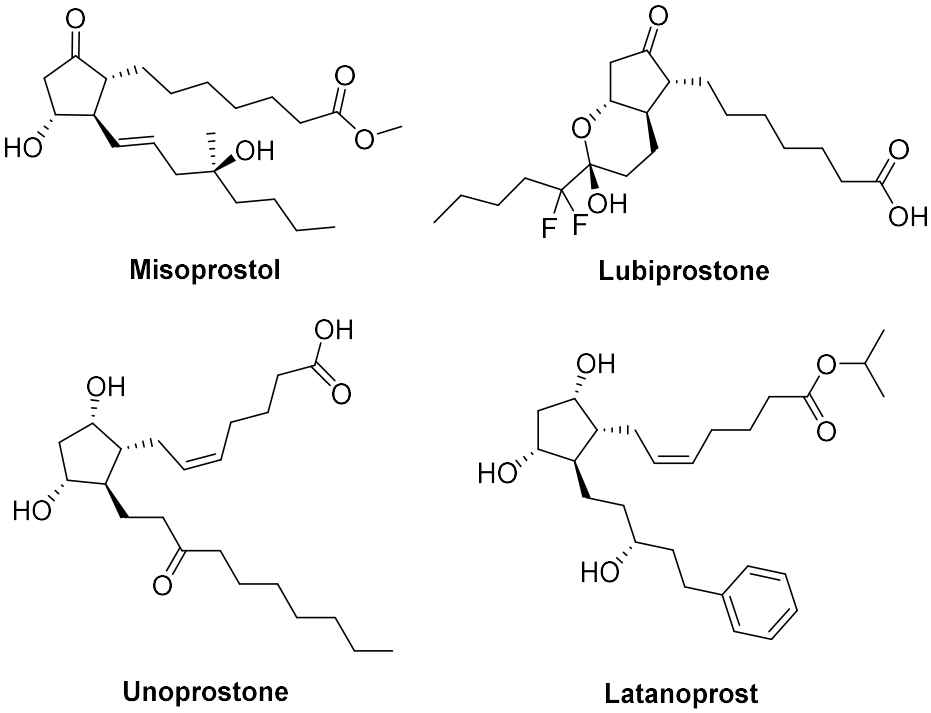

Figure 4.2. Examples of important drugs structurally related to Latanoprost.

RESULTS AND DISCUSSION

Latanoprost synthesis using Cu-catalysed ACA

We propose that Latanoprost could be synthesised using our newly developed ACA of using alkene **23** and cyclopentenone-3,5-dione monoacetal **18a** (Scheme 4.1). Once the primary chain is added to the cyclic core, we could add the second chain to the intermediate enolate **24** *via* tandem trapping to obtain ketone **25**. Then the ketone at position 2 could be selectively reduced to an enantioenriched alcohol followed by deprotection and reduction of the protected ketone at position 5 to obtain Latanoprost **22**.

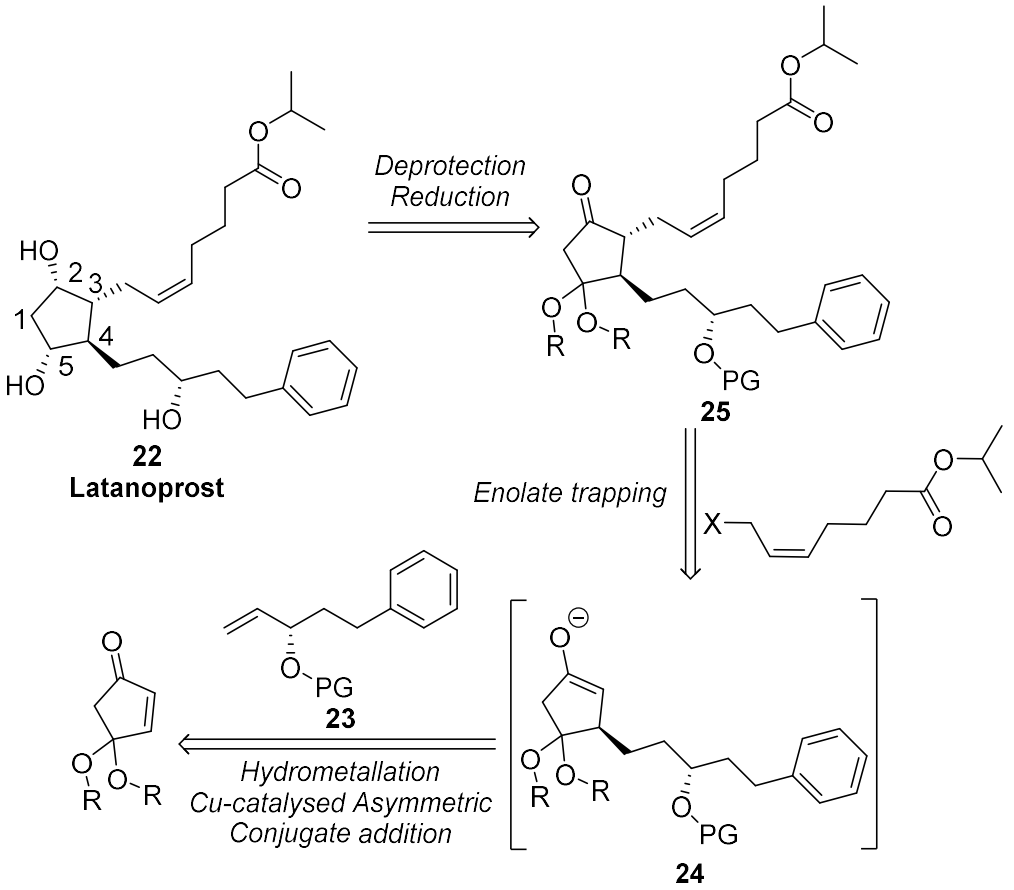

Scheme 4.1. Proposed retrosynthetic route for Latanoprost using our newly developed ACA of alkylzirconocene to cyclopentenone-3,5-dione monoacetal **18a**.

1) Synthesis of alkene

We first wanted to synthesise alkene **23**. The synthesis of the Latanoprost chain has already been described by Aggarwal[124]. Starting from alkene **16**, enantioenriched epoxide **26** is obtained by *m*CPBA epoxidation followed by a kinetic resolution of the epoxide using Jacobsen's Co^{II} Salen catalyst[124] (Scheme 4.2). We found out that those two steps can be carried out without purifying the epoxide obtaining a quantitative yield of 50% and very high ee (99.5%). Epoxide **26** is then opened using trimethylsulfoxonium iodide with retention of the ee to give allylic alcohol **27** in 85% yield[124]. Alkene **23** is obtained by protecting alcohol **27** via standard procedures.

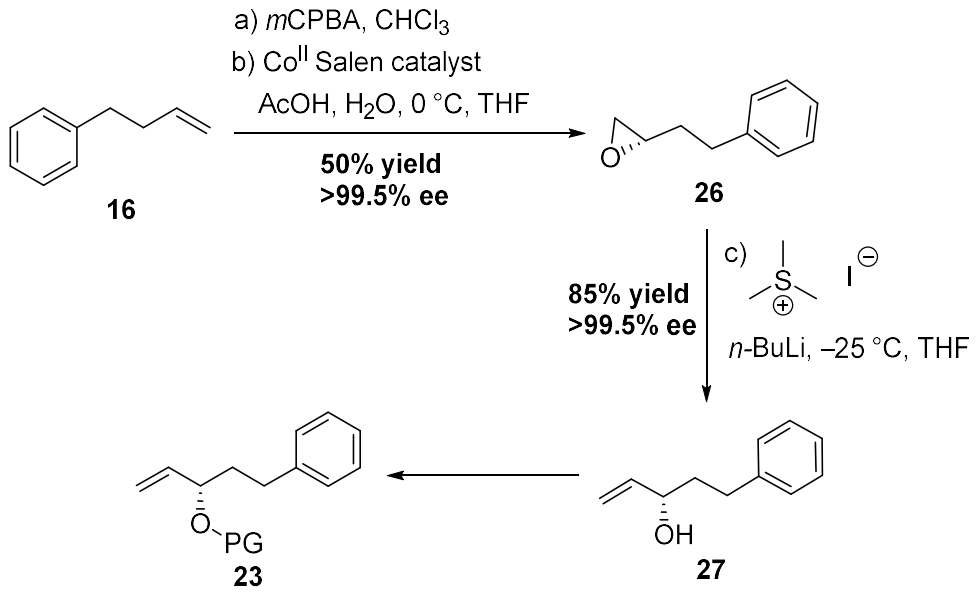

Scheme 4.2. Synthesis of Latanoprost alkene chain 23 following Aggarwal's procedures[124] to be used in the hydrometallation/Cu-catalysed ACA. Conditions: a) *m*CPBA (2.0 eq), 4-Phenyl-1-butene **16** (1.0 eq) in $CHCl_3$ 7 h at room temperature. b) (*S*, *S*) Jacobsen Co^{II} Salen catalyst (1 mol%), racemic-**26** (1.0 eq), acetic acid (0.02 eq), H_2O (0.52 eq), in THF 1 h, 0 °C. c) *n*BuLi (3.0 eq), trimethylsulfoxonium iodide (3.0 eq), **26** (1.0 eq) in THF overnight at –25 °C to room temperature.

2) ACA of cyclopentenone-3,5-dione monoacetal

Many protecting group for alcohol exist and we were uncertain about the impact of different protecting groups in the reactivity of the ACA. We tested three silyl protecting groups (PG) in our ACA[140] (Table 4.1). TMS, a very labile protecting group, was unstable to the reaction condition and yielded a moderate 38% of the deprotected product **28** without any traces of TMS protected product **29a** (entry 1). To our delight, the dr obtained for deprotected product **28** was high (93:7 *trans*:*cis*). TBS was also found to give mainly the deprotected product **28** in 31% yield with high 89:11 dr (entry 2). Some TBS protected product **29b** was recovered in low 10% yield. In order to avoid deprotection, we resolved to use the bulky TIPS protected group which exclusively gave product **29c** in a high 79% yield and good 85:15 dr (entry 3) and decided to use the TIPS protected alkene **23c** in subsequent analysis.

Table 4.1. Testing different protecting group in the ACA of the Latanoprost alkene 23 or 27.

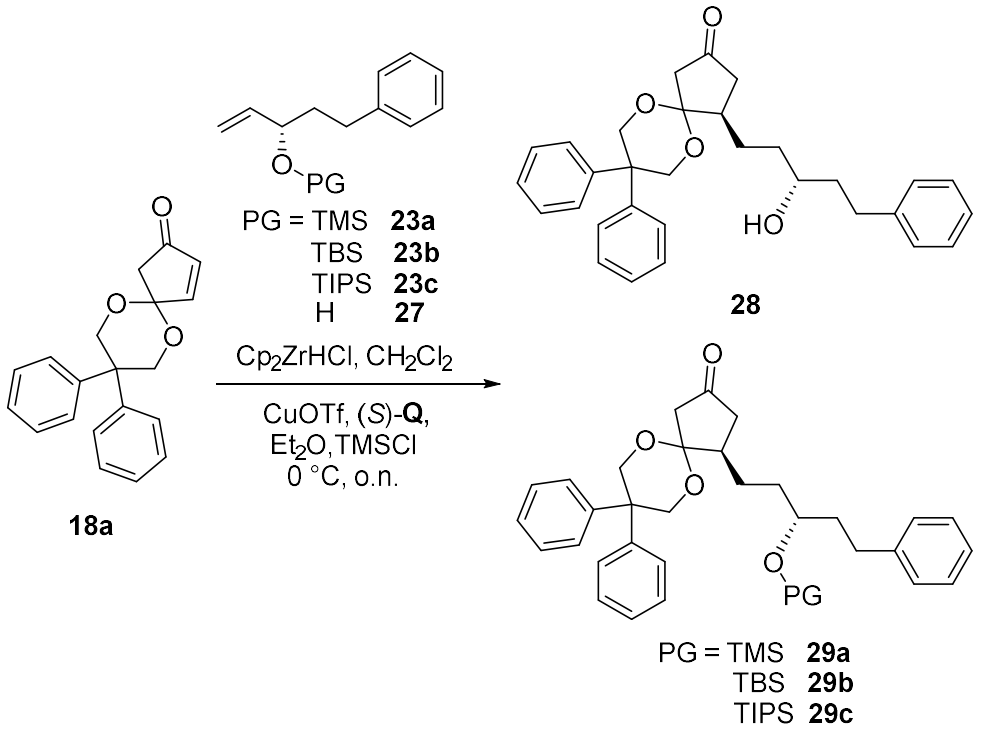

Entry	PG	28 (% yield)*	29 (% yield)*	dr (trans:cis)§
1	TMS	0	38	93:7
2	TBS	~10	31	89:11[a]
3	TIPS	79	0	85:15
4	H	-	39	90:10

Conditions: alkene **23** (3.5 eq), Cp_2ZrHCl (3.0 eq) in CH_2Cl_2, cyclopentenone-3,5-dione monoacetal **18a** (1.0 eq), CuCl (20 mol%), AgOTf (20 mol%), (*S*)-**Q** (22 mol%), TMSCl (5.0 eq), in Et_2O (0.1 M), at 0 °C. Condition for alkene **27**: alkene **27** (3.0 eq), Cp_2ZrHCl (6.0 eq) in CH_2Cl_2, cyclopentenone-3,5-dione monoacetal **18a** (1.0 eq), CuCl (20 mol%), AgOTf (20 mol%), (*S*)-**Q** (22 mol%), TMSCl (5.0 eq), in Et_2O (0.1 M), at 0 °C. *Isolated yield. §Dr determined by NMR of the isolated diastereomeric product mixture.

Based on the results obtained with TMS as a labile protecting group, we also examined the behaviour of non-protected alcohol **27**. When using the standard conditions, the hydrozirconation of alkene **27** did not proceed well. However, when we added 2.0 eq of Cp_2ZrHCl (6.0 eq) compared to alkene **27** (3.0 eq), the hydrozirconation worked well and fast (30 min). Subsequently, alcohol **27** was used in the hydrometallation/ACA reaction resulting in product **28** obtained in a moderate 39% yield and high 90:10 dr (entry 4).

Why some of the silyl protecting groups are stable to the hydrozirconation-ACA conditions (TIPS) while other are partially (TBS) or not at all (TMS) is unknown. We speculate that deprotection of the silyl group occurs due to the proximity of the alcohol to the hydrozirconation site (Scheme 4.3). Indeed, after hydrozirconation, the organometallic **30** could form the 5-membered chelate **31**. From **31**, the high oxophilicity of Zr[163] could be the driving force for the intramolecular silyl deprotection to form the 5-membered ring **32**. TIPS is such a bulky protecting group that steric clashes might disfavour the proposed intramolecular formation of 5-membered ring **32**, resulting in no deprotection of the TIPS group contrary to other silyl protecting groups.

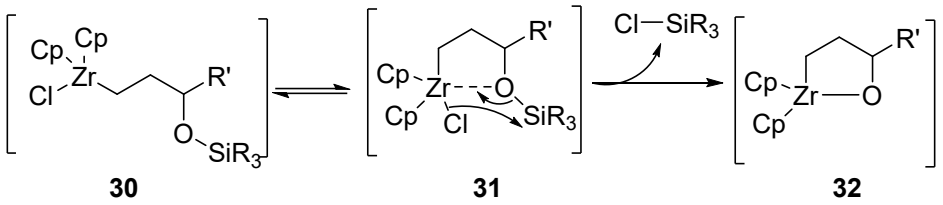

30 **31** **32**

Scheme 4.3. Proposed intramolecular deprotection of silyl protecting groups during hydrozirconation.

Finally, we wanted to scale up the hydrozirconation of **23c**. However, using 20 mol% catalyst and 3.5 eq of alkene **23c** is not ideal for large scale. Therefore we decided to optimise the reaction conditions when using alkene **23c**. Unfortunately the reaction did not reach completion when reducing the catalyst loading to 10 mol% giving only 55% yield in a moderate 62:38 dr. However, we managed to reduce the alkylzirconocene excess to only 1.5 eq (**23c** (1.8 eq), Cp_2ZrHCl (1.5 eq)) for a 75% yield and 85:15 dr at small scale and 47% yield and 85:15 dr on large scale (4.8 mmol). These conditions were used in subsequent studies.

3) Addition of a second chain

Trapping enolate with electrophiles

Three component reactions are highly efficient and have been used in many Cu-ACA of unstabilised organometallics[2,117-123,147,149,164]. Therefore having successfully added the complex Latanoprost first chain, we set out to test the trapping of various electrophiles in the ACA of alkylzirconocene to cyclopentenone-3,5-dione monoacetal **18a.**

Aldehydes are highly potent electrophiles and are thus frequently used in ACA tandem trapping[117,118,147,149]. As a proof of concept, we tested the ACA of alkylzirconocene tandem trapping of various aldehydes. We initially tested the addition of hydrocinnamaldehyde and then later the simpler acetaldehyde for clarity (Scheme 4.4). When the aldehyde was added at the beginning of the ACA reaction, as it is traditionally done, the ACA reaction did not proceed. The aldehyde must interfere with the reaction as we did not observe either the ACA product **29c** nor the trapping product **33**. We decided to add the aldehyde after the ACA reaction was finished (15 h after addition of cyclopentenone-3,5-dione monoacetal **18a**) prior to work up. In this case, the ACA product was obtained in good yields but despite some promising preliminary results (presence of the trapped product mass by mass spectrometry), the expected trapped product **33** was never isolated.

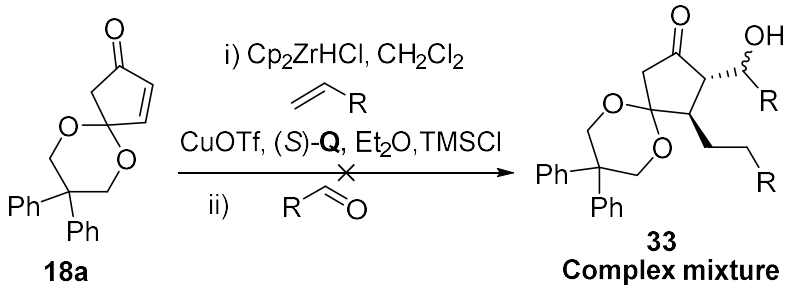

Scheme 4.4. Attempts at tandem ACA trapping of aldehyde on cyclopentenone-3,5-dione monoacetal 18a. Conditions: alkene **23c** (1.8 eq), Cp_2ZrHCl (1.5 eq) in CH_2Cl_2, cyclopentenone-3,5-dione monoacetal **18a** (1.0 eq), CuCl (20 mol%), AgOTf (20 mol%), (*S*)-**Q** (22 mol%), TMSCl (5.0 eq), in Et_2O (0.1 M), 15 h at 0 °C to room temperature then aldehyde (10.0 eq) at room temperature.

Alternatively, less reactive ethylene oxide or allylhalides could also be trapped. Trapping these electrophiles will be advantageous as the resulting product **34** or **35** could be easily transformed to aldehyde **36** by oxidation or ozonolysis respectively (Scheme 4.5). Then **36** could be modified to the Latanoprost precursor **37** using a Wittig reaction to selectively obtain a Z-alkene.

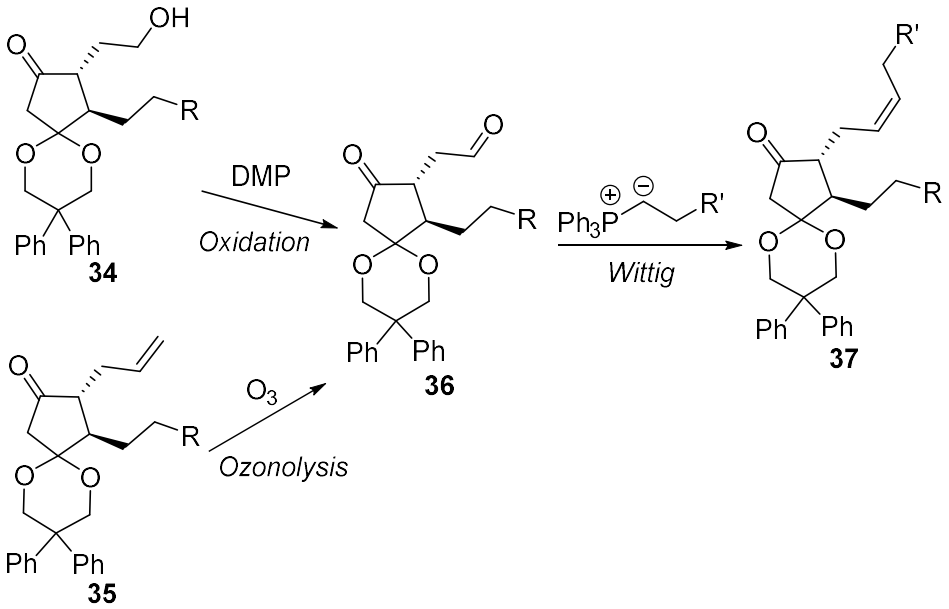

Scheme 4.5. Potential use of the ethylene oxide trapping product **34** or allylhalides trapping product **35** in the synthesis of Latanoprost **22**.

Unfortunately, despite various attempts (addition time, temperature, equivalents, activating agents, X groups etc.), ethylene oxide or allylhalides could

not be trapped to form product **34** or **35** in the tandem ACA-trapping to cyclopentenone-3,5-dione monoacetal **18a** (Scheme 4.6). Similarly to the results obtained when using an aldehyde, adding these electrophiles at the beginning of the ACA resulted in its inhibition. We also attempted to trap allyliodide using the TMS enolate derived from the ACA step without success[165].

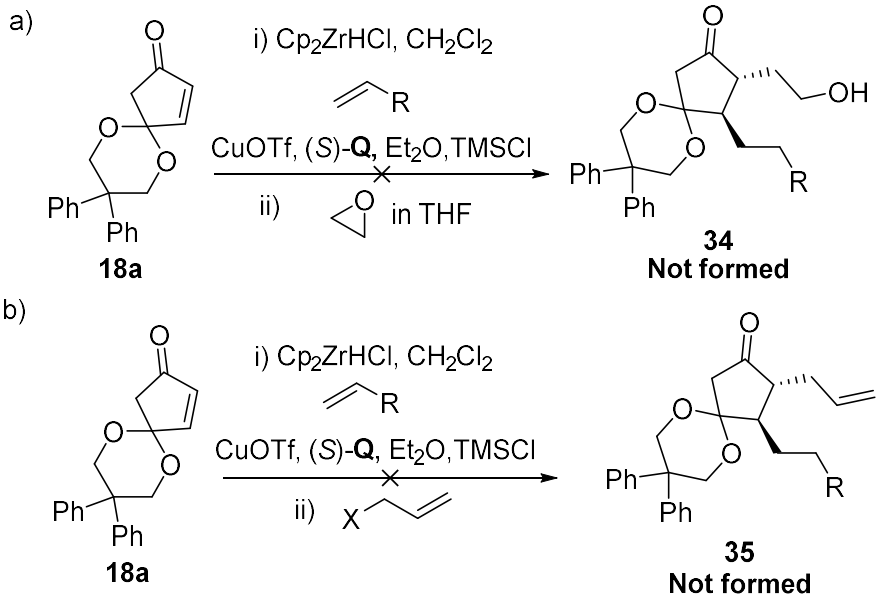

Scheme 4.6. Attempts at tandem ACA trapping of ethylene oxide (a) or allylhalides (b) on cyclopentenone-3,5-dione monoacetal 18a. Conditions: alkene **23c** (1.8 eq), Cp_2ZrHCl (1.5 eq) in CH_2Cl_2, cyclopentenone-3,5-dione monoacetal **18a** (1.0 eq), CuCl (20 mol%), AgOTf (20 mol%), (*S*)-**Q** (22 mol%), TMSCl (5.0 eq), in Et_2O (0.1 M), 15 h at 0 °C to room temperature then electrophile (10.0 eq) at room temperature.

Trapping electrophiles using ACA might be common for many organonucleophiles but has been a problem for organozirconocene nucleophiles. Indeed, we had also tested the trapping of electrophiles in various ACA systems using Zr-nucleophiles[85,142] and trapping was never observed. We thought that due to the high reactivity of the 5-membered ring enolate (Cf Chapter 3) tandem trapping electrophile in this case might be possible. However, the inability to add adding electrophiles by enolate trapping appears to be intrinsic to organozirconocenes. The origin of this lack of reactivity is puzzling as we have

shown (Cf Chapter 8) that enolates are indeed formed over the course of ACA and it seems reasonable to think that they should be able to trap electrophiles. Because this lack of reactivity was observed in this bulky 5-membered ring system as well as 6-membered ring tertiary and quaternary ACA[85,142] but not with alternative nucleophiles[147,149], we speculate that this issue probably does not originate from hindrance and/or conformational problems but more likely high stable enolate intermediates in the case of zirconocene nucleophiles, unable to react to form tandem trapping products.

Regioselective formation of enolate

The unfortunate inability to trap electrophiles during the ACA generates a regioselectivity issue and the desired enolate **38a** needs to be formed selectively over enolate **38b** (Scheme 4.7). The challenge originates from the lack of obvious differences in the two enolate sites, as they are both sp^3-hydridised. The difference in their respective reactivity would only be influenced sterically and electronically by the longer range effects of the acetal at position 5 and the aliphatic chain at position 4.

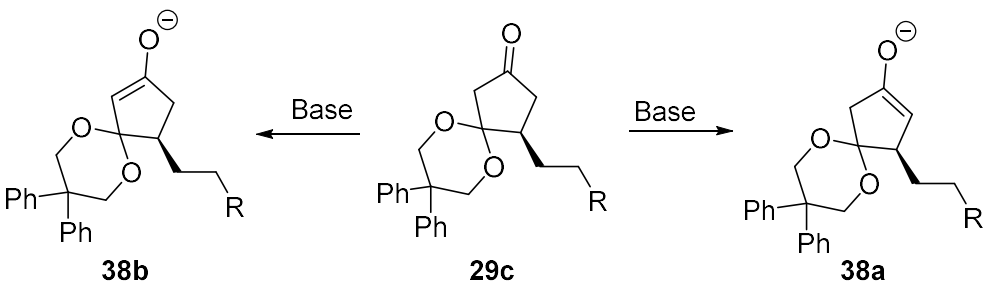

Scheme 4.7. Regioselective challenge of forming enolates from product 29c.

Using triethylamine as a mild base, we managed to form the desired TIPS enolate **39** in 24% yield (Scheme 4.8a). The low yield was due to poor conversion and attempts to improve the yield were unsuccessful. Deprotecting enolate **39** using TBAF to trap allylbromide to form **36** resulted in the decomposition of the starting material **39** (Scheme 4.8b). We also attempted to trap allylbromide directly, using Et_3N, which was unsuccessful even in the presence of Lewis acids and we solely recovered starting material **29c** (Scheme 4.8c).

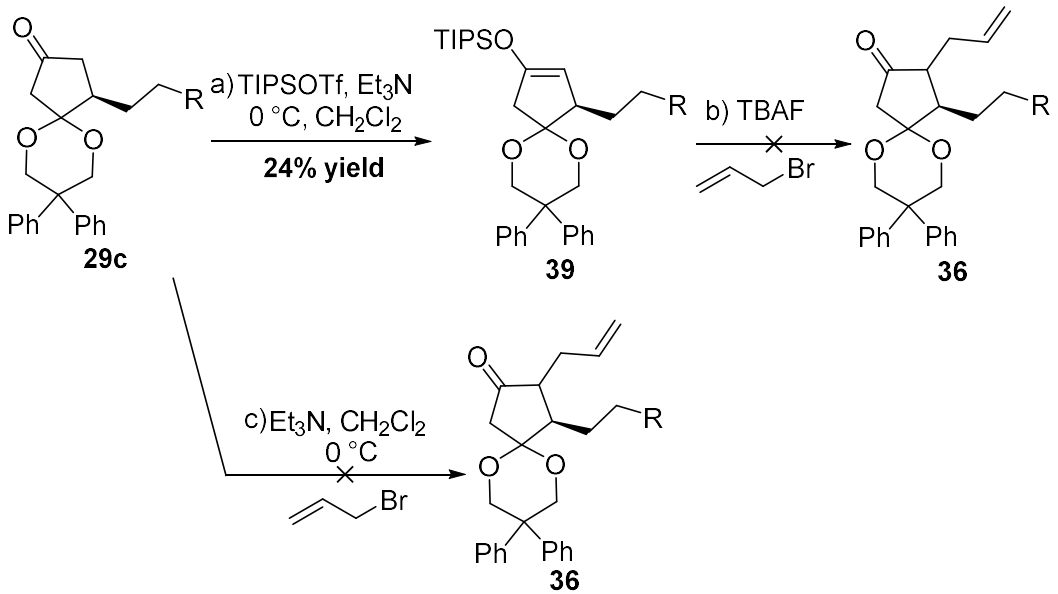

Scheme 4.8. Regioselectively forming enolate 38a using a mild base, Et_3N. Conditions: a) ketone **29c** (1.0 eq), TIPSOTf (2.5 eq), Et_3N (5.0 eq) in CH_2Cl_2 12 h from 0 °C to room temperature. b) enolate **39** (1.0 eq), allylbromide (2.5 eq), TBAF (1.1 eq) in THF 48 h from –78 °C to room temperature. c) ketone **29c** (1.0 eq), allylbromide (2.5 eq), Et_3N (5.0 eq) in THF 48 h from –78 °C to room temperature.

We initially attempted to form the TBS enolate rather than TIPS enolate **39** in order to differentiate the protecting groups (on the chain and on the enolate) during deprotection. However, when using TBSOTf, a complex mixture of TIPS and TBS protected starting material and products were recovered (Scheme 4.9).

Hence, we decided to from the TIPS protected enolate **39** in order to avoid any scrambling of protecting groups.

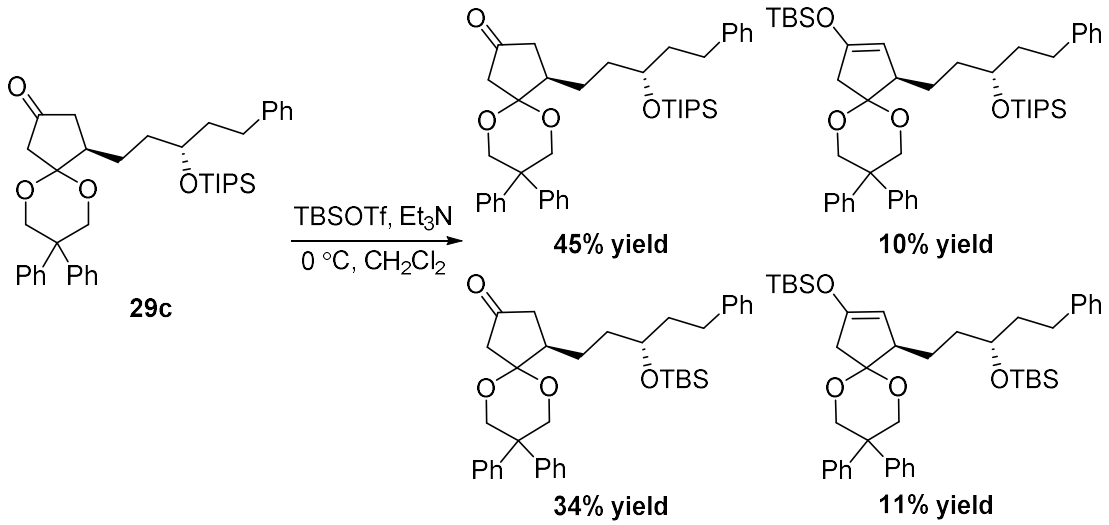

Scheme 4.9. Scrambling of protecting group when attempting to form the TBS enolate. Conditions: a) ketone **29c** (1.0 eq), TBSOTf (2.5 eq), Et_3N (5.0 eq) in CH_2Cl_2, 12 h from 0 °C to room temperature.

Circumventing regioselectivity – ring opening of cyclic acetal

Using stronger bases such as LiHMDS, *t*BuOK, or LDA to trap allylhalides resulted in the unwanted formation of enolate **38b**. When using LDA, the formation of product **40** was poor (7%) while the vast majority of enolate **38b** rapidly collapsed to form open acetal **41** in high yield (67%) (Scheme 4.10a). Other bases also opened the acetal to **41** and due to the presence of allylhalides, multiple trapping products were obtained depending on the conditions used. In the absence of allylbromide, the formation of the open acetal **41** was optimised to 90% yield (Scheme 4.10b).

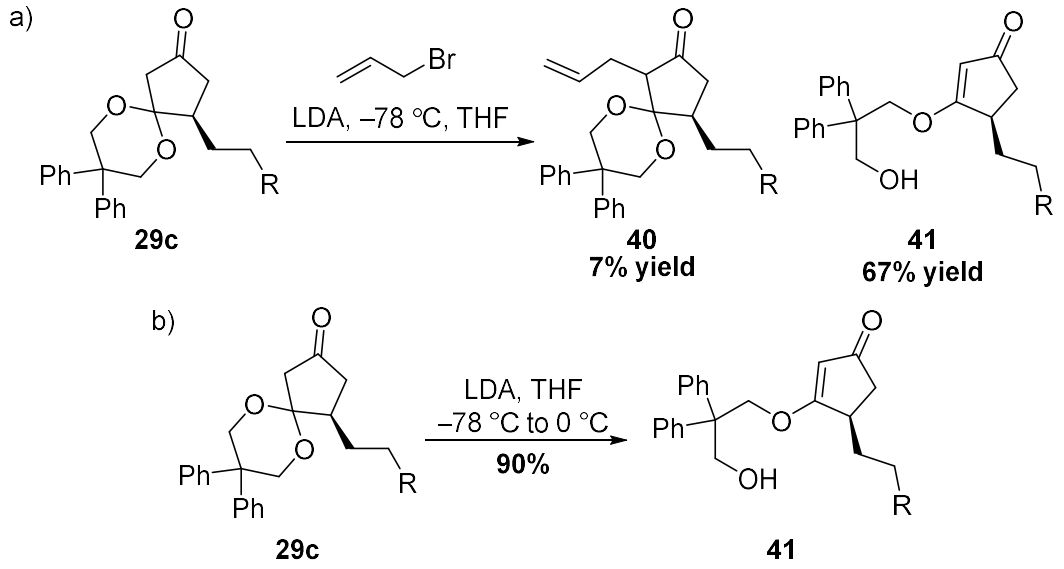

Scheme 4.10. Formation of the undesired product 40 and the open acetal 41 when using strong bases such as LDA. Conditions: a) Diisopropylamine (1.2 eq), *n*BuLi (1.2 eq) in THF, 15 min at –78 °C then **29c** (1.0 eq) in THF for 30 min, then allylbromide (5.0 eq), 10 h at –78 °C to 0 °C. b) Diisopropylamine (1.2 eq), *n*BuLi (1.2 eq) in THF, 15 min at –78 °C then **29c** (1.0 eq) in THF 10 h at –78 °C to 0 °C.

Nicolaou[166,167] described and patented an unusual synthesis of Δ^{12}-prostaglandin J_3 (Δ^{12}-PGJ_3), a potent anti-leukemic agent analogous to prostaglandins. Starting from cyclopentenone, his route consists of a Wittig reaction on an already substituted 5-membered ring to add the first chain, forming **42**, followed by an enolate alkylation to add the second chain (Scheme 4.11). This synthesis intelligently makes use of α,β-unsaturated ketone **42** to control the regioselectivity of the enolate alkylation.

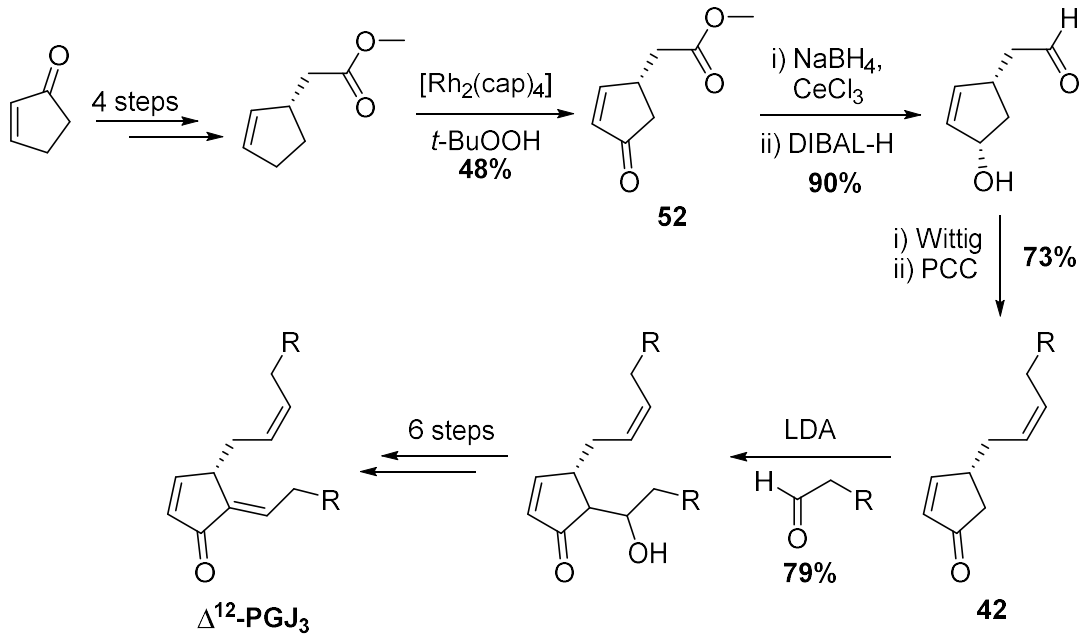

Scheme 4.11. Nicolaou's Δ^{12}-PGJ_3 synthesis[166,167].

We envisioned that in a similar fashion, we would use the formation of the α,β-unsaturated ketone **41** to block the undesired enolate **38b** site and trap an electrophile at the required 2-position. Before forming an enolate, open acetal **41** had to be protected. Based on the scrambling of protecting groups observed during the trapping of enolate **38a** with TBS (Scheme 4.9), we decided to protect open acetal **41** with TIPS and obtained product **43** in a high 86% yield (Scheme 4.12). In an attempt to reduce the number of synthetic steps, we tested a tandem acetal opening-TIPS protection step which gave the protected product **43** in only 14% yield.

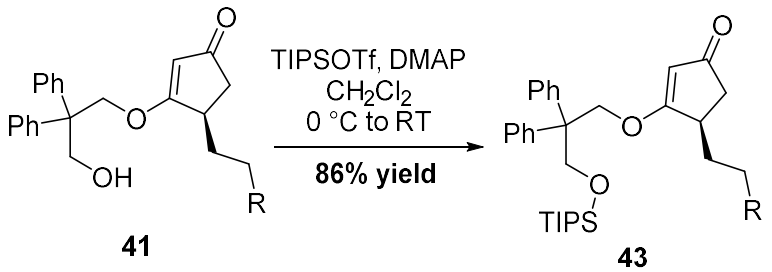

Scheme 4.12. Protection step of open acetal 41. Conditions: DMAP (2.0 eq), **41** (1.0 eq) TIPSOTf (2.5 eq) in CH_2Cl_2 2.5 h from 0 °C to room temperature.

When using LDA / allylbromide on α,β-unsaturated ketone **43**, desired **44** was formed in poor yield (11%) using model substrate **44a** and no product was formed on Latanoprost precursor **44b** (Scheme 4.13). The majority of starting material **43** was recovered. Different conditions were tested (electrophiles, equivalents, temperature etc.) without any improvements.

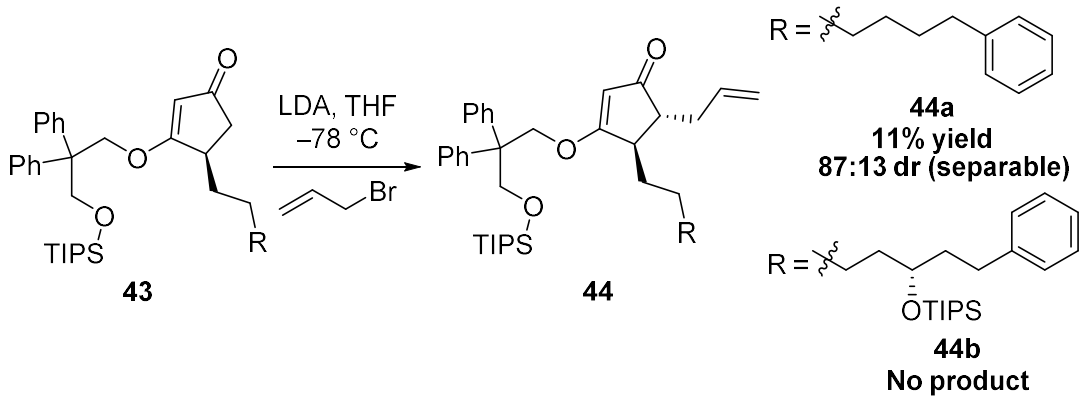

Scheme 4.13. Enolate trapping of allylbromide using LDA. Conditions: Diisopropylamine (1.2 eq), *n*BuLi (1.2 eq) in THF, 15 min at –78 °C then **43** (1.0 eq) in THF for 30 min, then allylbromide (5.0 eq), 12 h at –78 °C to room temperature.

The strength of LDA is well established so the lack of reactivity of ketone **43** was surprising. We speculate that the aliphatic chain at the 4 position of the cyclic core with a bulky TIPS protecting group and the bulky open acetal chain are blocking the enolate site. Using smaller bases such as NaH, or a complete different approach based on intramolecular α-allylic alkylation[168] were also

unsuccessful and only starting material was recovered. Due to the length of this synthesis, as well as a lack of obvious solution at this point, we decided to abandon this route.

Latanoprost synthesis using Cu-catalysed AAA

As detailed in Chapter 1, asymmetric allylic alkylation (AAA) is also highly proficient in the formation of new C-C bond enantioselectively. We recently reported a Cu-catalysed AAA using racemic cyclic allylchlorides **45** and alkylzirconocenes[4] (Scheme 4.14). Highly enantioenriched products are obtained at room temperature in high yield in convenient procedures. The method was used to synthesise bioactive natural product used as traditional treatments for tuberculosis and leprosy, as well as inhibit *p*-aminobenzoate biosynthesis. This reaction is later discussed in detail as we carried out extensive mechanistic studies by NMR (Chapter 5).

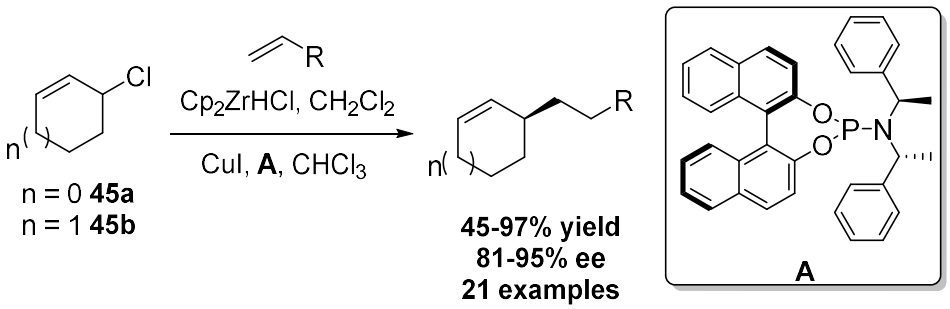

Scheme 4.14. Cu-AAA using racemic cyclic allylchlorides 45 and alkylzirconocenes[4].

This methodology worked well for 5-membered ring **45a** and has a high functional group tolerance. Therefore we decided to test this new AAA towards the synthesis of Latanoprost **22** to form **46** (Scheme 4.15). We envisioned that

following the AAA, allylic oxidation would yield product **47** following literature procedures[166,167,169-177]. Then the Latanoprost second chain could be installed by enolate trapping of an electrophile inspired by our previous route to form **48** with less steric constraints than **43**. Then a diastereoselective oxa-1,4-addition and stereoselective reduction of the ketone would provide Latanoprost **22**.

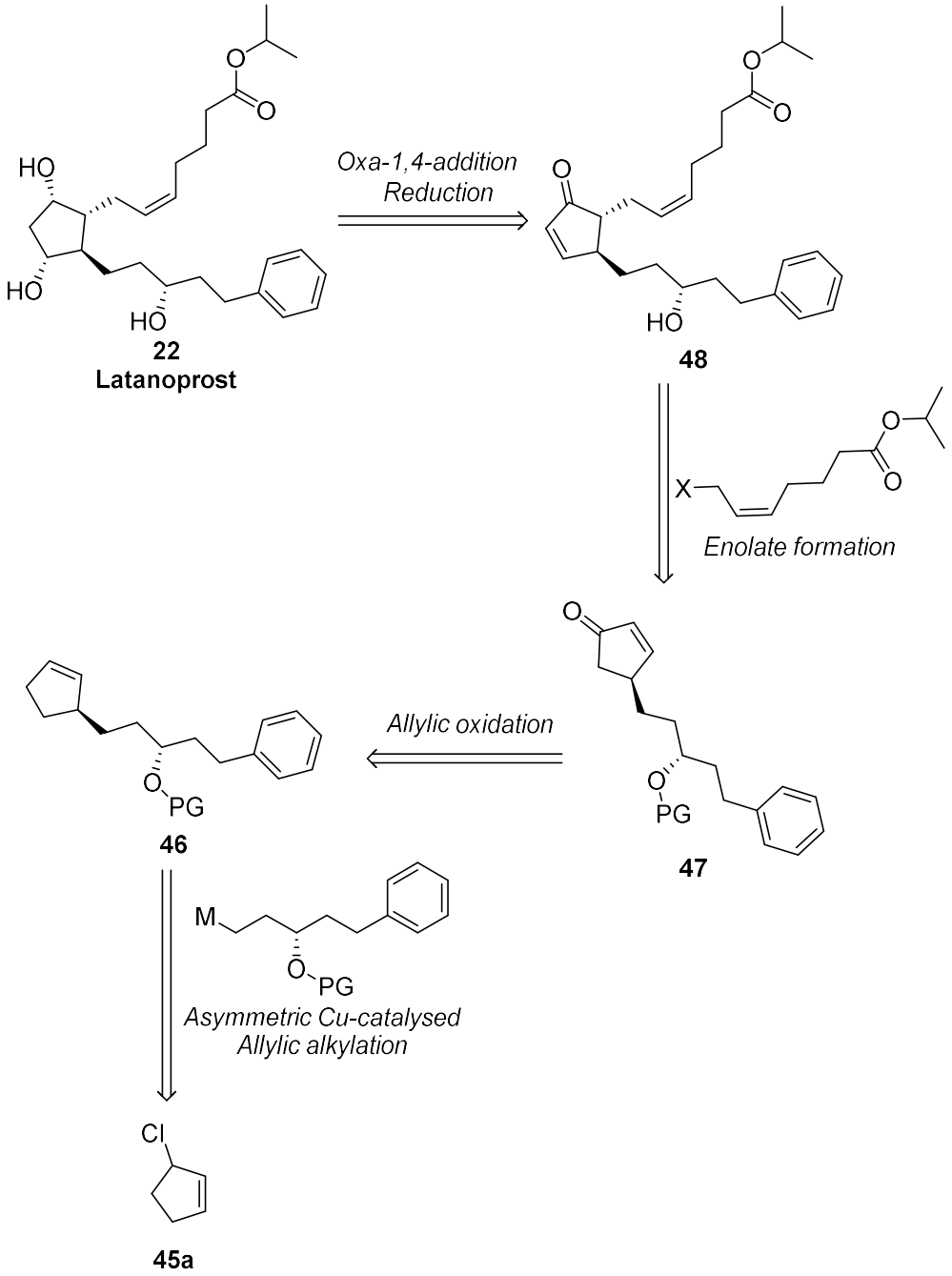

Scheme 4.15. Proposed retrosynthesis of Latanoprost **22** using our newly developed AAA of alkylzirconocene to allylchloride **45a**.

1) Cu-catalysed AAA

The hydrozirconation tandem AAA of TIPS protected alkene **23c** worked well. However, excess alkene was required to achieve high yield and ee, making purification of the product challenging as the AAA product **46**, excess alkene **23c** and alkane **49**, originating from the hydrozirconation of **23c**, have similar low polarity and boiling points. Isolated yields of pure AAA product **46** were low (22% yield) from an estimated 59% yield by NMR spectroscopy (Scheme 4.16).

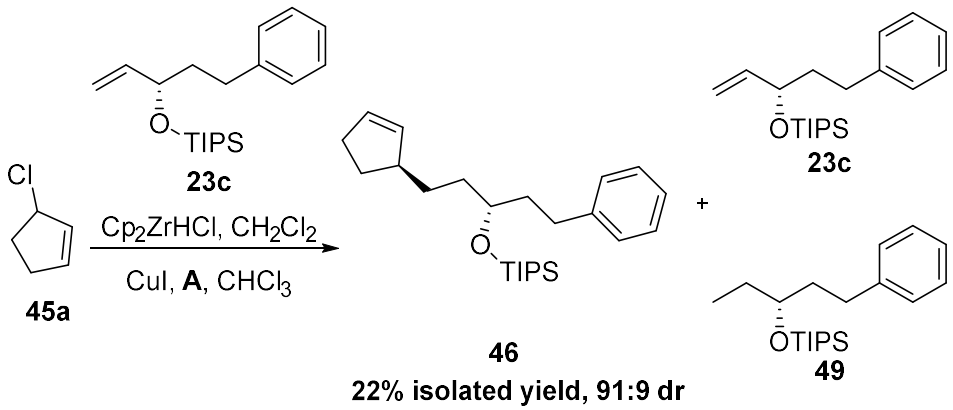

Scheme 4.16. Hydrometallation of alkene 23c / AAA products. Conditions: Alkene **23c** (2.5 eq), Cp_2ZrHCl (2.0 eq) in CH_2Cl_2, CuI (10 mol%), ligand **A** (10 mol%), allylchloride **45a** (1.0 eq), in $CHCl_3$ at room temperature.

Attempts to reduce the amount of initial alkene **23c** or alkylzirconocene to facilitate purification proved detrimental to the yields. In order to avoid this purification problem, we added TBAF to the crude AAA mixture to deprotect the AAA product **46**, alkene **23c** and alkane **49** and we could obtain pure alcohol **50** in 62% yield and an excellent 99:1 isolated dr over 2 steps (Scheme 4.17).

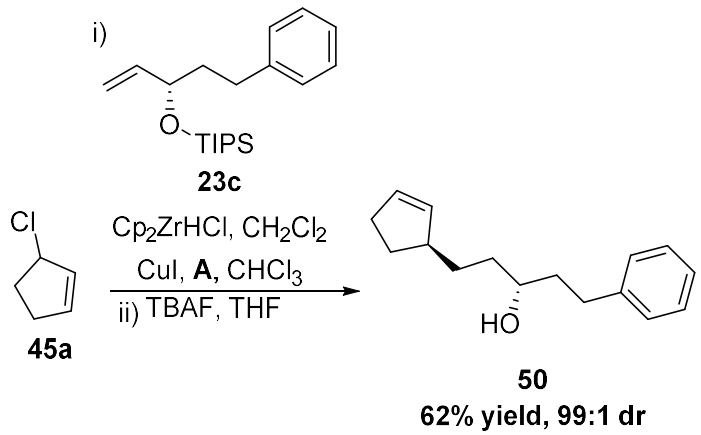

Scheme 4.17. Isolation of the AAA product by TBAF deprotection. Conditions: i) Alkene **23c** (2.5 eq), Cp_2ZrHCl (2.0 eq) in CH_2Cl_2, CuI (10 mol%), ligand **A** (10 mol%), allylchloride **45a** (1.0 eq), in $CHCl_3$ at room temperature. ii) TBAF (7.0 eq) in THF at room temperature.

When scaling the reaction to 4.0 mmol (10 times larger than the original screening), the yield drastically dropped to 4%. Because the AAA reaction is left overnight, we assumed some of the solvent evaporates. On small scales, small amounts of evaporation will significantly change the reaction concentration but on a large scale, solvent evaporation would be negligible. Therefore, we tuned the reaction conditions for the scale up by concentrating the reaction to 1.3 M rather than 0.5 M and cooling down the reaction to 0 °C, achieving 40% yield.

2) Allylic oxidation

We then set out to test the allylic oxidation of the AAA product **46** to form the oxidised product **47**. Allylic oxidation methodologies are commonly reported in literature[166,167,169-174,176,177] since the 1990s and therefore a variety of conditions exists. However, when following Nicolaou's[166,167] allylic oxidation procedure using a Rh-catalyst and *t*BuOOH as described in the synthesis of Δ^{12}-prostaglandin J_3 (Scheme 4.11), we obtained rearranged product **51** in 26% yield (Scheme 4.18).

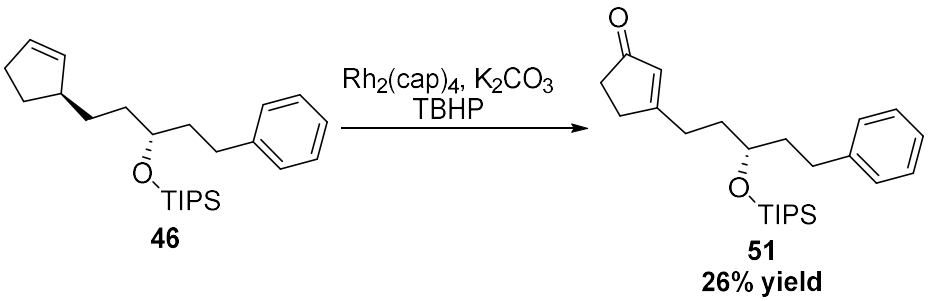

Scheme 4.18. Unwanted rearrangement during the allylic oxidation by $Rh_2(cap)_4$. Conditions: AAA product **46** (1.0 eq), K_2CO_3 (0.5eq), $Rh_2(cap)_4$ (1.0 mol%) *t*BuOOH (10.0 eq) in CH_2Cl_2, 1.5 h at room temperature.

This type of rearrangement is due to the preferential formation of the substituted radical and has been reported on many different substrates[166,167,169,170,172-175]. Most allylic oxidation actually uses substrates that prevent or disfavour rearrangement such as allylic quaternary centres, bridges, acetals etc[166,167,169-174,176,177]. Nicolaou[166,167] rationalised that substrate **52** (Scheme 4.11) does not rearrange to the more stable tertiary radical due the destabilising effect of proximal oxygens, favouring the secondary radical. In our case, the oxygen on the Latanoprost chain is apparently too distant to see this effect on the tertiary radical formation.

Unfortunately, the majority of allylic oxidation methodologies use a radical mechanism. Nonetheless, we tested a vast array of allylic oxidation conditions involving transition metal sources (Rh[41], Pd[170,177,178], Mn[166,173], Cr[179-181])[175], other catalyser (Se[175,177,181,182]), radical sources (*t*BuOOH[166,172,182], benzoquinone[181], TEMPO[183], *t*BuOO*t*Bu, UV)[175] and even P450 enzymes or combinations of literature procedures without success. For example we tested Cr^V, an uncommon oxidising reagent which mechanism is uncertain, described by Baran in the total synthesis of (−)-Taxuyunnanine D[177,181]. Cr^V gave us rearranged product **52** in 40% yield. We also tested $Pd(OAc)_2$ with MnO_2 and benzoquinone as Åkermark[169] described some mixed rearrangement of products suggesting that it

might be possible to synthesise **47**. In this case no reaction occurred and only starting material **46** was recovered. SeO_2 allylic oxidation undergo pericyclic mechanisms to give allylic alcohols or α,β-unsaturated ketones. We thoroughly investigated the use of SeO_2 under various conditions (equivalents, temperatures, solvents, additives, etc.)[175,177,181,182] but unfortunately all were unsuccessful. At temperature below 55 °C, no reaction occurred while at 55 °C a myriad of oxidation products were formed. We never succeeded in isolating the desired product **47**. After these complications and a lack of alternatives, we decided to halt the synthesis of Latanoprost via this pathway.

CONCLUSION

To conclude, using the ACA of alkylzirconocene to cyclopentenone-3,5-dione monoacetal **18a** we were able to add the first chain of Latanoprost **22** in high yield (79%) and good dr (85:15). Unfortunately *in situ* trapping of simple electrophiles was not successful and further experiments to add the second chain of Latanoprost did not succeed. Therefore we tested the AAA of alkylzirconocene to allylchloride on the Latanoprost alkene precursor **23c**. Initially we could not isolate the AAA product **46** but after optimisation we isolated the derived alcohol **50** in 62% yield and 99:1 dr. Unfortunately, the subsequent allylic oxidation was difficult and the route was abandoned.

Although we did not succeed in synthesising Latanoprost, the key enantioselectively C-C bond formation using both ACA and AAA of complex alkylzirconocenes was highly successful, proving the applicability of those

methods. Future works will be focused on circumventing the lack of reactivity of ketone **43** in the ACA pathway or the allylic oxidation difficulty in the AAA pathway. For example, we speculate that using substituted substrates or *meso*-bis-allylchloride substrates in the AAA might be successful. Furthermore, despite the huge variety of known allylic oxidation procedures, new allylic oxidation methodology to give products of type **46** is clearly lacking and should also be investigated.

PART II

MECHANISTIC NMR STUDIES OF CU-CATALYSED METHODOLOGY

INTRODUCTION

So far, we have discussed the development of new methodologies in Cu-asymmetric transformations and their application in the total synthesis of complex bioactive molecules. However, studying reaction mechanism is also an integral part of organic chemistry.

Many techniques have been developed to study mechanisms in solution (replicating the catalytic conditions) such as aliquot sampling / GC or HPLC analysis and ReactIR. However, such techniques only give limited structural information about intermediates, are prone to error and interpretation of results can be extremely difficult. Another technique, NMR, has been highly successful in structurally characterising inorganic and organometallic complexes of diverse metals in solution[91,184-186] and has the advantage to be able to follow reactions *in situ* in time with high precision in a non-invasive non-destructive way. Despite its clear advantages, mechanistic NMR studies are rare as complex organometallic catalytic systems in general are often inadequate (expensive deuterated solvent, cryogenic temperature, moisture sensitive systems etc.). Moreover, Cu has a large quadrupole moments rendering NMR studies challenging. Gschwind greatly contributed to the study of Cu-catalytic complexes in solution by NMR[91].

Organocopper (I) species are versatile, reactive and have a tendency to self-aggregate to complex mixtures (dimers, trimers, oligomers, polymers)[91]. Their aggregation and reactivity are dependent on solvent chelation, counterion effects, ligands stereo electronic properties and ratios of the species in solution, as well as other factors such as concentration and temperature[187] (Figure II.1).

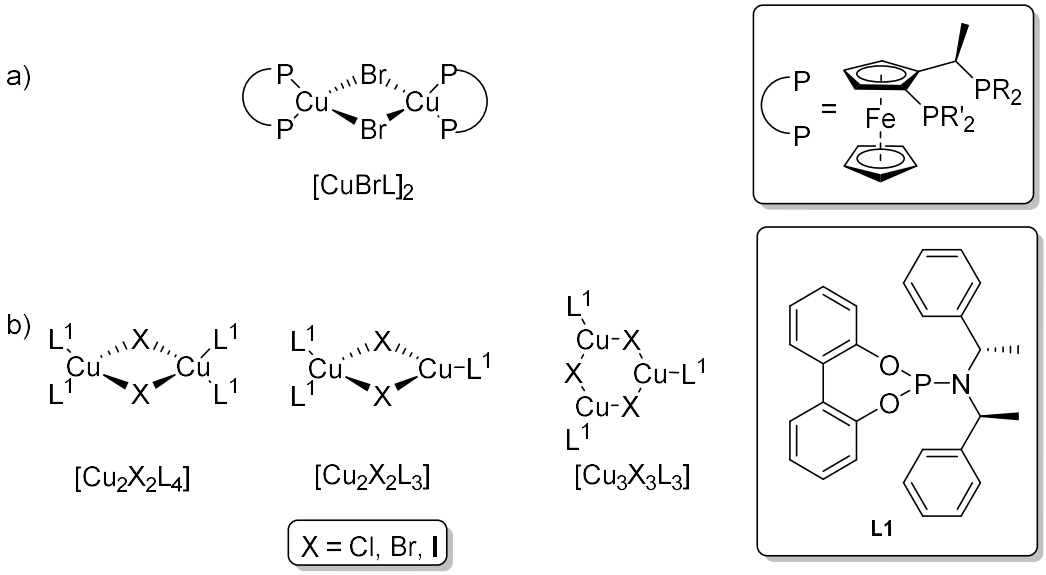

Figure II.1. Examples of pre-catalytic and catalytic complexes in various environements[91].

As exemplified in Figure II.1, the intrinsic nature of the ligand affects the solution aggregates in part because of how they bind to Cu (e.g. the bidentate ferrocene ligands (Figure II.1a) compared to the monodentate phosphoramidite ligands (Figure II.1b)). Moreover, pre-catalytic complexes can even be found in mixtures of aggregates. For example for the CuCl-**L*** complex depicted in Figure II.2, the major aggregate in solution was identified by ^{31}P NMR spectroscopy at 172 K as a binuclear pre-catalytic complex with mixed trigonal/tetrahedral geometry and a minor binuclear complex with tetrahedral coordination was also present[187].

Figure II.2. a) Representation of the pre-catalytic binuclear complex with mixed trigonal/tetragonal coordination. b) ^{31}P NMR spectra at 172 K of CuI-ligand showing presence of the trigonal/tetragonal complex and traces amount of binuclear complex with tetrahedral coordination. Reprinted with permission from Ruth M. Gschwind, Chemical Reviews, "*Organocuprates and Diamagnetic Copper Complexes: Structures and NMR Spectroscopic Structure Elucidation in Solution*"[91]. Copyright 2008 American Chemical Society.

The pre-catalytic Cu-aggregates also greatly vary from the catalyst species present during the reaction (Scheme II.1)[2,91,187,188]. All proposed mechanisms describe the transmetallation of the alkyl nucleophiles to the Cu species. However, as far as we are aware, spectroscopic proof of transmetallation has only been observed twice. Feringa[189] proposed that upon addition of Grignard, the pre-catalytic Cu-ferrocenyl dimer became a bimetallic transmetallation monomeric complex (Scheme II.1a). Further modifications upon addition of substrates and additives are clearly conceivable. Similarly, Gschwind[188] observed the transmetallation of diorganozinc nucleophiles with Cu-phosphoramidite

ligand complexes (Scheme II.1b). DFT calculations predicted that the resulting bimetallic zinc-cuprate transmetallation species would form yet more elaborate super-complexes binuclear in Cu upon addition of enone.

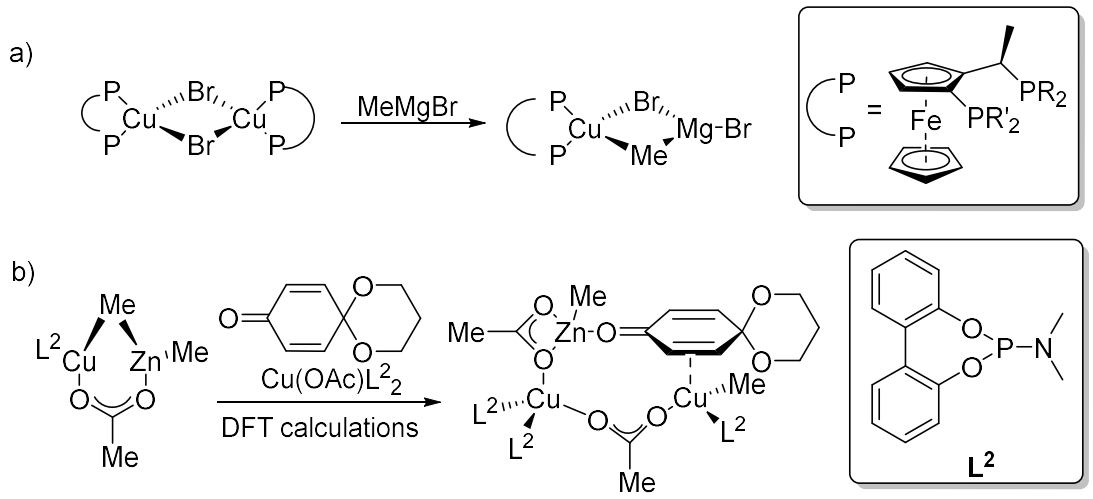

Scheme II.1. Proposed pre-catalytic and transmetallation complexes[188,189].

Therefore, structures of transmetallation intermediates vary significantly depending on the respective reactions and conditions. Hence, great care has to be taken into account in proposing general structural information as well as proposing mechanistic pathways, especially when moving from one system to another[91].

AIMS

In the second part of this thesis, we discuss the use of diverse NMR techniques to thoroughly study the mechanism of alkylzirconocenes in Cu-catalysed asymmetric transformations in the hope to understand their behaviour and reactivity and shed some light on their mechanistic pathways. Chapter 5 and

Chapter 6 discuss in detail the NMR study of Cu-catalysed AAA from allylchloride and allylphosphate respectively. In Chapter 7, we developed a new heterocyclic AAA and studied its mechanism by NMR to try to improve its reactivity. And finally Chapter 8 details the NMR study of the Cu-catalysed ACA of alkylzirconocenes.

CHAPTER 5

NMR MECHANISTIC STUDIES OF CU-CATALYSED ASYMMETRIC ALLYLIC ALKYLATION USING ALLYLCHLORIDE

Part of this Chapter has been published in Nature[4] and another manuscript is in preparation. Prof. Tim D. W. Claridge ran the selective inversion recovery and the SSTD and calculated the resulting exchange rates for these experiments. Dr Mireia Portela Sidera and Hengzhi You measured the ee of the product at 10 min, 2 h and at completion for CuI, CuCl and CuOTf catalysts and carried out the correlation between ee of the ligand and ee of product experiment (Figure 5.15).

INTRODUCTION

Over the past forty years a number of enantioselective catalytic strategies for inducing asymmetry have emerged[190,191]. Two strategies for generating single enantiomers have been widely embraced. The vast majority of asymmetric transformation converts prochiral starting materials to enantioenriched products. We have extensively discussed the use of prochiral substrates in Part I through Cu-catalysed asymmetric conjugate addition. However, efficient methods to produce enantioenriched compounds from racemic starting materials are also in high demand as racemic chiral substrates are more common than prochiral starting materials[192] and easily obtained by standard synthesis.

In the last decade, transition metal-catalysed asymmetric allylic alkylation (AAA) reactions have proven to be powerful tools for creating new C-C bonds

enantioselectively[193-198] and can accommodate both achiral and chiral substrates. In 1994, Trost first reported Pd-catalysed AAA reactions of chiral racemic substrates in high yield and ee using malonate anion[199] (Scheme 5.1). Since then, many more systems have been established using Pd and stabilised nucleophilic (pK_a <25) anions and have proven to be versatile and extremely valuable in synthesis[43,195,200,201].

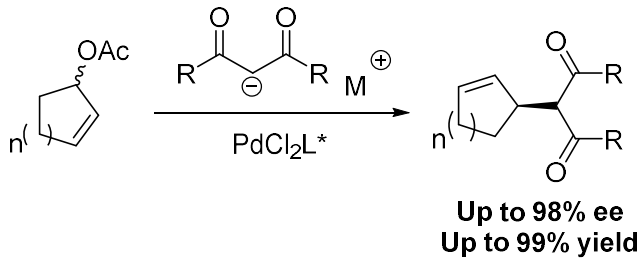

Scheme 5.1. Example of Pd-catalysed AAA of racemic allylacetates using malonate anion[199].

Expanding the scope of AAA to non-stabilised nucleophiles (pK_a >25)[195,202-204] such as Grignard reagents, organozincs, or organoaluminiums, has proven challenging. The difficulty is that there are significant mechanistic distinctions between stabilised and non-stabilised nucleophiles[193,196,202,203]. For stabilised nucleophiles, the C-C bond-making event occurs when the nucleophile attacks the π-allyl-metal intermediate[205], usually using Pd-catalysis. For non-stabilised nucleophiles, the C-C bond formation probably occurs through reductive elimination of an intermediate in which the nucleophile is already bound to the metal centre and in practice such reactions use Cu-catalysis[1,7].

Initially, Cu-AAA involved diastereoselective allylic alkylation using enantiopure chiral substrates[206] or chiral auxiliaries[207]. The drawbacks of these reactions are clear (expensive, long synthesis of enantiopure reagents,

compulsory chiral building blocks, etc.) but provided important insights for tuning the enantioselective Cu-AAAs that would follow[1,7]. In 1995, Bäckvall[50] described the first enantioselective Cu-AAA using Grignard reagents on prochiral acyclic allylic substrates, highlighting the important synergistic effect of the leaving group, temperature, ligand and ligand/metal ratio. Now, the enantioselective Cu-catalysed AAA to prochiral materials can be readily achieved and involve an array of nucleophiles, ligands, leaving groups and possible products[1,7,51,62,73,196,198,208-210]. However, Cu-AAAs using chiral racemic substrates are still limited and rare despite their desirability. Bäckvall[211] and then Alexakis[48,212,213] reported promising results with Grignard reagents (Scheme 5.2).

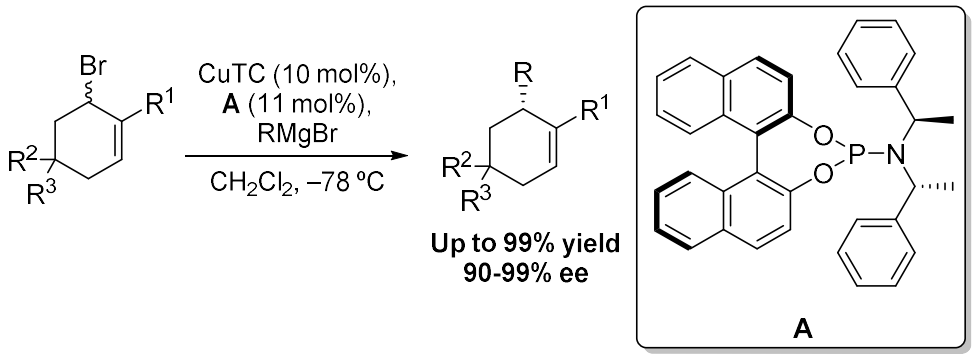

Scheme 5.2. Example of Cu-AAA of racemic allylbromides using Grignard nucleophiles[48,212,213].

Studies on the mechanisms of non-stabilised nucleophiles in Cu-AAA have proven more difficult than their Pd counterparts. Non-stabilised organometallics are typically very reactive, hindering the determination of intermediates or mechanistic pathways. However, Cu-AAAs are generally accepted to operate via regiospecific *anti*-addition mechanisms. A rate-limiting S_N2' oxidative addition step gives Cu^{III} intermediates, followed by a fast reductive elimination to form the final product[1,7,37]. Variants of this mechanism when using *syn*-directing

leaving group to overcome the preferential *anti*-S_N2' pathway have also been described[214].

Moreover, due to the racemic nature of the starting material, mechanistic complexities have to be taken into account due to the differences in the diastereomeric substrate-catalyst interactions. The mechanistic concepts behind such transformation can be narrowed down to four different pathways (Scheme 5.3)[215].

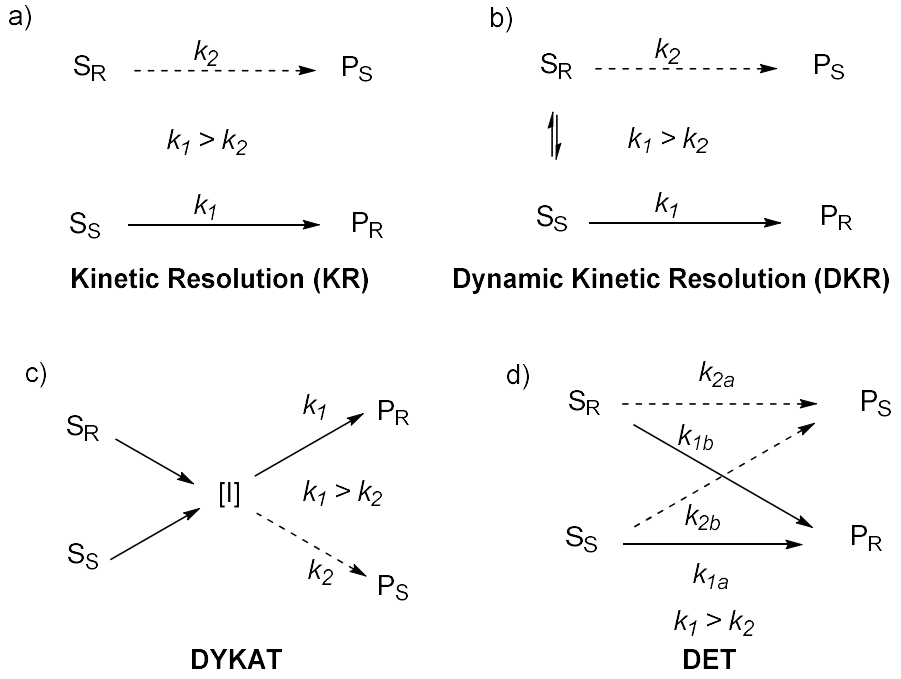

Scheme 5.3. Mechanistic schemes of the four different pathways for the asymmetric reaction of racemic substrate to enantioenriched products.

The vast majority of successful reactions involving racemic substrates and chiral catalyst are kinetic resolutions[216] (Scheme 5.3a). One enantiomer of the substrate reacts rapidly with the chiral catalyst to give an enantioenriched product whilst the other enantiomer of starting material is unreactive, presumably due to substrate-catalyst steric clashes. Only a maximum of 50%

enantioenriched product and 50% of enantioenriched starting material can be isolated [200,217-219].

To overcome the limitation of these incomplete conversions, elegant processes have been designed that can transform both enantiomers of the racemic starting material into a single enantiomer of product. Dynamic kinetic resolution[220-222] (DKR) involves the rapid racemisation of the starting material whilst only one of the enantiomer of the starting material is reactive. Through racemisation of the substrate, the most reactive enantiomer of the starting material is constantly replaced to obtain full conversion (Scheme 5.3b). DKR are commonly found chemically catalysed but have increasingly been designed to use transition metal (Pd, Ru or Rh) mediated racemisation coupled with an enzymatic resolution[221,223] as exemplified in Scheme 5.4.

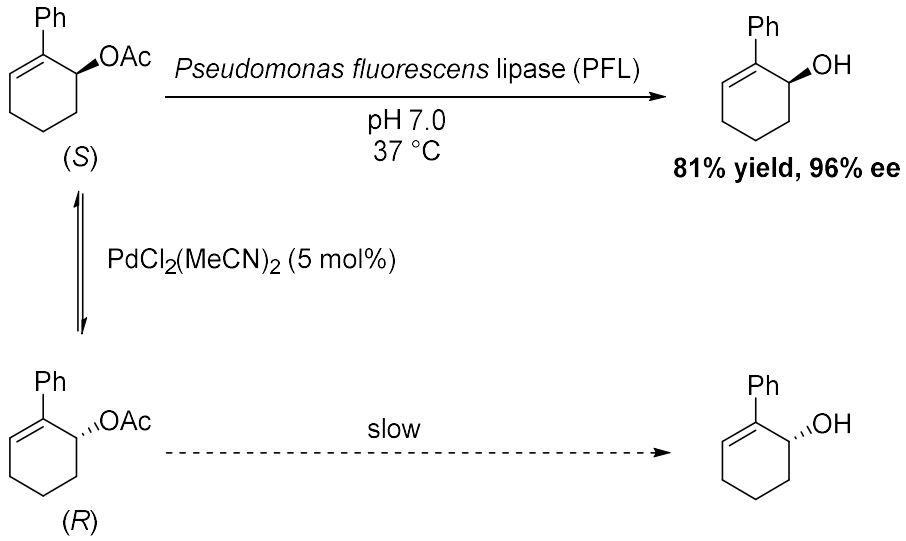

Scheme 5.4. Example of dynamic kinetic resolution using transition metal-catalysed (Pd or Ru) racemisation coupled with enzymatic resolution[221,223].

Here the Pd^{II}-catalyst allows the racemisation of the allylacetate while *Pseudomonas fluorescens* lipase selectively hydrolyses the (*S*)-allylacetate. This biocatalytic concept works particularly well due to the specificity of enzymes for

one enantiomer caused by their folding and binding pockets and the known ability of Pd^{II} to rapidly isomerise allylacetate.

Dynamic kinetic asymmetric transformation[42,43,195,202,212,224,225] (DYKAT) is a deracemisation/symmetrisation method (Scheme 5.3c). Both enantiomers of starting material are converted into a common intermediate, usually pseudo-*meso* or pseudo-prochiral catalytic π-complex, similar to the Pd- or Ir-intermediates observed with soft nucleophiles (Scheme 5.5). The symmetrical intermediate behaves as a prochiral system in enantioselective catalysis. Most AAAs with more than 50% yield are described as DYKAT such as the previously mentioned Pd-AAA by Trost[199] (Scheme 5.1).

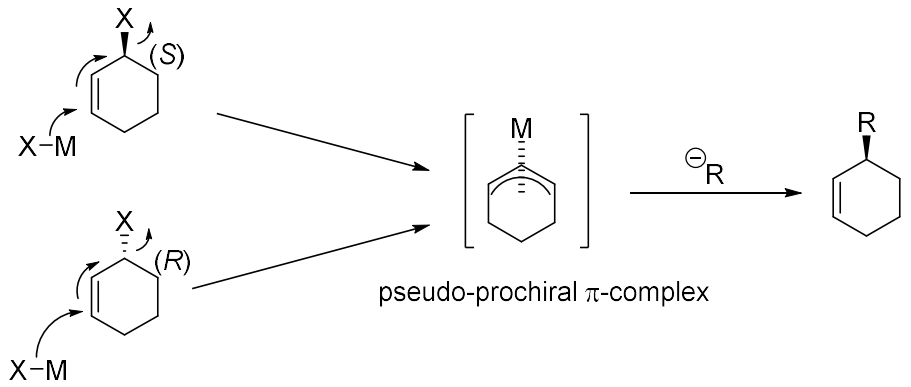

Scheme 5.5. Example of a dynamic kinetic asymmetric transformation (DYKAT) forming a pseudo prochiral π-complex as a common intermediate.

However, some substrates are not suitable for racemisation (DKR) or pseudo-symmetrical intermediates (DYKAT) and achieving >50% yield of enantioenriched product relies on the catalyst promoting two different reaction pathways for each enantiomer towards a common product. Those reactions are called direct enantioconvergent transformation[213,215] (DET) (Scheme 5.3d). The difficulty of DET is that the substrate-controlled stereoselectivity and the reagent-controlled enantioselectivity of the catalyst are in conflict with the

conversion of the lesser reactive enantiomer of starting material, usually resulting in kinetic resolution. The greater influence of reagent-controlled enantioselectivity over substrate-controlled stereoselectivity is crucial to achieve high ee and yields. Sawamura[215] described a Cu-AAA DET using boronic ester nucleophiles (Scheme 5.6). Based on computational modelling, the previously mentioned Cu-AAA of Grignard by Alexakis[212] (Scheme 5.2) is also thought to undergo a DET

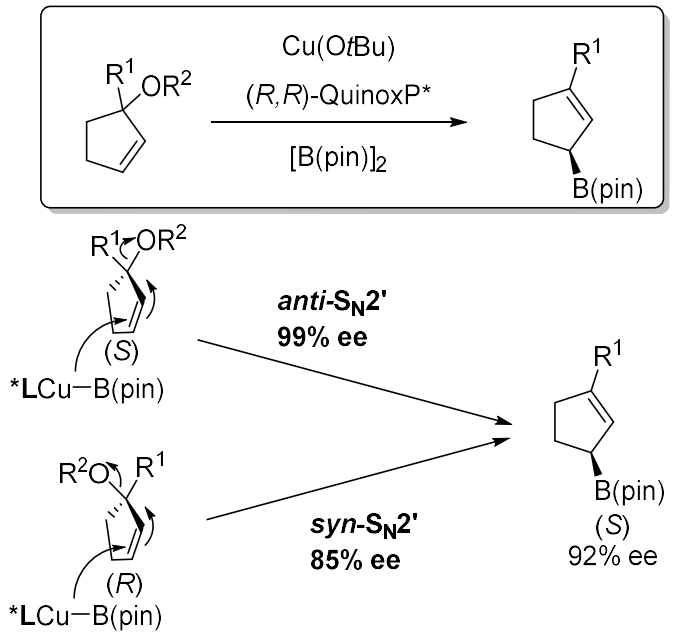

Scheme 5.6. Example of a direct enantioconvergent transformation (DET)[215].

We recently reported a Cu-catalysed AAA using racemic cyclic allylchlorides **45** with alkylzirconocenes[4] (Scheme 5.7). Clearly as >50% yield was consistently obtained, this reaction is not a kinetic resolution. Our aim was to identify the dynamic mechanistic pathways involved and we determined NMR to be the best technique to do so. Indeed, the reaction is carried out in $CHCl_3$ and

at room temperature, significantly reducing the issues encountered with other organometallic systems.

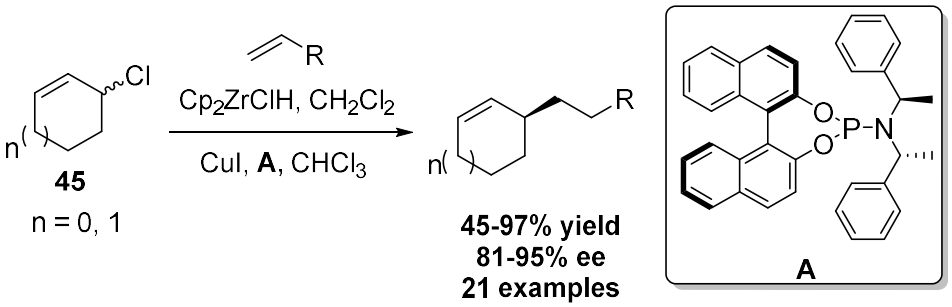

Scheme 5.7. Cu-AAA using racemic cyclic allylchloride 45 and alkylzirconocenes[4].

RESULTS AND DISCUSSION

Reaction Kinetics

We first followed the Cu-AAA reaction *in situ* using ^{1}H NMR spectroscopy. During this experiment we observed clean conversion of allylchloride **45b** (red) to the product **53** (blue) and the formation of low (~3%), but fairly constant, concentrations of allyliodide **54** (purple) (Figure 5.1). This reaction is very slow, with a half-life of 7 h and thus achieving only 85% conversion after 15 h.

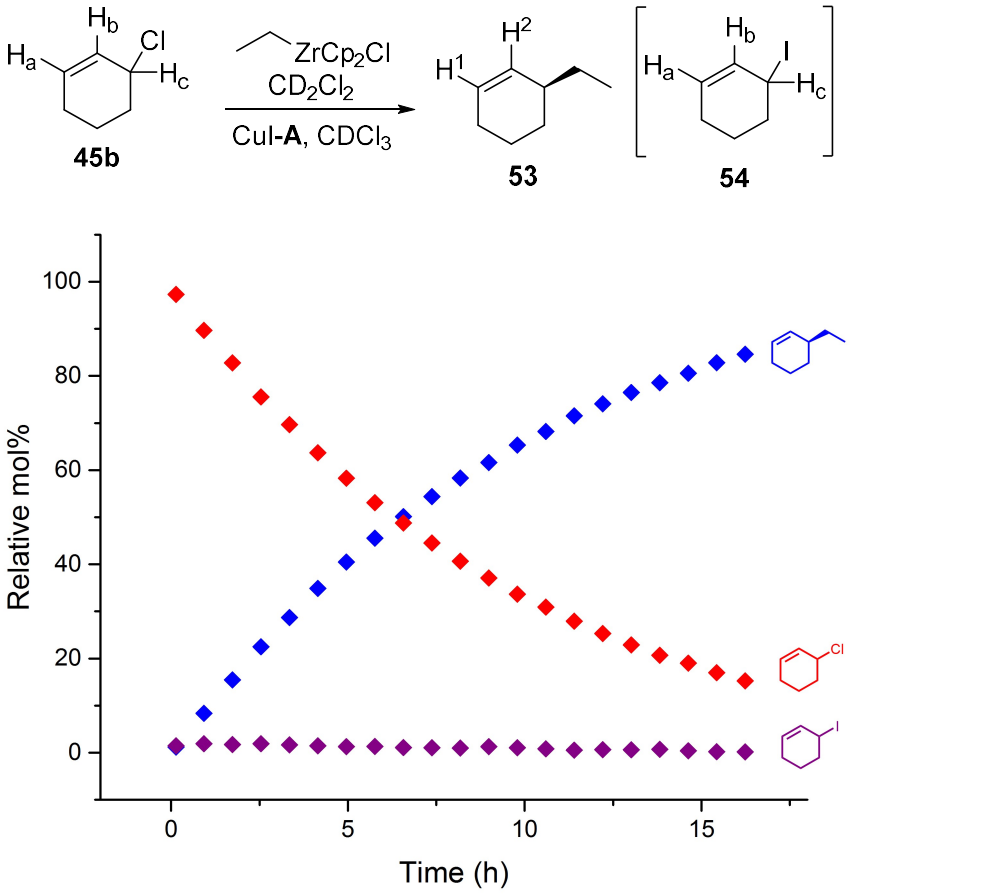

Figure 5.1. Cu-AAA reaction kinetics as monitored by in situ ^{1}H NMR spectroscopy from allylchloride 45b. Conditions: $Cp_2ZrEtCl$ (2.0 eq) in CD_2Cl_2, CuI (10 mol%), ligand **A** (10 mol%), allylchloride **45b** (1.0 eq), in $CDCl_3$, room temperature.

In the ^{31}P NMR spectrum we observed that the main pre-catalyst signal at 129.5 ppm (Figure 5.2– black), does not change upon addition of $Cp_2ZrEtCl$ (orange) or throughout the course of the reaction as shown 24 h after the addition of allylchloride **45b** (blue). At the end of the reaction (blue), the catalytic peak at 129.5 ppm is unchanged but three sharp peaks appeared at 73.8 ppm, 72.5 ppm and 12.5 ppm. Cu-ligated species are usually broad in ^{31}P NMR[188,226] and because of their sharper nature, we assume those peaks come from the catalyst degrading with time and are presumably ligand species, denuded of Cu. The peak at 12.5 ppm is most likely oxidised ligand, as the

chemical shift resembles that of pentavalent phosphorus and has been observed at this shift when phosphoramidite ligands have been oxidised.

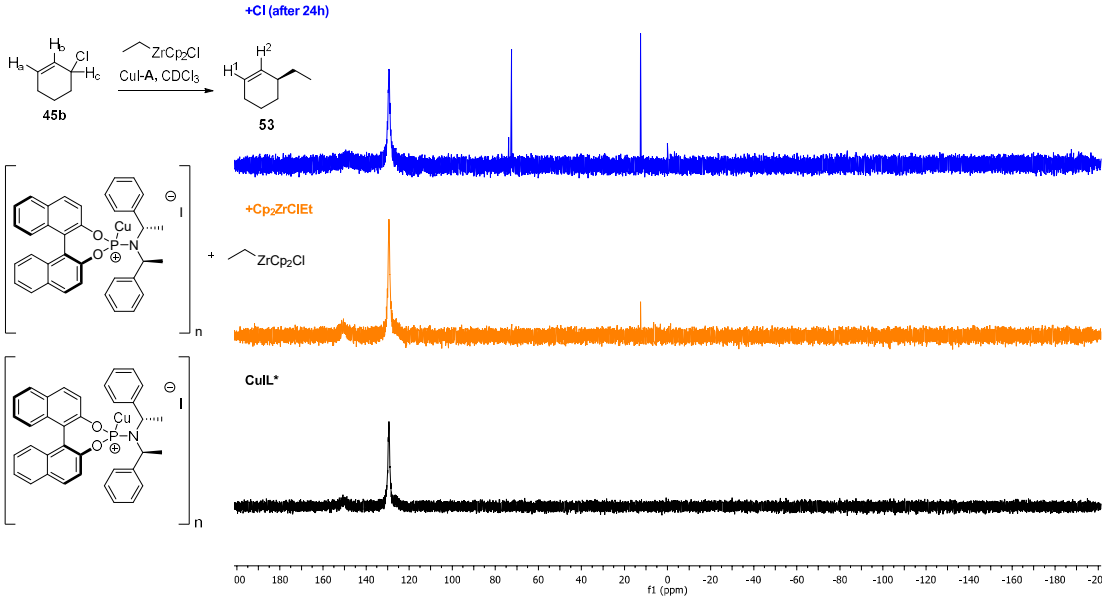

Figure 5.2. ^{31}**P NMR spectroscopy of the catalyst CuI-A (black), CuI-A+Cp_2ZrEtCl (orange) and at the end of the AAA-reaction (blue).** Conditions: Cp_2ZrEtCl (2.0 eq) in CD_2Cl_2, CuI (10 mol%), ligand **A** (10 mol%), allylchloride **45b** (1.0 eq), in $CDCl_3$, room temperature.

Allyliodide intermediate

1) Identification

A constant concentration of allyliodide **54** (purple) was observed during the reaction kinetics (Figure 5.1). Allyliodide **54** is also generated by mixing allylchloride **45b** with the CuI-**A** complex (in the absence of Cp_2ZrEtCl) as judged by ^{1}H NMR spectroscopy (Figure 5.3a).

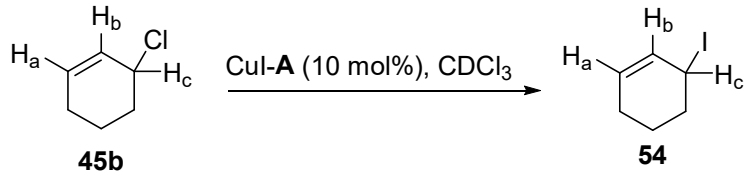

45b **54**

a)

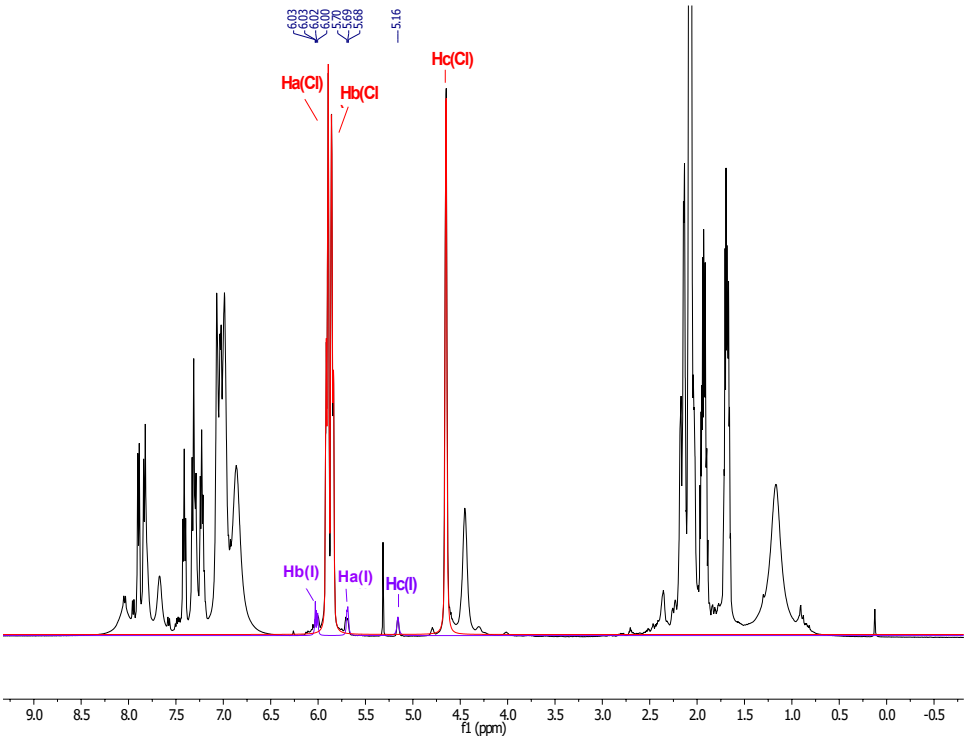

b)

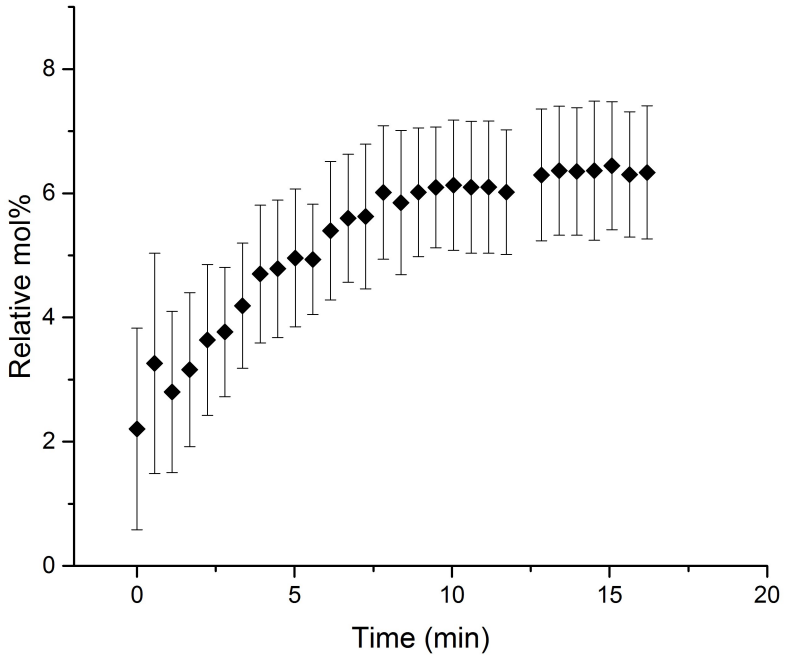

Figure 5.3. Formation of allyliodide 54 from allylchloride 45b and CuI-A as monitored by in situ ^{1}H NMR spectroscopy. a) ^{1}H NMR spectra; allyliodide **54** is shown in purple and allylchloride **45b** in red. b) Kinetic monitoring by ^{1}H NMR. Conditions: CuI (10 mol%), ligand **A** (10 mol%), allylchloride **45b** (1.0 eq), in $CDCl_3$, room temperature. The error bars are the standard deviation of the ^{1}H signal for H_a(I), H_b(I) and H_c(I).

Through this simplified ^{1}H NMR analysis we identified the intermediate allyliodide **54** using *in situ* characterisation (^{1}H, ^{13}C NMR, COSY, HSQC, TOCSY and HMBC) (see Experimental Section for details) despite low concentrations. Under these conditions, allyliodide **54** is formed rapidly reaching a maximum of ~6% within 10 min (Figure 5.3b). Allyliodide **54** was also generated upon addition of TBAI or TMSI to allylchloride **45b** in 4% yield and 70% yield respectively and compared to the signals generated when adding CuI-**A** to allylchloride **45b**.

2) EXSY exchanges

Examination of allyliodide **54** generated from allylchloride **45b** (1.0 eq) and CuI-**A** (10 mol%) complex in $CDCl_3$ using 2D exchange spectroscopy NMR (EXSY) shows that the H_a and H_c protons of **54** rapidly interconvert (as indicated by cross-peaks between these proton signals) (Figure 5.4).

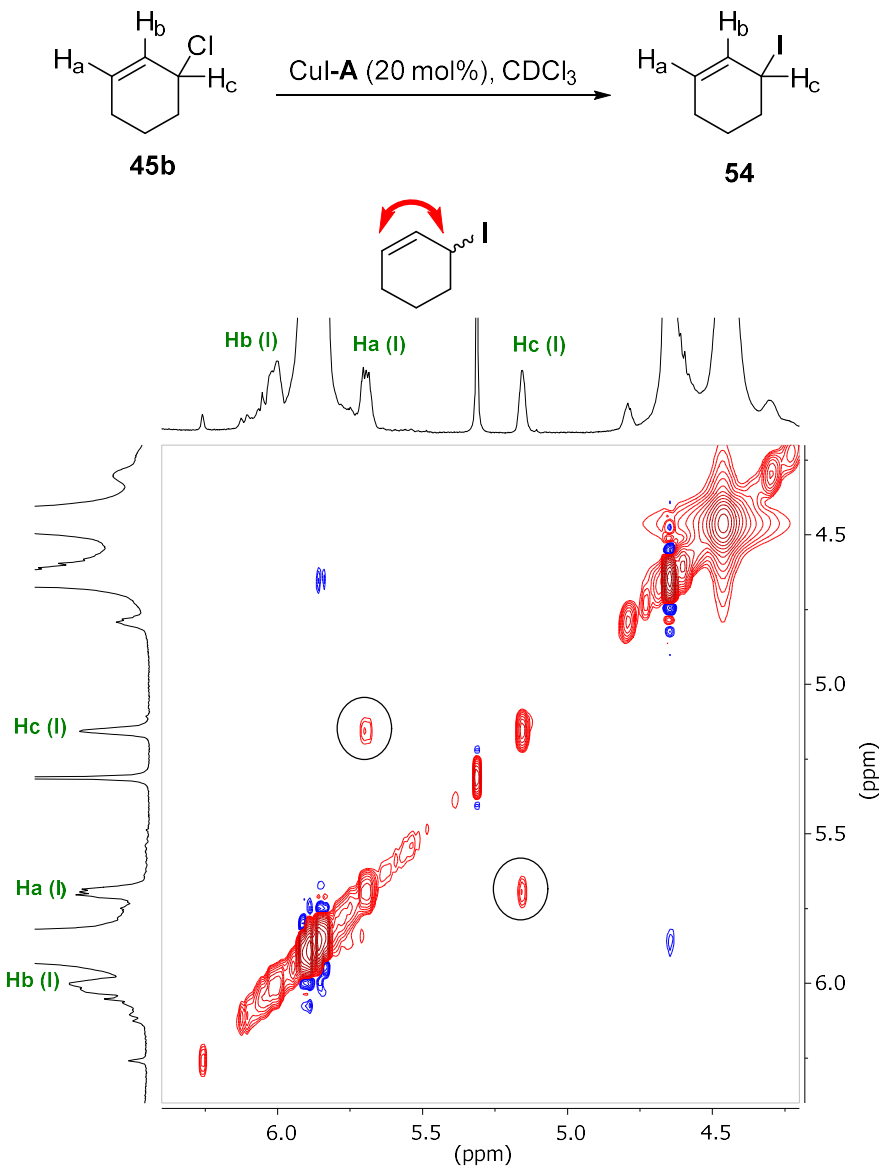

Figure 5.4. 2D exchange spectroscopy NMR (EXSY) of allyliodide 54 formed from allylchloride 45b and CuI-A complex. Conditions: CuI (20 mol%), ligand **A** (20 mol%), allylchloride **45b** (1.0 eq), in $CDCl_3$, room temperature.

A control experiment of allylchloride **45b** alone in $CDCl_3$, showed that what we identified as allyliodide **54** is absent and no exchanges are observed (Figure 5.5).

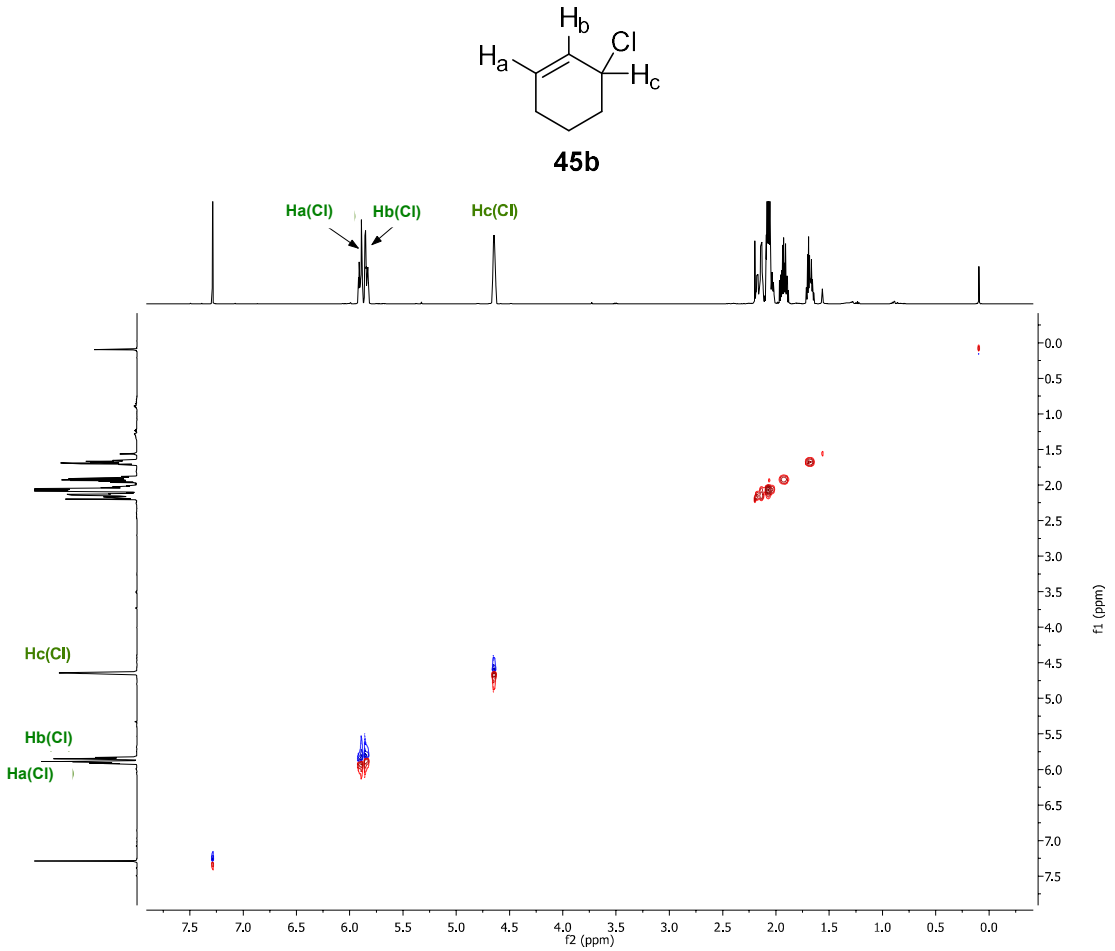

Figure 5.5. 2D exchange spectroscopy NMR (EXSY) of allylchloride 45b. Conditions: allylchloride **45b** (1.0 eq), in $CDCl_3$, room temperature.

Monitoring the actual AAA reaction to form **56** from **45b** by *in situ* EXSY demonstrated that allyliodide **54** undergoes dynamic isomerisation during the AAA itself (Figure 5.6).

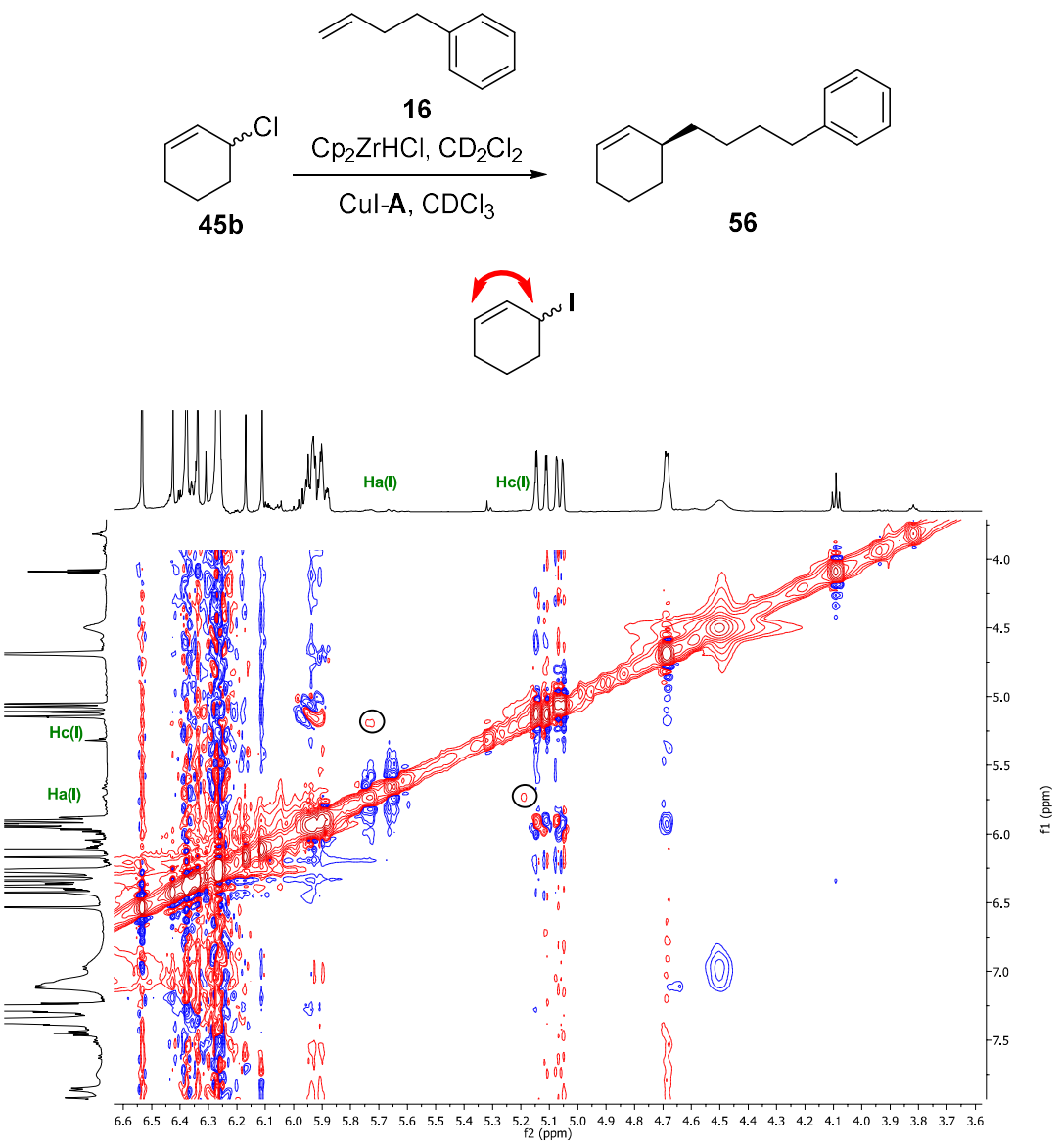

Figure 5.6. 2D exchange spectroscopy NMR (EXSY) during Cu-AAA reaction. Conditions: 4-phenyl-1-butene **16** (2.5 eq), Cp_2ZrHCl (2.0 eq) in CD_2Cl_2, CuI (10 mol%), ligand **A** (10 mol%), allylchloride **45b** (1.0 eq), in $CDCl_3$, room temperature.

The dynamic exchanges of allyliodide **54** generated from allylchloride **45b** and CuI-**A** complex in $CDCl_3$ were also examined at 55 °C (Figure 5.7). Under these conditions, **45b** and **54** undergo observable weak dynamic processes, demonstrating that the allyliodide **54** and allylchloride **45b** interconvert, but not fast enough to be detected on the NMR timescale at room temperature (Figure 5.4). Here **45b** was not observed to isomerise directly, possibly due to the absence of exchanges, or incompatibility with the NMR experiments

(timescale or S_N2 exchanges). S_N2 exchanges between the allyliodide **54** and allylchloride **45b** were also not observed.

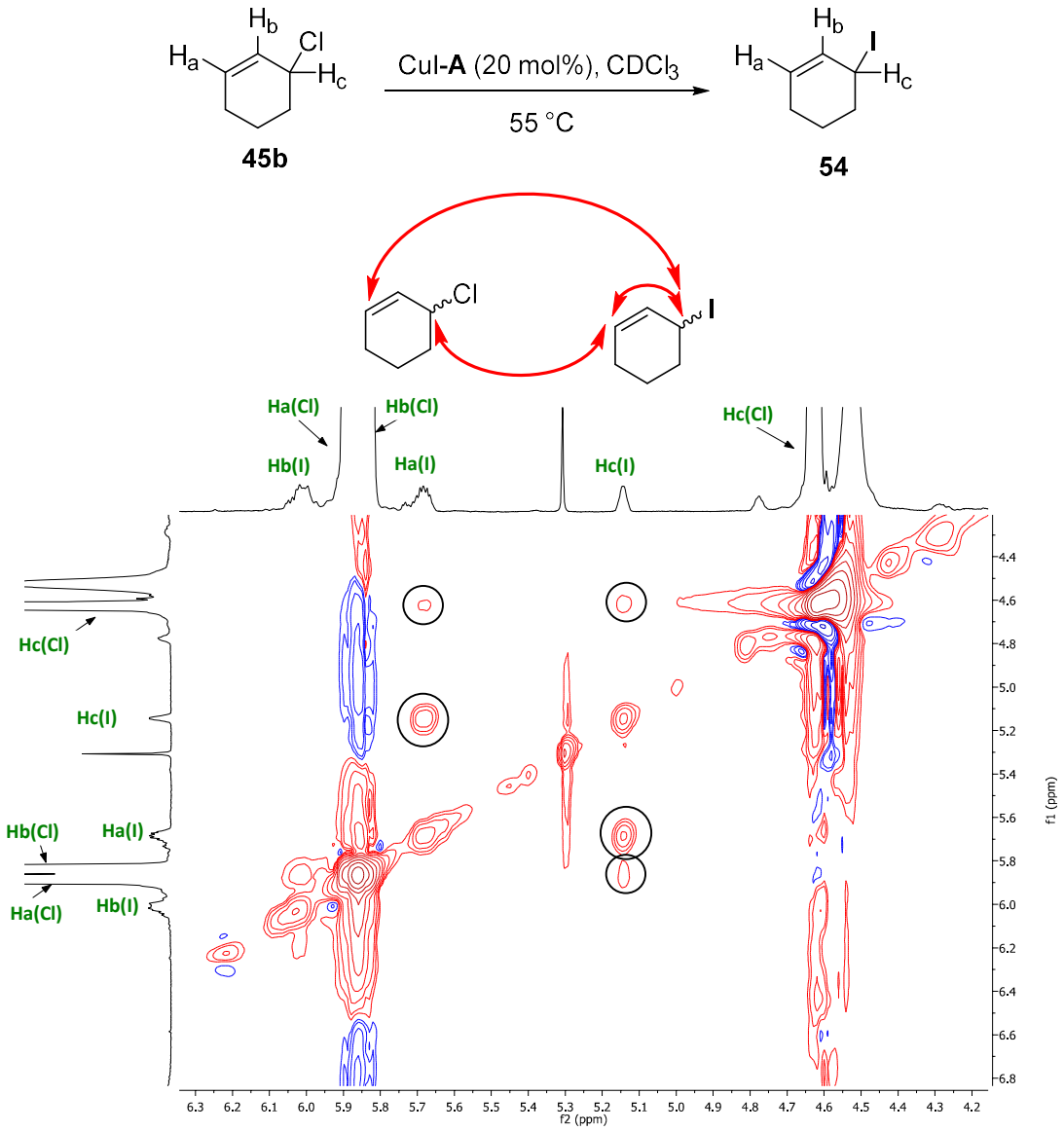

Figure 5.7. 2D exchange spectroscopy NMR (EXSY) of allyliodide 54 formed from allylchloride 45b and CuI-A complex at 55 °C. Conditions: CuI (20 mol%), ligand **A** (20 mol%), allylchloride **45b** (1.0 eq), in $CDCl_3$, 55 °C.

We also analysed allylbromide **55** under similar conditions. Allylbromide **55** itself in $CDCl_3$ does not show any S_N2' exchanges at room temperature by EXSY (Figure 5.8) contrary to a suggested isomerisation of allylbromide at room temperature by Alexakis[227,228].

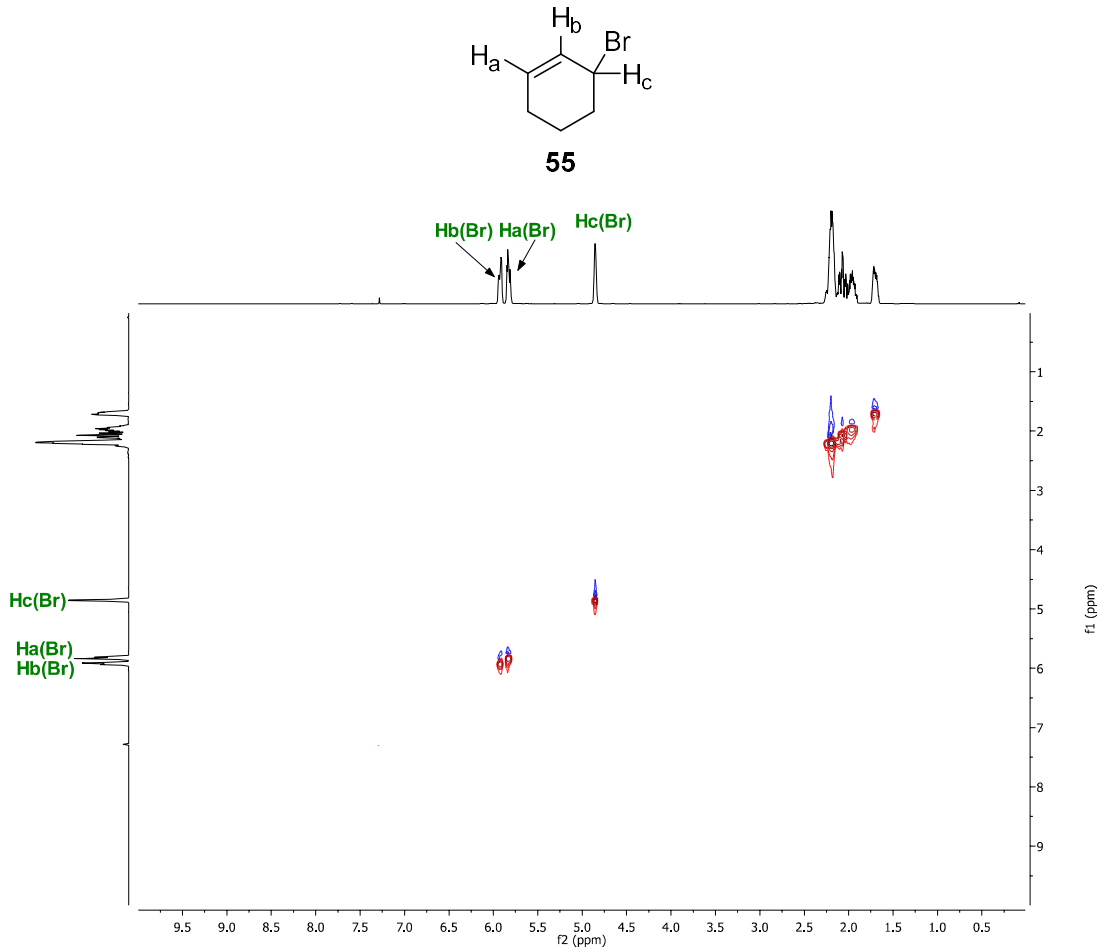

Figure 5.8. 2D exchange spectroscopy NMR (EXSY) of allylbromide 55. Conditions: allylbromide **55** (1.0 eq), in $CDCl_3$, room temperature.

In the presence of CuI-**A** complex (20 mol%) a variety of fast exchanges are observed (Figure 5.9). Allyliodide **54** is formed and rapidly isomerises (as indicated by cross peaks between H_a(I)/H_c(I)). Allylbromide **55** is also found to isomerise itself (cross-peaks between H_a(Br) and H_c(Br)). Rapid interconversion of allylbromide **55** and allyliodide **54** also occurs as indicated by cross peaks between H_a(Br)/H_c(I) and H_a(I)/H_c(Br). As cross peaks between H_c(Br)/H_c(I) (intermolecular S_N2) are not observed, interconversion appears to exclusively occur by S_N2' mechanisms. This observation suggests that intramolecular S_N2 exchanges within the allylbromide, which are not visible by NMR, also do not occur. By extrapolation the allylchloride **45b** system should behave similarly to

the allylbromide **55**, albeit with less reactivity. Thus based on our observation of the behaviour of allylbromide **55** and the allylchloride **45b** at 55 °C, it would seem that neither intermolecular nor intramolecular S_N2 exchanges occur in this AAA reaction.

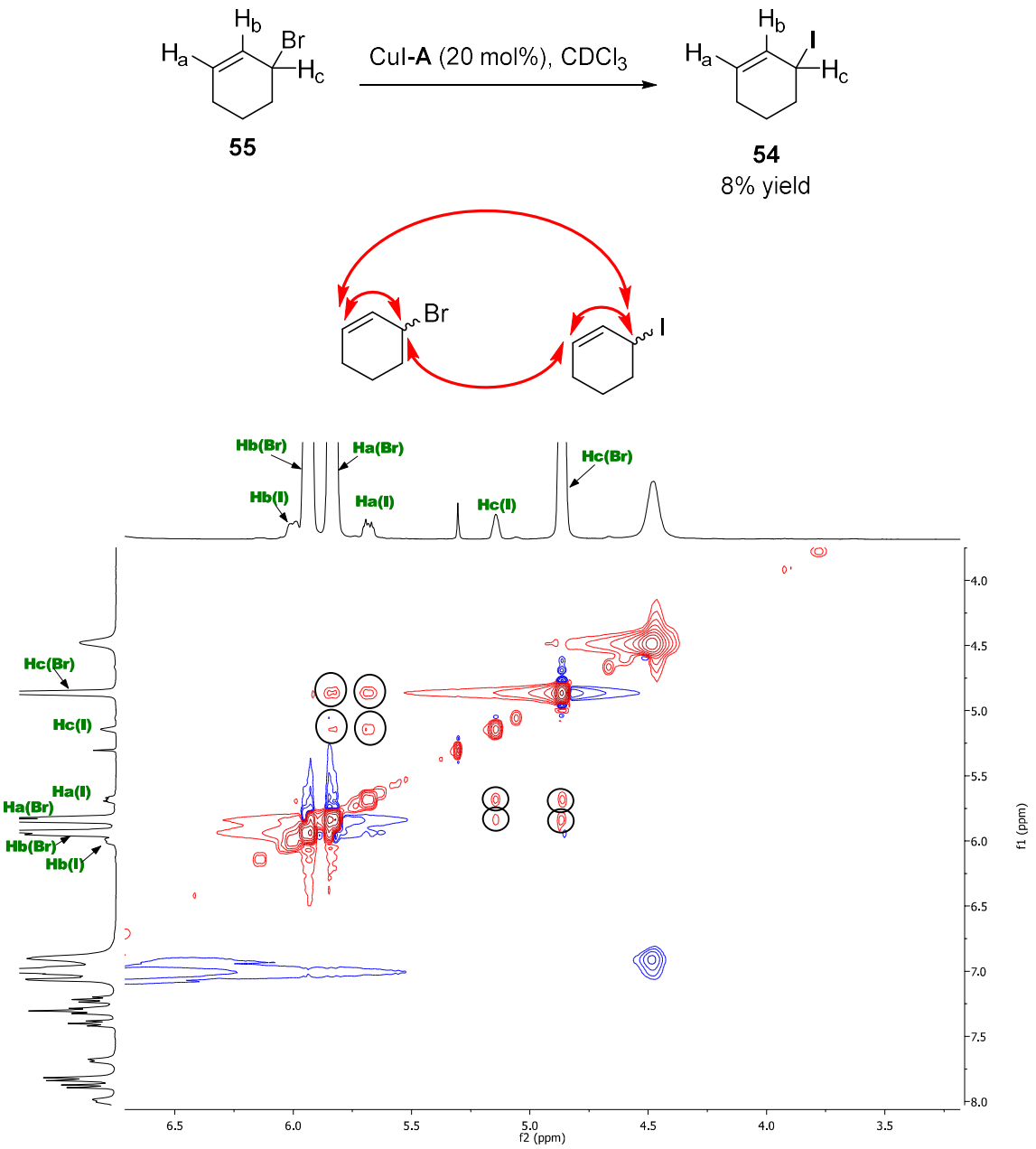

Figure 5.9. 2D exchange spectroscopy NMR (EXSY) of allyliodide 54 formed from allylbromide 55 and CuI-A complex. Conditions: CuI (20 mol%), ligand **A** (20 mol%), allylbromide **55** (1.0 eq), in $CDCl_3$, room temperature.

Generally, allylic substitutions are *anti*-selective unless the leaving group can coordinate to the Cu to form an ion pair, in which case they favour *syn*-S_N2' selectivity[37,229]. Anionic nucleophiles however favour an S_N2 mechanism but if they occur through S_N2' rearrangement, they are *anti*-selective[37,229]. Because only S_N2'-pathways are observed by EXSY, our studies are consistent with the Cu-mediated *syn*-S_N2' pathway shown in Scheme 5.8a. This *syn*-S_N2' displacement also suggests racemisation of allyliodide **54**. *Anti*-S_N2' displacements, which would not result in racemisation, are less likely as Cu and halide are known to form complexes[187,188,226,230]. The possible S_N2-inversion, which would also provide a racemisation mechanism (Scheme 5.8b), probably does not occur as intermolecular S_N2-pathways were not observed.

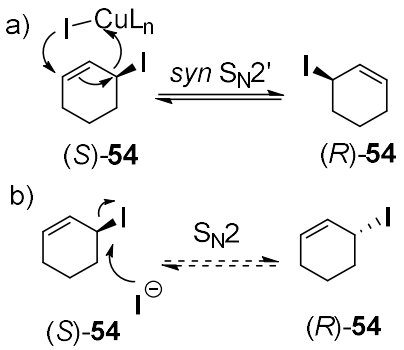

Scheme 5.8. Possible racemisation mechanisms. a) racemisation by metal assisted *syn*-S_N2' attack. b) racemisation by S_N2 attack.

Taken together, these studies point to a mechanism where selective AAA of one of the enantiomers of allylchlorides **45b** gives a product with high enantiomeric excess and **45b** indirectly racemises via allyliodide **54**. Because allylchloride **45b** was not observed to isomerise and its behaviour differs from allylbromide **55**, we assume allylchloride **45b** cannot racemise itself under these conditions. Thus the formation of **54** is responsible for the dynamic kinetic

transformation of allylchloride **45b** to product **53**. However, the question remains whether it is the allyliodide **54** or the allylchloride **45b** that undergoes AAA to give **53**.

Allylbromide **55**, which we know also forms intermediate allyliodide **54**, gives lower enantioselectivity (77 % ee) in the AAA. This lower ee may be due to less selectivity in the AAA step, as allylbromide **55** should be more reactive than allylchloride **45b**. One possible explanation for this observation would be that the energy barrier for the AAA of the less reactive enantiomer of allylbromide **55** is low enough in these conditions that it is achievable, overall lowering the observed ee of the product contrary to the AAA of the less reactive enantiomer of allylchloride **45b**. Unfortunately, allyliodide **54** is so unstable that, despite a variety of serious attempts, we could not isolate and carry out reactions with allyliodide **54** as the starting material. However, we assume the trend of reactivity of the allylhalides will be I>Br>Cl (Scheme 5.9) and speculate that as allyliodide is highly reactive, the AAA would be less selective due to achievable energy barriers of both enantiomers of allyliodide **54** and overall less stereocontrol over the reaction outcome to give lower ee of the product than for allylbromide **55** and allylchloride **45b**.

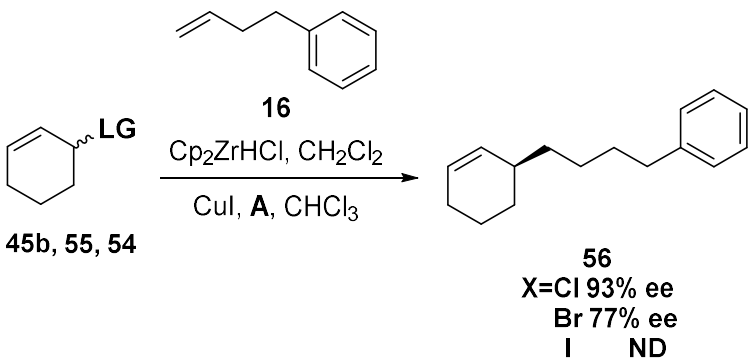

Scheme 5.9. Testing the outcome of AAA reaction when using different allylhalides. Conditions: 4-phenyl-1-butene **16** (2.5 eq), Cp_2ZrHCl (2.0 eq) in CH_2Cl_2, CuI (10 mol%), ligand **A** (10 mol%), allylhalides **45b**, **55** or **54** (1.0 eq), in $CHCl_3$, room temperature. ND: not determined.

When using Cu halides, higher enantioselectivities are obtained when the halide is a better nucleophile and leaving group (i.e. I > Br > Cl) (Scheme 5.10). This observation can be rationalised if we assume that CuX facilitates the interconversion of the allylchloride **45b** enantiomers. Using CuCl, resulted in a low 49% ee. CuCl does not readily racemise **45b**, as judged by no exchanges being observed by EXSY using these conditions (See Experimental Section), and in the absence of a racemising mechanism, the more reactive enantiomer of allylchloride **45b** would be depleted. Thus with time, the less reactive enantiomer of allylchloride **45b** can react to form the undesired enantiomer of the AAA product **56**, lowering the measured ee of the product. Depletion of ee of product **56** in time was observed and is discussed in detail later in this Chapter. Using CuBr would form allylbromide **55** which would racemise but not as well as allyliodide **54**. Slower racemisation of allylchloride **45b** via allylbromide **55** should result in a medium ee (73% ee is observed). Using CuI favours the formation of a low concentration of allyliodide **54**, which facilitates fast racemisation, continuously replenishing the more reactive enantiomer of allylchloride **45b**. In this case, the less reactive enantiomer of allylchloride **45b** would not react to give the undesired enantiomer of product as the more

reactive enantiomer of starting allylchloride **45b** is always present, resulting in a high ee (93% ee is observed).

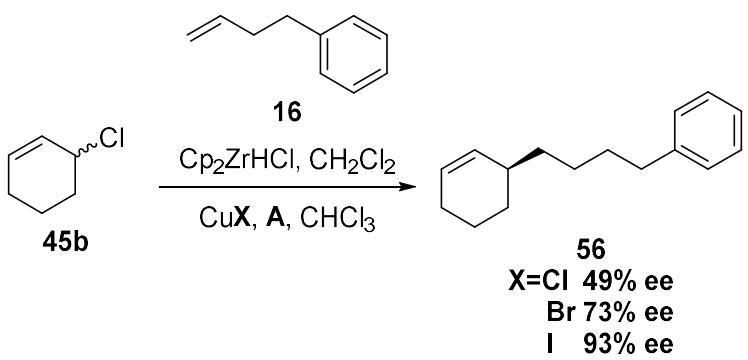

Scheme 5.10. Testing the outcome of the AAA reaction using different CuX sources. Conditions: 4-phenyl-1-butene **16** (2.5 eq), Cp_2ZrHCl (2.0 eq) in CH_2Cl_2, CuX (10 mol%), ligand **A** (10 mol%), allylchloride **45b** (1.0 eq), in $CHCl_3$, room temperature.

3) Sensitivity of exchanges

As the presence of allyliodide **54** and its isomerisation is a key component of the reaction, we decided to thoroughly investigate it. Allyliodide **54** was only observed when using allylchloride **45b** and CuI complexed with phosphine ligands (phosphoramidite ligand **A**, diphosphine ligand Binap or PPh_3) (Table 5.1 – entry 1, 2 and 3 respectively). The absence of ligand (entry 6) or other known ligands of Cu such as NHC ligands (entry 4) or DMS (entry 5) yielded no allyliodide **54**. Alternative source of iodide anion such as TBAI (entry 7) and TMSI (entry 8) both formed allyliodide **54** in 4% and 70% yield respectively.

Table 5.1. Testing the sensibility of the allyliodide 54 formation and exchanges.

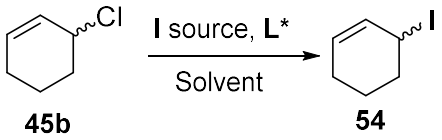

Entry	I^- source	Ligand	Solvent	Iodide	Exchanges
1	CuI	**A**	$CDCl_3$	Yes	Yes
2	CuI	Binap	$CDCl_3$	Yes	Yes
3	CuI	PPh_3	$CDCl_3$	Yes	Yes
4	CuI	NHC[a]	$CDCl_3$	No	-
5	CuI	DMS	$CDCl_3$	traces	No
6	CuI	-	$CDCl_3$	No	-
7	TBAI	-	$CDCl_3$	Yes	No
8	TMSI	-	$CDCl_3$	Yes	Yes
9	CuI	**A**	Benzene-d_6	Yes	Yes
10	CuI	**A**	THF-d_8	Yes	Yes
11	CuI	**A**	CD_3CN	Yes	Yes

Conditions: Iodide source (10 mol% for CuI, 1.0 eq for TMSI and TBAI), ligand (10 mol%), allylchloride **45b** (1.0 eq), in solvent, room temperature. [a]NHC ligand used: 1-(*S*)-Leucinol-3-(2,4,6-trimethylphenyl)-3*H*-imidazolium hexafluorophosphate.

Furthermore, even though allyliodide **54** was formed in the presence of TBAI, no exchanges by EXSY were observed (entry 7). All other cases (CuI-phosphorus based ligand and TMSI) showed isomerisation of the allyliodide **54** (entry 1, 2, 3, 8). The divergence between TBAI and TMSI was surprising but commercial TMSI is stabilised with Cu (<3%) and thus TMSI is not a true source of iodide anion devoid of Cu.

Thus it would seem that firstly the strong affinity of Cu for phosphorus permits the release of readily accessible iodide anion source similarly to TBAI and TMSI. In the absence of organophosphorus ligands, allyliodide **54** is not formed. Secondly, the isomerisation of allyliodide **54** is only possible in the presence of Cu, reinforcing our proposed Cu-mediated *syn*-S_N2' isomerisation of allyliodide **54** proposed in Scheme 5.8a. Surprisingly, the formation and

isomerisation of allyliodide **54** is robust to all type of solvents ($CDCl_3$, benzene-d_6, THF-d_8, CD_3CN) (entry 1, 9, 10, 11 respectively).

4) Rate of exchange

We wanted to quantify the rates of exchange of allyliodide **54**. We initially chose to measure these parameters by 1D Exchange Spectroscopy (1D-EXSY). However, we were not certain of the accuracy of the EXSY measured exchange rates, as NOE/EXSY experiments are usually used to measure differences in distances. Therefore, to obtain meaningful quantitative exchange rates and assess the accuracy and applicability of exchange rate measurements by NMR, we ran two other experiments: selective inversion recovery and spin saturation transfer difference (SSTD).

1D Exchange Spectroscopy (1D-EXSY)

NOE/EXSY is a common NMR technique used to determine adjacent ^1H distances through space. For example it is used in the identification of the precise relative 3D structure of a molecule to identifying different diastereomers, or other useful intra/intermolecular distances. NOE/EXSY works through saturation by strong radiofrequency pulse of a specific ^1H signal (H_c) and observing this saturation effect on other ^1H signals (H_a) to determine if there is any dipolar coupling between signals. By modifying the mixing times of the saturation, the coupled ^1H signals get a definite time to relax resulting in variable intensities. We can then plot H_a/H_c (H_c: irradiated signal; H_a: coupled signal) over

the mixing time and exchange rates can be calculated from the slope of the resulting curve[231-234].

We decided to carry out 1D-EXSY at different temperatures by irradiating H_c of allyliodide **54** and observing the ratio H_a/H_c at different mixing times (Figure 5.10). At 0 °C (blue) and room temperature (RT) (black), the mixing time is proportional to H_a/H_c, giving a linear plot and the R^2 are high (>0.99). At 40 °C (red), the resulting curve is non-linear, presumably due to decomposition and instability of allyliodide **54** at higher temperatures. Nonetheless, the rate of exchange could be calculated from the linear initial slope albeit with a bit less accuracy (R^2=0.98477).

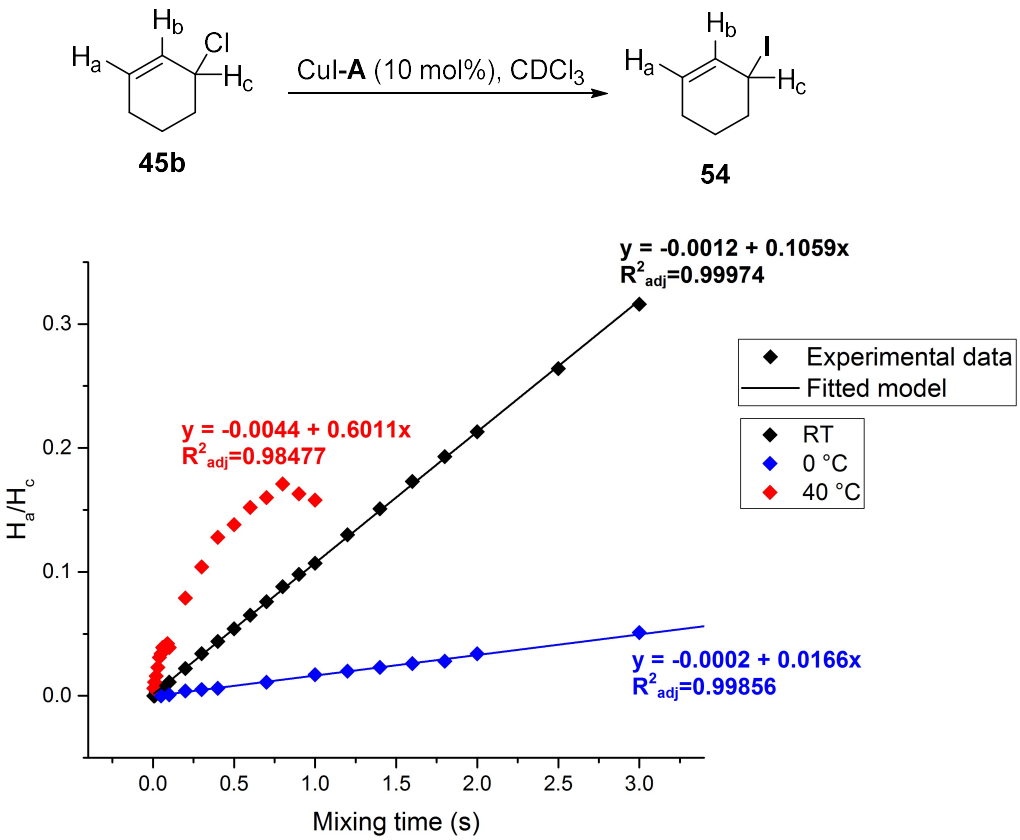

Figure 5.10. 1D-EXSY measurement of the rate of exchange of allyliodide 54 at different temperatures. Conditions: CuI (10 mol%), ligand **A** (10 mol%), allylchloride **45b** (1.0 eq), in $CDCl_3$, at specified temperature.

The rate of exchange of H_a and H_c of allyliodide is as expected greater the higher the temperature: 0.02 s^{-1} at 0 °C, 0.11 s^{-1} at room temperature and 0.60 s^{-1} at 40 °C. These results show an exponential increase in the exchange rate with respect to temperature. Therefore, above ambient temperature, small variations in temperature can have drastic effects on the rate of exchange of the allyliodide and thus, by extrapolation, the AAA reaction itself. 1D-EXSY rate and distance calculation are often criticised for inaccuracies caused by various perturbations[235]. However, in our system, normalisation[236] to compensate for relaxation effects gave us the same results (exchanges at room temperature were 0.108 s^{-1}).

Selective inversion recovery

The second type of experiment we ran to determine the exchange rate was a selective inversion recovery. Inversion recovery experiments are more complicated to calibrate and setup than EXSY experiments but produce more reliable results as they were specifically engineered for chemical exchange measurements. A specific ^1H signal (H_c) is selectively inverted (to the opposite initial z-magnetisation $-M_0$) and over time (T1) relaxes back to equilibrium (to the initial z-magnetisation $+M_0$). If H_c undergoes chemical exchange to H_a then H_a will get inverted (transient dip - blue) even if it was never pulsed and H_c will relax faster (faster recovery - red) from exchanges between the inverted H_c and the relaxed H_a (Figure 5.11)[232-234,237,238]. Data can then be fitted using Bain's CIFIT program to quantitatively calculate the exchange rate from the experimental data[237].

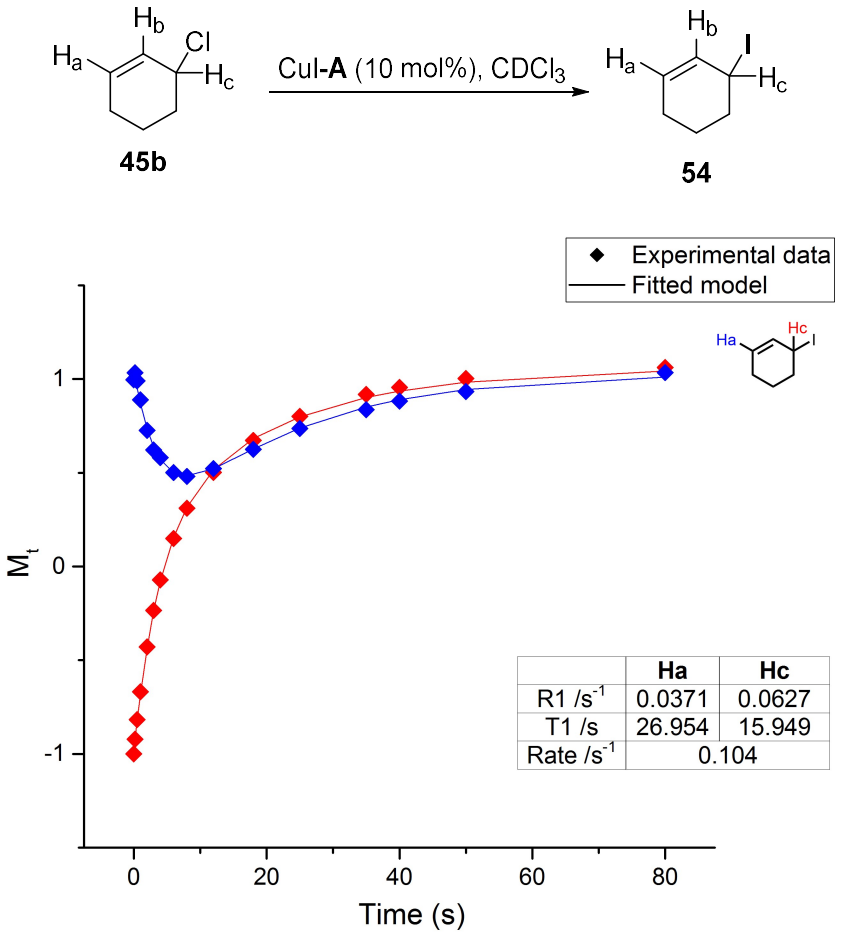

Figure 5.11. Selective inversion recovery measurement of the rate of exchange of allyliodide 54. Conditions: CuI (10 mol%), ligand **A** (10 mol%), allylchloride **45b** (1.0 eq), in $CDCl_3$, room temperature. *Note: The setup was performed by ER and the NMR experiment was performed by TDWC.*

We carried out selective inversion recovery by irradiating H_c(I) of allyliodide **54** (Figure 5.11). As allyliodide **54** is a minor species in the mixture, H_a(I) overlapped with satellite of the prominent H_b(Cl) and H_a(Cl) signals of allylchloride **45b**. Thus we remove the fixed intensity of the allylchloride **45b** satellite to obtain reliable data. The allyliodide **54** exchange rate measured was 0.104 s^{-1}. This value correlates well with the rate of 0.106 s^{-1} obtained by 1D-EXSY experiments at room temperature. The T1 value of allyliodide **54** obtained in this system are extremely high (27.0 s and 15.9 s for H_a and H_c respectively) and as the selective inversion recovery is dependent on the T1 of the molecule studied, the experiment were excessively long (~20 h).

Spin saturation transfer difference (SSTD)

A third type of exchange spectroscopy, spin saturation transfer difference (SSTD), a newly described technique[239], was also performed. This method is based on spin saturation transfer experiments (SST): saturation of H_a until it reaches a saturated steady state of spin H_c followed by an inversion-recovery experiment to determine T1. SSTD is the difference spectrum of equilibrium-saturated H_c intensity. The resulting curve is mathematically fitted to calculate the exchange rate parameter.

We set to carry out a SSTD of H_a (Figure 5.12). Similarly to inversion recovery, the H_a intensity from the SSTD trace was overlapping with the satellite of the H_a and H_b of allylchloride **45b**. Thus H_a was corrected by scaling by 1.64 to account for satellite overlap in reference to the ^1H spectrum. The data fitting was performed in OriginPro by BoxLucas1 fitting ($f(x)=a(1-e^{bx})$) to give the a and b parameters. The rate constant was calculated to be $k=a*b=0.080\ s^{-1}$, this exchange rate for the allyliodide signals was smaller than measured previously ($0.104\ s^{-1}$ for the inversion recovery and $0.106\ s^{-1}$ for 1D-EXSY) but still within the same order of magnitude.

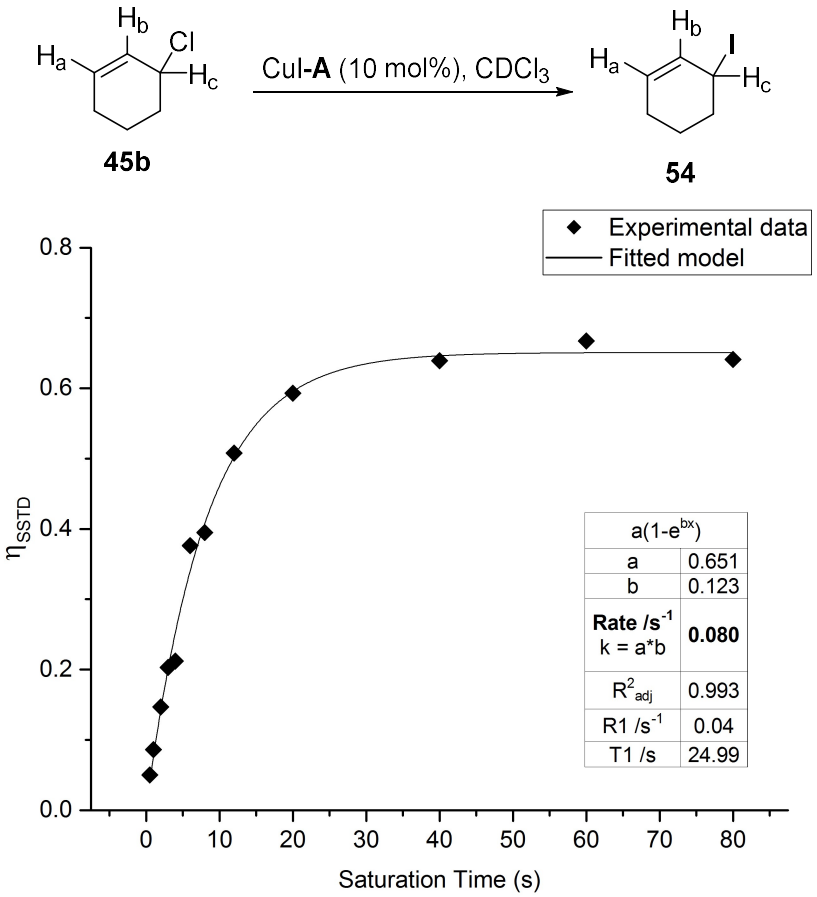

Figure 5.12. Spin saturation transfer difference (SSTD) measure of the rate of exchange of allyliodide 54. Conditions: CuI (10 mol%), ligand **A** (10 mol%), allylchloride **45b** (1.0 eq), in $CDCl_3$, room temperature. *Note: The setup was performed by ER and the NMR experiment was performed by TDWC.*

The average calculated rate of exchange of H_c and H_a of allyliodide **54** based on those three experiments (1D-EXSY, inversion recovery and SSTD) is 0.10±0.01 s^{-1}. Thus all three methods gave similar results emphasising the validity of each of them and the certainty of the results. This study also demonstrates that that the easily accessible and rapid 1D-EXSY experiments are an accurate method for quantitative exchange rate calculations. Thus we hope that this study will encourage exchange rate determinations in various systems in the future due to their accessibility.

Catalyst

After analysing the nature and reactivity of allyliodide **54** in detail we wanted to investigate the catalytic species in the reaction. Understanding the different catalytic species involved is essential to reveal the mechanism through the interaction of the catalyst with the substrate and the nucleophile. Cu-phosphoramidite pre-catalytic complexes have been extensively studied by Gschwind[2,91,187,188,226,230,240]. We are more interested in the complexes and aggregates formed during the reaction.

1) CuI-Cp_2ZrEtCl interactions

Identifying species formed from the interaction of Cu-phosphoramidite and Cp_2ZrEtCl would reveal the first catalytic aggregate (pre-reaction). However, upon addition of the alkylzirconocene nucleophile (Cp_2ZrEtCl, 2.0 eq), CuI-**A** (10 mol%) does not show any significant change in the ^{1}H (Figure 5.13a - orange) and ^{31}P NMR spectra (Figure 5.13b - orange). The only difference observed was a slight shielding of the benzylic signal of ligand **A** from 4.42 ppm to 4.31 ppm. This small shift might be an artefact of concentration effects on the Cu-ligand aggregate population. There was no colour change in the flask during this experiment, in contrast to using CuOTf-**A**, where the reaction mixture instantaneously turns brown upon addition of Cp_2ZrClR (see section 4 *CuI, CuCl and CuOTf comparison* and Chapter 8)

a)

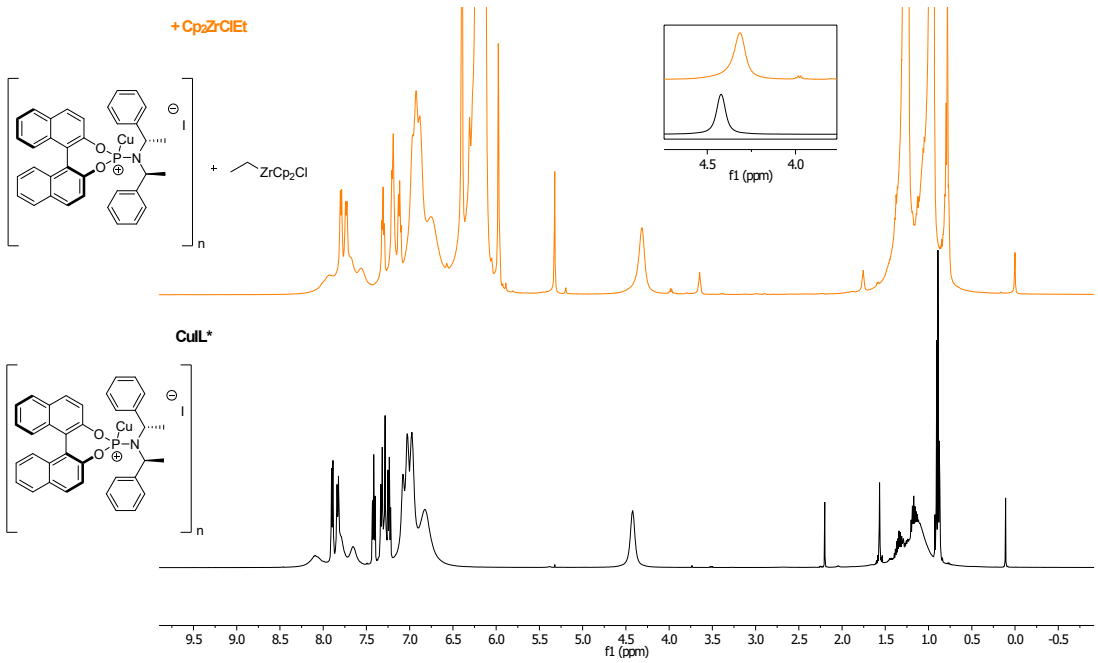

b)

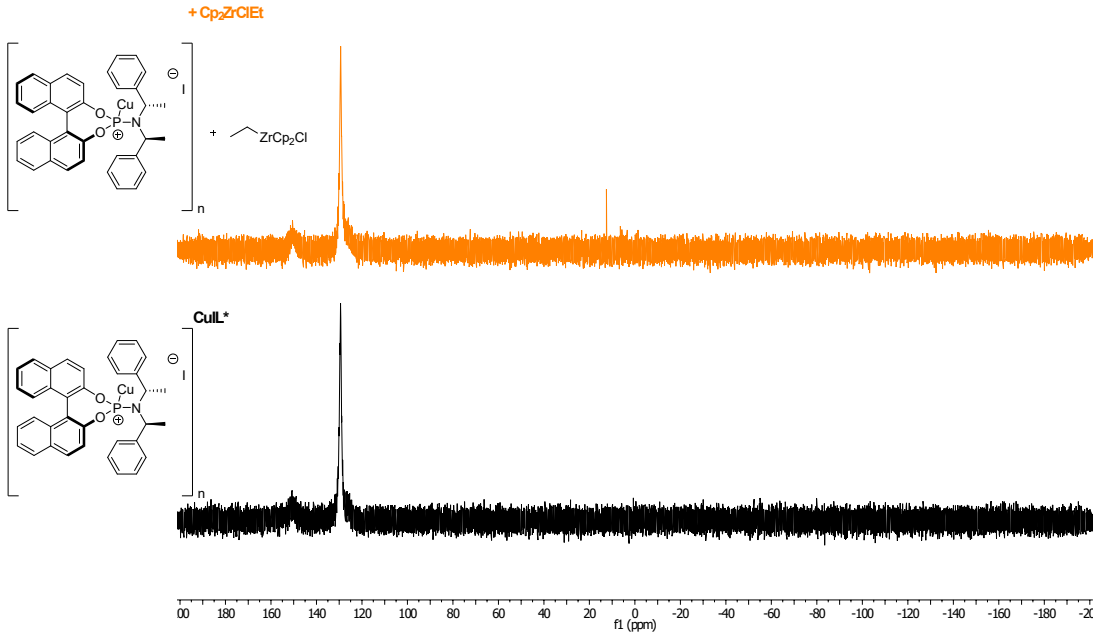

Figure 5.13. Comparison of ^{1}H (a) and ^{31}P (b) NMR spectroscopy of CuI-A complex (black) upon addition of $Cp_2ZrEtCl$ (orange). Conditions: $Cp_2ZrEtCl$ (2.0 eq) in CD_2Cl_2, CuI (10 mol%), ligand **A** (10 mol) in $CDCl_3$, room temperature.

As CuI-**A** is not modified as judged by ^{1}H and ^{31}P NMR spectroscopy by the addition of $Cp_2ZrEtCl$, we speculate that CuI-**A** and $Cp_2ZrEtCl$ do not interact at

least in the reaction-setup phase (before the addition of allylchloride **45b**). This is interesting as all mechanisms proposed with other related organometallic nucleophiles involve the initial transmetallation of the R group to the Cu before oxidative addition[1,7,55,188,189]. Therefore, it would seem that the Zr nucleophiles react differently than traditional nucleophiles (Al, Zn, Mg) at least with CuI-**A** catalyst and exhibit different reactivity patterns and behaviour. Transmetallation might occur only in the presence of starting allylchloride **45b** or not at all during the reaction.

2) Catalyst kinetic change

In situ kinetic ^{1}H NMR spectroscopy of the AAA-reaction shows a continuous shift (deshielding) in the benzylic proton signal of ligand **A** over time from 4.31 ppm to 4.45 ppm (Figure 5.14a). This change in catalyst as the AAA reaction progresses suggests that the Cu-ligand aggregates change during the reaction. When comparing the benzylic ^{1}H chemical shifts, we observe a shift from the initial characteristic $[L_nCuI]_n$ signal (I-anion bridges) at 4.42 ppm (blue) towards species resembling $[L_nCuCl]_n$ (Cl-anion bridges) at 4.65 ppm (green) (Figure 5.14b).

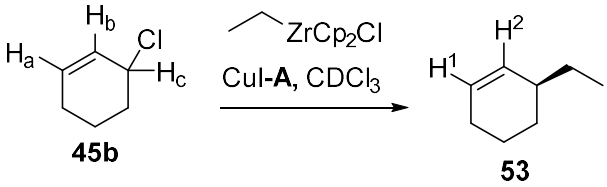

a)

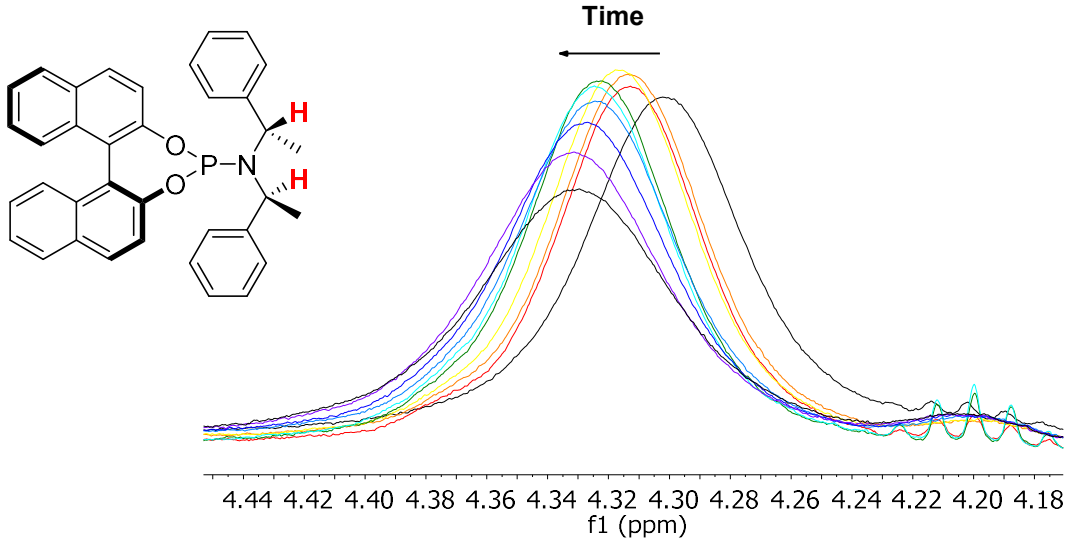

b)

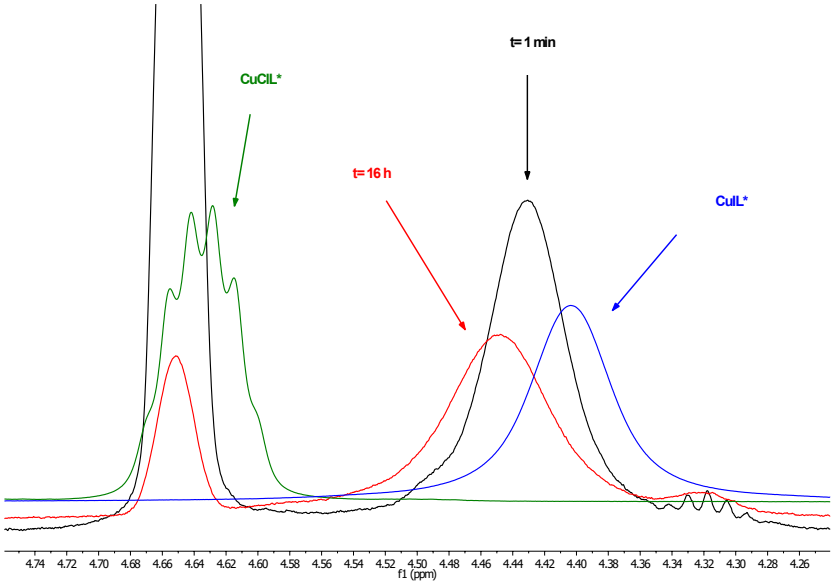

Figure 5.14. ^{1}H chemical shift of benzylic ^{1}H signal of the ligand during the AAA-reaction over time (a) and compared to CuI-A and CuCl-A complexes (b). a) Spectra taken at different times following the visible light spectrum of colour for clarity. b) CuI-**A** (blue); CuCl-**A** (green); AAA-reaction t= 1 min (black); AAA-reaction t = 16 h (red).

Furthermore, when studying the evolution of the ee of the AAA product **56** during the reaction, an increase in the enantiomeric excess was observed over

time: 85% ee at 10 min, 90% ee at 2 h and 95% ee overnight. This *in situ* change in ee over time can be correlated to the benzylic ^{1}H change in the ^{1}H NMR. These results suggest that as the AAA reaction progresses the catalyst species evolves to a more enantioselective system. Based on comparison of the benzylic signals of the CuI and CuCl ligand complexes (Figure 5.14b), the change in catalyst seems to suggest conversion of a $[Cu_aI_bL_c]$ species towards a Cl enriched catalyst $[Cu_aI_bCl_cL_d]$. An experiment performed using 10% **A** + 5% CuCl + 5% CuI ambiguously gave **56** with 90% ee (rather than 93% ee). Thus the identity of the proposed highly enantioselective catalyst is unclear.

As a black precipitate with a tendency to crystallise (identified as Cp_2ZrCl_2) is observed, salt effects may influence the catalytic species and affect the solubility of reaction components and the ee outcome by favouring the formation of certain Cu-ligand aggregates over others. Cu-halide phosphoramidite aggregates exhibit complex dynamic equilibria between several solution- and solid-phase species, which are sensitive to solvent as well as halide and salt effects[226,230] and so determining the actual composition of the Cu species generated in the reaction will require further work.

3) Diffusion-ordered spectroscopy (DOSY)

In an attempt to gain insight into the structure of the active catalysts we carried out diffusion NMR spectroscopy experiments. Gschwind extensively used these to study pre-catalytic Cu-phosphoramidite complexes at 220 K[230,240,241] and found that the diffusion coefficients obtained are accurate enough to determine the number of ligands in a complex, but not the number of salt units[226,230].

Morris[242] described a pragmatic correlation function using the concept of an effective mean density for solute and solvent molecules to estimate the molecular weight of small molecule based on their diffusion coefficients. We note that although the correlation was demonstrated only for molecules comprising light atoms (< Cl), the estimated molecular weights would nevertheless help establish the supramolecular assemblies of CuX-**A** complexes since the ligand unit makes up the bulk of the molecular weight (540 g.mol^{-1}) as opposed to the heavy atoms such as Cu (64 g.mol^{-1}) and halides (35 g.mol^{-1} for Cl, 127 g.mol^{-1} for I).

We carried out DOSY experiments with convection compensation[243,244] of different CuX-**A** complexes at 298 K in $CDCl_3$. Those experiments were measured in triplicate at 0.05 M, the same concentration as the catalytic species in the reaction. First as a control, we measured the diffusion coefficient of free ligand **A** to be 8.74±0.16 10^{-10} m^2.s^{-1} (Table 5.2 – entry 1). The diffusion coefficient of **A** correlates to an estimated molecular weight of 542±21 g.mol^{-1} using Morris' model, close to the actual value of 540 g.mol^{-1}.

Table 5.2. Diffusion coefficients D measured by DOSY and estimated molecular weight.

Entry	Catalyst	D (10^{-10} m^2.s^{-1})	Predicted MW[242]
1	**A**	8.74±0.16	542±21
2	CuI-**A**	6.13±0.05	1163±20
3	CuCl-**A**	5.87±0.09	1279±46
4	CuI/CuCl-**A**[a]	5.89±0.11	1269±55
5	CuI-**A** +$Cp_2ZrEtCl$[b]	5.95±0.18	1243±83
6a	CuOTf-**A**	6.70±0.11	956±36
6b[c]		5.83±0.17	1298±86

Conditions: CuX (10 mol%), (*S,S,S*)-**A** (10 mol%) in $CDCl_3$ at 298 K. [a]CuI (5 mol%), CuCl (5 mol%), (*S,S,S*)-**A** (10 mol%) in $CDCl_3$, 298 K. [b]Ethylene (1 atm), Cp_2ZrClH (2.0 eq) in CD_2Cl_2, CuX (10 mol%), (*S,S,S*)-**A** (10 mol%) in $CDCl_3$ at 298 K. [c]Calculated for a broader component at 7.07-6.76 ppm. The error values were calculated from the standard deviation of diffusion coefficient found for the CH-N signals at 4.65-4.31 ppm and the aromatic signals of the catalyst in each diffusion experiment. The diffusion experiments were run in triplicate.

The diffusion coefficient of CuI-**A** in $CDCl_3$ at 298 K was measured to be 6.13±0.05 10^{-10} $m^2.s^{-1}$ (entry 2) which correlates to an estimated molecular weight of 1163±20 $g.mol^{-1}$. This molecular weight is consistent with a Cu-ligand dimer as Cu$\mathbf{A}_2$ has a molecular weights of 1143 $g.mol^{-1}$, a close match to the experimental estimated molecular weight of CuI-**A**, whilst a Cu-**A** monomer (603 $g.mol^{-1}$) would be too small.

CuCl-**A** in $CDCl_3$ have a diffusion coefficient of 5.87±0.09 10^{-10} $m^2.s^{-1}$ (entry 3), which suggests a molecular weight of 1279±46 $g.mol^{-1}$. Again this molecular weight correlates to a dimer (Cu$\mathbf{A}_2$, 1143 $g.mol^{-1}$) rather than a monomer (Cu**A**, 603 $g.mol^{-1}$) or trimer (Cu$\mathbf{A}_3$, 1682 $g.mol^{-1}$). Regarding our observations of catalyst change during the course of the AAA-reaction, we also measured the diffusion coefficient of mixed CuI-**A**/CuCl-**A** complexes in a 1:1 ratio (entry 4) in an attempt to mimic the possible structure of the enhanced enantioselective catalyst generated during the CuI catalysed AAA. The diffusion coefficient was 5.89±0.11 10^{-10} $m^2.s^{-1}$, a value more similar to CuCl-**A** supramolecular complexes than CuI-**A**, and also corresponding to a dimer. This observation suggests that Cu-halide complexes might favour chloride anions and their oligomeric form over iodide anion aggregates and is consistent with our hypothesised change in catalyst during the AAA-reaction to species incorporating chloride anion.

We wanted to study the effect of $Cp_2ZrEtCl$ on the pre-catalyst CuI-**A** aggregates as these Cu-Zr aggregates may reflect the true catalytic species. When adding $Cp_2ZrClEt$ to CuI-**A**, the diffusion coefficient was 5.95±0.18 10^{-10} $m^2.s^{-1}$ (entry 5), within experimental error of the diffusion coefficient for CuI-**A**, which taken together with the lack of change observed in the ^1H and ^{31}P NMR spectra

when $Cp_2ZrClEt$ and CuI-**A** are mixed suggests that the aggregates do not change significantly in the presence of the nucleophile.

Finally, the diffusion coefficient of CuOTf-**A**, which the ^{1}H and ^{31}P NMR spectra suggest is two complexes in solution at 298 K, was $6.70\pm0.11\ 10^{-10}\ m^2.s^{-1}$ (entry 6a), associated with a molecular weight of 956±36 $g.mol^{-1}$. This value is too low for a dimer (Cu$\mathbf{A}_2$, 1143 $g.mol^{-1}$) but too high for a monomer (Cu**A**, 603 $g.mol^{-1}$) and the observed diffusion coefficient may be an average of the two CuOTf-**A** complexes found in solution. Measuring the diffusion coefficient for a broader component at 7.07-6.67 ppm resulted in a diffusion coefficient of $5.83\pm0.17\ 10^{-10}\ m^2.s^{-1}$, corresponding to molecular weight of 1298±86 (entry 6b) and thus a dimeric species. Due to extensive NMR signal overlap we were unable to obtain diffusion ordered (DOSY) data, in which each complex could be separated. A weighted 1:0.3 ratio of a dimer : monomer is consistent with 1018 $g.mol^{-1}$, a match to Morris' model. We note that CuOTf or other strongly dissociated counterions such as $CuNTf_2$ are usually necessary in order to achieve asymmetric conjugate addition with alkylzirconocene species[3,36,87,142,245] perhaps due to their different aggregation trends.

Studies on the relationship of ligand ee toward product ee showed a negative non-linear effect (Figure 5.15). This type of effect usually means that the active catalyst is an oligomer[246-248] which correlates to our observations by DOSY of the pre-catalytic complex CuI-**A** (entry 1), the mixed CuI/CuCl-**A** (entry 3) and the CuI-**A**/Zr complexes (entry 4), which were all consistent with these species being dimers.

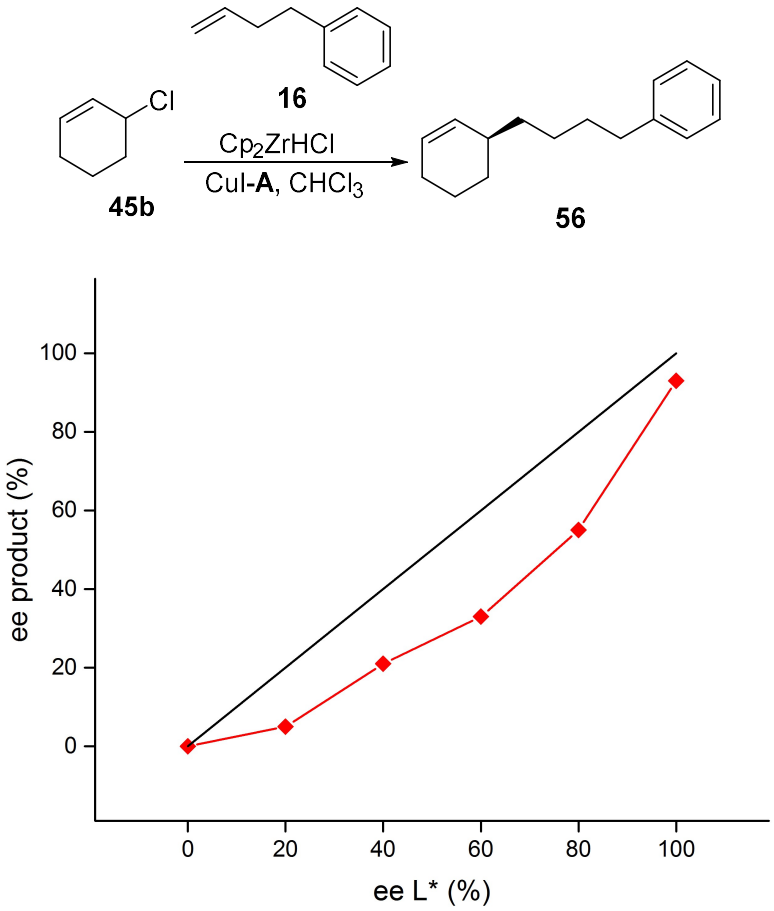

Figure 5.15. Negative non-linear effect observed in the AAA of allylchloride 45b. Conditions: 4-phenyl-1-butene **16** (2.5 eq), Cp_2ZrHCl (2.0 eq) in CD_2Cl_2, CuX (10 mol%), ligand **A** (10 mol%), allylchloride **45b** (1.0 eq), in $CDCl_3$, room temperature. *Note: This experiment was performed by HY.*

4) CuI, CuCl and CuOTf comparison

CuOTf system

We followed the Cu-AAA of allylchloride **45b** and $Cp_2ZrEtCl$ using CuOTf-**A** as the catalyst by *in situ* ^1H NMR spectroscopy. When using CuOTf, the AAA reaction goes to completion much faster (80 min) than with Cu halides (Figure 5.16). The reaction reaches its halfway point in 10 min compared to the 7 h halfway point of the CuI-AAA (Figure 5.1). Following the reaction in time showed that the ee of the product did not change over time (71% ee).

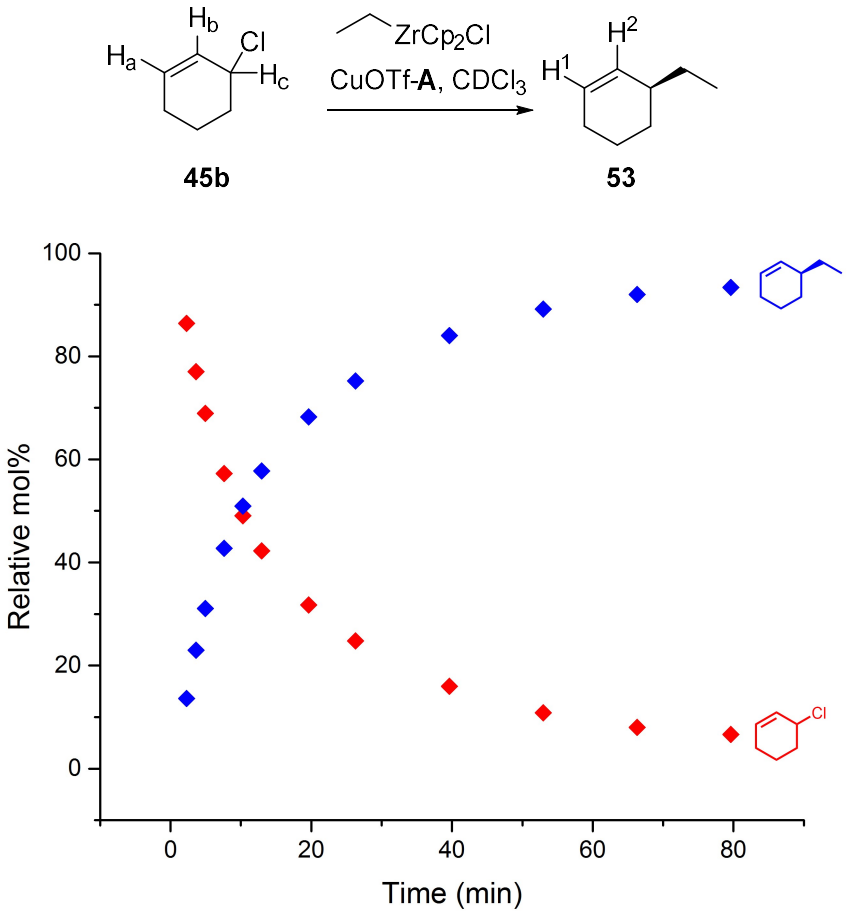

Figure 5.16. Cu-AAA reaction kinetics using CuOTf as monitored by *in situ* ^{1}H NMR spectroscopy from allylchloride 45b. Conditions: $Cp_2ZrEtCl$ (2.0 eq) in CD_2Cl_2, CuCl (10 mol%), AgOTf (11 mol%), ligand **A** (10 mol%), allylchloride **45b** (1.0 eq), in $CDCl_3$, room temperature.

It appears that CuOTf-**A** exist as at least 2 species in $CDCl_3$ as we can observe two distinct benzylic signals at 4.60 ppm and 4.38 ppm and two methyl signals at 1.84 ppm and 1.12 ppm in the ^{1}H NMR (Figure 5.17a – black). We also see two signals at 124.1 and 122.8 ppm in the ^{31}P NMR spectrum (Figure 5.17b – black). Upon addition of $Cp_2ZrEtCl$, the catalyst instantaneously changes in colour (brown) and changes can also be observed in the ^{1}H and ^{31}P NMR spectra (Figure 5.17 - purple). In the ^{1}H NMR, the aromatics are shifted and their multiplicities modified, the two benzylic signals of CuOTf-**A** become a single peak at 4.45 ppm and the methyl signals vanish entirely and are presumably underneath the ethyl signal of $Cp_2ZrEtCl$. Therefore it would seem that $Cp_2ZrEtCl$

modifies CuOTf-**A** to a single species. In the ^{31}P NMR (Figure 5.17b - purple), upon addition of $Cp_2ZrEtCl$ the two broad catalyst signals at 124.1 and 122.8 ppm disappear entirely presumably due to extreme broadening rendering their observation difficult. Also, five novel species appeared in the 80-50 ppm region. The identity of those phosphorylated species is unknown but due to their sharp nature, may be an artefact of catalyst decomposition.

a)

b)

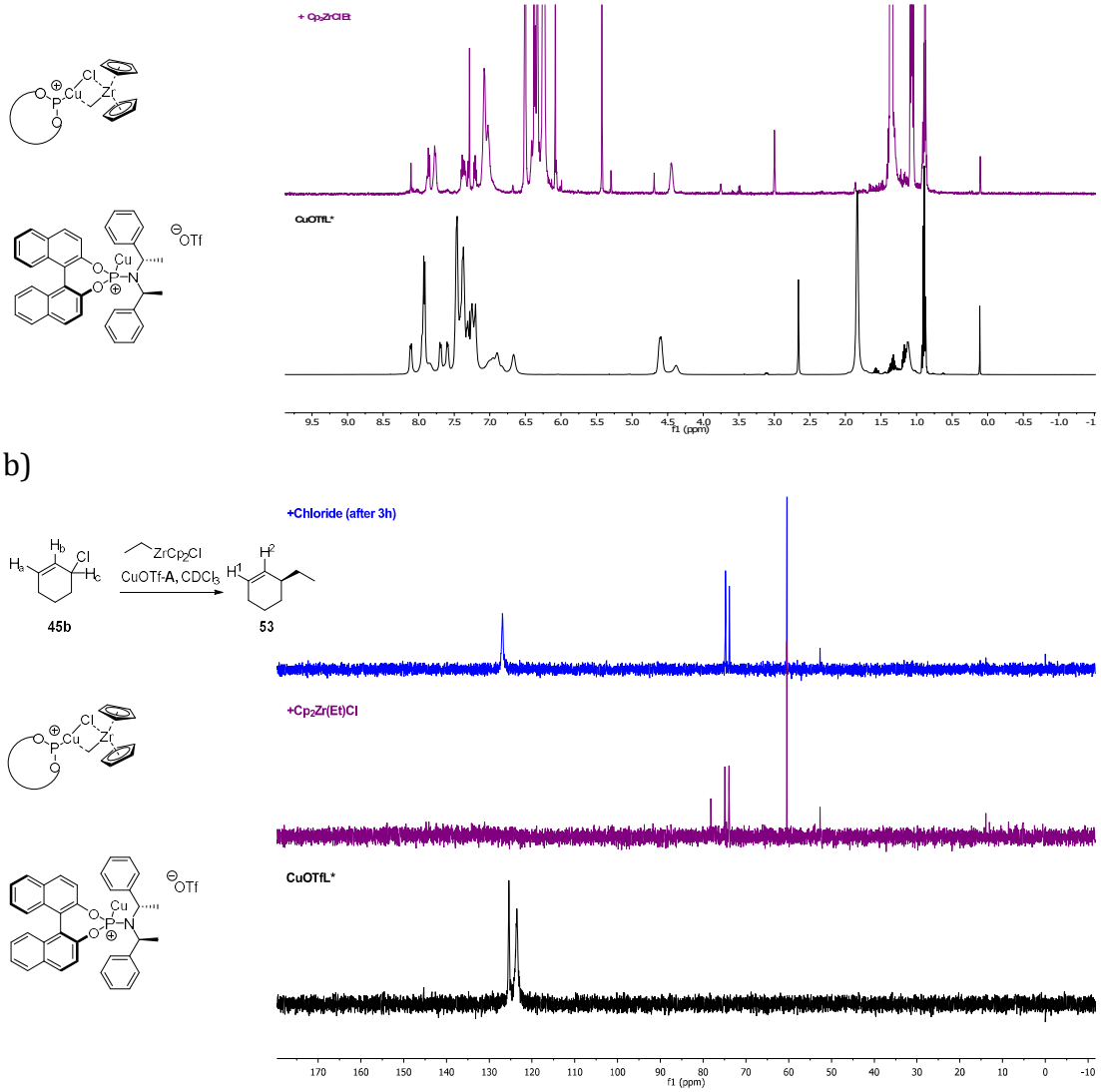

Figure 5.17. ^{1}H (a) and ^{31}P (b) NMR spectroscopy of CuOTf-A (black) and CuOTf-A+$Cp_2ZrEtCl$ (purple) and at the end of the AAA-reaction (blue). Conditions: $Cp_2ZrEtCl$ (2.0 eq) in CD_2Cl_2, CuCl (10 mol%), AgOTf (11 mol%), ligand **A** (10 mol%), allylchloride **45b** (1.0 eq) in $CDCl_3$, room temperature.

3h after the addition of allylchloride **45b** at completion of the CuOTf-AAA (Figure 5.17b – blue), the catalyst decomposition has not changed (peaks in the 80-50 ppm region) but a new species at 127.4 ppm can be observed. This broad signal diverges from the original 124.1 and 122.8 ppm signal of the CuOTf-**A** complex suggesting that a new species was formed over the course of the CuOTf-catalysed AAA.

Altogether, the modification of the CuOTf catalyst upon addition of $Cp_2ZrEtCl$, the fast conversion of the AAA reaction, the CuOTf-**A** pre-catalytic complexes forming mixture of oligomers and the constant ee of the product over time suggest that CuOTf–**A** behaves entirely differently than Cu-halides complexes.

Using non-linear least-squares regression using the DynaFit4 software[249], we attempted to model the CuOTf-catalysed AAA based on our experimental data shown in Figure 5.16 (Figure 5.18). This program uses Levenberg-Marquardt Algorithm to correlate reaction equations with rates based on kinetic data points.

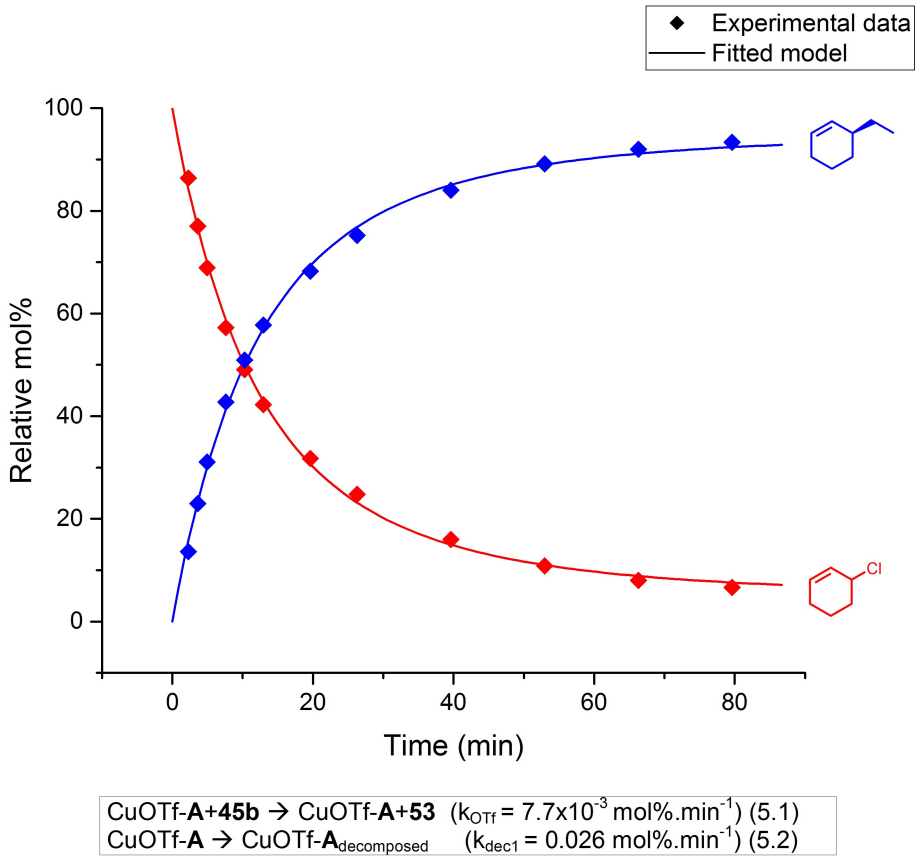

Figure 5.18. Modelling by non-linear least-squares regression of CuOTf-catalysed AAA based on kinetic experimental data collected by *in situ* ^{1}H NMR. The experimental data recorded by ^{1}H NMR are shown as diamonds. Based on those data points, modelling was performed using Dynafit4 software[249] and resulted fitted curves are shown as solid lines and the input equations with their rates below the graph.

According to the model, the CuOTf-**A** catalysed AAA goes at a rate of k_{OTf}=7.7x10^{-3} mol%.min^{-1} (Equation 5.1). Because the reaction did not go to completion we had to take into account the decomposition of catalyst over time in the modelling (might be an artefact of running the reaction in a sealed NMR tubes without stirring). We calculated the decomposition to be k_{dec1}=0.026 mol%.min^{-1} (Equation 5.2). Inhibition of the catalyst is three times faster than the reaction itself which is coherent with the instability and inherent reactivity of CuOTf. The model fitted the experimental data points well as the residuals were small and symmetrical showing the accuracy of the model (See Experimental Section for details).

CuCl system

We examined CuCl-**A** as catalyst in the AAA-reaction and followed it by *in situ* ^{1}H NMR spectroscopy (Figure 5.19). We observed clean conversion of allylchloride **45b** to product **53**. Reactions using CuCl are slower than with CuOTf but faster than with CuI and reach completion in 5 h with a half-life of 1 h.

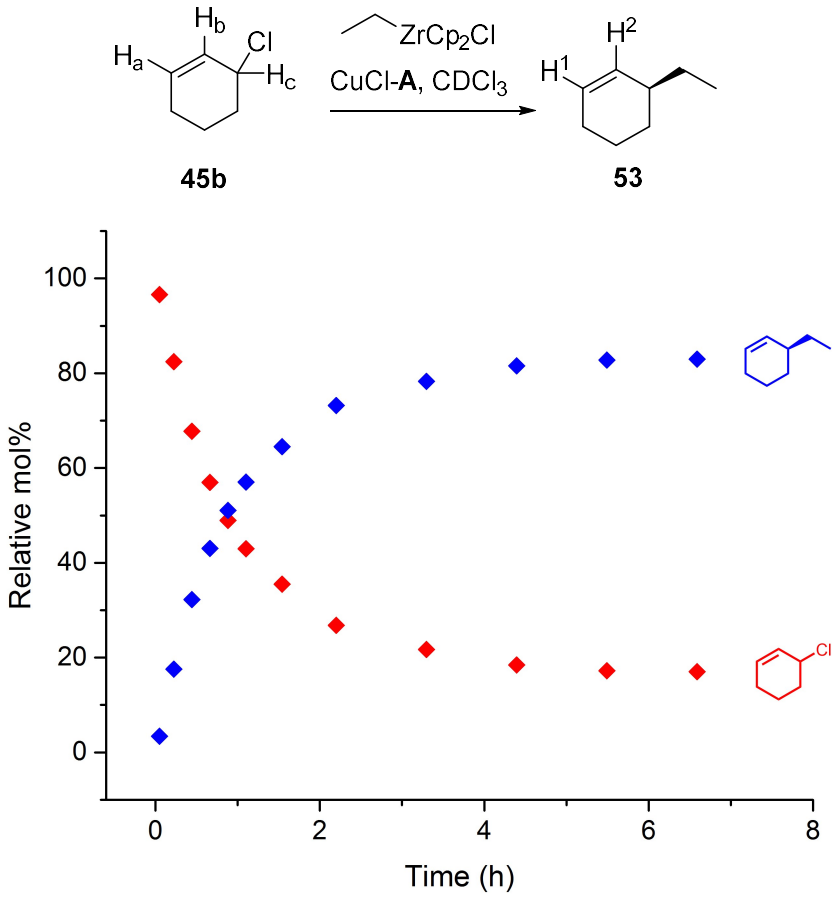

Figure 5.19. Cu-AAA reaction kinetics using CuCl as monitored by *in situ* ^{1}H NMR spectroscopy from allylchloride 45b. Conditions: $Cp_2ZrEtCl$ (2.0 eq), CuCl (10 mol%), ligand **A** (10 mol%), allylchloride **45b** (1.0 eq), in $CDCl_3$, room temperature.

In the case of CuCl, the ee of the product decreases over time: 82% ee at 10 min, 68% ee at 2 h and 54% ee at completion. We know that CuCl does not racemise **45b** at a rate that is detectable by EXSY. Therefore, we speculate that

when using CuCl, the rapidly reacting enantiomer of **45b** is consumed. However, the reacting enantiomer of **45b** is not replenished due to the absence of a racemising mechanism. The reaction with the minor enantiomer thus becomes significant and reduces the measured ee of **53** in time.

Upon addition of $Cp_2ZrEtCl$ to CuCl-**A**, the reaction mixture changed colour from yellow to dark brown in a few minutes. A change was also observed by ^1H NMR spectroscopy where the aromatics are shifted and their multiplicity were modified, the benzylic signal is shifted from 4.65 ppm to 4.39 ppm and the methyl signal from 1.65 to what is presumably a shielded species hidden by the ethyl signal of $Cp_2ZrEtCl$ (Figure 5.20a - green). In the ^{31}P NMR spectra, the CuCl-**A** catalyst peak drastically broadened without significant change of chemical shift (from 126.2 ppm to 128.8 ppm) (Figure 5.20b - green). Also, similarly to the CuOTf system, a myriad of species appeared in the 90-50 ppm region, presumably due to catalyst decomposition. Therefore, it seems that contrary to CuI-**A**, CuCl-**A** does interact with $Cp_2ZrEtCl$.

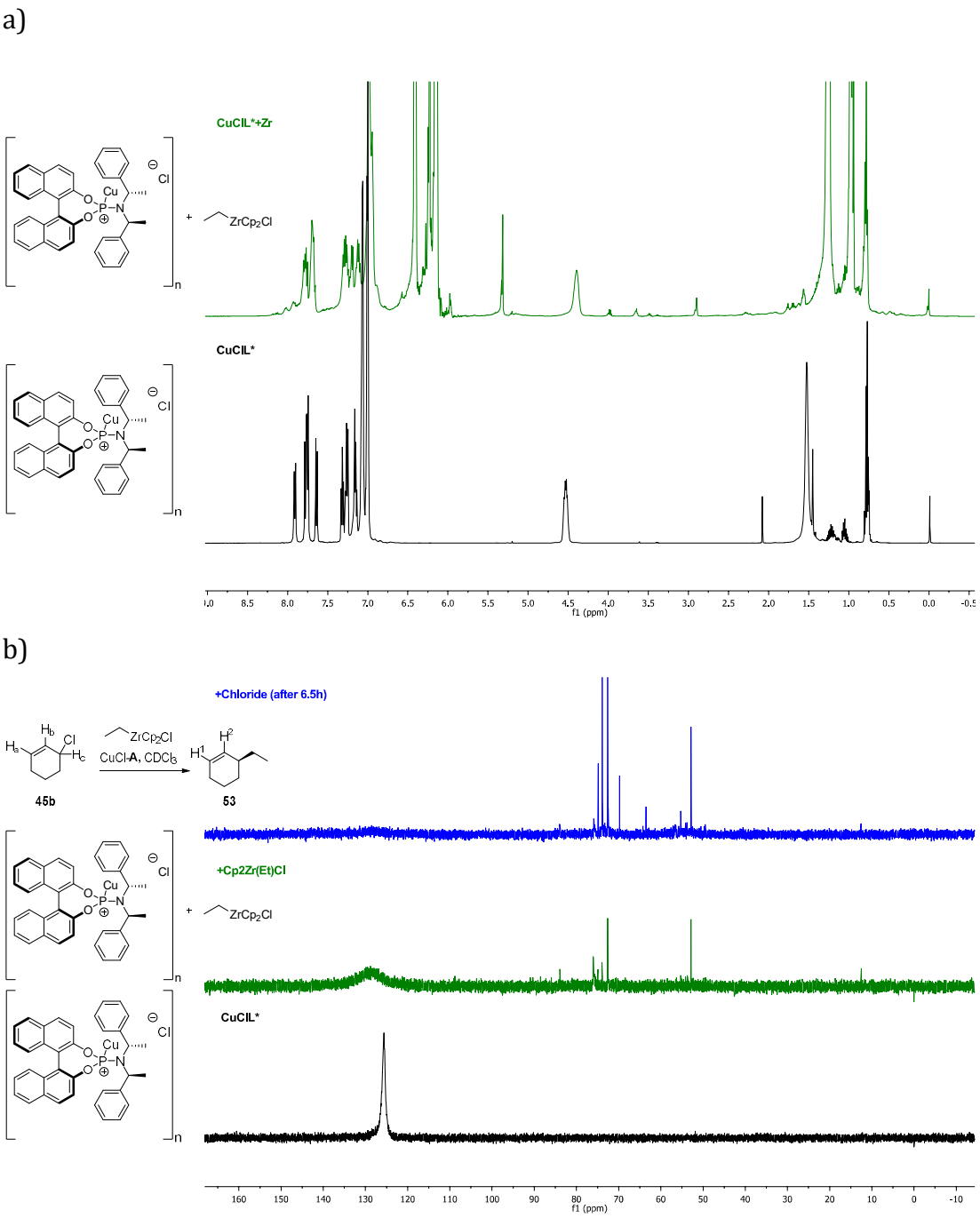

Figure 5.20. ^{1}H (a) and ^{31}P (b) NMR spectroscopy of CuCl-A (black) and CuCl-A+$Cp_2ZrEtCl$ (green) and at the end of the AAA-reaction using CuCl catalyst (blue). Conditions: $Cp_2ZrEtCl$ (2.0 eq) in CD_2Cl_2, CuCl (10 mol%), ligand **A** (10 mol%), allylchloride **45b** (1.0 eq) in $CDCl_3$, room temperature.

We also followed the CuCl catalysed AAA reaction by ^{31}P NMR spectroscopy (Figure 5.20b - blue). At completion, more species were observed in the 80-50 ppm region than already observed upon addition of $Cp_2ZrEtCl$ to CuCl-**A** complex. Moreover, the catalyst, primarily found at 140-120 ppm disappeared.

Therefore, the ^{31}P NMR clearly shows the catalyst decomposition, explaining why the reaction stopped at 80% conversion.

Based on the experimental CuCl-catalysed AAA data shown in Figure 5.19, a model was built using non-linear least-squares regression[249] (Figure 5.21). The resulting kinetic rate for the CuCl-catalysed AAA was $k_{Cl}=5.9x10^{-4}$ mol%.min^{-1} (Equation 5.3). Because the reaction did not reach completion, we also took into account catalyst decomposition. The rate of the catalyst decomposing was $k_{dec2}=0.46$ mol%.min^{-1} (Equation 5.4) thus 10^3 faster than the AAA reaction, accounting for the 80% conversion observed. Based on the kinetic rates, the CuCl-catalysed AAA is 10^1 slower than the CuOTf-catalysed AAA. The residuals were small and symmetrical showing that the model fitted well to the experimental data (See Experimental Section for details).

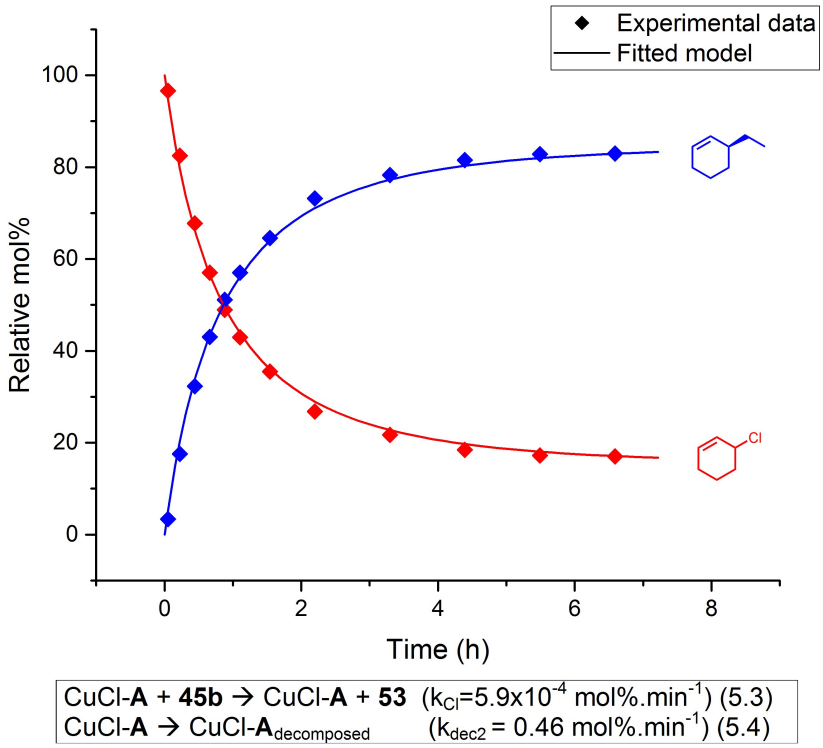

Figure 5.21. Modelling by non-linear least-squares regression of CuCl-catalysed AAA based on kinetic experimental data collected by *in situ* ^{1}H NMR. The experimental data recorded by ^{1}H NMR are shown as diamonds. Based on those data points, modelling was performed using Dynafit4 software[249] and resulted fitted curves are shown as solid lines and the input equations with their rates below the graph.

5) Modelling of Cu-AAA catalysed by CuI

Using non-linear least-squares regression[249], we attempted to build a simple model of the optimised CuI-catalysed AAA using the experimental data in Figure 5.1. However, not all interactions in the reaction can be modelled and only the key reactions were taken into account to obtain meaningful rates. We decided to model the reaction by taking into account the reversible formation of allyliodide **54**. We modelled formation of product **53** from allylchloride **45b** (Equation 5.5) coupled with the formation of allyliodide **54** (Equation 5.6) and the reverse reaction to regenerate allylchloride **45b** ((*R*) or (*S*)) (Equation 5.7). This model indirectly accounts for the racemisation of allyliodide **54** and **45b** without taking into account the enantiomers of each species. In order to donate an iodide anion we had to consider the modification of the catalyst from CuI-**A** to CuCl-**A** (Equation 5.6) and the regeneration of CuI-**A** upon release of chloride anion to allyliodide **54** to regenerate allylchloride **45b** (Equation 5.7). Attempts to fit this model led to divergence from the experimental data towards the end of the reaction (Figure 5.22).

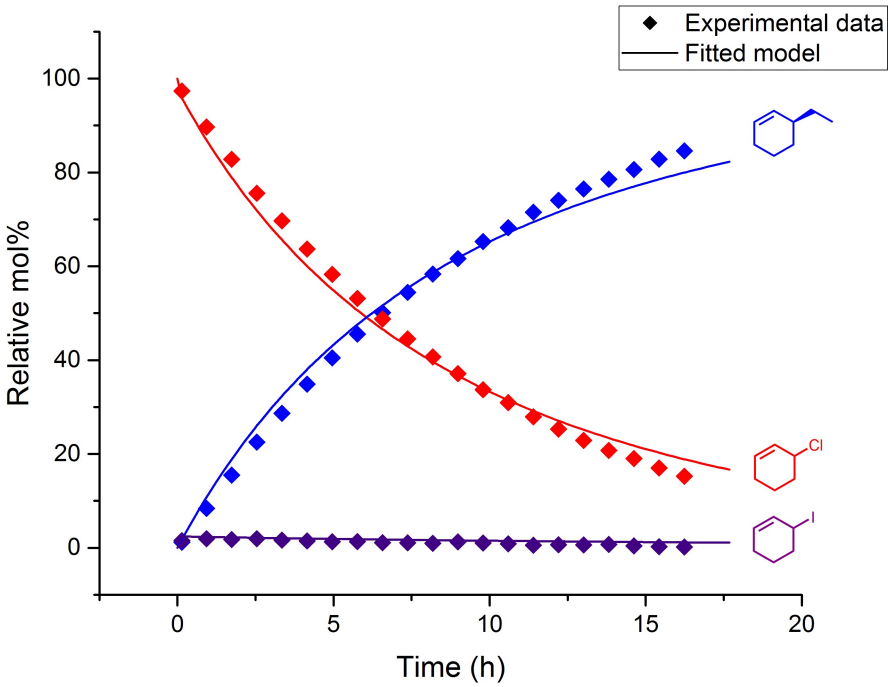

CuI-**A**+**45b**+$Cp_2ZrClEt$ → CuICl-**A**+**53** (k_I = 3.5x10^{-5} mol%.min^{-1}) (5.5)
CuI-**A**+**45b** → CuCl-**A**+**54** ($k_{allyliodide}$= 0.0080 mol%.min^{-1}) (5.6)
CuCl-**A**+**54** → CuI-**A**+**45b** ($k_{allylchloride}$= 0.029 mol%.min^{-1}) (5.7)

Figure 5.22. First attempt at modelling by non-linear least-squares regression of CuI-catalysed AAA based on kinetic experimental data collected by *in situ* ^{1}H NMR. The experimental data recorded by ^{1}H NMR are shown as diamonds. Based on those data points, modelling was performed using Dynafit4 software[249] and resulted fitted curves are shown as solid lines and the input equations with their rates below the graph.

In order to obtain a more accurate model, we had to take into account the modification of the catalyst observed by NMR during the reaction in Figure 5.14a (Figure 5.23)[4]. We speculate that the chloride leaving group generated in the CuI-**A** catalysed AAA (Equation 5.8) becomes incorporated into the catalyst, to generate a more enantioselective catalyst as the reaction proceeds, the simplest form of which would be "CuICl-**A**". A model using "CuICl-**A**" as a second 'reaction-enhanced' catalyst (Equation 5.9) suggested this AAA is three times faster than AAA with the starting catalyst (Equation 5.8), consistent with the increase in ee over time observed, as the major AAA pathway would preferentially involve the more selective catalyst CuICl-**A** once formed. Chemical exchange between allyliodide **54** and allylchloride **45b** is relatively fast: $k_{allyliodide}$=0.008 mol%.min^{-1}

for the formation allyliodide **54** (Equation 5.10) with regeneration of allylchloride **45b** being over three times faster ($k_{allylchloride}$=0.029 mol%.min^{-1}, Equation 5.11). This model supports the idea that AAA is slow compared to isomerization of allylchloride **45b** and allyliodide **54** (>10^2 times slower), allowing constant replenishing of the most reactive enantiomer of allylchloride **45b**.

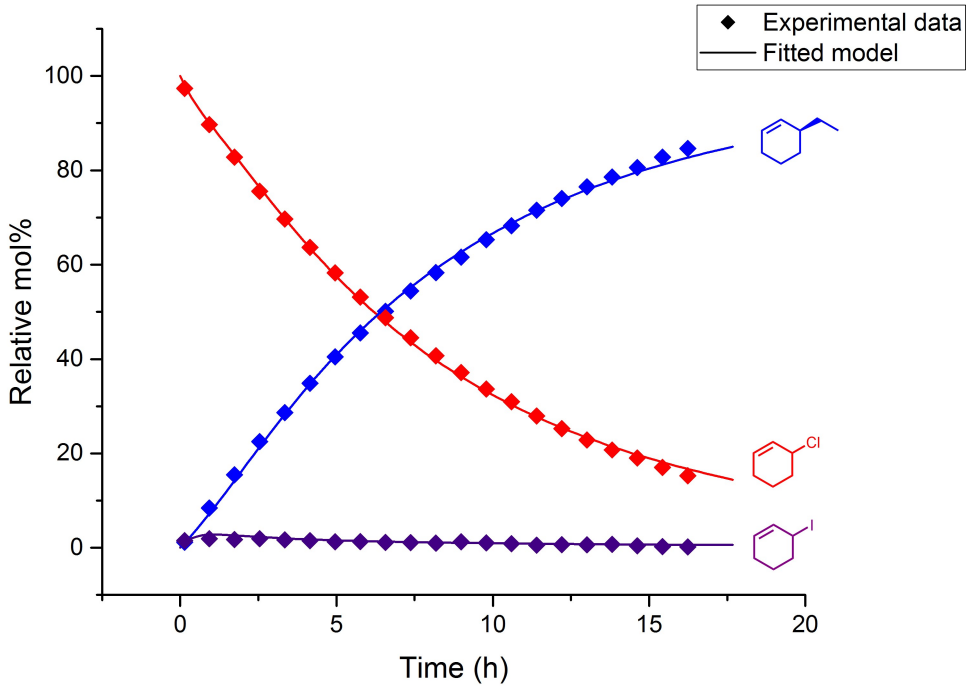

CuI-**A**+**45b**+$Cp_2ZrClEt$ → CuICl-**A**+**53** (k_I = 3.5x10^{-5} mol%.min^{-1}) (5.8)
CuICl-**A**+**45b**+$Cp_2ZrClEt$ → CuICl-**A**+**53**+Cl (k_{ICl}= 9.9x10^{-5} mol%.min^{-1}) (5.9)
CuI-**A**+**45b** → CuCl-**A**+**54** ($k_{allyliodide}$= 0.0080 mol%.min^{-1}) (5.10)
CuCl-**A**+**54** → CuI-**A**+**45b** ($k_{allylchloride}$= 0.029 mol%.min^{-1}) (5.11)

Figure 5.23. Modelling by non-linear least-squares regression of CuI-catalysed AAA based on kinetic experimental data collected by *in situ* ^{1}H NMR. The experimental data recorded by ^{1}H NMR are shown as diamonds. Based on those data points, modelling was performed using Dynafit4 software[249] and resulted fitted curves are shown as solid lines and the input equations with their rates below the graph.

The calculated rate of the AAA of alkylzirconocene to allylchloride **45b** is 10^1 times slower with CuI than with CuCl (k_{Cl}=5.9x10^{-4} mol%.min^{-1}) and 10^2 times slower than with CuOTf (k_{OTf}=7.7 x10^{-3} mol%.min^{-1}). Why the CuI catalysed

reaction is so much slower than when using the other counterion is unknown but might account for the high enantioselectivity of the system.

CONCLUSION AND PROPOSED MECHANISM

A plausible mechanism based on extensive experimental evidence gathered is shown in Figure 5.24. Firstly, we speculate that the active catalyst favours allylchloride **45b** over allyliodide **54** for the AAA reaction and presumably selects for one enantiomer of allylchloride **45b** due to steric effects, so that one enantiomer of **45b** reacts much faster than the other.

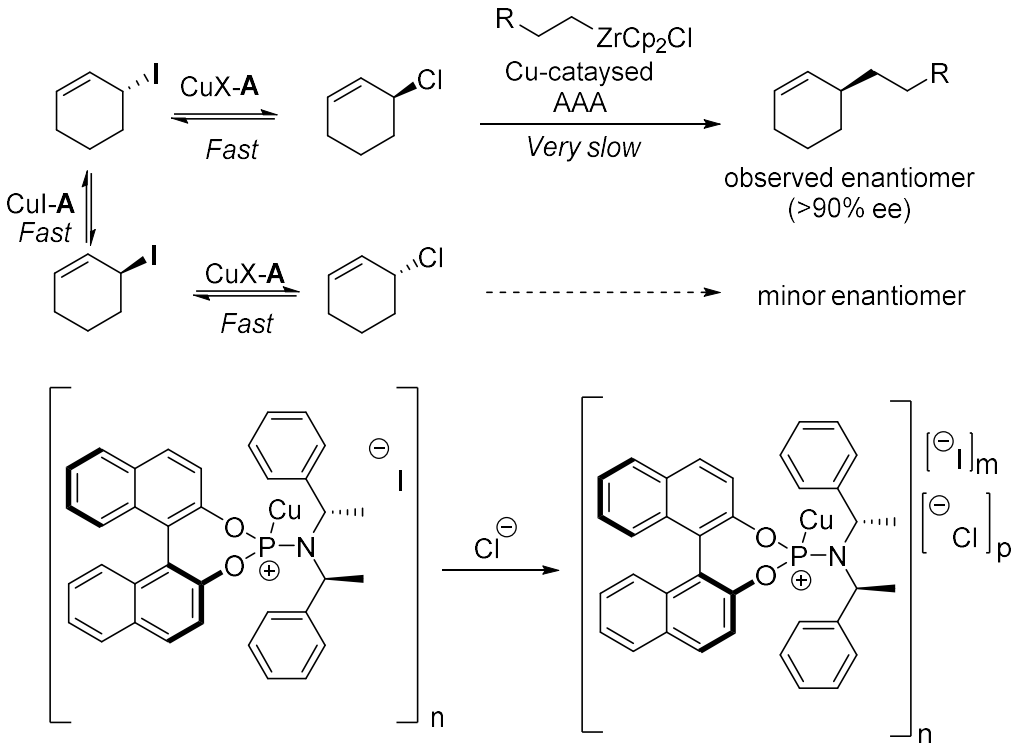

Figure 5.24. Proposed mechanism of Cu-catalysed AAA of allylchloride 45b using alkylzirconocenes.

The catalyst also enables the formation of allyliodide **54** from allylchloride **45b** and vice versa (^{1}H NMR and modelling) and allows fast racemisation of **54** (0.10±0.01 s^{-1}) (1D-EXSY, selective inversion recovery, Spin saturation transfer difference), for the AAA to proceed in high ee. We also showed by modelling that allylchloride **45b** and allyliodide **54** interchange much faster than the C-C bond forming event. Racemisation of allyliodide **54** coupled to interchanging to allylchloride **45b** enables constant replenishment of the more reactive enantiomer of **45b**.

The AAA reaction with CuI-**A** is slow, much slower than when using CuOTf or CuCl catalysts as judged by reaction kinetic and modelling, but why is still not clear. We speculate that CuOTf-catalysed reaction undergoes a different mechanism than with the Cu-halide systems.

Finally the exact catalytic species in the AAA catalytic cycle are unknown. ^{1}H and ^{31}P NMR spectra are unmodified upon addition of $Cp_2ZrEtCl$ to CuI-**A** and we speculate that, contrary to the traditional mechanism for Cu-catalysed reactions with other nucleophiles (Al, Zn, Mg), Zr nucleophiles might not transmetallate to Cu accounting for their different reactivity and behaviour. We observed that CuOTf interacts with $Cp_2ZrEtCl$ instantaneously (see Chapter 8 for further details), CuCl interacts with the organozirconocene nucleophile within a few minutes whereas CuI never shows any modifications upon addition of $Cp_2ZrEtCl$. These observations might explain the divergence in reaction rate for each counterion.

DOSY analysis showed that pre-catalytic species are dimers, an observation which is consistent with the negative non-linear effects observed during the reaction. We also observed a shift of the catalyst benzylic signal in the kinetic

^{1}H NMR experiments, accounting for a change in the catalyst over time which also correlated with an increase of enantioselectivity in the product in time (from 85 % ee to 95% ee). This modification, we hypothesise, is due to incorporation of Cl-anions in the catalyst which results in a more enantioselective catalyst species. Modelling of the kinetic data supports this hypothesis.

We hope that these results help the mechanistic understanding of Cu-catalysed transformations. Those results might guide DFT calculations to get a clearer idea about the AAA mechanism and shed light into the questions that this study generated. Furthermore, we hope that this study underlines the importance of detailed studies on mechanism and expand the use of mechanistic NMR.

CHAPTER 6

NMR MECHANISTIC STUDIES OF CU-CATALYSED ASYMMETRIC ALLYLIC ALKYLATION USING ALLYLPHOSPHATE

INTRODUCTION

Allylchloride is a reactive starting material, presumably explaining its success in the Cu-catalysed AAA described in Chapter 5. However, its instability sometimes renders mechanistic studies highly challenging. Indeed, non-symmetrical allylchloride substrates can only be isolated as multiple regioisomers and give rise to mixtures of products. New procedures using less reactive starting materials would be desirable. Such compounds would be chemically stable and less prone to isomerization during routine manipulations and mechanistic studies. From this perspective, another Cu-catalysed system was developed using racemic allylphosphate **57** (Scheme 6.1).

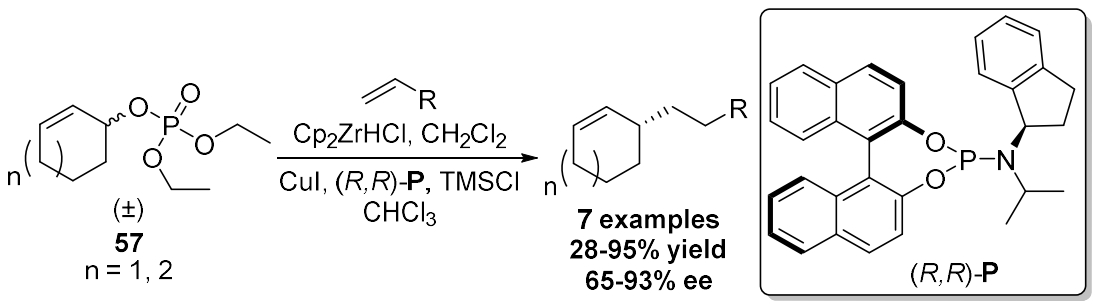

Scheme 6.1. Cu-AAA using racemic allylphosphate 57 and alkylzirconocenes.

This new method gives the same products as AAAs with allylchloride **45b** but unfortunately in lesser yield and ee. The allylphosphate method is however useful in preparing enantioenriched seven-membered ring products in 90% ee which gave poor results (23% ee) with the allylchloride system. Moreover, allylphosphates are generally easier to handle and more stable than allylchlorides. The lesser reactivity of allylphosphate **57** probably accounts for the difficulty to develop a method comparable to the Cu-catalysed AAA to allylchlorides **45b** but we could also carry out more advanced mechanistic testing. In this Chapter, we describe the study of the mechanism of this new allylphosphate **57** system by NMR spectroscopy in the hope that it would expand our understanding of Cu-catalysed AAA mechanisms.

RESULTS AND DISCUSSION

Reaction kinetics with TMSCl

We first followed the Cu-AAA reaction of allylphosphate **57** *in situ* using ^{1}H NMR spectroscopy. During this experiment we observed a clean conversion of allylphosphate **57** to product **53** (Figure 6.1). However, the kinetic rates did not match. Clearly allylphosphate **57** was consumed much more rapidly (1 h) than product **53** was formed (11 h to reach completion). We assumed there must be an intermediate formed from the allylphosphate **57**, which was the species, undergoing the Cu-AAA reaction.

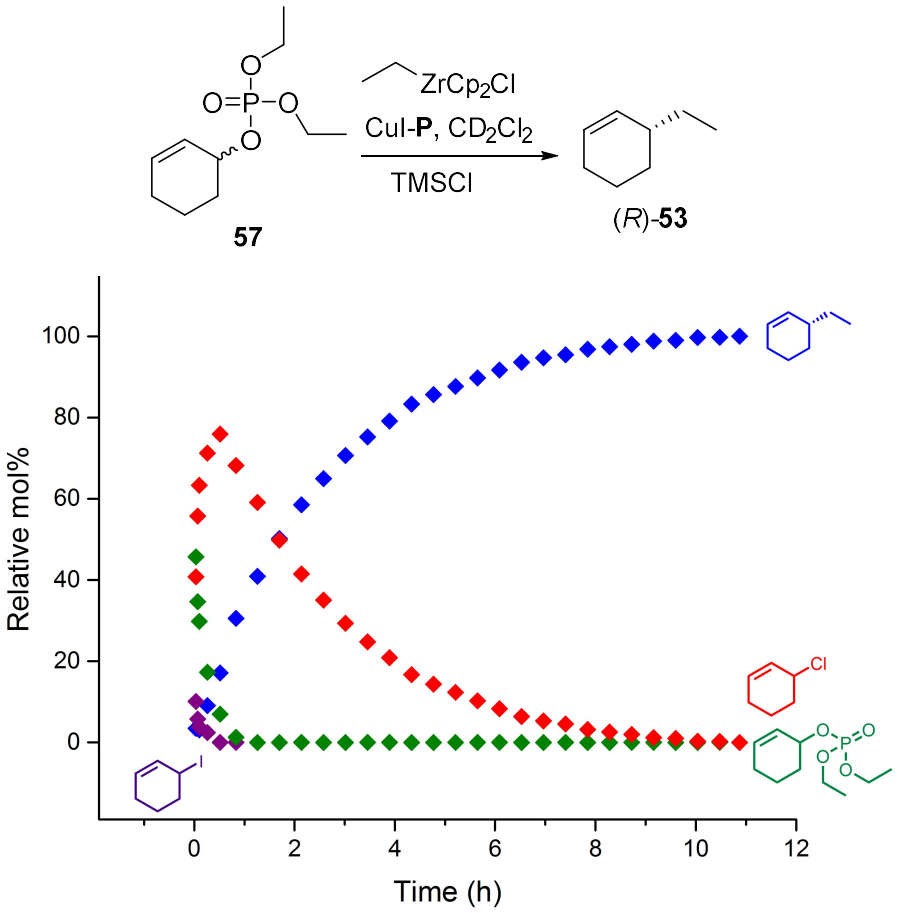

Figure 6.1. Reaction kinetics of Cu-AAA from allylphosphate 57 monitored by ^{1}H NMR spectroscopy. Conditions: $Cp_2ZrEtCl$ (2.0 eq) in CD_2Cl_2, CuI (10 allyliodide), **P** (10 mol%), allylphosphate **57** (1.0 eq), TMSCl (1.0 eq) in CD_2Cl_2, room temperature.

Upon comparison with spectra of isolated allylchloride **45b**, we identified this intermediate as allylchloride **45b** (Figure 6.2). The allylchloride **45b** was easily recognisable due to the allylic ^{1}H signal at 4.63 ppm and the olefinic signal and coupling pattern at 5.91-5.77 ppm. This observation was not entirely surprising due to the presence of TMSCl which could account for the rapid formation of allylchloride **45b** as depicted in Figure 6.1. As allylphosphate **57** is consumed rapidly over 1 h, allylchloride **45b** is formed to achieve its maximum observed quantity of 75 mol% at 1 h. Allylchloride **45b** is then slowly consumed to form the AAA product **53**, with a half-life of ~3 h and full conversion in 11 h.

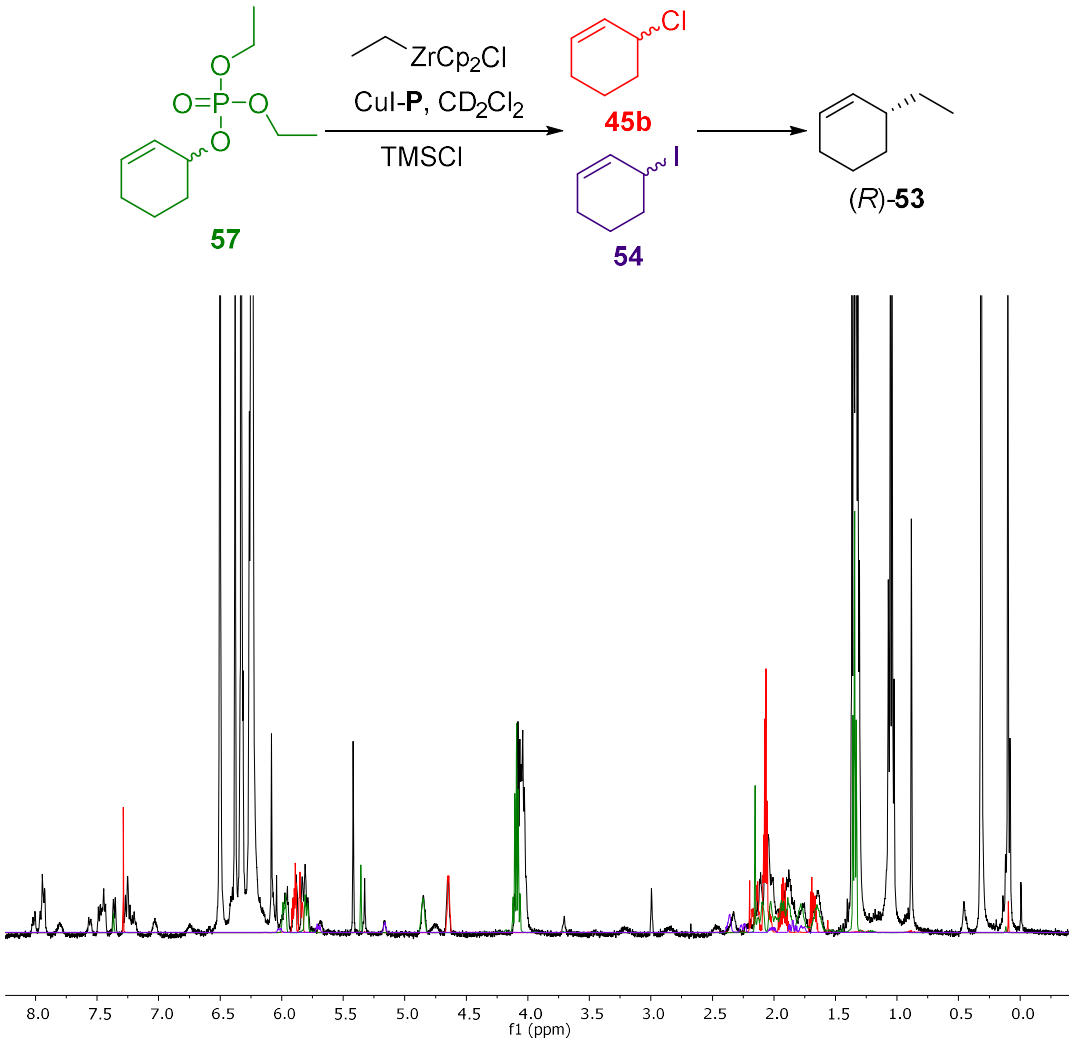

Figure 6.2. Example of a ^{1}H NMR during the AAA kinetics of allylphosphate 57 (black) compared to isolated allylphosphate 57 (green) and isolated allylchloride 45b (red) and allyliodide 54 (purple). Conditions: $Cp_2ZrEtCl$ (1.7 eq) in CD_2Cl_2, CuI (10 mol%), **P** (10 mol%), allylphosphate **57** (1.0 eq), TMSCl (1.0 eq) in CD_2Cl_2, room temperature.

The presence of allyliodide **54** was also observed but surprisingly, behaved differently than in the case of the AAA of allylchloride **45b** (Chapter 5). Indeed, in the AAA of allylchloride **45b**, a steady low 3 mol% of allyliodide **54** was constantly observed throughout the AAA reaction and was demonstrated to be a key component of the dynamic kinetic resolution of the AAA of allylchloride **45b**. However, in the AAA of allylphosphate **57**, allyliodide **54** is rapidly formed at the beginning of the reaction, reaching its observed maximum (10 mol%) 2 min after the addition of allylphosphate (Figure 6.1). Then allyliodide **54** is rapidly

consumed within 30 min. Despite the presence of allylchloride **45b** in the AAA of allylphosphate **57**, this new system does not require the constant presence of allyliodide **54** to obtain high yield and good ee.

To further investigate this Cu-AAA, we also followed the reaction by *in situ* ^{31}P NMR spectroscopy. In this case, we can follow any change in the catalyst (Figure 6.3) and the consumption or modification of allylphosphate **57** (Figure 6.4). As with AAAs of allylchloride **45b**, upon addition of $Cp_2ZrEtCl$, the Cu-ligand complex was not observed to change. Rationalisation of this observation was extensively discussed in Chapter 5 for ligand **A**. Upon addition of allylphosphate **57** and TMSCl, we also did not observe any shift in the catalyst initially (Figure 6.3 - green), but at completion (12 h) the original catalyst had entirely disappeared and two deshielded broad signals were observed at 141.4 and 145.8 ppm (blue). It is shown in other cases (below and Chapter 8), that TMSCl can modify the catalyst complex, so it is also possible that the species observed at 141.4 and 145.8 ppm originate from the presence of TMSCl.

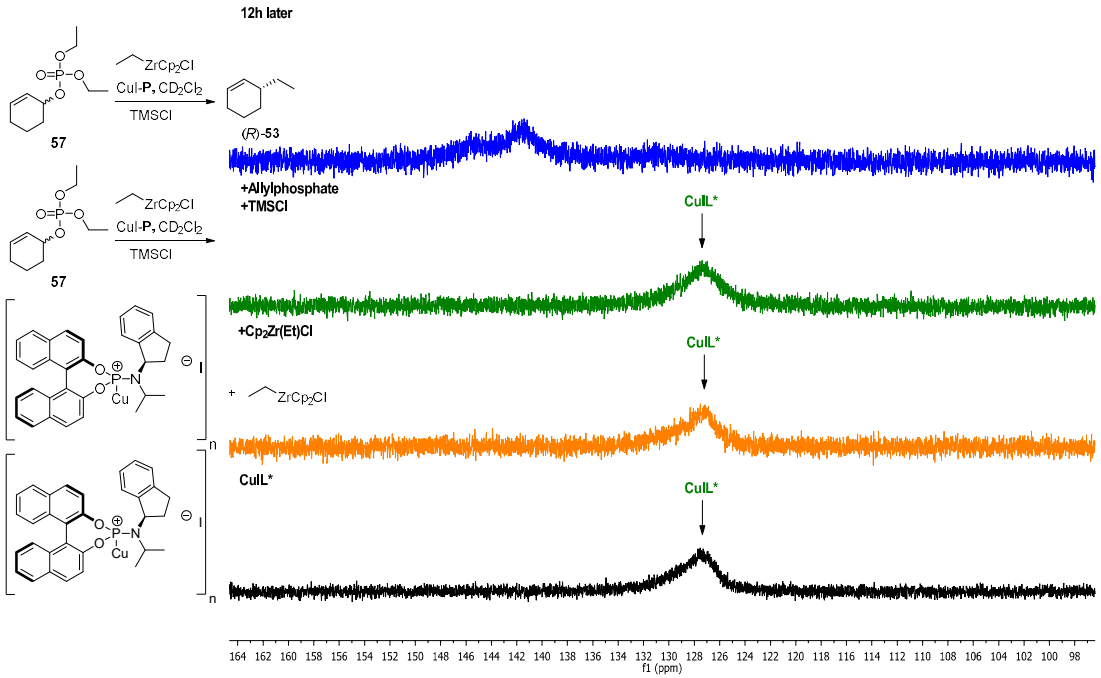

Figure 6.3. ^{31}P NMR spectroscopy from 164 to 100 ppm of the catalyst (CuI-P- black), CuI-P+$Cp_2ZrEtCl$ (orange) upon addition of allylphosphate 57 and TMSCl (green) and at the end of the AAA-reaction, 12 h after the addition of the substrate (blue). Conditions: $Cp_2ZrEtCl$ (2.0 eq) in CD_2Cl_2, CuI (10 mol%), **P** (10 mol%), allylphosphate **57** (1.0 eq), TMSCl (1.0 eq) in CD_2Cl_2, room temperature.

In the 2 to –10 ppm region of the ^{31}P NMR, we can observe the evolution of allylphosphate **57** (Figure 6.4). Upon addition of allylphosphate **57** and TMSCl, we observe the presence of allylphosphate **57** at –1.5 ppm as well as another species at –9.2 ppm (green). Based on the relative evolution of this second peak compared to the allylphosphate, the chemical shift and further evidence in other experiments, the species at –9.2 ppm seems to be the phosphate leaving group. At completion (blue), the phosphate leaving group is still present while the allylphosphate is fully consumed. New small unsymmetrical broad peaks can also be observed.

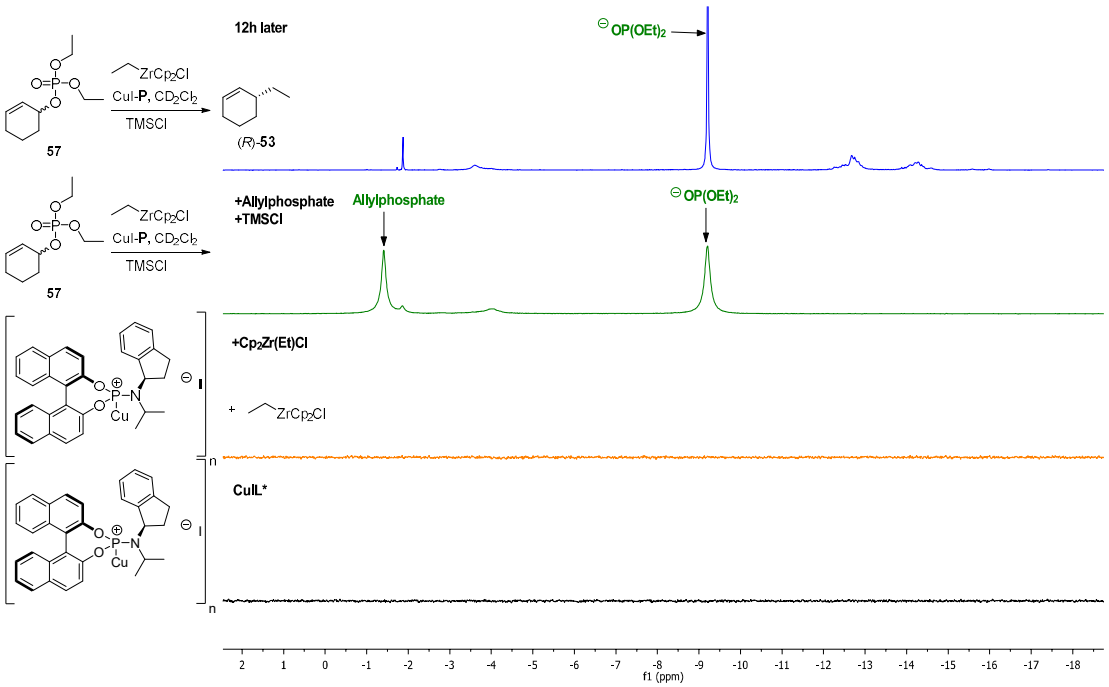

Figure 6.4. ^{31}P NMR spectroscopy from 2 to –18 ppm of the catalyst (CuI-P- black), CuI-P+$Cp_2ZrEtCl$ (orange) upon addition of allylphosphate 57 and TMSCl (green) and at the end of the AAA-reaction, 12 h after the addition of the substrate (blue). Conditions: $Cp_2ZrEtCl$ (2.0 eq) in CD_2Cl_2, CuI (10 mol%), **P** (10 mol%), allylphosphate **57** (1.0 eq), TMSCl (1.0 eq) in CD_2Cl_2, room temperature.

Based on our knowledge that the allylphosphate Cu-AAA form allylchloride **45b** *in situ*, we wanted to check if the mechanism is similar, whether the allylchloride **45b** is the primary substrate (Chapter 5) or formed *in situ* (this Chapter). A key component of the Cu-AAA with allylchloride **45b** was the formation of allyliodide **54** and racemisation. From the *in situ* ^{1}H NMR kinetic studies with allylphosphate **57** AAA, we know that allyliodide **54** appears completely consumed within 30 min. However trace amounts of species are challenging to observe in the complex kinetic ^{1}H NMR experiments. We carried out *in situ* EXSY during the Cu-AAA reaction search for the presence of isomerising allyliodide **54** (Figure 6.5). Despite multiple attempts and extensive NMR experiments tuning, signals characteristic of the S_N2' isomerisation process in allyliodide **54** were never observed in this system. Thus it is possible that the

AAA of allylphosphate **57** does not rely on the S_N2' isomerisation of allyliodide **54** as **54** intermediate cannot be detected after 30 min. The S_N2' isomerisation of allylchloride **45b**, as an alternative dynamic process was also not observed.

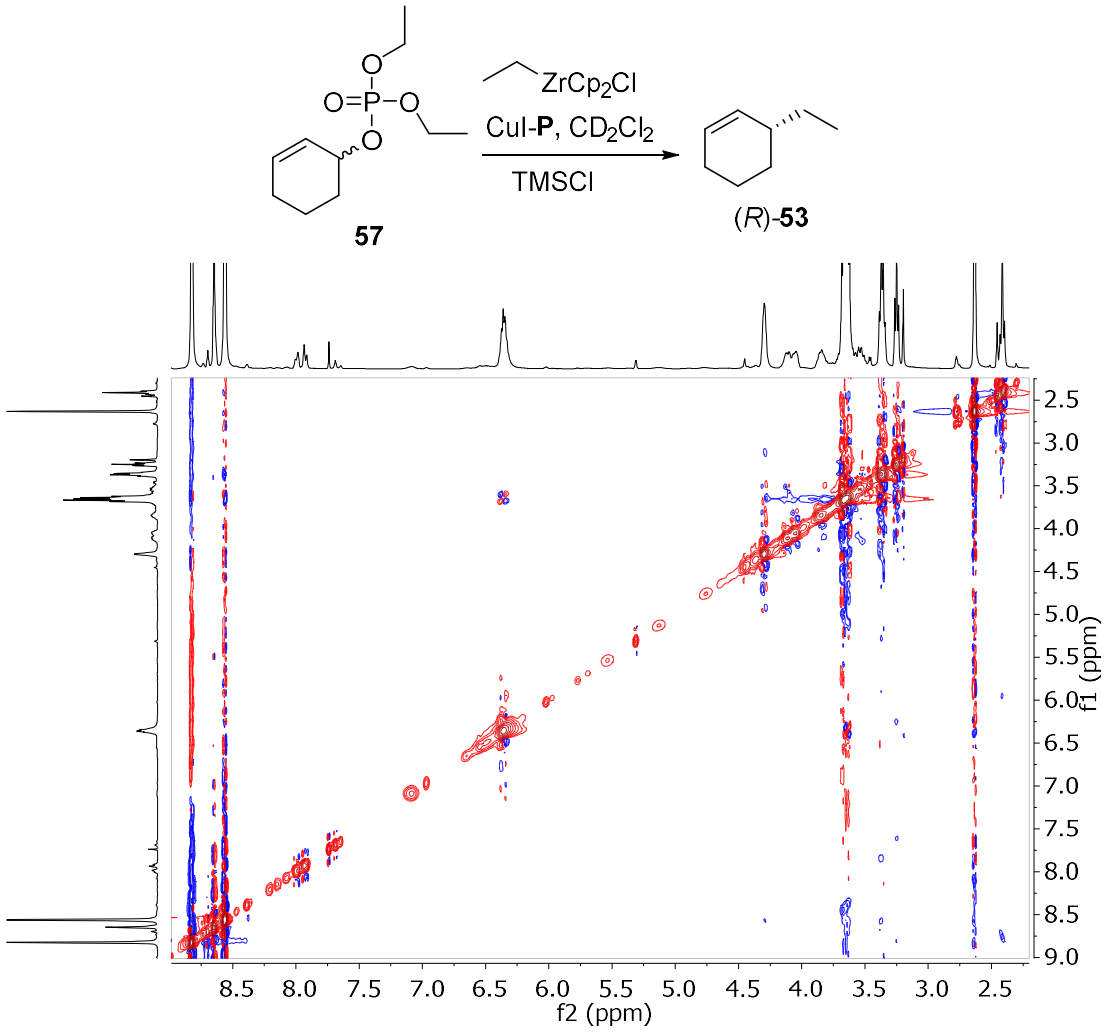

Figure 6.5. 2D exchange spectroscopy NMR (EXSY) during Cu-AAA reaction using allylphosphate 57. Conditions: $Cp_2ZrEtCl$ (2.0 eq) in CD_2Cl_2, CuI (10 mol%), **P** (10 mol%), allylphosphate **57** (1.0 eq), TMSCl (1.0 eq) in CD_2Cl_2, room temperature.

We decided to model the AAA data obtained through ^1H NMR kinetic studies of allylphosphate **57** (Figure 6.1) using non-linear least-squares regression[249] using DynaFit4 (Figure 6.6).

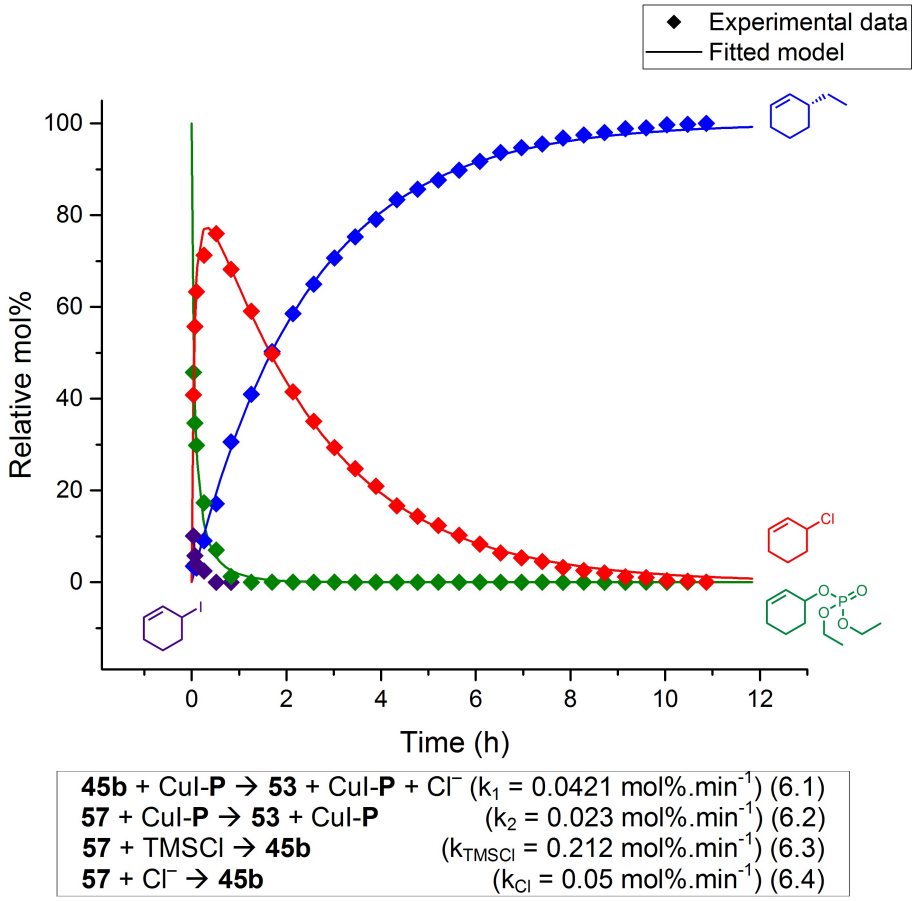

Figure 6.6. Modelling by non-linear least-squares regression of Cu-catalysed AAA of allylphosphate 57 based on kinetic experimental data collected by *in situ* ^{1}H NMR. The experimental data recorded by ^{1}H NMR are shown as diamonds. Based on those data points, modelling was performed using Dynafit4 software[249] and resulted fitted curves are shown as solid lines and the input equations with their rates below the graph.

As observed *in situ*, we assume the AAA reaction actually uses the newly synthesised allylchloride **45b** as the main substrate (Equation 6.1). However, we cannot rule out that some allylphosphate **57** undergoes allylic alkylation (Equation 6.2). The model fits the formation of product **53** from allylchloride **45b** being 20 times faster (k_1=0.042 mol%.min^{-1}) than from allylphosphate **57** (k_2=0.023 mol%.min^{-1}). Then, we assumed that TMSCl is responsible for the formation of allylchloride **45b** (Equation 6.3) (k_{TMSCl}=0.212 mol%.min^{-1}) five times faster than AAA. At this point, the model still showed divergence from the experimental data so we took into account that the formation of **53** from allylchloride **45b** generates a stoichiometric amount of chloride anion and that

these anions can react with allylphosphate **57** to generate more allylchloride **45b** (Equation 6.4). This reaction goes at a similar rate (k_{Cl}=0.05 mol%.min^{-1}) as the AAA reaction with allylchloride **45b**, presumably as each chloride anion is formed, they will react with allylphosphate **57**. The small and symmetrical spread of the residuals confirmed the model fitting to the experimental data (See Experimental Section for more details).

Allylchloride intermediate and components interactions

As the formation of allylchloride **45b** is a key step in formation of product **53** in the AAA of allylphosphate **57**, we wanted to further investigate it. Based on the experiments above, we assumed that TMSCl was essential in the formation of allylchloride **45b**. As expected, upon addition of TMSCl (1.0 eq), allylphosphate **57** (1.0 eq) gets fully transformed to allylchloride **45b** within 1 h, correlating perfectly with the 1 h consumption of allylphosphate **57** in the AAA reaction (Figure 6.7). However, in the presence of TMSCl, allylchloride **45b** was not observed to S_N2' isomerise by EXSY (see Experimental Section).

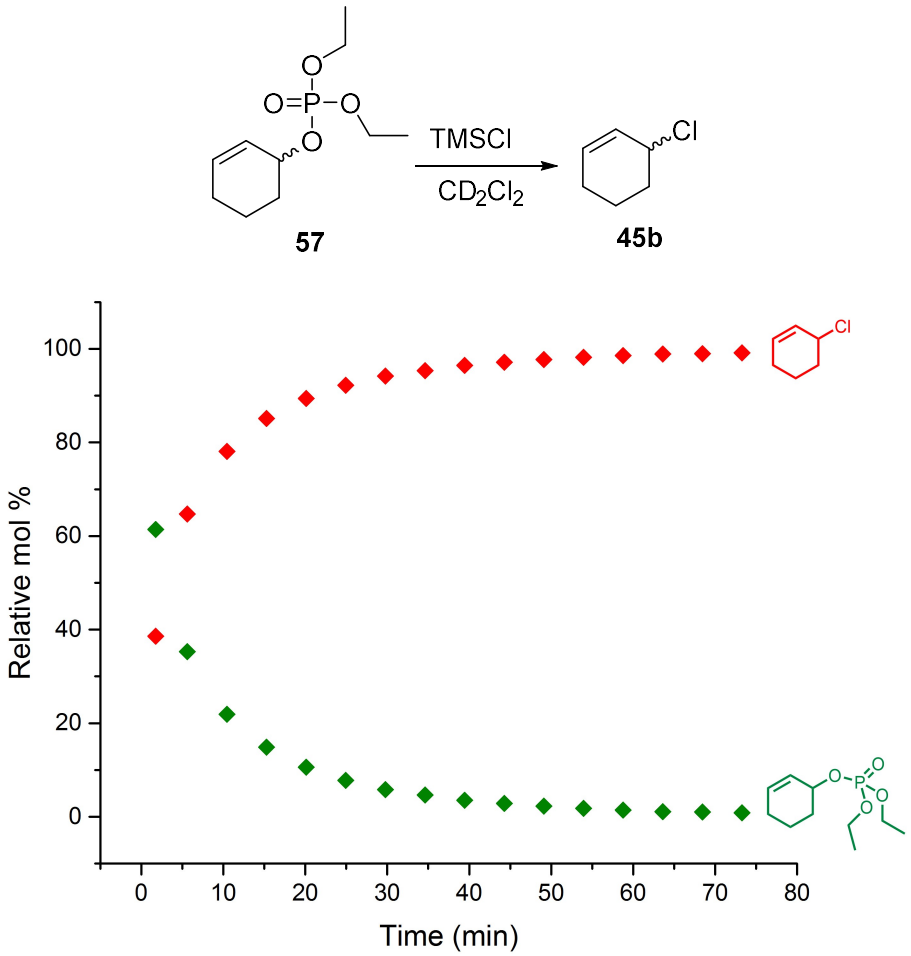

Figure 6.7. Reaction kinetics of allylphosphate 57 and TMSCl monitored by ^{1}H NMR Spectroscopy. Conditions: allylphosphate **57** (1.0 eq), TMSCl (1.0 eq) in CD_2Cl_2, room temperature.

We wanted to investigate the effect of other components present in the reaction on the formation of allylchloride **45b** from allylphosphate **57**. The addition of CuI-**P** complex (1.0 eq) to allylphosphate **57** did not result in any observable changes to the ^{1}H or ^{31}P NMR spectra (Figure 6.8 - blue).

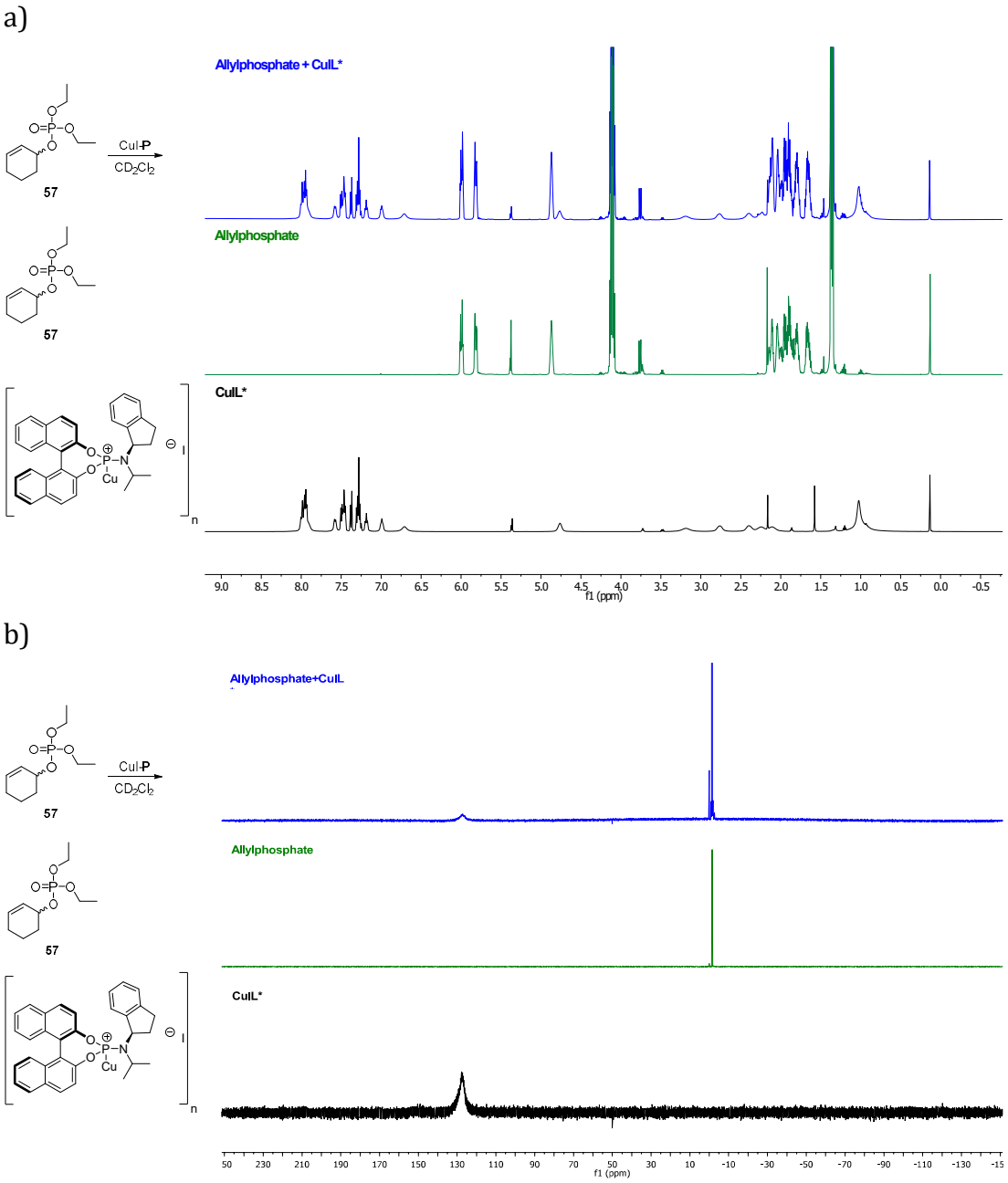

Figure 6.8. Comparison of ^{1}H (a) and ^{31}P (b) NMR spectroscopy of CuI-P complex (black), allylphosphate 57 (green) and allylphosphate + CuI-P (blue). Conditions: CuI (10 mol%), ligand **P** (10 mol%), allylphosphate **57** (1.0 eq), in CD_2Cl_2, room temperature.

Therefore unlike allylchloride **45b** (Chapter 5), allylphosphate **57** is not reactive enough to be directly interacting with the catalyst to form allyliodide **54**. The absence of the isomerising allyliodide was further suggested by EXSY experiments. However, upon addition of TMSCl (1.0 eq) to the CuI-**P** complex (0.10 eq) / allylphosphate **57** (1.0 eq) mixture, the allylphosphate is rapidly

transformed (7 min, eight times faster than without CuI-**P**) to allylchloride **45b** (Figure 6.9). Thus CuI-**P** clearly catalyses the formation of allylchloride **45b** from allylphosphate **57** in the absence of $Cp_2ZrEtCl$.

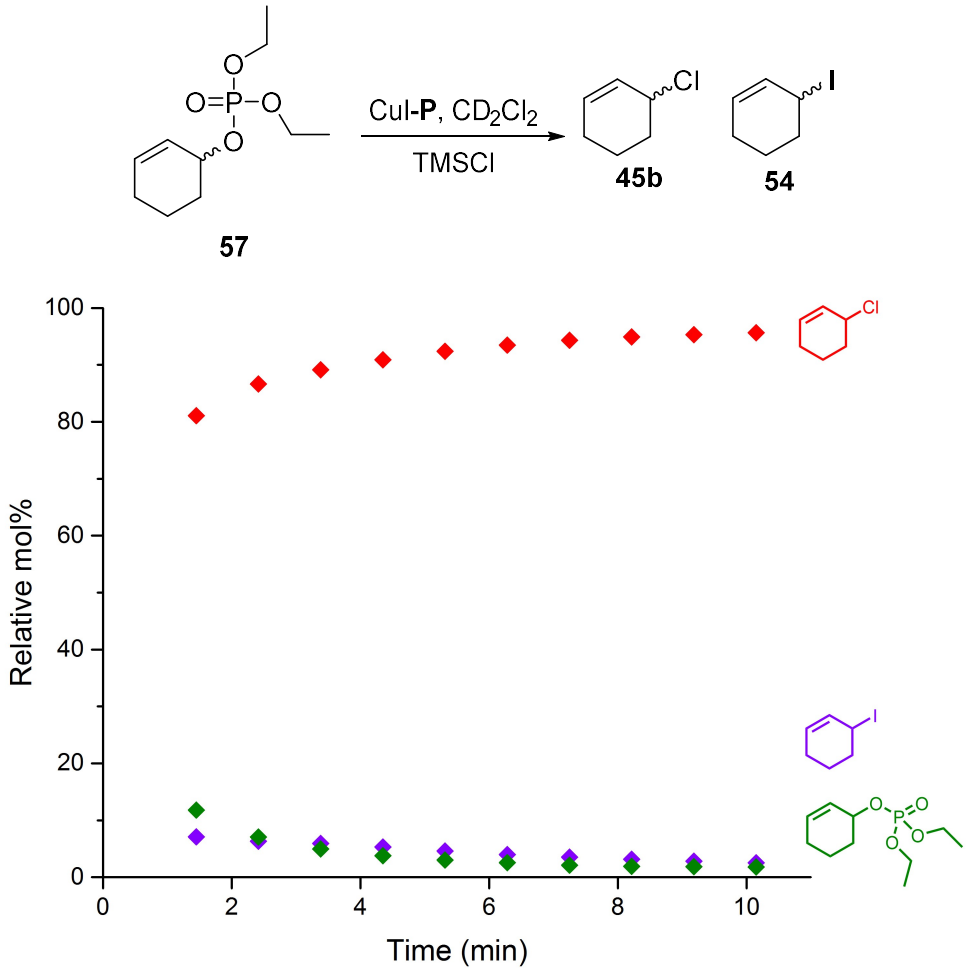

Figure 6.9. Reaction kinetics of allylphosphate 57 with TMSCl in the presence of CuI-P monitored by ^{1}H NMR spectroscopy. Conditions: CuI (10 mol%), **P** (10 mol%), allylphosphate **57** (1.0 eq), TMSCl (1.0 eq) in CD_2Cl_2, room temperature.

In these conditions, similarly to the Cu-AAA of allylphosphate **57**, allyliodide **54** is formed rapidly to reach a maximum 10 mol% and is then is consumed within 10 min in favour of allylchloride **45b**. In this case isomerisation of allyliodide **54** was observed by EXSY (Figure 6.10) contrasting with the

absence of allyliodide isomerisation being observed in the Cu-AAA itself. The potential S_N2' isomerisation of allylchloride **45b** was however not observed.

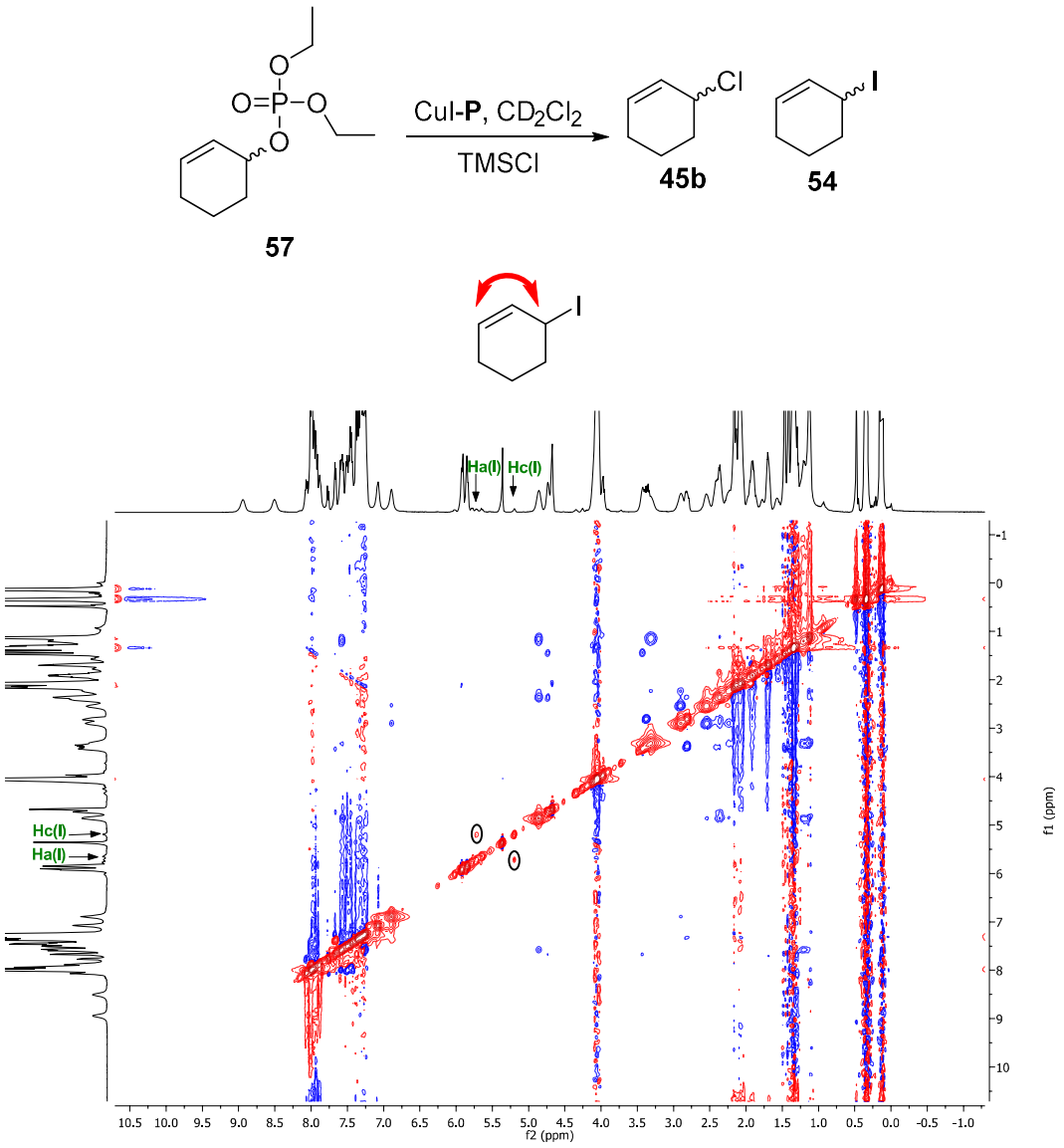

Figure 6.10. 2D exchange spectroscopy NMR (EXSY) of allylphosphate 57 with TMSCl in the presence of CuI-P. Conditions: CuI (10 mol%), **P** (10 mol%), allylphosphate **57** (1.0 eq), TMSCl (1.0 eq) in CD_2Cl_2, room temperature.

Upon mixing $Cp_2ZrEtCl$ (2.0 eq) to allylphosphate **57** (1.0 eq), the ^1H and ^{31}P NMR spectra remain unaffected, suggesting there is no interaction between those species. In the presence of $Cp_2ZrEtCl$, addition of TMSCl also transforms allylphosphate **57** to allylchloride **45b**. However, formation of allylchloride **45b**

only reached completion in 150 min, thus 2.5 times slower than without $Cp_2ZrEtCl$ (Figure 6.11). Therefore $Cp_2ZrEtCl$ appears to slow the formation of **45b** from **57**. In the presence of $Cp_2ZrEtCl$ and TMSCl, allylchloride **45b** was not observed to undergo S_N2' isomerisation by EXSY.

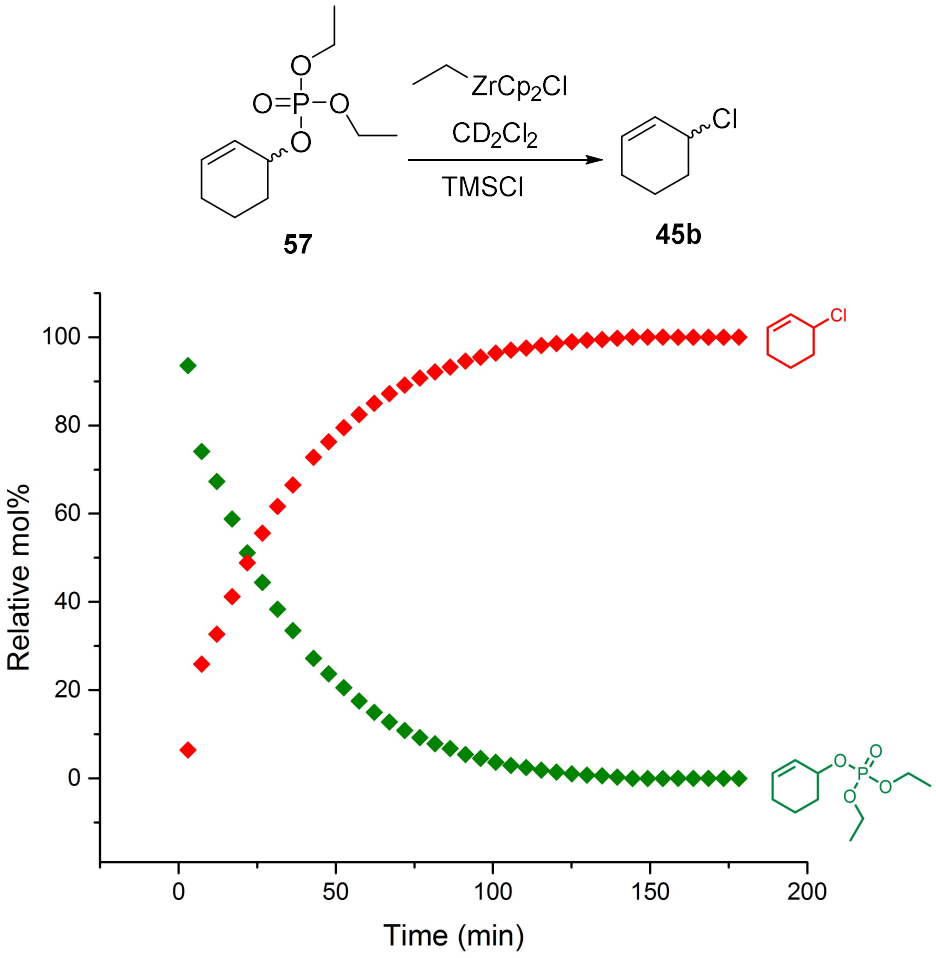

Figure 6.11. Reaction kinetics of allylphosphate 57 with TMSCl in the presence of $Cp_2ZrEtCl$ monitored by ^{1}H NMR spectroscopy. Conditions: $Cp_2ZrEtCl$ (2.0 eq) in CD_2Cl_2, allylphosphate **57** (1.0 eq), TMSCl (1.0 eq) in CD_2Cl_2, room temperature.

Thus based on those results, the formation of allylchloride **45b** clearly seems to originate from the addition of TMSCl. Indeed, in the absence of TMSCl we did not observe allylchloride **45b** being formed but the rate of allylchloride **45b** formation is however affected by the presence of those components: while

Cu catalyses the formation of allylchloride **45b**, $Cp_2ZrEtCl$ impairs it. How and why those components react together remains elusive. Despite their clear involvement in these tests, it is difficult to speculate whether the acceleration by CuI-**P** (10 min) and/or the impairing by $Cp_2ZrEtCl$ (150 min) play a role in the AAA itself or whether other more complex interactions are in place as catalytic species would differ from the pre-catalytic ones. Also, as no S_N2' isomerisation of **45b** is observed by EXSY, we do not have evidence on the mechanism of the dynamic kinetic transformation of allylphosphate **57** to product **53**.

Reaction kinetics without TMSCl

The AAA reaction of allylphosphate **57** also worked in the absence of TMSCl, albeit with a slightly lower 85% ee instead of 89% ee. We carried out AAA without TMSCl and monitored it by *in situ* ^{1}H NMR spectroscopy. To our surprise, the reaction proceeded through the same allylchloride **45b** intermediate (Figure 6.12). Allyliodide **54** was also briefly observed in <2 mol% and then consumed within the first 10 min of the AAA reaction.

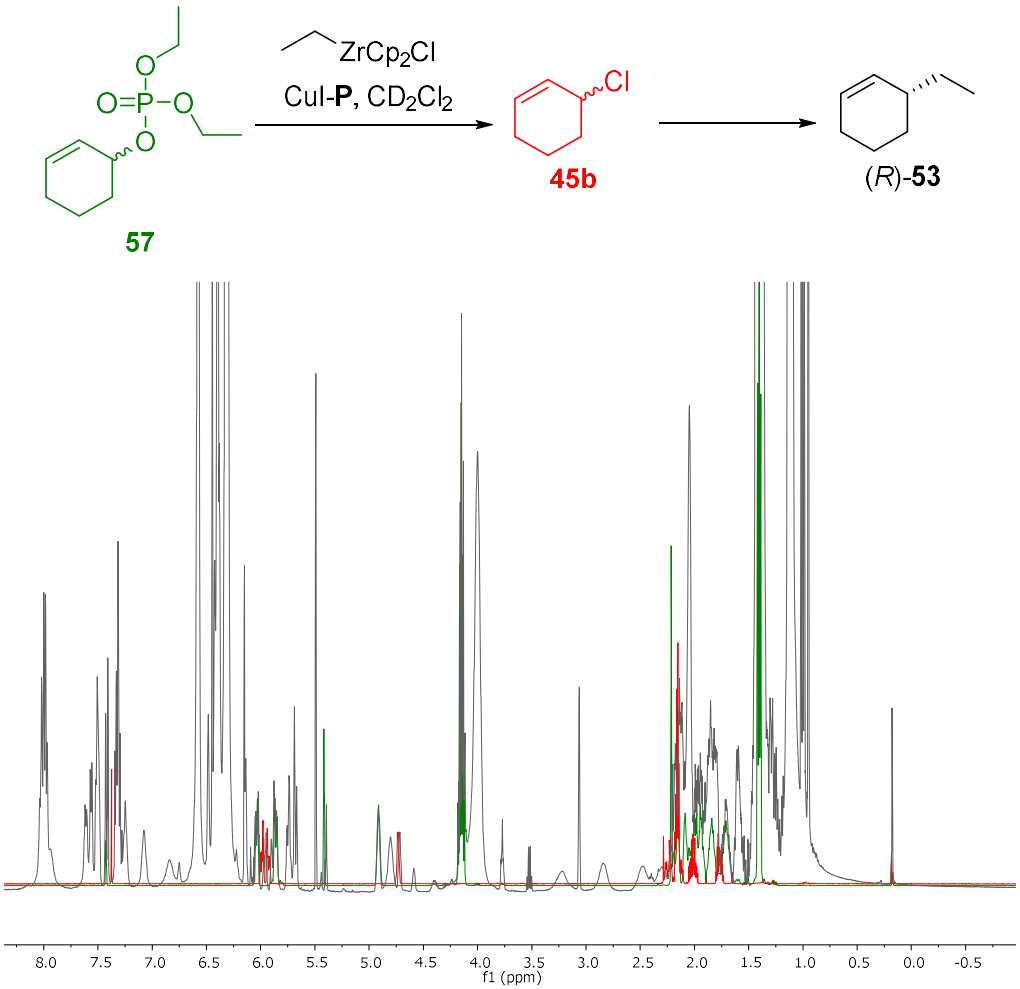

Figure 6.12. Example of a ^{1}H NMR during the AAA kinetics of allylphosphate 57 in the absence of TMSCl (grey) compared to isolated allylphosphate 57 (green) and isolated allylchloride 3 (red). Conditions: $Cp_2ZrEtCl$ (1.7 eq) in CD_2Cl_2, CuI (10 mol%), **P** (10 mol%), allylphosphate **57** (1.0 eq) in CD_2Cl_2, room temperature.

The reaction without TMSCl is fast, reaching completion at 3.5 h as opposed to 11 h in the presence of TMSCl with a half-life of 1.5 h similar to the TMSCl mediated AAA (Figure 6.13). As previously stated, TMSCl has usually been associated with accelerating effects[131-137], thus it is interesting that in this case TMSCl slows the reaction rate and might also be the case in other TMSCl-mediated Cu-catalysed addition. Clearly TMSCl has a bigger role in the reaction than purely generating allylchloride **45b**. We hypothesise that TMSCl might modify the catalyst, perhaps allowing a better stereocontrol in the rate determining step's transition state.

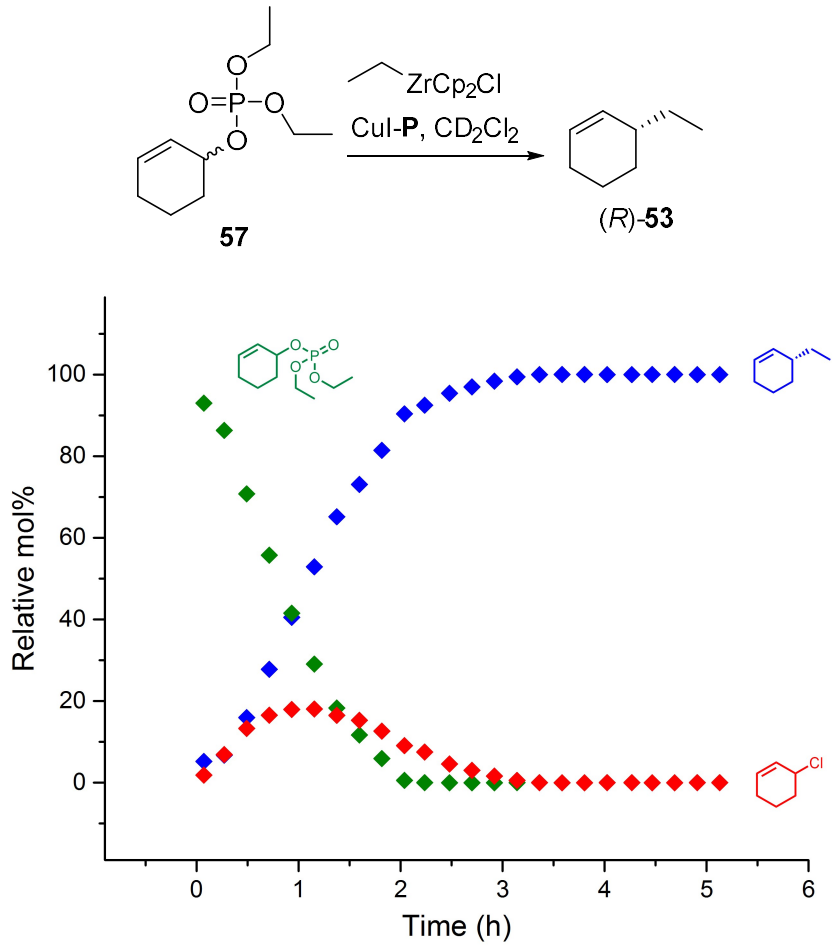

Figure 6.13. Reaction kinetics of Cu-AAA from allylphosphate 57 without TMSCl as monitored by ^{1}H NMR spectroscopy. Conditions: $Cp_2ZrEtCl$ (2.0 eq) in CD_2Cl_2, CuI (10 mol%), **P** (10 mol%), allylphosphate **57** (1.0 eq), in CD_2Cl_2, room temperature.

Unsurprisingly, in the absence of TMSCl, the consumption of allylphosphate **57** is much slower (2 h) than in the presence of TMSCl (1 h). The allylchloride only reaches a maximum of 20 mol% at 1 h (compared to 75 mol% at 1 h in the presence of TMSCl) presumably as it is getting transformed to product **53** simultaneously. In the previous testing, we only observed formation of **45b** in the presence of TMSCl. In absence of TMSCl, the sole sources of chloride are the solvent (CD_2Cl_2) or $Cp_2ZrEtCl$. However, how anion transfer is achieved is elusive and might originate from complex *in situ* mechanisms intrinsic to the AAA to generate nucleophilic chloride. Indeed, the transfer of the chloride anion was not

observed in simpler model systems such as adding CuI-**P** or $Cp_2ZrEtCl$ to allylphosphate **57** in CD_2Cl_2. Nonetheless, we observed that those species affect the rate of the formation of the allylchloride **45b** from allylphosphate **57** with TMSCl and we will also see other effects in the deuterium experiment section below.

We had already noticed the importance of using chlorinated solvent in the AAA of allylchloride as non-chlorinated solvent impaired the reaction[4]. We speculate that in both the AAA of allylphosphate **57** and allylchloride **45b**, the presence of chlorinated solvent is crucial for the formation of the product and in both systems, the optimised conditions somehow provide an essential source of chloride anions for the AAA reaction to proceed. Thus allylchloride **45b** seems to be a compulsory intermediate in the AAA of allylphosphate **57** and TMSCl facilitate this transformation.

To further investigate Cu-AAA without TMSCl, we followed the reaction *in situ* using ^{31}P NMR spectroscopy (Figure 6.14 and 6.15). Allylphosphate **57** alone does not initially change the Cu-Zr catalyst chemical shift at 127.5 ppm (Figure 6.14 - green). However, after 12 h (blue), the original catalyst at 127.5 ppm is replaced by two new broad deshielded signals at 151.3 ppm and 141.3 ppm respectively, presumably from the presence of competing phosphate leaving group. Those new signals do not correlate to the change in catalyst observed in the AAA of allylphosphate **57** in the presence of TMSCl (141.4 and 145.8 ppm), showing that the presence of TMSCl have an effect on the catalyst.

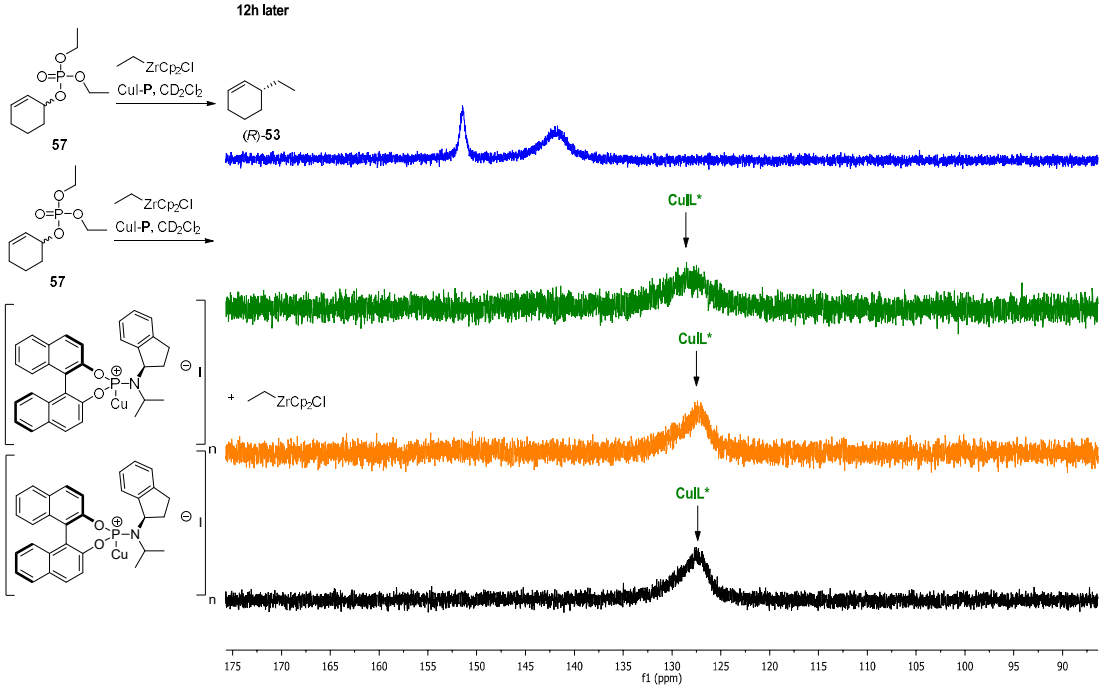

Figure 6.14. ^{31}P NMR spectroscopy from 175 to 90 ppm of the catalyst (CuI-P- black), CuI-P+$Cp_2ZrEtCl$ (orange) upon addition of allylphosphate 57 (green) and at the end of the AAA-reaction, 12 h after the addition of the substrate (blue). Conditions: $Cp_2ZrEtCl$ (2.0 eq) in CD_2Cl_2, CuI (10 mol%), **P** (10 mol%), allylphosphate **57** (1.0 eq), in CD_2Cl_2, room temperature.

In the 2 to –20 ppm region (Figure 6.15), the allylphosphate **57** at –1.5 ppm is consumed within 2 h in concordance with ^{1}H NMR kinetic studies (blue). Many non-symmetrical broad signals appeared in that region 12 h after the addition of allylphosphate **57** (Figure 6.15 - blue). This fact was surprising as in the presence of TMSCl, the corresponding ^{31}P NMR spectrum was relatively clean (Figure 6.4 – blue). Thus in absence of TMSCl, the allylphosphate reaction seems to produce many side-products containing phosphorus at –4.0 ppm, –12.7 ppm and –14.3 ppm. What we previously identified as the allylphosphate leaving group at –9.2 ppm, observed during ^{31}P NMR kinetics of the formation of allylchloride **45b** from allylphosphate **57** (Figure 6.4) was not observed here. This observation suggests that the phosphate leaving group binds to other entities during the AAA-reaction in absence of TMSCl and TMSCl might have a

beneficial effect on the control of the phosphate leaving group, which is not surprising considering the known affinity of Si for O. TMSCl role in the optimised conditions must be to generate allylchloride **45b** and inhibit the side-effect of having a stoichiometric amount of anionic phosphate ($OPO(OEt)_2^-$).

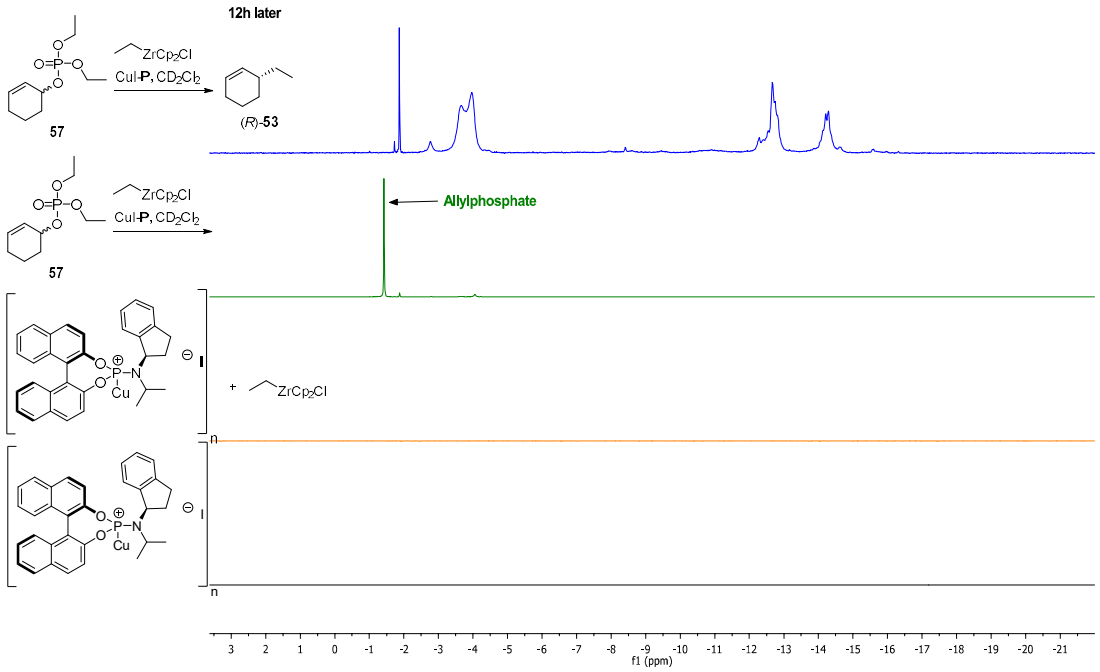

Figure 6.15. ^{31}P NMR spectroscopy from 3 to –21 ppm of the catalyst (CuI-P- black), CuI-P+$Cp_2ZrEtCl$ (orange) upon addition of allylphosphate 57 (green) and at the end of the AAA-reaction, 12 h after the addition of the substrate (blue). Conditions: $Cp_2ZrEtCl$ (2.0 eq) in CD_2Cl_2, CuI (10 mol%), **P** (10 mol%), allylphosphate **57** (1.0 eq), in CD_2Cl_2, room temperature.

Finally, we also tried to identify the presence of isomerising allyliodide **54** in the reaction without TMSCl by EXSY (Figure 6.16). Similarly to the AAA-reaction optimised with TMSCl, the reaction without TMSCl did not show any sign of the isomerisation of allyliodide or allylchloride as no EXSY cross-peaks were observed.

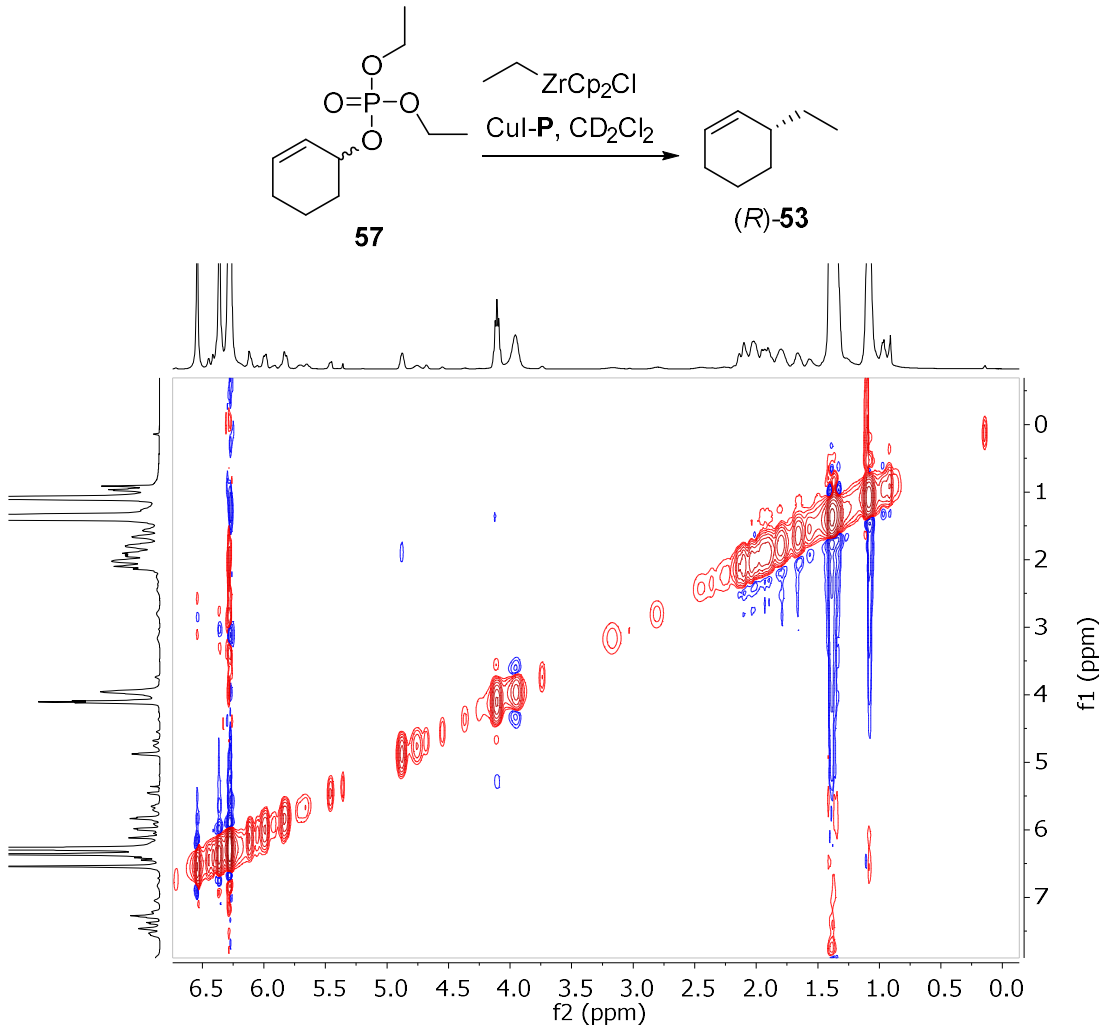

Figure 6.16. 2D exchange spectroscopy NMR (EXSY) during Cu-AAA reaction using allylphosphate 57 without TMSCl. Conditions: $Cp_2ZrEtCl$ (2.0 eq) in CD_2Cl_2, CuI (10 mol%), **P** (10 mol%), allylphosphate **57** (1.0 eq),) in CD_2Cl_2, room temperature.

We decided to model the AAA-reaction of allylphosphate **57** without TMSCl using non-linear least-squares regression[249] with DynaFit4 (Figure 6.17). As discussed in the modelling for the AAA-reaction of allylphosphate **57** with TMSCl, both allylphosphate **57** and allylchloride **45b** might undergo the allylic alkylation step (Equation 6.6 and 6.5 respectively). According to the model, in the absence of TMSCl, the formation of product **53** is 10 times faster (k_1=0.26 mol%.min^{-1}) from allylchloride **45b** than allylphosphate **57** (k_2=0.019 mol%.min^{-1}). This observation is coherent with the modelling of the

AAA reaction with TMSCl. However, whilst k_2 is still in the same order of magnitude as the model of AAA with TMSCl, the reaction rate k_1 of the AAA from allylchloride **45b** is extremely fast compared to the initial one in the presence of TMSCl (k_1=0.042 mol%.min^{-1}). This observation is perhaps due to the effect of TMSCl on the catalyst to obtain a slower but more enantioselective catalyst in the optimised conditions.

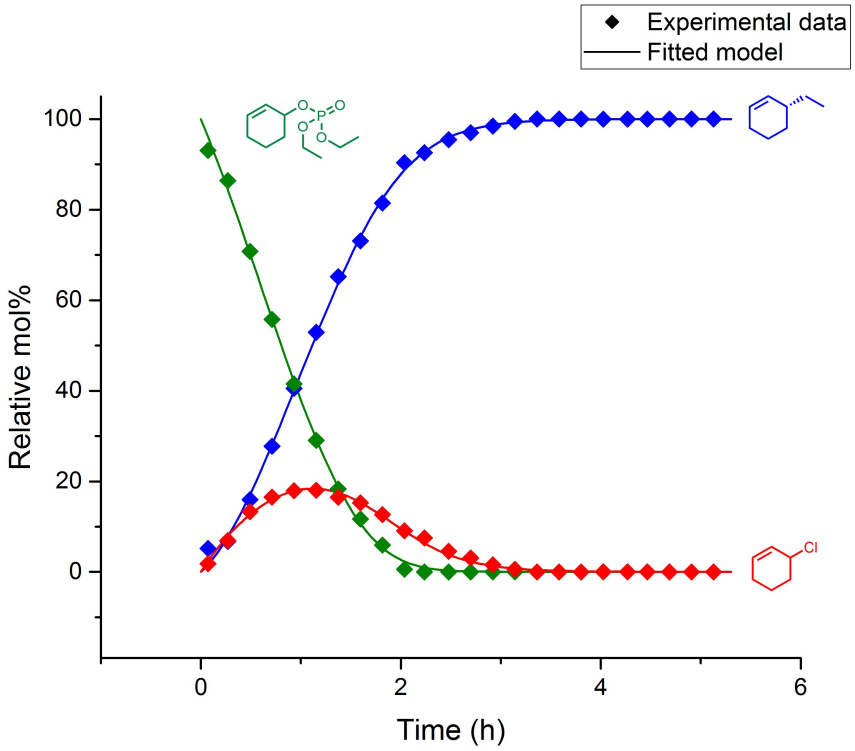

45b + CuI-**P** → **53** + CuI-**P** + Cl$^-$ (k_1 = 0.26 mol%.min^{-1}) (6.5)
57 + CuI-**P** → **53** + CuI-**P** (k_2 = 0.019 mol%.min^{-1}) (6.6)
57 + Cl source → **45b** (k_{Cl1} = 0.0018 mol%.min^{-1}) (6.7)
57 + Cl$^-$ →**45b** (k_{Cl2} = 0.18 mol%.min^{-1}) (6.8)

Figure 6.17. Modelling by non-linear least-squares regression of Cu-catalysed AAA of allylphosphate 57 without TMSCl based on kinetic experimental data collected by *in situ* ^{1}H NMR. The experimental data recorded by ^{1}H NMR are shown as diamonds. Based on those data points, modelling was performed using Dynafit4 software[249] and resulted fitted curves are shown as solid lines and the input equations with their rates below the graph.

We also wanted to model the formation of allylchloride **45b**. As $Cp_2ZrEtCl$ and CH_2Cl_2 are the only possible *initial* sources of chloride, we modelled the formation of **45b** using $Cp_2ZrEtCl$ as the source (Equation 6.7). Modelling

$Cp_2ZrEtCl$ (2.0 eq) is arguably easier than modelling a large excess of solvent (CH_2Cl_2) but the model is equally compatible with using CH_2Cl_2 as a source of nucleophilic chloride. The formation of allylchloride **45b** from $Cp_2ZrEtCl$ is very slow (k_{Cl1}=0.0018 mol%.min^{-1}). Thus to account for the divergence of the current model from the experimental data, we decided to also take into account the formation allylchloride **45b** from the chloride anion generated during the AAA step (Equation 6.8). This reaction is fast (k_{Cl2}=0.18 mol%.min^{-1}), in the same order of magnitude as the formation of product **53** from allylchloride **45b** (Equation 6.6), similarly observed in the model of the AAA with TMSCl. The model fit the data well and the small and symmetrical spread of residuals support the accuracy of the model (See Experimental Section for details).

TMSCl effect on the Catalyst

TMSCl has been observed to affect the catalyst here and in other systems (Chapter 2 and 8). Upon addition of TMSCl (1.0 eq), CuI-**P** (1.0 eq) instantaneously changed as observed in the ^{1}H and ^{31}P NMR spectra (Figure 6.18 - blue). In the ^{1}H NMR (Figure 6.18a - blue), the aromatics multiplicities are modified, the benzylic signal at 4.77 ppm is split into two entities at 4.83 ppm and 4.70 ppm, new signals appeared in the aliphatic region and the broad signal of isopropyl at 1.03 ppm is deshielded to 1.10 ppm and 1.40 ppm. In the ^{31}P NMR (Figure 6.18b - blue), the unique catalytic signal at 129.6 ppm (black) split into two entities at 127.7 ppm and 170.6 ppm. Both the ^{1}H and ^{31}P NMR suggest that upon the addition of TMSCl, the CuI-**P** pre-catalyst is transformed to two novel species. The presence of coexisting two catalytic species has also been observed

for CuOTf-**A** (Chapter 5) and will be discussed in the addition of TMSCl to CuOTf-**A** (Chapter 8).

a)

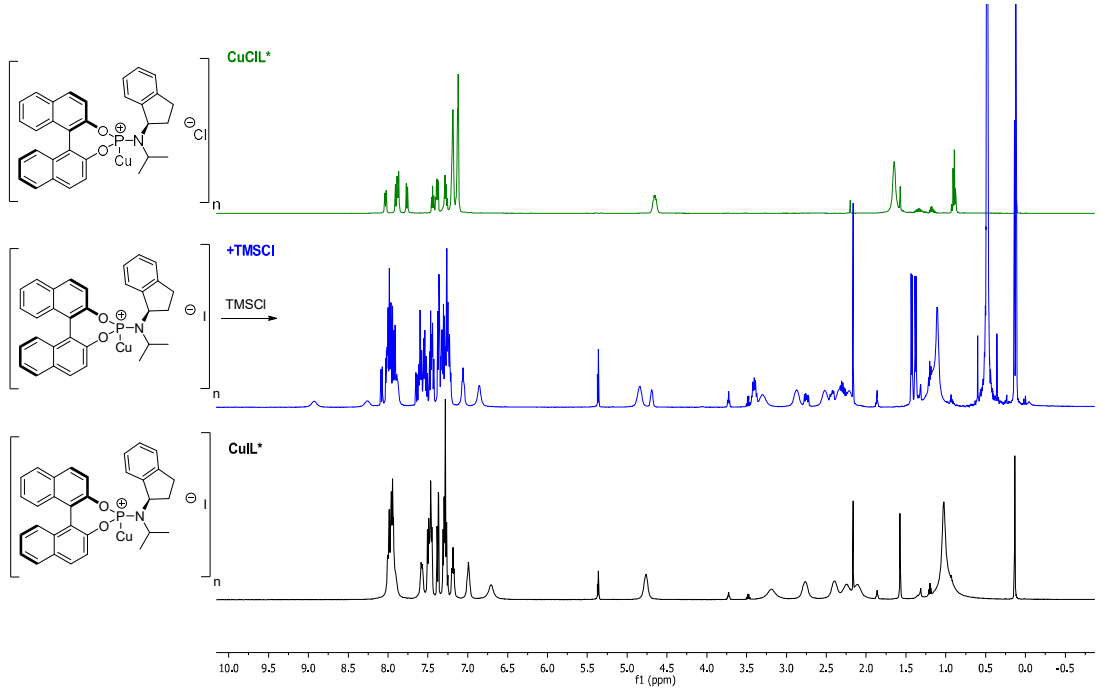

b)

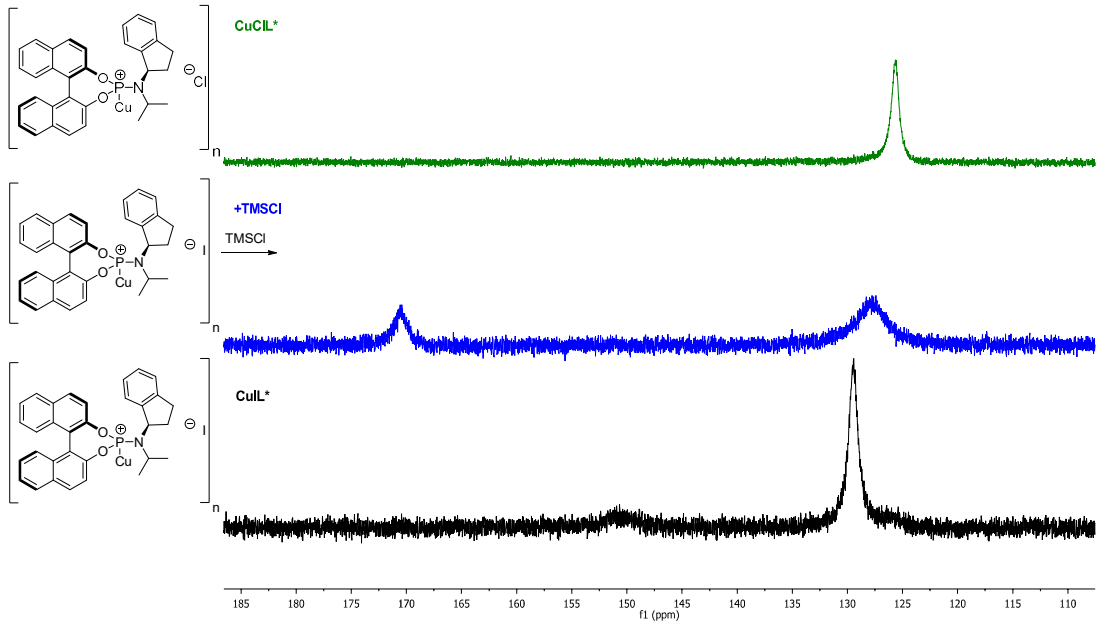

Figure 6.18. ^{1}H (a) and ^{31}P (b) NMR spectroscopy of the catalyst CuI-P (black), CuI-P+TMSCl (blue) and CuCl-P (green). Conditions: CuI (10 mol%), **P** (10 mol%), TMSCl (1.0 eq), in CD_2Cl_2, room temperature.

Furthermore, even though TMSCl is a source of chloride anion, the newly formed species do not resemble the CuCl-**P** complex alone (Figure 6.18 - green) nor the catalytic species formed during the AAA of allylphosphate **57** in the presence of TMSCl (Figure 6.3 - blue). Indeed, the benzylic signal of CuCl-**P** is found at 4.62 ppm (not at 4.83 ppm or 4.70 ppm) and its phosphorus signal is at 125.8 ppm (not at 127.7 ppm or 170.6 ppm). The AAA of allylphosphate **57** in the presence of TMSCl gave new catalytic signals at 141.4 and 145.8 ppm, not at 127.7 ppm and 170.6 ppm. Therefore the species formed when adding TMSCl to CuI-**P** remains unknown. Thus whether TMSCl influences the CuI-**P** catalyst during the AAA reaction itself is difficult to determine. Moreover, only 1.0 eq of TMSCl is necessary in the AAA to give 89% ee whereas using an excess of TMSCl (5.0 eq) lowered the ee to 80%. Therefore for optimal reactivity, the primary role of TMSCl seemed to be to fully convert allylphosphate **57** to allylchloride **45b** rapidly while any excess impairs the AAA presumably as modified CuI-**P** aggregates by TMSCl are disfavoured.

Deuterium studies

In order to obtain further mechanistic information, we synthesised deuterated allylphosphate **58**. These studies show the advantage of using phosphate leaving groups over chlorides due to the stability of the phosphates. Indeed, deuterated chlorides are difficult to obtain in pure form and can only be isolated as mixtures of regioisomers **59a** and **59b**. Thus the mechanistic behaviours of deuterated allylchloride are more difficult to interpret than deuterated allylphosphate **58**.

^{2}H NMR gives broader signal than ^{1}H NMR as ^{2}H has a spin quantum number I=1 and thus lower resolution. However, ^{2}H NMR only shows ^{2}H containing species as exemplified in Figure 6.19, simplifying the observation of only the desired species and largely removing the difficulty associated with overlapping signals.

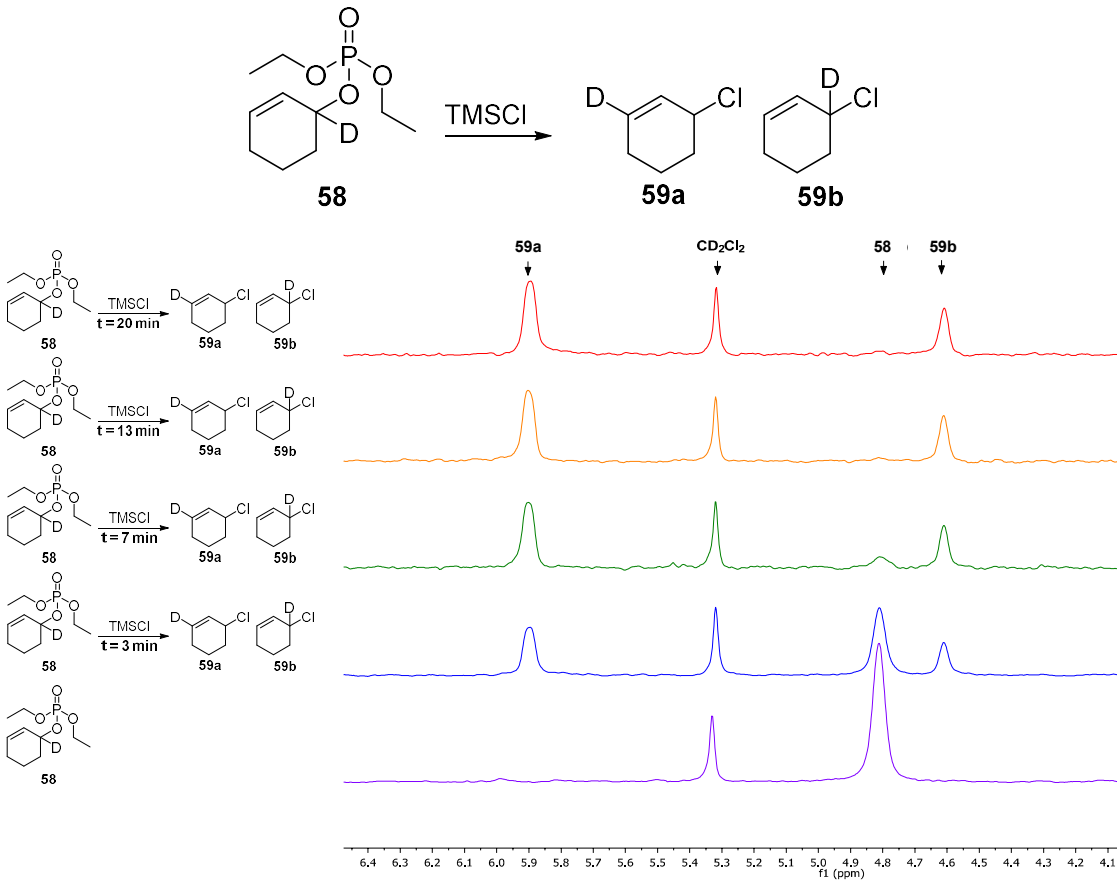

Figure 6.19. ^{2}H NMR spectroscopy of the kinetic addition of TMSCl to D-allylphosphate 58. Conditions: D-allylphosphate **58** (1.0 eq), TMSCl (1.0 eq) in CH_2Cl_2, room temperature.

Firstly, we wanted to carry out the optimised AAA reaction (with TMSCl) using D-allylphosphate **58** and monitor it using *in situ* ^{2}H spectroscopy. D-allylphosphate **58** is rapidly consumed to form D-allylchlorides **59a** and **59b** which in turn forms D-products **60a** and **60b** (Figure 6.20). D-allylchlorides **59a** and **59b** are produced from D-allylphosphate **58** in equal amount throughout the

reaction. As S_N2' isomerising mechanisms were not observed by EXSY under the optimised conditions, D-allylchloride **59** is equally formed through S_N2 and S_N2' mechanisms. D-product **60a** and **60b** are also formed in a 50:50 ratio. Unfortunately, because the D-allylchlorides **59a** and **59b** are scrambled, no information can be gathered on the mechanism of the AAA step (S_N2 or S_N2'). Due to the poor resolution of ^2H NMR and low amount of allyliodide generated in the AAA reaction, D-allyliodide **61** was not observed.

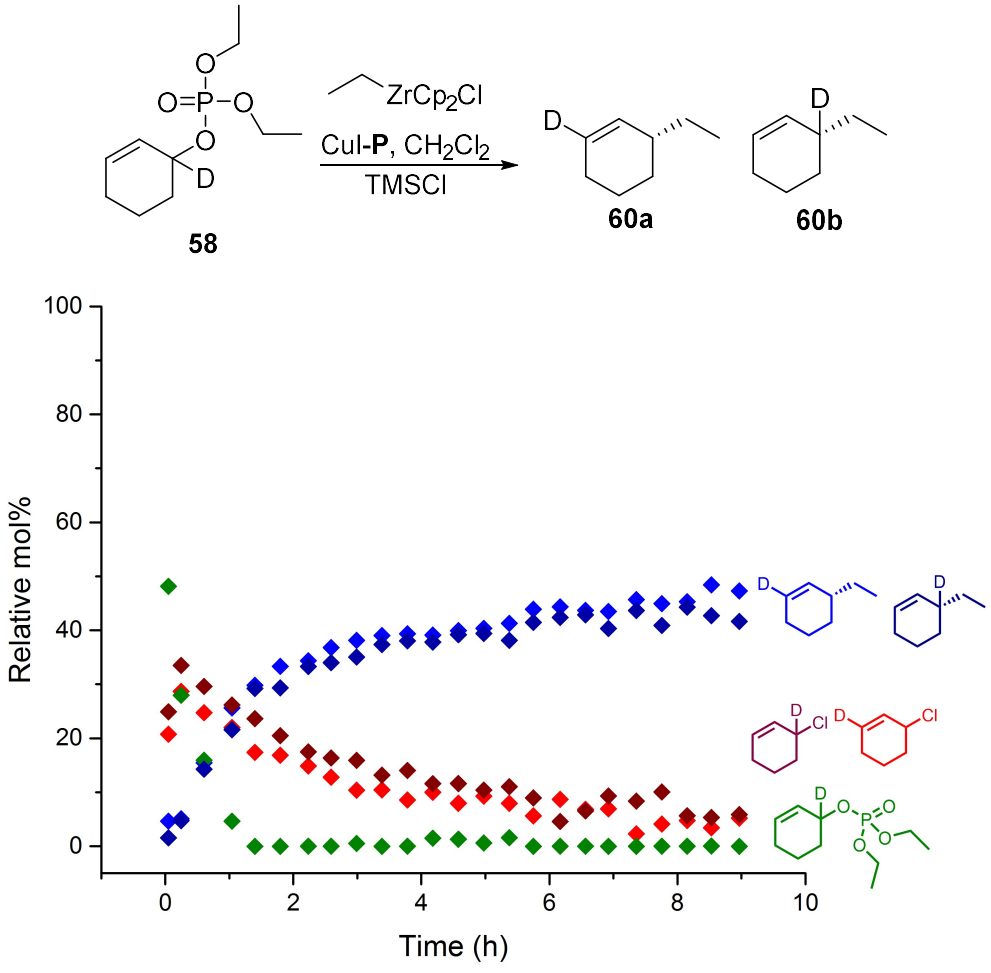

Figure 6.20. Reaction kinetics of Cu-AAA from D-allylphosphate 58 as monitored by ^2H NMR Spectroscopy. Conditions: $Cp_2ZrEtCl$ (2.0 eq) in CH_2Cl_2, CuI (10 mol%), **P** (10 mol%), D-allylphosphate **58** (1.0 eq), TMSCl (1.0 eq) in CH_2Cl_2, room temperature.

We also decided to carry out the *in situ* ^{2}H NMR kinetic of D-allylphosphate **58** without TMSCl (Figure 6.21). D-allylphosphate **58** is consumed slowly forming D-allylchlorides **59a** and **59b** in an equal ratio, which in turns form D-products **60a** and **60b** in equal amounts. Therefore the AAA reaction of allylphosphate **57** both with and without TMSCl share similar mechanistic aspects on the S_N2 and S_N2' control of the formation of allylchloride **45b**. D allyliodide was also not observed in the absence of TMSCl.

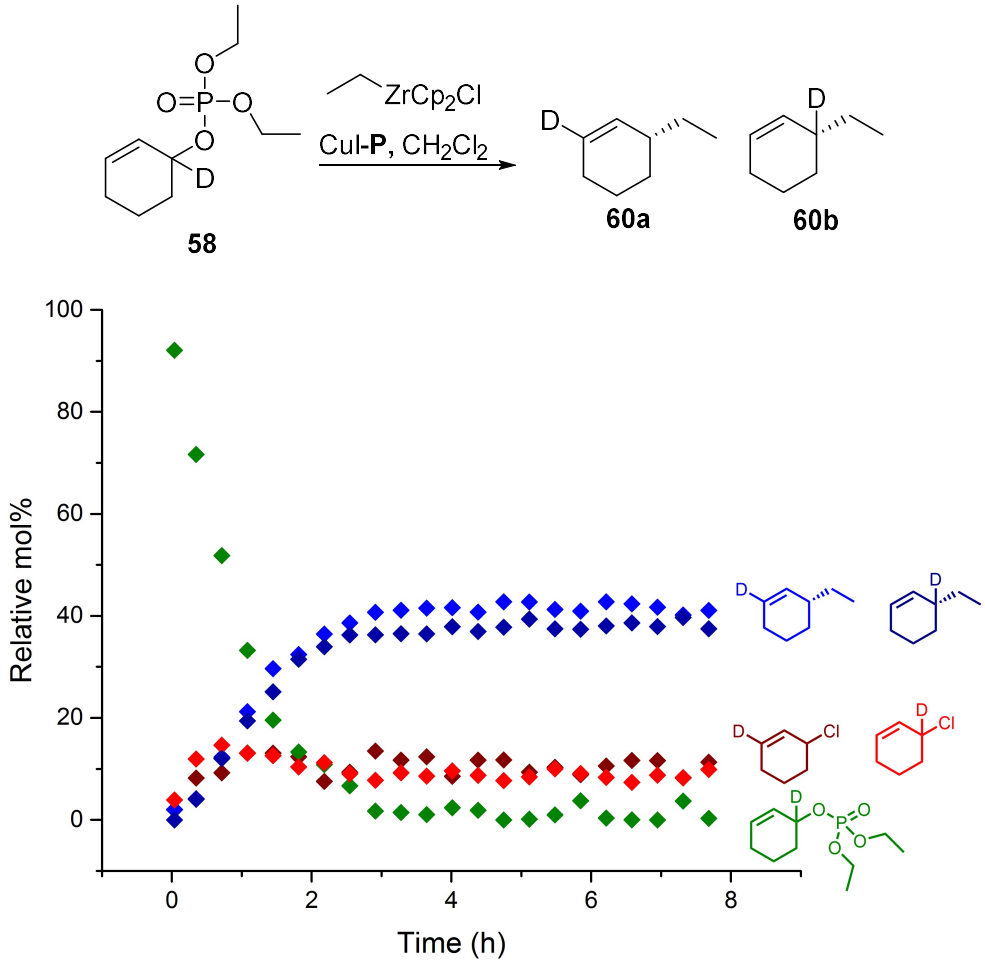

Figure 6.21. Reaction kinetics of Cu-AAA from D-allylphosphate 58 without TMSCl as monitored by ^{2}H NMR spectroscopy. Conditions: $Cp_2ZrEtCl$ (2.0 eq) in CH_2Cl_2, CuI (10 mol%), **P** (10 mol%), D-allylphosphate **58** (1.0 eq), in CH_2Cl_2, room temperature.

To further investigate the S_N2 and S_N2' formation of D-allylchlorides **59a** and **59b**, we decided to perform interaction studies. We first added TMSCl (1.0 eq) to D-allylphosphate **58** (1.0 eq) (Figure 6.22). D-allylchlorides **59a** and **59b** were formed in 20 min and 65 mol% of the β-deuterated isomer **59a** was formed while only 35 mol% of the geminal isomer **59b** was obtained at completion. This experiment clearly shows that while both S_N2' and S_N2 mechanisms occur, the nucleophilic attack of TMSCl alone favours S_N2' displacement over S_N2. Moreover, these conditions suggest that D-allylchloride **59** alone cannot isomerise via S_N2' pathways as the 50:50 mixture that would be expected is not observed. However, we do not have any information regarding isomerisation of allylchloride **45b** through S_N2 mechanisms as such behaviour would not be observable on D-allylchlorides **59a** and **59b**. This experiment exemplified that TMSCl alone is not responsible for the formation of the observed D-allylchloride ratio of **59a** and **59b** during the AAA reaction itself. Indeed, in the AAA reaction, D-allylchlorides **59a** and **59b** are formed in equal amounts whereas here TMSCl favours S_N2' displacement of the phosphate leaving group.

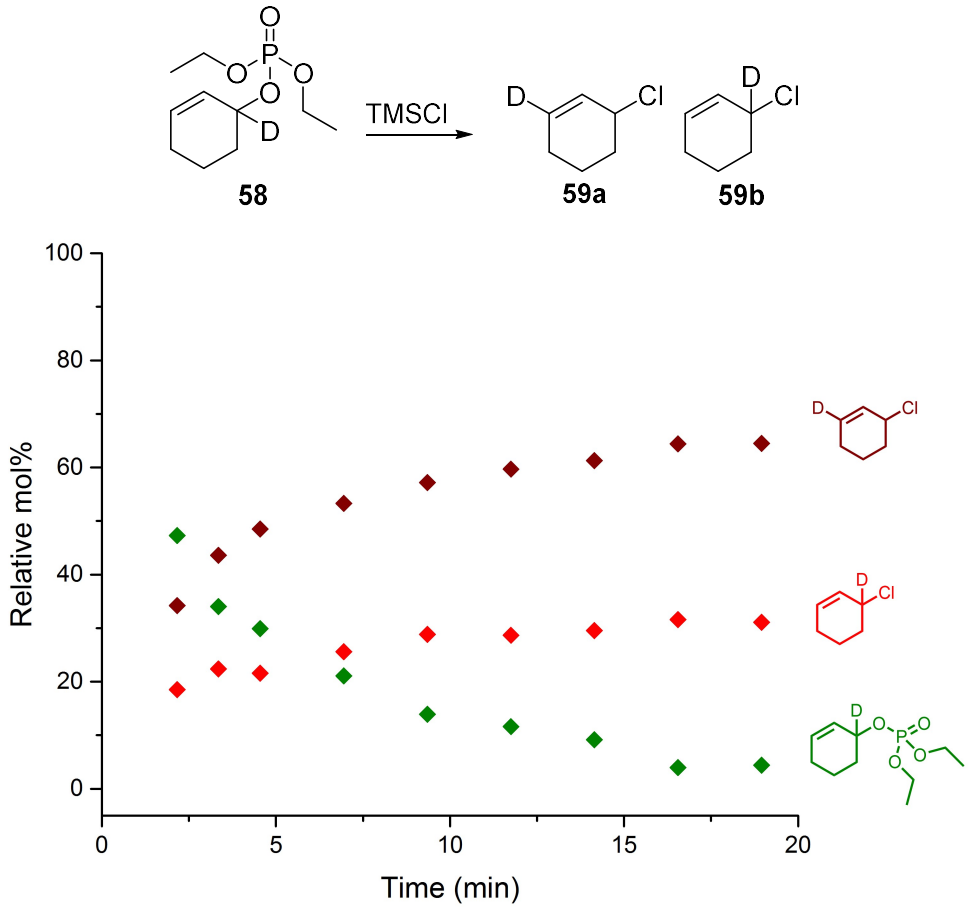

Figure 6.22. Reaction kinetics of D-allylphosphate 58 and TMSCl as monitored by ^{2}H NMR spectroscopy. Conditions: D-allylphosphate **58** (1.0 eq), TMSCl (1.0 eq) in CH_2Cl_2, room temperature.

Secondly, we studied the effect of $Cp_2ZrEtCl$ (2.0 eq) on the formation of D-allylchlorides **59a** and **59b** by TMSCl (1.0 eq) (Figure 6.23). **59a** and **59b** were formed in 200 min and 65 mol% of the geminal isomer **59b** was formed while only 35 mol% of the β-deuterated isomer **59a** was obtained at completion. In the presence of $Cp_2ZrEtCl$ the mechanistic selectivity was reversed, TMSCl favours the formation of D-allylchloride **59** through S_N2 pathways over S_N2'. Based on the divergence from the AAA itself (equal amounts of **59a** and **59b** formed), it would seem that $Cp_2ZrEtCl$ and TMSCl alone are not the only forces involved in the formation and isomerisation of allylchloride **45b** in the AAA of allylphosphate **57**.

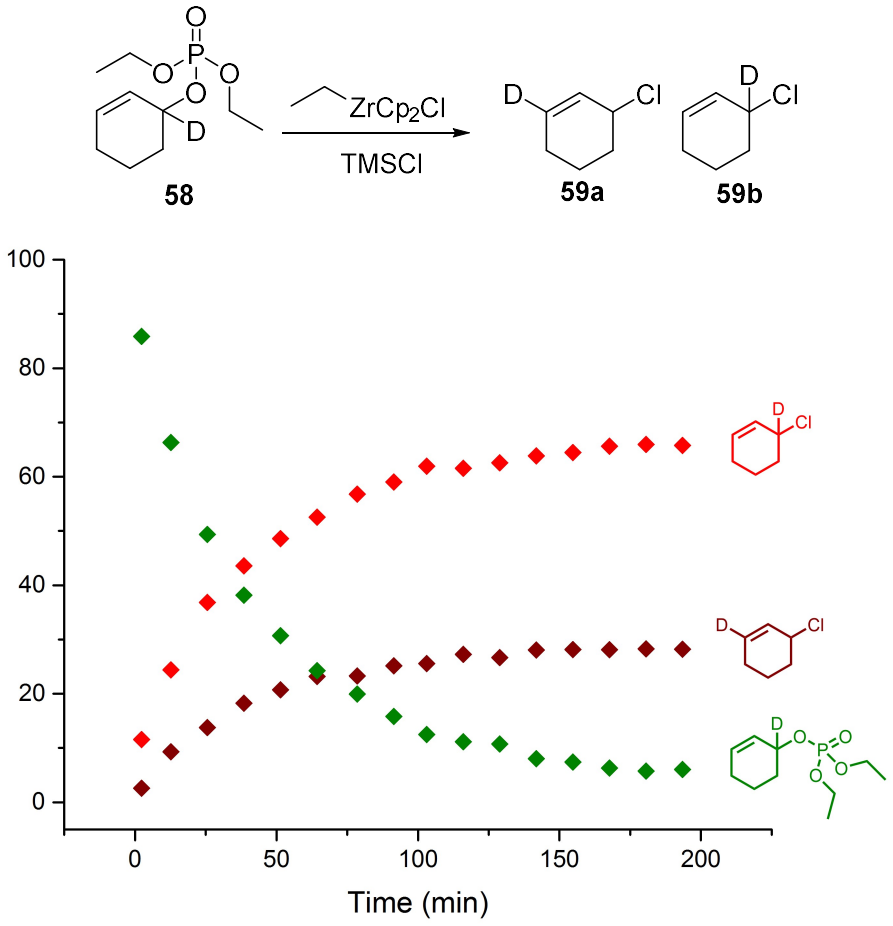

Figure 6.23. Reaction kinetics of D-allylphosphate 58 with TMSCl in the presence of $Cp_2ZrEtCl$ as monitored by ^2H NMR spectroscopy. Conditions: $Cp_2ZrEtCl$ (2.0 eq) in CH_2Cl_2, D-allylphosphate **58** (1.0 eq), TMSCl (1.0 eq) in CH_2Cl_2, room temperature.

Finally, we investigated the effect of CuI-**P** (10 mol%) on the formation of D-allylchlorides **59a** and **59b** from D-allylphosphate **58** by TMSCl (Figure 6.24). Without TMSCl, we did not observe the isomerisation of D-allylphosphate **58**, in agreement with previous observations. Upon the addition of TMSCl, rapid equal formation of D-allylchloride geminal isomer **59a** and β-deuterated isomer **59b** is observed within 5 min as well as traces amount of D-allyliodides **61a** and **61b**. Thus in the presence of CuI-**P**, the nucleophilic attack of TMSCl on D-allylphosphate **58** equally favours S_N2 and S_N2' pathways or once formed, CuI-**P** catalyses the S_N2' isomerisation of D-allylchlorides **59a** and **59b**, presumably through formation and subsequent *syn*-S_N2' racemisation of iodides **61a** and

61b. Direct S_N2' isomerisation of D-allylchlorides **59a** and **59b** is improbable as allylchloride **45b** was not observed to isomerise by EXSY. Reactions of TMSCl with D-allylphosphate **58** in the presence of CuI-**P** best fit the behaviour associated with formation of chlorides **59a** and **59b** in the AAA reaction (with and without TMSCl). Hence CuI-**P** mediates the formation of allylchlorides via S_N2 and S_N2' pathways.

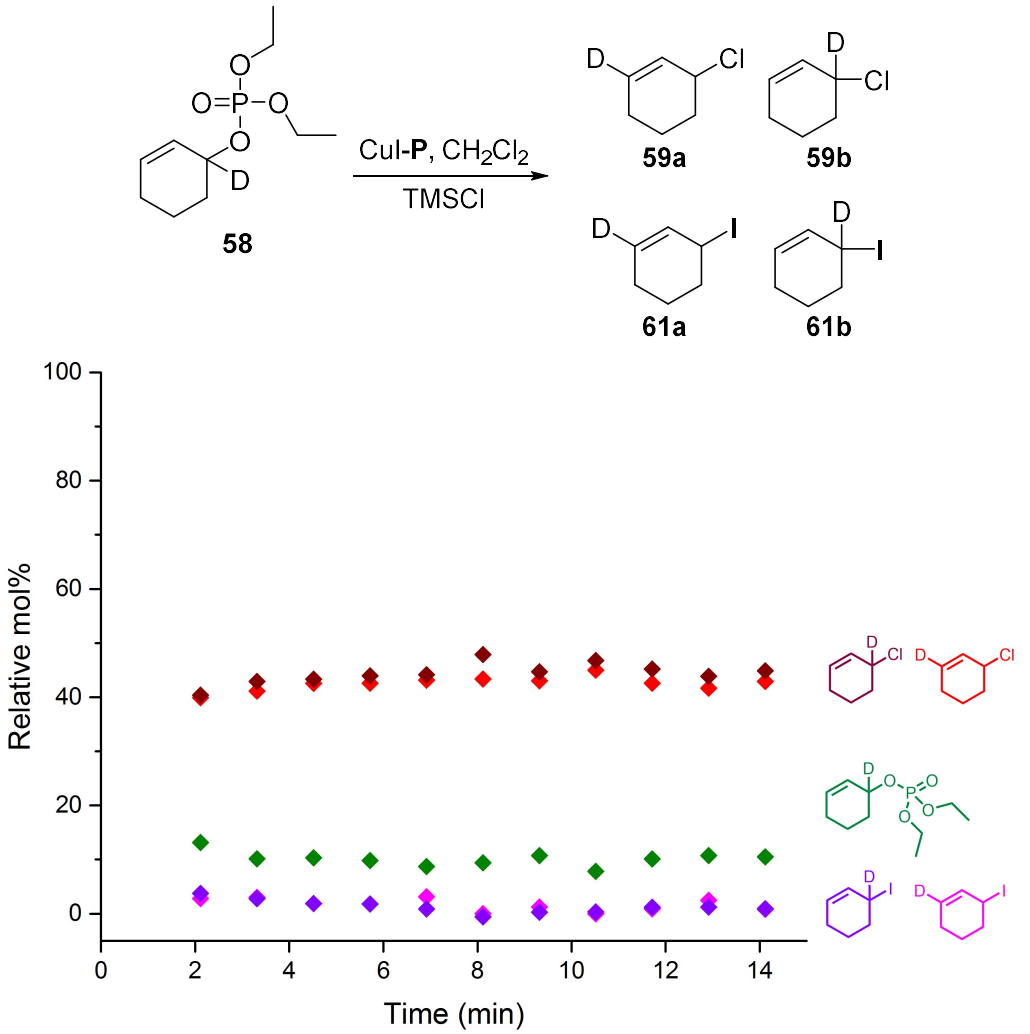

Figure 6.24. Reaction kinetics of D-allylphosphate 58 with TMSCl in the presence of CuI-P as monitored by ^{2}H NMR Spectroscopy. Conditions: CuI (10 mol%), **P** (10 mol%), D-allylphosphate **58** (1.0 eq), TMSCl (1.0 eq) in CH_2Cl_2, room temperature.

CONCLUSION AND PROPOSED MECHANISM

To conclude, we have shown that allylphosphate **57** is rapidly transformed (1 h) to allylchloride **45b** during the AAA of allylphosphate **57**, remarkably even in the absence of TMSCl (Scheme 6.2). Therefore, it would seem that allylchloride is the favoured substrate for the AAA of alkylzirconocenes. The origin of nucleophilic chloride in the absence of TMSCl remains elusive. However, surprisingly the AAA of allylphosphate **57** and the AAA of allylchloride **45b** may follow different mechanisms.

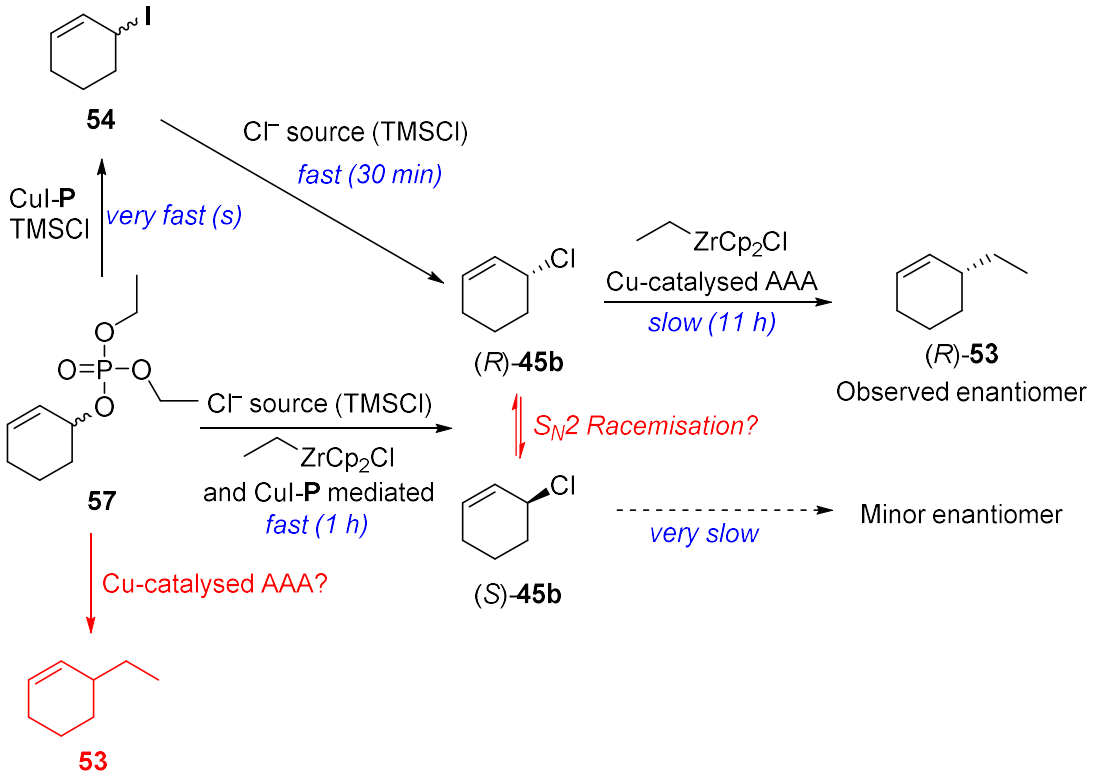

Scheme 6.2. Proposed mechanism of the AAA of alkylzirconocene to allylphosphate 57.

Indeed, contrary to the proposed mechanism of the AAA of allylchloride **45b**, we did not observe the constant presence of allyliodide **54** nor its S_N2' isomerisation by EXSY. However, allyliodide **54** was instantaneously formed and

then rapidly consumed within 30 min of the addition of allylphosphate **57**. We suspect initially the formation of allyliodide **54** is faster than allylchloride **45b** thus reaching its theoretical maximum of 10 mol%. We know that allyliodide **54** is not formed from the interaction of CuI-**P** and allylphosphate **57** alone and requires the presence of TMSCl and might also be influenced by the presence of $Cp_2ZrEtCl$. However, as the reaction progresses, the non-reversible formation of allylchloride **45b** from **57** was demonstrated and, also, the allyliodide **54** is probably transformed to allylchloride **45b**.

Many questions remain on the mechanism of the AAA of allylphosphate **57**. Such as, if the allyliodide **54** is not present throughout the reaction, how is the allylchloride **45b** racemising to achieve AAA with high ee? Throughout our studies, we did not observe the S_N2' isomerisation of allylchloride **45b** directly. In Chapter 5, we have dismissed the S_N2 racemisation of allyliodide **54** and allylchloride **45b** on the basis that cross-species S_N2 pathways were not observed. However, the AAA of allylphosphate **57** is a different system with different species present in the reaction thus it is conceivable that in this system, allylchloride **45b** is isomerising through S_N2 pathways only, providing direct racemisation of allylchloride **45b** (Scheme 6.3). At this point we do not have further evidence for the mechanistic pathway of the dynamic kinetic transformation of allylphosphate **57** to product **53** and a DYKAT pathway via a pseudo prochiral intermediate or a DET mechanism are also conceivable.

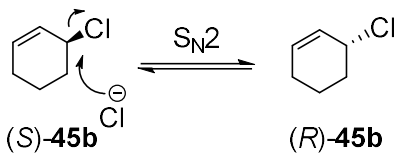

Scheme 6.3. Possible S_N2 racemisation mechanisms.

The study on the formation of allylchloride **45b** from allylphosphate **57** showed that the catalyst and the alkylzirconocene have a significant impact on the rate of their formation and their mechanistic pathways (S_N2 or S_N2'). $Cp_2ZrEtCl$ slows the formation of allylchloride **45b** with TMSCl and reverse its S_N2-S_N2' mechanistic selectivity. CuI-**P** not only catalyses the formation of allylchloride **45b**, it also mediates its formation through equal S_N2 and S_N2' selectivity, mimicking the observed behaviour of D-allylchloride **59** in the AAA of D-allylphosphate **58**. Therefore CuI-**P** and TMSCl play a crucial role in the mechanism of the AAA reaction beyond the catalytic formation of product. These observations highlight the hidden intrinsic components' interactions and their importance on the overall mechanism as well as a possible indirect evidence for the origin of the formation of allylchloride **45b** without TMSCl.

Another aspect of the AAA of allylphosphate **57** is whether or not allylphosphate **57** is reactive enough to undergo the AAA step. We did not observe any strong evidence either for or against this pathway and modelling of the system in the presence and in the absence of TMSCl suggests that AAA of allylphosphate **57** directly is disfavoured and slow. However, it is possible that some allylphosphate **57** react with the alkylzirconocene to give product **53**. Therefore, despite the fact that the AAA of allylphosphate **57** forms allylchloride **45b**, the mechanisms of the AAA of allylphosphate **57** and allylchloride **45b** diverge. This analysis emphasises the challenges of studying mechanisms and importance of limiting extrapolation between different systems due to the astonishing variability in mechanisms and the influence of the reaction environment.

CHAPTER 7

CU-CATALYSED ASYMMETRIC ALLYLIC ADDITION OF ALKYLZIRCONOCENES TO RACEMIC 3,6-DIHYDRO-2*H*-PYRANS

This chapter has been published in the Beilstein Journal of Organic Chemistry[5].

INTRODUCTION

Heterocycles are a frequent moiety found in pharmaceuticals compounds and natural products[250-252]. Tetrahydropyrans are also commonly used as synthetic intermediates[253]. However, the direct asymmetric derivatisation of pyrans is rare[254] and enantiomerically enriched tetrahydropyrans are often obtained by ring closing methods[255,256]. For example, Hoveyda described the Zr-catalysed kinetic resolution of derivatised-3,6-dihydro-2*H*-pyran obtained by ring closing metathesis[254]. Inspired by the success of our previous AAA methods (Chapter 5 and 6), we decided to examine the AAA of alkylzirconocene to racemic 3,6-dihydro-2*H*-pyrans **62** (Scheme 7.1).

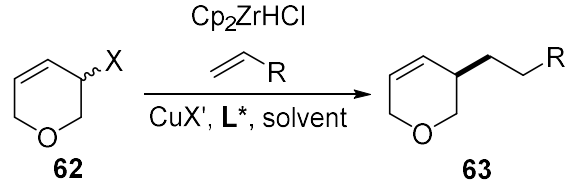

Scheme 7.1. AAA of alkylzirconocenes to racemic 3,6-dihydro-2*H*-pyran 62.

This method was envisaged to be challenging as the presence of the oxygen atom in the ring would modify the electronics and the reactivity of the starting material compared to carbocyclic systems. Moreover, due to the oxophilicity of the various reaction components[163], the oxygen lone pairs on 3,6-dihydro-2*H*-pyrans **62** could potentially interact with the Cu-catalyst or alkylzirconocene.

RESULTS AND DISCUSSION

We first examined the *in situ* hydrometallation/AAA of 4-phenyl-1-butene **16** to racemic 3-chloro-3,6-dihydro-2*H*-pyran **62a** (Table 7.1). No product was formed using our previous reported conditions[4] for AAA to racemic carbocyclic substrates (CuI, ligand **A**, $CHCl_3$, entry 1) and only unreacted starting material was recovered. Different Cu salts were examined (entries 2-7) and more strongly electron-withdrawing counterions were found to provide the desired product, with $CuClO_4$ giving the best ee (70% ee, entry 3).

Table 7.1. Asymmetric allylic alkylation to 3-chloro-3,6-dihydro-2*H*-pyran 62a.

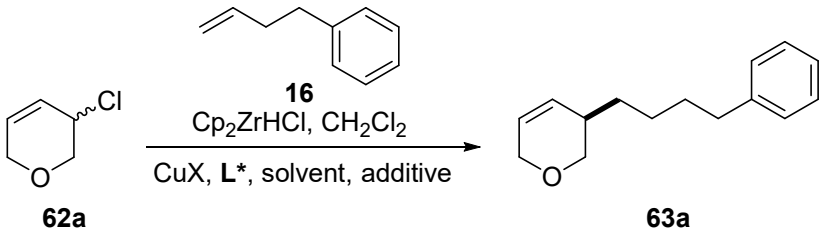

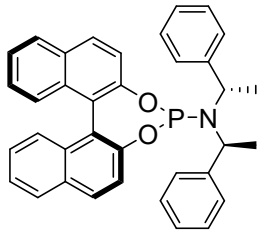

A

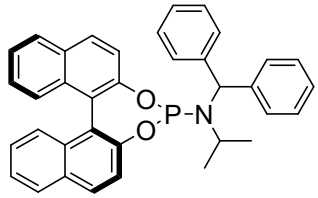

Q

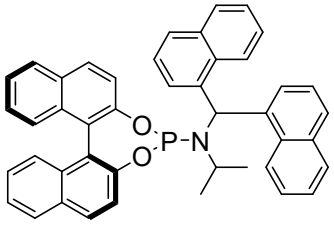

T

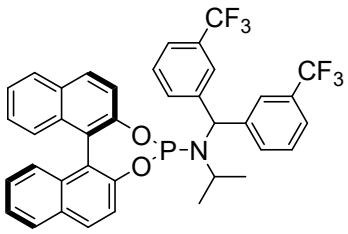

U

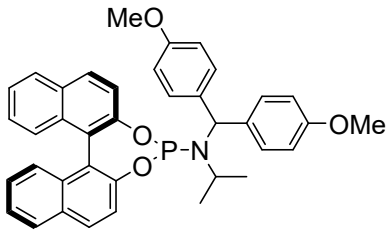

V

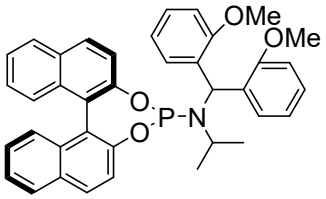

W

Entry	CuX	L*	Solvent	Additive	ee[§]
1	CuI	**A**	$CHCl_3$		**NP**
2	$CuClO_4$	**A**	CH_2Cl_2		**68%**
3	$CuClO_4$	**Q**	CH_2Cl_2		**70%**
4	CuOTf	**Q**	CH_2Cl_2		**64%**
5	$CuNTf_2$	**Q**	CH_2Cl_2		**52%**
6	CuTC	**Q**	CH_2Cl_2		**12%**
7	$CuSbF_6$	**Q**	CH_2Cl_2		**NP**
8	$CuClO_4$	**Q**	Et_2O		**55%**
9	$CuClO_4$	**Q**	Me-THF		**38%**
10	$CuClO_4$	**Q**	$CHCl_3$		**67%**
11	$CuClO_4$	**T**	CH_2Cl_2		**53%**
12	$CuClO_4$	**U**	CH_2Cl_2		**–36%**
13	$CuClO_4$	**V**	CH_2Cl_2		**–12%**
14	$CuClO_4$	**Q**	CH_2Cl_2	TMSCl	**73%**
15	$CuClO_4$	**Q**	CH_2Cl_2	$Si(OEt)_4$	**63%**
16	$CuClO_4$	**Q**	CH_2Cl_2	$Ti(OiPr)_4$	**25%**
17	$CuClO_4$	**Q**	CH_2Cl_2	$AlCl_3$	**15%**
18	$CuClO_4$	**Q**	CH_2Cl_2	$B(OiPr)_3$	**80%**
19	$CuClO_4$	**T**	CH_2Cl_2	$B(OiPr)_3$	**78%**
20	$CuClO_4$	**V**	CH_2Cl_2	$B(OiPr)_3$	**–47%**
21	$CuClO_4$	**W**	CH_2Cl_2	$B(OiPr)_3$	**–83%**

Conditions: 4-phenyl-1-butene **16** (2.5 eq), Cp_2ZrHCl (2.0 eq), CH_2Cl_2, allylchloride **62a** (1.0 eq), CuX (10 mol%), **L*** (10 mol%), additive (1.0 eq), in specified solvent, room temperature. [§]ee determined by HPLC. NP = no product.

A solvent screen lead us to the conclusion that chlorinated solvents give better results (CH_2Cl_2 (70% ee) and $CHCl_3$ (67% ee), entries 7 and 10 respectively). Extensive examination of phosphoramidite ligands (for example, entries 2 and 11-13) did not improve the ee. We then tested many additives (TMSCl, AgOTf, borates, $ZrCl_4$, $Si(OEt)_4$, etc.) (for examples, entries 14-18). Using $B(O\textit{i}Pr)_3$, which presumably acts as a Lewis acid, improved the ee to 80% (entry 18). We decided to re-examine different ligands using $CuClO_4$ in CH_2Cl_2 with $B(O\textit{i}Pr)_3$ (entries 19-21). Derivatives of ligand **Q** were tested and ligand **W** gave 83% ee (entry 21), while electronically similar **V** was much less selective (47% ee, entry 20). The effects of concentration (0.1-0.4 M), temperature (0-40 °C), catalyst loading (5-20 mol%), ligand to Cu ratio (0.5-2.0 eq of **L*** for 1.0 eq of Cu) and equivalent of $B(O\textit{i}Pr)_3$ (0.5-2.0 eq) were also investigated (not shown) with no improvement on the enantioselectivity.

Thus after extensive optimisation, the highest enantiomeric excess obtained was only 83% ee, so we decided to examine other leaving groups (Table 7.2). Like allylchloride **62a**, allylbromide **62b** gave no desired product when using our previously reported conditions[4] (entry 2) and only gave low ee with the conditions optimised above (38% ee, entry 1). Allylacetate **62c** did not give the desired product under any conditions examined, however, allylphosphate **62d** was found to provide product **63a** with good selectivity (77% ee, entry 5). 3,6-dihydro-2*H*-pyran-3-yl diethyl phosphate **62d** was also the only substrate to react using the all-carbon substrate AAA conditions (CuI, ligand **A**, $CHCl_3$)[4], albeit with poor enantioselectivity (29% ee, entry 6).

Table 7.2. Effect of the leaving groups.

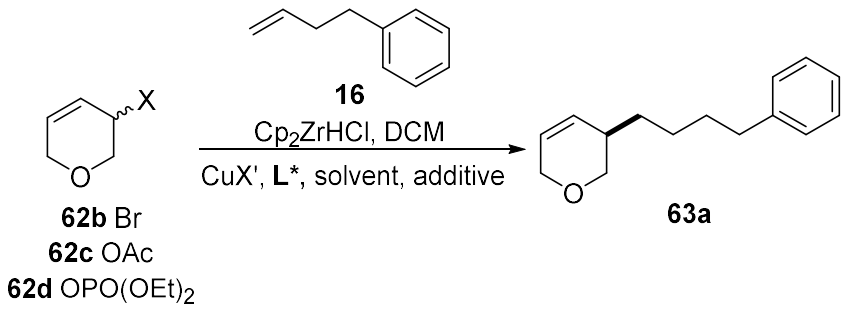

Entry	X	CuX'	L*	Solvent	Additive	ee[§]
1	Br	$CuClO_4$	**W**	CH_2Cl_2	$B(OiPr)_3$	**–38%**
2	Br	CuI	**A**	$CHCl_3$		**NP**
3	OAc	$CuClO_4$	**W**	CH_2Cl_2	$B(OiPr)_3$	**NP**
4	OAc	CuI	**A**	$CHCl_3$		**NP**
5	$OPO(OEt)_2$	$CuClO_4$	**W**	CH_2Cl_2	$B(OiPr)_3$	**–77%**
6	$OPO(OEt)_2$	CuI	**A**	$CHCl_3$		**29%**

Conditions: 4-phenyl-1-butene **16** (2.5 eq), Cp_2ZrHCl (2.0 eq), CH_2Cl_2, **62** (1.0 eq), CuX' (10 mol%), **L***(10 mol%), additive (1.0 eq), in specified solvent, room temperature. [§]ee determined by HPLC. NP = no product.

Design of experiments (DoE)[257-263] is a powerful tool for efficient screening and is commonly used in industry, since traditional one-factor-at-a-time optimisation poorly covers all potential conditions due to components' interactions. As DoE rapidly explores the response space efficiently and can reveal interdependence of factors at no extra experimental cost, we decided to setup a DoE for the optimisation of this complex asymmetric transformation using allylphosphate **62d**. We note that there are limits to this investigation as understanding what interactions give rise to asymmetric induction (particularly in transformations where mechanisms are not understood) is extremely challenging and it is not obvious how to parameterise the multiple variables present in key factors such as ligand structures[264].

A principal component analysis using JMP® 12.1.0 (SAS) was carried out using allylphosphate **62d**. In each factor, the most promising levels were chosen based on results from published methods[4,88,142,245], the conditions used for all

carbon allylphosphate (Chapter 6), the procedure optimised for allylchloride **62a** (above) and the results of previous waves.

The first wave was as a third factorial design with three categories: ligand (**A**, **Q**, **T**, **W** and **P**), counterion (ClO_4, I and OTf) and solvent (CH_2Cl_2, Et_2O and TBME) (entries 1-17, ●) (Figure 7.1). Neither CuI nor TBME were good fits for the reaction as both consistently gave low ee, 1-29% ee for CuI and 2-26% for TBME. The combination of CuOTf in CH_2Cl_2 gave the best enantioselectivity, up to 83% ee (entry 3) with ligand **P**. $CuClO_4$ did not give better ee with allylphosphate **62d** than the previously optimised conditions (77% ee, Table 7.2, entry 5). Et_2O gave mixed results with some low (e.g. 1% ee, entry 1) and moderate (e.g. 56% ee, entry 6) ee values obtained.

Based on those results, a second wave of DoE was designed as a 6th factorial design with 4 factors: ligand (**P**, **X**, **O** and **F**), counterion (OTf and NTf_2), solvent (CH_2Cl_2, Et_2O and $CHCl_3$) and TMSCl equivalent (0, 1 and 5) (entries 18-30, ◆). As mixed results were obtained with Et_2O, we decided to investigate it more thoroughly. This second study emphasises the intrinsic challenge of finding optimum conditions in complex asymmetric reactions. Whereas CuOTf seems to work best with CH_2Cl_2 as a solvent, $CuNTf_2$ gave better enantioselectivity in Et_2O. $CHCl_3$ consistently provided lower enantioselectivity than CH_2Cl_2. In the small selection of ligands examined, **P** generally gave the best results.

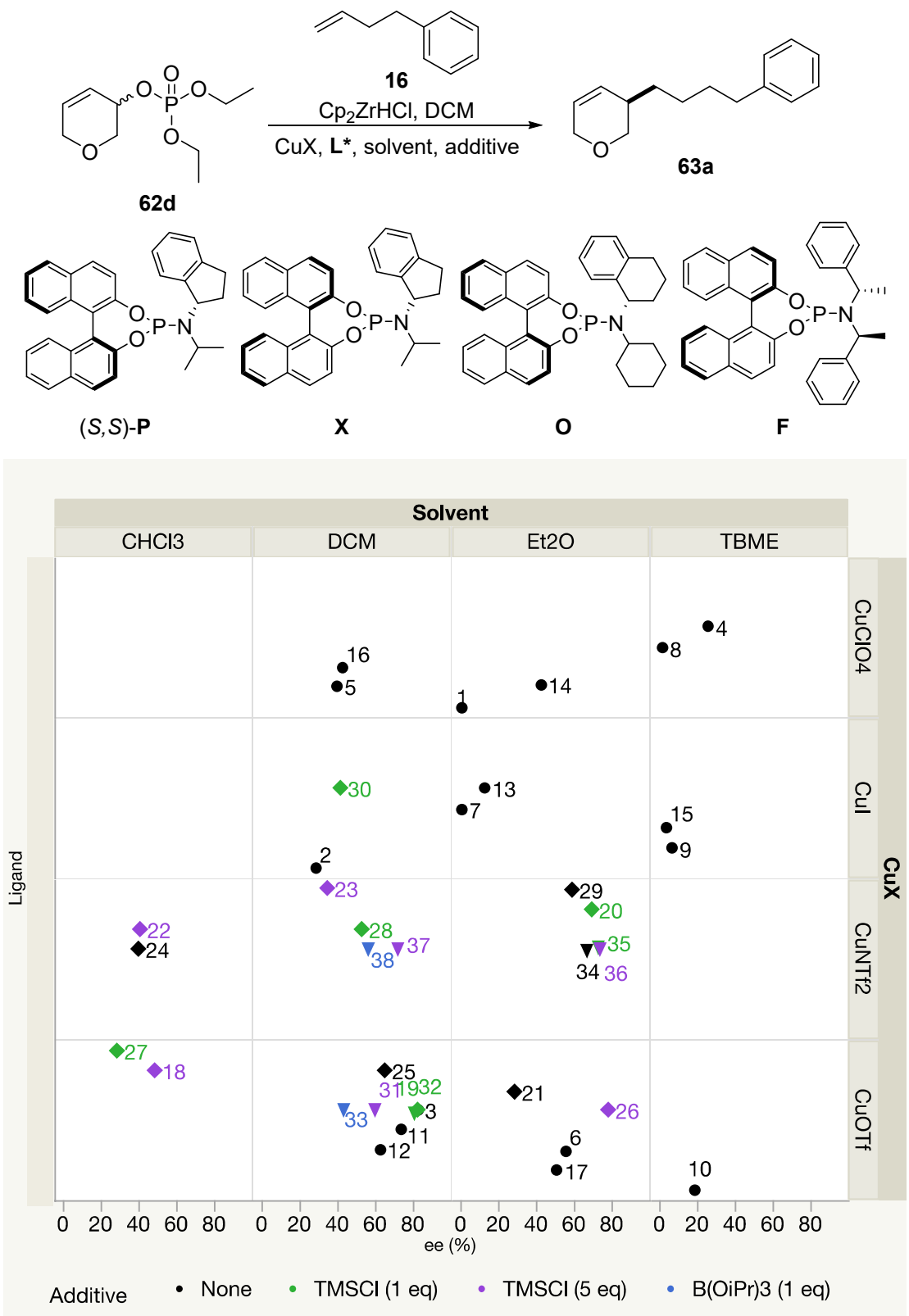

Figure 7.1. DoE from 3,6-dihydro-2*H*-pyran-3-yl diethyl phosphate 62d. Conditions: 4-phenyl-1-butene **16** (2.5 eq), Cp_2ZrHCl (2.0 eq), allylphosphate **62d** (1.0 eq), CuX (10 mol%), **L*** (10 mol%), additive (1.0 eq or 5.0 eq), in specified solvent, room temperature. ee determined by HPLC. ● (Wave 1, entries 1-17), ◆ (Wave 2, entries 18-30), ▼ (Wave 3, entries 31-38).

We designed a final study to investigate the role of various equivalents of additive (TMSCl and B(O*i*Pr)$_3$) with CuOTf and CuNTf$_2$ in their respective favoured solvents (CH_2Cl_2 and Et_2O) (entries 31-38, ▼). In this case, B(O*i*Pr)$_3$ significantly lowered the ee to 44% ee (entry 33) emphasising the synergy between B(O*i*Pr)$_3$ and $CuClO_4$ similar to TMSCl in etherated solvents. The influence of TMSCl on the reaction was highly dependent on the other reaction parameters. Indeed, CuNTf$_2$ in Et_2O with no additive gave 67% ee (entry 34), while adding 1.0 eq of TMSCl gave a slight improvement to 73% ee (entry 35) but no further improvement was observed by adding more TMSCl such as 5.0 eq which gave 74% ee (entry 36). On the other hand, using 1.0 eq of TMSCl with CuOTf in CH_2Cl_2 does not modify the ee (81% ee, entry 32), while adding 5.0 eq of TMSCl was detrimental to the ee, giving only 60% ee (entry 31).

Despite our efforts to optimise this second system, the highest enantioselectivity obtained was 83% ee. It became clear that when using alkylzirconocene nucleophiles in Cu catalysis, derivatised 3,6-dihydro-2*H*-pyrans are difficult to obtain in high ee. Moreover, both optimised systems gave poor yield: 25% yield with 100% conversion was obtained for allylchloride **62a** and 17% yield with 31% conversion for allylphosphate **62d**.

Various alkenes were examined using the allylchloride **62a** system (Scheme 7.2). The reaction showed tolerance to functional groups such as CF_3 in 75% ee (**63b**) Cl in 77% ee (**63c**) and cyclohexane in 88% ee (**63d**). Electron rich allylsilane could also be used to introduce a TMS group giving a high 93% ee (**63e**), but all the yields were poor.

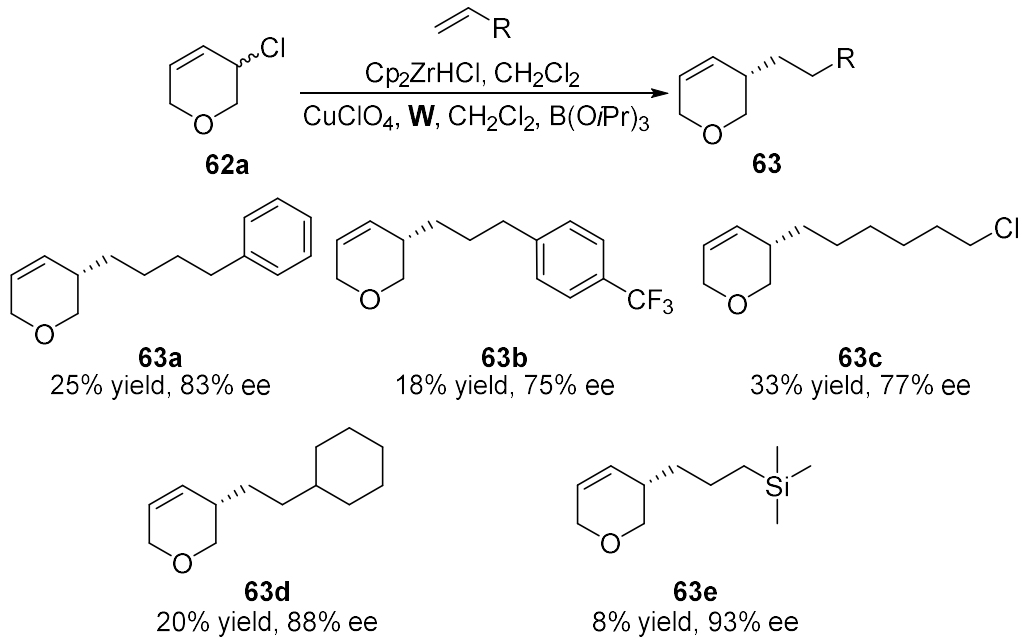

Scheme 7.2. Scope of nucleophiles. Conditions: alkene (2.5 eq), Cp_2ZrHCl (2.0 eq) in CH_2Cl_2, 3-chloro-3,6-dihydro-2*H*-pyran **62a** (1.0 eq), CuCl (10 mol%), $AgClO_4$ (11 mol%), **W** (10 mol%), B(O*i*Pr)3 (1.0 eq), in CH_2Cl_2, room temperature. Isolated yields. ee determined by HPLC or GC.

To investigate why we obtained such poor yields and possibly shed light into the reaction mechanism, we decided to follow both reactions in time using *in situ* ^{1}H NMR spectroscopy (Figures 7.2 and 7.3). Through these kinetic studies, it is clear that the allylchloride **62a** system fails because the starting material dimerises to give **64** as the major reaction product in 60% isolated yield (Figure 7.2). This is consistent with the observed full conversion but low product yields. Presumably dimer **64** arises from the homocoupling of allylchloride **62a** in the presence of a reductant. However, how a reductant can be formed *in situ* in these heterocyclic AAA remains elusive and would require further studies. Although both the conditions and leaving groups differ in the two reactions it is unclear why allylchloride **62a**, but not allylphosphate **62d** or allylchloride **45b** dimerises. Moreover, dimer **64** can exists as 3 isomers: a *meso* compound and two enantiomers. Upon comparison to literature data[265], we concluded that we form a mixture of all three as a 1:1:1 mixture of *meso* and racemic materials. Our

sample did not rotate the plane of the polarised light ($[\alpha]_D^{25}$ was 0), emphasising the racemic nature of the sample and suggesting that dimer **64** is formed through a completely non-selective pathway.

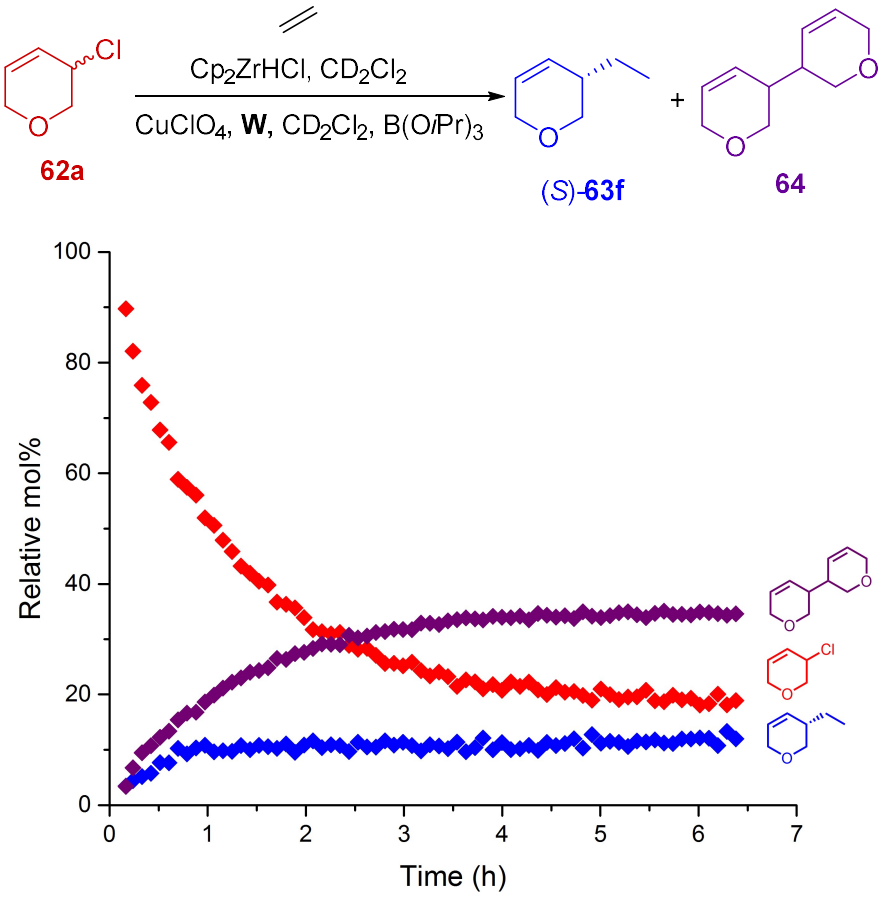

Figure 7.2. Reaction kinetics of allylchloride 62a monitored by ^{1}H NMR Spectroscopy. Conditions: ethylene (1 atm), Cp_2ZrHCl (2.0 eq) in CD_2Cl_2 then CuCl (10 mol%), $AgClO_4$ (11 mol%), **W** (10 mol%), 3-chloro-3,6-dihydro-2*H*-pyran **62a** (1.0 eq), $B(OiPr)_3$ (1.0 eq) in CD_2Cl_2, room temperature.

In the case of allylphosphate **62d**, the system appears to lack reactivity and the reaction quickly dies, so that product **63f** (Figure 7.3) is poorly. We speculate that over time the phosphate leaving group inhibits the catalyst which would explain why only 17% of product is formed.

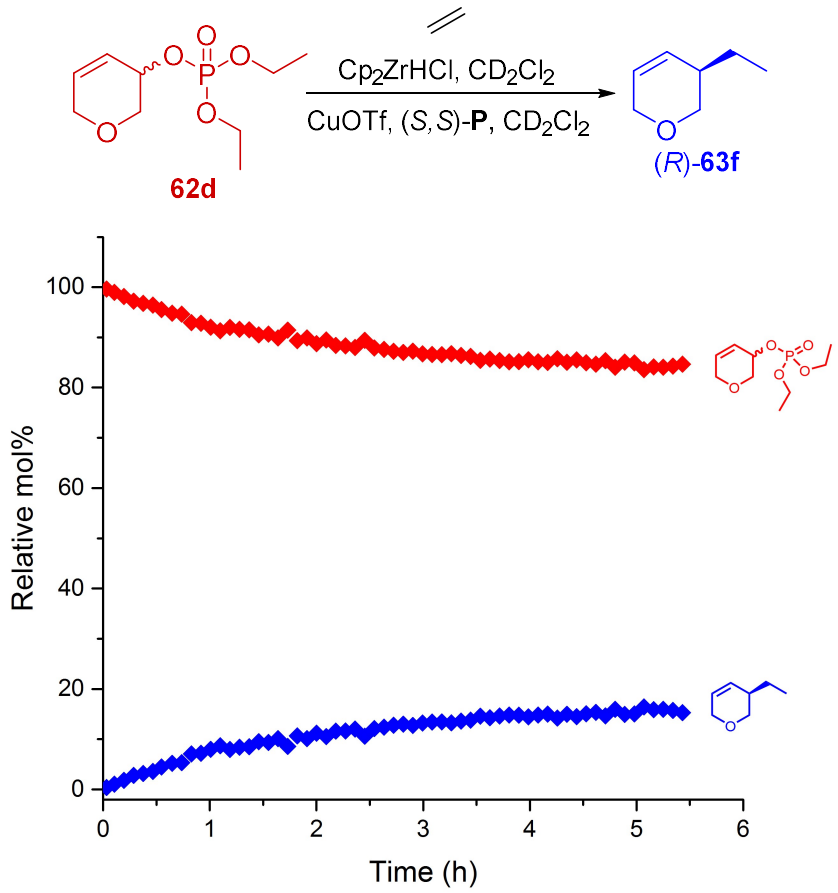

Figure 7.3. Reaction kinetics of allylphosphate 62d as monitored by ^{1}H NMR Spectroscopy. Conditions: ethylene (1 atm), Cp_2ZrHCl (2.0 eq) in CD_2Cl_2 then CuCl (10 mol%), AgOTf (11 mol%), (*S,S*)-**P** (10 mol%), 3,6-dihydro-2*H*-pyran-3-yl diethyl phosphate **62d** (1.0 eq) in CD_2Cl_2, room temperature.

To obtain further mechanistic information we followed the ee of these reactions in time (Figure 7.4 and 7.5). In the system using allylchloride **62a**, the ee of product **63a** remains constant throughout the reaction (~78% ee, Figure 7.4). Starting allylchloride **62a** was found to be quite stable so that we could also determine its enantiomeric excess during the course of the reaction. Initially allylchloride **62a** is racemic but becomes scalemic to reach 34% ee at completion (~12 hours). From these observations and our experimental observation that allylchloride **62a** is much more stable than all-carbocyclic **45b**, it appears that allylchloride **62a** undergoes kinetic resolution. However, this system is clearly complicated by the fact that the majority of allylchloride **62a** is consumed during the by-product **64** formation.

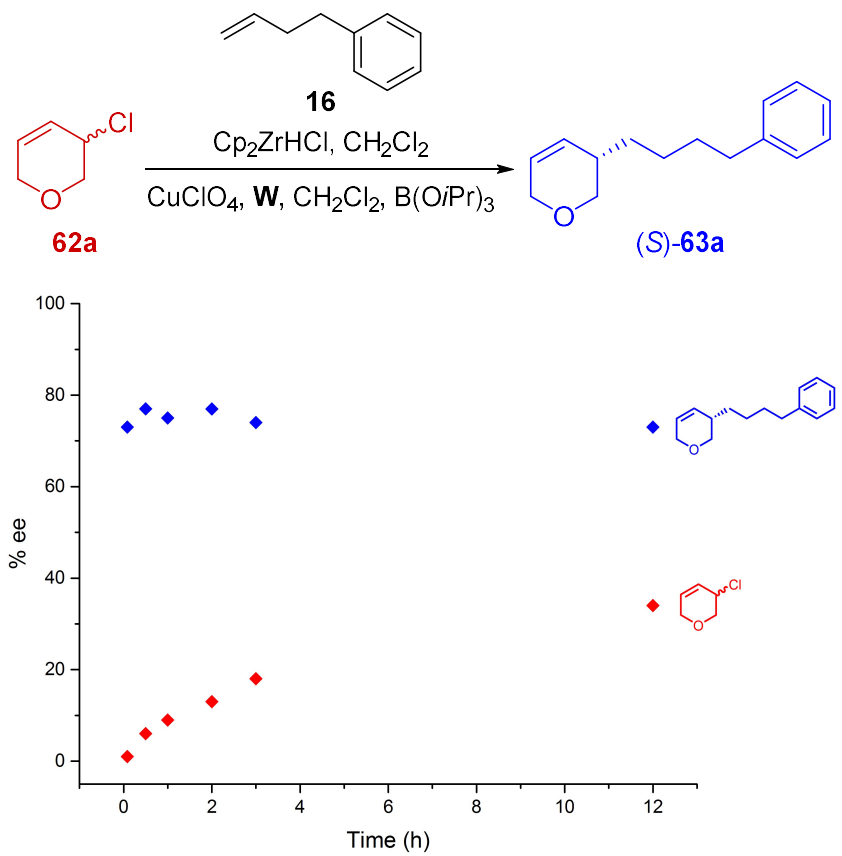

Figure 7.4. Kinetic ee analysis using allylchloride 62a. The ee were measured by aliquot samplings of the same reaction. Conditions: 4-phenyl-1-butene **16** (2.5 eq), Cp_2ZrHCl (2.0 eq) in CH_2Cl_2 then CuCl (10 mol%), $AgClO_4$ (11 mol%), **W** (10 mol%), 3-chloro-3,6-dihydro-2*H*-pyran **62a** (1.0 eq), $B(OiPr)_3$ (1.0 eq) in CH_2Cl_2, room temperature.

In the phosphate system based on allylphosphate **62d**, the ee of product **63a** was found to increase during the course of the reaction (Figure 7.5) so that **63a** was 26% ee after a few minutes and increase to 82% ee after 5 hours. Unfortunately, analytical conditions to separate the enantiomers of allylphosphate **62d**, so we could measure the enantiomeric excess of this starting material, could not be found.

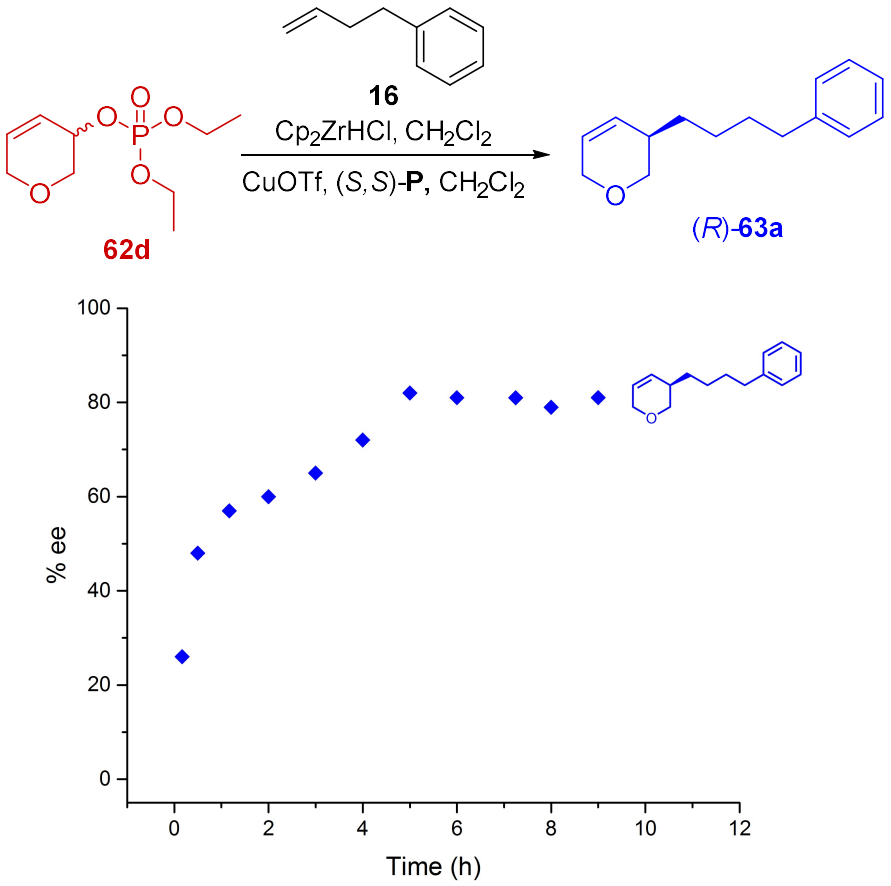

Figure 7.5. Kinetic ee analysis using allylphosphate 62d. The ee were measured by aliquot samplings of the same reaction. Conditions: 4-phenyl-1-butene **16** (2.5 eq), Cp_2ZrHCl (2.0 eq) in CH_2Cl_2 then CuCl (10 mol%), AgOTf (11 mol%), (*S,S*)-**P** (10 mol%), 3,6-dihydro-2*H*-pyran-3-yl diethyl phosphate **62d** (1.0 eq) in CH_2Cl_2, room temperature.

CONCLUSION

The Cu-catalysed AAA of alkylzirconium reagents to racemic heterocyclic electrophiles was explored. After extensive examination, two different methods for obtaining 3,6-dihydro-2*H*-pyran derivatives **63** with respectable 83% ee were developed. Unfortunately, the yields were poor in both cases. Kinetic studies were performed to help understand the difficulties associated with these reactions. At this stage it is not possible to provide a full mechanistic rationalisation of these reactions. It is also not immediately obvious how to

improve yields and enantiomeric excesses. The kinetic studies suggest that the two reactions work through very different mechanisms, revealing remarkable mechanistic diversity in Cu-catalysed asymmetric alkylation reactions in seemingly equivalent reactions.

CHAPTER 8

MECHANISTIC NMR STUDIES OF AN ASYMMETRIC CONJUGATE ADDITION BY CU-PHOSPHORAMIDITE COMPLEXES USING ORGANOZIRCONOCENES AS NUCLEOPHILES.

I would like to thank Kilian Garrec for providing $Cp_2ZrMeCl$, the pure isolated products and deuterated compounds as well as interesting discussion and suggestions. A manuscript on this chapter is in preparation.

INTRODUCTION

Cu-catalysed asymmetric conjugate additions (Cu-ACA) have been widely developed and a mechanism has been commonly accepted for all conditions (Cu counterions, organometallic nucleophiles, solvent, temperature etc.)[2,37,189,230] as described in Chapter 1. However when looking more in detail, many different pre-catalytic complexes, nucleophiles complexes and complexing to enones have been described (Schemes 8.1, 8.2, 8.3).

With Grignard reagents, Feringa[189] proposed a mixed Cu-Mg complex with transmetallation of the R group from Mg to Cu (Scheme 8.1). The authors observed that this complex requires a bromide ion, either from the Grignard or the Cu to carry out the reaction in high ee and yield. Upon addition of the enone, the Mg act as a Lewis acid and the Cu interacts with the olefin through d-π* back donation.

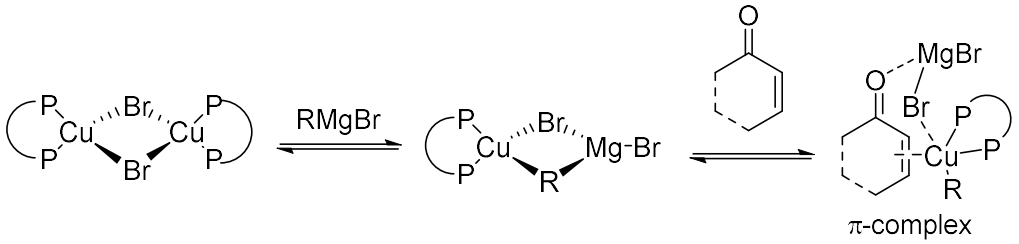

Scheme 8.1. Proposed pre-catalytic, catalytic and enone complexes using Grignard reagents[189].

In the case of cuprates (Scheme 8.2), Cu and Li are known to form complex lattices[37,266-269]. Their interaction to the enone, even though electronically similar to the π-complex previously described, is more intricate, where the cuprate is believed to act as a Lewis acid and is involved in double coordination to the oxygen atom *via* Li atoms. A twice transmetallated Cu^{III} species coordinates to the olefin while also forming a σ-bond at the 1,4-addition site. The study seems to suggest that no π-complex is formed.

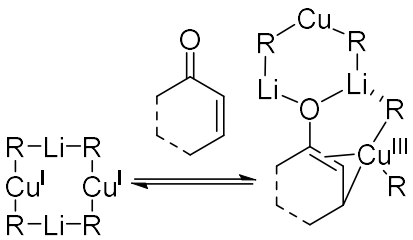

Scheme 8.2. Proposed pre-catalytic, catalytic and enone complexes using cuprates[37].

Finally Gschwind thoroughly investigated pre-catalytic and catalytic species with dialkylzinc nucleophiles[230] (Scheme 8.3). Zn also forms intricate dual-metal catalytic complexes involving the counterions with transmetallation of one of the R groups to Cu. The transmetallated Cu interact with the olefin, while Zn acts as a Lewis acid to facilitate the reductive elimination. In this case,

Zn is associated to an extended $Cu_2L_3X_2R$ complex bimolecular in Cu, forming large aggregates with the enone.

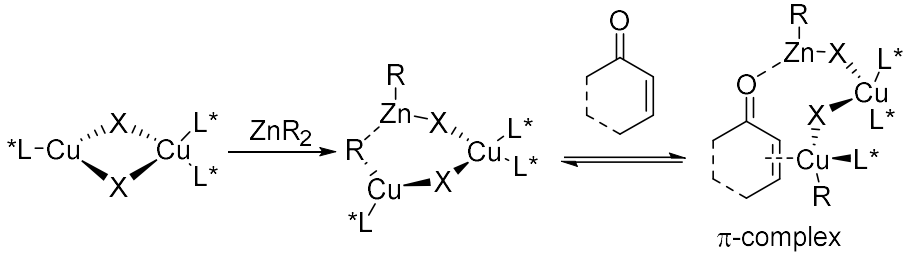

Scheme 8.3. Proposed pre-catalytic, catalytic and enone complexes using dialkylzinc reagents[230].

Despite all the Cu-ACA methodologies published and numerous mechanistic speculations, physical proof of catalytic species and intermediates in solution is scarce. And to the best of our knowledge only Gschwind[188] and Feringa[189] carried out extensive studies on Cu-ACA. Gschwind performed many elegant studies on Cu-phosphoramidite complexes, notably in the case of the conjugate addition of diorganozinc[230] and thoroughly investigated the effect of Cu salt, solvent and ligand in pre-catalytic complexes. These studies emphasise the importance of investigating a system with the exact same conditions in the NMR, as in a flask, in order to obtain genuinely useful mechanistic information.

We wanted to gain insight into the mechanism of our published Cu-ACA method using alkylzirconocenes[245,270] (Scheme 8.4). Based on the success of our NMR studies on asymmetric allylic alkylation (AAA) systems[5,271] (Chapter 5, 6, 7), we decided to carry out extensive NMR studies on this ACA.

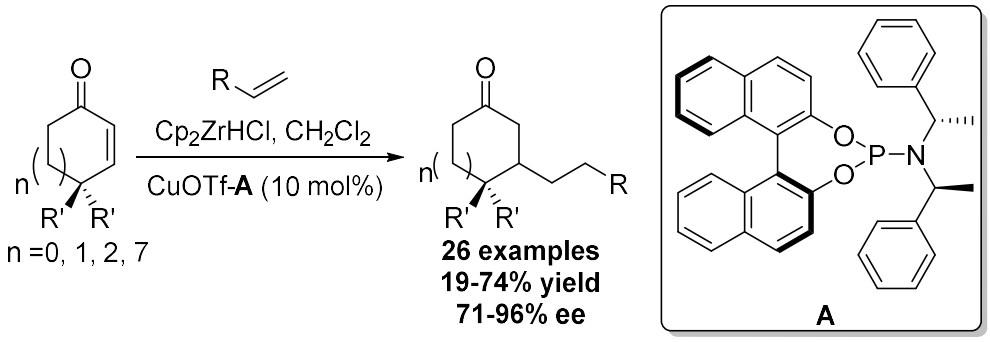

Scheme 8.4. Catalytic asymmetric conjugate addition using alkylzircononcenes[245].

One of the challenges we had to face was that Et_2O-d_{10} is excruciatingly expensive and thus could only see limited use. However, CH_2Cl_2 showed promising results in the presence (35% yield, 85% ee (entry 4, Table 8.1)) or absence of TMSCl (35% yield, 81% ee (entry 1))[36,85], comparable to Et_2O (entry 2 and 5). 5.0 eq of TMSCl seems to be optimal for the system as 1.0 eq only gave 20% yield, 78% ee in CH_2Cl_2 (entry 3). In a more recently developed system[270], CH_2Cl_2 also showed good results with good 58% yield and good 76% ee (entry 6) comparable to Et_2O (21% yield, 91% ee, entry 7)[270]. Bearing in mind that solvent has an important impact on mechanistics[5,230], we still decided to perform the mechanistic study in CD_2Cl_2 and correlate them to a minimal number of experiments in Et_2O.

Table 8.1. Effect of solvent and additive.

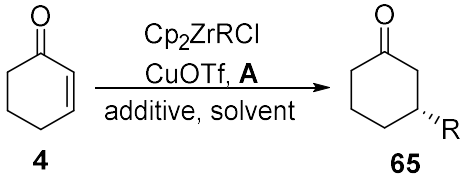

4 **65**

Entry	R	Solvent	Additive	Yield (%)*	ee (%)§
1	-$(CH_2)_4$-Ph	CH_2Cl_2	-	35	81
2	-$(CH_2)_4$-Ph	Et_2O	-	37	79
3	-$(CH_2)_4$-Ph	CH_2Cl_2	TMSCl (1 eq)	20	78
4	-$(CH_2)_4$-Ph	CH_2Cl_2	TMSCl (5 eq)	35	85
5	-$(CH_2)_4$-Ph	Et_2O	TMSCl (5 eq)	59	90
6	-CH_3	CH_2Cl_2	TMSCl (5 eq)	58	76
7	-CH_3	Et_2O	TMSCl (5 eq)	21	91

Conditions: Entries 1-5: 4-phenyl-1-butene **16** (2.5 eq), Cp_2ZrHCl (2.0 eq) in CH_2Cl_2, $(CuOTf)_2{\cdot}PhH$ (5 mol%), ligand **A** (10 mol%), cyclohex-2-en-1-one **4** (1.0 eq), TMSCl (as specified), in specified solvent, room temperature. Entries 6-7: $Cp_2ZrMeCl$ (1.7 eq) in CH_2Cl_2, CuCl (10 mol%), AgOTf (11 mol%), ligand **A** (10 mol%),cyclohex-2-en-1-one **4** (1.0 eq), TMSCl (as specified), in specified solvent, room temperature. *Isolated yield. §ee determined by HPLC.

RESULTS AND DISCUSSION

In situ ^{1}H NMR spectroscopy Kinetics without TMSCl

We first followed the Cu-ACA reaction *in situ* using ^{1}H NMR spectroscopy without TMSCl for simplification of analysis. In the normal set-up, different enones gave similar ees and yields[245,270] and could be tested using NMR kinetics without modification to the mechanism (Scheme 8.5).

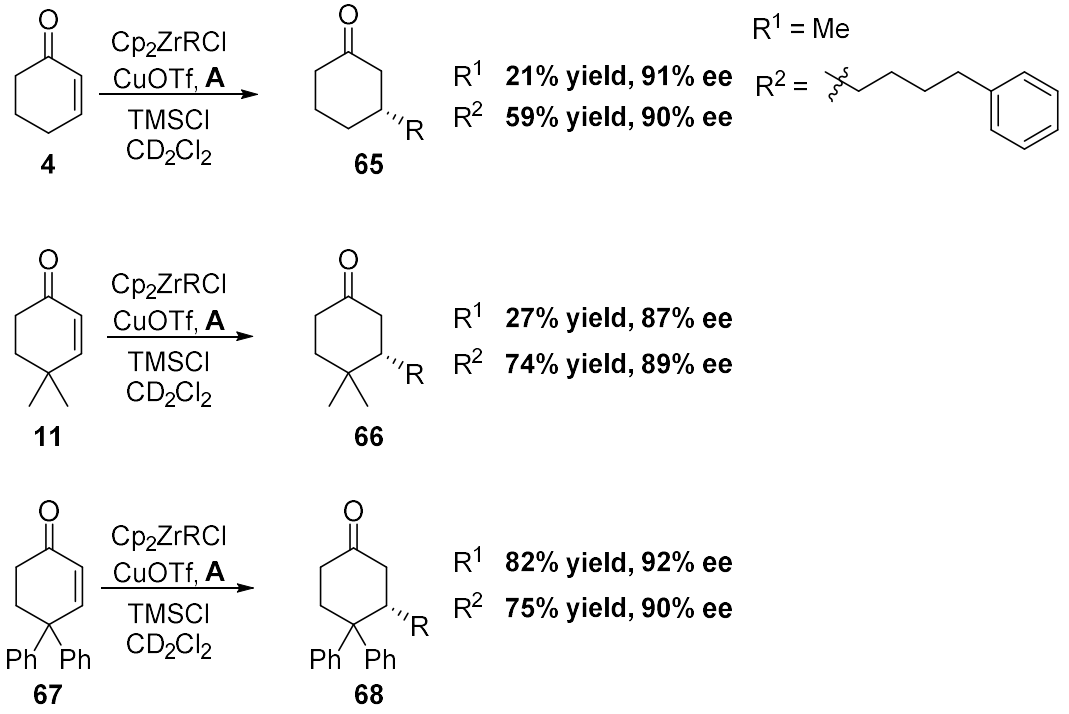

Scheme 8.5. Scope of enone. R=-$(CH_2)_4$-Ph Conditions: 4-phenyl-1-butene **16** (2.5 eq), Cp_2ZrHCl (2.0 eq) in CH_2Cl_2, $(CuOTf)_2$·PhH (5 mol%), ligand **A** (10 mol%),enone **4**, **11** or **67** (1.0 eq), TMSCl (5.0 eq) in Et_2O, room temperature. R=Me Conditions: $Cp_2ZrMeCl$ (1.7 eq) in CH_2Cl_2, CuCl (10 mol%), AgOTf (11 mol%), ligand **A** (10 mol%), enone **4**, **11** or **67** (1.0 eq), TMSCl (5.0 eq), in Et_2O, room temperature. Isolated yield. ee determined by HPLC.

In order to simplify the setup and NMR analysis, we decided to use $Cp_2ZrMeCl$ as the nucleophile. Using $Cp_2ZrMeCl$ also results in simpler ^1H NMR spectra then when using longer chains, limiting coupling and reducing the number of signals. Furthermore once $Cp_2ZrMeCl$ is synthesised[270], no further modification is required and can be used directly as opposed to hydrozirconated alkenes which have to be prepared fresh. Nonetheless, some tests were carried out with $Cp_2ZrEtCl$ obtained from the hydrozirconation of ethylene depending on the availability of $Cp_2ZrMeCl$.

The ACA of enones **4** and **11** were highly difficult to monitor by *in situ* ^1H NMR spectroscopy due to overlapping signals of the starting materials **4** or **11** and the products **65** or **66**. However, enone **67** gave clean resolved signals with

minimal overlap for effective kinetic monitoring by ^{1}H NMR spectroscopy (Figure 8.1).

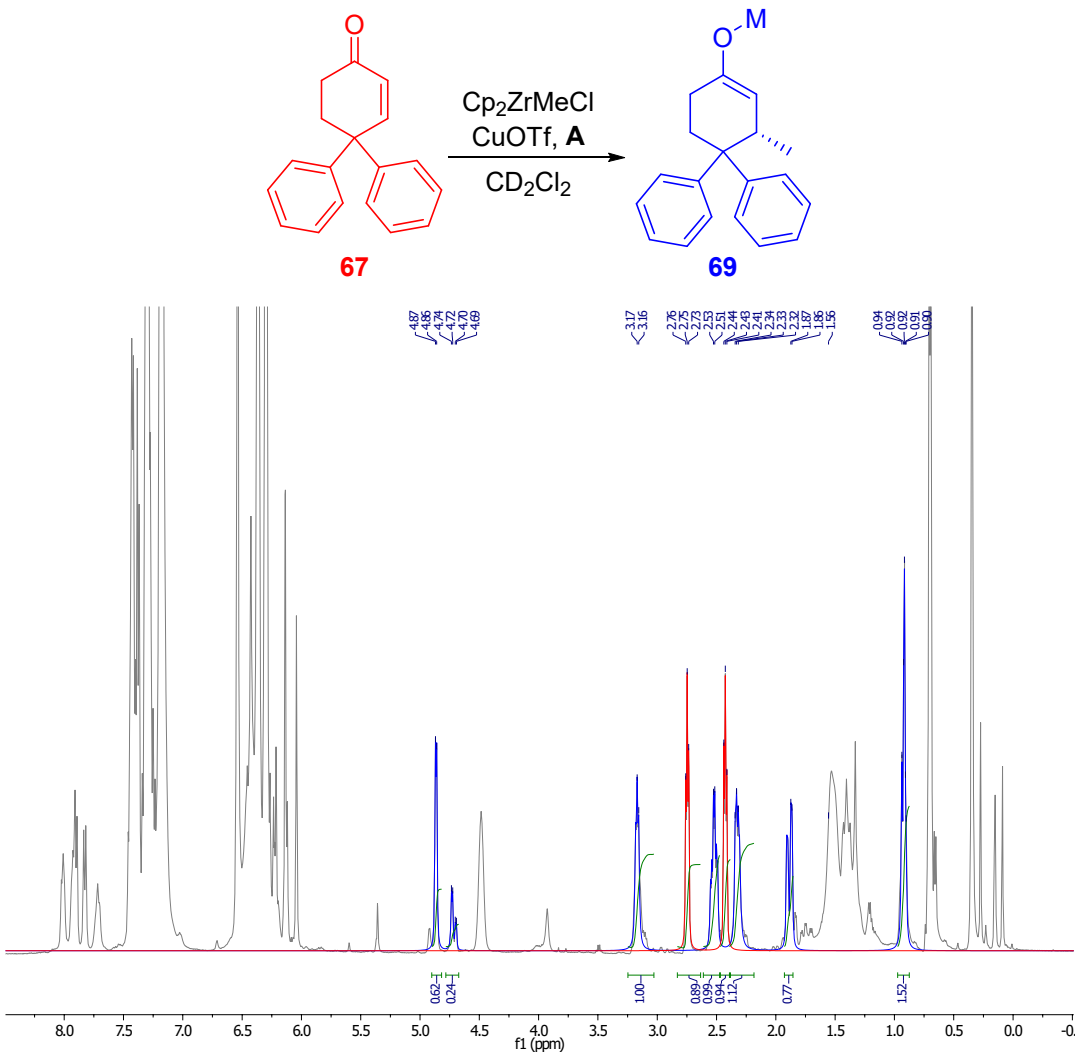

Figure 8.1. Example of a ^{1}H NMR during kinetics. Conditions: $Cp_2ZrMeCl$ (1.7 eq) in CD_2Cl_2, CuCl (20 mol%), AgOTf (22 mol%), ligand **A** (20 mol%), 4,4-diphenyl-2-cyclohexen-1-one **67** (1.0 eq), in CD_2Cl_2, room temperature. Product **69** is shown in blue and starting material **67** in red.

During these experiments we observed the disappearance of enone **67** (in red) and the formation of two unknown species (in blue), which were not product **68**. The unknown species had a ^{1}H signals at 4.86 and 4.73 ppm, a characteristic shift of alkenes. Through *in situ* characterisation by COSY, HSQC

and NOESY we determined that two products were formed in a 78:22 ratio and that they were most likely enolates **69**.

The only divergence between the normal setup and the NMR setup was the lack of work-up. If products **69** were indeed enolate they would, on work-up, give isolated product **68**. In order to further validate their identity, we added 1.0 eq of H_2O to the Cu-ACA at completion (Figure 8.2). Figure 8.2 clearly shows that the NMR product **69** (black) is instantaneously transformed upon addition of H_2O (blue). The new signals resemble those of the isolated 1,4-addition product **68** (red). Thus the products we observed in the *in situ* NMR kinetic ACA represents the true product of the ACA and evidence suggests they are enolates.

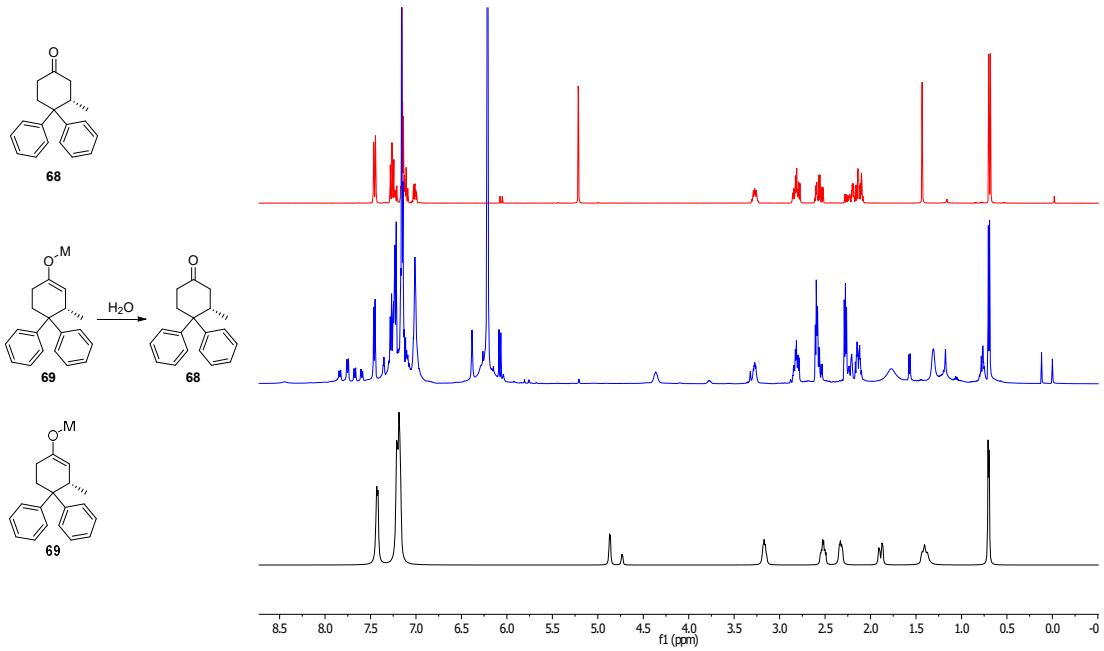

Figure 8.2. Comparison of the isolated signal of the enolate **69** (black), the NMR product upon addition of H_2O (1.0 eq) (blue) and the isolated 1,4-addition product **68** (in flask with standard work-up and flash chromatography) (red).

Despite our best efforts, COSY, NOESY and HMBC correlations did not reveal the exact nature of the entities present on the oxygen and thus remain elusive. We speculate that the major enolate is most likely zirconium enolate **69a**

(78%) (Figure 8.3). Zr is notorious for its oxophilicity[163] and DFT calculations by Prof. Robert Paton predicted that in these conditions[272], the zirconium enolate **69a** would be formed[36]. We speculate that the minor enolate species is Cu-enolate **69b**. As ~20% of this species was observed, it would seem that Cu-enolate **69b** is primarily formed and then Cu is displaced to form the Zr-enolate **69a**, for the catalytic turnover. The exact nature of the substituents on Zr or Cu is unknown, simple enolate such as $ZrCp_2(Cl)$ or Cu-**A** are possible as well as mixed Cu-Zr enolates or modified substituents on Zr or Cu. Unfortunately, *in situ* attempts at synthesising $ZrCp_2(Cl)$ enolate **69a**[273] or Cu-**A** enolate **69b**[274] for comparison were unsuccessful.

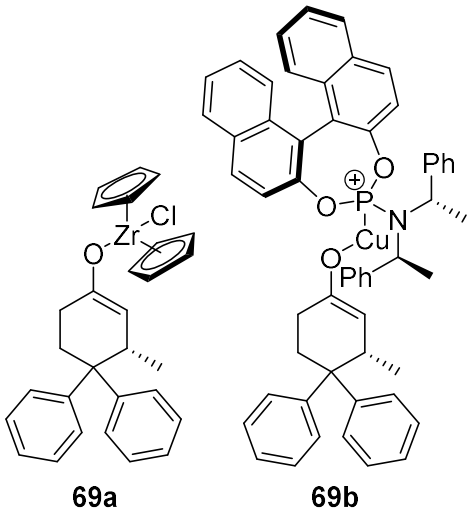

Figure 8.3. Structure of the proposed Zr-enolate 69a and Cu-enolate 69b products.

A kinetic overview could be drawn (Figure 8.4) by *in situ* ^{1}H NMR and shows the clean conversion of enone **67** to enolate **69**. In order to check for consistency within the ^{1}H NMR signals, we decided to plot each of the resolved signals of enolate **69** (Figure 8.4a). We were pleased to see that even though some divergences were observed, the standard deviation between the signal was

small (Figure 8.4b). The integration differences between the enolate proton (in green) and the rest of the signals can be attributed to the slower relaxation of ^{1}H on sp^{2}-hybridised centres[275]. This observation strengthens the idea that the product is enolate **69**, as the ^{1}H signals were calibrated accordingly and the data is coherent. The reaction reached completion in 5 h with a half-life of 1 h.

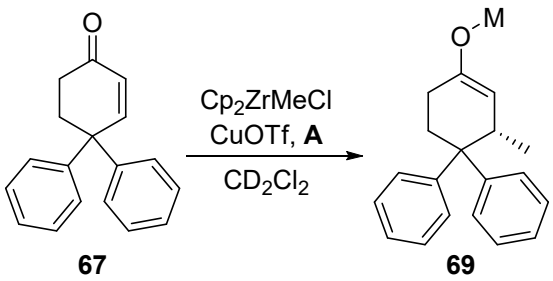

67 **69**

a)

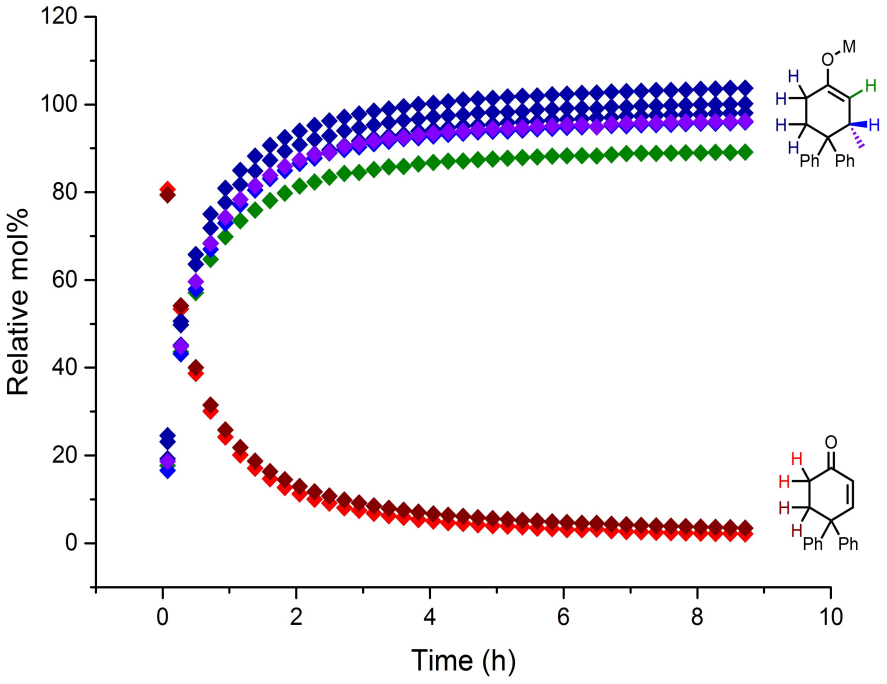

b)

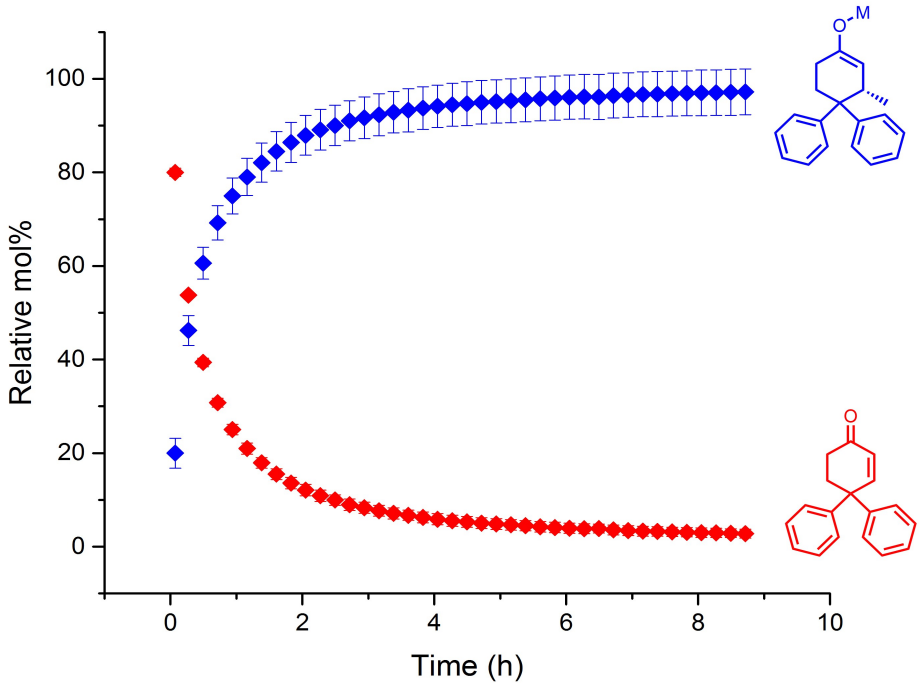

Figure 8.4. Reaction kinetics as monitored by in situ ^{1}H NMR spectroscopy from 4,4-diphenyl-2-cyclohexen-1-one 67. a) Reaction kinetic of all resolved signal. b) reaction kinetic with standard deviation as error bars. Conditions: $Cp_2ZrMeCl$ (1.7 eq) in CD_2Cl_2, CuCl (10 mol%), AgOTf (11 mol%), ligand **A** (10 mol%), 4,4-diphenyl-2-cyclohexen-1-one **67** (1.0 eq), in CD_2Cl_2, room temperature.

In situ ^{1}H NMR spectroscopy kinetics with TMSCl

Similarly, we followed the Cu-catalysed ACA of alkylzirconocene in CD_2Cl_2 with TMSCl using *in situ* ^{1}H NMR spectroscopy (Figure 8.5). During this experiment we observed the conversion of enone **67** to a major new unknown species (95%). A small amount of what we identified as the zirconium enolate **69a** was also observed but none of what we believe was the Cu-enolate **69b** was found. The unknown product was characterised *in situ* using COSY, NOESY, HSQC and HMBC correlations and was transformed to the isolated 1,4-addition product **68** upon addition of H_2O (1.0 eq). We identify this unknown product as TMS-enolate **69c** with a characteristic enolate ^{1}H signal at 5.20-5.15 ppm, similar to the reported isolated enolate 1-trimethylsiloxy-4,4-diphenylcyclohexene[276].

Thus, in the presence of TMSCl, the formation of the TMS-enolate **69c** is favoured over the zirconium enolate **69a** and the Cu-enolate **69b** (TMS:Zr:Cu 95:5:0).

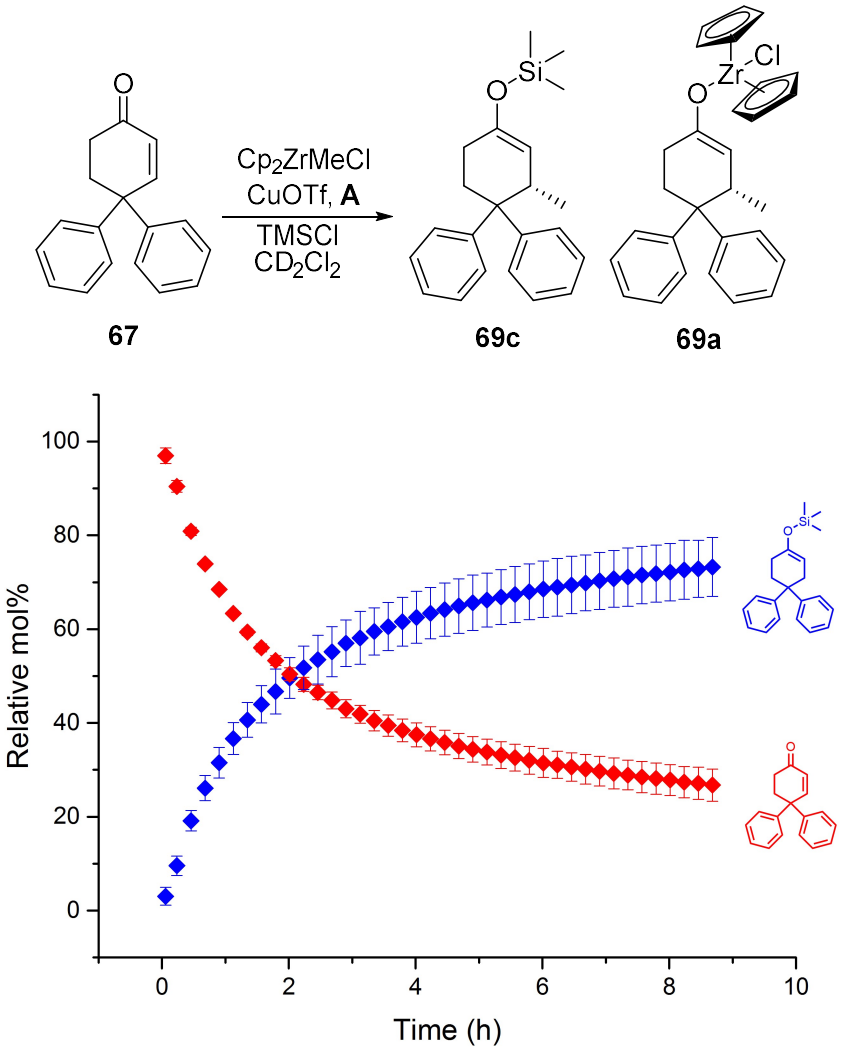

Figure 8.5. Reaction kinetics with TMSCl as monitored by in situ ^{1}H NMR spectroscopy from 4,4-diphenyl-2-cyclohexen-1-one 67. The errors bars are the standard deviation of all the observed, non-overlapping signals. Conditions: $Cp_2ZrMeCl$ (1.7 eq) in CD_2Cl_2, CuCl (10 mol%), AgOTf (11 mol%), ligand **A** (10 mol%), 4,4-diphenyl-2-cyclohexen-1-one **67** (1.0 eq), TMSCl (5.0 eq) in CD_2Cl_2, room temperature.

Similarly to the ^{1}H NMR kinetics without TMSCl (Figure 8.4), in the reaction with TMSCl (Figure 8.5), the resolved ^{1}H peaks of starting enone **67** and enolate **69c** are internally consistent, with small errors. However, the ACA of alkylzirconocenes in CD_2Cl_2 with TMSCl did not reach completion in the NMR tube despite multiple attempts. It has been commonly observed that this ACA

system is unpredictable in CH_2Cl_2 whereas it is highly robust in Et_2O, justifying the lack of full conversion in the NMR setup. When compared to the ACA without TMSCl (Figure 8.4), the ACA seems much slower with TMSCl, reaching half conversion at 2 h rather than 40 min without TMSCl, again emphasising the unusual deceleration of the kinetic rate by TMSCl in these systems (Chapter 6).

Stoichiometric studies using achiral CuBr·DMS without ligand or TMSCl in CD_2Cl_2 show the reaction favours a different enolate, so that Zr enolate **69a** is the minor (93:7) species, but the reaction conversion was poor (18%). The new enolate however shows different ^{1}H signals to Cu-phosphoramidite enolate **69b**, with the key sp^2-enolate ^{1}H signal at 5.01 ppm. We rationalise that this product is the CuBr·DMS enolate. This observation shows that in the presence of stoichiometric Cu (100%), the Cu-enolate is favoured to 93%, similar to the ~20% of Cu-Phosphoramidite enolate **69b** formed in the presence of 20 mol% catalyst. Therefore we speculate that Cu-enolates are the ACA initial products and can be transformed to the zirconium **69a** or TMS **69c** enolates over time.

^{31}P NMR spectroscopy kinetics

We also followed the reaction by ^{31}P NMR spectroscopy (Figure 8.6 and 8.7). Once the pre-catalyst is modified by the addition of $Cp_2ZrMeCl$ (discussed later), the catalyst does not change over time without TMSCl (Figure 8.6 - blue). No subtle intermediate catalytic species were observed in the ^{31}P NMR, presumably due to the extreme broadening of the ^{31}P signals caused by Cu.

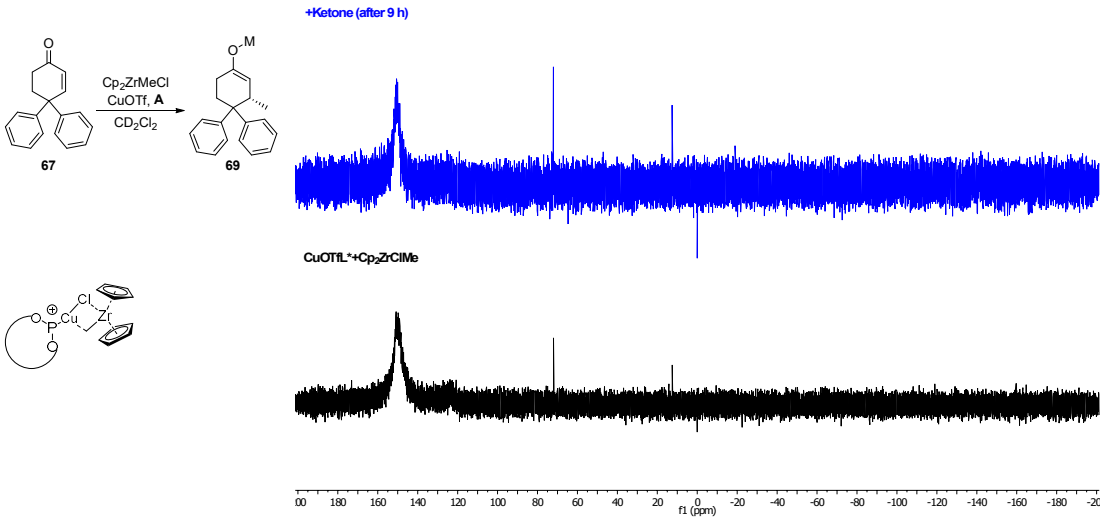

Figure 8.6. ^{31}P NMR spectroscopy at the end of the ACA-reaction without TMSCl (blue) compared to the Cu-Zr species (black). Conditions: $Cp_2ZrMeCl$ (1.7 eq) in CD_2Cl_2, CuCl (10 mol%), AgOTf (11 mol%), ligand **A** (10 mol%), 4,4-diphenyl-2-cyclohexen-1-one **67** (1.0 eq), in CD_2Cl_2, room temperature.

In the presence of TMSCl, the catalyst also stays the same over the course of the reaction but various sharp signals appeared (Figure 8.7 - purple). However, those peaks are probably due to catalyst degradation as they lack broadening. Notably the strong signal at 8.1 ppm resembles the ^{31}P signal of oxidised ligand **A**. These observations probably account for the temperamental behaviour of the ACA with TMSCl in CH_2Cl_2.

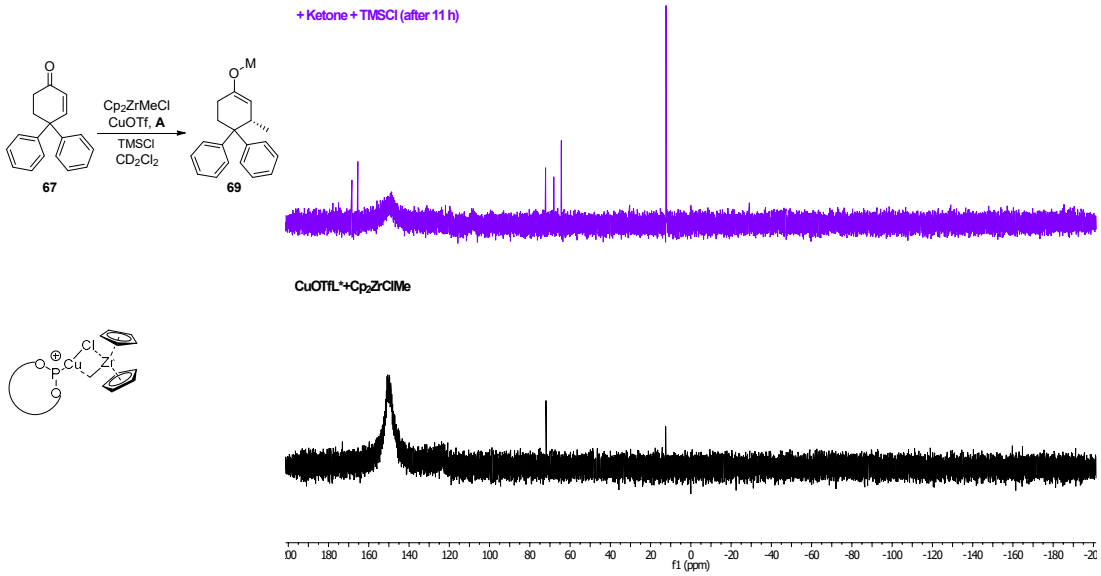

Figure 8.7. ^{31}P NMR spectroscopy at the end of the ACA-reaction with TMSCl (purple) compared to the Cu-Zr species (black). Conditions: $Cp_2ZrMeCl$ (1.7 eq) in CD_2Cl_2, CuCl (10 mol%), AgOTf (11 mol%), ligand **A** (10 mol%), 4,4-diphenyl-2-cyclohexen-1-one **67** (1.0 eq), TMSCl (5.0 eq) in CD_2Cl_2, room temperature.

Interactions

Modification of the starting material

In order to further investigate the reaction mechanism, we wanted to compare the different components' interactions. When TMSCl (5.0 eq) or $Cp_2ZrMeCl$ (1.7 eq) are added to 4,4-diphenylcyclohexenone **67** (1.0 eq), the starting enone **67** remained unaffected. This observation seemed surprising as the Lewis acid would be expected to modify the α,β-unsaturated ketone moiety and to be visible by ^{1}H or ^{13}C NMR spectroscopy.

When pre-mixing the enone and TMSCl, the ACA reaction gave a only 22% yield but a good ee (85% ee) showing that the possible interactions between TMSCl and enone **67** prior to interactions between enone **67** and the Cu-Zr complex are disfavoured. Therefore addition of TMSCl at the end of the setup is optimal as TMSCl's primary role is not to interact with enone **67** to facilitate the oxidative addition step of the 1,4-addition. These observations are consistent

with TMSCl enabling the formation of TMS-enolate **69c** only when Cu-enolate **69b** and/or Zr enolate **69a** have been formed, releasing Cu and Zr for the reaction turnover.

Because 5.0 eq of TMSCl greatly improves the yield to 35% and ee to 85% (Table 8.1 entry 3), compared to 1.0 eq of TMSCl (20% yield, 78% ee, Table 8.1 entry 4), the role of TMSCl in the system has to be more than just to form the TMS-enolate product **69c**. TMSCl presumably interacts with the catalyst to form a new catalyst with better stereoselectivity and reactivity, improving the ee and yield outcome, which we observed in the AAA of alkylzirconocene to allylphosphate (Chapter 6) and is discuss later in this Chapter.

We then investigated the effect of CuOTf-**A** (1.0 eq) to 4,4-diphenylcyclohexenone **67** (1.0 eq). We decided to use a stoichiometric amount of catalyst to facilitate observation of any subtle changes in the catalyst. Contrary to TMSCl or $Cp_2ZrMeCl$, CuOTf-**A** clearly modifies the starting enone **67** (Figure 8.8a - purple). The catalyst signals (blue) remain almost unaffected in the ^{1}H, ^{13}C and ^{31}P NMRs, but the ^{1}H signals of enone **67** (black) are all shifted (purple). In the ^{1}H NMR, the olefinic and aliphatic signals are all shielded notably from 6.21 to 5.71 ppm for the visible alkene ^{1}H signal and from 2.74 to 2.23 ppm and 2.41 to 1.92 ppm for the CH_2. Moreover, in the ^{13}C NMR, the ketone was deshielded from 198.3 (black) to 201.1 ppm (Figure 8.8b - purple).

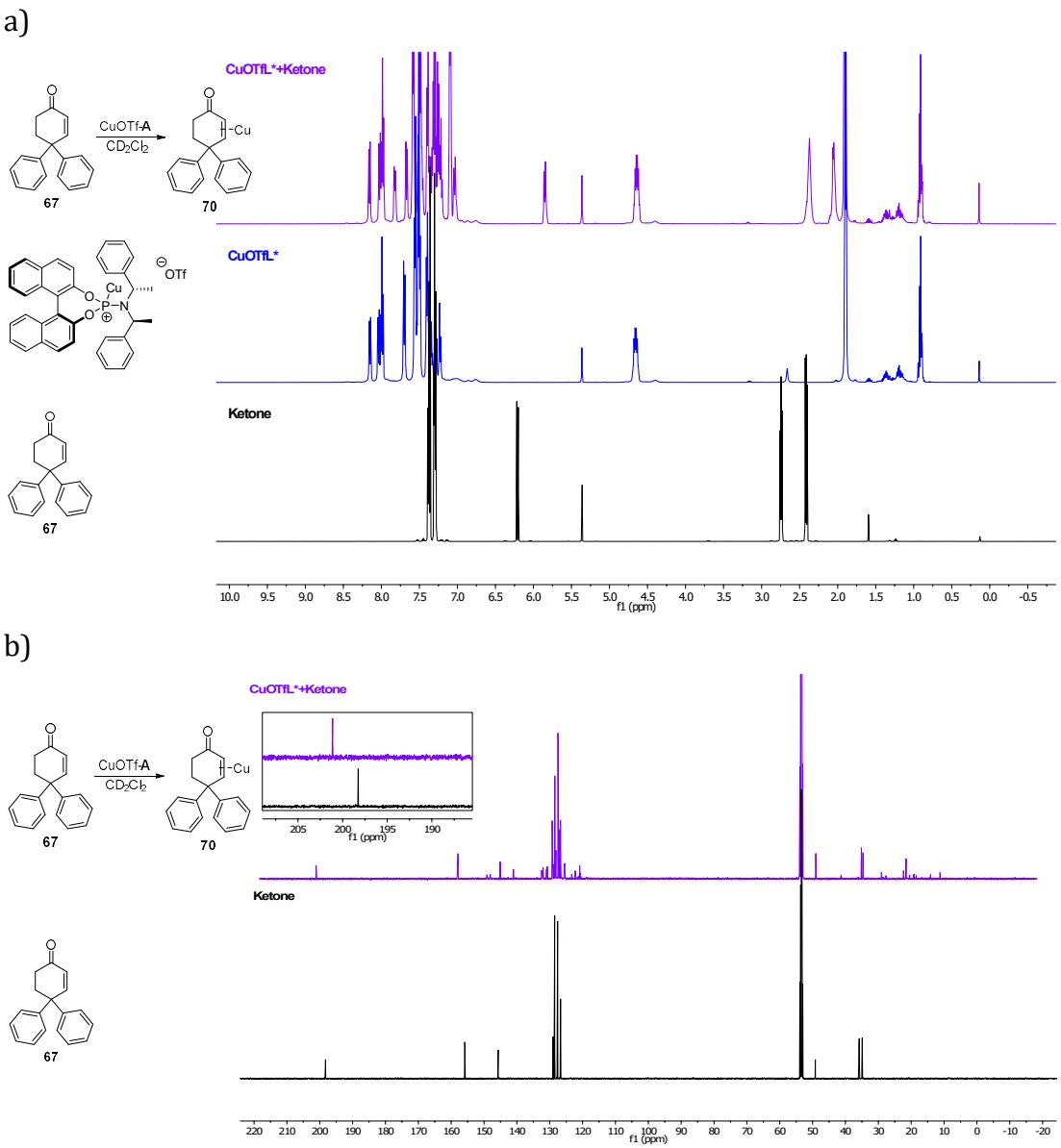

Figure 8.8. ^{1}H (a) and ^{13}C (b) NMR spectroscopy of the CuOTf-A (1.0 eq) interaction with 4,4-diphenyl-2-yclohexen-1-one 67 (1.0 eq) (purple) compared to CuOTf-A (blue) and 67 alone (black). Conditions: CuCl (10 mol%), AgOTf (11 mol%), ligand **A** (10 mol%), 4,4-diphenyl-2-cyclohexen-1-one **67** (0.1 eq), in CD_2Cl_2, room temperature.

This suggests that upon mixing enone **67** and CuOTf-**A**, a Cu-π-complex **70** is formed such as depicted in Figure 8.9. The d-π* back donation of the Cu would render the olefin less conjugated thus formerly giving the α,β-unsaturated ketone moiety, typically 198-200 ppm, a more non-conjugated ketone character, typically observed to be 211-213 ppm in the 1,4-addition products (see Experimental Section).

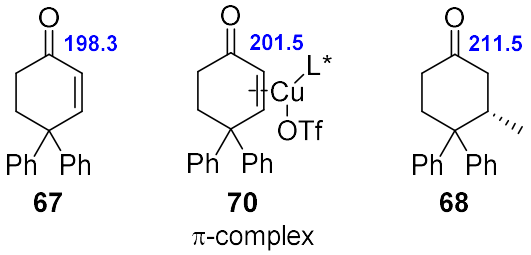

Figure 8.9. Comparison of the ketone ^{13}C NMR shift of the α,β-unsaturated ketone 67, π-complex 70 and 1,4-addition product 68.

To more closely mimic the reaction conditions we added catalytic CuOTf-**A** complex (20 mol%) to 4,4-diphenylcyclohexenone **67** (1.0 eq). To our surprise, here the signals observed are also shifted (Figure 8.10 - red) and their chemical shift is roughly 20% more shielded than the free starting enone **67** (black) compared to the stoichiometric Cu-enone complex **70** (blue). This observation is particularly striking for the most resolve alkene signal at 6.08 ppm for the free starting enone **67** (black), 5.54 ppm for the stoichiometric Cu-enone complex **70** (blue) and 5.97 ppm for 20 mol% Cu-catalyst. . Surprisingly, temperature studies showed that even between −60 °C to 40 °C, the most resolve alkene signal at 5.97 ppm is unchanged. When testing different catalyst loading, we obtained a gradual shift of the observed alkene signal from 5.97 ppm for 20 mol% (20% shielded), 5.80 ppm for 50 mol% (50% shielded) and 5.65 ppm for 80 mol% (80% shielded). This observation suggests that the NMR signal observed is the outcome of a rapid equilibrium on the NMR time scale between the free enone and the enone-Cu complex. The equilibrium of those species is so fast that chemical exchanges still occur at temperature as low as −60 °C.

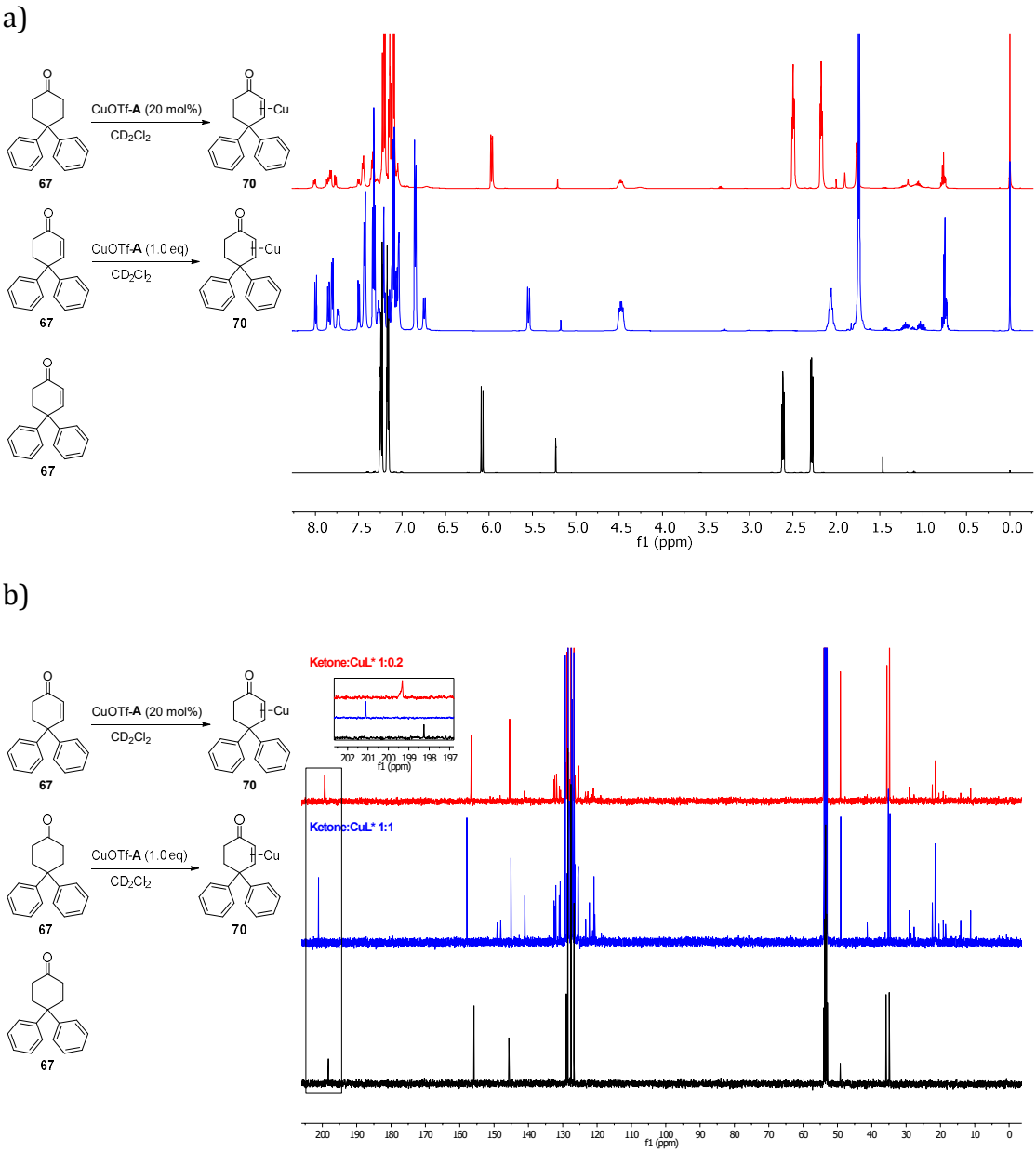

Figure 8.10. ^{1}**H (a) and** ^{13}**C (b) NMR spectroscopy of the CuOTf-A (0.1 eq) interaction with 4,4-diphenyl-2-yclohexen-1-one 67 (1.0 eq) (red) compared to CuOTf-A (1.0 eq)+ 67 (1.0 eq) (blue) and 67 alone (black).** Conditions: CuCl (10 mol%), AgOTf (11 mol%), ligand **A** (10 mol%), 4,4-diphenyl-2-cyclohexen-1-one **67** (1.0 eq), in CD_2Cl_2, room temperature.

Interestingly, the modification of enone **67** by CuOTf-**A** is not observed by ^{1}H NMR spectroscopy during the reaction. We hypothesise that the π-complex is formed in such trace amounts, with a short life-span, that it is difficult to observe by NMR. Although it is also possible that in the presence of $Cp_2ZrMeCl$, the Cu-catalyst behaves differently and does not form a π-complex with the enone.

When adding $Cp_2ZrMeCl$ (1.7 eq) to the **67**-Cu complex **70** (20 mol% CuOTf-**A**, 1.0 eq **67**) (red), the starting enone **67** appears unbound and the ACA reaction proceeds as normal (Figure 8.11 - orange). Thus CuOTf-**A** appears to have more affinity for $Cp_2ZrMeCl$ than enone **67** and the pre-formation of the **67**-Cu complex **70** does not disrupt the reaction.

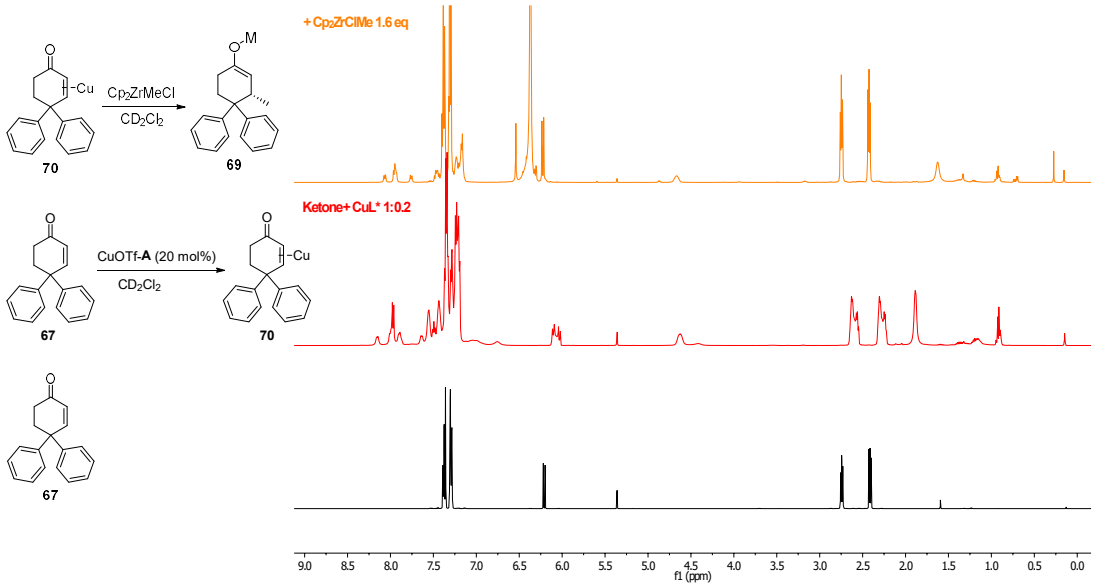

Figure 8.11. ^{1}H NMR spectroscopy of the $Cp_2ZrMeCl$ interaction with the CuOTf-A (0.2 eq), 4,4-diphenyl-2-yclohexen-1-one complex 70 (orange) compared to the CuOTf-A+67 (red) and 67 alone (black). Conditions: CuCl (20 mol%), AgOTf (22 mol%), ligand **A** (20 mol%), 4,4-diphenyl-2-cyclohexen-1-one **67** (1.0 eq), in CD_2Cl_2 then $Cp_2ZrMeCl$ (1.7 eq) in CD_2Cl_2, room temperature.

Similarly, when adding TMSCl (5.0 eq) to the **67**-Cu complex **70** (20 mol% CuOTf-**A**, 1.0 eq **67**) (Figure 8.12 - purple), the starting material **67** is released and the catalyst is modified as observed in the ^{1}H and ^{31}P NMR spectra. Thus surprisingly TMSCl has more affinity for the catalyst than the enone. The same modification of the catalyst was observed when adding TMSCl (5.0 eq) to the CuOTf-**A** catalyst alone (20 mol%) (orange). In the ^{1}H NMR (Figure 8.12a - orange), the aromatic signals of the catalyst are shifted, the benzylic CH-N signal, originally at 4.60 ppm, splits in two signals at 4.67 ppm and at 3.90 ppm and the

Me groups at 1.84 ppm, also splits into two shielded signals at 1.72 ppm and 1.63 ppm. In the ^{31}P NMR spectra (Figure 8.12b – orange), the original catalytic peak (black) is deshielded from 122.6 ppm to 152.6 ppm and a new broad weak signal can be found at 155.6 ppm. Clearly TMSCl has an important impact on the nature of the catalyst and due to the splitting of signal, seems to form at least two different species or aggregates.

a)

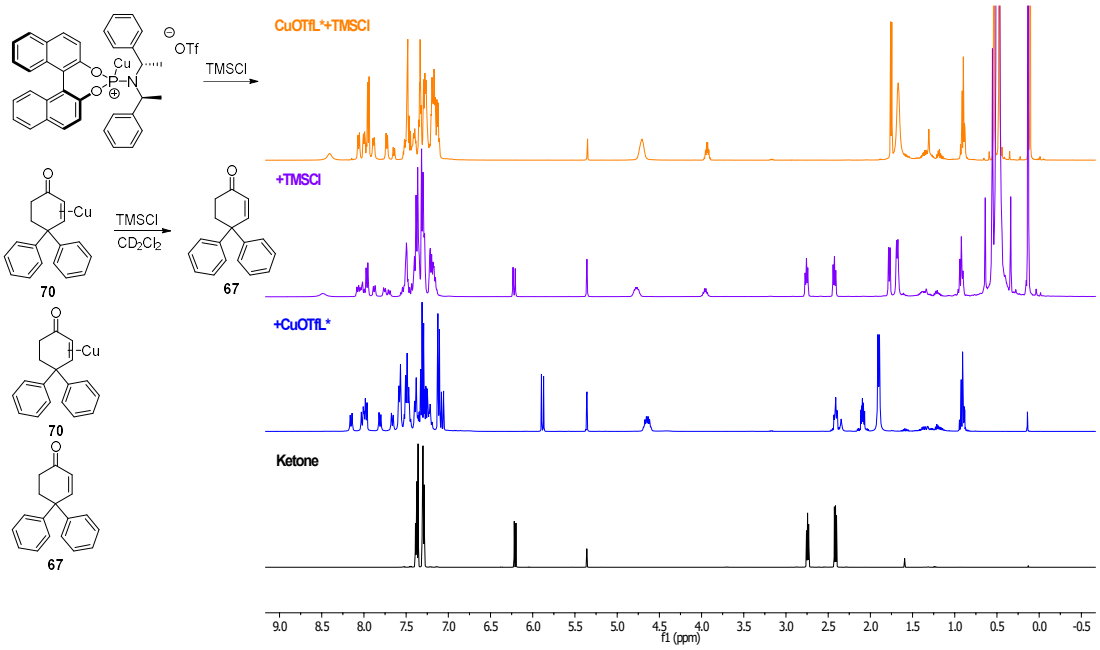

b)

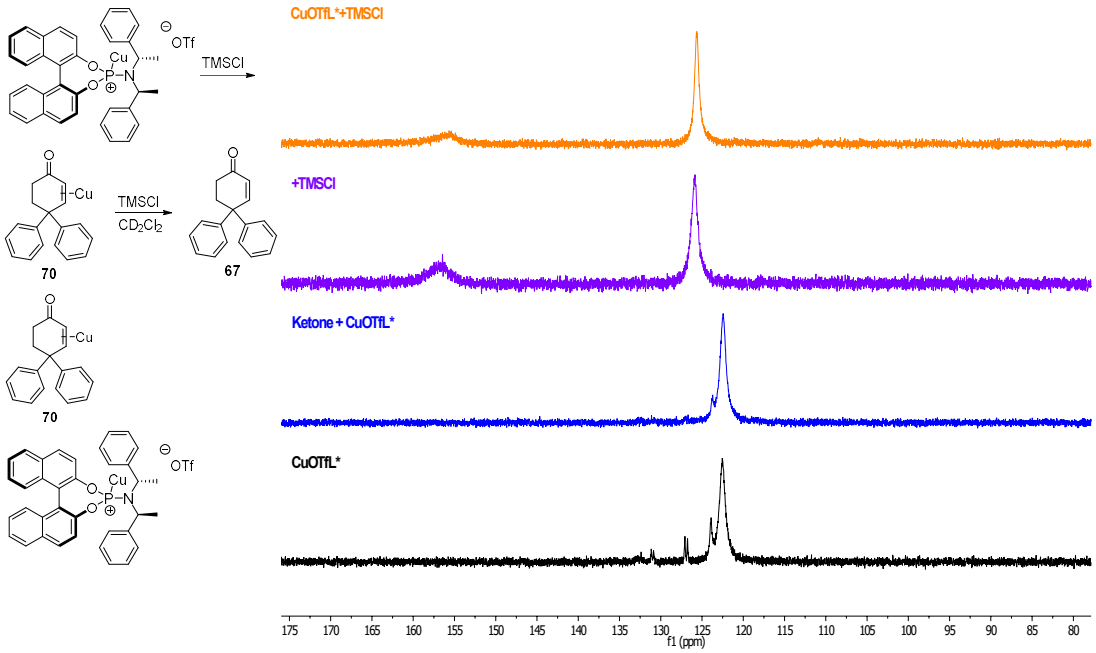

Figure 8.12 ^{1}H (a) and ^{31}P (b) NMR spectroscopy of the TMSCl interaction with the CuOTf-A + 4,4-diphenyl-2-yclohexen-1-one 67 (purple) compared to 70 (blue), CuOTf-A (black) and CuOTf-A+TMSCl (orange). Conditions: CuCl (20 mol%), AgOTf (22 mol %), ligand **A** (20 mol%), 4,4-diphenyl-2-cyclohexen-1-one **67** (1.0 eq), in CD_2Cl_2 then TMSCl (5.0 eq) in CD_2Cl_2, room temperature.

When we added TMSCl (5.0 eq) to the Cu-Zr catalyst complex (1.7 eq $Cp_2ZrMeCl$, 20 mol% CuOTf-**A**), no change were observed in the ^{1}H or ^{31}P NMR spectra (Figure 8.13 - purple). Thus it would appear that TMSCl might not affect the catalyst once it has been modified by $Cp_2ZrMeCl$ (black). As the ACA reaction proceeds, whether TMSCl has an impact on the catalyst remains unknown.

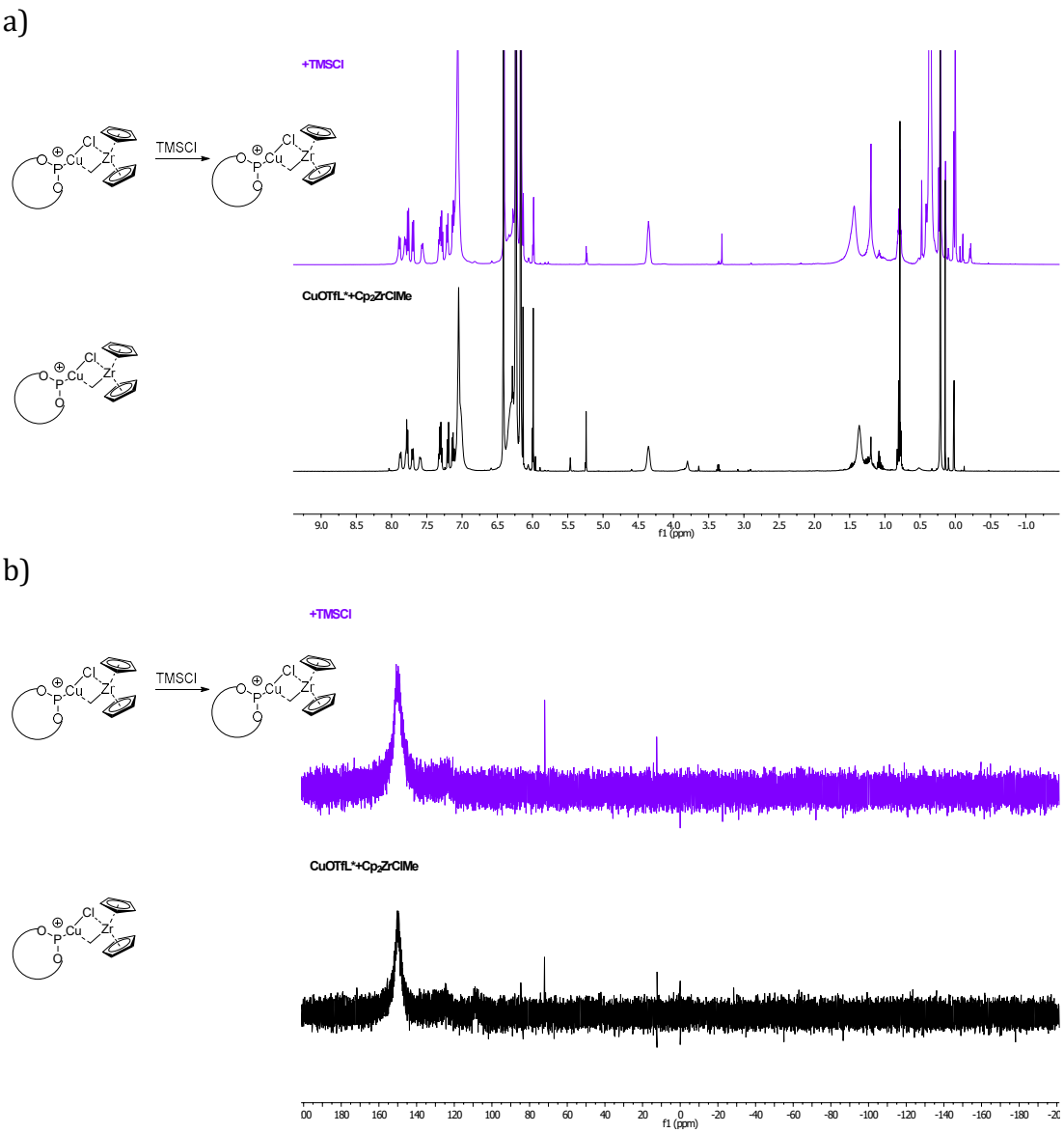

Figure 8.13. ^{1}H (a) and ^{31}P (b) NMR spectroscopy of the TMSCl interaction with the CuOTf-A/$Cp_2ZrMeCl$ supramolecular complex (purple) compared to CuOTf-A/$Cp_2ZrMeCl$ complex alone (black). Conditions: $Cp_2ZrMeCl$ (1.7 eq) in CD_2Cl_2, CuCl (20 mol%), AgOTf (22 mol %), ligand **A** (20 mol%) in CD_2Cl_2 then TMSCl (5.0 eq), room temperature.

Catalytic species

One of the most difficult aspects of mechanistic studies is the identification of the catalytic species that result in high ee. Information on the pre-catalytic species is easier to obtain in the solid-state or in solution. However, those intricate oligomeric structures are highly malleable and easily influenced by

small changes in the environment. Understanding the different catalytic species involved in the reaction is fundamental to revealing the mechanism.

*CuOTf-**A** and $Cp_2ZrMeCl$ transmetallation?*

Every mechanism involving other nucleophiles (Zn, Mg, Al) has been proposed to involve transmetallation to Cu[1,7,55,188] but to our knowledge only Gschwind found experimental evidence of transmetallation when using diethylzinc[188]. We were interested in the Cu-phosphoramidite/$Cp_2ZrMeCl$ interactions and to determine whether transmetallation occurred in this methodology. Upon addition of the zirconocene nucleophile (1.7 eq of $Cp_2ZrMeCl$) to the CuOTf-**A** catalyst (20 mol% CuOTf-**A**) changes in the ^{1}H and ^{31}P NMR spectra are observed (Figure 8.14 - orange) as well as drastic changes of colour from clear yellow to dark brown.

a)

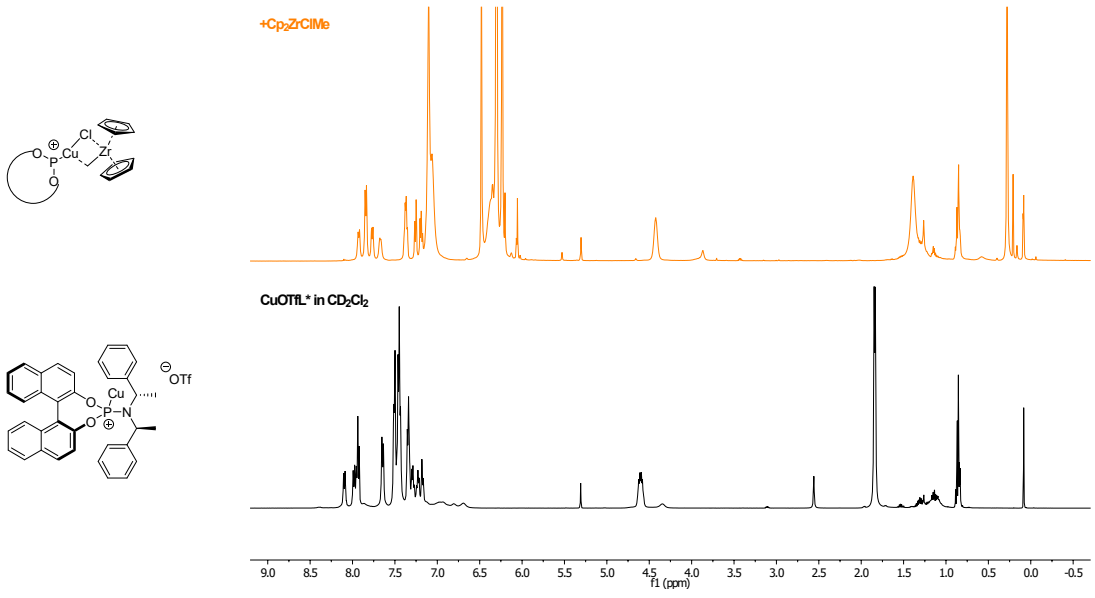

b)

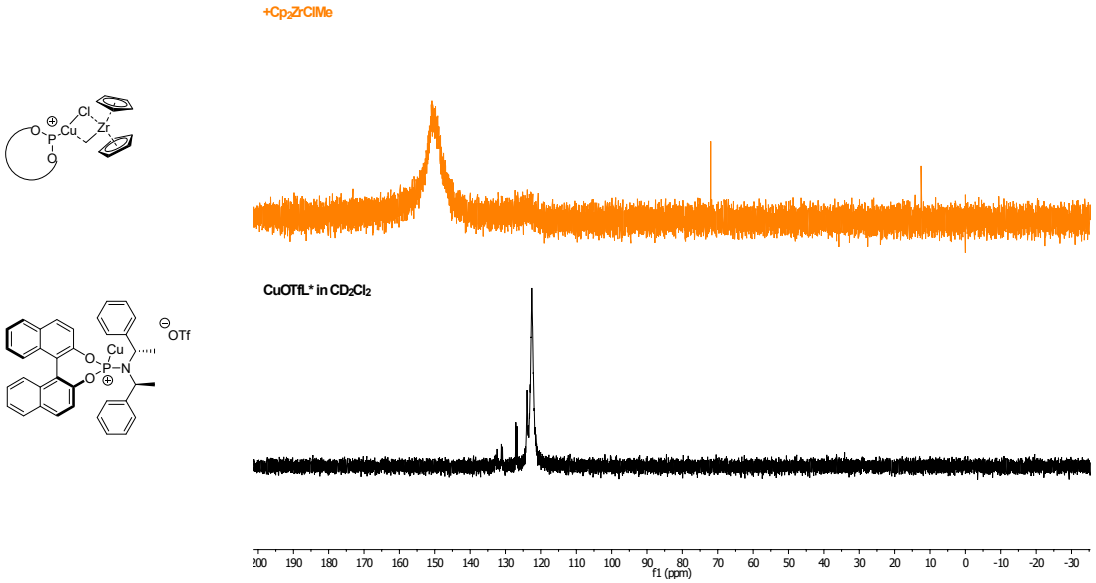

Figure 8.14. ^{1}H (a) and ^{31}P (b) NMR spectroscopy of the CuOTf-A (0.2 eq) $Cp_2ZrMeCl$ (1.7 eq) interactions in CD_2Cl_2 (orange) compared to CuOTf (black) Conditions: CuCl (20 mol%), AgOTf (22 mol%), ligand **A** (20 mol%), in CD_2Cl_2 then $Cp_2ZrMeCl$ (1.7 eq) in CD_2Cl_2, room temperature.

In the ^{1}H NMR (Figure 8.14a -orange), the aromatic signals rearrange and their multiplicity changes, the benzylic signal is shielded from 4.60 ppm to 4.48 ppm and the Me-signal of the ligand is shielded from a doublet at 1.84 ppm to a broad singlet at 1.49 ppm. In the ^{31}P NMR (Figure 8.14b -orange) an array of species with a major peak at 122.5 ppm change to a broad deshielded peak at 150.4 ppm upon addition of $Cp_2ZrMeCl$. Another weak broad signal observed at 123.6 ppm is reminiscent of the original pre-catalyst.

We also decided to analyse the stoichiometric addition of $Cp_2ZrMeCl$ to the catalyst (Figure 8.15). This type of study, even though diverging from the reaction conditions, helps estimate the effect of CuOTf-**A** on $Cp_2ZrMeCl$ as there is no excess nucleophile obstructing the visualisation of changes. The Me of $Cp_2ZrMeCl$ (orange) does not shift but get broad both in the ^{1}H and ^{13}C NMR (blue).

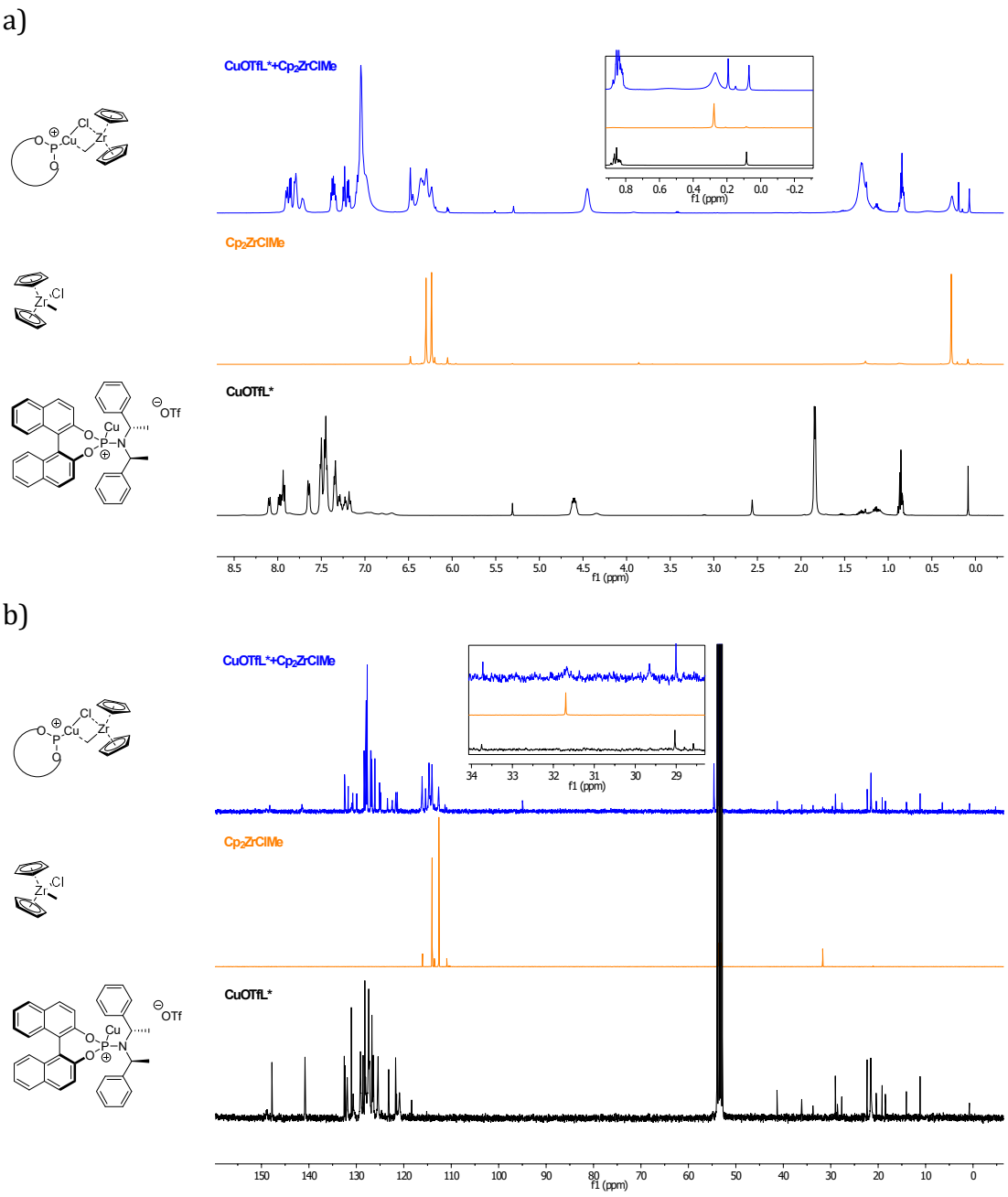

Figure 8.15. ^{1}H (a) and ^{13}C (b) NMR spectroscopy of the CuOTf-A (1.0 eq) $Cp_2ZrMeCl$ (1.0 eq) interactions in CD_2Cl_2 (blue) compared to $Cp_2ZrMeCl$ alone (orange) and CuOTf-A (black). Conditions: CuCl (1.0 eq), AgOTf (1.1 eq), ligand **A** (1.0 eq), in CD_2Cl_2 then $Cp_2ZrMeCl$ (1.0 eq) in CD_2Cl_2, room temperature.

These observations altogether showed a clear interaction between the $Cp_2ZrMeCl$ and the CuOTf-**A** complex. However, the lack of shifting in the ^{1}H and ^{13}C NMR spectra of the $Cp_2ZrMeCl$'s Me group was surprising. Cu (1.90) is more electronegative than Zr (1.33)[277] and in the case of transmetallation, we would expect the Me group originally on $Cp_2ZrMeCl$ to shift downfield as it bonds to Cu.

$(PR_3)_nCuMe$ type neutral alkylcopper species have chemical shifts of +0.3 to –0.9 ppm[189,278] in benzene and $LiCuMe_2$ species –1.0 to –4.0 ppm[14] but as far as we are aware the ^1H NMR shift of alkyl on Cu-phosphoramidite has never been reported and thus its chemical shift is unknown. Nonetheless, we did not observe any signal in the negative region of the ^1H NMR. These observations suggest no covalent changes have occurred between the $Cp_2ZrMeCl$ and the Cu-phosphoramidite complex. However, the broadening of the $Cp_2ZrMeCl$'s Me group indicates the presence of Cu and $Cp_2ZrMeCl$ and Cu-phosphoramidite may form a supramolecular complex. Transmetallation of the Me group on the Zr to the Cu is possible but evidence (lack of shifting of the Me group) suggest otherwise. Therefore whether the Me is formerly attached to Cu or Zr or shared between the metals is unknown. We decided to describe those species as an equilibrium between those possible Zr-Cu complexes (Figure 8.16).

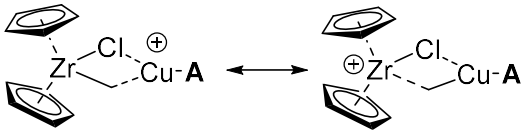

Figure 8.16. Proposed primary catalytic species.

In order to investigate these species under the actual reaction conditions, we added $Cp_2ZrMeCl$ (1.7 eq) in CD_2Cl_2 to CuOTf-**A** (20 mol%) in Et_2O-h_{10} (Figure 8.17). The ^{31}P NMR spectra show an instantaneous change from three different aggregates at 136.4, 131.1 and 123.9 ppm respectively to a single, sharper species at 151.1 ppm. Thus the interaction of the Cu-phosphoramidite/$Cp_2ZrMeCl$ (orange) is even more striking and clean in Et_2O than in CH_2Cl_2, emphasising the influence and importance of solvent.

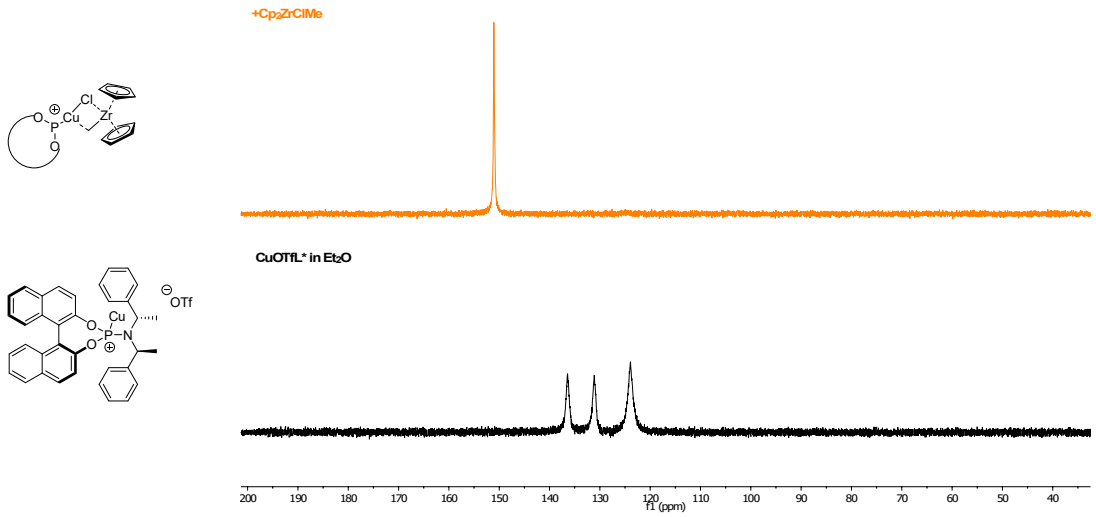

Figure 8.17. ^{31}P NMR spectroscopy of the CuOTf-A (0.2 eq) $Cp_2ZrMeCl$ (1.7 eq) interactions in Et_2O (orange) compared to CuOTf-A alone (black). Conditions: CuCl (20 mol%), AgOTf (22 mol%), ligand **A** (20 mol%), in Et_2O then $Cp_2ZrMeCl$ (1.7 eq) in CD_2Cl_2, room temperature.

Diffusion spectroscopy

Similarly to our AAA system, we decided to carry out DOSY on CuOTf-**A** in order to estimate supramolecular assemblies of the catalyst aggregates. Similarly to CuOTf-**A** in $CDCl_3$, CuOTf-**A** in CD_2Cl_2 is forming two complexes in solution at 298 K and we were only able to obtain diffusion ordered data for the principal complex. We found that the diffusion coefficient of the major oligomer of CuOTf-**A** in CD_2Cl_2 is 9.15±0.07 10^{-10} $m^2.s^{-1}$ (Table 8.2).

Table 8.2. Diffusion coefficients and their predicted molecular weight.

	D (10^{-10} $m^2.s^{-1}$)	Predicted MW[242]
CuOTf-A	9.15±0.07	821±14
CuOTf-A + $Cp_2ZrMeCl$	8.72±0.36	914±95

Conditions: CuCl (10 mol%), AgOTf (11 mol%), ligand **A** (10 mol%), in CD_2Cl_2 then $Cp_2ZrMeCl$ (1.7 eq) in CD_2Cl_2, room temperature.

According to Morris[242] calculations, we estimated the molecular weight of the major pre-catalytic CuOTf-**A** complex to be roughly 821±14 $g.mol^{-1}$. This size of complex corresponds to a monomer of Cu-**A** (603 $g.mol^{-1}$) as the smallest

dimer Cu**A**$_2$ has a molecular weight of 1143 g.mol^{-1}. Upon addition of $Cp_2ZrMeCl$ (1.7 eq), the diffusion coefficient drops to 8.72±0.36 10^{10} m^2.s^{-1}, an estimated molecular weight of 914±95 g.mol^{-1}. Due to the complexity of this system, especially as greater variations could be observed in the measured diffusion coefficient when adding $Cp_2ZrMeCl$ due to the behavioural unpredictability and instability of the reaction components in CD_2Cl_2, it is difficult to judge whether this value is still within the experimental errors or significantly smaller. The molecular weight appear too low to accommodate a dimer (>1143 g.mol^{-1}) but a CuOTf-**A**-$Cp_2ZrMeCl$ supramolecular complex has a molecular weight of 911 g.mol^{-1}, a close match to the predicted 914 g.mol^{-1}. Thus the measured diffusion coefficient fits the hypothesised Cu-Zr supramolecular complex determined in previous testing. The exact nature of the catalytic species during the reaction are unknown but linear effect studies on similar system, correlate to the active catalyst to be also a monomer[36].

CONCLUSION AND PROPOSED MECHANISM

During the ACA of organozirconocene nucleophiles to cyclic enones, the immediate product appears to be an enolate and different enolates are formed depending on the conditions. In the presence of TMSCl, the principal product is TMS-enolate **69c** (95%) whereas in the absence of TMSCl, we speculated that a mixture of Zr-enolate **69a** (78%) and Cu-enolate **69b** (22%) are observed (Scheme 8.6). In the absence of TMSCl, the formation of the Cu-enolate **69b** seems faster than formation of the Zr-enolate **69a** and some mechanisms must

enable the transformation of Cu- to Zr-enolate to explain the turnover observed. We speculate that organocopper species **71** is initially formed followed by its tautomerisation to the Cu-enolate **69b**. The formation of Cu-enolate **69b** could also be a key event in the TMSCl mediated ACA before getting converted to the TMS-enolate **69c** (Scheme 8.6 – blue) rationalising the poor reactivity (22% yield) obtained when using pre-mixed TMSCl and enone in the ACA. Alternatively each enolate could be formed through different pathways as shown in red.

A π-complex is formed when mixing the starting enone and the Cu-catalyst but was not observed during the ACA. The π-complex might not be observed as it is transient, highly different from the Cu-enone complex **70** or formed in traces amounts. Finally, even though there is no clear evidence of transmetallation, (^{1}H NMR, ^{31}P NMR, DOSY) our observations suggest that a monomeric Zr-Cu supramolecular complex is formed rapidly in both CD_2Cl_2 and Et_2O. We also discussed the intriguing dual role of TMSCl for achieving high ee and good yields. TMSCl clearly is involved in the formation of TMS-enolate **69c** but it also has been found to be able to modify pre-catalytic complexes and can also influence in-reaction catalytic ones in this case and in previous examples (Chapter 2, 3 and 6).

These NMR studies gave us a clearer picture of the mechanism of the ACA of alkylzirconocene, however, we did not gather evidence on the mechanisms involved in the Zr-Cu supramolecular complex interactions with the enone **67**. Further work should be carried out to identify these mechanisms presumably in correlation with DFT calculations.

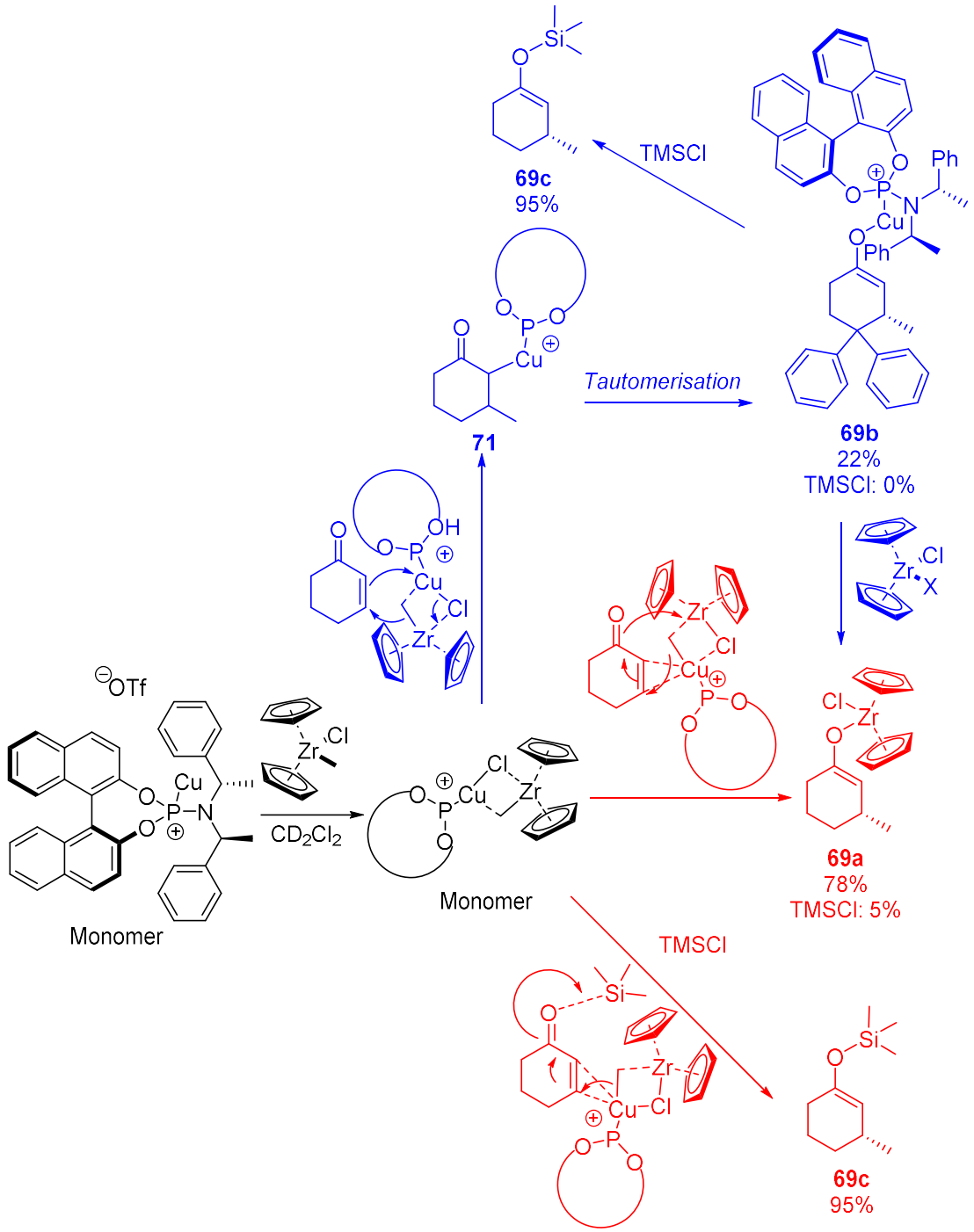

Scheme 8.6. Proposed mechanisms for the ACA of alkylzirconocenes to secondary enone 67.

CHAPTER 9

CONCLUSION AND FUTURE WORKS

CONCLUSIONS

In the course of this thesis, we primarily set out to study the applicability of Cu-catalysed asymmetric additions to the synthesis of prostaglandins (Part I). We discussed the difficulty associated with using alkenylzirconocenes in Cu-catalysed ACA (Chapter 2) (Scheme 9.1).

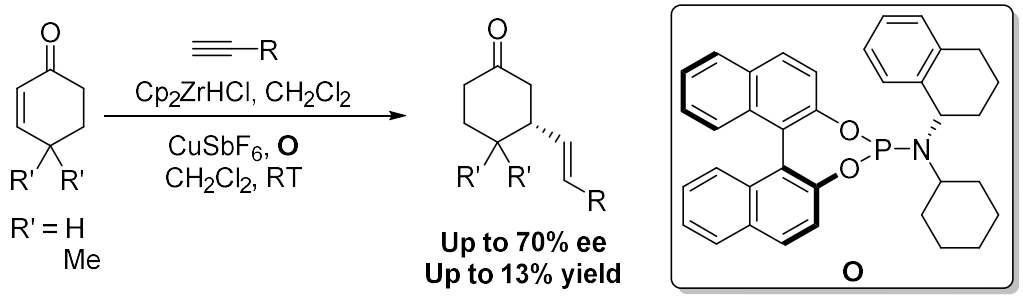

Scheme 9.1. Using alkenylzirconocenes in Cu-Catalysed ACA (Chapter 2).

Then despite the challenges associated with using reactive 5-membered ring in ACA, we successfully developed a tolerant and mild new methodology for the ACA of alkylzirconocenes to cyclopentenone derivatives, cyclopentene-3,5-dione monoacetal **18a** (Chapter 3) (Scheme 9.2)[140].

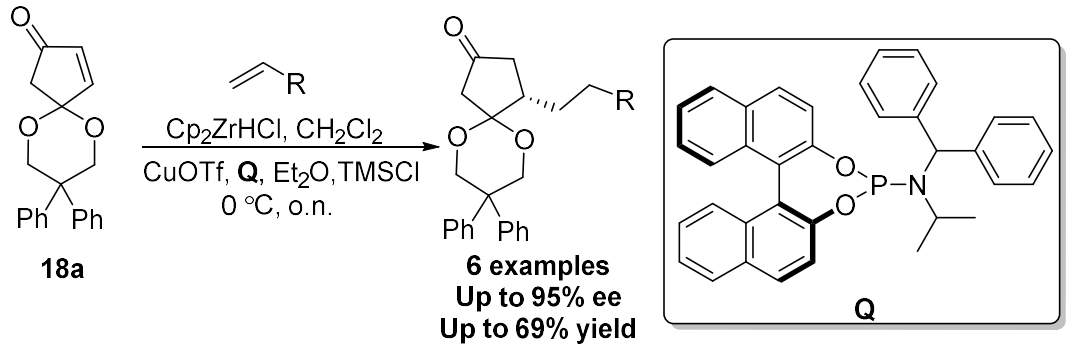

Scheme 9.2. Cu-Catalysed ACA of alkylzirconocenes to cyclopentene-3,5-dione monoacetal 18a (Chapter 3)[140].

We then decided to apply this methodology and a recently developed AAA towards the total synthesis of Latanoprost, a prostaglandin analogue. The addition of complex enantioenriched alkylzirconocene nucleophiles was successful in both ACA and AAA but unfortunately further derivatisation failed (Chapter 4).

In the second part of this thesis (Part II), our aims were to study the mechanism of diverse Cu-catalysed asymmetric additions of alkylzirconocenes by NMR. The AAA of allylchloride **45b** was thoroughly investigated and gave us remarkable insight into these poorly understood mechanisms (Chapter 5). We experimentally observed and investigated the formation of allyliodide **54** *in situ* and its isomerisation. The isomerisation of allyliodide **54** is thought to be at the fundamental step for the dynamic kinetic transformation of this AAA (Scheme 9.3)[4].

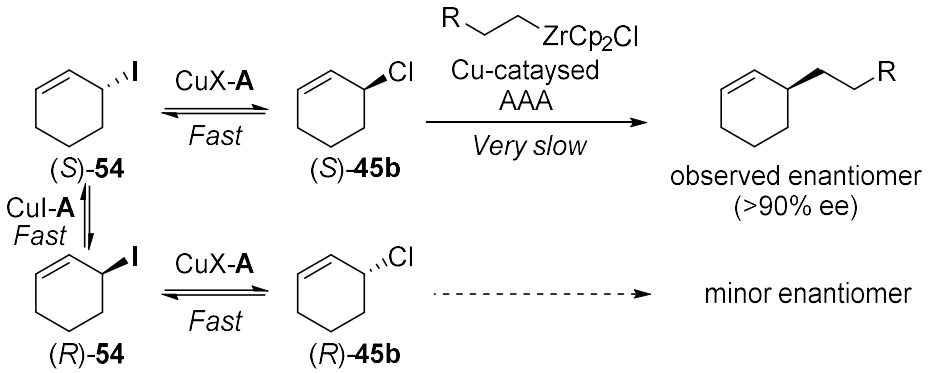

Scheme 9.3. Proposed mechanism based on our NMR mechanistic studies of the AAA of alkylzirconocenes to cyclic allylchloride 45b (Chapter 5)[4].

After the study of the AAA of allylchloride **45b**, mechanistic questions remain. Therefore we decided to study the AAA of more stable allylphosphate **57** (Chapter 6). We observed that this system form allylchloride **45b** *in situ* but the mechanism seems to differ from the original AAA of allylchloride **45b**.

Then we developed and study the mechanism of an heterocyclic AAA of alkylzirconocenes (Chapter 7)[5]. After extensive examination, two different methods for obtaining 3,6-dihydro-2*H*-pyran derivatives were obtained, achieving a good 83% ee but poor yields (Scheme 9.4). These methodologies could not be improved but reveals remarkable mechanistic diversity in Cu-catalysed asymmetric alkylation reactions.

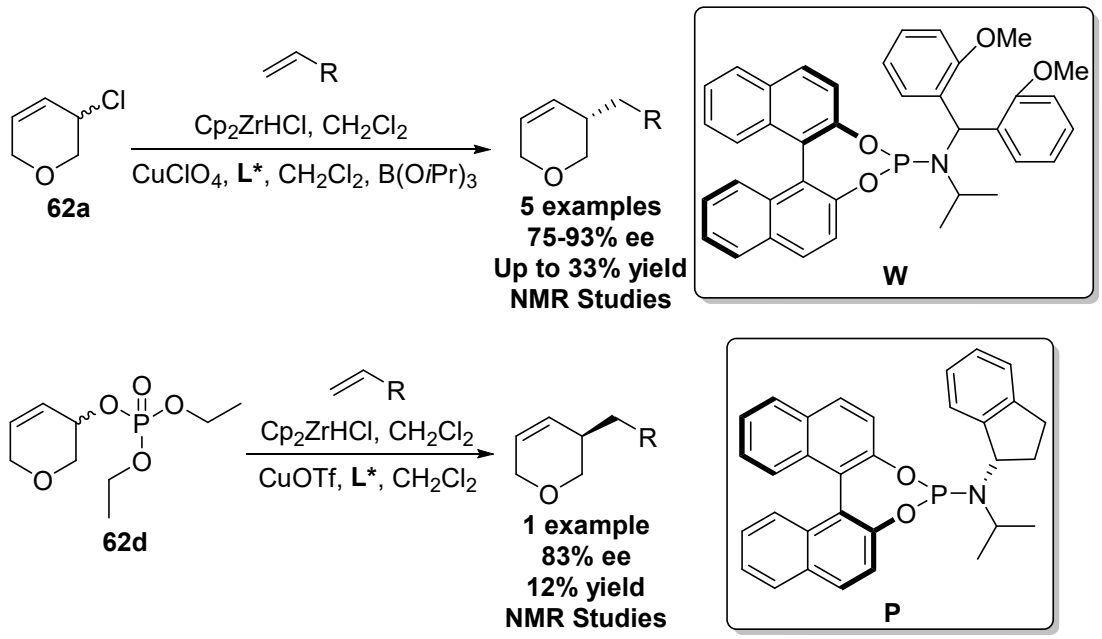

Scheme 9.4. Development of two methodologies for the AAA of alkylzirconocenes to racemic 3,6-dihydro-2*H*-pyrans 62 (Chapter 7)[5].

Finally, we used NMR mechanistic studies to gain insight into the mechanism of the ACA of alkylzirconocenes (Chapter 8) and exemplified the formation of various enolates in diverse conditions (Scheme 9.5). We also noticed the divergence in catalytic species and interaction with alkylzirconocenes depending on the Cu counterions. The intricate role of TMSCl was also detailed.

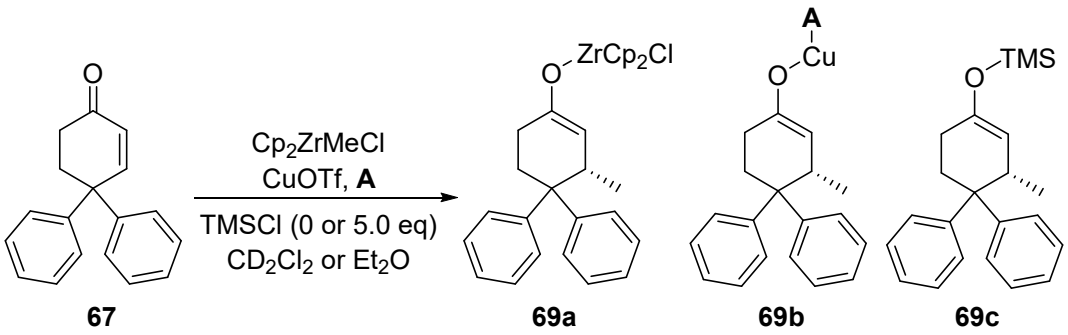

Scheme 9.5. NMR mechanistic studies of the ACA of alkylzirconocenes (Chapter 8).

FUTURE WORKS

Based on the work carried out in this thesis, we envisioned that future work in the Fletcher group will continue on the development of new asymmetric methodologies towards implementing a novel and practical platform for the synthesis of prostaglandins analogues notably Latanoprost. New Cu-catalysed addition of alkylzirconocene nucleophiles methodologies such as the AAA of alkylzirconocene to complex substituted substrates (e.g. *meso*-bis-allylchloride substrates(Scheme 9.6a)) or the use of alternative nucleophiles such as vinyl boronic acids (Scheme 9.6b) similarly to our newly developed Rh-catalysed AAA of aryl boronic acid[139] might be successful in the total synthesis of prostaglandins and circumvent the allylic oxidation issue.

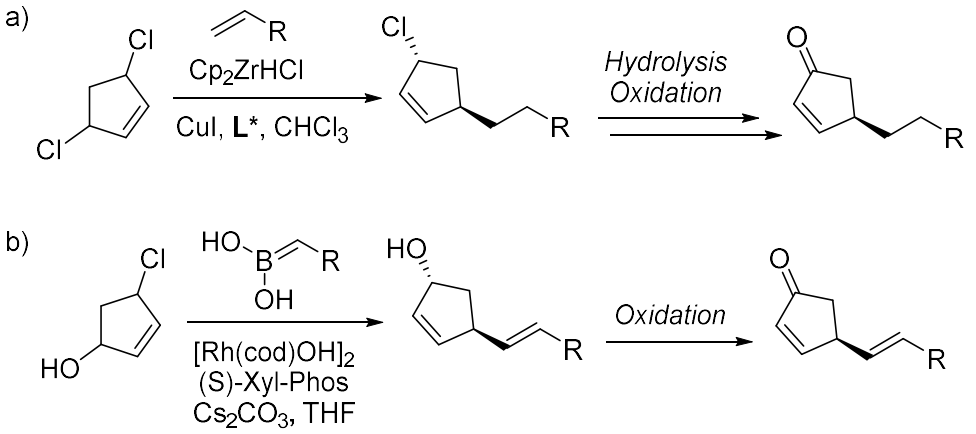

Scheme 9.6. Proposed alternative synthesises of prostaglandin analogues. a) Synthesis using the AAA of alkylzirconocenes to *meso*-bis-allylchloride substrates. b) Synthesis using the AAA of vinyl boronic acids to substituted allylchloride.

Moreover, we hope that our demonstration of the success and advantages of using NMR in mechanistic studies will inspire more similar studies and promote the thriving of better mechanistic understanding of complex organometallic systems. We envisioned that in our group the ACA of alkylzirconocenes to tertiary enone[142], lactone[87], linear substrates[88], the AAA of boronic acids[139] and yet to be developed methodologies could be studied by NMR for mechanistic examination and optimisation. Furthermore, we foresee great advantages in correlating this thesis work on the AAA of alkylzirconocenes to allylchlorides **45b** (Chapter 5) and the ACA of alkylzirconocenes to enone (Chapter 8) with DFT calculations. DFT calculations usually lack experimental evidences and such comparative studies will further extend our understanding of the mechanism of these complex well-designed methodologies.

EXPERIMENTAL DATA AND ANALYSIS

I. General Information

All reactions involving oxygen/moisture sensitive reagents were performed with anhydrous solvents in flame-dried glassware under a positive pressure of anhydrous argon, using standard Schlenk techniques. Cooling of reaction mixtures to –78 °C was achieved using an acetone/dry ice bath; to 0 °C using an ice/water bath; to other temperatures using a Julabo FT902 immersion cooler. Heating was performed using Drysyn® heating blocks.

In the cases where silver salts were used, the resulting solutions were filtered using syringe filters PTFE (0.2 μm, 13 mm diameter) from Camlab.

Analytical thin-layer chromatography was performed on glassplates pre-coated with silica gel (Silica Gel 60 F_{254}; Merck). Plates were visualised using UV light (λ=254 nm) and then stained with either aqueous ceric ammonium molybdate (CAM), aqueous basic potassium permanganate ($KMnO_4$) or anysaldehyde and developed upon heating.

Flash chromatography was performed using silica gel (Apollo Scientific 60 (40-63 μm), Sigma Aldrich (Davisil® grade 636, pore size 60 Å, 35-60 mesh), Merck 60 Å or VWR (40-63 μm)). Pressure was applied at the column head via a flow of nitrogen with solvent systems used in parentheses.

Nuclear magnetic resonance spectra were acquired in deuterated solvents at room temperature on Bruker: AVIIIHD 400 nanobay, AVIIIHD 500, AVII 500, AVII 500 with cryoprobe spectrometers. Chemical shifts (δ) are reported in ppm from the residual solvent. Coupling constants (*J*) are quoted in Hertz (Hz) and are recorded to the nearest 0.1 Hz. Resonances are descried as singlet (s), doublet (d), triplet (t), quartet (q), quintet (quint), doublet of doublets (dd), doublet of

doublets of doublets (ddd), doublet of triplets (dt), multiplet and broad (br.). Assignments were made with the assistance of gCOSY, DEPT-Q, gHSQC and gHMBC NMR spectra.

Low resolution (LRMS) and high resolution (HRMS) mass spectral analyses were acquired by electrospray ionisation (ESI), electron impact (EI), field ionisation (FI). Low resolution ESI were recorded using an Agilent 6120 quadrupole LC/MS. High resolution accurate ESI were recorded using a Thermo Exactive 1.1 SP5 Benchtop orbitrap MS and EI/FI on a Waters GTC Temperature programmed solid probe inlet within the department of chemistry, University of Oxford.

Infrared spectroscopy (IR) measurements (neat, thin film) were carried out using a Bruker Tensor 27 FTIR with internal calibration in the range of 4000-600 cm^{-1}. Absorption maxima are reported as wavenumbers (cm^{-1}).

Optical rotations were recorded using a Schmidt Haensch Unipol L2000 Polarimeter.

Chiral HPLC separations were achieved using an Agilent 1260 Infinity series normal phase HPLC unit and HP Chemstation software. Chiralpak® columns (250 × 4.6 mm), fitted with matching Chiralpak® Guard Cartridges (10 × 4 mm), were used as specified. Solvents used were of HPLC grade (Fisher Scientific, Sigma Aldrich or Rathburn). All eluent systems were isocratic.

Chiral GC separations were achieved using an Agilent 7820A GC and HP Chemstation software. Columns from Macherey-Nagel, Supelco and Agilent were used using He as a carrier gas and constant pressure (10 psi).

Low temperature[279] (150 K) single-crystal X-ray diffraction data were collected using or an Oxford Diffraction (Agilent) SuperNova A diffractometer.

Raw frame data were reduced using the instrument manufacturer supplied software CrysAlisPro[280]. All structures could be solved *ab initio* using SuperFlip[281] and full-matrix least-squares refinement was carried out using CRYSTALS[282-284]. All non-hydrogen atoms were refined using anisotropic displacement ellipsoids and hydrogen atoms were visible in the difference map. Once the heavy atoms structure was complete, hydrogen atoms were positioned geometrically then refined separately using soft restraints prior to inclusion in the final refinement using a riding model[285]. The ORTEP plots show thermal ellipsoids at 50% probability level.

II. CHEMICALS

Chemicals and reagents were obtained from Sigma Aldrich, Alfa-Aesar, Apollo Scientific, Strem chemicals, Acros Organics, TCI UK and Fluorochem and were used as received unless otherwise stated. Deuterated solvents were purchased from Sigma-Aldrich ($CDCl_3$, Et_2O-d_{10}) and Fluorochem (CD_2Cl_2, THF-d_8, benzene–d_6, Et_2O-d_{10}, CD_3CN).

Dry dichloromethane (CH_2Cl_2), diethyl ether (Et_2O), tetrahydrofuran (THF), dimethylformamide (DMF), benzene and acetonitrile were collected fresh from a solvent purification system (MBraun, SPS-800) having been passed through anhydrous alumina columns. Chloroform ($CHCl_3$) was obtained by filtration through activated alumina (powder ~150 mesh, pore size 58 Å, basic, Sigma-Aldrich) columns. Dry *tert*-butyl methyl ether, 2-methyltetrahydrofuran, acetone, methanol and chloroform were purchased from Acros Organics with an

AcroSeal® or Sigma Aldrich with a similar seal as advertised dry solvent stored under inert atmosphere.

TMSCl was distilled before use and stored in Schlenk flasks under an argon atmosphere containing CaH_2. Schwartz reagent was prepared according to a literature procedure[286] from Cp_2ZrCl_2 provided by Strem Chemicals. $(CuOTf)_2 \cdot PhH$ was synthesised using a modified literature[287] procedure and carefully maintained under inter atmosphere. Phosphoramidite ligands were synthesised according to in-house procedures[36].

WARNING: Perchlorates are explosive and should be handled with caution.

III. NMR EXPERIMENTS

NMR experiments were carried out on Bruker AVIIIHD 400 nanobay, AVIIIHD 500, and AVII 500 spectrometers equipped with conventional or cryo-probes. Processing was performed using Topspin 3.2. Kinetic NMR experiments were performed by pre-tuning, locking and shimming the NMR sample before adding the substrate. No re-tuning and re-shimming was performed after the addition of the substrate to facilitate fast data collection unless stated. Kinetics integrations were calibrated on the assumption that at any t_n, the sum of starting material and products was 100%. All solvents were dried over molecular sieves and degassed under a flow of argon for a minimum of 30 min. $CDCl_3$ was dried by stirring over CaH_2 and K_2CO_3 for 30 min before distillation under an argon atmosphere onto molecular sieves. The solvents were stored at 0 °C, in a Schlenk on molecular sieves, protected from light.

IV. EXPERIMENTALS CHAPTER 2

*(R, E)-3-(5-phenylpent-1-en-1-yl)cyclohexanone (**6**)*

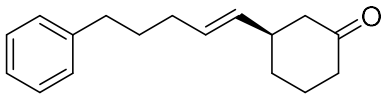

6

Cp_2ZrHCl (210 mg, 0.80 mmol, 2.0 eq) was added in one portion to a stirred solution of 5-phenyl-1-pentyne **5** (0.15 µL, 1.0 mmol, 2.5 eq) in CH_2Cl_2 (0.4 mL) and stirred until a clear yellow solution was obtained (~15 min). Simultaneously, in a different flask, CuCl (3.8 mg, 40 µmol, 10 mol%) and ligand **O** (20.2 mg, 40.0 µmol, 10.0 mol%) were dissolved in CH_2Cl_2 (2.0 mL) and stirred for 1 h. $AgSbF_6$ (15.2 mg, 44.0 µmol, 11.0 mol%)) was then added to the freshly formed Cu complex and stirring was continued for an additional 15 min. The resulting catalyst complex mixture was then taken up into a syringe, the needle was fitted with a syringe filter and the mixture was injected into the freshly prepared alkenylzirconocene species. After 10 min, cyclohex-2-en-1-one **4** (39 µL, 0.40 mmol, 1.0 eq) was added to the resulting black solution and stirring was continued for 12 h. The reaction mixture was diluted with Et_2O (2 mL) and then 1 M aqueous NH_4Cl (~3 mL) was added. The mixture was partitioned and the aqueous phase was extracted with Et_2O (3 x 10 mL). The combined organic extracts were washed with $NaHCO_3$ (aq., sat.), dried over $MgSO_4$, filtered and concentrated under reduced pressure. Purification by flash column chromatography (SiO_2, EtOAc:hexane 1:9) yielded the title product **6** (13 mg,

54 μmol, 13%, 70% ee) as a colourless oil. **^{1}H NMR** (400 MHz, $CDCl_3$) δ_H/ppm 7.33-7.24 (m, 2H, Ar-**H**), 7.20-7.11 (m, 3H, Ar-**H**), 5.51-5.32 (m, 2H, C**H**=C**H**), 2.59 (t, *J*=7.6 Hz, 2H, C**H$_2$**-Ph), 2.51-2.30 (m, 3H, C**H**$_2$-C**H**-CH_2-CH_2-C**H**$_2$-CO), 2.30-2.24 (m, 1H, CH_2-C**H**$_2$-CO), 2.23-2.13 (m, 1H, CO-C**H**$_2$-CH), 2.10-1.98 (m, 3H, C**H$_2$**-CH=CH, CH-CH_2-C**H**$_2$-CH_2-CO), 1.94-1.83 (m, 1H, CH-C**H**$_2$-CH_2) 1.77-1.60 (m, 3H, C**H$_2$**-CH_2-CH=CH, CH-CH_2-C**H**$_2$-CH_2-CO) 1.56-1.39 (m, 1H, CH-C**H**$_2$-CH_2); **^{13}C NMR** (100 MHz, $CDCl_3$) δ_C/ppm 211.5 (**C**=O), 142.4 (**C**q-Ar), 133.5 (CH=**C**H-CH), 129.4 (**C**H=CH-CH), 128.5 (**C**H-Ar), 128.3 (**C**H-Ar), 125.7 (**C**H-Ar), 47.7 (CO-**C**H_2-CH), 41.6 (CH=CH-**C**H), 41.3 (CH_2-**C**H_2-CO), 35.3 (**C**H_2-Ph), 32.0 (**C**H_2-CH=CH), 31.6 (CH-**C**H_2-CH_2), 31.1 (**C**H_2-CH_2-Ph), 25.0 (CH-CH_2-**C**H_2-CH_2-CO); **HRMS** (ESI) *m/z* calcd for $C_{17}H_{22}ONa$ $[M+Na]^+$: 265.1563, found: 265.1564; **IR (neat)** νmax/cm^{-1} 2929, 1712, 1451, 1222, 968, 747, 699; **$[\alpha]_D^{25}$** = +4.2° (*c* 1.0, $CHCl_3$, 70% ee).

The enantiomeric excess of 70% ee was determined by HPLC [Chiralpak® IA; hexane:*i*PrOH 99:1; 1.0 mL.min^{-1}, λ= 210 nm, t_R = 8.7 min (major enantiomer), t_R = 10.1 min (minor enantiomer)].

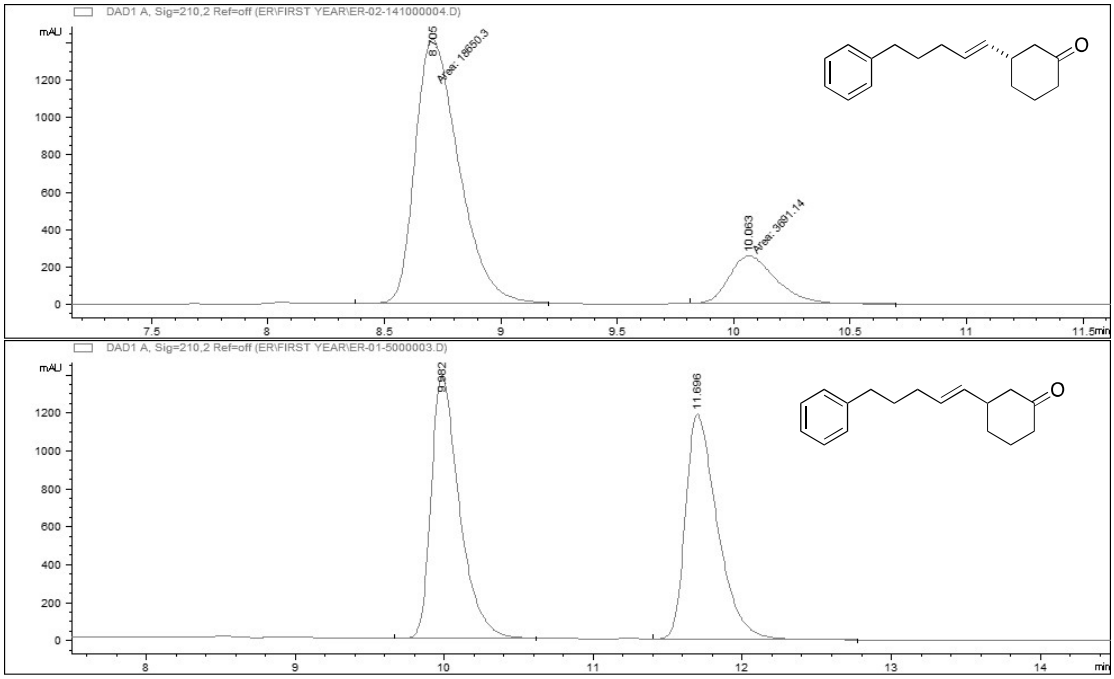

*(E)-3-(5-phenylpent-1-en-1-yl)cyclohex-2-en-1-ol (**8**)*

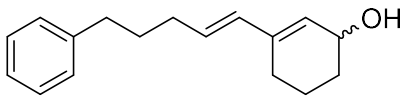

8

From the previous conditions, alcohol **8** (11 mg, 47 μmol, 12%) was also isolated. **^{1}H NMR** (400 MHz, $CDCl_3$) δ_H/ppm 7.33-7.25 (m, 2H, Ar-**H**), 7.23-7.15 (m, 3H, Ar-**H**), 6.06 (d, *J*=15.7 Hz, 1H, CH=C**H**-C=CH), 5.77-5.64 (m, 2H, C**H**=CH-C=C**H**), 4.30 (br. s, 1H, C**H**-OH), 2.63 (t, *J*=7.6 Hz, 2H, C**H$_2$**-Ph), 2.24-2.01 (m, 4H, C**H$_2$**-CH=CH-C(C**H$_2$**)=CH), 1.96-1.85 (m, 1H, C**H**$_2$-CH-OH), 1.85-1.78 (m, 1H, C**H**$_2$-CH$_2$-CH-OH), 1.78-1.69 (m, 2H, C**H$_2$**-CH$_2$-Ph), 1.68-1.52 (m, 2H, C**H**$_2$-C**H**$_2$-CH-OH);

^{13}C NMR (100 MHz, $CDCl_3$) δ_C/ppm 142.4 (**C**q-Ar), 138.6 (CH=CH-**C**(CH_2)=CH), 132.9 (CH=**C**H-C(CH_2)=CH), 129.7 (**C**H=CH-C(CH_2)=CH), 128.5 (**C**H-Ar), 128.4 (CH=CH-C(CH_2)=**C**H) 128.3 (**C**H-Ar), 125.7 (**C**H-Ar), 66.3 (**C**H-OH), 35.4 (**C**H_2-Ph), 32.4 (**C**H_2-CH=CH), 32.2 (CH_2-**C**H_2-CH-OH), 31.1 (**C**H_2-CH_2-Ph), 24.6 (CH=CH-C(**C**H_2)=CH), 18.9 (**C**H_2-CH_2-CH-OH); **HRMS** (ESI) *m/z* calcd for $C_{17}H_{22}ONa$ $[M+Na]^+$: 265.1563, found: 265.1566; **IR (neat)** νmax/cm^{-1} 3338 (br.), 3025, 2928, 2857, 2361, 1496, 1454, 1261, 1031, 965, 914, 800, 746, 699.

*(E)-3-(hex-1-en-1-yl)cyclohexan-1-one (**10**)*

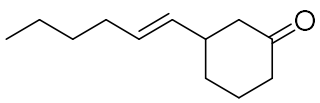

10

In analogy to a published procedure[288,289], Cp_2ZrHCl (110 mg, 0.44 mmol, 1.1 eq) was added in one portion to a stirred solution of 1-hexyne **9** (0.15 mL, 1.0 mmol, 2.5 eq) in THF (1.7 mL) and stirred until a clear yellow solution was obtained (5 min). Cyclohex-2-en-1-one **4** (39 µL, 0.40 mmol, 1.0 eq) was added to the solution followed by CuBr·DMS (82.2 mg, 40.0 µmol, 1.00 eq) 5 min later. The resulting black solution was stirred at 40 °C for 3 h. The reaction mixture was diluted with Et_2O (2 mL) and NH_4Cl (aq., 1 M, 5 mL) was added. The mixture was partitioned and the aqueous phase was extracted with Et_2O (3 x 10 mL). The combined organic extracts were washed with $NaHCO_3$ (aq., sat., 10 mL), dried over $MgSO_4$, filtered and concentrated under reduced pressure. Purification by flash column chromatography (SiO_2, Et_2O:hexane 5:95) yielded the title product

10 (27 mg, 0.15 mmol, 38%) as a colourless oil. **^{1}H NMR** (400 MHz, $CDCl_3$) δ_H/ppm 5.49-5.30 (m, 2H, C**H**=C**H**), 2.54-2.12 (m, 5H, C**H**$_2$-C**H**-CH_2-CH_2-C**H**$_2$-CO), 2.10-1.93 (m, 3H, C**H$_2$**-CH=CH, C**H**$_2$-CH_2-CO), 1.89 (dddt, *J*=13.3, 6.5, 3.4, 3.4, 1.5 Hz, 1H, CH-C**H**$_2$-CH_2), 1.68 (dddt, *J*=13.3, 11.7, 11.7, 5.0, 3.6 Hz, 1H, C**H**$_2$-CH_2-CO), 1.56-1.38 (m, 1H, CH-C**H**$_2$-CH_2), 1.36-1.17 (m, 4H, C**H$_2$**-C**H$_2$**-CH_3), 0.88 (t, *J*=7.6 Hz, 3H, C**H$_3$**); **^{13}C NMR** (100 MHz, $CDCl_3$) δ_C/ppm 211.5 (**C**=O), 132.9 (**C**H=CH-CH), 129.9 (CH=**C**H-CH), 47.7 (CO-**C**H_2-CH), 41.6 (CH=CH-**C**H), 41.3 (CH_2-**C**H_2-CO), 32.1 (**C**H_2-CH=CH), 31.6 (CH-**C**H_2-CH_2), 31.5 (**C**H_2-CH_2-CH_3), 25.0 (CH-CH_2-**C**H_2-CH_2-CO), 22.1 (**C**H_2-CH_3), 13.9 (**C**H_3); **HRMS** (ESI) *m/z* calcd for $C_{12}H_{20}NaO$ $[M+Na]^+$: 203.1399, found: 203.1406. Spectral data were in agreement with literature[290].

*(E)-4,4-dimethyl-1-(5-phenylpent-1-en-1-yl)cyclohex-2-en-1-ol (**12**)*

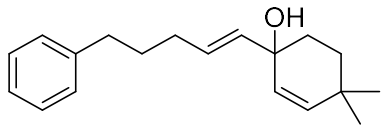

12

Cp_2ZrHCl (210 mg, 0.80 mmol, 2.0 eq) was added in one portion to a stirred solution of 5-phenyl-1-pentyne **5** (0.15 mL, 1.0 mmol, 2.5 eq) in CH_2Cl_2 (0.4 mL) and stirring was continued until a clear yellow solution was obtained (~15 min). Simultaneously, in a different flask, $Cu(MeCN)_2OTf$ (11.8 mg, 40.0 μmol, 10.0 mol%) and ligand **A** (21.6 mg, 40.0 μmol, 10.0 mol%) were dissolved in CH_2Cl_2 (2.0 mL) and stirred for 1 h. The resulting catalyst complex mixture was then added to the freshly prepared alkenylzirconocene species. After 10 min, 4,4-

dimethylcyclohex-2-en-1-one **11** (53 µL, 0.40 mmol, 1.0 eq) was added to the resulting black solution and stirred for 12 h. The reaction mixture was diluted with Et_2O (2 mL) and NH_4Cl (aq., 1 M) was added. The mixture was partitioned, then the aqueous phase was extracted with Et_2O (3 x 10 mL). The combined organic extracts were washed with $NaHCO_3$ (aq., sat.), dried over $MgSO_4$, filtered and concentrated under reduced pressure. Purification by flash column chromatography (SiO_2, EtOAc:hexane 5:95) yielded the title product **12** (46 mg, 0.17 mmol, 43%, 0% ee) as a yellow oil. **^{1}H NMR** (400 MHz, $CDCl_3$) δ_H/ppm 7.40-7.33 (m, 2H, Ar-**H**), 7.30-7.23 (m, 3H, Ar-**H**), 5.77-5.67 (m, 1H, C**H**=CH-Cq-OH), 5.66-5.59 (m, 2H, CH=C**H**-Cq(OH), Cq-CH=C**H**-Cq-OH or Cq-C**H**=CH-Cq-OH), 5.48 (d, *J*=10.1 Hz, 1H, Cq-CH=C**H**-Cq-OH or Cq-C**H**=CH-Cq-OH), 2.70 (t, *J*=7.5 Hz, 2H, C**H$_2$**-Ph), 2.18 (app. q, 2H, C**H$_2$**-CH=CH), 1.88-1.46 (m, 6H, C**H$_2$**-CH_2-Ph, Cq-OH-C**H$_2$**-C**H$_2$**), 1.11 (s, 3H, C**H$_3$**) 1.06 (s, 3H, C**H$_3$**); **^{13}C NMR** (100 MHz, $CDCl_3$) δ_C/ppm 142.4 (**Cq**-Ar), 139.8 (Cq-**C**H=CH-Cq-OH or Cq-CH=**C**H-Cq-OH), 136.1 (CH=**C**H-Cq(OH)), 129.4 (**C**H=CH-Cq(OH)), 129.1 (Cq-**C**H=CH-Cq-OH or Cq-CH=**C**H-Cq-OH), 128.4 (**C**H-Ar), 128.2 (**C**H-Ar), 125.6 (**C**H-Ar), 70.9 (**Cq**-OH), 35.3 (**C**H_2-Ph), 33.9 (Cq-OH-**C**H_2-CH_2 or Cq-OH-CH_2-**C**H_2), 33.6 (Cq-OH-**C**H_2-CH_2 or Cq-OH-CH_2-**C**H_2), 31.8 (**Cq**$(CH_3)_2$), 31.7 (**C**H_2-CH=CH), 31.0 (**C**H_2-CH_2-Ph), 29.0 (C**H$_3$**), 28.9 (C**H$_3$**); **HRMS** (ESI) *m/z* calcd for $C_{19}H_{26}O$ $[M]^+$: 270.1984, found: 270.1984; **IR (neat)** νmax/cm^{-1} 3421, 2926, 1720, 1717, 1496, 1030, 748, 699.

The enantiomeric excess of 0% ee was determined by HPLC [Chiralpak® IC; hexane:*i*PrOH 98:2; 1.0 mL.min^{-1}, λ= 210 nm, t_R = 10.6 min, 11.5 min].

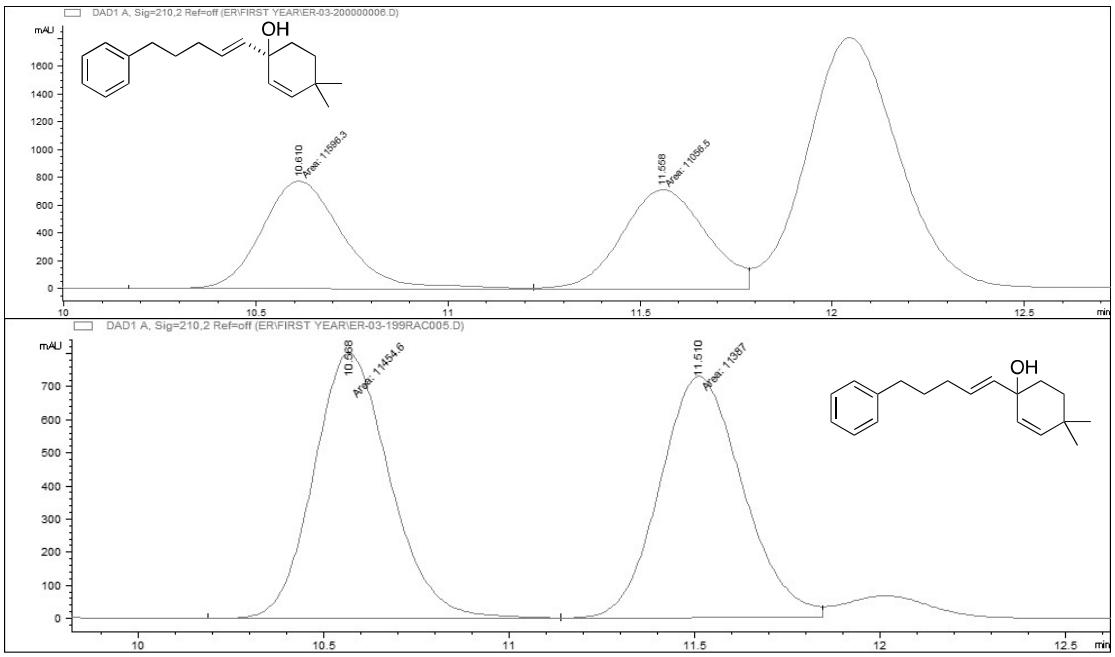

*(E)-4,4-dimethyl-3-(5-phenylpent-1-en-1-yl)cyclohexan-1-one (**13**)*

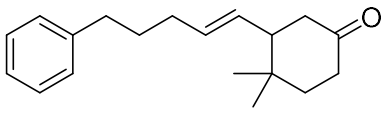

13

Cp_2ZrHCl (210 mg, 0.80 mmol, 2.0 eq) was added in one portion to a stirred solution of 5-phenyl-1-pentyne **5** (0.15 mL, 1.0 mmol, 2.5 eq) in CH_2Cl_2 (0.4 mL) and stirred until a clear yellow solution was obtained (15 min). The resulting alkenylzirconocene species was added to a solution of CuBr·DMS (82.2 mg, 40.0 μmol, 1.00 eq) in CH_2Cl_2 (2.0 mL) previously stirred for 20 min. After 10 min, 4,4-dimethylcyclohex-2-en-1-one **11** (53 μL, 0.40 mmol, 1.0 eq) was added to the resulting black solution and stirred for 12 h. The reaction mixture

was diluted with Et_2O (2 mL) and NH_4Cl (aq., 1 M) was added. The mixture was partitioned, then the aqueous phase was extracted with Et_2O (3 x 10 mL). The combined organic extracts were washed with $NaHCO_3$ (aq., sat.), dried over $MgSO_4$, filtered and concentrated under reduced pressure. Purification by flash column chromatography (SiO_2, EtOAc:petrol 5:95) yielded the title racemic product **13** (9.4 mg, 30 μmol, 9%) as a pale green oil. **^{1}H NMR** (400 MHz, $CDCl_3$) δ_H/ppm 7.25-7.17 (m, 2H, Ar-**H**), 7.15-7.07 (m, 3H, Ar-**H**), 5.42-5.31 (m, 1H, CH=C**H**-CH), 5.31-5.19 (m, 1H, C**H**=CH-CH), 2.53 (t, *J*=7.9 Hz, 2H, C**H$_2$**-Ph), 2.44-2.09 (m, 5H, C**H$_2$**-CO-C**H$_2$**, CH=CH-C**H**), 1.98 (app. q, 2H, C**H$_2$**-CH=CH), 1.72-1.46 (m, 4H, C**H$_2$**-CH_2-Ph, Cq-C**H$_2$**-CH_2-CO), 0.94 (s, 3H, C**H$_3$**), 0.93 (s, 3H, C**H$_3$**); **^{13}C NMR** (100 MHz, $CDCl_3$) δ_C/ppm 211.8 (**C**=O), 142.4 (**C**q-Ar), 131.9 (CH=**C**H-CH), 130.2 (**C**H=CH-CH), 128.4 (**C**H-Ar), 128.3 (**C**H-Ar), 125.7 (**C**H-Ar), 50.6 (CH=CH-**C**H), 44.0 (CO-**C**H_2-CH), 39.7 (**C**H_2-CH_2-CO), 38.2 (CH_2-**C**H_2-CO), 35.3 (**C**H_2-Ph), 32.8 (**Cq**$(CH_3)_2$), 32.1 (**C**H_2-CH=CH), 31.2 (**C**H_2-CH_2-Ph), 29.0 (C**H$_3$**), 20.1 (C**H$_3$**); **HRMS** (ESI) *m/z* calcd for $C_{19}H_{26}NaO$ $[M+Na]^+$: 293.1876, found: 293.1879; **IR (neat)** νmax/cm^{-1} 2927, 2360, 1713, 1454, 1148, 970, 747, 699.

The enantiomeric excess of 0% ee was determined by HPLC [Chiralpak® IA; hexane:*i*PrOH 98:2; 1.0 mL.min^{-1}, λ= 210 nm, t_R = 18.1 min, 18.8 min].

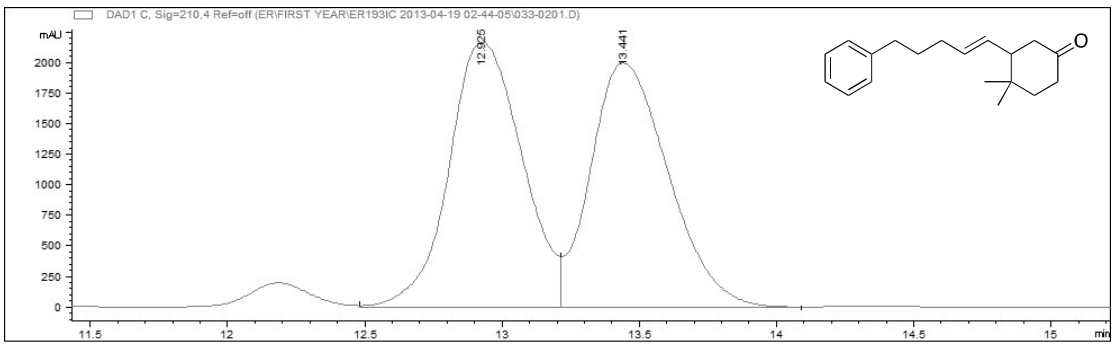

*(S)-N-(1-(naphthalen-2-yl)ethyl)cyclohexanamine (**72**)*

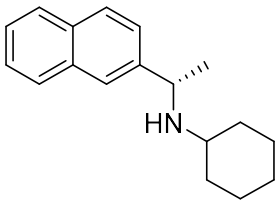

72

According to a modified procedure[291], cyclohexanone (0.31 mL, 3.0 mmol, 1.5 eq) was added to a stirring solution of (*S*)-1-(naphthalen-2-yl)ethan-1-amine (342 mg, 2.00 mmol, 1.00 eq) in THF (15 mL) at room temperature. After 5 min, $NaB(OAc)_3H$ (636 mg, 3.00 mmol, 1.50 eq) was tipped into the reaction mixture at room temperature and the resulting suspension was stirred for 48 h. Et_2O (10 mL) and $NaHCO_3$ (aq. sat., ca 10 mL) were added to the suspension and stirring was continued for 30 min. The mixture was partitioned between the aqueous and Et_2O layers and the aqueous phase extracted with Et_2O (3 × 10 mL). The combined organic phase was concentrated under reduced pressure to a small volume (~15 mL) and 2 M aqueous HCl (1 mL) was then added dropwise. The mixture was partitioned between the aqueous and Et_2O layers and the organic phase extracted with 2 M aqueous HCl (15 mL). Then CH_2Cl_2 (10 mL) was added to the combined aqueous phases and 2 M aqueous NaOH (10 mL) and then saturated aqueous NaCl (10 mL) were added until the mixture became basic (pH paper, pH >14). The mixture was partitioned between the aqueous and CH_2Cl_2 layers and the aqueous phase extracted with CH_2Cl_2 (3 × 10 mL). The combined organic phase was dried over $MgSO_4$, filtered and concentrated under reduced pressure to afford the desired title product **72** (402 mg, 1.58 mmol,

79%) as a yellow oil. **^{1}H NMR** (400 MHz, $CDCl_3$) δ_H/ppm 7.84 (d, *J*=7.8, 1.3 Hz, 3H, Ar-**H**), 7.74 (br. s, 1H, Ar-**H**), 7.51-7.44 (m, 3H, Ar-**H**), 4.16 (q, *J*=6.6 Hz, 1H, C**H**-CH_3), 2.35-2.30 (m, 1H, C**H**-cyclohexane), 2.06 (m, 1H, C**H**$_2$-cyclohexane), 1.75-1.64 (m, 3H, C**H**$_2$-cyclohexane), 1.59-1.52 (m, 1H, C**H**$_2$-cyclohexane), 1.43 (d, *J*=6.6 Hz, 3H, C**H$_3$**), 1.18-1.00 (m, 5H, C**H**$_2$-cyclohexane); **^{13}C NMR** (100 MHz, $CDCl_3$) δ_C/ppm 143.8 (**C**q-Ar), 133.5 (**C**q-Ar), 132.7 (**C**q-Ar), 128.1 (**C**H-Ar), 127.7 (**C**H-Ar), 127.6 (**C**H-Ar), 125.9 (**C**H-Ar), 125.3 (**C**H-Ar), 125.0 (**C**H-Ar), 124.8 (**C**H-Ar), 54.6 (**C**H-CH_3), 53.7 (**C**H-cyclohexane), 34.6 (**C**H$_2$-cyclohexane), 33.2 (**C**H$_2$-cyclohexane), 26.1 (**C**H$_2$-cyclohexane), 25.2 (**C**H$_2$-cyclohexane), 25.0 (**C**H$_3$), 24.9 (**C**H$_2$-cyclohexane); **LRMS** (ESI) 254.2 (100) $[M+H]^+$; **$[\alpha]_D^{25}$** = -62.1° (*c* 0.9 in $CHCl_3$). Spectral data were in agreement with literature[292].

*(S)-N-isopropyl-1,2,3,4-tetrahydronaphthalen-1-amine (**73**)*

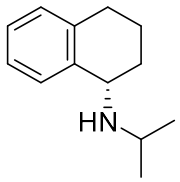

73

According to a modified procedure[291], acetone (2.6 mL, 35 mmol, 5.0 eq) was added to a stirring solution of (*S*)-1-(naphthalen-2-yl)ethan-1-amine (2.5 mL, 18 mmol, 1.0 eq) in THF (15 mL) at room temperature. After 5 min, $NaB(OAc)_3H$ (5.6 g, 26 mmol, 1.5 eq) was tipped into the reaction mixture at room temperature and the resulting suspension was stirred for 48 h. Et_2O (200 mL) and $NaHCO_3$ (aq. sat., ca 200 mL) were added to the suspension and

stirring was continued for 30 min. The mixture was partitioned between the aqueous and Et_2O layers and the aqueous phase extracted with Et_2O (3 × 50 mL). The combined organic phase was dried ($MgSO_4$), filtered and concentrated under reduced pressure to afford the desired title product **73** (2.6 g, 14 mmol, 79%) as a yellow oil. **^{1}H NMR** (400 MHz, $CDCl_3$) δ_H/ppm 7.30-7.25 (m, 1H, Ar-**H**), 7.10-7.02 (m, 2H, Ar-**H**), 7.01-6.96 (m, 1H, Ar-**H**), 3.73 (app. t, *J*=4.6 Hz, 1H, C**H**-NH), 2.97 (dt, *J*=12.5, 2x 6.2 Hz, 1H, C**H**$(CH_3)_2$), 2.79-2.58 (m, 2H, C**H$_2$**-Ar), 1.92-1.59 (m, 4H, C**H$_2$**-C**H$_2$**), 1.05 (d, *J*=6.2 Hz, 3H, C**H$_3$**), 1.03 (d, *J*=6.2 Hz, 3H, C**H$_3$**); **^{13}C NMR** (100 MHz, $CDCl_3$) δ_C/ppm 140.2 (**C**q-Ar), 137.2 (**C**q-Ar), 129.0 (**C**H-Ar), 128.9 (**C**H-Ar), 126.5 (**C**H-Ar), 125.8 (**C**H-Ar), 52.4 (Ar-**C**H-NH), 45.9 (**C**H$(CH_3)_2$), 29.4 (**C**H_2-Ar), 29.0 (CH-**C**H_2-CH_2), 24.2 (**C**H_3), 22.9 (**C**H_3), 18.9 (CH-CH_2-**C**H_2); **HRMS** (ESI) *m/z* calcd for $C_{13}H_{20}N$ $[M]^+$: 190.1590, found: 190.1590; **IR (neat)** νmax/cm^{-1} 3486, 2999, 2970, 1738, 1442, 1367, 1216, 738; **$[\alpha]_D^{25}$** = +1.4° (*c* 1.1 in $CHCl_3$).

*(11bS)-N-isopropyl-N-((S)-1,2,3,4-tetrahydronaphthalen-1-yl)dinaphtho[2,1-d:1',2'-f][1,3,2]dioxaphosphepin-4-amine (**Y**)*

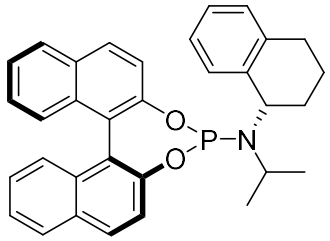

Y

According to a modified procedure from Trost[293], triethylamine (1.3 mL, 9.2 mmol, 1.5 eq) was added dropwise to an ice-cooled solution of PCl_3 (0.16 mL, 1.8 mmol, 1.0 eq) in CH_2Cl_2 (10 mL). The ice bath was removed and the solution left to warm to room temperature before (*S*)-N-isopropyl-1,2,3,4-tetrahydronaphthalen-1-amine **78** (0.35 mg, 1.8 mmol, 1.0 eq) was added to the stirring solution. (*S*)-binaphthol (0.53 mg, 1.8 mmol, 1.0 eq) was added to the suspension after 5 h and the subsequent mixture was left stirring 12 h. The solution was then filtered on a small pad of silica and Celite® and washed with CH_2Cl_2. The resulting solution was concentrated under reduced pressure to afford a yellow residue. After flash column chromatography (SiO_2, 88:17:1 Petrol:CH_2Cl_2:Et_3N), the title ligand **Y** (540 mg, 1.10 mmol, 60%) was obtained as a crystalline white solid. **^{1}H NMR** (500 MHz, $CDCl_3$) δ_H/ppm 7.96 (d, *J*=8.6 Hz, 1H, Ar-**H**), 7.92-7.84 (m, 3H, Ar-**H**), 7.80 (d, *J*=8.8 Hz, 1H, Ar-**H**), 7.51 (d, *J*=8.8 Hz, 2H, Ar-**H**), 7.42-7.35 (m, 3H, Ar-**H**), 7.35-7.15 (m, 5H, Ar-**H**), 7.06 (d, *J*=7.6 Hz, 1H, Ar-**H**), 4.41 (dt, *J*=11.1, 5.2 Hz, 1H, Ar-C**H**-N), 3.36-3.24 (m, 1H, C**H**(CH_3)$_2$), 2.87-2.77 (m, 1H, C**H**$_2$-cyclohexane), 2.72-2.63 (m, 1H, C**H**$_2$-cyclohexane), 2.24-2.12 (m, 1H,

C**H**$_2$-cyclohexane), 2.03-1.95 (m, 1H, C**H**$_2$-cyclohexane), 1.95-1.87 (m, 1H, C**H**$_2$-cyclohexane), 1.56-1.48 (m, 1H, C**H**$_2$-cyclohexane), 1.34 (d, *J*=6.6 Hz, 3H, C**H**$_3$), 1.27 (d, *J*=6.6 Hz, 3H, C**H**$_3$); **^{13}C NMR** (125 MHz, $CDCl_3$) δ_C/ppm 151.1 (d, *J*=9.3 Hz, O-**C**q-Ar), 150.4 (O-**C**q-Ar), 138.9 (**C**q-Ar), 133.3 (**C**q-Ar), 133.1 (**C**q-Ar), 131.7 (**C**q-Ar), 130.8 (**C**q-Ar), 130.7 (**C**q-Ar), 129.9 (**C**q-Ar), 129.4 (**C**q-Ar), 129.1 (**C**H-Ar), 128.7 (**C**H-Ar), 128.6 (**C**H-Ar), 127.7 (**C**H-Ar), 127.6 (**C**H-Ar) 127.0 (**C**H-Ar), 126.4 (**C**H-Ar), 126.2 (**C**H-Ar), 126.1 (**C**H-Ar), 125.1 (**C**H-Ar), 124.7 (**C**H-Ar) 124.6 (**C**H-Ar), 124.5 (**C**H-Ar), 122.9 (**C**H-Ar), 122.6 (**C**H-Ar), 121.7 (**C**H-Ar), 47.3 (Ar-**C**H-N), 47.2 (**C**H(CH_3)$_2$), 34.0 (**C**H$_2$-cyclohexane), 30.2 (**C**H$_3$), 26.5 (**C**H$_2$-cyclohexane), 23.9 (**C**H$_2$-cyclohexane), 22.8 (**C**H$_3$); **^{31}P NMR** (200 MHz, CD_2Cl_2) δ_P/ppm 153.9 (s, 1P); **HRMS** (EI/FI) *m/z* calcd for $C_{33}H_{30}NO_2P$ $[M]^+$: 503.2014, found: 503.2017; **IR (neat)** νmax/cm^{-1} 3486 (br.), 2970, 1739, 1366, 1229, 1217, 1152, 1072, 949, 815, 790, 748, 693, 627; **$[\alpha]_D^{25}$** = +175.1 (*c* 1.8 in $CHCl_3$); **Mp** 232-234 °C.

*(S)-N-cyclohexyl-1,2,3,4-tetrahydronaphthalen-1-amine (**74**)*

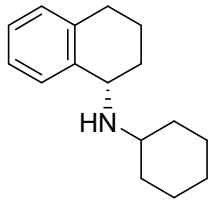

74

According to a modified procedure[291], cyclohexanone (0.70 mL, 7.0 mmol, 2.0 eq) was added to a stirring solution of (*S*)-1,2,3,4-tetrahydronaphthalen-1-amine (0.50 mL, 3.5 mmol, 1.0 eq) in THF (20 mL) at room temperature. After

5 min, $NaB(OAc)_3H$ (1.1 g, 5.3 mmol, 1.5 eq) was tipped into the reaction mixture at room temperature and the resulting suspension was stirred for 48 h. Et_2O (10 mL) and $NaHCO_3$ (aq. sat., ca 10 mL) were added to the suspension and stirring was continued for 30 min. The mixture was partitioned between the aqueous and Et_2O layers and the aqueous phase extracted with Et_2O (3 × 10 mL). The combined organic phase was dried with $MgSO_4$, filtered and concentrated under reduced pressure to afford the desired title product **74** (761 mg, 3.30 mmol, 95%) as an orange oil. **^{1}H NMR** (400 MHz, $CDCl_3$) δ_H/ppm 7.26 (d, *J*= 7.7 Hz, 1H, Ar-**H**), 7.10-7.01 (m, 2H, Ar-**H**), 6.97 (d, *J*= 7.7 Hz, 1H, Ar-**H**), 3.78 (app. t, *J*=4.7 Hz, 1H, Ar-C**H**-NH), 2.77-2.68 (m, 1H, NH-C**H**-cyclohexane), 2.67-2.52 (m, 2H, C**H**$_2$-cyclohexane), 1.99-1.50 (m, 9H, C**H**$_2$-cyclohexane), 1.29-1.00 (m, 5H, C**H**$_2$-cyclohexane); **^{13}C NMR** (100 MHz, $CDCl_3$) δ_C/ppm 139.9 (**C**q-Ar), 136.9 (**C**q-Ar), 128.6 (**C**H-Ar), 128.5 (**C**H-Ar), 126.0 (**C**H-Ar), 125.4 (**C**H-Ar), 53.8 (NH-**C**H-cyclohexane), 51.5 (Ar-**C**H-NH), 34.5 (**C**H$_2$-cyclohexane), 33.1 (**C**H$_2$-cyclohexane), 29.0 (**C**H$_2$-cyclohexane), 28.7 (**C**H$_2$-cyclohexane), 25.9 (**C**H$_2$-cyclohexane), 24.9 (**C**H$_2$-cyclohexane), 24.6 (**C**H$_2$-cyclohexane), 18.5 (**C**H$_2$-cyclohexane); **HRMS** (ESI) *m/z* calcd for $C_{16}H_{24}N$ $[M]^+$: 230.1903, found: 230.1903; **IR (neat)** νmax/cm^{-1} 3302, 2924, 851, 1488, 1448, 1109, 888, 766, 739, 694; **$[\alpha]_D^{25}$** = +1.4 (*c* 1.1 in $CHCl_3$).

*(11bS)-N-cyclohexyl-N-((S)-1,2,3,4-tetrahydronaphthalen-1-yl)dinaphtho[2,1-d:1',2'-f][1,3,2]dioxaphosphepin-4-amine (**O**)*

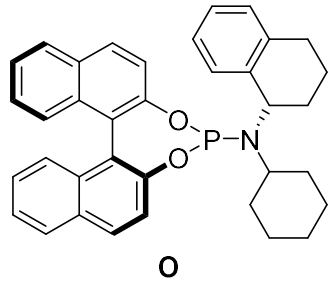

O

According to a modified procedure from Trost[293], triethylamine (1.52 mL, 10.9 mmol, 1.50 eq) was added dropwise to an ice-cooled solution of PCl_3 (0.19 mL, 2.2 mmol, 1.0 eq) in CH_2Cl_2 (15 mL). The ice bath was removed and the solution left to warm to room temperature before (*S*)-N-cyclohexyl-1,2,3,4-tetrahydronaphthalen-1-amine **79** (0.50 mg, 2.2 mmol, 1.0 eq) was added to the stirring solution. (*S*)-binaphthol (0.62 mg, 2.2 mmol, 1.0 eq) was added to the suspension after 5 h and the subsequent mixture was left stirring 12 h. The solution was then filtered on a small pad of silica and Celite® and washed with CH_2Cl_2. The resulting solution was concentrated under reduced pressure to afford a yellow residue. After flash column chromatography (SiO_2, 78:17:1 Petrol:CH_2Cl_2:Et_3N), the title ligand **O** (692 mg, 13.7 mmol, 58%) was obtained as a crystalline white solid. **^{1}H NMR** (500 MHz, $CDCl_3$) δ_H/ppm 7.96 (d, *J*=8.5 Hz, 1H, Ar-**H**), 7.90 (dd, *J*=8.6, 5.3 Hz, 2H, Ar-**H**), 7.85 (d, *J*=7.9 Hz, 1H, Ar-**H**), 7.78 (d, *J*=8.8 Hz, 1H, Ar-**H**), 7.50 (dd, *J*=9.7, 8.9 Hz, 2H, Ar-**H**), 7.43-7.36 (m, 3H, Ar-**H**), 7.35-7.29 (m, 2H, Ar-**H**), 7.28-7.15 (m, 3H, Ar-**H**), 7.06 (d, *J*=7.6 Hz, 1H, Ar-**H**), 4.41 (dt, *J*=10.9, 5.4 Hz, 1H, Ar-C**H**-N), 2.87-2.61 (m, 3H, C**H**-cyclohexane, C**H**$_2$-

cyclohexane), 2.21-2.13 (m, 1H, C**H**$_2$-cyclohexane), 2.09 (d, *J*=12.3 Hz, 1H, C**H**$_2$-cyclohexane), 2.03 (d, *J*=11.7 Hz, 1H, C**H**$_2$-cyclohexane), 1.98-1.85 (m, 2H, C**H**$_2$-cyclohexane), 1.84-1.75 (m, 1H, C**H**$_2$-cyclohexane), 1.71 (dd, *J*=12.9, 1.9 Hz, 1H, C**H**$_2$-cyclohexane), 1.64 (d, *J*=12.3 Hz, 1H, C**H**$_2$-cyclohexane), 1.59-1.43 (m, 3H, C**H**$_2$-cyclohexane), 1.40-1.25 (m, 1H, C**H**$_2$-cyclohexane), 1.10-0.99 (m, 1H, C**H**$_2$-cyclohexane), 0.98-0.91 (m, 1H, C**H**$_2$-cyclohexane); **^{13}C NMR** (125 MHz, $CDCl_3$) δ_C/ppm 151.2 (d, *J*=9.3 Hz, O-**C**q-Ar), 150.4 (O-**C**q-Ar), 139.1 (**C**q-Ar), 138.8 (**C**q-Ar), 133.3 (**C**q-Ar), 133.3 (**C**q-Ar), 133.1 (**C**q-Ar), 131.7 (**C**q-Ar), 130.8 (**C**q-Ar), 130.7 (**C**H-Ar), 130.0 (**C**H-Ar), 129.4 (**C**H-Ar), 129.0 (**C**q-Ar), 128.7 (**C**H-Ar), 128.5 (**C**H-Ar), 127.6 (**C**H-Ar), 126.9 (**C**H-Ar), 126.4 (**C**H-Ar), 126.2 (**C**H-Ar), 126.0 (**C**H-Ar), 125.1 (**C**H-Ar), 124.7 (**C**H-Ar), 124.6 (**C**H-Ar), 122.9 (**C**H-Ar), 122.5 (**C**H-Ar), 121.7 (**C**H-Ar), 55.8 (d, *J*=11.1 Hz, N-**C**H-Cyclohexane) 55.3 (d, *J*=10.9 Hz, N-**C**H-Ar), 37.6 (**C**H_2-cyclohexane), 34.5 (**C**H_2-cyclohexane), 34.1 (**C**H_2-cyclohexane), 30.2 (**C**H_2-cyclohexane), 26.9 (**C**H_2-cyclohexane), 26.8 (**C**H_2-cyclohexane), 25.9 (**C**H_2-cyclohexane), 22.8 (**C**H_2-cyclohexane); **^{31}P NMR** (200 MHz, CD_2Cl_2) δ_P/ppm 153.9 (s, 1P); **HRMS** (EI/FI) *m/z* calcd for $C_{36}H_{34}NO_2P$ $[M]^+$: 543.2327, found: 543.2212; **IR (neat)** νmax/cm^{-1} 3474, 2928, 2160, 2022, 2001, 1590, 1328, 1229, 946, 819, 789, 746, 694, 679, 625; **$[\alpha]_D^{25}$** = +141.2 (*c* 1.0 in $CHCl_3$); **Mp** 109-111 °C.

V. EXPERIMENTALS CHAPTER 3

a) Starting materials

*2,2-diphenylpropane-1,3-diol (**75**)*

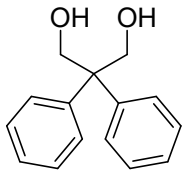

75

According to a procedure of Burgers[294], formaldehyde (13 mL, 37 wt% in H_2O, 170 mmol, 3.3 eq) and K_2CO_3 (3.5 g, 25 mmol, 0.5 eq) were added to a solution of diphenylacetaldehyde (8.9 mL, 50 mmol, 1.0 eq), in water (10 mL) and ethanol (50 mL) and refluxed for 15 h. The reaction mixture was quenched with H_2O (300 mL) and washed with EtOAc (3 x 150 mL). The combined organic layers were dried over $MgSO_4$, filtered and concentrated under reduced pressure to afford the crude product as a yellow oil. The product was recrystallized in hexane to afford the title product **75** (10.8 g, 47.3 mmol, 95%) as a white crystalline solid. **^{1}H NMR** (400 MHz, $CDCl_3$) δ_H/ppm 7.40-7.32 (m, 4H, Ar-**H**), 7.32-7.22 (m, 6H, Ar-**H**), 4.38 (s, 4H, C**H$_2$**-OH), 2.21 (br. s, 2H, O**H**); **^{13}C NMR** (100 MHz, $CDCl_3$) δ_C/ppm 142.9 (**Cq**-Ar), 128.6 (**C**H-Ar), 128.2 (**C**H-Ar), 126.9 (**C**H-Ar), 68.6 (**Cq**-(Ph_2)(CH_2)$_2$), 53.3 (**C**H_2); **HRMS** (ESI) *m*/z calcd for $C_{15}H_{16}O_2Na$ $[M+Na]^+$: 251.10425, found: 251.10420; **IR (neat)** ν_{max}/cm^{-1} 3297,

1039, 1023, 1004, 989, 696, 630. Spectral data was in accordance with literature[294].

*8,8-dimethyl-6,10-dioxaspiro[4.5]dec-3-en-2-one (**18b**)*

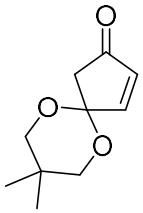

18b

According to a modified procedure of Feringa[147], $BF_3.Et_2O$ (2.5 mL, 20 mmol, 1.0 eq) was added dropwise to a solution of 4-cyclopentene-1,3-dione (1.92 g, 20.0 mmol, 1.00 eq) in $CHCl_3$ (50 mL). 2,2-dimethylpropanediol (2.50 g, 24.0 mmol, 1.20 eq) was then added at 0 °C and stirred overnight. The reaction mixture was washed with $CHCl_3$ (30 mL), quenched with NH_4Cl (*aq. sat.*, 50 mL), partitioned and the aqueous phase extracted with $CHCl_3$ (30 mL). The combined organic layers were dried over $MgSO_4$, filtered and concentrated under reduced pressure to afford the crude product as a yellow oil. Purification by flash column chromatography (SiO_2, 40% Et_2O in pentane) yielded the title product **18b** (1.54 g, 8.40 mmol, 42%) as a foamy white crystalline solid. **^{1}H NMR** (400 MHz, $CDCl_3$) δ_H/ppm 7.57 (d, *J*=6.0 Hz, 1H, OCCH=C**H**), 6.26 (d, *J*=5.8 Hz, 1H, OCC**H**=CH), 3.64 (d, *J*=11.7 Hz, 2H, C**H$_2$**-O), 3.54 (d, *J*=11.5 Hz, 2H, C**H$_2$**-O), 2.64 (s, 2H, C**H$_2$**-C=O), 1.14 (s, 3H, C**H$_3$**), 0.93 (s, 3H, C**H$_3$**); **^{13}C NMR** (100 MHz, $CDCl_3$) δ_C/ppm 204.1 (**C**=O), 157.2 (OCCH=**C**H), 135.4 (OC**C**H=CH), 104.0 (**Cq**-O_2), 73.1 (2 x **C**H_2-O), 44.2 (**C**H_2-C=O), 30.2 (**Cq**-Me_2), 22.5 (**C**H_3), 22.4 (**C**H_3); **HRMS** (ESI)

m/z calcd for $C_{10}H_{14}O_3Na$ $[M+Na]^+$: 205.08352, found: 205.0838; **IR (neat)** ν_{max}/cm^{-1} 2958, 2864, 1714, 1281, 1131, 1074, 1042, 995. Spectral data was in accordance with literature[147].

*8,8-diphenyl-6,10-dioxaspiro[4.5]dec-3-en-2-one (**18a**)*

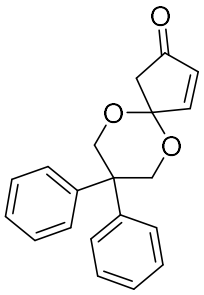

18a

According to a modified procedure of Feringa[147], $BF_3.Et_2O$ (0.81 mL, 6.6 mmol, 1.0 eq) was added dropwise to a solution of 4-cyclopentene-1,3-dione (633 mg, 6.60 mmol, 1.00 eq) in $CHCl_3$ (30 mL). 2,2-diphenylpropanediol **75** (1.50 g, 6.60 mmol, 1.00 eq) was then added at 0 °C and stirred overnight. The reaction mixture was washed with $CHCl_3$ (30 mL), quenched with NH_4Cl (*aq. sat.*, 50 mL), partitioned and the aqueous phase extracted with $CHCl_3$ (30 mL). The combined organic layers were dried over $MgSO_4$, filtered and concentrated under reduced pressure to afford the crude product as a yellow oil. Purification by flash column chromatography (SiO_2, 40% Et_2O in pentane) yielded the title product **18a** (1.36 g, 4.44 mmol, 67%) as a foamy white crystalline solid. **^{1}H NMR** (400 MHz, $CDCl_3$) δ_H/ppm 7.41 (d, *J*=5.6 Hz, 1H, OCCH=**C**H), 7.36-7.02 (m, 10H, Ar-**H**), 6.14 (d, *J*=5.6 Hz, 1H, OC**C**H=CH), 4.53 (d, *J*=11.5 Hz, 2H, C**H$_2$**-O), 4.28 (d, *J*=11.7 Hz, 2H, C**H$_2$**-O), 2.60 (s, 2H, C**H$_2$**-C=O); **^{13}C NMR** (100 MHz, $CDCl_3$) δ_C/ppm

203.8 (**C**=O), 157.0 (OCCH=**C**H), 143.7 (**Cq**-Ar), 143.5 (**Cq**-Ar), 135.6 (OC**C**H=CH), 128.8 (Ar-**C**H), 128.6 (Ar-**C**H), 127.9 (Ar-**C**H), 127.1 (Ar-**C**H), 127.0 (Ar-**C**H), 126.8 (Ar-**C**H), 104.4 (**Cq**-O_2), 70.7 (2 x **C**H_2-O), 44.8 (**Cq**-Ph_2), 44.3 (**C**H_2-C=O); **HRMS** (ESI) *m*/z calcd for $C_{20}H_{18}O_3Na$ $[M+Na]^+$: 329.11482, found: 329.1149; **IR (neat)** ν_{max}/cm^{-1} 2871, 1718, 1494, 1276, 1134, 1030, 1019, 753, 697. Spectral data was in accordance with literature[147].

b) General Procedures

Preparation of premade complex[87]

$(CuOTf)_2$·PhH (240 mg, 0.48 mmol, 0.50 eq) and (*R*)-**Q** (513 mg, 0.950 mmol, 1.00 eq) were added to a flame-dried Schlenk, dissolved in CH_2Cl_2 (10 mL) and stirred at room temperature for 1 h. The resulting clear solution was filtered over a syringe filter into another Schlenk flask before the solvent was slowly removed under high vacuum. The resulting white solid was dried for 3 h and then stored under an atmosphere of argon.

Procedure when using premade complex

In a flame-dried flask under an argon atmosphere, Cp_2ZrHCl (3.0 eq) was added to a solution of alkene (3.5 eq) in CH_2Cl_2 (2.0 M in alkene) and the resulting mixture was vigorously stirred until a clear yellow solution was obtained (20-40 min). Simultaneously, in another flask under an inert atmosphere, premade CuOTf/(*R*)-**Q** complex (20 mol%) was dissolved in Et_2O (0.2 M in **18**) and stirred for 15 min at room temperature. The freshly prepared alkylzirconocene species was then added to the catalyst complex. After 10 min,

solid cyclopentene-3,5-dione monoacetal **18** (1.0 eq) was added in one portion by quickly tipping the solid into the black solution. TMSCl (5.0 eq) was then added dropwise and the reaction mixture was stirred overnight. The reaction mixture was diluted with Et_2O (2 mL) and quenched with NH_4Cl (3 mL, 1 M). The mixture was partitioned and the aqueous phase was extracted with Et_2O (3 x 10 mL). The combined organic extracts were washed with $NaHCO_3$ (aq. sat. 30 mL), dried over $MgSO_4$, filtered and concentrated under reduced pressure. Purification by flash column chromatography yielded the enantioenriched products.

Procedure when using AgX at RT

In a flame-dried flask under an argon atmosphere, Cp_2ZrHCl (3.0 eq) was added to a solution of alkene (3.5 eq) in CH_2Cl_2 (2.0 M in alkene) and vigorously stirred until a clear yellow solution was obtained (20-40 min). Simultaneously, in another flask under an inert atmosphere, CuCl (20 mol%) and (*R*)-**Q** (22 mol%) were covered in Et_2O (0.2 M in **18**) and stirred for 1 h at room temperature. AgX (20 mol%) was added to the freshly formed Cu-ligand containing solution and stirring was continued for an additional 1 h. The resulting catalyst complex mixture was taken up by syringe and injected through a filter into the freshly prepared alkylzirconocene species. After 10 min, solid cyclopentene-3,5-dione monoacetal **18** (1.0 eq) was added in one portion by quickly tipping the solid into the black solution. TMSCl (5.0 eq) was then added dropwise and the reaction mixture was stirred overnight. The reaction mixture was diluted with Et_2O (2 mL) and quenched with NH_4Cl (3 mL, 1 M). The mixture was partitioned and the aqueous phase was extracted with Et_2O (3 x 10 mL). The combined organic

extracts were washed with $NaHCO_3$ (aq. sat. 30 mL), dried over $MgSO_4$, filtered and concentrated under reduced pressure. Purification by flash column chromatography yielded the enantioenriched products.

Procedure for synthesising racemic products

In a flame-dried flask under inert atmosphere, Cp_2ZrHCl (3.0 eq) was added to a solution of alkene (3.5 eq) in CH_2Cl_2 (2.0 M in alkene) under an argon atmosphere and stirred vigorously until a clear yellow solution was obtained (20-40 min). The hydrozirconated mixture was dissolved in CH_2Cl_2 (0.2 M in **18**) and then CuBr·DMS (1.0 eq) was added. After 10 min, cyclopentene-3,5-dione monoacetal **18** (1.0 eq) was added quickly as a solid to the resulting black solution and stirred overnight. The reaction mixture was diluted with Et_2O (2 mL) and quenched with NH_4Cl (3 mL, 1 M). The mixture was partitioned and the aqueous phase was extracted with Et_2O (3 x 10 mL). The combined organic extracts were washed with $NaHCO_3$ (aq., sat., 30 mL), dried over $MgSO_4$, filtered and concentrated under reduced pressure. Purification by flash column chromatography yielded the racemic products.

c) Specific procedures

*(S)-8,8-dimethyl-4-(4-phenylbutyl)-6,10-dioxaspiro[4.5]decan-2-one (**20a**)*

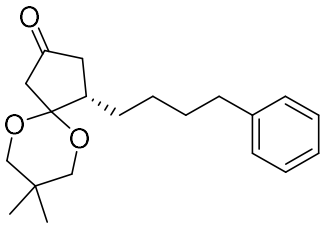

20a

In a flame-dried flask under an argon atmosphere, Cp_2ZrHCl (310 mg, 1.2 mmol, 3.0 eq) was added to a solution of 4-phenyl-1-butene **16** (0.21 mL, 1.4 mmol 3.5 eq) in CH_2Cl_2 (0.5 mL) and vigorously stirred until a clear yellow solution was obtained (15 min). Simultaneously, in another flask under argon, CuCl (7.9 mg, 80 μmol, 20 mol%) and (*R*)-**Q** (47.5 mg, 88.0 μmol, 22.0 mol%) were covered in Et_2O (2.2 mL) and stirred for 1 h at room temperature. AgOTf (20.6 mg, 80.0 μmol, 20.0 mol%) was added to the freshly formed Cu-ligand containing solution and stirring continued for an additional 15 min. The resulting catalyst mixture was taken up by syringe and injected through a filter into the freshly prepared alkylzirconocene species. After 10 min, solid 8,8-dimethyl-6,10-dioxaspiro[4.5]dec-3-en-2-one **18b** (73.0 mg, 0.400 mmol, 1.00 eq) was added in one portion by quickly tipping the solid into the black solution. TMSCl (0.25 mL, 2.0 mmol, 5.0 eq) was then added dropwise and the reaction mixture was stirred overnight. The reaction mixture was diluted with Et_2O (2 mL) and quenched with NH_4Cl (3 mL, 1 M). The mixture was partitioned and the aqueous phase was extracted with Et_2O (3 x 10 mL). The combined organic extracts were washed

with $NaHCO_3$ (aq. sat. 30 mL), dried over $MgSO_4$, filtered and concentrated under reduced pressure. Purification by flash column chromatography (SiO_2, Et_2O 5-10% in pentane) yielded the title product **20a** (61 mg, 0.19 mmol, 48%, 87% ee) as a clear oil. **^{1}H NMR** (500 MHz, $CDCl_3$) δ_H/ppm 7.23-7.17 (m, 2H, Ar-**H**), 7.13-7.08 (m, 3H, Ar-**H**), 3.46-3.34 (m, 4H, O-C**H$_2$**), 2.89 (d, *J*= 18.2 Hz, 1H, C**H$_2$**), 2.62-2.50 (m, 2H, C**H$_2$**), 2.41 (dd, *J*= 17.7, 8.0 Hz, 1H, C**H$_2$**), 2.27-2.19 (m, 2H, C**H** and C**H$_2$**), 2.02 (dd, *J*= 18.2 Hz, 10.7 Hz, 1H, C**H$_2$**), 1.86-1.77 (m, 1H, C**H$_2$**), 1.66-1.53 (m, 2H, C**H$_2$**), 1.42-1.23 (m, 3H, C**H$_2$**), 1.10 (s, 3H, C**H$_3$**), 0.70 (s, 3H, C**H$_3$**); **^{13}C NMR** (126 MHz, $CDCl_3$) δ_C/ppm 213.7 (**C**=O), 142.7 (**Cq**-Ar), 128.5 (**C**H-Ar), 128.4 (**C**H-Ar), 125.8 (**C**H-Ar), 104.3 (**Cq**-O_2), 73.1 (O-**C**H_2), 71.5 (O-**C**H_2), 46.1 (**C**H), 44.3 (**C**H_2-C=O), 43.2 (**C**H_2), 36.0 (**C**H_2), 31.8 (**C**H_2), 30.4 (**Cq**-Me_2), 27.9 (**C**H_2), 27.5 (**C**H_2), 22.8 (**C**H_3), 22.2 (**C**H_3); **HRMS** (ESI) *m*/z calcd for $C_{20}H_{29}O_3$ $[M+H]^+$: 317.21112, found: 317.21117; **IR (neat)** ν_{max}/cm^{-1} 2931, 2858, 1748, 1466, 1396, 1285, 1186, 1118, 1055, 1017, 979, 747, 700; **$[\alpha]_D^{25}$** = +67.9° (c= 1.0 in $CHCl_3$, 87% ee).

The enantiomeric excess of 87% ee was determined by HPLC [Chiralpak® IC; hexane:*i*PrOH 95:5; 1.0 mL.min^{-1}, λ= 210 nm, t_R = 11.8 min (major enantiomer), t_R = 15.6 min (minor enantiomer)].



*(S)-8,8-diphenyl-4-(4-phenylbutyl)-6,10-dioxaspiro[4.5]decan-2-one (**21a**)*

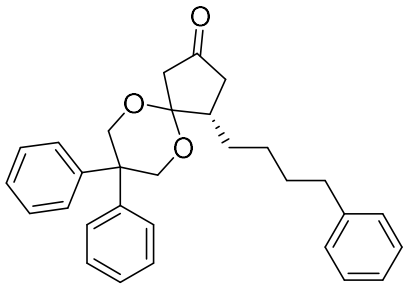

21a

In a flame-dried flask under an argon atmosphere, Cp_2ZrHCl (310 mg, 1.2 mmol, 3.0 eq) was added to a solution of 4-phenyl-1-butene **16** (0.21 mL, 1.4 mmol 3.5 eq) in CH_2Cl_2 (0.5 mL) and vigorously stirred until a clear yellow solution was obtained (15 min). Simultaneously, in another flask under an argon atmosphere, CuCl (7.9 mg, 80 μmol, 20 mol%) and (*R*)-**Q** (47.5 mg, 88.0 μmol,

22.0 mol%) were covered in Et_2O (2.2 mL) and stirred for 1 h at room temperature. AgOTf (20.6 mg, 80.0 μmol, 20.0 mol%) was added to the freshly formed Cu-ligand containing solution and stirring continued for an additional 1 h. The resulting catalyst mixture was taken up by syringe and injected through a filter into the freshly prepared alkylzirconocene species and then the reaction flask was cooled to 0 °C using an ice/water bath. After 10 min, solid 8,8-diphenyl-6,10-dioxaspiro[4.5]dec-3-en-2-one **18a** (120 mg, 0.400 mmol, 1.00 eq) was added in one portion by quickly tipping the solid into the black solution. TMSCl (0.25 mL, 2.0 mmol, 5.0 eq) was then added dropwise and the reaction mixture was stirred overnight and allowed to slowly warm to RT. The reaction mixture was diluted with Et_2O (2 mL) and quenched with NH_4Cl (3 mL, 1 M). The mixture was partitioned and the aqueous phase was extracted with Et_2O (3 x 10 mL). The combined organic extracts were washed with $NaHCO_3$ (aq. sat. 30 mL), dried over $MgSO_4$, filtered and concentrated under reduced pressure. Purification by flash column chromatography (SiO_2, Et_2O 10-20% in pentane) yielded the title product **21a** (108 mg, 0.240 mmol, 61%, 92% ee) as a white solid. **^{1}H NMR** (500 MHz, $CDCl_3$) δ_H/ppm 7.51 (d, *J*= 8.0 Hz, 2H, Ar-**H**), 7.37 (d, *J*= 7.5 Hz, 2H, Ar-**H**), 7.35-7.19 (m, 7H, Ar-**H**), 7.18 (d, *J*= 7.6 Hz, 2H, Ar-**H**), 7.11 (d, *J*= 7.6 Hz, 2H, Ar-**H**), 4.67-4.60 (m, 2H, C**H**$_2$-O-Cq-O-C**H**$_2$), 4.36 (d, *J*= 12.0 Hz, 1H, C**H**$_2$-O-Cq-O-CH_2), 4.24 (d, *J*= 12.0 Hz, 1H, CH_2-O-Cq-O-C**H**$_2$), 3.13 (d, *J*= 18.0 Hz, 1H, Cq-C**H**$_2$-CO), 2.60-2.51 (m, 2H, CH_2-C**H$_2$**-Ph), 2.50 (d, *J*= 8.4 Hz, 1H, CH-C**H**$_2$-CO), 2.43 (d, *J*= 18.0 Hz, 1H, Cq-C**H**$_2$-CO), 2.35-2.26 (m, 1H, C**H**-CH_2-CO), 2.15 (dd, *J*= 18.1, 11.0 Hz, 1H, CH-C**H**$_2$-CO), 1.70-1.59 (m, 1H, CH-CH_2-C**H**$_2$), 1.55 (app. quint., 2H, C**H$_2$**-CH_2-Ph), 1.36-1.13 (m, 3H, CH-C**H**$_2$-CH_2, CH-CH_2-C**H**$_2$); **^{13}C NMR** (126 MHz, $CDCl_3$) δ_C/ppm 213.2 (**C**=O), 143.7 (**Cq**-Ar), 143.4 (**Cq**-Ar), 142.8 (**Cq**-Ar), 128.8

(Ar-**C**H), 128.7 (Ar-**C**H), 128.5, (Ar-**C**H) 128.4 (Ar-**C**H), 128.2 (Ar-**C**H), 127.1 (Ar-**C**H), 126.5 (Ar-**C**H), 126.5 (Ar-**C**H), 125.7 (Ar-**C**H), 104.8 (O-**Cq**-O), 70.9 (**C**H_2-O), 68.9 (**C**H_2-O), 46.0 (**C**H-CH_2-CO), 45.0 (Cq-**C**H_2-CO), 44.8 (**Cq**-Ph_2), 43.4 (CH-**C**H_2-CO), 35.8 (CH_2-**C**H_2-Ph), 31.8 (**C**H_2-CH_2-Ph), 27.7 (CH-**C**H_2-CH_2), 27.5 (CH-CH_2-**C**H_2); **HRMS** (ESI) *m*/z calcd for $C_{30}H_{32}O_3Na$ $[M+Na]^+$: 463.22437, found: 463.22410; **IR (neat)** (ν_{max}/cm^{-1}) 3026, 2933, 1749, 1400, 1279, 1132, 1044, 751, 699; **$[\alpha]_D^{25}$** = +50.4 (c= 1.1 in $CHCl_3$, 92% ee); **Mp** 80-84 °C.

The enantiomeric excess of 92% ee was determined by HPLC [Chiralpak® IA; hexane:*i*PrOH 90:10; 1.0 mL.min^{-1}, λ= 210 nm, t_R = 7.6 min (major enantiomer), t_R = 13.4 min (minor enantiomer)].



X-Ray Crystal structure (for absolute configuration determination)

The absolute configuration was determined by X-ray crystallography. (*S*)-8,8-diphenyl-4-(4-phenylbutyl)-6,10-dioxaspiro[4.5]decan-2-one **21a** was recrystallized from CH_2Cl_2/pentane.

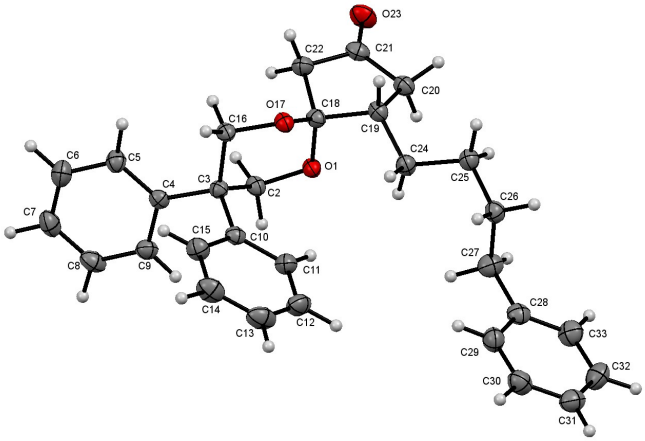

Crystal Data

a = 6.27440(10) Å α = 90°
b = 18.51590(10) Å β = 90°
c = 20.23140(10) Å γ = 90°

Volume	2350.41(4) Å³	Crystal Class	orthorhombic
Space group	P 2_1 2_1 2_1	Z =	4
Formula	C_{30} H_{32} O_3	M_r	440.58
Cell determined from	61381 reflections	Cell θ range =	3 - 76°
Temperature	150K		
Shape	needles		
Colour	clear_pale_colourless	Size	0.05 × 0.16 × 0.20 mm
D_x	1.24 mg m^{-3}	F000	944.000
μ	0.618 mm^{-1}		
Absorption correction	multi-scan		
T_{min}	0.80	T_{max}	0.97

Data Collection

Diffractometer	multi-scan
Scan type	ω scans
Reflections measured	91715
Independent reflections	4913
Rint	0.0254
θ_{max}	76.4153
h =	-7 → 6
k =	-23 → 23
l =	-25 → 25

Refinement

$\Delta\rho_{min}$ =	-0.14 e Å^{-3}
$\Delta\rho_{max}$ =	0.17 e Å^{-3}
Reflections used	4892
Cutoff: I >	-3.00σ(I)
Parameters refined	299
S =	1.00
R-factor	0.027
weighted R-factor	0.068
Δ/σ_{max}	0.0005
Flack parameter	0.04(12)
Refinement on	F^2
w =	$1/[\sigma^2(F_{obs}^2) + (0.037 \times P)^2 + 0.406 \times P + 0.000 + 0.000 \times \sin\theta]$, $P = 0.333 \times \max(F_{obs}^2,0) + 0.667 \times F_{calc}^2$

Parameters

Label	*x*	*y*	*z*	$U_{iso/equiv}$	Occupancy
O1	0.19664(11)	0.48293(4)	0.52345(3)	0.0231	1.0000
C2	0.09302(16)	0.52317(5)	0.57453(5)	0.0232	1.0000
C3	0.12629(16)	0.55262(5)	0.55401(5)	0.0207	1.0000
C4	0.22982(16)	0.58300(5)	0.61654(5)	0.0219	1.0000
C5	0.41425(17)	0.55494(6)	0.64398(5)	0.0277	1.0000
C6	0.50645(19)	0.58651(7)	0.69983(6)	0.0354	1.0000
C7	-0.4129(2)	0.64568(7)	0.72930(5)	0.0364	1.0000
C8	-0.2256(2)	0.67341(6)	0.70320(5)	0.0339	1.0000

C9	0.13550(18)	0.64268(6)	0.64729(5)	0.0277	1.0000
C10	0.11831(17)	0.61184(5)	0.50106(5)	0.0228	1.0000
C11	0.06112(19)	0.62680(6)	0.46320(5)	0.0298	1.0000
C12	0.0542(2)	0.68055(6)	0.41471(6)	0.0382	1.0000
C13	-0.1293(2)	0.71947(7)	0.40392(6)	0.0417	1.0000
C14	-0.3084(2)	0.70551(6)	0.44146(6)	0.0386	1.0000
C15	0.30294(19)	0.65180(6)	0.48941(5)	0.0307	1.0000
C16	0.24715(16)	0.48730(5)	0.52612(5)	0.0230	1.0000
O17	0.12802(11)	0.45619(4)	0.47265(3)	0.0233	1.0000
C18	0.06906(16)	0.42807(5)	0.49376(5)	0.0227	1.0000
C19	0.19360(17)	0.39998(5)	0.43342(5)	0.0243	1.0000
C20	0.35557(18)	0.34728(6)	0.46398(5)	0.0274	1.0000
C21	0.24488(18)	0.31730(5)	0.52444(5)	0.0277	1.0000
C22	0.04984(18)	0.36227(5)	0.53965(5)	0.0277	1.0000
O23	0.30121(15)	0.26490(4)	0.55586(4)	0.0377	1.0000
C24	0.28915(18)	0.45915(5)	0.39018(5)	0.0267	1.0000
C25	0.43480(19)	0.43083(6)	0.33545(5)	0.0278	1.0000
C26	0.50771(18)	0.49027(6)	0.28792(5)	0.0277	1.0000
C27	0.6456(2)	0.54907(6)	0.31963(5)	0.0338	1.0000
C28	0.71629(19)	0.60372(6)	0.26889(5)	0.0296	1.0000
C29	0.5732(2)	0.65440(6)	0.24425(6)	0.0344	1.0000
C30	0.6314(2)	0.70292(7)	0.19506(6)	0.0375	1.0000
C31	0.8358(2)	0.70174(7)	0.16964(6)	0.0374	1.0000
C32	0.9807(2)	0.65234(8)	0.19397(6)	0.0407	1.0000
C33	0.9212(2)	0.60392(7)	0.24355(6)	0.0372	1.0000
H22	0.19721(16)	0.56340(5)	0.58268(5)	0.0286	1.0000
H21	0.06205(16)	0.49073(5)	0.61504(5)	0.0290	1.0000
H51	0.48897(17)	0.51178(6)	0.62459(5)	0.0353	1.0000
H61	0.63956(19)	0.56605(7)	0.71940(6)	0.0462	1.0000
H71	-0.4841(2)	0.66922(7)	0.76843(5)	0.0456	1.0000
H81	-0.1652(2)	0.71556(6)	0.72592(5)	0.0448	1.0000
H91	0.01156(18)	0.66340(6)	0.62861(5)	0.0345	1.0000
H111	0.18549(19)	0.60085(6)	0.47252(5)	0.0382	1.0000
H121	0.1885(2)	0.69083(6)	0.38790(6)	0.0476	1.0000
H131	-0.1342(2)	0.75711(7)	0.37266(6)	0.0547	1.0000
H141	-0.4441(2)	0.73244(6)	0.43688(6)	0.0496	1.0000
H151	0.42428(19)	0.64276(6)	0.51468(5)	0.0400	1.0000
H162	0.26402(16)	0.44907(5)	0.56086(5)	0.0282	1.0000

H161	0.38805(16)	0.50221(5)	0.50812(5)	0.0282	1.0000
H191	0.08662(17)	0.37003(5)	0.40682(5)	0.0310	1.0000
H201	0.49157(18)	0.37329(6)	0.47777(5)	0.0355	1.0000
H202	0.39540(18)	0.30801(6)	0.43080(5)	0.0332	1.0000
H221	0.03638(18)	0.37590(5)	0.58727(5)	0.0361	1.0000
H222	0.08031(18)	0.33473(5)	0.52947(5)	0.0375	1.0000
H241	0.36862(18)	0.49085(5)	0.41923(5)	0.0339	1.0000
H242	0.17324(18)	0.48708(5)	0.36752(5)	0.0357	1.0000
H251	0.56201(19)	0.40789(6)	0.35367(5)	0.0349	1.0000
H252	0.35688(19)	0.39045(6)	0.31186(5)	0.0350	1.0000
H261	0.37974(18)	0.51388(6)	0.26548(5)	0.0362	1.0000
H262	0.59633(18)	0.46729(6)	0.25542(5)	0.0365	1.0000
H271	0.5607(2)	0.57624(6)	0.35260(5)	0.0463	1.0000
H272	0.7702(2)	0.52586(6)	0.34205(5)	0.0465	1.0000
H291	0.4301(2)	0.65380(6)	0.26046(6)	0.0426	1.0000
H301	0.5203(2)	0.73843(7)	0.17852(6)	0.0473	1.0000
H311	0.8735(2)	0.73630(7)	0.13636(6)	0.0503	1.0000
H321	1.1237(2)	0.65086(8)	0.17384(6)	0.0506	1.0000
H331	1.0290(2)	0.56806(7)	0.26207(6)	0.0469	1.0000

Thermal Parameters

Label	U_{11}	U_{22}	U_{33}	U_{23}	U_{13}	U_{12}
O1	0.0196(3)	0.0237(3)	0.0262(3)	-0.0044(3)	-0.0004(3)	-0.0002(3)
C2	0.0218(5)	0.0242(5)	0.0236(4)	-0.0033(4)	-0.0021(4)	0.0010(4)
C3	0.0192(5)	0.0206(4)	0.0222(4)	-0.0003(4)	-0.0009(4)	-0.0006(4)
C4	0.0242(5)	0.0209(4)	0.0207(4)	0.0014(3)	-0.0025(4)	0.0027(4)
C5	0.0232(5)	0.0318(5)	0.0280(5)	-0.0026(4)	-0.0003(4)	0.0008(4)
C6	0.0315(6)	0.0425(6)	0.0320(6)	-0.0014(5)	0.0068(5)	0.0023(5)
C7	0.0451(7)	0.0370(6)	0.0270(5)	-0.0038(4)	0.0044(5)	0.0095(5)
C8	0.0497(7)	0.0254(5)	0.0268(5)	-0.0040(4)	-0.0046(5)	0.0010(5)
C9	0.0331(6)	0.0237(5)	0.0262(5)	0.0012(4)	-0.0003(4)	-0.0025(4)
C10	0.0274(5)	0.0207(4)	0.0204(4)	-0.0022(4)	-0.0021(4)	-0.0017(4)
C11	0.0322(6)	0.0256(5)	0.0316(5)	0.0000(4)	0.0033(5)	-0.0019(4)
C12	0.0506(7)	0.0320(6)	0.0318(5)	0.0029(5)	0.0079(5)	-0.0088(5)
C13	0.0660(9)	0.0291(5)	0.0300(6)	0.0062(4)	-0.0027(6)	-0.0020(6)
C14	0.0484(7)	0.0325(6)	0.0350(6)	0.0058(5)	-0.0074(6)	0.0078(5)
C15	0.0322(6)	0.0306(5)	0.0292(5)	0.0026(4)	-0.0022(4)	0.0038(4)

C16	0.0195(4)	0.0232(4)	0.0263(5)	-0.0036(4)	-0.0009(4)	-0.0015(4)
O17	0.0204(3)	0.0246(3)	0.0249(3)	-0.0046(3)	-0.0022(3)	0.0009(3)
C18	0.0225(5)	0.0210(4)	0.0246(4)	-0.0018(4)	-0.0014(4)	-0.0003(4)
C19	0.0250(5)	0.0228(4)	0.0250(5)	-0.0031(4)	-0.0013(4)	0.0019(4)
C20	0.0282(5)	0.0233(4)	0.0306(5)	-0.0016(4)	0.0001(4)	0.0036(4)
C21	0.0327(5)	0.0220(4)	0.0284(5)	-0.0027(4)	-0.0054(4)	-0.0008(4)
C22	0.0314(5)	0.0223(5)	0.0295(5)	0.0015(4)	0.0022(4)	-0.0004(4)
O23	0.0482(5)	0.0281(4)	0.0368(4)	0.0047(3)	-0.0038(4)	0.0077(4)
C24	0.0289(5)	0.0262(5)	0.0251(5)	0.0002(4)	0.0016(4)	0.0032(4)
C25	0.0295(5)	0.0272(5)	0.0266(5)	-0.0018(4)	0.0020(4)	0.0009(4)
C26	0.0297(5)	0.0293(5)	0.0241(5)	-0.0022(4)	0.0018(4)	0.0008(4)
C27	0.0370(6)	0.0355(6)	0.0289(5)	0.0017(4)	-0.0043(5)	-0.0052(5)
C28	0.0333(6)	0.0287(5)	0.0268(5)	-0.0035(4)	-0.0036(4)	-0.0038(5)
C29	0.0320(6)	0.0362(6)	0.0351(5)	-0.0014(5)	0.0042(5)	0.0036(5)
C30	0.0454(7)	0.0320(6)	0.0350(6)	0.0005(5)	0.0002(5)	0.0045(5)
C31	0.0456(7)	0.0343(6)	0.0323(5)	0.0003(5)	0.0003(5)	-0.0079(5)
C32	0.0311(6)	0.0497(7)	0.0411(6)	0.0015(6)	0.0037(5)	-0.0064(5)
C33	0.0310(6)	0.0399(6)	0.0407(6)	0.0018(5)	-0.0035(5)	0.0017(5)

Distances

O1	C2	1.4302(11)Å		O1	C18	1.4260(11)Å
C2	C3	1.5373(13)Å		C2	H22	1.005Å
C2	H21	1.035Å		C3	C4	1.5293(13)Å
C3	C10	1.5338(13)Å		C3	C16	1.5351(13)Å
C4	C5	1.3847(14)Å		C4	C9	1.3994(14)Å
C5	C6	1.3975(15)Å		C5	H51	1.006Å
C6	C7	1.3786(18)Å		C6	H61	0.999Å
C7	C8	1.3867(18)Å		C7	H71	1.008Å
C8	C9	1.3866(15)Å		C8	H81	0.982Å
C9	H91	0.946Å		C10	C11	1.3896(15)Å
C10	C15	1.3946(15)Å		C11	C12	1.3982(16)Å
C11	H111	0.936Å		C12	C13	1.376(2)Å
C12	H121	1.020Å		C13	C14	1.381(2)Å
C13	H131	0.942Å		C14	C15	1.3897(16)Å
C14	H141	0.991Å		C15	H151	0.932Å
C16	O17	1.4354(12)Å		C16	H162	1.003Å
C16	H161	0.995Å		O17	C18	1.4081(12)Å

C18	C19	1.5399(13)Å		C18	C22	1.5364(14)Å
C19	C20	1.5387(14)Å		C19	C24	1.5248(14)Å
C19	H191	1.024Å		C20	C21	1.5122(15)Å
C20	H201	1.019Å		C20	H202	1.021Å
C21	C22	1.5119(15)Å		C21	O23	1.2127(13)Å
C22	H221	0.999Å		C22	H222	0.985Å
C24	C25	1.5284(14)Å		C24	H241	0.969Å
C24	H242	1.003Å		C25	C26	1.5314(14)Å
C25	H251	0.976Å		C25	H252	1.013Å
C26	C27	1.5313(15)Å		C26	H261	1.021Å
C26	H262	0.961Å		C27	C28	1.5084(15)Å
C27	H271	0.991Å		C27	H272	1.001Å
C28	C29	1.3908(16)Å		C28	C33	1.3840(17)Å
C29	C30	1.3895(17)Å		C29	H291	0.957Å
C30	C31	1.3817(19)Å		C30	H301	1.015Å
C31	C32	1.3806(19)Å		C31	H311	0.958Å
C32	C33	1.3963(18)Å		C32	H321	0.986Å
C33	H331	1.019Å				

Angles

C2	O1	C18	114.85(7)°		O1	C2	C3	113.37(8)°
O1	C2	H22	102.063°		C3	C2	H22	111.335°
O1	C2	H21	110.809°		C3	C2	H21	104.576°
H22	C2	H21	115.006°		C2	C3	C4	106.70(8)°
C2	C3	C10	114.39(8)°		C4	C3	C10	109.19(7)°
C2	C3	C16	105.19(7)°		C4	C3	C16	112.59(8)°
C10	C3	C16	108.82(8)°		C3	C4	C5	123.26(9)°
C3	C4	C9	118.60(9)°		C5	C4	C9	118.14(9)°
C4	C5	C6	120.86(10)°		C4	C5	H51	122.090°
C6	C5	H51	117.041°		C5	C6	C7	120.39(11)°
C5	C6	H61	120.523°		C7	C6	H61	119.076°
C6	C7	C8	119.36(10)°		C6	C7	H71	119.626°
C8	C7	H71	120.979°		C7	C8	C9	120.28(10)°
C7	C8	H81	116.287°		C9	C8	H81	123.418°
C4	C9	C8	120.94(10)°		C4	C9	H91	119.357°
C8	C9	H91	119.655°		C3	C10	C11	123.64(9)°
C3	C10	C15	118.05(9)°		C11	C10	C15	118.30(9)°

C10	C11	C12	120.23(11)°		C10	C11	H111	117.534°
C12	C11	H111	122.204°		C11	C12	C13	120.68(12)°
C11	C12	H121	118.696°		C13	C12	H121	120.617°
C12	C13	C14	119.72(10)°		C12	C13	H131	121.426°
C14	C13	H131	118.798°		C13	C14	C15	119.87(12)°
C13	C14	H141	123.605°		C15	C14	H141	116.521°
C10	C15	C14	121.21(11)°		C10	C15	H151	119.362°
C14	C15	H151	119.426°		C3	C16	O17	109.63(7)°
C3	C16	H162	110.514°		O17	C16	H162	107.452°
C3	C16	H161	110.777°		O17	C16	H161	107.345°
H162	C16	H161	111.004°		C16	O17	C18	112.15(7)°
O1	C18	O17	110.93(7)°		O1	C18	C19	106.84(8)°
O17	C18	C19	109.27(8)°		O1	C18	C22	110.75(8)°
O17	C18	C22	114.06(8)°		C19	C18	C22	104.55(8)°
C18	C19	C20	103.34(8)°		C18	C19	C24	114.32(8)°
C20	C19	C24	115.25(9)°		C18	C19	H191	105.486°
C20	C19	H191	107.498°		C24	C19	H191	110.212°
C19	C20	C21	104.74(8)°		C19	C20	H201	111.303°
C21	C20	H201	109.671°		C19	C20	H202	110.443°
C21	C20	H202	112.522°		H201	C20	H202	108.175°
C20	C21	C22	109.53(8)°		C20	C21	O23	125.73(10)°
C22	C21	O23	124.75(10)°		C18	C22	C21	104.49(8)°
C18	C22	H221	112.887°		C21	C22	H221	113.805°
C18	C22	H222	110.445°		C21	C22	H222	110.089°
H221	C22	H222	105.216°		C19	C24	C25	113.85(8)°
C19	C24	H241	106.829°		C25	C24	H241	109.855°
C19	C24	H242	110.330°		C25	C24	H242	106.217°
H241	C24	H242	109.757°		C24	C25	C26	112.77(8)°
C24	C25	H251	111.374°		C26	C25	H251	107.796°
C24	C25	H252	107.815°		C26	C25	H252	112.266°
H251	C25	H252	104.548°		C25	C26	C27	114.61(9)°
C25	C26	H261	110.613°		C27	C26	H261	109.041°
C25	C26	H262	106.518°		C27	C26	H262	105.952°
H261	C26	H262	109.919°		C26	C27	C28	110.98(9)°
C26	C27	H271	109.855°		C28	C27	H271	105.995°
C26	C27	H272	109.022°		C28	C27	H272	111.511°
H271	C27	H272	109.438°		C27	C28	C29	120.44(11)°
C27	C28	C33	121.81(11)°		C29	C28	C33	117.71(11)°

C28	C29	C30	121.55(12)°		C28	C29	H291	118.391°
C30	C29	H291	119.990°		C29	C30	C31	120.02(12)°
C29	C30	H301	118.328°		C31	C30	H301	121.650°
C30	C31	C32	119.26(12)°		C30	C31	H311	118.686°
C32	C31	H311	122.029°		C31	C32	C33	120.37(12)°
C31	C32	H321	118.074°		C33	C32	H321	121.486°
C28	C33	C32	121.07(12)°		C28	C33	H331	118.610°
C32	C33	H331	120.321°					

The enantiomer of the measured crystal was checked by HPLC [Chiralpak® IA; hexane:*i*PrOH 90:10; 1.0 mL.min^{-1}, λ= 210 nm] t_R = 7.6 min (major enantiomer), t_R = 13.4 min (minor enantiomer)] and is representative of the whole sample.

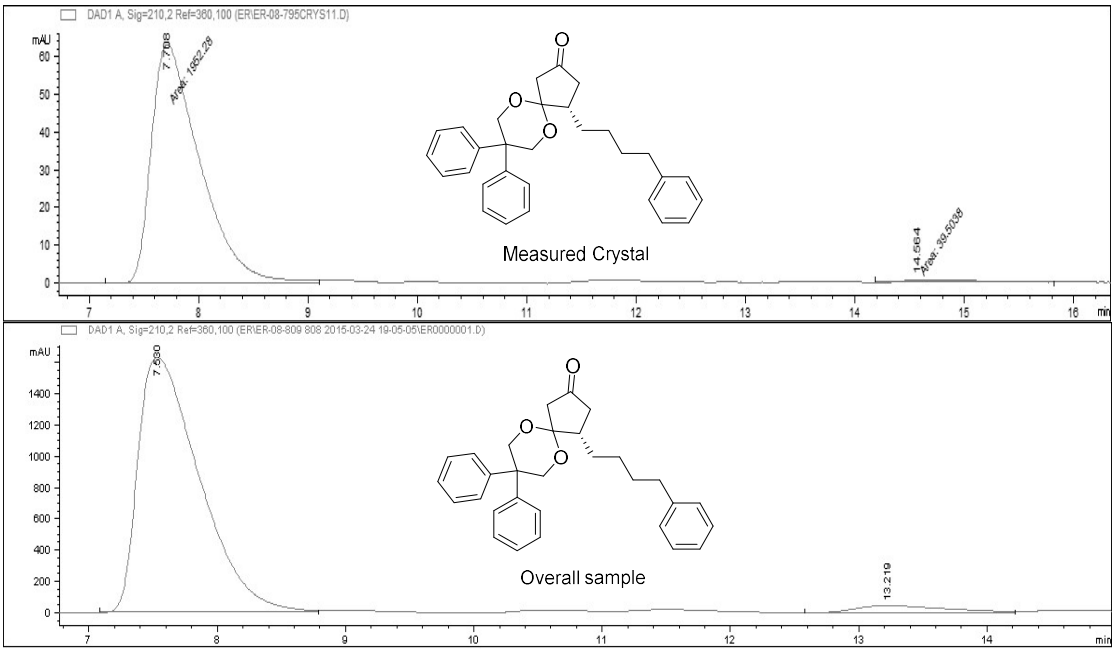

A second crystal in the sample was run in order to check that the first X-ray crystal structured determined absolute configuration is representative of the whole sample.

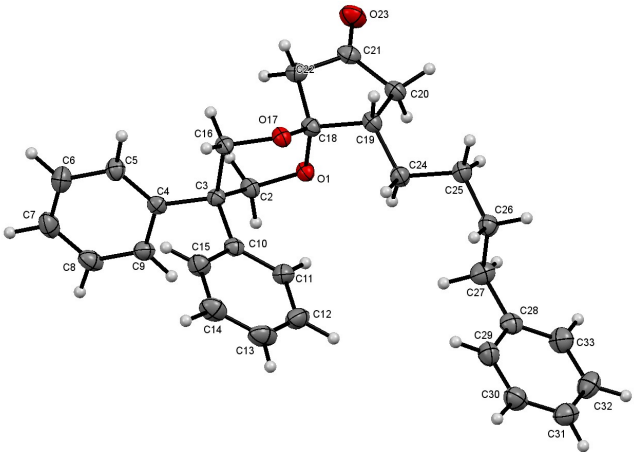

Crystal Data

a = 6.27460(10) Å α = 90°
b = 18.52660(10) Å β = 90°
c = 20.24350(10) Å γ = 90°

Volume	2353.25(4) Å³	Crystal Class	orthorhombic
Space group	P 2_1 2_1 2_1	Z =	4
Formula	C_{30} H_{32} O_3	M_r	440.58
Cell determined from	59601 reflections	Cell θ range =	3 - 76°
Temperature	150K		
Shape	needles		
Colour	clear_pale_colourless	Size	0.07 × 0.18 × 0.22 mm
D_x	1.24 mg m^{-3}	F000	944.000
μ	0.617 mm^{-1}		
Absorption correction	multi-scan		
T_{min}	0.81	T_{max}	0.96

Data Collection

Diffractometer	multi-scan
Scan type	ω scans
Reflections measured	92194
Independent reflections	4921
Rint	0.0277
θ_{max}	76.4540
h =	-7 → 7
k =	-23 → 23
l =	-25 → 25

Refinement

$\Delta\rho_{min}$ =	-0.13 e Å^{-3}
$\Delta\rho_{max}$ =	0.18 e Å^{-3}
Reflections used	4900
Cutoff: I >	-3.00σ(I)
Parameters refined	299
S =	0.99
R-factor	0.028
weighted R-factor	0.069
Δ/σ_{max}	0.0004
Flack parameter	0.02(13)
Refinement on	F^2
w =	$1/[\sigma^2(F_{obs}^2) + (0.035 \times P)^2 + 0.499 \times P + 0.000 + 0.000 \times \sin\theta]$, $P = 0.333 \times \max(F_{obs}^2,0) + 0.667 \times F_{calc}^2$

Parameters

Label	*x*	*y*	*z*	$U_{iso/equiv}$	Occupancy
O1	0.30308(11)	0.48294(4)	0.47656(4)	0.0236	1.0000
C2	0.40652(17)	0.52319(6)	0.42553(5)	0.0236	1.0000
C3	0.62595(17)	0.55269(5)	0.44601(5)	0.0208	1.0000
C4	0.72947(17)	0.58303(5)	0.38343(5)	0.0220	1.0000
C5	0.91373(18)	0.55505(6)	0.35604(5)	0.0279	1.0000
C6	1.0060(2)	0.58663(7)	0.30014(6)	0.0357	1.0000
C7	0.9124(2)	0.64577(7)	0.27083(6)	0.0371	1.0000
C8	0.7249(2)	0.67349(6)	0.29688(6)	0.0342	1.0000
C9	0.63487(19)	0.64272(6)	0.35273(5)	0.0278	1.0000

C10	0.61793(18)	0.61184(5)	0.49892(5)	0.0229	1.0000
C11	0.4387(2)	0.62679(6)	0.53679(6)	0.0300	1.0000
C12	0.4456(2)	0.68051(7)	0.58525(6)	0.0385	1.0000
C13	0.6288(3)	0.71939(7)	0.59601(6)	0.0421	1.0000
C14	0.8081(2)	0.70540(7)	0.55849(6)	0.0389	1.0000
C15	0.8026(2)	0.65175(6)	0.51057(6)	0.0307	1.0000
C16	0.74666(16)	0.48735(5)	0.47382(5)	0.0232	1.0000
O17	0.62779(12)	0.45627(4)	0.52728(4)	0.0236	1.0000
C18	0.43066(17)	0.42812(5)	0.50625(5)	0.0235	1.0000
C19	0.30635(18)	0.40004(6)	0.56656(5)	0.0251	1.0000
C20	0.14433(19)	0.34732(6)	0.53601(5)	0.0281	1.0000
C21	0.25497(19)	0.31734(6)	0.47561(6)	0.0285	1.0000
C22	0.44986(19)	0.36231(6)	0.46037(5)	0.0286	1.0000
O23	0.19866(16)	0.26490(4)	0.44419(4)	0.0388	1.0000
C24	0.21097(19)	0.45915(6)	0.60975(5)	0.0273	1.0000
C25	0.0652(2)	0.43089(6)	0.66456(5)	0.0282	1.0000
C26	0.00760(19)	0.49025(6)	0.71203(5)	0.0282	1.0000
C27	-0.1455(2)	0.54897(7)	0.68040(6)	0.0340	1.0000
C28	-0.2161(2)	0.60365(6)	0.73112(5)	0.0299	1.0000
C29	-0.0734(2)	0.65431(7)	0.75582(6)	0.0348	1.0000
C30	-0.1316(2)	0.70277(7)	0.80492(6)	0.0382	1.0000
C31	-0.3358(2)	0.70160(7)	0.83038(6)	0.0381	1.0000
C32	-0.4808(2)	0.65218(8)	0.80605(7)	0.0414	1.0000
C33	-0.4210(2)	0.60385(7)	0.75646(7)	0.0379	1.0000
H22	0.30010(17)	0.56310(6)	0.41720(5)	0.0295	1.0000
H21	0.43761(17)	0.49097(6)	0.38509(5)	0.0298	1.0000
H51	0.99092(18)	0.51264(6)	0.37566(5)	0.0355	1.0000
H61	1.1374(2)	0.56561(7)	0.27942(6)	0.0463	1.0000
H71	0.9862(2)	0.66936(7)	0.23212(6)	0.0465	1.0000
H81	0.6641(2)	0.71513(6)	0.27383(6)	0.0451	1.0000
H91	0.51300(19)	0.66338(6)	0.37174(5)	0.0343	1.0000
H111	0.3140(2)	0.60176(6)	0.52666(6)	0.0378	1.0000
H121	0.3093(2)	0.69123(7)	0.61150(6)	0.0483	1.0000
H131	0.6325(3)	0.75700(7)	0.62610(6)	0.0563	1.0000
H141	0.9431(2)	0.73230(7)	0.56279(6)	0.0495	1.0000
H151	0.9240(2)	0.64254(6)	0.48546(6)	0.0397	1.0000
H162	0.88713(16)	0.50130(5)	0.49170(5)	0.0280	1.0000
H161	0.76289(16)	0.44899(5)	0.43911(5)	0.0283	1.0000

H191	0.41518(18)	0.37012(6)	0.59304(5)	0.0323	1.0000
H201	0.10568(19)	0.30796(6)	0.57008(5)	0.0341	1.0000
H202	0.00620(19)	0.37330(6)	0.52238(5)	0.0363	1.0000
H221	0.57938(19)	0.33489(6)	0.46993(5)	0.0396	1.0000
H222	0.46565(19)	0.37633(6)	0.41261(5)	0.0380	1.0000
H241	0.32750(19)	0.48742(6)	0.63299(5)	0.0367	1.0000
H242	0.12900(19)	0.49068(6)	0.58121(5)	0.0346	1.0000
H251	0.1449(2)	0.39061(6)	0.68832(5)	0.0357	1.0000
H252	-0.0618(2)	0.40755(6)	0.64684(5)	0.0345	1.0000
H261	0.11766(19)	0.51431(6)	0.73588(5)	0.0368	1.0000
H262	0.09892(19)	0.46680(6)	0.74305(5)	0.0373	1.0000
H271	-0.0586(2)	0.57604(7)	0.64813(6)	0.0474	1.0000
H272	-0.2685(2)	0.52629(7)	0.65766(6)	0.0473	1.0000
H291	0.0689(2)	0.65323(7)	0.74093(6)	0.0426	1.0000
H301	-0.0183(2)	0.73784(7)	0.82156(6)	0.0483	1.0000
H311	-0.3750(2)	0.73653(7)	0.86284(6)	0.0512	1.0000
H321	-0.6242(2)	0.65076(8)	0.82654(7)	0.0520	1.0000
H331	-0.5300(2)	0.56839(7)	0.73746(7)	0.0469	1.0000

Thermal Parameters

Label	U_{11}	U_{22}	U_{33}	U_{23}	U_{13}	U_{12}
O1	0.0197(3)	0.0242(3)	0.0268(4)	0.0044(3)	-0.0007(3)	-0.0001(3)
C2	0.0225(5)	0.0245(5)	0.0238(5)	0.0033(4)	-0.0023(4)	-0.0011(4)
C3	0.0195(5)	0.0207(4)	0.0223(4)	0.0004(4)	-0.0011(4)	0.0005(4)
C4	0.0242(5)	0.0213(4)	0.0206(4)	-0.0015(4)	-0.0030(4)	-0.0027(4)
C5	0.0235(5)	0.0320(5)	0.0281(5)	0.0026(4)	-0.0006(4)	-0.0012(4)
C6	0.0327(6)	0.0426(7)	0.0319(6)	0.0016(5)	0.0069(5)	-0.0022(5)
C7	0.0465(7)	0.0374(6)	0.0272(5)	0.0036(5)	0.0046(5)	-0.0100(6)
C8	0.0504(7)	0.0251(5)	0.0271(5)	0.0036(4)	-0.0044(5)	-0.0012(5)
C9	0.0331(6)	0.0237(5)	0.0267(5)	-0.0014(4)	-0.0002(5)	0.0026(5)
C10	0.0274(5)	0.0208(4)	0.0206(5)	0.0022(4)	-0.0022(4)	0.0020(4)
C11	0.0329(6)	0.0256(5)	0.0316(6)	-0.0002(4)	0.0033(5)	0.0021(5)
C12	0.0513(8)	0.0322(6)	0.0320(6)	-0.0028(5)	0.0080(6)	0.0090(6)
C13	0.0671(9)	0.0287(6)	0.0304(6)	-0.0062(5)	-0.0029(6)	0.0024(6)
C14	0.0489(8)	0.0327(6)	0.0353(6)	-0.0058(5)	-0.0073(6)	-0.0078(6)
C15	0.0324(6)	0.0302(5)	0.0295(5)	-0.0024(4)	-0.0024(5)	-0.0039(5)
C16	0.0192(5)	0.0235(5)	0.0268(5)	0.0035(4)	-0.0009(4)	0.0015(4)

O17	0.0207(3)	0.0249(3)	0.0253(3)	0.0047(3)	-0.0023(3)	-0.0008(3)
C18	0.0232(5)	0.0215(5)	0.0257(5)	0.0020(4)	-0.0015(4)	0.0000(4)
C19	0.0256(5)	0.0232(5)	0.0264(5)	0.0036(4)	-0.0015(4)	-0.0020(4)
C20	0.0292(6)	0.0238(5)	0.0313(5)	0.0018(4)	-0.0001(4)	-0.0036(4)
C21	0.0339(6)	0.0222(5)	0.0293(5)	0.0031(4)	-0.0056(5)	0.0009(4)
C22	0.0322(6)	0.0229(5)	0.0306(5)	-0.0014(4)	0.0020(5)	0.0005(4)
O23	0.0496(5)	0.0286(4)	0.0381(4)	-0.0049(4)	-0.0042(4)	-0.0078(4)
C24	0.0295(6)	0.0265(5)	0.0259(5)	0.0002(4)	0.0014(4)	-0.0032(4)
C25	0.0299(6)	0.0276(5)	0.0271(5)	0.0021(4)	0.0021(5)	-0.0011(5)
C26	0.0308(6)	0.0295(6)	0.0244(5)	0.0024(4)	0.0018(4)	-0.0009(5)
C27	0.0368(7)	0.0356(6)	0.0296(6)	-0.0015(5)	-0.0047(5)	0.0052(5)
C28	0.0339(6)	0.0289(5)	0.0269(5)	0.0041(4)	-0.0038(5)	0.0039(5)
C29	0.0318(6)	0.0364(6)	0.0362(6)	0.0019(5)	0.0040(5)	-0.0036(5)
C30	0.0464(7)	0.0325(6)	0.0357(6)	-0.0004(5)	0.0008(6)	-0.0046(6)
C31	0.0466(8)	0.0346(6)	0.0331(6)	-0.0003(5)	0.0001(6)	0.0079(6)
C32	0.0308(6)	0.0505(8)	0.0428(7)	-0.0009(6)	0.0038(5)	0.0065(6)
C33	0.0315(6)	0.0406(7)	0.0414(7)	-0.0013(5)	-0.0036(5)	-0.0017(5)

Distances

O1	C2	1.4298(12)Å		O1	C18	1.4261(12)Å
C2	C3	1.5384(14)Å		C2	H22	1.011Å
C2	H21	1.032Å		C3	C4	1.5306(14)Å
C3	C10	1.5332(14)Å		C3	C16	1.5350(13)Å
C4	C5	1.3831(15)Å		C4	C9	1.4005(15)Å
C5	C6	1.3993(16)Å		C5	H51	1.005Å
C6	C7	1.3776(19)Å		C6	H61	1.003Å
C7	C8	1.3876(19)Å		C7	H71	1.010Å
C8	C9	1.3867(16)Å		C8	H81	0.979Å
C9	H91	0.938Å		C10	C11	1.3891(16)Å
C10	C15	1.3944(16)Å		C11	C12	1.3981(17)Å
C11	H111	0.932Å		C12	C13	1.374(2)Å
C12	H121	1.026Å		C13	C14	1.382(2)Å
C13	H131	0.926Å		C14	C15	1.3893(16)Å
C14	H141	0.987Å		C15	H151	0.932Å
C16	O17	1.4349(12)Å		C16	H162	0.987Å
C16	H161	1.005Å		O17	C18	1.4082(13)Å
C18	C19	1.5393(14)Å		C18	C22	1.5374(15)Å

C19	C20	1.5395(15)Å		C19	C24	1.5239(15)Å
C19	H191	1.030Å		C20	C21	1.5118(16)Å
C20	H201	1.033Å		C20	H202	1.029Å
C21	C22	1.5116(16)Å		C21	O23	1.2137(14)Å
C22	H221	0.978Å		C22	H222	1.006Å
C24	C25	1.5302(15)Å		C24	H241	1.015Å
C24	H242	0.969Å		C25	C26	1.5303(15)Å
C25	H251	1.019Å		C25	H252	0.975Å
C26	C27	1.5305(16)Å		C26	H261	1.024Å
C26	H262	0.955Å		C27	C28	1.5089(16)Å
C27	H271	0.988Å		C27	H272	0.992Å
C28	C29	1.3902(17)Å		C28	C33	1.3843(18)Å
C29	C30	1.3884(18)Å		C29	H291	0.943Å
C30	C31	1.381(2)Å		C30	H301	1.021Å
C31	C32	1.381(2)Å		C31	H311	0.954Å
C32	C33	1.3964(19)Å		C32	H321	0.992Å
C33	H331	1.023Å				

Angles

C2	O1	C18	114.91(8)°		O1	C2	C3	113.38(8)°
O1	C2	H22	101.666°		C3	C2	H22	112.105°
O1	C2	H21	110.942°		C3	C2	H21	104.488°
H22	C2	H21	114.581°		C2	C3	C4	106.69(8)°
C2	C3	C10	114.39(8)°		C4	C3	C10	109.25(8)°
C2	C3	C16	105.08(8)°		C4	C3	C16	112.57(8)°
C10	C3	C16	108.88(8)°		C3	C4	C5	123.29(9)°
C3	C4	C9	118.51(9)°		C5	C4	C9	118.19(10)°
C4	C5	C6	120.88(11)°		C4	C5	H51	122.519°
C6	C5	H51	116.565°		C5	C6	C7	120.30(12)°
C5	C6	H61	121.037°		C7	C6	H61	118.605°
C6	C7	C8	119.48(11)°		C6	C7	H71	118.889°
C8	C7	H71	121.567°		C7	C8	C9	120.21(11)°
C7	C8	H81	116.159°		C9	C8	H81	123.631°
C4	C9	C8	120.91(11)°		C4	C9	H91	119.072°
C8	C9	H91	119.939°		C3	C10	C11	123.69(10)°
C3	C10	C15	118.03(10)°		C11	C10	C15	118.27(10)°
C10	C11	C12	120.25(12)°		C10	C11	H111	117.313°

C12	C11	H111	122.326°		C11	C12	C13	120.70(12)°
C11	C12	H121	118.351°		C13	C12	H121	120.918°
C12	C13	C14	119.71(11)°		C12	C13	H131	121.303°
C14	C13	H131	118.868°		C13	C14	C15	119.85(12)°
C13	C14	H141	123.751°		C15	C14	H141	116.383°
C10	C15	C14	121.21(12)°		C10	C15	H151	119.342°
C14	C15	H151	119.448°		C3	C16	O17	109.67(8)°
C3	C16	H162	111.621°		O17	C16	H162	107.022°
C3	C16	H161	110.570°		O17	C16	H161	107.234°
H162	C16	H161	110.558°		C16	O17	C18	112.17(8)°
O1	C18	O17	110.89(8)°		O1	C18	C19	106.89(8)°
O17	C18	C19	109.30(8)°		O1	C18	C22	110.73(8)°
O17	C18	C22	114.05(9)°		C19	C18	C22	104.53(8)°
C18	C19	C20	103.32(8)°		C18	C19	C24	114.28(8)°
C20	C19	C24	115.29(9)°		C18	C19	H191	104.991°
C20	C19	H191	107.781°		C24	C19	H191	110.398°
C19	C20	C21	104.76(9)°		C19	C20	H201	109.559°
C21	C20	H201	112.867°		C19	C20	H202	111.542°
C21	C20	H202	109.982°		H201	C20	H202	108.154°
C20	C21	C22	109.51(9)°		C20	C21	O23	125.75(11)°
C22	C21	O23	124.74(11)°		C18	C22	C21	104.50(9)°
C18	C22	H221	110.949°		C21	C22	H221	110.214°
C18	C22	H222	112.564°		C21	C22	H222	114.721°
H221	C22	H222	104.033°		C19	C24	C25	113.88(9)°
C19	C24	H241	110.720°		C25	C24	H241	105.736°
C19	C24	H242	107.416°		C25	C24	H242	108.740°
H241	C24	H242	110.346°		C24	C25	C26	112.82(9)°
C24	C25	H251	107.441°		C26	C25	H251	112.104°
C24	C25	H252	111.939°		C26	C25	H252	107.811°
H251	C25	H252	104.459°		C25	C26	C27	114.64(9)°
C25	C26	H261	112.312°		C27	C26	H261	108.772°
C25	C26	H262	105.374°		C27	C26	H262	105.032°
H261	C26	H262	110.390°		C26	C27	C28	111.00(9)°
C26	C27	H271	108.976°		C28	C27	H271	105.738°
C26	C27	H272	109.442°		C28	C27	H272	111.833°
H271	C27	H272	109.757°		C27	C28	C29	120.59(11)°
C27	C28	C33	121.77(12)°		C29	C28	C33	117.59(12)°
C28	C29	C30	121.63(12)°		C28	C29	H291	118.747°

C30	C29	H291	119.471°		C29	C30	C31	120.08(13)°
C29	C30	H301	117.678°		C31	C30	H301	122.230°
C30	C31	C32	119.21(12)°		C30	C31	H311	119.014°
C32	C31	H311	121.702°		C31	C32	C33	120.30(12)°
C31	C32	H321	117.791°		C33	C32	H321	121.835°
C28	C33	C32	121.17(12)°		C28	C33	H331	118.666°
C32	C33	H331	120.153°					

*(S)-4-phenethyl-8,8-diphenyl-6,10-dioxaspiro[4.5]decan-2-one (**21b**)*

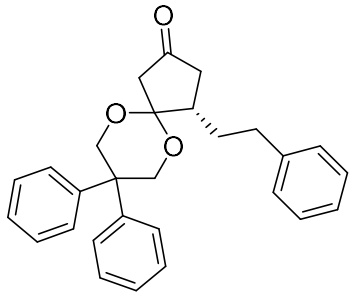

21b

In a flame-dried flask under an argon atmosphere, Cp_2ZrHCl (310 mg, 1.2 mmol, 3.0 eq) was added to a solution of styrene (0.16 mL, 1.4 mmol 3.5 eq) in CH_2Cl_2 (0.5 mL) and vigorously stirred until a clear red solution was obtained (5 min). Simultaneously, in another flask under an argon atmosphere, CuCl (7.9 mg, 80 μmol, 20 mol%) and (*R*)-**Q** (47.5 mg, 88.0 μmol, 22.0 mol%) were covered in Et_2O (2.2 mL) and stirred for 1 h at room temperature. AgOTf (20.6 mg, 80.0 μmol, 20.0 mol%) was added to the freshly formed Cu-ligand containing solution and stirring was continued for an additional 1 h. The resulting catalyst mixture was taken up by syringe and injected through a filter into the freshly prepared alkylzirconocene species and the reaction flask was cooled to 0 °C using a water/ice bath. After 10 min, solid 8,8-diphenyl-6,10-

dioxaspiro[4.5]dec-3-en-2-one **18a** (120 mg, 0.40 mmol, 1.0 eq) was added in one portion by quickly tipping the solid into the black solution. TMSCl (0.25 mL, 2.0 mmol, 5.0 eq) was then added dropwise and the reaction mixture was stirred overnight and allowed to slowly warm up to RT. The reaction mixture was diluted with Et_2O (2 mL) and quenched with NH_4Cl (3 mL, 1 M). The mixture was partitioned and the aqueous phase was extracted with Et_2O (3 x 10 mL). The combined organic extracts were washed with $NaHCO_3$ (aq. sat. 30 mL), dried over $MgSO_4$, filtered and concentrated under reduced pressure. Purification by flash column chromatography (SiO_2, Et_2O 10-20% in pentane) yielded the title product **21b** (64 mg, 0.15 mmol, 36%, 95% ee) as a white oil. **^{1}H NMR** (500 MHz, $CDCl_3$) δ_H/ppm 7.51 (d, *J*= 8.7, 2H, Ar-**H**), 7.42-7.20 (m, 9H, Ar-**H**), 7.15 (d, *J*= 8.4, 2H, Ar-**H**), 7.12 (d, *J*= 7.6, 2H, Ar-**H**), 4.66 (ddd, *J*= 12.2, 3.0, 2.7 Hz, 2H, O-C**H$_2$**), 4.38 (d, *J*= 11.9 Hz, 1H, O-C**H$_2$**), 4.28 (d, *J*= 12.2 Hz, 1H, O-C**H$_2$**), 3.17 (d, *J*= 17.9 Hz, 1H, C**H$_2$**), 2.63-2.50 (m, 3H, C**H$_2$**), 2.47 (d, *J*= 18.0 Hz, 1H, C**H$_2$**), 2.43-2.35 (m, 1H, C**H**), 2.22 (dd, *J*= 17.8, 10.9 Hz, 1H, C**H$_2$**), 2.07-1.98 (m, 1H, C**H$_2$**), 1.68-1.58 (m, 1H, C**H$_2$**); **^{13}C NMR** (126 MHz, $CDCl_3$) δ_C/ppm 213.0 (**C**=O), 143.7 (**Cq**-Ar), 143.4 (**Cq**-Ar), 142.1 (**Cq**-Ar), 128.9 (**C**H-Ar), 128.7 (**C**H-Ar), 128.4 (**C**H-Ar), 128.4 (**C**H-Ar), 128.3 (**C**H-Ar), 127.1 (**C**H-Ar), 126.6 (**C**H-Ar), 126.5 (**C**H-Ar), 125.9 (**C**H-Ar), 104.9 (**Cq**-O_2), 70.9 (O-**C**H_2), 68.9 (O-**C**H_2), 45.2 (**C**H), 45.0 (**C**H_2), 44.9 (**Cq**-Ph_2), 43.4 (**C**H_2), 33.9 (**C**H_2), 29.1 (**C**H_2); **HRMS** (ESI) *m*/z calcd for $C_{28}H_{28}O_3Na$ $[M+Na]^+$: 435.19307, found: 435.19317; **IR (neat)** νmax/cm^{-1} 3026, 2924, 1749, 1602, 1496, 1448, 1400, 1279, 1188, 1132, 1032, 970, 753, 699; **$[\alpha]_D^{25}$** = +65.6° (c= 1.0 in $CHCl_3$, 95% ee).

The enantiomeric excess of 95% ee was determined by HPLC [Chiralpak® IA; hexane:*i*PrOH 90:10; 1.0 mL.min^{-1}, λ= 210 nm, t_R = 7.8 min (major enantiomer), t_R = 16.5 min (minor enantiomer)].

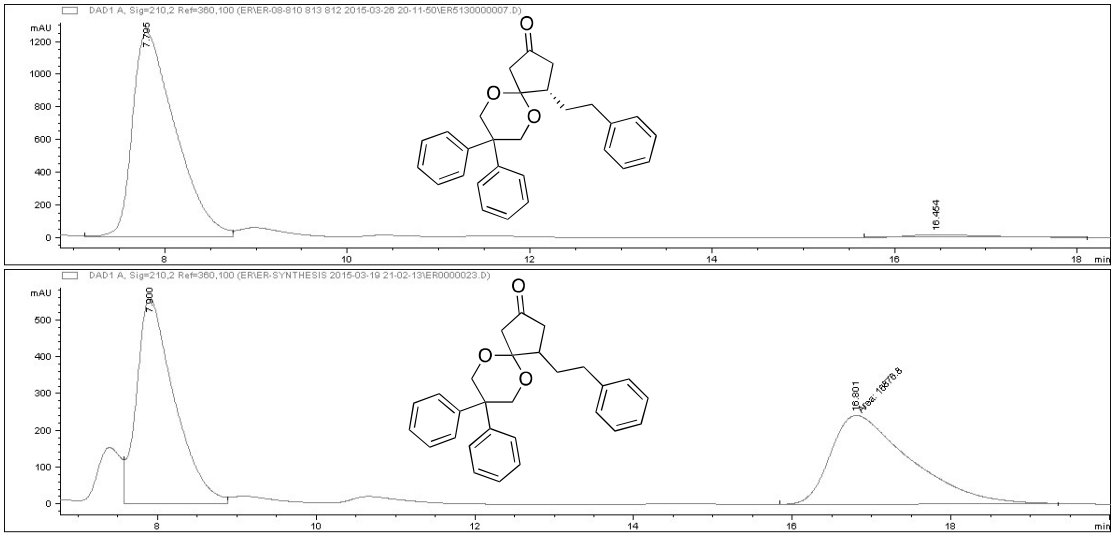

*(S)-4-hexyl-8,8-diphenyl-6,10-dioxaspiro[4.5]decan-2-one (**21c**)*

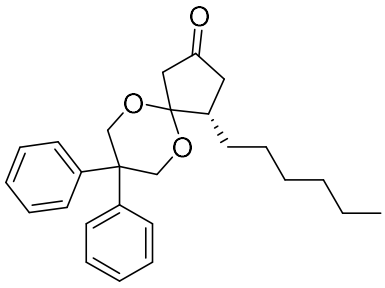

21c

In a flame-dried flask under an argon atmosphere, Cp_2ZrHCl (310 mg, 1.2 mmol, 3.0 eq) was added to a solution of 1-hexene (0.21 mL, 1.4 mmol 3.5 eq) in CH_2Cl_2 (0.5 mL) and vigorously stirred until a clear orange/yellow solution was obtained (10 min). Simultaneously, in another flask under an argon atmosphere, CuCl (7.9 mg, 80 μmol, 20 mol%) and (*R*)-**Q** (47.5 mg, 88.0 μmol,

22.0 mol%) were covered in Et_2O (2.2 mL) and stirred for 1 h at room temperature. AgOTf (20.6 mg, 80.0 μmol, 20.0 mol%) was added to the freshly formed Cu-ligand containing solution and stirring continued for an additional 1 h. The resulting catalyst mixture was taken up by syringe and injected through a filter into the freshly prepared alkylzirconocene species and the reaction flask was cooled to 0 °C. After 10 min, solid 8,8-diphenyl-6,10-dioxaspiro[4.5]dec-3-en-2-one **18a** (120 mg, 0.40 mmol, 1.0 eq) was added in one portion by quickly tipping the solid into the black solution. TMSCl (0.25 mL, 2.0 mmol, 5.0 eq) was then added dropwise and the reaction mixture was stirred overnight and allowed to slowly warm to RT. The reaction mixture was diluted with Et_2O (2 mL) and quenched with NH_4Cl (3 mL, 1 M). The mixture was partitioned and the aqueous phase was extracted with Et_2O (3 x 10 mL). The combined organic extracts were washed with $NaHCO_3$ (aq. sat. 30 mL), dried over $MgSO_4$, filtered and concentrated under reduced pressure. Purification by flash column chromatography (SiO_2, Et_2O 10-20% in pentane) yielded the title product **21c** (99 mg, 0.25 mmol, 63%, 89% ee) as a yellow oil. **^{1}H NMR** (500 MHz, $CDCl_3$) δ_H/ppm 7.47 (d, *J*= 7.9, 2H, Ar-**H**), 7.37-7.20 (m, 6H, Ar-**H**), 7.10 (d, *J*= 7.2, 2H, Ar-**H**), 4.64-4.57 (m, 2H, O-C**H$_2$**), 4.34 (d, *J*= 12.0 Hz, 1H, O-C**H$_2$**), 4.22 (d, *J*= 12.0 Hz, 1H, O-C**H$_2$**), 3.09 (d, *J*= 17.9 Hz, 1H, C**H$_2$**), 2.52 (dd, *J*= 17.9, 8.0 Hz, 1H, C**H$_2$**), 2.42 (d, *J*= 18.2 Hz, 1H, C**H$_2$**), 2.34-2.25 (m, 1H, C**H**), 2.13 (dd, *J*= 17.9, 10.7 Hz, 1H, C**H$_2$**), 1.63-1.51 (m, 1H, C**H$_2$**), 1.35-1.07 (m, 9H, C**H$_2$**), 0.89 (t, *J*= 7.5 Hz, 3H, **C**H$_3$); **^{13}C NMR** (126 MHz, $CDCl_3$) δ_C/ppm 213.4 (**C**=O), 143.8 (**Cq**-Ar), 143.5 (**Cq**-Ar), 128.8 (**C**H-Ar), 128.7 (**C**H-Ar), 128.2 (**C**H-Ar), 127.1 (**C**H-Ar), 126.6 (**C**H-Ar), 126.5 (**C**H-Ar), 104.9 (**Cq**-O_2), 70.9 (O-**C**H$_2$), 69.0 (O-**C**H$_2$), 46.0 (**C**H), 45.0 (**C**H$_2$), 44.9 (**Cq**-Ph_2), 43.4 (**C**H$_2$), 31.8 (**C**H$_2$), 29.6 (**C**H$_2$), 28.0 (**C**H$_2$), 27.8 (**C**H$_2$), 22.8

(**C**H_2), 14.2 (**C**H_3); **HRMS** (ESI) *m*/z calcd for $C_{26}H_{33}O_3$ $[M+H]^+$: 393.24242, found: 393.24238; **IR (neat)** νmax/cm^{-1} 2926, 2856, 2360, 1750, 1496, 1464, 1399, 1280, 1188, 1129, 1035, 771, 699, 642; **$[\alpha]_D^{25}$** = +89.0° (c= 1.4 in $CHCl_3$, 89% ee).

The enantiomeric excess of 89% ee was determined by HPLC [Chiralpak® IA; hexane:*i*PrOH 90:10; 1.0 mL.min^{-1}, λ= 210 nm, t_R = 5.9 min (major enantiomer), t_R = 10.6 min (minor enantiomer)].

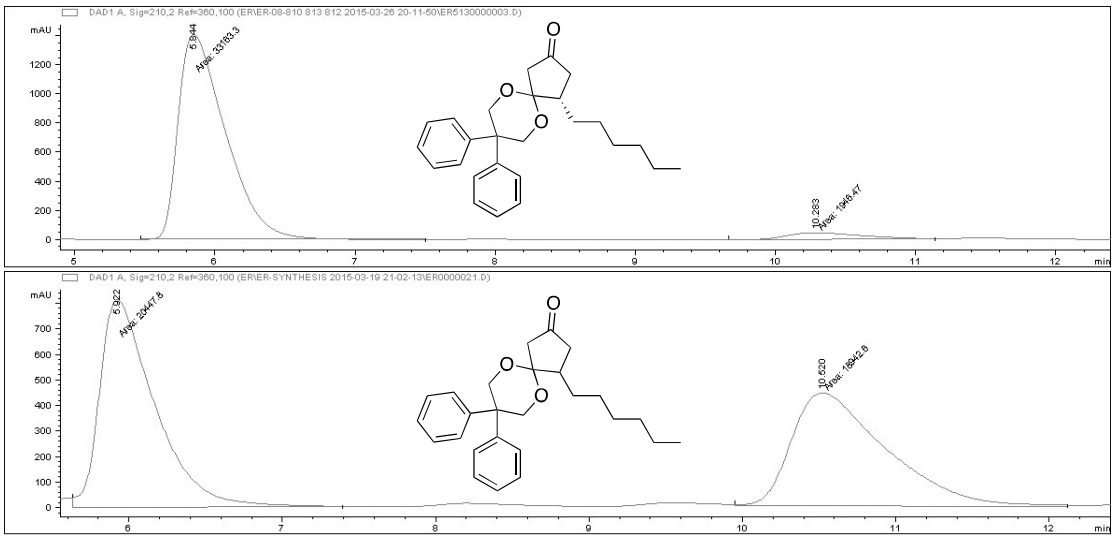

*(S)-4-(6-chlorohexyl)-8,8-diphenyl-6,10-dioxaspiro[4.5]decan-2-one (**21d**)*

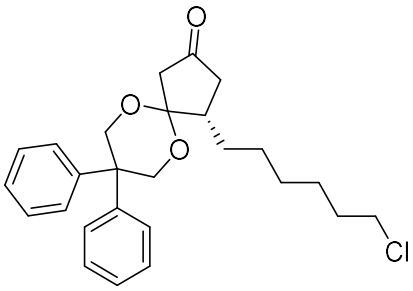

21d

In a flame-dried flask under an argon atmosphere, Cp_2ZrHCl (310 mg, 1.2 mmol, 3.0 eq) was added to a solution of 6-chlorohexene (0.19 mL, 1.4 mmol 3.5 eq) in CH_2Cl_2 (0.5 mL) and vigorously stirred until a clear yellow solution was obtained (15 min). Simultaneously, in another flask under an argon atmosphere, CuCl (7.9 mg, 80 μmol, 20 mol%) and (*R*)-**Q** (47.5 mg, 88.0 μmol, 22.0 mol%) were covered in Et_2O (2.2 mL) and stirred for 1 h at room temperature. AgOTf (20.6 mg, 80.0 μmol, 20.0 mol%) was added to the freshly formed Cu-ligand containing solution and stirring continued for an additional 1 h. The resulting catalyst mixture was taken up by syringe and injected through a filter into the freshly prepared alkylzirconocene species and the reaction flask was then cooled to 0 °C using an ice/water bath. After 10 min, solid 8,8-diphenyl-6,10-dioxaspiro[4.5]dec-3-en-2-one **18a** (120 mg, 0.40 mmol, 1.0 eq) was added in one portion by quickly tipping the solid into the black solution. TMSCl (0.25 mL, 2.0 mmol, 5.0 eq) was then added dropwise and the reaction mixture was stirred overnight and allowed to slowly warm to RT. The reaction mixture was diluted with Et_2O (2 mL) and quenched with NH_4Cl (3 mL, 1 M). The mixture was partitioned and the aqueous phase was extracted with Et_2O (3 x 10 mL). The

combined organic extracts were washed with $NaHCO_3$ (aq. sat. 30 mL), dried over $MgSO_4$, filtered and concentrated under reduced pressure. Purification by flash column chromatography (SiO_2, Et_2O 10-20% in pentane) yielded the title product **21d** (96 mg, 0.23 mmol, 56%, 91% ee) as a white oil. **^{1}H NMR** (500 MHz, $CDCl_3$) δ_H/ppm 7.48 (d, *J*= 7.3 Hz, 2H, Ar-**H**), 7.38-7.21 (m, 6H, Ar-**H**), 7.10 (d, *J*= 7.3 Hz, 2H, Ar-**H**), 4.66-4.58 (m, 2H, O-C**H$_2$**), 4.35 (d, *J*= 11.6 Hz, 1H, O-C**H$_2$**), 4.22 (d, *J*= 11.6 Hz, 1H, O-C**H$_2$**), 3.52 (t, *J*= 6.8 Hz, 2H, C**H$_2$**-Cl), 3.12 (d, *J*= 17.7 Hz, 1H, C**H$_2$**), 2.51 (dd, *J*= 17.9, 8.3 Hz, 1H, C**H$_2$**), 2.42 (d, *J*= 18.1 Hz, 1H, C**H$_2$**), 2.33-2.25 (m, 1H, C**H**), 2.14 (dd, *J*= 17.6, 11.1 Hz, 1H, C**H$_2$**), 1.78-1.70 (app. quint., 2H, C**H$_2$**), 1.64-1.53 (m, 1H, C**H$_2$**), 1.39-1.08 (m, 7H, C**H$_2$**); **^{13}C NMR** (126 MHz, $CDCl_3$) δ_C/ppm 213.1 (**C**=O), 143.7 (**Cq**-Ar), 143.3 (**Cq**-Ar), 128.8 (**C**H-Ar), 128.7 (**C**H-Ar), 128.2 (**C**H-Ar), 127.1 (**C**H-Ar), 126.5 (**C**H-Ar), 126.4 (**C**H-Ar), 104.8 (**Cq**-O_2), 70.9 (O-**C**H_2), 68.9 (O-**C**H_2), 46.0 (**C**H), 45.2 (**C**H_2), 44.9 (**Cq**-Ph_2), 44.8 (**C**H_2-Cl), 43.4 (**C**H_2), 32.7 (**C**H_2), 29.1 (**C**H_2), 27.8 (**C**H_2), 27.6 (**C**H_2), 26.7 (**C**H_2); **HRMS** (ESI) *m*/z calcd for $C_{26}H_{31}O_3ClNa$ $[M+Na]^+$: 449.18539, found: 449.18561. **IR (neat)** νmax/cm^{-1} 2931, 2859, 1769, 1727, 1275, 1130, 699; **$[\alpha]_D^{25}$** = +66.5° (c= 0.9 in $CHCl_3$, 91% ee).

The enantiomeric excess of 91% ee was determined by HPLC [Chiralpak® IA; hexane:*i*PrOH 90:10; 1.0 mL.min^{-1}, λ= 210 nm, t_R = 8.1 min (major enantiomer), t_R = 16.5 min (minor enantiomer)].



(S)-8,8-diphenyl-4-(3-(trimethylsilyl)propyl)-6,10-dioxaspiro[4.5]decan-2-one ***(21e)***

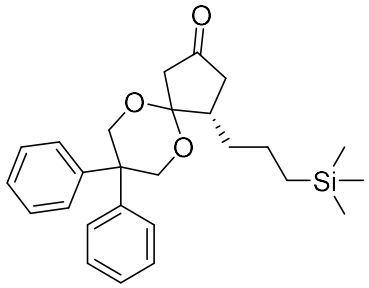

21e

In a flame-dried flask under an argon atmosphere, Cp_2ZrHCl (310 mg, 1.2 mmol, 3.0 eq) was added to a solution of allyltrimethylsilane (0.22 mL, 1.4 mmol 3.5 eq) in CH_2Cl_2 (0.5 mL) and vigorously stirred until a clear orange solution was obtained (10 min). Simultaneously, in another flask under inert

atmosphere, CuCl (7.9 mg, 80 μmol, 20 mol%) and (*R*)-**Q** (47.5 mg, 88.0 μmol, 22.0 mol%) were covered in Et_2O (2.2 mL) and stirred for 1 h at room temperature. AgOTf (20.6 mg, 80.0 μmol, 20.0 mol%) was added to the freshly formed Cu-ligand containing solution and stirring continued for an additional 1 h. The resulting catalyst mixture was taken up by syringe and injected through a filter into the flask containing the freshly prepared alkylzirconocene species, which was cooled to 0 °C. After 10 min, solid 8,8-diphenyl-6,10-dioxaspiro[4.5]dec-3-en-2-one **18a** (120 mg, 0.40 mmol, 1.0 eq) was added in one portion by quickly tipping the solid into the black solution. TMSCl (0.25 mL, 2.0 mmol, 5.0 eq) was then added dropwise and the reaction mixture was allowed to warm to room temperature while stirring was continued overnight. The reaction mixture was diluted with Et_2O (2 mL) and quenched with NH_4Cl (3 mL, 1 M). The mixture was partitioned and the aqueous phase was extracted with Et_2O (3 x 10 mL). The combined organic extracts were washed with $NaHCO_3$ (aq. sat. 30 mL), dried over $MgSO_4$, filtered and concentrated under reduced pressure. Purification by flash column chromatography (SiO_2, Et_2O 10-20% in pentane) yielded the title product **21e** (66 mg, 0.16 mmol, 39%, 92% ee) as a clear oil. **^{1}H NMR** (500 MHz, $CDCl_3$) δ_H/ppm 7.46 (d, *J*= 7.6 Hz, 2H, Ar-**H**), 7.37-7.21 (m, 6H, Ar-**H**), 7.09 (d, *J*= 7.8 Hz, 2H, Ar-**H**), 4.64-4.55 (m, 2H, O-C**H$_2$**), 4.34 (d, *J*= 12.6 Hz, 1H, O-C**H$_2$**), 4.21 (d, *J*= 12.6 Hz, 1H, O-C**H$_2$**), 3.08 (d, *J*= 17.6 Hz, 1H, C**H$_2$**), 2.52 (dd, *J*= 18.1, 8.1 Hz, 1H, C**H$_2$**), 2.42 (d, *J*= 18.1 Hz, 1H, C**H$_2$**), 2.38-2.27 (m, 1H, C**H**), 2.14 (dd, *J*= 17.8, 10.4 Hz, 1H, C**H$_2$**), 1.63-1.54 (m, 1H, C**H$_2$**), 1.35-1.20 (m, 2H, C**H$_2$**), 1.20-1.08 (m, 1H, C**H$_2$**), 0.48-0.35 (m, 2H, C**H$_2$**), -0.06 (s, 9H, Si(C**H$_3$**)$_3$); **^{13}C NMR** (126 MHz, $CDCl_3$) δ_C/ppm 231.4 (**C**=O), 143.9 (**Cq**-Ar), 143.5 (**Cq**-Ar), 128.8 (**C**H-Ar), 128.7 (**C**H-Ar), 128.3 (**C**H-Ar), 127.1 (**C**H-Ar), 126.6 (**C**H-

Ar), 126.5 (**C**H-Ar), 104.9 (**Cq**-O_2), 70.9 (O-**C**H_2), 69.0 (O-**C**H_2), 45.6 (**C**H), 44.9 (**Cq**-Ph_2), 44.8 (**C**H_2), 43.3 (**C**H_2), 31.5 (**C**H_2), 22.5 (**C**H_2), 16.8 (**C**H_2), -1.5 (Si(**C**H_3)$_3$); **HRMS** (ESI) *m*/z calcd for $C_{26}H_{34}O_3NaSi$ $[M+Na]^+$: 445.21694, found: 445.21689; **IR (neat)** νmax/cm^{-1} 2951, 2870, 1749, 1259, 1130, 835, 752, 697; **$[\alpha]_D^{25}$** = +144.3° (c= 1.2 in $CHCl_3$, 92% ee).

The enantiomeric excess of 92% ee was determined by HPLC [Chiralpak® IA; hexane:*i*PrOH 90:10; 1.0 mL.min^{-1}, λ= 210 nm, t_R = 5.0 min (major enantiomer), t_R = 7.3 min (minor enantiomer)].

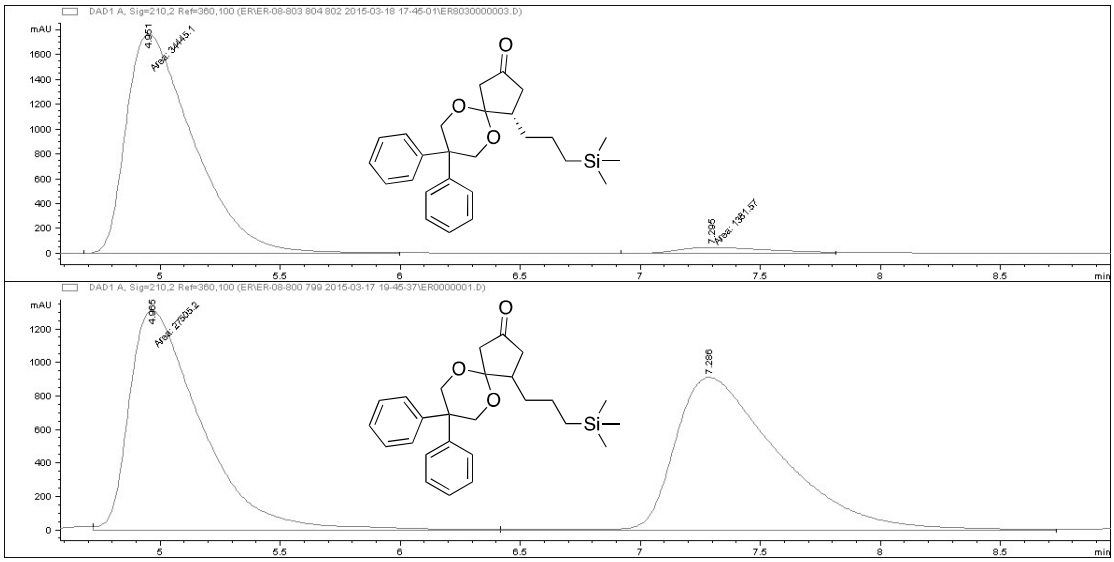

*(S)-4-(4-(benzyloxy)butyl)-8,8-diphenyl-6,10-dioxaspiro[4.5]decan-2-one (**21f**)*

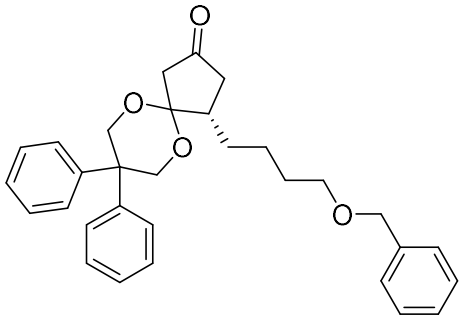

21f

In a flame-dried flask under an argon atmosphere, Cp_2ZrHCl (310 mg, 1.2 mmol, 3.0 eq) was added to a solution of ((but-3-en-1-yloxy)methyl)benzene (0.23 mL, 1.4 mmol 3.5 eq) in CH_2Cl_2 (0.5 mL) and stirred vigorously at 40 °C until a clear yellow solution was obtained (~45 min). Simultaneously, in another flask under inert atmosphere, CuCl (7.9 mg, 80 μmol, 20 mol%) and (*R*)-**Q** (47.5 mg, 88.0 μmol, 22.0 mol%) were covered in Et_2O (2.2 mL) and stirred for 1 h at room temperature. AgOTf (20.6 mg, 80.0 μmol, 20.0 mol%) was added to the freshly formed Cu-ligand containing solution and stirring continued for an additional 1 h. The resulting catalyst mixture was taken up by syringe and injected through a filter into the flask containing the freshly prepared alkylzirconocene species, which was then cooled to 0 °C using an ice/water bath. After 10 min, solid 8,8-diphenyl-6,10-dioxaspiro[4.5]dec-3-en-2-one **18a** (120 mg, 0.40 mmol, 1.0 eq) was added in one portion by quickly tipping the solid into the black solution. TMSCl (0.25 mL, 2.0 mmol, 5.0 eq) was then added dropwise and the reaction mixture was stirred overnight whilst being allowed to slowly warm to RT. The reaction mixture was diluted with Et_2O (2 mL) and

quenched with NH_4Cl (3 mL, 1 M). The mixture was partitioned and the aqueous phase was extracted with Et_2O (3 x 10 mL). The combined organic extracts were washed with $NaHCO_3$ (aq. sat. 30 mL), dried over $MgSO_4$, filtered and concentrated under reduced pressure. Purification by flash column chromatography (SiO_2, Et_2O 10-20% in pentane) yielded the title product **21f** (130 mg, 0.28 mmol, 69%, 89% ee) as a yellow oil. **^{1}H NMR** (500 MHz, $CDCl_3$) δ_H/ppm 7.45 (d, *J*= 7.5 Hz, 2H, Ar-**H**), 7.40-7.18 (m, 11H, Ar-**H**), 7.09 (d, *J*= 7.5 Hz, 2H, Ar-**H**), 4.64-4.57 (m, 2H, O-C**H$_2$**), 4.49 (s, 2H, O-C**H$_2$**), 4.33 (d, *J*= 11.8 Hz, 1H, O-C**H$_2$**), 4.20 (d, *J*= 12.5 Hz, 1H, O-C**H$_2$**), 3.38 (t, *J*= 6.8 Hz, 2H, O-C**H$_2$**), 3.10 (d, *J*= 17.9 Hz, 1H, C**H$_2$**), 2.51 (dd, *J*= 17.9, 8.0 Hz, 1H, C**H$_2$**), 2.41 (d, *J*= 17.9 Hz, 1H, C**H$_2$**), 2.34-2.24 (m, 1H, C**H**), 2.13 (dd, *J*= 17.3, 10.5 Hz, 1H, C**H$_2$**), 1.63-1.49 (m, 3H, C**H$_2$**), 1.34-1.12 (m, 3H, C**H$_2$**); **^{13}C NMR** (126 MHz, $CDCl_3$) δ_C/ppm 213.2 (**C**=O), 143.7 (**Cq**-Ar), 143.4 (**Cq**-Ar), 138.8 (**Cq**-Ar), 128.8 (**C**H-Ar), 128.7 (**C**H-Ar), 128.5 (**C**H-Ar), 128.3 (**C**H-Ar), 127.8 (**C**H-Ar), 127.7 (**C**H-Ar), 127.1 (**C**H-Ar), 126.6 (**C**H-Ar), 126.5 (**C**H-Ar), 104.8 (**Cq**-O_2), 73.0 (O-**C**H_2), 71.0 (O-**C**H_2), 70.3 (O-**C**H_2), 68.9 (O-**C**H_2), 46.1 (**C**H), 45.0 (**C**H_2), 44.8 (**Cq**-Ph_2), 43.4 (**C**H_2), 30.1 (**C**H_2), 27.6 (**C**H_2), 24.7 (**C**H_2); **HRMS** (ESI) *m*/z calcd for $C_{31}H_{35}O_4$ $[M+H]^+$: 471.25299, found: 471.25290. **IR (neat)** νmax/cm^{-1} 2929, 2862, 1748, 1496, 1448, 1278, 1188, 1131, 1049, 752, 699, 642; **$[\alpha]_D^{25}$** = +58.3° (c= 1.1 in $CHCl_3$, 89% ee).

The enantiomeric excess of 89% ee was determined by HPLC [Chiralpak® IA; hexane:*i*PrOH 90:10; 1.0 mL.min^{-1}, λ= 210 nm, t_R = 9.9 min (major enantiomer), t_R = 16.0 min (minor enantiomer)].

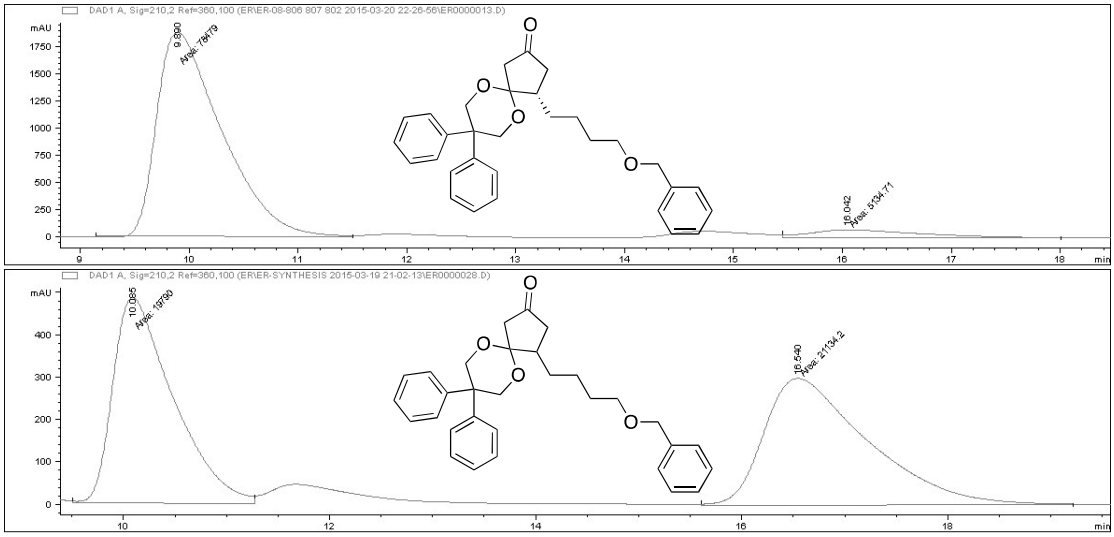

VI. EXPERIMENTALS CHAPTER 4

*(S)-2-phenethyloxirane (**26**)*

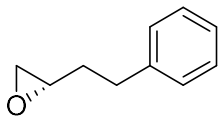

26

In analogy to a published procedure by Aggarwal[124], *m*CPBA (70%, 46 g, 230 mmol, 2.0 eq) was added in portions to a solution of 4-phenyl-1-butene **16** (17.4 mL, 116 mmol, 1.00 eq) in $CHCl_3$ (600 mL) in a flame-dried flask under argon atmosphere. After stirring for 7 h, the resulting white suspension was concentrated under reduced pressure, quenched with NaOH (aq., 1 M, 100 mL)

and $Na_2S_2O_3$ (aq., sat. 100 mL) and washed with $CHCl_3$ (3 x 50 mL). The combined organic layers were washed with brine (sat., 100 mL), dried over $MgSO_4$, filtered and concentrated under reduced pressure to afford the crude product as a pale yellow oil and used as such for the next step.

In analogy to a modified procedure by Aggarwal[124], (*S,S*)-(+)-*N,N'*-Bis(3,5-di-*tert*-butylsalicylidene)-1,2-cyclohexanediaminocobalt(II) (700 mg, 1.2 mmol, 1.0 mol%) was added to a solution of racemic 2-phenethyloxirane (17.2 g, 116 mmol, 1.00 eq) in THF (17 mL) in a flame-dried flask under argon atmosphere. After cooling to 0 °C, acetic acid (0.13 mL, 2.3 mmol, 2.0 mol%) and H_2O (1.1 mL, 60 mmol, 0.52 eq) were added. The reaction mixture was stirred for 1 h at 0 °C and then overnight at room temperature. The red solution was filtered over Celite® and washed with Et_2O (200 mL) and concentrated under reduced pressure to obtain the crude product as a red oil. Purification by flash column chromatography (SiO_2, 0→10% Et_2O in pentane) yielded the title product (*S*)-**26** (8.54 g, 57.6 mmol, 50%, >99.5% ee) as a red oil. **^{1}H NMR** (500 MHz, $CDCl_3$) δ_H/ppm 7.33-7.27 (m, 2H, Ar-**H**), 7.24-7.18 (m, 3H, Ar-**H**), 3.00-2.93 (m, 1H, C**H**-O), 2.88-2.72 (m, 3H, C**H$_2$**-Ph and C**H$_2$**-O), 2.46 (dd, *J*=5.0, 2.7 Hz, 1H, C**H$_2$**-O), 1.93-1.79 (m, 2H, C**H$_2$**-CH-O); **^{13}C NMR** (100 MHz, $CDCl_3$) δ_C/ppm 141.4 (**Cq**-Ar), 128.6 (Ar-**C**H), 128.5 (Ar-**C**H), 126.2 (Ar-**C**H), 51.9 (**C**H-O), 47.4 (**C**H_2-O), 34.4 (**C**H_2-CH-O), 32.4 (**C**H_2-Ph); **HRMS (ESI)** *m*/z calcd for $C_{10}H_{12}ONa$ $[M+Na]^+$: 171.07804, found: 171.0781; **IR (neat)** ν_{max}/cm^{-1} 3027,2921, 2860,1496, 1431, 820, 751, 699; **$[\alpha]_D^{25}$** = -15.4 (c= 1.1 in $CHCl_3$, >99.5% ee). The spectral data was in accordance with literature[124].

The enantiomeric excess of >99.5% ee was determined by HPLC [Chiralpak® IB; hexane:*i*PrOH 99.2:0.8; 1.0 mL.min^{-1}, λ= 210 nm, t_R = 6.6 min (minor enantiomer), t_R = 9.0 min (major enantiomer)].

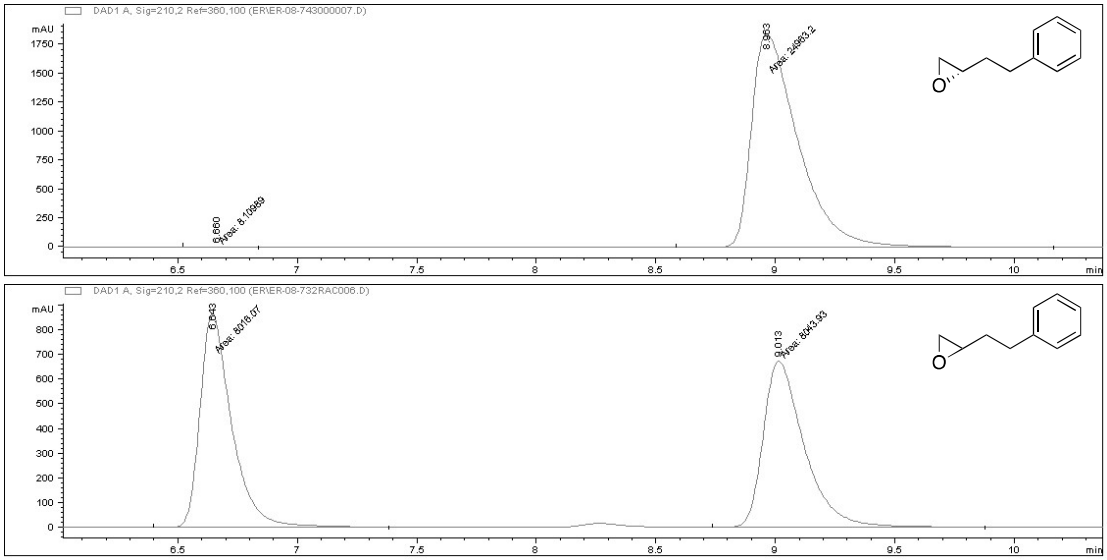

*(S)-5-phenylpent-1-en-3-ol (**27**)*

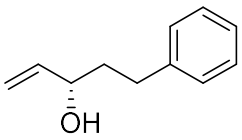

27

In analogy to a published procedure by Aggarwal[124], *n*-BuLi (69 mL, 2.5 M in hexane, 170 mmol, 3.0 eq) was added dropwise at –25 °C to a suspension of trimethylsulfoxonium iodide (35 g, 170 mmol, 3.0 eq) in THF (420 mL) in a flame-dried flask under argon atmosphere. The resulting pale yellow cloudy solution was stirred for 1 h at –25 °C. Then a solution of (*S*)-2-phenethyloxirane **26** (8.5 g, 57 mmol, 1.0 eq, >99.5% ee) in THF (73 mL) was added slowly and stirred for 1 h at –25 °C. The reaction was stirred overnight while the cooling

bath was let to warm up to room temperature. The reaction mixture was quenched with H_2O (200 mL) and washed with Et_2O (3 x 100 mL). The combined organic layers were washed with brine (100 mL), dried over $MgSO_4$, filtered and concentrated under reduced pressure to afford the crude product as an orange oil. Purification by flash column chromatography (SiO_2, 0→25% Et_2O in pentane) yielded the title product **27** (7.9 g, 49 mmol, 85%, >99.5% ee) as a pale yellow oil. **^{1}H NMR** (500 MHz, $CDCl_3$) δ_H/ppm 7.33-7.26 (m, 2H, Ar-**H**), 7.24-7.16 (m, 3H, Ar-**H**), 5.91 (ddd, *J*= 17.2, 9.8, 6.1 Hz, 1H, C**H**=CH_2), 5.25 (ddd, *J*=17.2, 1.6, 1.4 Hz, 1H, CH=C**H**$_2^{\mathbf{trans}}$), 5.14 (ddd, *J*=10.5, 1.6, 1.2 Hz, 1H, CH=C**H**$_2^{\mathbf{cis}}$), 4.14 (dt, 1H, *J*=11.2, 5.5 Hz, 1H, C**H**-O), 2.80-2.64 (m, 2H, C**H$_2$**-Ph), 1.90-1.82 (m, 2H, C**H$_2$**-CH-OH); **^{13}C NMR** (125 MHz, $CDCl_3$) δ_C/ppm 142.0 (**Cq**-Ar), 141.2 (**C**H=CH_2), 128.6 (Ar-**C**H), 128.5 (Ar-**C**H), 126.0 (Ar-**C**H), 115.1 (CH=**C**H_2), 72.6 (**C**H-OH), 38.6 (**C**H_2-CH-OH), 31.7 (**C**H_2-Ph); **HRMS** (ESI) *m*/z calcd for $C_{11}H_{14}ONa$ $[M+Na]^+$: 185.09369, found: 185.0939; **IR (neat)** ν_{max}/cm^{-1} 3346 (br.), 3027, 2925, 2860, 1496, 1454, 1031, 990, 922, 748, 699; **$[\alpha]_D^{25}$** = -6.0 (c= 1.0 in $CHCl_3$, >99.5% ee). The spectral data was in accordance with literature[295].

The enantiomeric excess of >99.5% ee was determined by HPLC [Chiralpak® IB; hexane:*i*PrOH; 95:5, 1.5 mL.min^{-1}, λ= 210 nm, t_R = 5.9 min (major enantiomer), t_R = 7.9 min (minor enantiomer)].

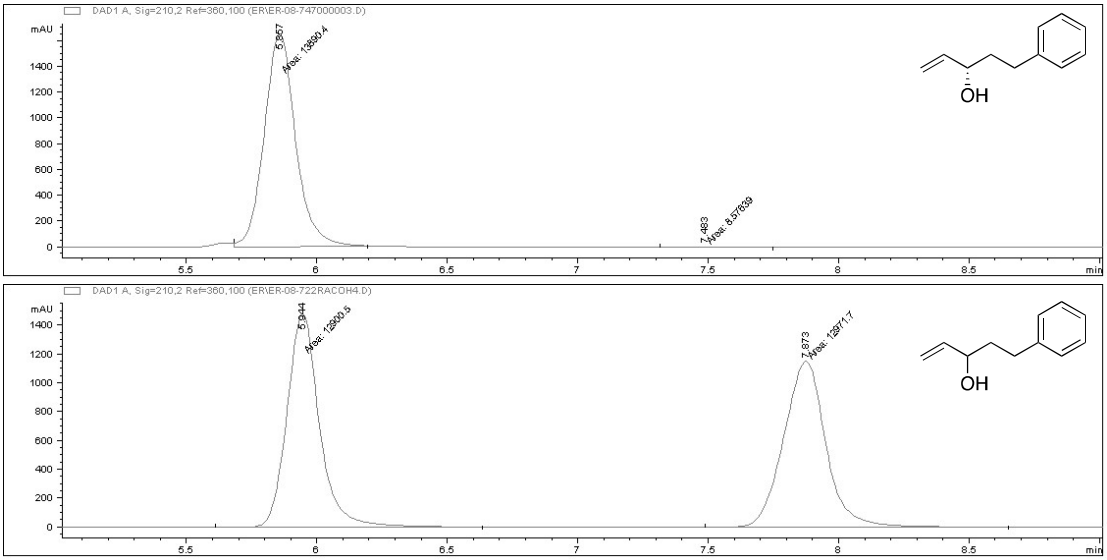

*(S)-tert-butyldimethyl((5-phenylpent-1-en-3-yl)oxy)silane (**23b**)*

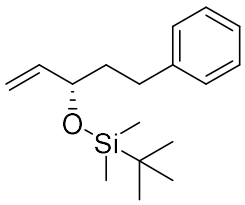

23b

In analogy to a modified procedure by Aggarwal[124], TBSCl (5.6 g, 37 mmol, 2.0 eq) and imidazole (3.0 g, 42 mmol, 2.3 eq) were added to a solution of (*S*)-5-phenylpent-1-en-3-ol **27** (3.0 g, 19 mmol, 1.0 eq, >99.5 % ee) in CH_2Cl_2 (60 mL) at 0 °C in a flame-dried flask under argon atmosphere. After 10 min at 0 °C, the reaction mixture was stirred overnight at room temperature. The resulting white suspension solution was quenched with HCl (aq., 10%, 30 mL) and washed with

CH_2Cl_2 (3 x 20 mL). The combined organic layers were washed with brine (sat., 30 mL), dried over $MgSO_4$, filtered and concentrated under reduced pressure to afford the crude product as a yellow oil. Purification by flash column chromatography (SiO_2, 100% pentane) yielded the title product **23b** (4.9 g, 18 mmol, 95%, >99.5% ee) as a colourless oil. **^{1}H NMR** (400 MHz, $CDCl_3$) δ_H/ppm 7.31-7.24 (m, 2H, Ar-**H**), 7.21-7.15 (m, 3H, Ar-**H**), 5.85 (ddd, 1H, *J*= 17.2, 10.1, 6.2 Hz, C**H**=CH_2), 5.18 (ddd, 1H, *J*=17.2, 2.0, 1.6 Hz, CH=C**H**$_2^{\mathbf{cis}}$), 5.07 (ddd, 1H, *J*=10.4, 2.0, 1.3 Hz, CH=C**H**$_2^{\mathbf{trans}}$), 4.16 (app. q, 1H, C**H**-O), 2.73-2.57 (m, 2H, C**H$_2$**-CH-O), 1.89-1.73 (m, 2H, C**H$_2$**-Ph), 0.92 (s, 9H, Si$(CH_3)_2$C**$(CH_3)_3$**), 0.06 (s, 3H Si-**CH_3**), 0.04 (s, 3H, Si-**CH_3**); **^{13}C NMR** (100 MHz, $CDCl_3$) δ_C/ppm 142.5 (**Cq**-Ar), 141.5 (**C**H=CH_2), 128.4 (Ar-**C**H), 128.3 (Ar-**C**H), 125.7 (Ar-**C**H), 114.0 (CH=**C**H_2), 73.4 (**C**H-O), 39.8 (**C**H_2-Ph), 31.5 (**C**H_2-CH=CH), 25.9 (Si$(CH_3)_2$C(**C**$H_3)_3$), 18.3 (Si$(CH_3)_2$**C**$(CH_3)_3$), -4.30 (Si-**C**H_3), -4.79 (Si-**C**H_3); **HRMS** (ESI) *m*/z calcd for $C_{17}H_{28}ONaSi$ $[M+Na]^+$: 299.18016, found: 299.18020; **IR (neat)** ν_{max}/cm^{-1} 2929, 2857, 1497, 1252, 1084, 921, 834, 774, 697; **$[\alpha]_D^{25}$** = +8.7 (c= 1.0 in $CHCl_3$). The spectral data was in accordance with literature[124].

*(S)-trimethyl((5-phenylpent-1-en-3-yl)oxy)silane (**23a**)*

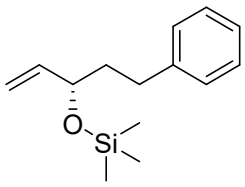

23a

DMAP (1.3 g, 11 mmol, 2.5 eq) was added to a solution of (*S*)-5-phenylpent-1-en-3-ol **27** (680 mg, 4.2 mmol, 1.0 eq, >99.5 % ee) in CH_2Cl_2 (15 mL) at room temperature in a flame-dried flask under argon atmosphere. After the solid had fully dissolved to obtain a clear pale yellow solution, TMSCl (1.1 mL, 8.4 mmol, 2.0 eq) was added dropwise and the reaction mixture was stirred for 3 h at room temperature. The yellow solution was concentrated under reduced pressure, quenched with brine (20 mL) and washed with Et_2O (3 x 10 mL). The combined organic layers were washed with brine (sat., 20 mL), dried over $MgSO_4$, filtered and concentrated under reduced pressure to afford the crude product as a yellow oil. Purification by short flash column chromatography (SiO_2, 100% pentane) yielded the title product **23a** (850 mg, 3.6 mmol, 87%, >99.5% ee) as a colourless oil. **^{1}H NMR** (400 MHz, $CDCl_3$) δ_H/ppm 7.20-7.11 (m, 2H, Ar-**H**), 7.10-7.02 (m, 3H, Ar-**H**), 5.73 (ddd, *J*= 17.3, 10.0, 6.6 Hz, 1H, C**H**=CH_2), 5.05 (d, *J*=17.2 Hz, 1H, CH=C$\mathbf{H_2^{cis}}$), 4.95 (d, *J*=10.0 Hz, 1H, CH=C$\mathbf{H_2^{trans}}$), 4.00 (dd, *J*=13.6, 6.4 Hz, 1H, C**H**-O), 2.66-2.41 (m, 2H, C$\mathbf{H_2}$-CH-O), 1.79-1.59 (m, 2H, C$\mathbf{H_2}$-Ph), 0.00 (s, 9H, Si$\mathbf{(CH_3)_3}$); **^{13}C NMR** (100 MHz, $CDCl_3$) δ_C/ppm 141.9 (**Cq**-Ar), 141.0 (**C**H=CH_2), 128.1 (Ar-**C**H), 128.0 (Ar-**C**H), 125.4 (Ar-**C**H), 113.8 (CH=**C**H_2), 73.0 (**C**H-O), 39.2 (**C**H_2-Ph), 31.5 (**C**H_2-CH=CH), 0.0 (Si(**C**H_3)$_3$); **HRMS** (EI/FI) *m*/z calcd for

$C_{14}H_{22}OSi$ $[M]^+$:234.1440, found: 234.1345; **IR (neat)** ν_{max}/cm^{-1} 2955, 1250, 1123, 837, 747, 697; $\mathbf{[\alpha]_D^{25}}$ = +6.9 (c= 1.1 in $CHCl_3$).

*(S)-triisopropyl((5-phenylpent-1-en-3-yl)oxy)silane (**23c**)*

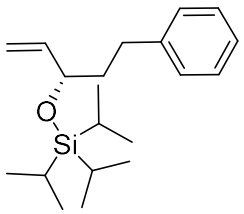

23c

DMAP (14.9 g, 122 mmol, 2.50 eq) was added to a solution of (*S*)-5-phenylpent-1-en-3-ol **27** (7.9 g, 49 mmol, 1.0 eq, >99.5 % ee) in CH_2Cl_2 (175 mL) at room temperature in a flame-dried flask under argon atmosphere. After the solid had fully dissolved to obtain a clear pale yellow solution, TIPSCl (21 mL, 97 mmol, 2.0 eq) was added. The reaction mixture was stirred overnight at room temperature. TIPSOTf (6.6 mL, 25 mmol, 0.50 eq) was added and the reaction was stirred for a further 9 h. The yellow solution was concentrated under reduced pressure, quenched with H_2O (100 mL) and washed with $CHCl_3$ (3 x 50 mL). The combined organic layers were washed with brine (sat., 100 mL), dried over $MgSO_4$, filtered and concentrated under reduced pressure to afford the crude product as a yellow oil. Purification by flash column chromatography (SiO_2, 100% pentane) yielded the title product **23c** (12.4 g, 38.8 mmol, 79%, >99.5% ee) as a colourless oil. For better results, the title product was degassed (bubbling Ar for 30 min) before being used in the subsequent steps. **^{1}H NMR** (400 MHz, $CDCl_3$) δ_H/ppm 7.23-7.17 (m, 2H, Ar-**H**), 7.14-7.07 (m, 3H, Ar-**H**), 5.80

(ddd, *J*= 6.5, 10.4, 17.3 Hz, 1H, C**H**=CH_2), 5.12 (d, *J*= 17.3 Hz, 1H, CH=C$\mathbf{H_2^{cis}}$), 5.03 (d, *J*= 10.4 Hz, 1H, CH=C$\mathbf{H_2^{trans}}$), 4.22 (m, 1H, C**H**-O), 2.68-2.48 (m, 2H, C$\mathbf{H_2}$-CH-O), 1.89-1.72 (m, 2H, C$\mathbf{H_2}$-Ph), 0.99 (s, 21H, Si(C**H**(C$\mathbf{H_3}$)$_2$)$_3$); **^{13}C NMR** (100 MHz, $CDCl_3$) δ_C/ppm 142.6 (**Cq**-Ar), 141.5 (**C**H=CH_2), 128.4 (Ar-**C**H), 128.3 (Ar-**C**H), 125.6 (Ar-**C**H), 114.3 (CH=**C**H_2), 73.6 (**C**H-O), 40.1 (**C**H_2-Ph), 30.9 (**C**H_2-CH=CH), 18.1 (Si(**C**H(CH_3)$_2$)$_3$), 12.4 (Si(CH(**C**H_3)$_2$)$_3$); **HRMS** (EI/FI) *m*/z calcd for $C_{20}H_{34}OSi$ $[M]^+$: 318.2379, found: 318.2369; **IR (neat)** ν_{max}/cm^{-1} 2943, 2867, 1463, 1089, 1064, 992, 882, 746, 678; **$[\alpha]_D^{25}$** = +13.9 (c= 1.1 in $CHCl_3$).

*(R)-4-((R)-3-((tert-butyldimethylsilyl)oxy)-5-phenylpentyl)-8,8-diphenyl-6,10-dioxaspiro[4.5]decan-2-one (**29b**)*

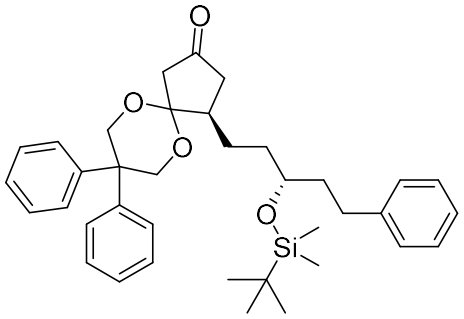

29b

In a flame-dried flask under argon atmosphere, Cp_2ZrHCl (310 mg, 1.2 mmol, 3.0 eq) was added to a solution of (*S*)-*tert*-butyldimethyl((5-phenylpent-1-en-3-yl)oxy)silane **23b** (390 mg, 1.4 mmol 3.5 eq) in CH_2Cl_2 (0.5 mL) and vigorously stirred at 40 °C until a clear orange solution was obtained (ca 30 min). Simultaneously, in another flask under argon atmosphere, CuCl (7.9 mg, 80 μmol, 20 mol%) and (*S*)-**Q** (47.5 mg, 88.0 μmol, 22.0 mol%)

were covered in Et_2O (2.2 mL) and stirred for 1 h at room temperature. AgOTf (20.6 mg, 80.0 μmol, 20.0 mol%) was added to the freshly formed Cu-ligand containing solution and stirring continued for an additional 1 h. The resulting catalyst mixture was taken up by syringe and injected through a filter into the freshly prepared alkylzirconocene species and then the reaction flask was cooled to 0 °C using an ice/water bath. After 10 min, solid 8,8-diphenyl-6,10-dioxaspiro[4.5]dec-3-en-2-one (120 mg, 0.40 mmol, 1.0 eq) was added in one portion by quickly tipping the solid into the black solution. TMSCl (0.25 mL, 2.0 mmol, 5.0 eq) was then added dropwise and the reaction mixture was stirred overnight and allowed to slowly warm to RT. The reaction mixture was diluted with Et_2O (2 mL) and quenched with NH_4Cl (3 mL, 1 M). The mixture was partitioned and the aqueous phase was extracted with Et_2O (3 x 10 mL). The combined organic extracts were washed with $NaHCO_3$ (aq. sat. 30 mL), dried over $MgSO_4$, filtered and concentrated under reduced pressure. Purification by flash column chromatography (SiO_2, Et_2O 0→20% in pentane) yielded the title protected alcohol product *(R,R)*-**29b** and its diastereomer (24 mg, 40 μmol, 21%, 85:15 dr) as a yellow oil and the deprotected alcohol **28** and its diastereomer (59 mg, 0.12 mmol, 31%, 89:11 dr) as a colourless oil. **^{1}H NMR** (500 MHz, $CDCl_3$) δ_H/ppm 7.39 (d, *J*= 8.1 Hz, 2H, Ar-**H**), 7.29-7.10 (m, 11H, Ar-**H**), 7.03 (d, *J*= 7.3 Hz, 2H, Ar-**H**), 4.60-4.50 (m, 2H, C**H**$_2$-O-Cq-O-C**H**$_2$), 4.30 (d, *J*=11.8 Hz, 1H, C**H**$_2$-O), 4.13 (d, *J*=11.8 Hz, 1H, C**H**$_2$-O), 3.64-3.56 (m, 1H, C**H**-OTBS), 3.04 (d, *J*=17.8 Hz, 1H, Cq-C**H**$_2$-C=O), 2.70-2.54 (m, 1H, C**H$_2$**-Ph), 2.53-2.42 (m, 1H, C**H$_2$**-Ph), 2.39 (dd, *J*=18.1, 8.1 Hz, 1H, CH-C**H**$_2$-C=O), 2.30 (d, *J*=17.9 Hz, 1H, Cq-C**H**$_2$-C=O), 2.27-2.16 (m, 1H, C**H**-CH_2-C=O), 2.07 (dd, *J*=17.9, 11.0 Hz, 1H, CH-C**H**$_2$-C=O), 1.63-1.53 (m, 3H, C**H$_2$**), 1.53-1.35 (m, 3H, C**H**$_2$), 0.87 (s, 9H, Si(CH_3)$_2$C(C**H$_3$**)$_3$), -0.00 (s, 3H,

Si(C**H**$_3$)$_2$C(CH$_3$)$_3$), -0.03 (s, 3H, Si(C**H**$_3$)$_2$C(CH$_3$)$_3$); **^{13}C NMR** (100 MHz, $CDCl_3$) δ_C/ppm 213.1 (**C**=O), 143.7(**C**q-Ar), 143.4 (**C**q-Ar), 142.9 (**C**q-Ar), 128.8 (**C**H-Ar), 128.7 (**C**H-Ar), 128.6 (**C**H-Ar), 128.5 (**C**H-Ar), 128.4 (**C**H-Ar), 128.3 (**C**H-Ar), 127.1 (**C**H-Ar), 126.4 (**C**H-Ar), 125.9 (**C**H-Ar), 104.7 (**C**q-O$_2$), 71.7 (**C**H-OH), 70.9 (**C**H$_2$-O), 68.8 (**C**H$_2$-O), 46.0 (**C**H-CH$_2$-C=O), 45.0 (Cq-**C**H$_2$-C=O), 44.8 (**C**q-Ph$_2$), 43.3 (CH-**C**H$_2$-C=O), 38.7 (**C**H$_2$-CH-OH), 35.3 (C**H**$_2$-CH$_2$-Ph), 32.2 (**C**H$_2$-Ph), 26.1 (Si(CH$_3$)$_2$C(**C**H$_3$)$_3$), 22.7 (CH-**C**H$_2$-CH$_2$-CH-OH), 18.2 (Si(CH$_3$)$_2$**C**(CH$_3$)$_3$), -4.1 (Si-**C**H$_3$), -4.4 (Si-**C**H$_3$); **HRMS** (ESI) *m*/z calcd for $C_{37}H_{48}O_4NaSi$ $[M+Na]^+$: 607.32141, found: 607.32116; **IR (neat)** ν_{max}/cm^{-1} 2957, 2927, 2855, 1751, 1496, 1458, 1189, 1133, 836, 774, 699; **$[\alpha]_D^{25}$** = +29.4 (c= 1.0 in $CHCl_3$).

The diastereomeric ratio of 85:15 was determined by ^{1}H NMR of the isolated diastereomeric mixture: 0.14 ppm (minor diastereomer), 0.07 ppm (major diastereomer).

*(R)-4-((R)-3-hydroxy-5-phenylpentyl)-8,8-diphenyl-6,10-dioxaspiro[4.5]decan-2-one (**28**)*

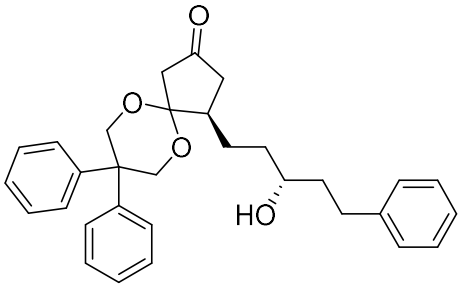

28

Procedure from TBS protected alcohol 23b

In a flame-dried flask under argon atmosphere, Cp_2ZrHCl (310 mg, 1.2 mmol, 3.0 eq) was added to a solution of (*S*)-*tert*-butyldimethyl((5-phenylpent-1-en-3-yl)oxy)silane **23b** (390 mg, 1.4 mmol 3.5 eq) in CH_2Cl_2 (0.5 mL) and vigorously stirred at 40 °C until a clear orange solution was obtained (ca 30 min). Simultaneously, in another flask under argon atmosphere, CuCl (7.9 mg, 80 μmol, 20 mol%) and (*S*)-**Q** (47.5 mg, 88.0 μmol, 22.0 mol%) were covered in Et_2O (2.2 mL) and stirred for 1 h at room temperature. AgOTf (20.6 mg, 80.0 μmol, 20.0 mol%) was added to the freshly formed Cu-ligand containing solution and stirring continued for an additional 1 h. The resulting catalyst mixture was taken up by syringe and injected through a filter into the freshly prepared alkylzirconocene species and then the reaction flask was cooled to 0 °C using an ice/water bath. After 10 min, solid 8,8-diphenyl-6,10-dioxaspiro[4.5]dec-3-en-2-one (120 mg, 0.40 mmol, 1.0 eq) was added in one portion by quickly tipping the solid into the black solution. TMSCl (0.25 mL, 2.0 mmol, 5.0 eq) was then added dropwise and the reaction mixture was stirred

overnight and allowed to slowly warm to RT. The reaction mixture was diluted with Et_2O (2 mL) and quenched with NH_4Cl (3 mL, 1 M). The mixture was partitioned and the aqueous phase was extracted with Et_2O (3 x 10 mL). The combined organic extracts were washed with $NaHCO_3$ (aq. sat. 30 mL), dried over $MgSO_4$, filtered and concentrated under reduced pressure. Purification by flash column chromatography (SiO_2, Et_2O 5→100% in pentane) yielded the title product (*R,R*)-**28** and its diastereomer (58.5 mg, 0.124 mmol, 31%, 89:11 dr) as a colourless oil.

Procedure from TMS protected alcohol 23a

In a flame-dried flask under argon atmosphere, Cp_2ZrHCl (310 mg, 1.2 mmol, 3.0 eq) was added to a solution of (*S*)-trimethyl((5-phenylpent-1-en-3-yl)oxy)silane **23a** (340 mg, 1.4 mmol 3.5 eq) in CH_2Cl_2 (0.5 mL) and vigorously stirred at 40 °C until a clear orange solution was obtained (ca 40 min). Simultaneously, in another flask under argon atmosphere, CuCl (7.9 mg, 80 μmol, 20 mol%) and (*S*)-**Q** (47.5 mg, 88.0 μmol, 22.0 mol%) were covered in Et_2O (2.2 mL) and stirred for 1 h at room temperature. AgOTf (20.6 mg, 80.0 μmol, 20.0 mol%) was added to the freshly formed Cu-ligand containing solution and stirring continued for an additional 1 h. The resulting catalyst mixture was taken up by syringe and injected through a filter into the freshly prepared alkylzirconocene species and then the reaction flask was cooled to 0 °C using an ice/water bath. After 10 min, solid 8,8-diphenyl-6,10-dioxaspiro[4.5]dec-3-en-2-one (120 mg, 0.40 mmol, 1.0 eq) was added in one portion by quickly tipping the solid into the black solution. TMSCl (0.25 mL, 2.0 mmol, 5.0 eq) was then added dropwise and the reaction mixture was stirred overnight and allowed to slowly

warm to RT. The reaction mixture was diluted with Et_2O (2 mL) and quenched with NH_4Cl (3 mL, 1 M). The mixture was partitioned and the aqueous phase was extracted with Et_2O (3 x 10 mL). The combined organic extracts were washed with $NaHCO_3$ (aq. sat. 30 mL), dried over $MgSO_4$, filtered and concentrated under reduced pressure. Purification by flash column chromatography (SiO_2, Et_2O 0→100% in pentane) yielded the title product (*R, R*)-**28** and its diastereomer (72 mg, 0.15 mmol, 38%, 93:7 dr) as a colourless oil.

Procedure from non-protected alcohol 27

In a flame-dried flask under argon atmosphere, Cp_2ZrHCl (620 mg, 2.4 mmol, 6.0 eq) was added to a solution of (*S*)-5-phenylpent-1-en-3-ol **27** (190 mg, 1.2 mmol, 3.0 eq) in CH_2Cl_2 (0.9 mL) and vigorously stirred until a clear orange solution was obtained (ca 30 min). Simultaneously, in another flask under argon atmosphere, CuCl (7.9 mg, 80 μmol, 20 mol%) and (*S*)-**Q** (47.5 mg, 88.0 μmol, 22.0 mol%) were covered in Et_2O (3.0 mL) and stirred for 1 h at room temperature. AgOTf (20.6 mg, 80.0 μmol, 20.0 mol%) was added to the freshly formed Cu-ligand containing solution and stirring continued for an additional 1 h. The resulting catalyst mixture was taken up by syringe and injected through a filter into the freshly prepared alkylzirconocene species and then the reaction flask was cooled to 0 °C using an ice/water bath. After 10 min, solid 8,8-diphenyl-6,10-dioxaspiro[4.5]dec-3-en-2-one (120 mg, 0.40 mmol, 1.0 eq) was added in one portion by quickly tipping the solid into the black solution. TMSCl (0.25 mL, 2.0 mmol, 5.0 eq) was then added dropwise and the reaction mixture was stirred overnight and allowed to slowly warm to RT. The reaction mixture was diluted with Et_2O (2 mL) and quenched with NH_4Cl (3 mL, 1 M). The mixture was

partitioned and the aqueous phase was extracted with Et_2O (3 x 10 mL). The combined organic extracts were washed with $NaHCO_3$ (aq. sat. 30 mL), dried over $MgSO_4$, filtered and concentrated under reduced pressure. Purification by flash column chromatography (SiO_2, Et_2O 20→100% in pentane) yielded the title product (*R, R*)-**28** and its diastereomer (74 mg, 0.16 mmol, 39%, dr 90:10) as a colourless oil. **^{1}H NMR** (400 MHz, $CDCl_3$) δ_H/ppm 7.37-7.28 (m, 2H, Ar-**H**), 7.20-6.99 (m, 11H, Ar-**H**), 6.91 (d, 2H, *J*=7.5 Hz, Ar-**H**), 4.53-4.43 (m, 2H, C**H**$_2$-O-Cq-O-C**H**$_2$), 4.15 (d, *J*=11.7 Hz, 1H, C**H**$_2$-O), 4.04 (d, *J*=12.1 Hz, 1H, C**H**$_2$-O), 3.34-3.25 (m, 1H, C**H**-OH), 2.98 (d, *J*=18.0 Hz, 1H, Cq-C**H**$_2$-C=O), 2.65-2.54 (m, 1H, C**H**$_2$-Ph), 2.50-2.39 (m, 1H, C**H**$_2$-Ph), 2.34 (dd, *J*= 17.8, 7.9 Hz, 1H, CH-C**H**$_2$-C=O), 2.24 (d, *J*=17.8 Hz, 1H, Cq-C**H**$_2$-C=O), 2.18-2.06 (m, 1H, C**H**-CH$_2$-C=O), 1.96 (dd, *J*= 18.1, 11.6 Hz, 1H, CH-C**H**$_2$-C=O), 1.56-1.38 (m, 3H, CH-C**H**$_2$-C**H$_2$**-CH-OH), 1.25-1.09 (m, 3H, C**H**$_2$-CH$_2$-CH(OH)-C**H$_2$**-CH$_2$-Ph); **^{13}C NMR** (100 MHz, $CDCl_3$) δ_C/ppm 212.9 (**C**=O), 143.6 (**C**q-Ar), 143.0 (**C**q-Ar), 142.3 (**C**q-Ar), 128.8 (**C**H-Ar), 128.7 (**C**H-Ar), 128.5 (**C**H-Ar), 128.5 (**C**H-Ar), 128.3 (**C**H-Ar), 128.2 (**C**H-Ar), 127.1 (**C**H-Ar), 126.4 (**C**H-Ar), 125.8 (**C**H-Ar), 104.7 (**C**q-O$_2$), 71.5 (**C**H-OH), 70.9 (**C**H$_2$-O), 68.7 (**C**H$_2$-O), 46.0 (**C**H-CH$_2$-C=O), 45.0 (Cq-**C**H$_2$-C=O), 44.8 (**C**q-Ph$_2$), 43.5 (CH-**C**H$_2$-C=O), 38.7 (**C**H$_2$-CH-OH), 35.8 (C**H**$_2$-CH$_2$-Ph), 32.1 (**C**H$_2$-Ph), 23.8 (CH-**C**H$_2$-CH$_2$-CH-OH); **HRMS** (ESI) *m*/z calcd for $C_{31}H_{34}O_4Na$ $[M+Na]^+$: 493.23493, found: 493.23476; **IR (neat)** ν_{max}/cm^{-1} 3443 (br.), 2870, 2856, 1748, 1091, 752, 699; **$[\alpha]_D^{25}$** = -59.2 (c= 1.1 in $CHCl_3$).

The diastereomeric ratio of 90:10 was determined by ^{13}C NMR of the isolated diastereomeric mixture: 143.1 ppm (minor diastereomer), 143.0 (major diastereomer).

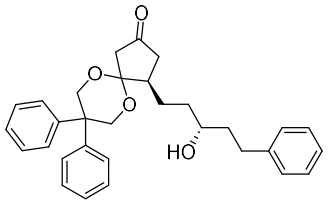

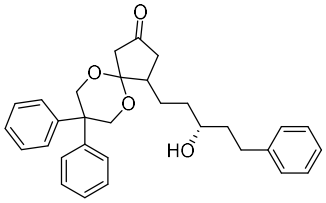

*(R)-8,8-diphenyl-4-((R)-5-phenyl-3-((triisopropylsilyl)oxy)pentyl)-6,10-dioxaspiro[4.5]decan-2-one (**29c**)*

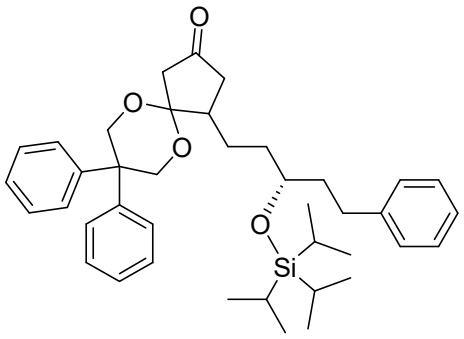

29c

In a flame-dried flask under argon atmosphere, Cp_2ZrHCl (160 mg, 0.60 mmol, 1.5 eq) was added to a solution of (*S*)-triisopropyl((5-phenylpent-1-en-3-yl)oxy)silane **23c** (220 mg, 0.72 mmol 1.8 eq) in CH_2Cl_2 (0.35 mL) and vigorously stirred at 42 °C sealed until a clear yellow solution was obtained (ca 1 h). Simultaneously, in another flask under argon atmosphere, CuCl (7.9 mg, 80 μmol, 20 mol%) and (*S*)-**Q** (47.5 mg, 88.0 μmol, 22.0 mol%) were covered in Et_2O (3.0 mL) and stirred for 1 h at room temperature. AgOTf (20.6 mg, 80.0 μmol, 20.0 mol%) was added to the freshly formed Cu-ligand containing solution and stirring continued for an additional 1 h. The resulting catalyst mixture was taken up by syringe and injected through a filter into the freshly prepared alkylzirconocene species and then the reaction flask was cooled to 0 °C using an ice/water bath. After 10 min, solid 8,8-diphenyl-6,10-dioxaspiro[4.5]dec-3-en-2-one (120 mg, 0.40 mmol, 1.0 eq) was added in one portion by quickly tipping the solid into the black solution. TMSCl (0.25 mL, 2.0 mmol, 5.0 eq) was then added dropwise and the reaction mixture was stirred

overnight and allowed to slowly warm to RT. The reaction mixture was diluted with Et_2O (2 mL) and quenched with NH_4Cl (3 mL, 1 M). The mixture was partitioned and the aqueous phase was extracted with Et_2O (3 x 10 mL). The combined organic extracts were washed with $NaHCO_3$ (aq. sat. 30 mL), dried over $MgSO_4$, filtered and concentrated under reduced pressure. Purification by flash column chromatography (SiO_2, Et_2O 0→20% in pentane) yielded the title product **29c** and its diastereomer (190 mg, 0.30 mmol, 75%, 85:15 dr) as a sticky colourless oil. **^{1}H NMR** (500 MHz, $CDCl_3$) δ_H/ppm 7.46-7.44 (m, 2H, Ar-**H**), 7.33-7.11 (m, 11H, Ar-**H**), 7.10-7.05 (m, 2H, Ar-**H**), 4.65-4.55 (m, 2H, C**H**$_2$-O-Cq-O-C**H**$_2$), 4.34 (d, *J*= 11.3 Hz, 1H, C**H**$_2$-O), 4.17 (d, *J*= 12.0 Hz, 1H, C**H**$_2$-O), 3.86-3.77 (m, 1H, C**H**-OTIPS), 3.09 (d, *J*= 18.2 Hz, 1H, Cq-C**H**$_2$-C=O), 2.64-2.53 (m, 2H, C**H$_2$**-Ph), 2.53-2.48 (m, 1H, CH-C**H**$_2$-C=O), 2.44 (d, *J*= 17.4 Hz, 1H, Cq-C**H**$_2$-C=O), 2.32-2.20 (m, 1H, C**H**-CH$_2$-C=O), 2.12 (dd, *J*= 10.6, 19.0 Hz, 1H, CH-C**H**$_2$-C=O), 1.75-1.63 (m, 2H, C**H$_2$**-CH-OTIPS), 1.51-1.38 (m, 2H, CH-C**H**$_2$-CH$_2$-CH-OH and C**H**$_2$-CH$_2$-Ph), 1.35-1.27 (m, 2H, CH-C**H**$_2$-CH$_2$-CH-OH and C**H**$_2$-CH$_2$-Ph), 0.98 (s, 21H, TIPS-**H**); **^{13}C NMR** (125 MHz, $CDCl_3$) δ_C/ppm 213.1 (**C**=O), 143.7 (**C**q-Ar), 143.4 (**C**q-Ar), 142.9 (**C**q-Ar), 128.9 (**C**H-Ar), 128.7 (**C**H-Ar), 128.5 (**C**H-Ar), 128.5 (**C**H-Ar), 128.3 (**C**H-Ar), 127.1 (**C**H-Ar), 126.6 (**C**H-Ar), 126.5 (**C**H-Ar), 125.8 (**C**H-Ar), 104.7 (**C**q-O$_2$), 71.7 (**C**H-OTIPS), 71.0 (**C**H$_2$-O), 68.9 (**C**H$_2$-O), 46.3 (**C**H-CH$_2$-C=O), 45.0 (Cq-**C**H$_2$-C=O), 44.8 (**C**q-(CH$_2$)$_2$Ph$_2$), 43.3 (CH-**C**H$_2$-C=O), 38.0 (**C**H$_2$-CH-OTIPS), 34.8 (**C**H$_2$-CH$_2$-Ph), 31.6 (**C**H$_2$-Ph), 22.4 (CH-**C**H$_2$-CH$_2$-CH-OH), 18.4 (Si-(CH-(**C**H$_3$)$_2$)$_3$), 12.8 (Si-(**C**H-(CH$_3$)$_2$)$_3$); **HRMS** (ESI) *m*/z calcd for $C_{40}H_{54}O_4NaSi$ $[M+Na]^+$: 649.36836, found: 649.36783; **IR (neat)** ν_{max}/cm^{-1} 2943, 2865, 1751, 1496, 1462, 1133, 1095, 1060, 883, 699; **$[\alpha]_D^{25}$** = -50.6 (c= 1.0 in $CHCl_3$, 85:15 dr).

The diastereomeric ratio of 85:15 was determined by ^{1}H NMR of the isolated diastereomeric mixture: 4.41 and 4.30 ppm (major diastereomer), 4.29 and 4.24 ppm (minor diastereomer).

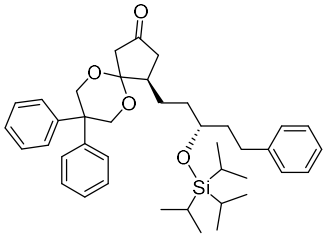

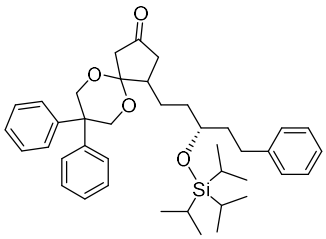

*(R)-((8,8-diphenyl-4-(4-phenylbutyl)-6,10-dioxaspiro[4.5]dec-1-en-2-yl)oxy)triisopropylsilane (**39**)*

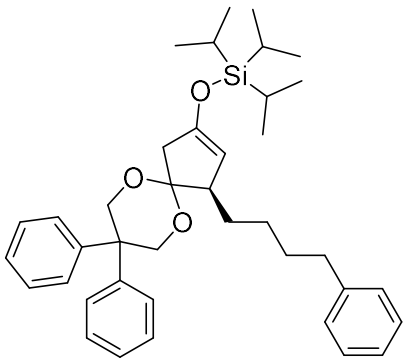

39

TIPSOTf (81 µL, 0.30 mmol, 1.5 eq) and Et_3N (39 µL, 0.28 mmol, 1.4 eq) were added to a solution of (*S*)-8,8-diphenyl-4-(4-phenylbutyl)-6,10-dioxaspiro[4.5]decan-2-one **21a** (88 mg, 0.20 mmol, 1.0 eq, 92% ee) in CH_2Cl_2 (1.0 mL) at 0 °C in a flame-dried flask under argon atmosphere. The reaction mixture was stirred overnight and let to slowly warm up to room temperature. The resulting yellow solution was quenched with brine (sat, 5 mL) and washed with $CHCl_3$ (3 x 5 mL). The combined organic layers were dried over $MgSO_4$, filtered and concentrated under reduced pressure to afford the crude product. Purification by flash column chromatography (SiO_2, 0→100% Et_2O in pentane) yielded the title product **39** (24 mg, 40 µmol, 20%) as a colourless oil. **^{1}H NMR** (400 MHz, $CDCl_3$) δ_H/ppm 7.49 (d, *J*= 7.8 Hz, 2H, Ar-**H**), 7.39-7.12 (m, 13H, Ar-**H**), 4.63 (d, *J*= 1.9 Hz, 1H, C**H**=Cq), 4.57 (d, *J*= 11.5 Hz, 2H, C**H**$_2$-O-Cq-C**H**$_2$-O), 4.42 (d, *J*= 11.5 Hz, 1H, C**H**$_2$-O), 4.34 (d, *J*= 11.8 Hz, 1H, C**H**$_2$-O), 2.76 (app. q, 2H, CO-C**H**$_2$-Cq), 2.70-2.63 (m, 1H, C**H**-CH_2-CH_2), 2.54 (t, *J*= 7.8 Hz, 2H, CH_2-C**H$_2$**-Ph), 1.64-1.51 (m, 3H, CH-C**H**$_2$-CH_2, C**H$_2$**-CH_2-Ph) 1.35-1.14 (m, 6H, CH-C**H**$_2$-C**H$_2$**, Si-

(C**H**$(CH_3)_2)_3$), 1.14-1.07 (m, 18H, Si-(CH(**C**$H_3)_2)_3$); **^{13}C NMR** (100 MHz, $CDCl_3$) δ_C/ppm 150.8 (O-**Cq**=CH), 144.5 (**Cq**-Ar), 144.2 (**Cq**-Ar), 143.2 (**Cq**-Ar), 128.7 (Ar-**C**H), 128.7 (Ar-**C**H), 128.5 (Ar-**C**H), 128.3 (Ar-**C**H), 128.2 (Ar-**C**H), 126.9 (Ar-**C**H), 126.7 (Ar-**C**H), 126.3 (Ar-**C**H), 125.6 (Ar-**C**H), 106.8 (Cq=**C**H), 104.6 (**C**q-O_2), 69.8 (**C**H_2-O), 69.3 (**C**H_2-O), 52.1 (**C**H-CH_2-CH_2), 45.1 (**Cq**-Ph_2), 40.6 (CO-**C**H_2-Cq), 35.9 (CH_2-**C**H_2-Ph), 31.9 (**C**H_2-CH_2-Ph), 29.6 (CH-**C**H_2-CH_2), 27.7 (CH-CH_2-**C**H_2), 18.0 (Si-(CH(**C**$H_3)_2)_3$), 12.6 (Si-(**C**$H(CH_3)_2)_3$); **HRMS** (ESI) *m*/z calcd for $C_{39}H_{52}O_3SiNa$ $[M+Na]^+$: 619.35779, found: 619.3577; **IR (neat)** ν_{max}/cm^{-1} 2941, 2865, 1652, 1496, 1463, 1332, 1127, 883, 806, 751, 698; **$[\alpha]_D^{25}$** = -38.6 (c= 1.0 in $CHCl_3$).

(R)-3-(3-hydroxy-2,2-diphenylpropoxy)-4-(4-phenylbutyl)cyclopent-2-en-1-one ***(41a)***

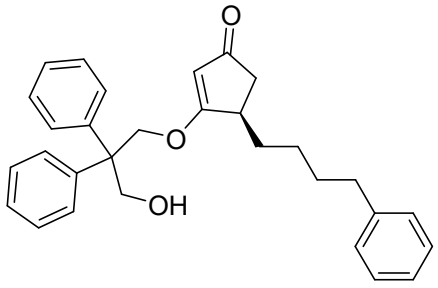

41a

Diisopropylamine (85 µL, 0.60 mmol, 1.2 eq) was dissolved in THF (3.3 mL) at −78 °C in a flame-dried flask under argon atmosphere. The reaction mixture was stirred at that temperature for 15 min. (*S*)-8,8-diphenyl-4-(4-phenylbutyl)-6,10-dioxaspiro[4.5]decan-2-one **21a** (220 mg, 0.50 mmol, 1.0 eq) in THF (2.5 mL) was added dropwise at −78 °C. After 10 min, the reaction mixture was

warmed up to 0 °C and stirred for 10 h. The resulting yellow solution was quenched with NH_4Cl (sat, 5 mL) and washed with CH_2Cl_2 (3 x 3 mL). The combined organic layers were dried over $MgSO_4$, filtered and concentrated under reduced pressure to afford the crude product. Purification by flash column chromatography (SiO_2, 0→100% Et_2O in pentane then 10% MeOH in $CHCl_3$) yielded the title product **41a** (198 mg, 45.0 μmol, 90%) as a pale yellow oil. **^{1}H NMR** (400 MHz, $CDCl_3$) δ_H/ppm 7.40-7.53 (m, 4H, Ar-**H**), 7.33-7.26 (m, 4H, Ar-**H**), 7.24-7.18 (m, 5H, Ar-**H**), 7.16 (d, *J*=7.1 Hz, 2H, Ar-**H**), 5.37 (s, 1H, C**H**=Cq), 4.70 (d, *J*=9.5 Hz, 1H, C**H**$_2$-O-Cq), 4.55 (d, *J*=9.5 Hz, 1H, C**H**$_2$-O-Cq), 4.38 (d, *J*=11.1 Hz, 1H, C**H**$_2$-OH), 4.34 (d, *J*=11.1 Hz, 1H, C**H**$_2$-OH), 2.81-2.72 (m, 1H, C**H**-CH_2), 2.58-2.50 (m, 3H, C**H$_2$**-Ph, CO-C**H**$_2$), 2.07 (dd, *J*=18.0, 2.4 Hz, 1H, CO-C**H**$_2$), 1.70-1.48 (m, 3H, CH-C**H**$_2$-CH_2-C**H$_2$**-CH_2-Ph) 1.26-1.19 (m, 3H, C**H$_2$**-C**H**$_2$-CH); **^{13}C NMR** (100 MHz, $CDCl_3$) δ_C/ppm 204.9 (**C**=O), 191.7 (**C**q=CH), 142.4 (**C**q-Ar), 142.4 (**C**q-Ar), 142.4 (**C**q-Ar), 128.6 (**C**H-Ar), 128.5 (**C**H-Ar), 128.3 (**C**H-Ar x2), 128.0 (**C**H-Ar x2), 127.2 (**C**H-Ar), 127.2 (**C**H-Ar), 125.8 (**C**H-Ar), 104.7 (**C**H=Cq), 74.5 (**C**H_2-O-Cq), 66.6 (**C**H_2-OH), 52.4 (**Cq-**Ph_2), 40.6 (**C**H-CH_2), 40.3 (**C**H_2-CO), 35.7 (**C**H_2-Ph), 31.9 (**C**H_2-CH_2-Ph), 31.4 (CH-**C**H_2), 26.1 (**C**H_2-CH_2-CH); **HRMS** (ESI) *m*/z calcd for $C_{30}H_{33}O_3$ $[M+H]^+$: 441.24242, found: 441.24243; **IR (neat)** ν_{max}/cm^{-1} 3397, 2927, 2856, 1675, 1587, 1249, 1189, 909, 732, 699; **$[\alpha]_D^{25}$** = +3.8 (c= 1.0 in $CHCl_3$).

*(R)-3-(3-hydroxy-2,2-diphenylpropoxy)-4-((R)-5-phenyl-3-((triisopropylsilyl)oxy)pentyl)cyclopent-2-en-1-one (**41b**)*

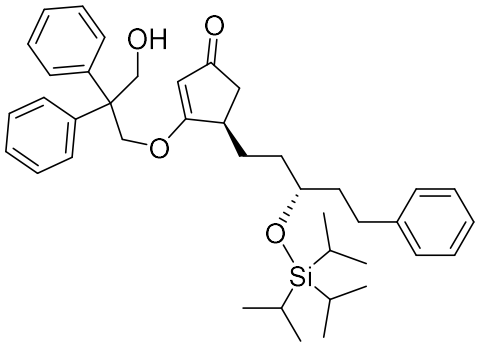

41b

Diisopropylamine (85 µL, 0.60 mmol, 1.2 eq) was dissolved in THF (3.3 mL) at −78 °C in a flame-dried flask under argon atmosphere. *n*BuLi (0.24 mL, 2.5 M in THF, 0.60 mmol, 1.2 eq) was added dropwise to the reaction mixture at −78 °C and stirred at that temperature for 15 min. (*R*)-8,8-diphenyl-4-((*R*)-5-phenyl-3-((triisopropylsilyl)oxy)pentyl)-6,10-dioxaspiro[4.5]decan-2-one **29c** (220 mg, 0.50 mmol, 1.0 eq) in THF (2.5 mL) was added dropwise at −78 °C. After 10 min, the reaction mixture was warmed up to 0 °C and stirred for 10 h. The resulting yellow solution was quenched with NH_4Cl (sat, 3 mL) and washed with CH_2Cl_2 (5 x 1 mL). The combined organic layers were dried over $MgSO_4$, filtered and concentrated under reduced pressure to afford the crude product. Purification by flash column chromatography (SiO_2, 50→100% Et_2O in pentane then 5% MeOH in $CHCl_3$) yielded the title product **41b** (200 mg, 0.45 mmol, 90%, dr 86:14) as a pale yellow oil. **^{1}H NMR** (400 MHz, $CDCl_3$) δ_H/ppm 7.37-7.26 (m, 7H, Ar-**H**), 7.26-7.13 (m, 8H, Ar-**H**), 5.39 (s, 1H, C**H**=Cq), 4.69 (d, *J*=10.1 Hz, 1H, C**H**$_2$-O), 4.59 (d, 1H, *J*=9.6 Hz, C**H**$_2$-O), 4.41-4.32 (m, 2H, C**H**$_2$-O), 3.88-3.79 (m, 1H, C**H**-OTIPS),

2.79-2.70 (m, 1H, C**H**-CH_2-CH_2-CH-OTIPS), 2.66-2.53 (m, 3H, C**H**$_2$-Ph, C**H**$_2$-CO), 2.08 (dd, *J*=18.1, 2.2 Hz, 1H, C**H**$_2$-CO), 1.81-1.57 (m, 3H, C**H**$_2$-CH_2-Ph, CH-C**H**$_2$), 1.55-1.38 (m, 2H, CH-CH_2-CH_2-C**H$_2$**-CH-OTIPS), 1.38-1.17 (m, 1H, CH-C**H**$_2$-CH_2), 1.08 (s, 21H, ((C**H**(C**H$_3$**)$_2$)$_3$Si); **^{13}C NMR** (100 MHz, $CDCl_3$) δ_C/ppm 204.8 (**C**=O), 191.6 (**C**q=CH), 142.5 (**C**q-Ar), 142.5 (**C**q-Ar), 128.7 (**C**H-Ar), 128.6 (**C**H-Ar), 128.5 (**C**H-Ar), 128.4 (**C**H-Ar), 128.0 (**C**H-Ar), 128.0 (**C**H-Ar), 127.3 (**C**H-Ar), 127.2 (**C**H-Ar), 125.9 (**C**H-Ar), 104.8 (**C**H=Cq), 74.6 (**C**H_2-O-Cq), 71.6 (**C**H-OTIPS), 66.7 (**C**H_2-OH), 52.5 (**Cq-**Ph_2), 40.8 (**C**H_2-CO), 40.6 (**C**H-CH_2-CH_2-CH-OTIPS), 38.4 (**C**H_2-CH_2-Ph), 33.7 (CH_2-CH_2-**C**H_2-CH-OTIPS), 31.4 (**C**H_2-Ph), 27.6 (CH-**C**H_2-CH_2), 18.3 ((CH(**C**H_3)$_2$)$_3$Si), 12.8 ((**C**H$(CH_3)_2$)$_3$Si); **HRMS** (ESI) *m*/z calcd for $C_{40}H_{55}O_4Si$ $[M+H]^+$:627.38641, found:627.38614; **IR (neat)** ν_{max}/cm^{-1} 3384 (br.), 2942, 2865, 1677, 1588, 1463, 1339, 1248, 1188, 1093, 1060, 883, 699; **$[\alpha]_D^{25}$** = +8.6 (c= 1.0 in $CHCl_3$).

The diastereomeric ratio of 86:14 was determined by ^{13}C NMR of the isolated diastereomeric mixture: 71.7 ppm (minor diastereomer) and 71.6 ppm (major diastereomer) [**C**H-OTIPS].

*(R)-3-(2,2-diphenyl-3-((triisopropylsilyl)oxy)propoxy)-4-(4-phenylbutyl)cyclopent-2-en-1-one (**43a**)*

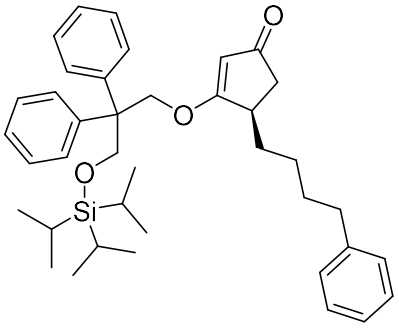

43a

DMAP (110 mg, 0.86 mmol, 2.0 eq) was added to a solution of (*R*)-3-(3-hydroxy-2,2-diphenylpropoxy)-4-(4-phenylbutyl)cyclopent-2-en-1-one **41a** (180 mg, 0.40 mmol, 1.0 eq) in CH_2Cl_2 (2.0 mL) at room temperature in a flame-dried flask under argon atmosphere. After the solid had fully dissolved to obtain a clear solution, TIPSCl (0.23 mL, 1.1 mmol, 2.5 eq) was added at 0 °C. After 10 min at 0 °C, the reaction mixture was stirred overnight at room temperature. TIPSOTf (0.29 mL, 1.1 mmol, 2.5 eq) was added and the reaction was stirred for a further 3.5 h. The yellow solution was concentrated under reduced pressure, quenched with brine (5 mL) and washed with $CHCl_3$ (3 x 3 mL). The combined organic layers were dried over $MgSO_4$, filtered and concentrated under reduced pressure to afford the crude product as a yellow oil. Purification by flash column chromatography (SiO_2, 20→50% Et_2O in pentane) yielded the title product **43a** (160 mg, 0.27 mmol, 68%) as a yellow oil. **^{1}H NMR** (400 MHz, $CDCl_3$) δ_H/ppm 7.27-7.03 (m, 15H, C**H**-Ar), 5.27 (s, 1H, C**H**=Cq), 4.63 (d, *J*=9.3 Hz, 1H, C**H$_2$**-O-Cq), 4.49 (d, *J*=9.3 Hz, 1H, C**H$_2$**-O-Cq), 4.33 (s, 2H, C**H$_2$**-O-Si), 2.66-2.58 (br. m, 1H, C**H**-

CH_2-CH_2), 2.49-2.39 (m, 3H, C**H**$_2$-C=O, C**H$_2$**-Ph), 1.98 (dd, *J*=17.9, 2.3 Hz, 1H, C**H**$_2$-C=O), 1.56-1.47 (m, 1H, CH-C**H**$_2$-CH_2), 1.47-1.38 (m, 2H, C**H**$_2$-CH_2-Ph), 1.17-1.06 (m, 3H, CH-C**H**$_2$-C**H$_2$**), 1.03-0.92 (m, 3H, (Si(C**H**$(CH_3)_2)_3$), 0.92-0.86 (m, 18H, (Si(CH(C**H$_3$**$)_2)_3$); **^{13}C NMR** (100 MHz, $CDCl_3$) δ_C/ppm 205.2 (**C**=O), 192.0 (**Cq**=CH), 143.6 (**Cq**-Ar), 143.5 (**Cq**-Ar), 142.3 (**Cq**-Ar), 128.5 (2C, **C**H-Ar), 128.3 (**C**H-Ar), 128.3 (**C**H-Ar), 128.2 (**C**H-Ar), 128.1 (**C**H-Ar), 126.9 (**C**H-Ar), 125.9 (**C**H-Ar), 104.6 (Cq=**C**H), 74.2 (**C**H_2-O-Cq), 67.5 (**C**H_2-O-Si), 52.4 (**Cq-**Ph_2), 40.8 (**C**H_2-C=O), 40.5 (**C**H-CH_2-CH_2), 35.8 (**C**H_2-Ph), 32.2 (CH-**C**H_2-CH_2), 31.5 (Ph-CH_2-**C**H_2), 26.5 (CH-CH_2-**C**H_2), 18.0 (Si(**C**H$(CH_3)_2)_3$), 12.1 (Si(CH(**C**$H_3)_2)_3$); **HRMS** (ESI) *m*/z calcd for $C_{39}H_{53}O_3Si$ $[M+H]^+$:597.37585, found: 597.37566; **IR (neat)** ν_{max}/cm^{-1} 2925, 2864, 1695, 1593, 1463, 1245, 1184, 1113, 882, 698; **$[\alpha]_D$ ^{25}** = -0.9 (c= 0.9 in $CHCl_3$).

*(R)-3-(2,2-diphenyl-3-((triisopropylsilyl)oxy)propoxy)-4-((R)-5-phenyl-3-((triisopropylsilyl)oxy)pentyl)cyclopent-2-en-1-one (**43b**)*

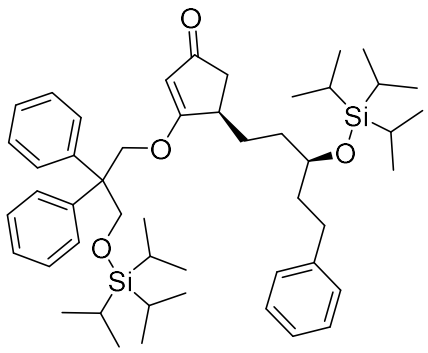

43b

DMAP (83 mg, 0.68 mmol, 2.0 eq) was added to a solution of (*R*)-3-(3-hydroxy-2,2-diphenylpropoxy)-4-((*R*)-5-phenyl-3-((triisopropylsilyl)oxy)pentyl)

cyclopent-2-en-1-one **41b** (210 mg, 0.34 mmol, 1.0 eq) in CH_2Cl_2 (2.0 mL) at room temperature in a flame-dried flask under argon atmosphere. After the solid had fully dissolved to obtain a clear solution, TIPSOTf (0.23 mL, 0.85 mmol, 2.5 eq) was added at 0 °C. After 1 h at 0 °C, the reaction mixture was stirred for 2.5 h at room temperature. The yellow solution was concentrated under reduced pressure, quenched with brine (5 mL) and washed with CH_2Cl_2 (3 x 3 mL). The combined organic layers were dried over $MgSO_4$, filtered and concentrated under reduced pressure to afford the crude product as a yellow oil. Purification by flash column chromatography (SiO_2, 20→30% Et_2O in pentane) yielded the title product **43b** (230 mg, 0.29 mmol, 86%, dr 73:27) as a yellow oil. **^{1}H NMR** (400 MHz, $CDCl_3$) δ_H/ppm 7.31-7.10 (m, 15H, Ar-**H**), 5.35 (s, 1H, C**H**=Cq), 4.69 (d, 1H, *J*=9.4 Hz, C**H**$_2$-O), 4.58 (d, 1H, *J*=9.4 Hz, C**H**$_2$-O), 4.38 (s, 2H, C**H**$_2$-OTIPS), 3.83-3.76 (m, 1H, C**H**-OTIPS), 2.71-2.62 (m, 1H, C**H**-CH_2-CH_2-CH-OTIPS), 2.60-2.50 (m, 3H, C**H**$_2$-Ph, C**H**$_2$-CO), 2.06 (dd, 1H, *J*=17.8, 2.3 Hz, C**H**$_2$-CO), 1.73-1.60 (m, 3H, C**H**$_2$-CH_2-Ph, CH-C**H**$_2$), 1.52-1.35 (m, 2H, CH-CH_2-CH_2-C**H**$_2$-CH-OTIPS), 1.25-1.15 (m, 1H, CH-C**H**$_2$-CH_2), 1.06-1.01 (s, 21H, ((C**H**(C**H**$_3$)$_2$)$_3$Si)), 0.96 (s, 12H, Si(C**H**(C**H**$_3$)$_2$)$_3$), 0.94 (s, 9H, Si(C**H**(C**H**$_3$)$_2$)$_3$); **^{13}C NMR** (100 MHz, $CDCl_3$) δ_C/ppm 204.8 (**C**=O), 191.8 (**C**q=CH), 143.6 (**C**q-Ar), 143.4 (**C**q-Ar), 142.6 (**C**q-Ar), 128.5 (**C**H-Ar), 128.4 (**C**H-Ar), 128.3 (2C, **C**H-Ar), 128.2 (**C**H-Ar), 128.1 (**C**H-Ar), 126.9 (**C**H-Ar), 125.9 (**C**H-Ar), 104.6 (**C**H=Cq), 74.2 (**C**H_2-O-Cq), 71.5 (**C**H_2-OTIPS), 67.5 (**C**H-OTIPS), 52.5 (**Cq-**Ph_2), 40.9 (**C**H_2-CO), 40.7 (**C**H-CH_2-CH_2-CH-OTIPS), 38.3 (**C**H_2-CH_2-Ph), 33.9 (CH_2-CH_2-**C**H_2-CH-OTIPS), 31.5 (**C**H_2-Ph), 27.5 (CH-**C**H_2-CH_2), 18.4 ((CH(**C**H_3)$_2$)$_3$Si), 18.0 ((CH(**C**H_3)$_2$)$_3$Si), 18.0 ((CH(**C**H_3)$_2$)$_3$Si), 12.8 ((**C**H$(CH_3)_2$)$_3$Si), 12.1 ((**C**H$(CH_3)_2$)$_3$Si); **HRMS** (ESI) *m*/z calcd for $C_{49}H_{75}O_4Si_2$

[M+H]$^+$:783.51984, found: 783.51978; **IR (neat)** ν_{max}/cm^{-1} 2942, 2865, 1698, 1594, 1463, 1110, 882, 698, 682; $\mathbf{[\alpha]_D^{25}}$ = +1.3 (c= 1.0 in $CHCl_3$).

The diastereomeric ratio of 73:27 was determined by ^{13}C NMR of the isolated diastereomeric mixture: 71.6 ppm (minor diastereomer) and 71.4 ppm (major diastereomer) [**C**H-OTIPS].

*(4R,5R)-5-allyl-3-(2,2-diphenyl-3-((triisopropylsilyl)oxy)propoxy)-4-(4-phenylbutyl)cyclopent-2-en-1-one (**44a**)*

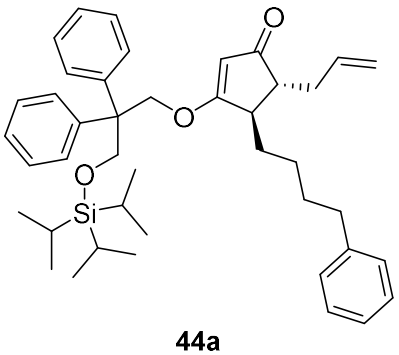

44a

Diisopropylamine (17 µL, 0.12 mmol, 1.2 eq) was dissolved in THF (0.66 mL) at –78 °C in a flame-dried flask under argon atmosphere. *n*BuLi (48 µL,

2.5 M in THF, 0.12 mmol, 1.2 eq) was added dropwise to the reaction mixture at –78 °C and stirred at that temperature for 15 min. (*R*)-3-(2,2-diphenyl-3-((triisopropylsilyl)oxy)propoxy)-4-(4-phenylbutyl)cyclopent-2-en-1-one **43a** (60 mg, 0.10 mmol, 1.0 eq) in THF (0.50 mL) was added dropwise at –78 °C. After stirring at that temperature for 30 min, allylbromide (17 µL, 0.20 mmol, 2.0 eq) was added. The reaction mixture was stirred for 3 h at –78 °C. The resulting yellow solution was quenched with NH_4Cl (sat, 2 mL) and washed with CH_2Cl_2 (3 x 1 mL). The combined organic layers were dried over $MgSO_4$, filtered and concentrated under reduced pressure to afford the crude product (dr 83:17). Purification by flash column chromatography (SiO_2, 0→20% Et_2O in pentane) yielded the title product **44a** as a single diastereomer (6.8 mg, 0.010 mmol, 11%) as a pale yellow oil. **^{1}H NMR** (400 MHz, $CDCl_3$) δ_H/ppm 7.36-7.11 (m, 15H, Ar-**H**), 5.79-5.61 (m, 1H, C**H**=CH_2), 5.34 (s, 1H, C**H**=Cq), 5.11-4.98 (m, 2H, CH=C**H$_2$**), 4.75 (d, 1H, *J*=9.2 Hz, C**H$_2$**-O), 4.56 (d, 1H, *J*=9.4 Hz, C**H$_2$**-O), 4.46-4.37 (m, 2H, C**H$_2$**-O), 2.58-2.39 (m, 4H, CH-C**H**$_2$-CH=CH_2, C**H**-CH_2-CH_2-CH_2-C**H$_2$**-Ph), 2.32-2.12 (m, 2H, C**H**-C**H**$_2$-CH=CH_2), 1.60-1.42 (m, 3H, CH-C**H**$_2$-CH_2-C**H$_2$**-CH_2-Ph), 1.35-1.26 (m, 1H, CH-C**H**$_2$-CH_2-CH_2-CH_2-Ph), 1.26-1.12 (m, 2H, CH-CH_2-C**H$_2$**-CH_2-CH_2-Ph), 1.12-1.03 (m, 3H, Si(C**H**$(CH_3)_2)_3$), 0.99 (d, *J*=6.8 Hz, 18H, Si(CH(C**H$_3$**$)_2)_3$); **^{13}C NMR** (100 MHz, $CDCl_3$) δ_C/ppm 206.6 (**C**=O), 191.1 (**Cq**=CH), 143.6 (**Cq**-Ar), 143.4 (**Cq**-Ar), 142.6 (**Cq**-Ar), 135.5 (**C**H=CH_2), 128.4 (**C**H-Ar), 128.4 (**C**H-Ar), 128.3 (**C**H-Ar), 128.3 (**C**H-Ar), 128.2 (**C**H-Ar), 128.0 (**C**H-Ar), 126.9 (**C**H-Ar), 125.9 (**C**H-Ar), 117.3 (CH=**C**H_2), 103.7 (Cq=**C**H), 74.0 (**C**H_2-O-Cq), 67.4 (**C**H_2-O-Si), 52.4 (**Cq-**Ph_2), 51.1 (**C**H-CH_2-CH=CH_2), 45.4 (**C**H-CH_2-CH_2-CH_2-CH_2-Ph), 35.9 (CH-**C**H_2-CH=CH_2), 35.8 (**C**H_2-Ph), 31.9 (CH-CH_2-CH_2-**C**H_2-CH_2-Ph), 31.6 (CH-**C**H_2-CH_2-CH_2-CH_2-Ph), 26.3 (CH-CH_2-**C**H_2-CH_2-CH_2-Ph), 18.1 (Si(CH(**C**$H_3)_2)_3$), 12.1 (Si(**C**$H(CH_3)_2)_3$);

HRMS (ESI) *m*/z calcd for $C_{42}H_{57}O_3Si$ $[M+H]^+$:637.40715, found: 637.40709; **IR (neat)** ν_{max}/cm^{-1} 2926, 2864, 1694, 1591, 1113, 698; $\mathbf{[\alpha]_D^{25}}$ = -0.4 (c= 1.0 in $CHCl_3$).

The diastereomeric ratio of 83:17 was determined by crude ^{13}C NMR: 208.5 ppm (major diastereomer) and 205.1 ppm (minor diastereomer)). [**C**=O]

A diastereomeric ratio of 97:3 was obtained after flash column chromatography.

*Cyclopent-2-en-1-ol (**76**)*

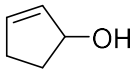

76

In analogy to a modified procedure by Nicolaou[166], $LiAlH_4$ (38 mL, 4.0 M in Et_2O, 150 mmol, 0.50 eq) was added to a solution of cyclopent-2-en-1-one (25.0 g, 304 mmol, 1.00 eq) in Et_2O (450 mL) at 0 °C in a flame-dried flask under argon atmosphere. After stirring 30 min at rt, the reaction mixture was quenched with ice (50 mL) and let to warm up at room temperature. The resulting yellow suspension was washed with HCl (1 M, 200 mL) and extracted with Et_2O (3 x 50 mL). The combined organic layers were washed with $NaHCO_3$ (sat., 50 mL) and then brine (sat., 50 mL), dried over $MgSO_4$, filtered and concentrated under reduced pressure (>400 mbar) to afford the product **76** (17.3 g, 205 mmol, 68%) as a 2.9 M solution in Et_2O. The crude product was used as such in the subsequent step. **^{1}H NMR** (400 MHz, $CDCl_3$) δ_H/ppm 6.02-5.93 (m, 1H, C**H**=CH-CH-OH), 5.87-5.79 (m, 1H, CH=C**H**-CH-OH), 4.86 (br. s, 1H, C**H**-OH), 2.58-2.42 (m, 1H, C**H**$_2$-CH=CH), 2.34-2.19 (m, 2H, OH-CH-C**H**$_2$-C**H**$_2$-CH=CH), 1.74-1.62 (m, 1H, OH-CH-C**H**$_2$), 1.48 (br. s, 1H, O**H**); **^{13}C NMR** (100 MHz, $CDCl_3$) δ_C/ppm 135.3 (**C**H=CH-CH-OH), 133.4 (CH=**C**H-CH-OH), 77.8 (**C**H-OH), 33.4 (OH-CH-**C**H$_2$-CH$_2$-CH=CH), 31.1 (OH-CH-CH$_2$-**C**H$_2$-CH=CH); **HRMS** (CI, Ammonia) *m*/z calcd for $C_5H_{12}ON$ $[M+NH_4]^+$: 102.0913, found: 102.0918; **IR (neat)** ν_{max}/cm^{-1} 3425 (br.), 2954, 2361, 1734, 1048, 773.

*3-chlorocyclopent-1-ene (**45a**)*

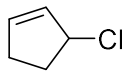

45a

Freshly distilled PCl_3 (2.2 mL, 25 mmol, 1.5 eq) was slowly added to a solution of crude cyclopent-2-en-1-ol **76** (5.8 g, 2.9 M in Et_2O, 17 mmol, 1.0 eq) and pyridine (0.55 mL, 6.8 mmol, 0.40 eq) at 0 °C in a flame-dried flask under argon atmosphere rapidly turning black. The reaction mixture was stirred at 0 °C for 5 min. The non-viscous layer of the resulting solution was purified by Kugelrohr distillation (18 mbar, 40 °C) to afford the title product **45a** (1.3 g, 13 mmol, 72%) as a clear oil. (**Caution**: store the title product away from light at –78 °C and minimise time out of the freezer as it can rapidly polymerise to a black residue). **^{1}H NMR** (400 MHz, $CDCl_3$) δ_H/ppm 6.09-6.02 (m, 1H, CH_2-C**H**=CH), 5.94-5.87 (m, 1H, CH=C**H**-CH-Cl), 5.09-4.99 (m, 1H, C**H**-Cl), 2.71-2.55 (m, 1H, C**H**$_2$), 2.44-2.30 (m, 2H, C**H**$_2$), 2.25-2.12 (m, 1H, C**H**$_2$); **^{13}C NMR** (100 MHz, $CDCl_3$) δ_C/ppm 136.3 (CH_2-**C**H=CH), 132.3 (CH=**C**H-CH-Cl), 65.8 (**C**H-Cl), 34.7 (**C**H_2), 31.2 (**C**H_2). The spectral data was in accordance with literature[296-298].

*(((R)-1-((S)-cyclopent-2-en-1-yl)-5-phenylpentan-3-yl)oxy)triisopropylsilane (**46**)*

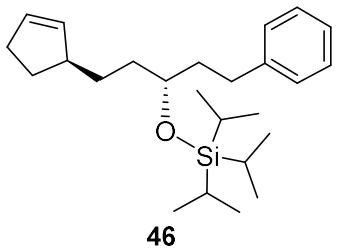

46

In a flame-dried flask under argon atmosphere, Cp_2ZrHCl (100 mg, 0.40 mmol, 2.0 eq) was added to a solution of (*S*)-triisopropyl((5-phenylpent-1-en-3-yl)oxy)silane **23c** (160 mg, 0.50 mmol 2.5 eq) in CH_2Cl_2 (0.3 mL) and vigorously stirred at 42 °C sealed until a clear yellow solution was obtained (ca 1 h). Simultaneously, in another flask under argon atmosphere, CuI (3.8 mg, 20 μmol, 10 mol%) and (*S, S, S*)-**A** (10.8 mg, 20.0 μmol, 10.0 mol%) were covered in $CHCl_3$ (0.4 mL) to obtain a cloudy white solution and stirred for 1 h at room temperature. The freshly prepared alkylzirconocene was added dropwise to the catalyst mixture species and cool to 0 °C after 10 min at room temperature. After 10 min at 0 °C, 3-chlorocyclopent-1-ene (41 μL, 0.40 mmol, 1.0 eq) was added to the yellow mixture and stirred overnight at room temperature. The reaction mixture was diluted with pentane (2 mL) and quenched with NH_4Cl (3 mL, 1 M). The mixture was partitioned and the aqueous phase was extracted with pentane (3 x 10 mL). The combined organic extracts were washed with $NaHCO_3$ (aq. sat. 10 mL), dried over $MgSO_4$, filtered and concentrated under reduced pressure (NMR yield: 59%, dr 91:9). Purification by flash column chromatography (SiO_2, 100% pentane) yielded the title product **46** (17 mg, 40 μmol, 22% isolated yield) as a yellow oil. **Note:** Many fractions were lost to obtain the product pure due to

co-spotting with alkene and alkane. **^{1}H NMR** (500 MHz, $CDCl_3$) δ_H/ppm 7.23-7.16 (m, 2H, Ar-**H**), 7.14-7.07 (m, 3H, Ar-**H**), 5.68-5.63 (m, 1H, C**H**=CH), 5.63-5.58 (m, 1H, C**H**=CH), 3.81 (tt, *J*= 11.1, 5.5 Hz, 1H, C**H**-OTIPS), 2.63-2.50 (m, 3H, C**H**-C**H$_2$**-CH_2-CH-OTIPS), 2.32-2.14 (m, 2H, C**H$_2$**-CH=CH), 2.02-1.93 (m, 1H, CH-C**H**$_2$-CH_2-CH=CH), 1.82-1.64 (m, 2H, CH-CH_2-C**H$_2$**-CH-OTIPS), 1.57-1.48 (m, 2H, OTIPS-CH-C**H$_2$**-C**H$_2$**-Ph), 1.44-1.16 (m, 3H, OTIPS-CH-C**H$_2$**-C**H$_2$**-Ph, CH-C**H**$_2$-CH_2-CH=CH), 1.00 (s, 21H, TIPS); **^{13}C NMR** (125 MHz, $CDCl_3$) δ_C/ppm 143.0 (**Cq**-Ar), 135.3 (**C**H=CH), 130.5 (**C**H=CH), 128.5 (Ar-**C**H), 128.5 (Ar-**C**H), 125.8 (Ar-**C**H), 72.3 (**C**H-OTIPS), 45.9 (CH=CH-**C**H-CH_2), 38.6 (CH-CH_2-**C**H_2-CH-OTIPS), 34.9 (TIPSO-CH-**C**H_2-CH_2-Ph), 32.2 (CH-**C**H_2-CH_2-CH-OTIPS), 31.4 (**C**H_2-CH=CH, C**H$_2$**-Ph), 30.0 (CH-**C**H_2-CH_2-CH=CH), 18.4 (($CH(\mathbf{C}H_3)_2)_3Si$), 18.4 (($CH(\mathbf{C}H_3)_2)_3Si$), 12.9 (($\mathbf{C}H(CH_3)_2)_3Si$); **HRMS** (CI, methane) *m*/z calcd for $C_{25}H_{42}OSi$ $[M+H]^+$:387.3078, found:387.3064; **IR (neat)** ν_{max}/cm^{-1} 2941, 2965, 1456, 1095, 1060, 882, 719, 697, 676; **$[\alpha]_D^{25}$** = -40.2 (c=1.0 in $CHCl_3$).

Protection from (R)-1-((S)-cyclopent-2-en-1-yl)-5-phenylpentan-3-ol (50)

DMAP (1.1 g, 9.3 mmol, 2.5 eq) was added to a solution of (*R*)-1-((*S*)-cyclopent-2-en-1-yl)-5-phenylpentan-3-ol **50** (860 mg, 3.7 mmol, 1.0 eq) in CH_2Cl_2 (15 mL) at room temperature in a flame-dried flask under argon atmosphere. After the solid had fully dissolved to obtain a clear pale yellow solution, TIPSOTf (2.3 mL, 7.4 mmol, 2.0 eq) was added. The reaction mixture was stirred overnight at room temperature. The yellow solution was concentrated under reduced pressure, quenched with H_2O (10 mL) and washed with $CHCl_3$ (3 x 10 mL). The combined organic layers were washed with brine (sat., 30 mL), dried over $MgSO_4$, filtered and concentrated under reduced

pressure to afford the crude product as a yellow oil. Purification by flash column chromatography (SiO_2, 0→2% Et_2O in pentane) yielded the title product **46** (1.0 g, 2.6 mmol, 71%, 86:14 dr) as a colourless oil.

The diastereomeric ratio of 91:9 was determined by ^{13}C NMR of the crude mixture: 34.9 ppm (major diastereomer) and 34.8 ppm (minor diastereomer).

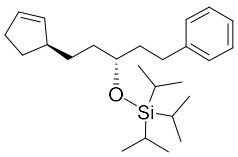

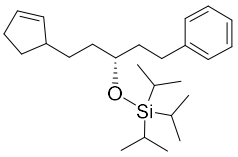

*(R)-1-((S)-cyclopent-2-en-1-yl)-5-phenylpentan-3-ol (**50**)*

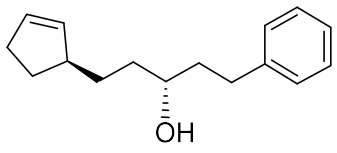

50

In a flame-dried flask under argon atmosphere, Cp_2ZrHCl (520 mg, 2.0 mmol, 2.0 eq) was added to a solution of (*S*)-triisopropyl((5-phenylpent-1-en-3-yl)oxy)silane **23c** (770 mg, 2.5 mmol 2.5 eq) in CH_2Cl_2 (1.5 mL) and vigorously stirred at 42 °C sealed until a clear yellow solution was obtained (ca 35 min). Simultaneously, in another flask under argon atmosphere, CuI (19.0 mg, 0.10 mmol, 10 mol%) and (*S, S, S*)-**A** (54 mg, 0.10 mmol, 10 mol%) were covered in $CHCl_3$ (1.0 mL) to obtain a cloudy white solution and stirred for 1 h at room temperature. The freshly prepared alkylzirconocene was added dropwise to the catalyst mixture species and then after10 min cooled at 0 °C. After 10 min at 0 °C, 3-chlorocyclopent-1-ene (126 mg, 1.00 mmol, 1.00 eq) was added to the yellow mixture and stirred overnight at 0°C to room temperature. The reaction mixture was diluted with pentane (10 mL) and quenched with NH_4Cl (10 mL, 1 M). The mixture was partitioned and the aqueous phase was extracted with pentane (3 x 10 mL). The combined organic extracts were washed with $NaHCO_3$ (aq. sat. 20 mL), dried over $MgSO_4$, filtered and concentrated under reduced pressure to obtain (*R*)-3-(5-phenyl-3-((triisopropylsilyl)oxy)pentyl)cyclopent-2-en-1-one **46** as a crude mixture.

The crude of (*R*)-3-(5-phenyl-3-((triisopropylsilyl)oxy)pentyl)cyclopent-2-en-1-one **46** was dissolved in THF (5.0 mL). TBAF (3.5 mL, 1 M in THF, 0.7 mmol,

3.5 eq) was added dropwise turning the reaction red/black. The reaction mixture was stirred for 2 h at room temperature and another portion of TBAF (3.5 mL, 1 M in THF, 0.7 mmol, 3.5 eq) was added. The reaction mixture was stirred for a further 2 h then diluted in Et_2O (10 mL) and quenched with brine (10 mL, sat). The mixture was partitioned and the aqueous phase was extracted with Et_2O (3 x 10 mL). The combined organic extracts were washed with brine (aq. sat. 30 mL), dried over $MgSO_4$, filtered and concentrated under reduced pressure. Purification by flash column chromatography (SiO_2, 0→5% EtOAc in cyclohexane) yielded the title product **50** (143 mg, 0.620 mmol, 62%, 99:1 dr) as a yellow oil. **^{1}H NMR** (400 MHz, $CDCl_3$) δ_H/ppm 7.34-7.28 (m, 2H, Ar-**H**), 7.26-7.19 (m, 3H, Ar-**H**), 5.77-5.73 (m, 1H, C**H**=CH), 5.71-5.67 (m, 1H, C**H**=CH), 3.70-3.61 (br. m, 1H, C**H**-OH), 2.87-2.78 (m, 1H, CH-C**H**$_2$-CH$_2$-CH-OH), 2.75-2.62 (m, 2H, C**H**-C**H**$_2$-CH$_2$-CH-OH), 2.41-2.24 (m, 2H, C**H$_2$**-CH=CH), 2.11-2.02 (m, 1H, CH-C**H**$_2$-CH$_2$-CH=CH), 1.88-1.72 (m, 2H, CH-CH$_2$-C**H$_2$**-CH-OH), 1.62-1.39 (m, 5H, OH-CH-C**H$_2$**-C**H$_2$**-Ph, CH-C**H**$_2$-CH$_2$-CH=CH), 1.39-1.35 (br. m, 1H, O**H**); **^{13}C NMR** (100 MHz, $CDCl_3$) δ_C/ppm 142.2 (**Cq**-Ar), 134.9 (**C**H=CH), 130.5 (**C**H=CH), 128.4 (Ar-**C**H x2), 125.8 (Ar-**C**H), 71.5 (**C**H-OH), 45.5 (CH=CH-**C**H-CH$_2$), 39.1 (CH-CH$_2$-**C**H$_2$-CH-OH), 35.8 (OH-CH-**C**H$_2$-CH$_2$-Ph), 32.1 (CH-**C**H$_2$-CH$_2$-CH-OH), 32.0 (**C**H$_2$-CH=CH), 31.9 (C**H$_2$**-Ph), 29.7 (CH-**C**H$_2$-CH$_2$-CH=CH); **HRMS** (ESI) *m*/z calcd for $C_{16}H_{23}O$ $[M+H]^+$:231.17434, found:231.17443; **IR (neat)** ν_{max}/cm^{-1} 3345 (br.), 2929, 2851, 1496, 1454, 1031, 912, 718, 698; **$[\alpha]_D^{25}$** = -74.2 (c=1.0 in $CHCl_3$).

The diastereomeric ratio of 99:1 was determined by ^{1}H NMR of the isolated diastereomeric mixture: 5.91 ppm (minor diastereomer) and 5.75 ppm (major diastereomer).

*(R)-3-(5-phenyl-3-((triisopropylsilyl)oxy)pentyl)cyclopent-2-en-1-one (**51**)*

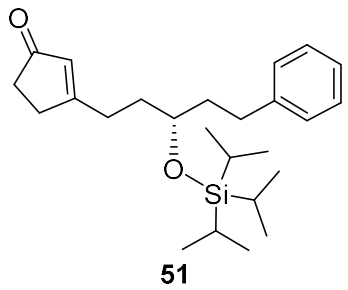

51

According to a modified procedure by Nicolaou[166], (*R*)-3-(5-phenyl-3-((triisopropylsilyl)oxy)pentyl)cyclopent-2-en-1-one **46** (250 mg, 0.50 mmol, 1.0 eq) was dissolved in CH_2Cl_2 at room temperature in a flame-dried flask under argon atmosphere. K_2CO_3 (35 mg, 0.25 mmol, 0.50 eq) and $Rh_2(cap)_4$ (1.6 mg, 2.5 μmol, 5.0 mol%) were added sequentially at room temperature to give a purple solution. *t*BuOOH (0.46 mL, 5.5 M in decane, 2.5 mmol, 5.0 eq) was added

slowly to give a dark purple solution. After 1 h, another portion of $Rh_2(cap)_4$ (1.6 mg, 2.5 μmol, 5.0 mol%) and *t*BuOOH (0.46 mL, 5.5 M in decane, 2.5 mmol, 5.0 eq) were added. Stirring was continued for 1.5 h then the mixture was filtered through a plug of SiO_2, washed with Et_2O and concentrated under reduced pressure. Purification by flash column chromatography (SiO_2, 10→20% Et_2O in pentane) yielded the title product **51** (52 mg, 0.13 mmol, 26% yield) as a pale yellow oil. **^{1}H NMR** (400 MHz, $CDCl_3$) δ_H/ppm 7.34-7.26 (m, 2H, Ar-**H**), 7.25-7.17 (m, 3H, Ar-**H**), 5.98 (s, 1H, Cq=C**H**), 4.00 (tt, *J*= 11.0, 5.5 Hz, 1H, C**H**-OTIPS), 2.73-2.65 (m, 2H, C**H$_2$**-Ph), 2.64-2.59 (m, 2H, C**H$_2$**-C=O), 2.55-2.48 (m, 2H, C**H$_2$**-Cq=CH), 2.46-2.41 (m, 2H, C**H$_2$**-CH_2-C=O), 1.94-1.78 (m, 4H, C**H$_2$**-CH_2-Ph, C**H$_2$**-CH-OTIPS), 1.10 (s, 21H, TIPS); **^{13}C NMR** (100 MHz, $CDCl_3$) δ_C/ppm 210.1 (**C**=O), 183.1 (**Cq**=CH), 142.2 (**Cq**-Ar), 129.5 (**C**H=Cq), 128.6 (Ar-**C**H), 128.4 (Ar-**C**H), 126.0 (Ar-**C**H), 71.3 (**C**H-OTIPS), 38.4 (**C**H_2-CH-OTIPS), 35.4 (**C**H_2-CH_2-C=O), 33.8 (**C**H_2-CH-OTIPS), 31.8 (**C**H_2-C=O), 31.6 (**C**H_2-Ph), 28.7 (**C**H_2-Cq=CH), 18.3 ((CH(**C**H_3)$_2$)$_3$Si), 12.8 ((**C**H(CH$_3$)$_2$)$_3$Si); **HRMS** (ESI) *m*/z calcd for $C_{25}H_{41}O_2Si$ $[M+Na]^+$: 401.28703, found: 401.28705; **IR (neat)** ν_{max}/cm^{-1} 2942, 2866, 1709, 1676, 1617, 1456, 1098, 1064, 883, 699, 679; **$[\alpha]_D^{25}$** = +5.8 (c=1.0 in $CHCl_3$).

*3-hexylcyclopent-2-en-1-one (**77**)*

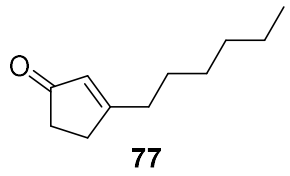

77

In analogy to a published procedure by Baran[181], MnO_2 (1.4 g, 16 mmol, 50 eq) and Sodium bis(2-hydroxy-2-methylbutyrato)oxochromate(V) (530 mg, 1.6 mmol, 5.0 eq) were added to a flame-dried flask under argon atmosphere. The flask was purged (3 x vacuum/Argon cycles) and then α,α,α-trifluorotoluene (21.1 mL), *(R)*-3-hexylcyclopent-1-ene (50.0 mg, 0.330 mmol, 1.00 eq) and 15-crown-5 (0.44 mL, 2.2 mmol, 6.8 eq) were added. After stirring 35 h at room temperature, the reaction was heated up to 55 °C overnight, then 80 °C for 12 h then 105 °C for 12 h. Despite not reaching completion, the mixture was filtered through a plug of Celite® and SiO_2, washed with Et_2O and concentrated under reduced pressure. Purification by flash column chromatography (SiO_2, 20% Et_2O in pentane) yielded the title product **77** (22 mg, 0.13 mmol, 40% yield) as a colourless oil. **^{1}H NMR** (400 MHz, $CDCl_3$) δ_H/ppm 5.93 (s, 1H, Cq=C**H**), 2.60-2.52 (m, 2H, C**H$_2$**), 2.44-2.34 (m, 4H, C**H$_2$**), 1.62-1.51 (m, 2H, C**H$_2$**), 1.39-1.22 (m, 6H, C**H$_2$**), 0.87 (t, *J*=6.8 Hz, 3H, C**H$_3$**); **^{13}C NMR** (100 MHz, $CDCl_3$) δ_C/ppm 210.4 (**C**=O), 183.5 (**Cq**=CH), 129.6 (Cq=**C**H), 35.4 (**C**H_2), 33.7 (**C**H_2), 31.7 (**C**H_2), 31.6 (**C**H_2), 29.1 (**C**H_2), 27.2 (**C**H_2), 22.7 (**C**H_2), 14.2 (**C**H_3); **HRMS** (ESI) *m*/z calcd for $C_{11}H_{19}O$ $[M+H]^+$: 167.14304, found: 167.14306; **IR (neat)** ν_{max}/cm^{-1} 2956, 2927, 2858, 1707, 1675, 1615, 1235, 841, 731.

VII. EXPERIMENTALS CHAPTER 5

a) Starting material

*3-chlorocyclohexene (**45b**)*

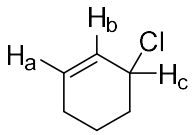

45b

Prepared in analogy to a published procedure[299], phosphorus trichloride (0.92 mL, 11 mmol, 0.37 eq) was added dropwise at 0 °C to a solution of cyclohex-2-en-1-ol (2.8 mL, 28.5 mmol, 1.0 eq) and pyridine (0.23 mL, 2.9 mmol, 0.10 eq). After vigorously stirring at 0 °C for 15 min, the solution was allowed to warm up to room temperature and stirred overnight. The resulting mixture was concentrated under reduced pressure and purified by Kulgelrohr distillation (60 mbar, 110 °C) to afford the title product **45b** (3.5 g, 30 mmol, 79% yield) as a colourless oil. **^{1}H NMR** (500 MHz, $CDCl_3$): δ_H/ppm 5.94-5.85 (m, 1H, H*a*), 5.85-5.79 (m, 1H, H*b*), 4.62 (br dd, *J*=11.5, 4.3 Hz, 1H, H*c*), 2.18 -2.08 (m, 1H, C**H**$_2$), 2.08-2.01 (m, 3H, C**H**$_2$), 1.96-1.83 (m, 1H, C**H**$_2$), 1.71-1.61 (m, 1H, C**H**$_2$); **^{13}C NMR** (125 MHz, $CDCl_3$) δ_C/ppm 131.3 (**C**H=CH-CH), 128.1 (CH=**C**H-CH), 55.5 (C**H**-Cl), 32.4 (**C**H$_2$), 24.7 (**C**H$_2$), 18.4 (**C**H$_2$); **HRMS** (EI/FI) *m/z* calcd for C_6H_9Cl $[M]^+$: 116.0393; found: 116.0390. Spectral data were in agreement with literature[299].

b) General Methods

Procedure used in the synthesis of racemic products

In a flame dried flask, Cp_2ZrHCl (210 mg, 0.80 mmol, 2.0 eq) was added to a stirred solution of alkene (1.0 mmol, 2.5 eq) in CH_2Cl_2 (2.0 mL) under an argon atmosphere at room temperature and stirred until a clear yellow solution was obtained (15-60 min). CuBr·DMS (82 mg, 0.40 mmol 1.0 eq), was added to the hydrozirconation solution and the resulting black mixture was allowed to stir for an additional 10 min before a cyclic allylchloride **45** (0.40 mmol, 1.0 eq) was added via microsyringe. Stirring at room temperature was continued arbitrarily overnight before the reaction was diluted and quenched by addition of Et_2O (3 mL) and then NH_4Cl (1 M aq., 2 mL). The mixture was partitioned and the aqueous phase extracted with Et_2O (3 × 10 mL). The combined organic phase was washed with $NaHCO_3$ (aq. sat. ca 10 mL), dried ($MgSO_4$), filtered and concentrated under reduced pressure to give the crude product. Flash column chromatography of the residue (SiO_2; Et_2O/pentane) gave the desired cyclic allylic product. In most cases, Kugelrohr distillation was used to remove excess starting alkene.

Procedure used in the synthesis of asymmetric products

In a flame dried flask, CuI (7.7 mg, 40 μmol, 10 mol%) and the ligand **A** (21.2 mg, 40.0 μmol, 10.0 mol%) were dissolved in $CHCl_3$ (0.8 mL) under an argon atmosphere and allowed to stir for 1 h at room temperature. In another flask, Cp_2ZrHCl (210 mg, 0.80 mmol, 2.0 eq) was added to a stirred solution of corresponding alkene (1.0 mmol, 2.5 eq) in CH_2Cl_2 (0.40 mL) under an argon

atmosphere until the solution was clear (20-60 min). The hydrozirconation solution was transferred to the Cu-**A** complex. The resulting dark mixture was allowed to stir for an additional 10 min before cyclic allylchloride **45** (0.40 mmol, 1.0 eq) was added dropwise *via* microsyringe and the reaction was stirred overnight. The reaction mixture was diluted and quenched by addition of Et_2O (3 mL) and then NH_4Cl (1 M aq., ca 2 mL). The mixture was partitioned and the aqueous phase extracted with Et_2O (3 × 10 mL). The combined organic phase was washed with $NaHCO_3$ (aq. sat. ca 10 mL), dried ($MgSO_4$), filtered and concentrated under reduced pressure to give the crude product. Flash column chromatography of the residue (SiO_2; Et_2O/pentane) gave the desired cyclic allylic product. In most cases, Kugelrohr distillation was used to remove the excess of starting alkene.

Derivatisation to the corresponding epoxides for ee determination

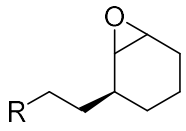

In a flame dried flask, the isolated product (1.0 eq) was dissolved in CH_2Cl_2 (0.07 M for 0.4 mmol scale). *m*-CPBA (2.0 eq) and Na_2HPO_4 (3.0 eq) were added and the reaction mixture was stirred for 2 h before being diluted in Et_2O (10 mL) and quenched by $Na_2S_2O_3$ (aq. sat., 10 mL). The organic layer was washed with NaOH (1 M aq., 3× 5mL), dried over mg_2SO_4, filtered and concentrated under reduced pressure. The crude mixture of diastereomeric epoxides was directly analysed by GC chromatography using a chiral stationary phase.

c) Scope and setup

*(R)-(+)-3-(6-Chlorohexyl)cyclohex-1-ene (**78**)*

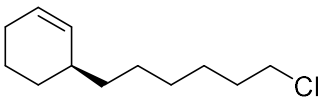

78

In a flame-dried flash under argon atmosphere, Cp_2ZrHCl (210 mg, 0.80 mmol, 2.0 eq) was added to a stirred solution of 6-chlorohex-1-ene (0.11 mL, 1.0 mmol, 2.5 eq), in CH_2Cl_2 (0.4 mL) and stirred until a clear yellow solution was obtained (20 min). Simultaneously, in a different flame-dried flash under argon atmosphere, CuI (7.6 mg, 40 μmol, 10 mol%) and (*S,S,S*)-**A** (21.6 mg, 40.0 μmol, 10.0 mol%) were dissolved in $CHCl_3$ (0.8 mL) and stirred for 1 h. The resulting catalyst complex mixture was then added to the freshly prepared alkenylzirconocene species. After 10 min, 3-chlorocyclohex-1-ene **45b** (46.6 mg, 0.400 mmol, 1.00 eq) was added to the resulting solution and stirred overnight. The reaction mixture was diluted in Et_2O (2 mL) and quenched in NH_4Cl (aq., 1 M). The mixture was partitioned, then the aqueous phase was extracted with Et_2O (3 x 10 mL). The combined organic extracts were washed with $NaHCO_3$ (aq., sat.), dried over $MgSO_4$, filtered and concentrated under reduced pressure. After flash column chromatography (SiO_2; 100% pentane), the title product **78** (66 mg, 0.34 mmol, 84%) was obtained as a colourless oil. **^{1}H NMR** (400 MHz, $CDCl_3$) δ_H/ppm 5.72-5.62 (m, 1H, C**H**=CH), 5.61-5.53 (m, 1H, C**H**=CH), 3.54 (t, *J*=6.8 Hz, 2H, C**H$_2$**-Cl), 2.09-2.00 (m, 1H, C**H**), 2.00-1.91 (m, 2H, C**H$_2$**), 1.83-1.74 (m, 3H,

C**H₂**), 1.73-1.66 (m, 1H, C**H₂**), 1.55-1.48 (m, 1H, C**H₂**), 1.48-1.39 (m, 2H, C**H₂**), 1.38-1.28 (m, 5H, C**H₂**), 1.28-1.15 (m, 2H, C**H₂**); **^{13}C NMR** (100 MHz, $CDCl_3$) δ_C/ppm 132.2 (**C**H=CH), 126.8 (**C**H=CH), 45.2 (**C**H_2-Cl), 36.3 (**C**H_2), 35.1 (**C**H), 32.6 (**C**H_2), 29.1 (**C**H_2), 29.1 (**C**H_2), 26.9 (**C**H_2), 26.8 (**C**H_2), 25.4 (**C**H_2), 21.5 (**C**H_2); **HRMS** (EI/FI) *m/z* calcd for $C_{12}H_{21}Cl$ $[M]^+$: 200.1335; found: 200.1332; **IR (neat)** νmax/cm^{-1} 2924, 2855, 1648, 1446, 1310, 885, 721, 698, 675, 653; **$[\alpha]_D^{25}$** = +14.9° (*c* 0.5 in $CHCl_3$, 91% ee).

The enantiomeric excess 91%, was determined by GC on a chiral stationary phase after derivatisation into the corresponding epoxides [Hydrodex 6-TBDM, 60-165 °C at 1 °C/min, 165 °C for 30 min, 10 psi] t_R = 1st diastereomer: 107.4 min, 2nd diastereomer: 113.8 min (major enantiomer), 116.2 min (minor enantiomer).

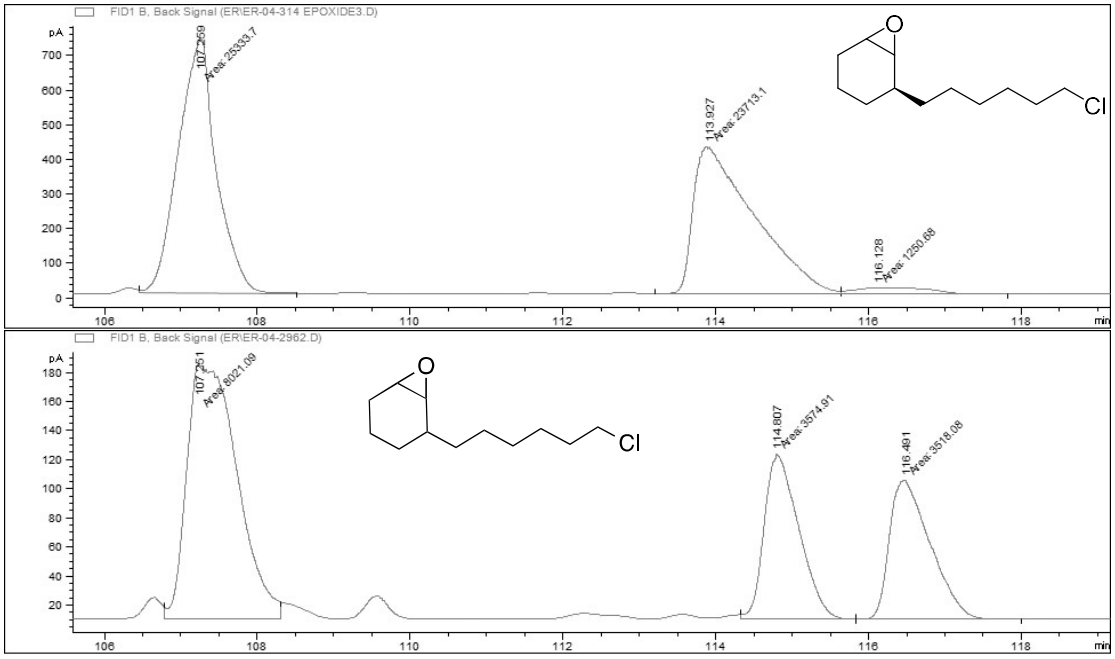

*(S)-(+)-4-(Cyclohex-2-en-1-yl)butan-1-ol (**79**)*

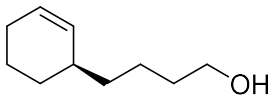

79

In a flame-dried flash under argon atmosphere, Cp_2ZrHCl (210 mg, 0.80 mmol, 2.0 eq) was added to a stirred solution of (but-3-en-1-yloxy)(tert-butyl)diphenylsilane (310 mg, 1.0 mmol, 2.5 eq) in CH_2Cl_2 (0.4 mL) and stirred until a clear yellow solution was obtained (20 min). Simultaneously, in a different flame-dried flash under argon atmosphere, CuI (7.7 mg, 40 μmol, 10 mol%) and (*S,S,S*)-**A** (21.6 mg, 40.0 μmol, 10.0 mol%) were dissolved in $CHCl_3$ (0.8 mL) and stirred for 1 h. The resulting catalyst complex mixture was then added to the freshly prepared alkenylzirconocene species. After 10 min, 3-chlorocyclohex-1-ene **45b** (48 μL, 0.40 mmol, 1.0 eq) was added to the resulting black solution and stirred for 12 h. The reaction mixture was diluted with Et_2O (2 mL) and NH_4Cl (aq., 1 M) was added. The mixture was partitioned, then the aqueous phase was extracted with Et_2O (3 x 10 mL). The combined organic extracts were washed with $NaHCO_3$ (aq., sat.), dried over $MgSO_4$, filtered and concentrated under reduced pressure. After flash column chromatography (SiO_2, 0-2% Et_2O in pentane), a mixture of (*S*)-tert-butyl(4-(cyclohex-2-en-1-yl) butoxy)diphenylsilane and (but-3-en-1-yloxy)(tert-butyl)diphenylsilane was obtained as a pale yellow oil. TBAF in THF (0.80 mL, 1 M, 0.80 mmol, 2.0 eq) was added dropwise the yellow oil dissolved in THF (3 mL) and stirred for 3h30. The reaction mixture was diluted with Et_2O (1 mL) and NaCl (aq., sat.) was added.

The mixture was partitioned, then the aqueous phase was extracted with Et_2O (3 x 3 mL). The combined organic extracts were dried over $MgSO_4$, filtered and concentrated under reduced pressure. After flash column chromatography (SiO_2; 30% Et_2O in hexane), the title product **79** (34 mg, 0.22 mmol, 55%) was obtained as a colourless oil. **^{1}H NMR** (400 MHz, $CDCl_3$) δ_H/ppm 5.71-5.64 (m, 1H, C**H**=CH), 5.58 (dd, *J*=9.8, 2.1 Hz, 1H, C**H**=CH), 3.66 (t, *J*=6.6 Hz, 2H, C**H$_2$**-OH), 2.11-2.01 (m, 1H, C**H**), 2.01-1.94 (m, 2H, C**H$_2$**), 1.84-1.67 (m, 2H, C**H$_2$**), 1.64-1.55 (m, 2H, C**H$_2$**), 1.55-1.45 (m, 1H, C**H$_2$**), 1.45-1.37 (m, 2H, C**H$_2$**), 1.37-1.28 (m, 1H, C**H$_2$**), 1.28-1.16 (m, 2H, C**H$_2$**); **^{13}C NMR** (100 MHz, $CDCl_3$) δ_C/ppm 132.0 (**C**H=CH), 126.9 (**C**H=CH), 63.0 (**C**H_2-OH), 36.1 (**C**H_2), 35.1 (**C**H), 33.0 (**C**H_2), 29.1 (**C**H_2), 25.4 (**C**H_2), 23.1 (**C**H_2), 21.5 (**C**H_2); **HRMS** (EI/FI) *m/z* calcd for $C_{10}H_{18}O$ $[M]^+$: 154.1358; found: 154.1354; **IR (neat)** νmax/cm^{-1} 3327, 3016, 2928, 2858, 1447, 1059, 720, 675; **$[\alpha]_D^{25}$** = +26.6° (*c* 1.0 in $CHCl_3$, 89% ee).

The enantiomeric excess of 89% ee, was determined by GC on a chiral stationary phase after derivatisation into the corresponding epoxides [Hydrodex 6-TBDM, 60-165 °C at 1 °C/min, 165 °C for 30 min, 10psi] t_R = 95.5, 104.6 min (major enantiomer), t_R = 94.8, 107.5 min (minor enantiomer).

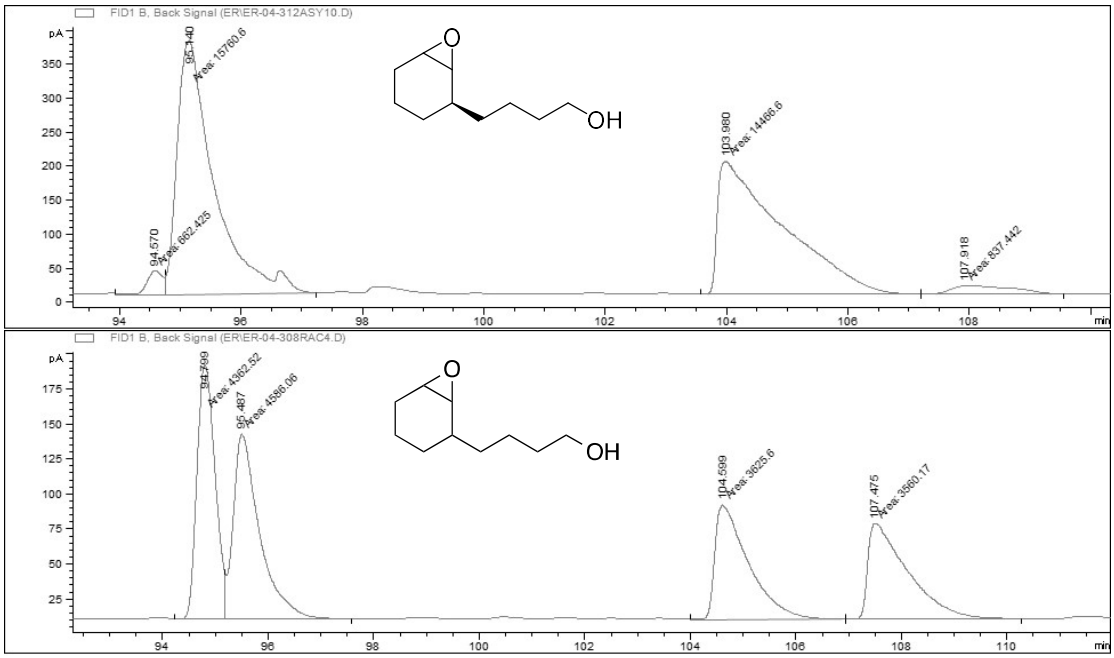

*Reaction using allylbromide **55***

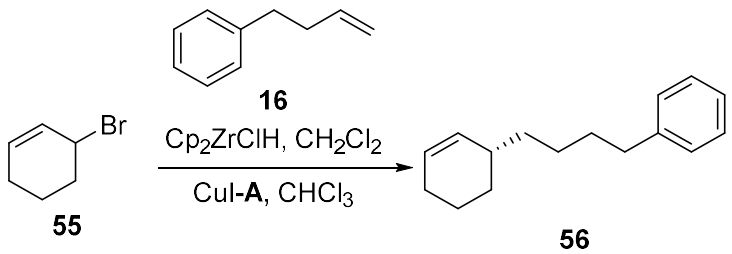

In a flame-dried flask under argon atmosphere, CuI (7.7 mg, 0.04 0mmol, 10 mol%) and (*R,R,R*)-**A** (21.6 mg, 40.0 μmol, 10 mol%) were dissolved in $CHCl_3$ (0.8 mL) and stirred for 1 h. Simultaneously, in another a flame-dried flask under argon atmosphere, Cp_2ZrHCl (210 mg, 0.80 mmol, 2.0 eq) was added to a

solution of 4-phenyl-1-butene **16** (0.15 mL, 1.0 mmol, 2.5 eq) in CH_2Cl_2 (0.2 mL) and stirred until a clear yellow solution was obtained (20 min). The resulting catalyst complex mixture was then added to the freshly prepared alkenylzirconocene species. The resulting yellow mixture was allowed to stir for an additional 10 min before 3-bromocyclohex-1-ene **55** (46 μL, 0.40 mmol, 1.0 eq) was added dropwise via a microsyringe and the reaction was allowed to continue stirring overnight. Afterwards, the reaction mixture was diluted and quenched by addition of pentane (3 mL) and then NH_4Cl (1 M aq., 3 mL). The mixture was partitioned and the aqueous phase extracted with pentane (3 × 10 mL). The combined organic phase was washed with $NaHCO_3$ (aq. sat. 10 mL), dried over $MgSO_4$, filtered and concentrated under reduced pressure to give the crude product. The product was purified by flash column chromatography (SiO_2; 100% pentane) to give product **56** (76 mg, 0.36 mmol, 89%, 77% ee) as a colourless oil. **^{1}H NMR** (400 MHz, $CDCl_3$) δ_H/ppm 7.36-7.27 (m, 2H, Ar-**H**), 7.25-7.18 (m, 3H, Ar-**H**), 5.72-5.65 (m, 1H, C**H**=CH), 5.64-5.57 (m, 1H, C**H**=CH), 2.65 (t, *J*= 7.7 Hz, 2H, C**H$_2$**), 2.13-2.03 (m, 1H, C**H**), 2.03-1.95 (m, 2H, C**H$_2$**), 1.84-1.17 (m, 10H, C**H$_2$**). **^{13}C NMR** (100 MHz, $CDCl_3$) δ_C/ppm: 143.0 (**Cq**-Ar), 132.4 (**C**H=CH), 128.5 (**C**H-Ar), 128.4 (**C**H-Ar), 126.9 (**C**H-CH), 125.7 (**C**H-Ar), 36.4 (**C**H_2), 36.1 (**C**H_2), 35.3 (**C**H), 31.9 (**C**H_2), 29.2 (**C**H_2), 26.8 (**C**H_2), 25.5 (**C**H_2), 21.7 (**C**H_2); **HRMS** (ESI) *m*/z calcd for $C_{16}H_{22}$ $[M]^+$: 214.1721, found: 214.1717; **IR (neat)** νmax/cm^{-1} 2926, 2855, 1739, 1454, 1366, 1229, 1217, 698; **$[\alpha]_D^{25}$** = +11.8 (c=0.4 in $CHCl_3$, 93% ee).

The enantiomeric excess of 77% was determined by HPLC [Chiralpak® IA; flow: 0.6 mL/min; hexane; λ = 210 nm; minor enantiomer t_R = 8.3 min; major enantiomer t_R = 8.8 min].

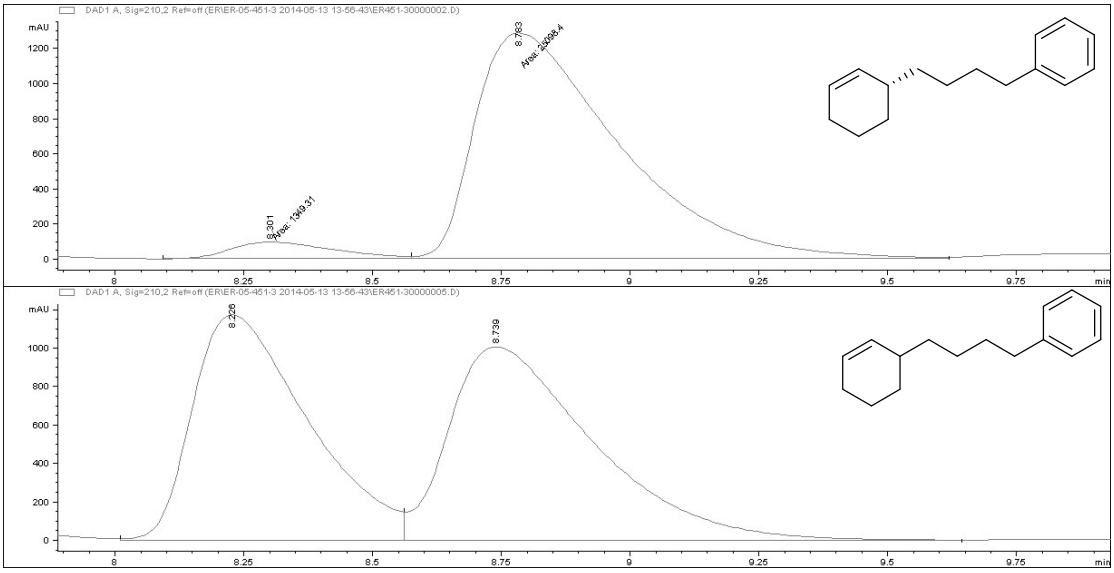

*Addition of allylchloride **45b** to the catalyst before the organozirconocene*

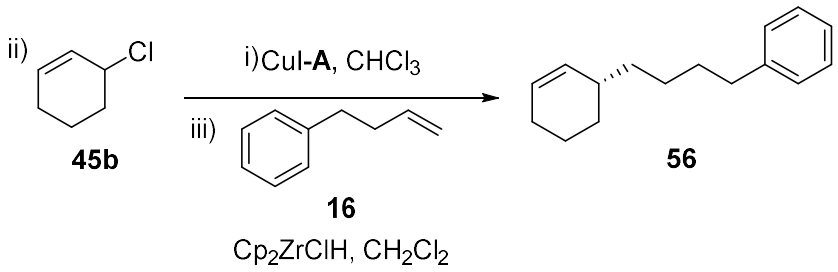

In a 5ml flame dried flask, CuI (7.7 mg, 40 μmol, 10 mol%) and (*R,R,R*)-**A** (21.6 mg, 40.0 μmol, 10.0 mol%) were dissolved in $CHCl_3$ (0.8 mL) under an argon atmosphere and allowed to stir for 1 h at room temperature. In another flask, Cp_2ZrHCl (210 mg, 0.80 mmol, 2.0 eq) was added to a stirred, room temperature, solution of 4-phenyl-1-butene **16** (0.15 mL, 1.0 mmol, 2.5 eq) in CH_2Cl_2 (0.20 mL) under an argon atmosphere. 3-Chlorocyclohex-1-ene **45b**

(47 mg, 0.40 mmol, 1.0 eq) was added dropwise via a microsyringe to the Cu-complex solution and was allowed to stir for an additional 10 min before the resulting clear hydrozirconation solution (stirred for 20 to 40 min) was transferred via syringe over about 1 min to the stirred Cu-complex and substrate solution. The reaction was arbitrarily allowed to continue stirring overnight. Afterwards, the reaction mixture was diluted and quenched by addition of Petrol (ca 3 mL) and then NH_4Cl (1 M aq., ca 1.5 mL). The mixture was partitioned between water and Petrol and the aqueous phase extracted with Petrol (3 × 10 mL). The combined organic phase was washed with $NaHCO_3$ (aq. sat. ca 10 mL), dried ($MgSO_4$), filtered and concentrated under reduced pressure to give the crude product. Flash column chromatography of the residue (SiO_2, 100% pentane) gave product **56** (75 mg, 0.35 mmol, 87%, 90% ee) as a colourless oil. **^{1}H NMR** (400 MHz, $CDCl_3$) δ_H/ppm 7.36-7.27 (m, 2H, Ar-**H**), 7.25-7.18 (m, 3H, Ar-**H**), 5.72-5.65 (m, 1H, C**H**=CH), 5.64-5.57 (m, 1H, C**H**=CH), 2.65 (t, *J*= 7.7 Hz, 2H, C**H$_2$**), 2.13-2.03 (m, 1H, C**H**), 2.03-1.95 (m, 2H, C**H$_2$**), 1.84-1.17 (m, 10H, C**H$_2$**). **^{13}C NMR** (100 MHz, $CDCl_3$) δ_C/ppm: 143.0 (**Cq**-Ar), 132.4 (**C**H=CH), 128.5 (**C**H-Ar), 128.4 (**C**H-Ar), 126.9 (**C**H-CH), 125.7 (**C**H-Ar), 36.4 (**C**H_2), 36.1 (**C**H_2), 35.3 (**C**H), 31.9 (**C**H_2), 29.2 (**C**H_2), 26.8 (**C**H_2), 25.5 (**C**H_2), 21.7 (**C**H_2); **HRMS** (ESI) *m*/z calcd for $C_{16}H_{22}$ $[M]^+$: 214.1721, found: 214.1717; **IR (neat)** νmax/cm^{-1} 2926, 2855, 1739, 1454, 1366, 1229, 1217, 698; **$[\alpha]_D^{25}$** = +11.8 (c=0.4 in $CHCl_3$, 93% ee).

The enantiomeric excess of 90% was determined by HPLC [Chiralpak® IA; flow: 0.6 mL/min; hexane; λ = 210 nm; minor enantiomer t_R = 8.3 min; major enantiomer t_R = 8.8 min].

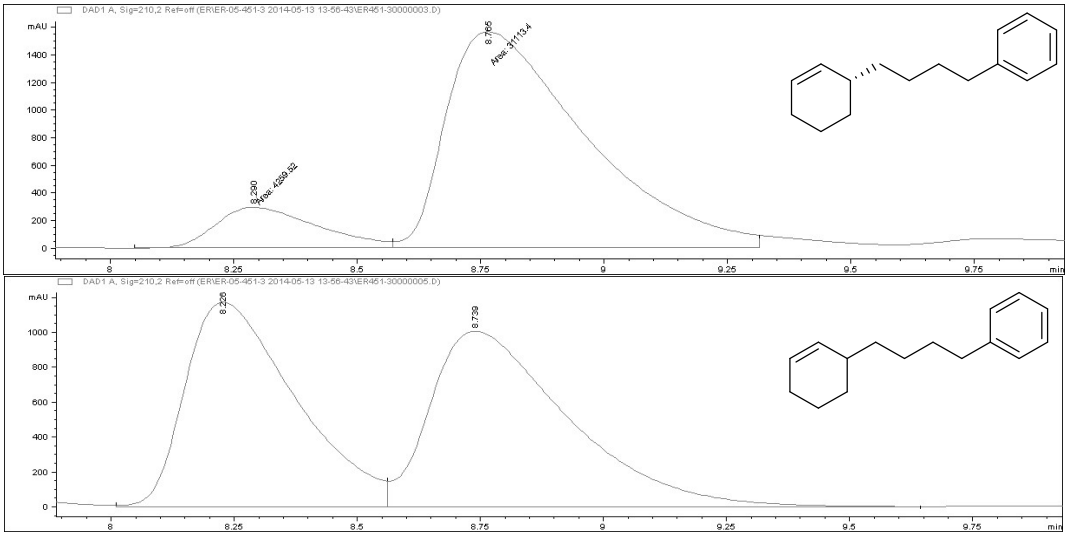

d) Mechanistic Studies

1) Characterisation

*3-chlorocyclohexene (**45b**)*

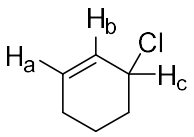

45b

^{1}H NMR (500 MHz, CD_2Cl_2) δ_H/ppm 5.91-5.84 (m, 1H, H*b*), 5.83–5.77 (m, 1H, H*a*), 4.63 (br dd, *J*= 11.5, 4.4 Hz, 1H, Hc), 2.17–1.95 (m, 4H, C**H**$_2$), 1.93–1. 18 (m, 1H,

C**H**$_2$), 1.70-1.60 (m, 1H, C**H**$_2$). **^{13}C NMR** (125 MHz, CD_2Cl_2) δ_C/ppm 131.7 (**C**H=CH), 128.4 (**C**H=CH), 56.1 (**C**H-Cl), 32.8 (**C**H$_2$), 25.0 (**C**H$_2$), 18.8 (**C**H$_2$).

Dynamics of 3-chlorocyclohex-1-ene ***45b***

Summary of EXSY Exchanges

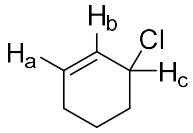

(none)

2D EXSY (gradient NOE t_{mix}= 800 ms)

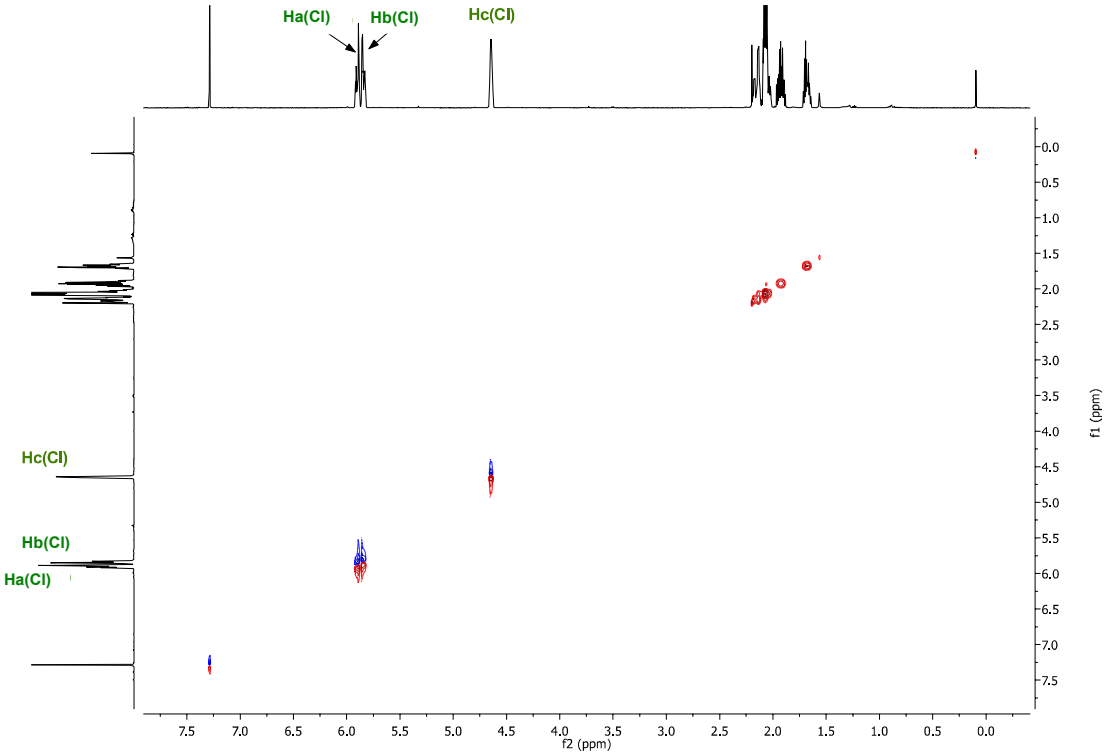

*3-Bromocyclohex-1-ene (**55**)*

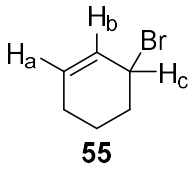

55

^{1}H NMR (400 MHz, $CDCl_3$) δ_H/ppm 5.94-5.87 (m, 1H, H*b*), 5.84-5.77 (m, 1H, H*a*), 4.83 (br dd, *J*= 11.5, 4.6 Hz, 1H, H*c*), 2.29-1.89 (m, 5H, C**H**$_2$), 1.73-1.63 (m, 1H, C**H**$_2$); **^{13}C NMR** (126 MHz, $CDCl_3$) δ_C/ppm 131.1 (CH=**C**H-CH), 128.9 (**C**H=CH-CH), 49.0 (**C**H-Br), 32.7 (**C**H$_2$), 24.7 (**C**H$_2$), 18.5 (**C**H$_2$).

Dynamics of 3-bromocyclohex-1-ene ***55***

Summary of EXSY Exchanges

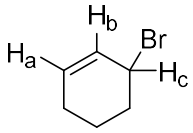

(none)

2D EXSY (gradient NOE t_{mix}=600 ms)

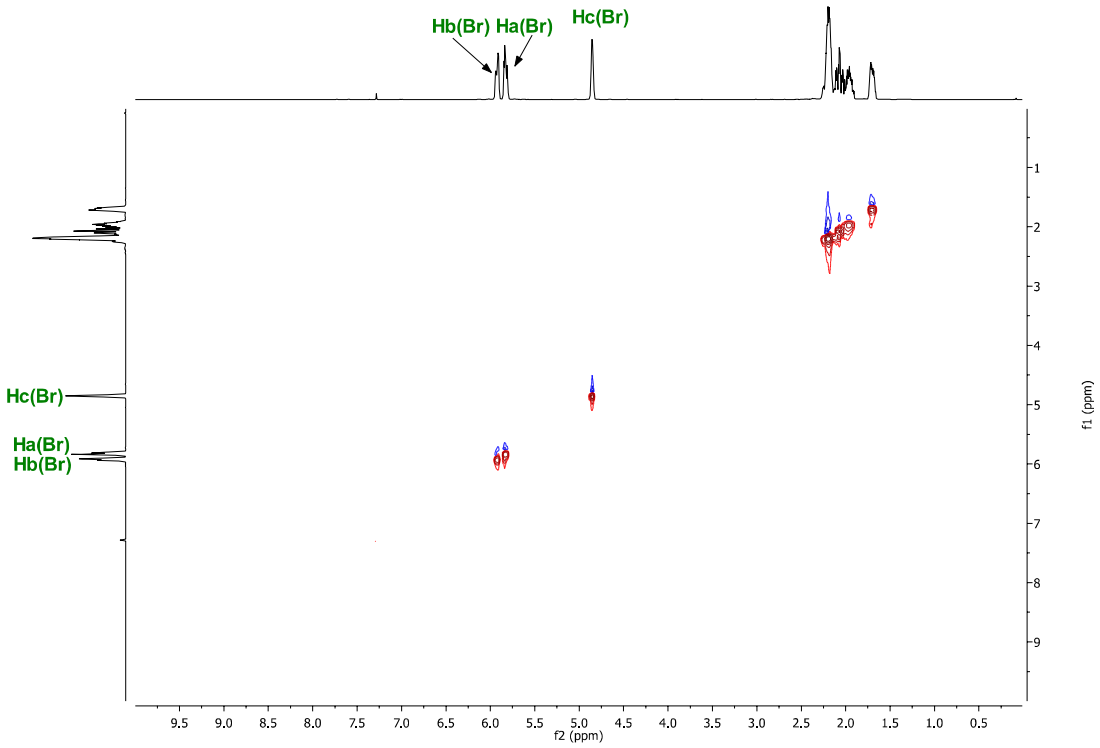

*(11bS)-N,N-bis((S)-1-phenylethyl)dinaphtho[2,1-d:1',2'-f][1,3,2]dioxaphosphepin-4-amine (**A**)*

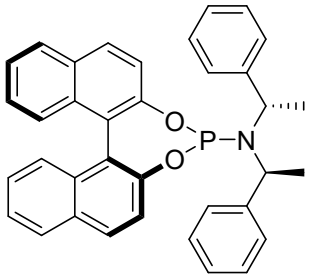

A

^{1}H NMR (500 MHz, $CDCl_3$) δ_H/ppm 8.03 (d, *J*= 8.7 Hz, 1H, Ar-**H**), 7.95 (d, *J*= 8.0, 1H, Ar-**H**), 7.84 (dd, *J*=8.7, 1.2 Hz, 1H, Ar-**H**), 7.76 (d, *J*= 8.8 Hz, 1H, Ar-**H**), 7.60 (d, *J*= 8.7 Hz, 1H, Ar-**H**), 7.44 (ddd, *J*= 8.1, 6.5, 1.3 Hz, 1H, Ar-**H**), 7.42–7.33 (m, 3H, Ar-**H**), 7.35–7.15 (m, 13H, Ar-**H**), 4.45 (dq, *J*= 10.8, 7.1 Hz, 2H, 2 x C**H**-N), 1.72 (d, *J*= 7.1 Hz, 6H, 2 x C**H$_3$**); **^{13}C NMR** (125 MHz, $CDCl_3$) δ_C/ppm 150.6 (**Cq**-Ar), 150.5 (**Cq**-Ar), 149.8 (**Cq**-Ar), 143.1 (**Cq**-Ar), 132.9 (**Cq**-Ar), 132.9 (**Cq**-Ar), 132.8 (**Cq**-Ar), 131.4 (**Cq**-Ar), 130.4 (**C**H-Ar), 130.4 (**Cq**-Ar), 129.6 (**C**H-Ar), 128.3 (**C**H-Ar), 128.1 (**C**H-Ar), 128.0 (**C**H-Ar), 128.0 (**C**H-Ar), 127.8 (**C**H-Ar), 127.2 (**C**H-Ar), 127.2 (**C**H-Ar), 126.7 (**C**H-Ar), 126.0 (**C**H-Ar), 125.8 (**C**H-Ar), 124.8 (**C**H-Ar), 124.3 (**C**H-Ar), 124.2 (**Cq**-Ar), 124.2 (**Cq**-Ar), 122.5 (**C**H-Ar), 122.4 (d, *J*=2.6 Hz, **C**H-Ar), 121.2 (d, *J*=2.8 Hz, **Cq**-Ar), 54.6 (**C**H-N), 54.5 (**C**H-N), 23.1 (**C**H_3), 23.0 (**C**H_3); **^{31}P NMR** (202 MHz, $CDCl_3$) δ_P/ppm 150.4 (s, 1P).

^{1}H NMR (500 MHz, CD_2Cl_2) δ_H/ppm 8.08 (d, *J*= 8.7 Hz, 1H, Ar-**H**), 8.00 (d, *J*= 8.3 Hz, 1H, Ar-**H**), 7.89 (d, *J*= 8.2 Hz, 1H, Ar-**H**), 7.83 (d, *J*= 8.8 Hz, 1H, Ar-**H**), 7.64 (d, *J*= 8.8 Hz, 1H, Ar-**H**), 7.52–7.39 (m, 3H, Ar-**H**), 7.37 (d, *J*= 8.4 Hz, 1H, Ar-**H**), 7.32–7.18 (m, 13H, Ar-**H**), 4.47 (dq, *J*= 10.9, 7.1 Hz, 2H, 2 x C**H**-N), 1.73 (d, *J*=

7.1 Hz, 6H, 2 x C**H**$_3$); **^{13}C NMR** (126 MHz, CD_2Cl_2) δ_C/ppm 150.9 (**Cq**-Ar), 150.8 (**Cq**-Ar), 150.2 (**Cq**-Ar), 143.5 (**Cq**-Ar), 133.2 (d, *J*=1.8 Hz, **Cq**-Ar), 133.2 (**Cq**-Ar), 131.8 (**Cq**-Ar), 130.9 (**C**H-Ar), 130.0 (**C**H-Ar), 128.8 (**C**H-Ar), 128.5 (**C**H-Ar), 128.4 (**C**H-Ar), 128.4 (**C**H-Ar), 128.1 (**C**H-Ar), 127.4 (**C**H-Ar), 127.3 (**C**H-Ar), 127.1 (**C**H-Ar), 126.5 (**C**H-Ar), 126.3 (**C**H-Ar), 125.2 (**C**H-Ar), 124.8 (**C**H-Ar), 124.5 (**Cq**-Ar), 124.4 (**Cq**-Ar), 122.9 (**C**H-Ar), 122.7 (d, *J*=2.1 Hz, **C**H-Ar), 121.4 (d, *J*=2.8 Hz, **Cq**-Ar), 54.9 (**C**H-N), 54.8 (**C**H-N), 25.2 (**C**H$_3$), 23.1 (**C**H$_3$); **^{31}P NMR** (202 MHz, CD_2Cl_2) δ_P/ppm 151.0 (s, 1P).

*Dynamics of ligand **A***

Summary of EXSY Exchanges

(none)

2D EXSY (gradient NOE t_{mix}= 800 ms)

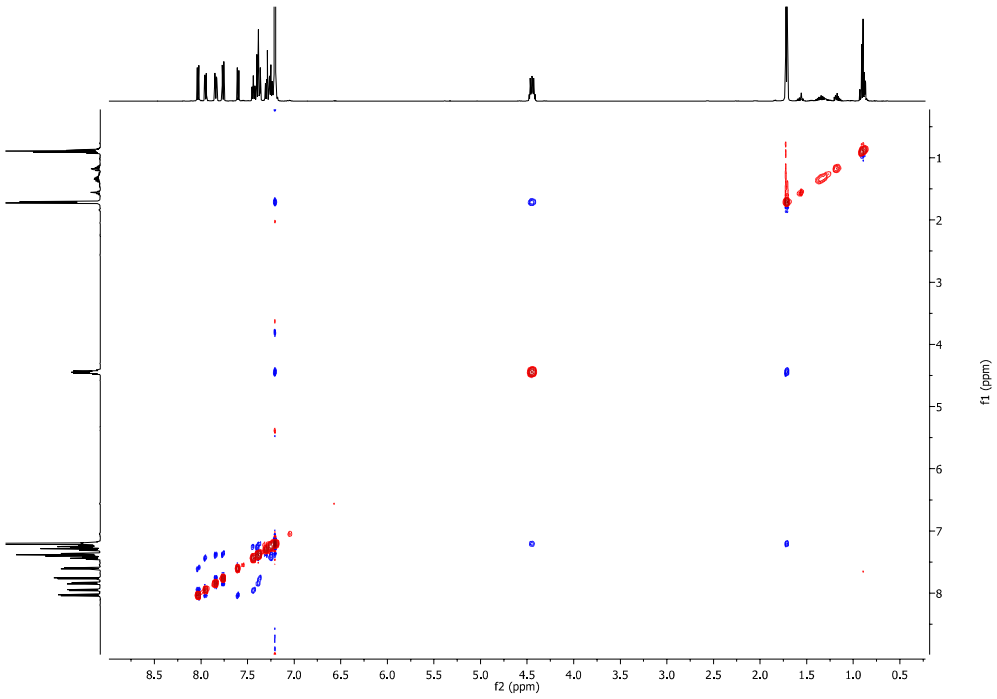

*CuI-Ligand **A** complex*

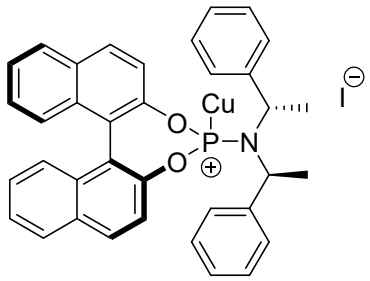

In a flame-dried flask, protected from light, under an argon atmosphere, CuI (7.7 mg, 0.040 μmol, 1.0 eq) and (*S, S, S*)-**A** (21.6 mg, 40.0 μmol, 1.00 eq) were dissolved in $CDCl_3$ (0.8 mL) and allowed to stir for 1 h at room temperature. Then the Cu-Complex solution was transferred to a flame-dried NMR tube under argon atmosphere equipped with a septa. **^{1}H NMR** (500 MHz, $CDCl_3$) δ_H/ppm 8.29-7.97 (br. m, 1H, Ar-**H**), 7.90 (d, *J*=7.8 Hz, 1H, Ar-**H**), 7.83 (d, *J*=8.4 Hz, 1H, Ar-**H**), 7.81-7.73 (br. m, 1H, Ar-**H**), 7.65 (br. s, 1H, Ar-**H**), 7.42 (t, *J*=7.4 Hz, 1H, Ar-**H**), 7.37-7.21 (m, 3H, Ar-**H**), 7.19-6.55 (br. m, 13H, Ar-**H**), 4.42 (br. s, 2H, C**H**-N), 1.16 (br, s, 6H, 2 x C**H$_3$**); **^{13}C NMR** (126 MHz, $CDCl_3$) δ_C/ppm 148.9 (br. s, **Cq**-Ar), 148.3 (br. s, **Cq**-Ar), 141.3 (br. s, **Cq**-Ar), 132.6 (**Cq**-Ar), 132.3, (**Cq**-Ar) 131.6 (**Cq**-Ar), 130.8 (**C**H-Ar), 129.8 (**C**H-Ar), 128.4 (**C**H-Ar), 128.2 (**C**H-Ar), 128.1 (**C**H-Ar), 127.5 (**C**H-Ar), 127.2 (**C**H-Ar), 126.7 (**C**H-Ar), 126.2 (**C**H-Ar), 125.9 (**C**H-Ar), 124.9 (**C**H-Ar), 123.5 (br. s, **Cq**-Ar), 122.0 (**Cq**-Ar), 54.9 (**C**H-N), 21.5 (br. S, **C**H_3); **^{31}P NMR** (202 MHz, $CDCl_3$) δ_P/ppm 151.5 (br. s), 129.5 (br. s, 1P).

*Dynamics of CuI-**A** complex*

Summary of EXSY Exchanges

A few in aromatic region

2D EXSY (gradient NOE t_{mix}= 800 ms)

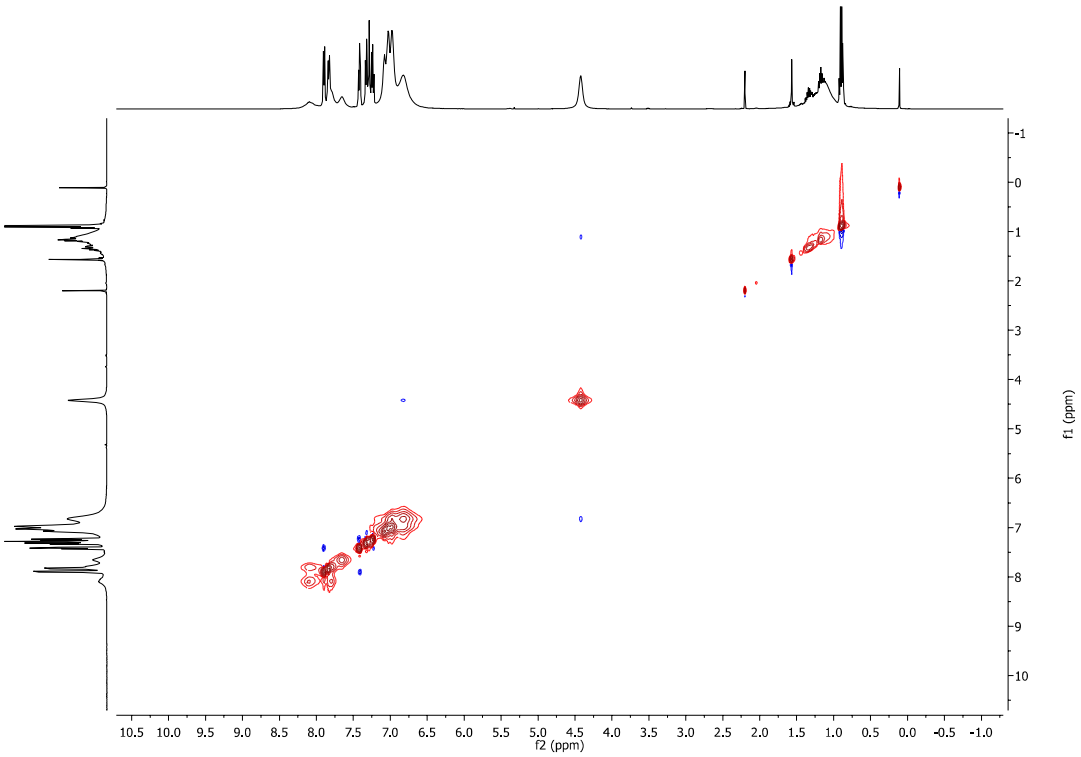

*CuCl-**A** complex*

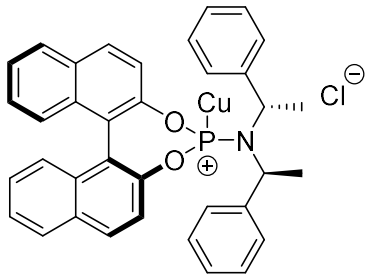

In a flame-dried flask, protected from light, under an argon atmosphere, CuCl (3.8 mg, 40 μmol, 10 mol%) and (*S, S, S*)-**A** (21.6 mg, 40.0 μmol, 1.00 eq) were dissolved in $CDCl_3$ (0.8 mL) and allowed to stir for 1 h at room temperature. Then the Cu-Complex solution was transferred to a flame-dried NMR tube under argon atmosphere equipped with a septa. **^{1}H NMR** (500 MHz, $CDCl_3$) δ_H/ppm 8.03 (d, *J*= 8.8 Hz, 1H, Ar-**H**), 7.93–7.85 (m, 3H, Ar-**H**), 7.76 (d, *J*= 8.8 Hz, 1H, Ar-**H**), 7.44 (t, *J*= 7.5 Hz, 1H, Ar-**H**), 7.39 (td, *J*= 8.0, 3.0 Hz, 2H, Ar-**H**), 7.28 (q, *J*= 7.7, 6.9 Hz, 2H, Ar-**H**), 7.24-7.16 (m, 6H, Ar-**H**), 7.16-7.09 (m, 6H, Ar-**H**), 4.65 (2 x q, *J*= 7.1 Hz, 2H, 2 x C**H**-N), 1.65 (br. s, 6H, 2 x C**H$_3$**); **^{13}C NMR** (126 MHz, $CDCl_3$) δ_C/ppm 149.0 (**Cq**-Ar), 148.9 (**Cq**-Ar), 148.1 (**Cq**-Ar), 141.1 (**Cq**-Ar), 132.6 (**Cq**-Ar), 132.5 (**Cq**-Ar), 131.9 (**Cq**-Ar), 131.0 (**C**H-Ar), 130.8 (**Cq**-Ar), 130.0 (**C**H-Ar), 128.5 (**C**H-Ar), 128.2 (**C**H-Ar), 128.1 (**C**H-Ar), 128.1 (**C**H-Ar), 127.4 (**C**H-Ar), 127.1 (**C**H-Ar), 126.3 (**C**H-Ar), 126.2 (**C**H-Ar), 125.2 (**C**H-Ar), 125.1 (**C**H-Ar), 123.3 (**Cq**-Ar), 122.8 (**C**H-Ar), 121.8 (**C**H-Ar), 121.5 (**Cq**-Ar), 54.3 (**C**H-N), 54.2 (**C**H-N), 21.7 (**C**H$_3$ x2); **^{31}P NMR** (202 MHz, $CDCl_3$) δ_P/ppm 126.2 (br. s, 1P).

*Dynamics of CuCl-**A** complex*

Summary of EXSY Exchanges

(none)

2D EXSY (gradient NOE t_{mix}= 800 ms)

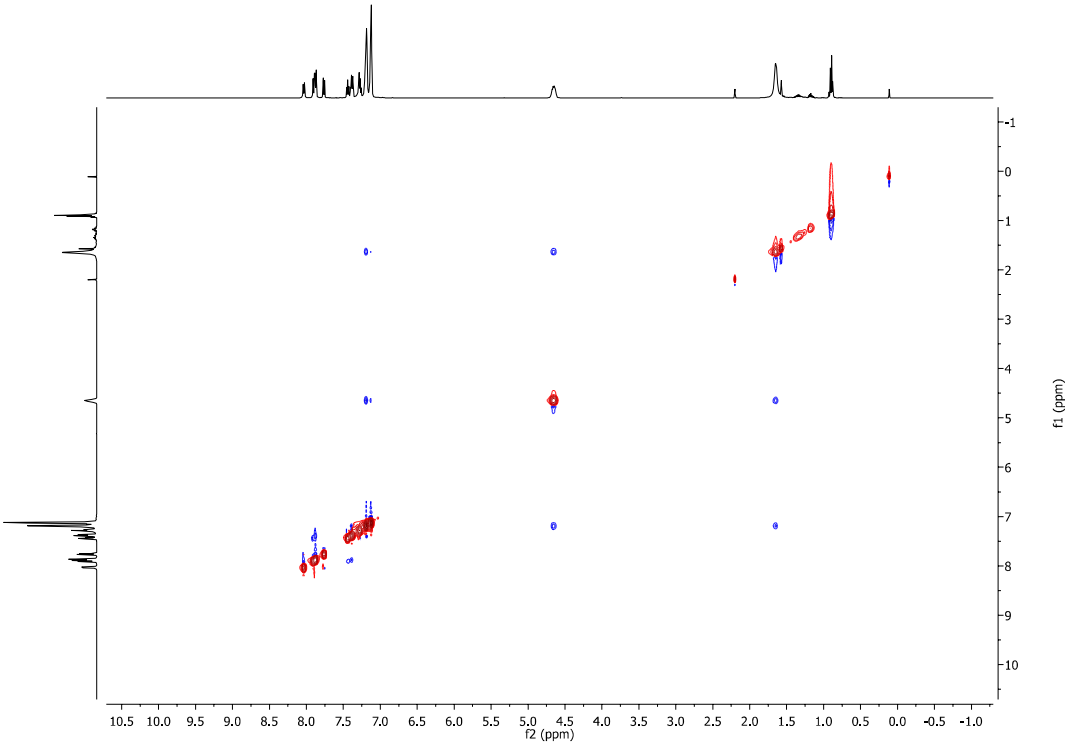

*CuOTf-**A** complex*

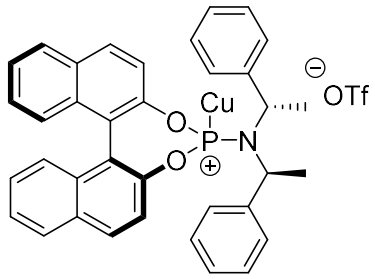

In a flame-dried flask, protected from light, under an argon atmosphere, CuCl (3.8 mg, 40 μmol, 1.0 eq) and (*S, S, S*)-**A** (21.6 mg, 40.0 μmol, 1.00 eq) were dissolved in $CDCl_3$ (0.8 mL) and allowed to stir for 1 h at room temperature. Then AgOTf (11.3 mg, 44.0 μmol, 11.0 mol%) was added to the Cu-complex and stirred for 15 min before filtering to a flame-dried NMR tube under argon atmosphere equipped with a septa. **^{1}H NMR** (500 MHz, $CDCl_3$) δ_H/ppm 8.11 (br. d, *J*= 8.4 Hz, 1H, Ar-**H**), 8.02–7.78 (br. m, 4H, Ar-**H**), 7.69 (br. d, *J*= 8.0 Hz, 1H, Ar-**H**), 7.59 (br. d, *J*= 7.8 Hz, 1H, Ar-**H**), 7.55-7.13 (m, 17H, Ar-**H**), 7.11-6.77 (m, 3H, Ar-**H**), 6.67 (br. s, 1H, Ar-**H**), 4.60 (br. dd, *J*= 15.0, 7.4 Hz, 2H, 2 x C**H**-N), 4.38 (br. s, 0.5H, 2 x C**H**-N(m)), 1.83 (br. d, *J*= 4.8 Hz, 6H, 2 x C**H$_3$**), 1.12 (br. s, 1.5H, 2 x C**H$_3$**(m)); **^{13}C NMR** (126 MHz, $CDCl_3$) δ_C/ppm 149.1 (br. s, **Cq**-Ar), 149.0 (br. s, **Cq**-Ar), 147.9 (**Cq**-Ar), 140.9 (**Cq**-Ar), 132.6 (**Cq**-Ar), 132.4 (**Cq**-Ar), 132.0 (br. s, **C**H-Ar), 130.9 (**Cq**-Ar), 130.5 (br. s, **C**H-Ar), 129.1 (br. s, **C**H-Ar), 128.6 (br. s, **C**H-Ar), 128.2 (br. s, **C**H-Ar), 128.0 (br. s, **C**H-Ar), 127.5 (br. s, **C**H-Ar), 126.8 (br. s, **C**H-Ar), 126.6 (br. s, **C**H-Ar), 126.4 (br. s, **C**H-Ar), 125.4 (br. s, **C**H-Ar), 123.7 (br. s, **C**H-Ar), 123.1 (br. s, **Cq**-Ar), 122.1 (br. s, **C**H-Ar), 121.2 (br. s, **Cq**-Ar), 121.0 (br. s, **C**H-Ar), 118.6 (**Cq**-Ar), 55.2 (br. s, 2 x **C**H-N (m)), 53.8 (br. d, *J*= 8.3 Hz, 2 x **C**H-N),

21.7 (br. s, 2 x **C**H_3 and 2 x **C**H_3 (m)); **^{31}P NMR** (202 MHz, $CDCl_3$) δ_P/ppm 124.1 (br. s, 0.5P(m)), 122.7 (br. s, 1P); **^{19}F NMR** (470 MHz, $CDCl_3$) δ_F/ppm -77.6 (s).

*Dynamics of CuOTf-**A** complex*

Summary of EXSY Exchanges

Many in aromatic region, CH-N of 2 species at 4.60 and 4.38 ppm, Me of 2 species at 1.83 and 1.12 ppm.

2D EXSY (gradient NOE t_{mix}= 800 ms)

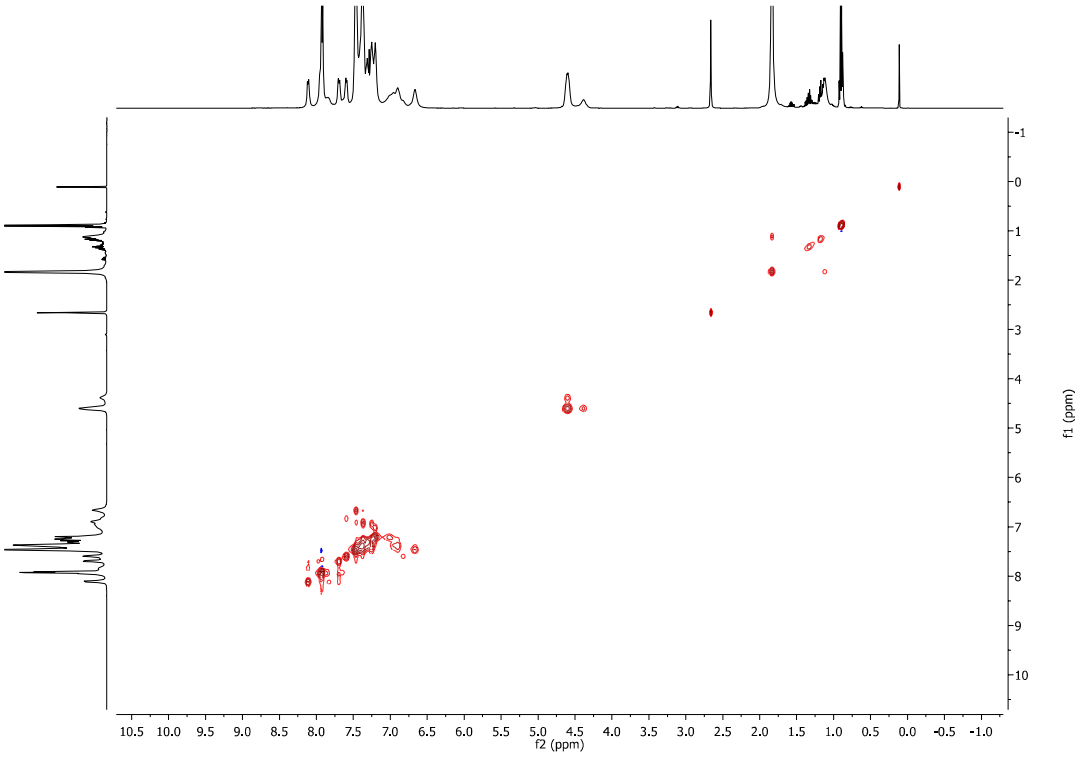

Hydrozirconation

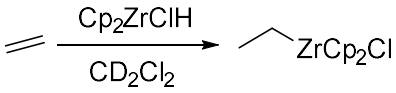

In a flame-dried flask, ethylene (1 atm) was bubbled through a solution of Cp_2ZrHCl (210 mg, 0.80 mmol, 1.0 eq) in CD_2Cl_2 (0.5 mL) for 30 s and then stirred at room temperature under ethylene atmosphere until the solution went clear (15-20 min). The clear yellow hydrozirconation solution was transferred via syringe to the NMR tube under argon atmosphere, equipped with a septa. **^{1}H NMR** (500 MHz, CD_2Cl_2) δ_H/ppm 6.29 (s, app. 7H, Cp-**H**), 1.42 (t, *J*= 7.1 Hz, 3H, C**H$_3$**), 1.11 (q, *J*= 7.1 Hz, 2H, C**H$_2$**); **^{13}C NMR** (125 MHz, CD_2Cl_2) $\delta_{C/ppm}$ 112.7 (Cp-**C**), 47.2 (**C**H_2), 18.1 (**C**H_3).

2) 3-Iodocyclohex-1-ene (54)

*i) Generated from 3-Chlorocyclohex-1-ene **45b** and CuI-**A** complex*

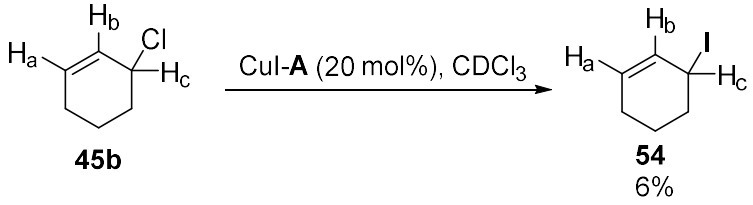

45b **54** 6%

In a flame-dried flask, protected from light, under an argon atmosphere, CuI (7.7 mg, 40 μmol, 20 mol%) and (*S, S, S*)-**A** (21.6 mg, 40.0 μmol, 20.0 mol%) were dissolved in $CDCl_3$ (0.8 mL) and allowed to stir for 1 h at room temperature. The

cloudy white solution containing the Cu-complex was transferred via syringe to a flame-dried NMR tube under argon atmosphere equipped with a septa. A preliminary ^{1}H NMR was run with locking and shimming. Then 3-chlorocyclohex-1-ene **45b** (24 µL, 0.20 mmol, 1.0 eq) was added dropwise via a microsyringe to the NMR tube and shaken vigorously, further analysis were carried out without re-locking and shimming.

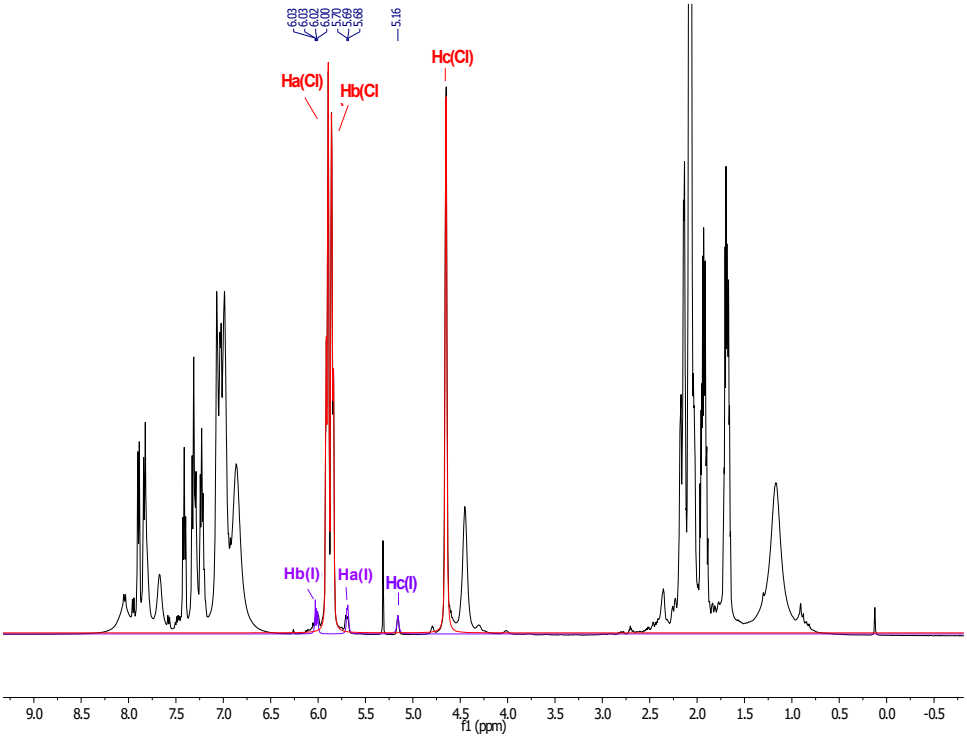

Rate of formation

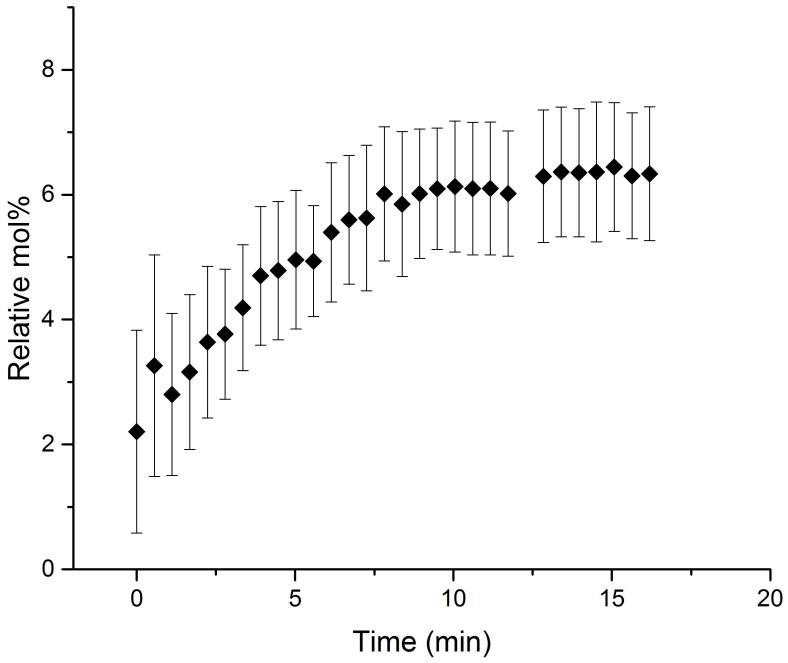

In situ characterisation of 3-Iodocyclohex-1-ene ***54***

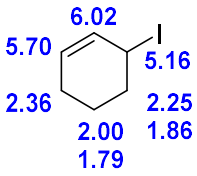

^{1}H NMR (500 MHz, $CDCl_3$) δ_H/ppm 6.02 (m, 1H, H*b*), 5.70 (m, 1H, H*a*), 5.16 (br. s, 1H, H*c*), 2.36 (m, 2H, C**H**$_2$CHCH), 2.25 (m, 1H, C**H**$_2$), 2.00(m, 1H, C**H**$_2$), 1.86 (m, 1H, C**H**$_2$), 1.79 (m, 1H, C**H**$_2$).

COSY Correlations

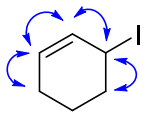

COSY NMR

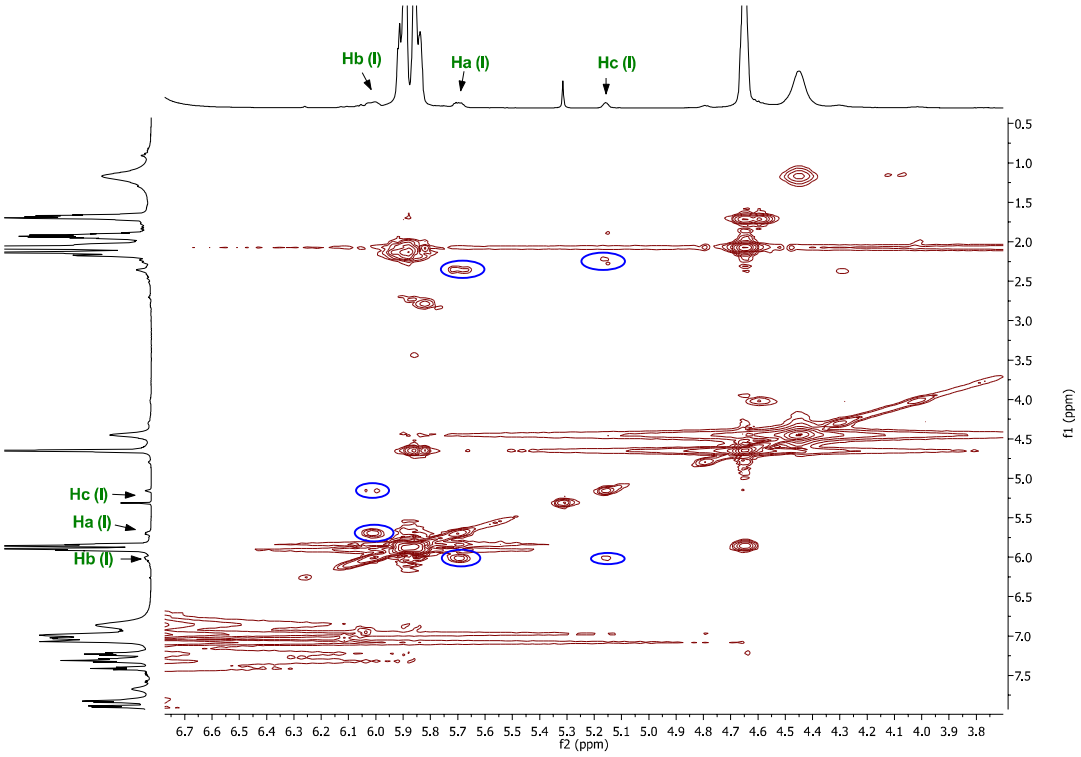

TOCSY Correlations

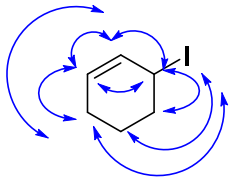

TOCSY NMR

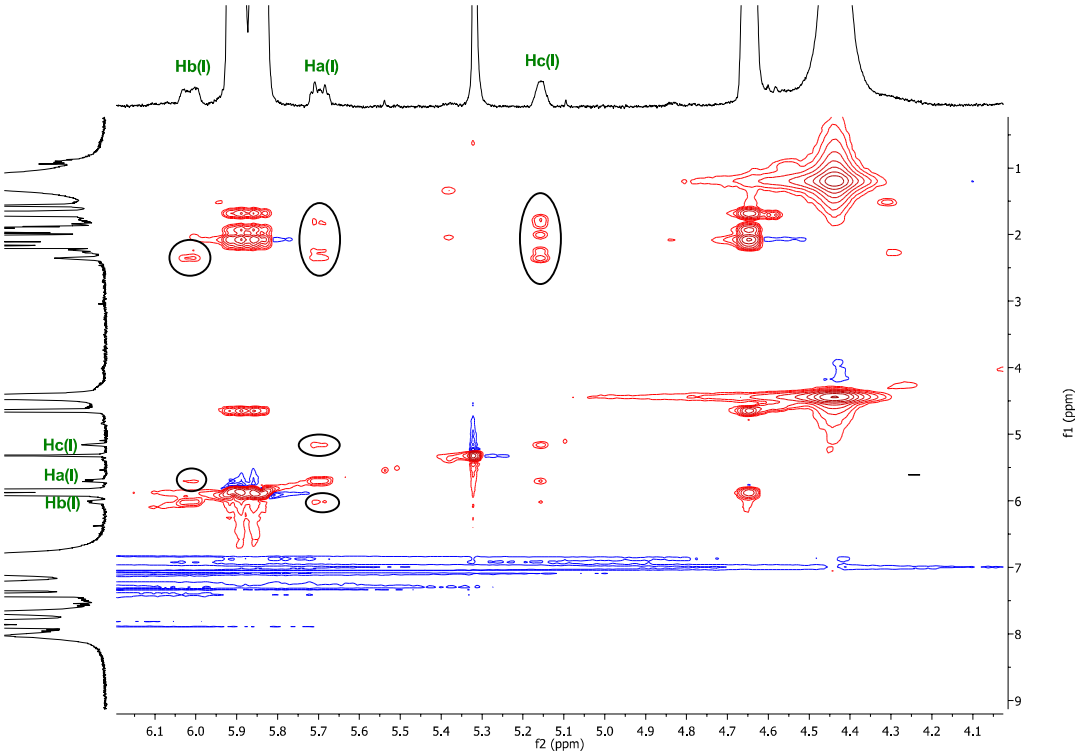

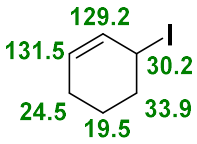

^{13}C NMR (125 MHz, $CDCl_3$) δ_C/ppm 131.5 (Ca), 129.2 (Cb), 33.9 (**C**H_2-CHI), 30.2 (Cc), 24.5 (**C**H_2-CH=CH), 19.5 (CH_2-**C**H_2-CH_2).

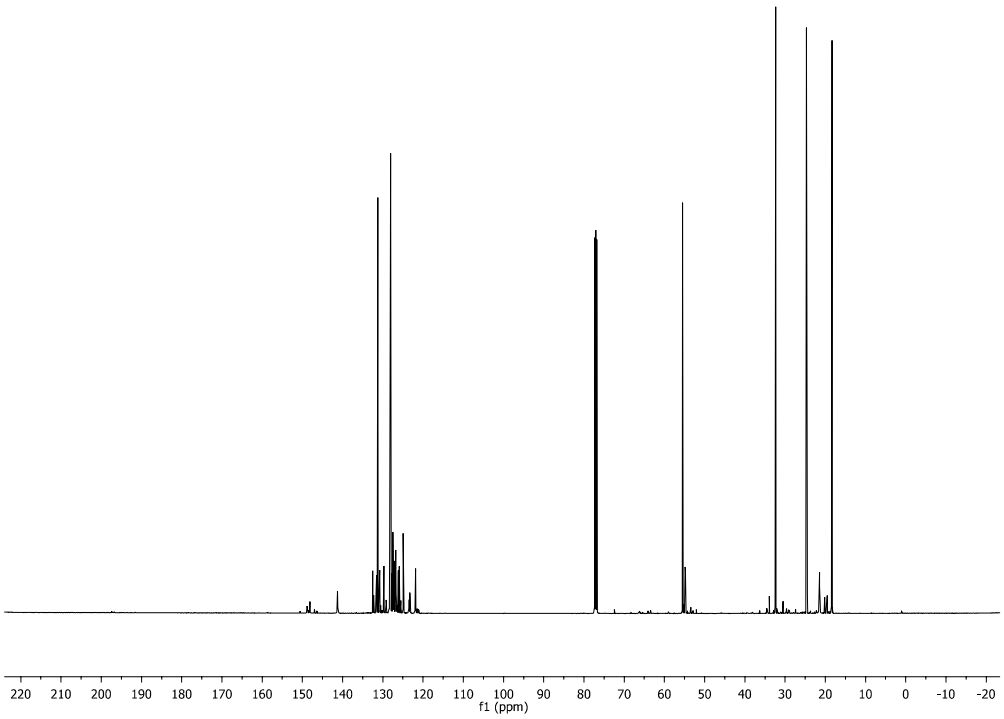
220 210 200 190 180 170 160 150 140 130 120 110 100 90 80 70 60 50 40 30 20 10 0 -10 -20
f1 (ppm)

HSQC NMR

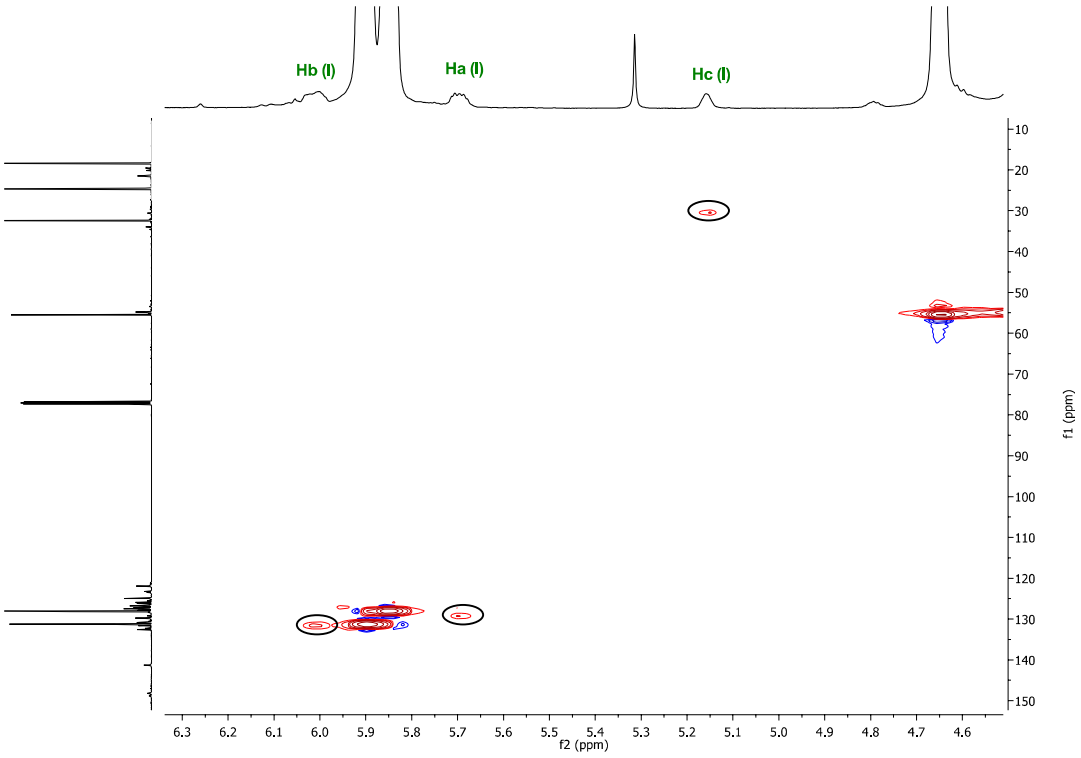
Hb (I)
Ha (I)
Hc (I)
10 20 30 40 50 60 70 80 90 100 110 120 130 140 150
f1 (ppm)
6.3 6.2 6.1 6.0 5.9 5.8 5.7 5.6 5.5 5.4 5.3 5.2 5.1 5.0 4.9 4.8 4.7 4.6
f2 (ppm)

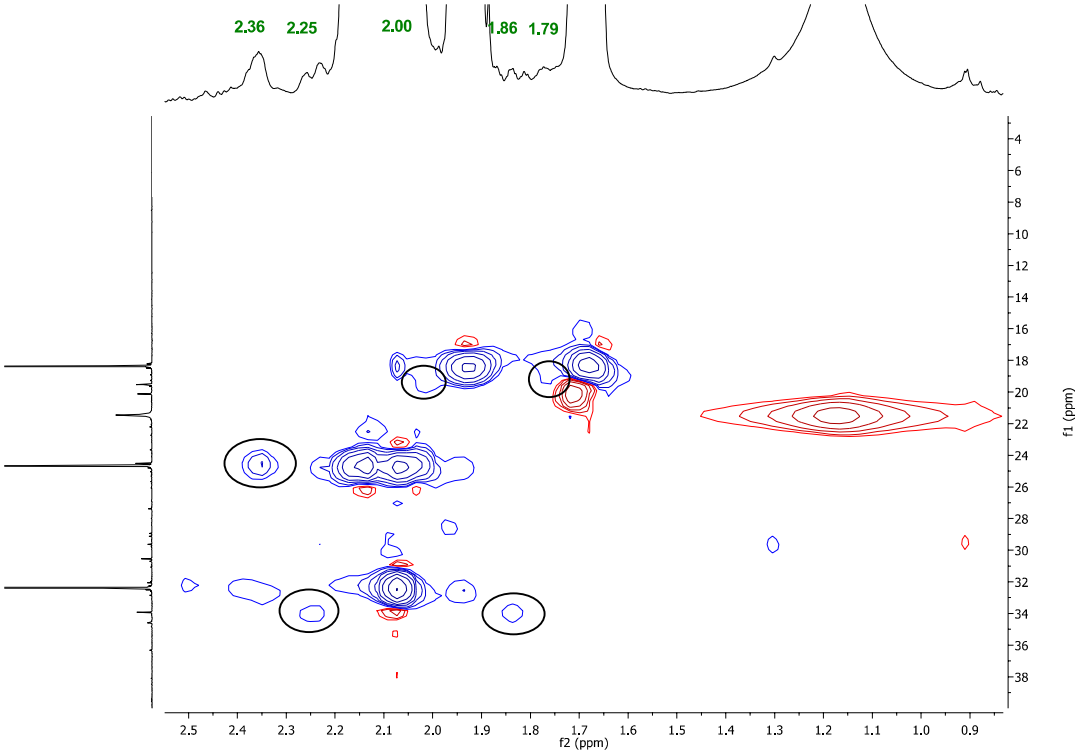
2.36
2.25
2.00
1.86
1.79
f1 (ppm)
f2 (ppm)

*Dynamics of 3-iodocyclohex-1-ene **54** generated from 3-chlorocyclohex-1-ene **45b** and CuI-**A***

Summary of exchanges observed by EXSY

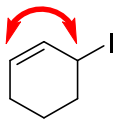

2D EXSY (gradient NOE t_{mix}= 800 ms)

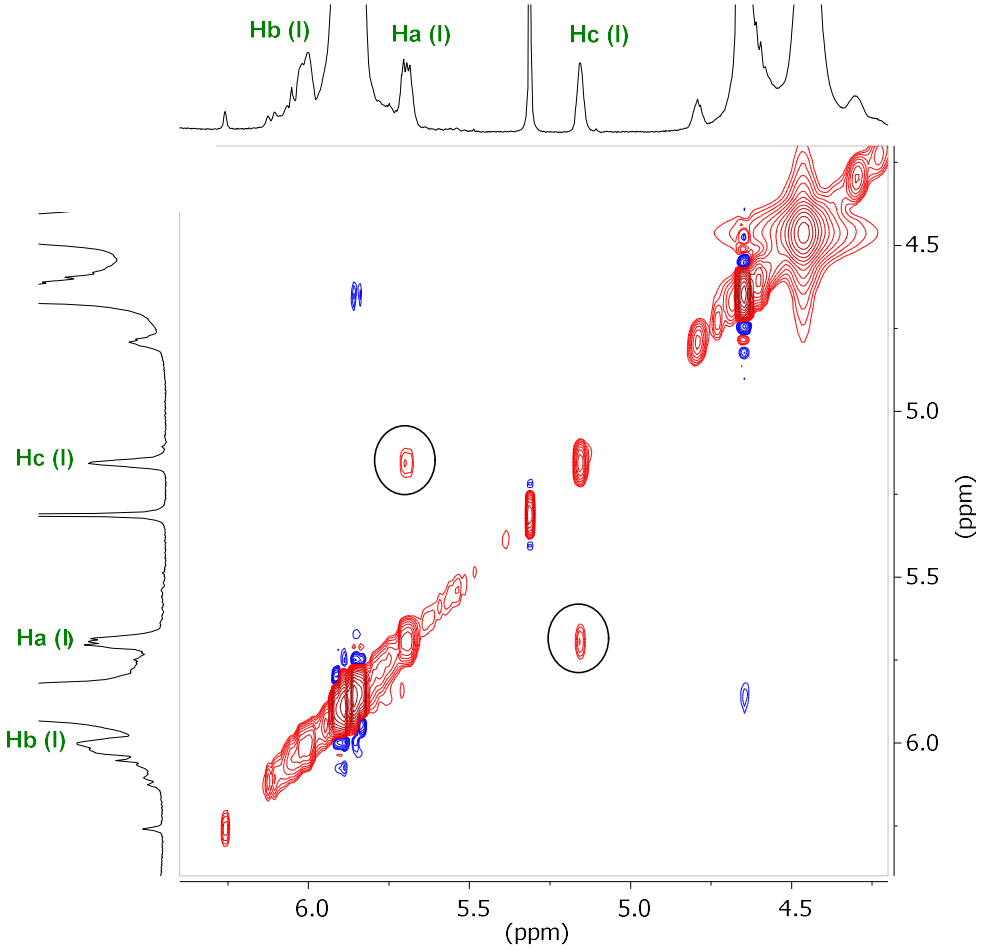

Summary of EXSY Exchanges at elevated temperature (328 K)

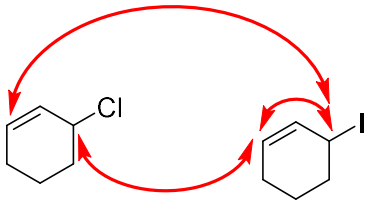

2D EXSY at 328 K (gradient NOE t_{mix}= 800 ms)

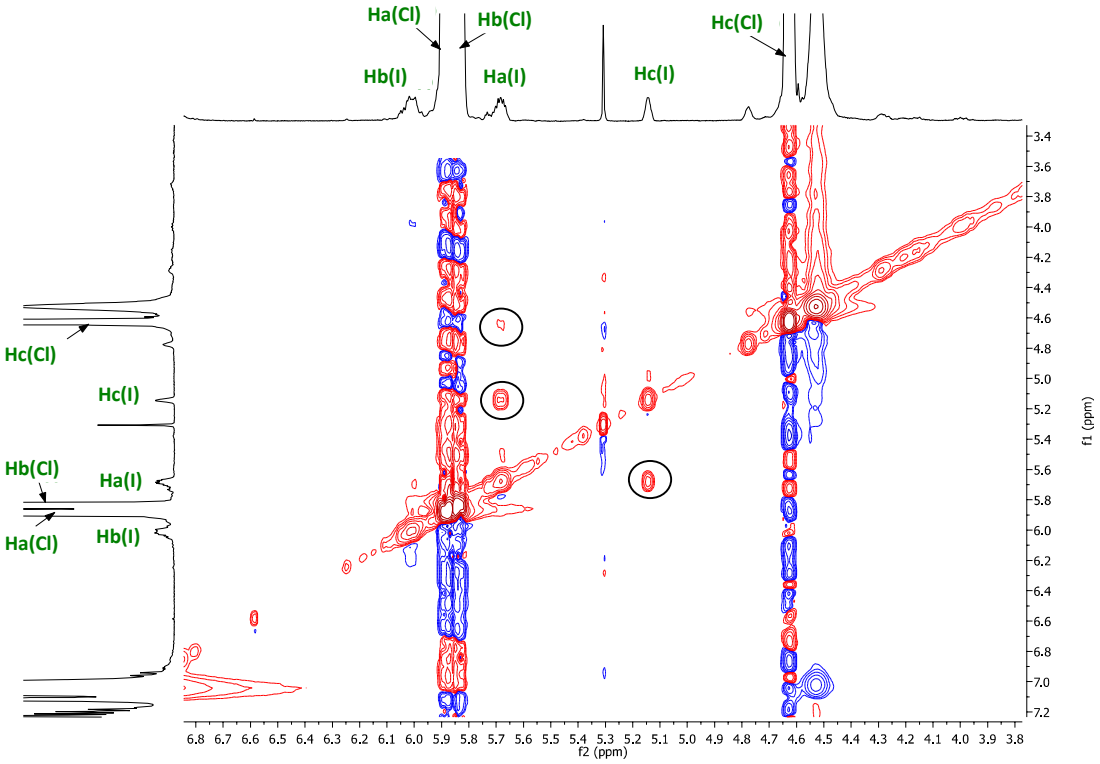

2D EXSY at 353 K (gradient NOE t_{mix}= 800 ms)

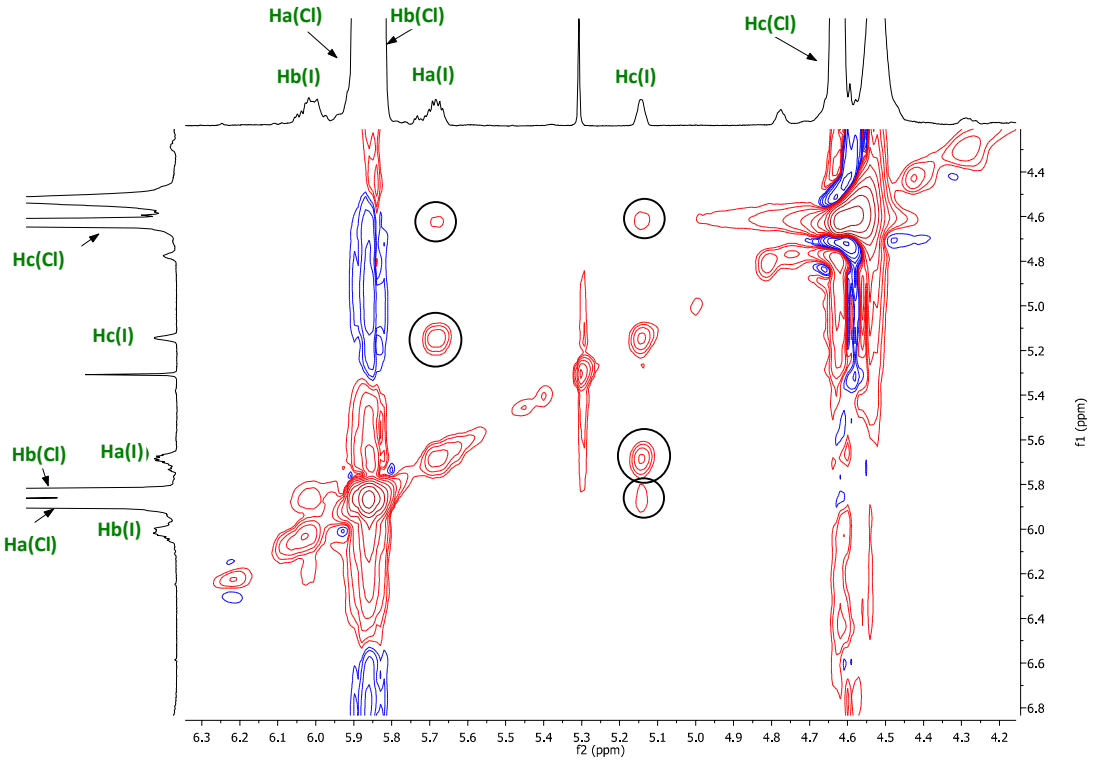

iii) *Generated from 3-bromocyclohex-1-ene **55** and CuI-**A** complex*

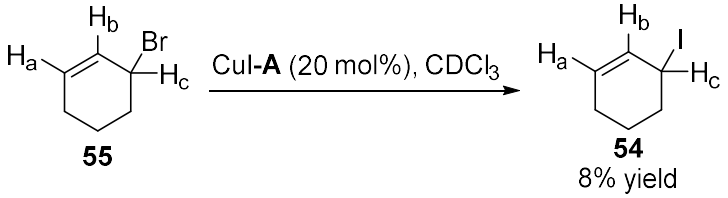

55 **54**
8% yield

In a flame-dried flask, protected from light, under an argon atmosphere, CuI (7.7 mg, 40 μmol, 20 mol%) and (*S, S, S*)-**A** (21.6 mg, 40.0 μmol, 20.0 mol%) were dissolved in $CDCl_3$ (0.8 mL) and allowed to stir for 1 h at room temperature. The cloudy white solution containing the Cu-complex was transferred via syringe to a flame-dried NMR tube under argon atmosphere equipped with a septa. A

preliminary ^{1}H NMR was run with locking and shimming. Then 3-bromocyclohex-1-ene **55** (23 μL, 0.20 mmol, 1.0 eq) was added dropwise via a microsyringe to the NMR tube and shaken vigorously, further analysis were carried out without re-locking and shimming.

*Dynamics of 3-iodocyclohex-1-ene **54** generated from 3-bromoyclohex-1-ene **55**.*

Summary of EXSY Exchanges

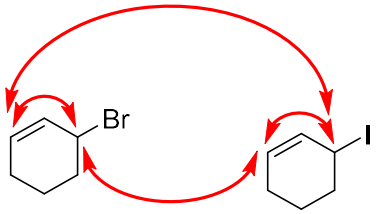

2D EXSY (gradient NOE t_{mix}= 600 ms)

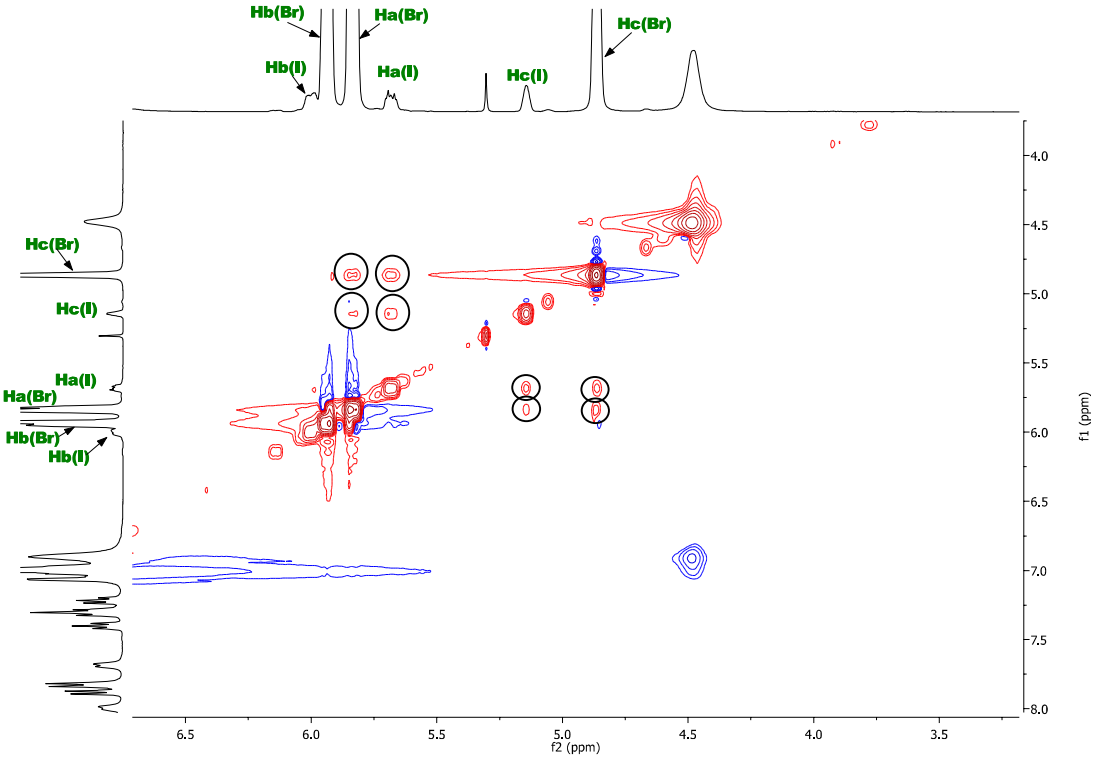

*iv) 3-Iodocyclohex-1-ene **54** in reaction*

*(i) Formation of 3-iodocyclohex-1-ene **54** in reaction*

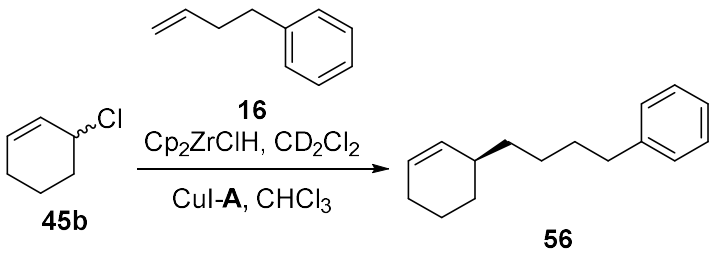

In a flame-dried flask, protected from light, under an argon atmosphere, CuI (7.7 mg, 40 μmol, 10 mol%) and (*S, S, S*)-**A** (21.6 mg, 40.0 μmol, 10.0 mol%) were dissolved in $CDCl_3$ (0.8 mL) and allowed to stir for 1 h at room temperature. In another flask under argon atmosphere, Cp_2ZrHCl (210 mg, 0.80 mmol, 2.0 eq) was added to a solution of 4-phenyl-1-butene **16** (0.15 mL, 1.0 mmol, 2.5 eq) in in CD_2Cl_2 (0.4 mL) and stirred at room temperature until a clear yellow solution was obtained (20 to 40 min). The cloudy white solution containing the Cu-complex was transferred via syringe to a flame-dried NMR tube under argon atmosphere equipped with a septa. The clear yellow hydrozirconation solution was transferred via syringe to the NMR tube under argon atmosphere and vigorously shaken. A preliminary ^1H NMR was run with locking and shimming. Then 3-chlorocyclohex-1-ene **45b** (47 μL, 0.40 mmol, 1.0 eq) was added dropwise via a microsyringe to the NMR tube and shaken vigorously, the kinetic was run without further locking and shimming.

*(ii) Dynamics of 3-Iodocyclohex-1-ene **54** in reaction*

Summary of EXSY Exchanges

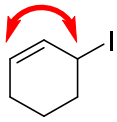

2D EXSY (gradient NOE t_{mix}=800 ms)

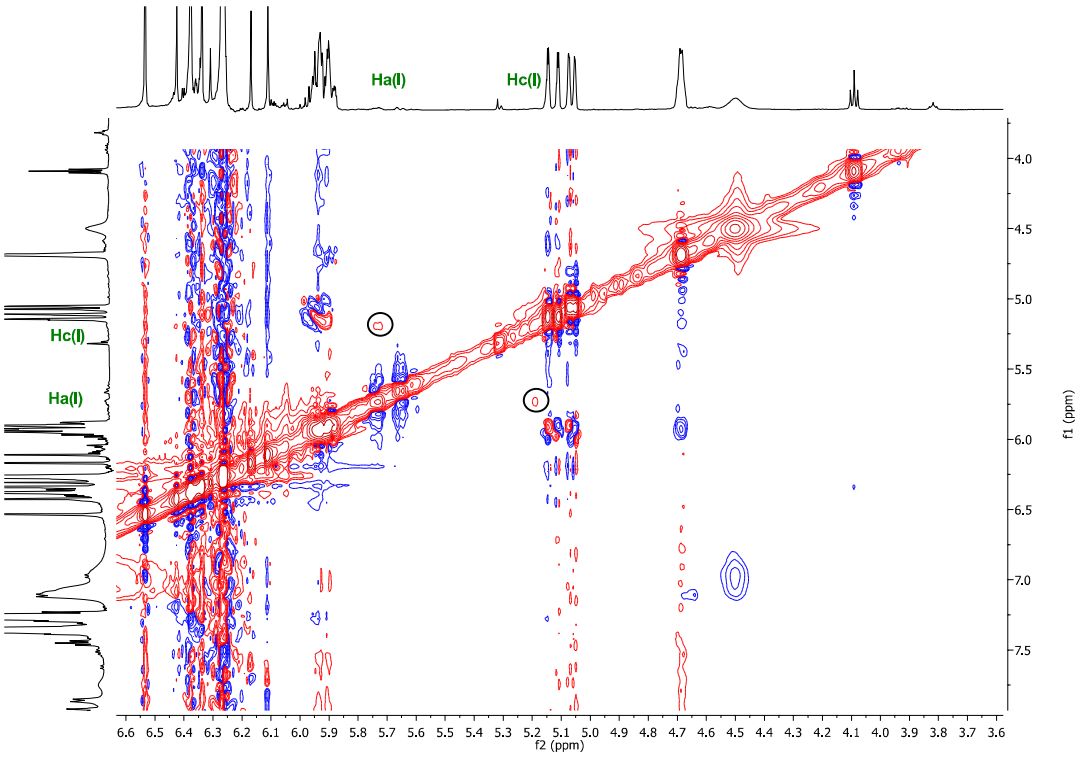

*v) Sensitivity of allyliodide **54** exchanges*

General procedure

In a flame-dried flask, protected from light, under an argon atmosphere, a source of iodide (40 μmol, 20 mol%) and ligand (40.0 μmol, 20.0 mol%) were dissolved in deuterated solvent (0.8 mL) and allowed to stir for 1 h at room temperature. The solution was transferred via syringe to a flame-dried NMR tube under argon atmosphere equipped with a septa. A preliminary ^{1}H NMR was run with locking and shimming. Then 3-chlorocyclohex-1-ene **45b** (24 μL, 0.20 mmol, 1.0 eq) was added dropwise via a microsyringe to the NMR tube and shaken vigorously, further analysis were carried out without re-locking and shimming.

*3-Chlorocyclohex-1-ene **45b** and CuI-(S)-Binap*

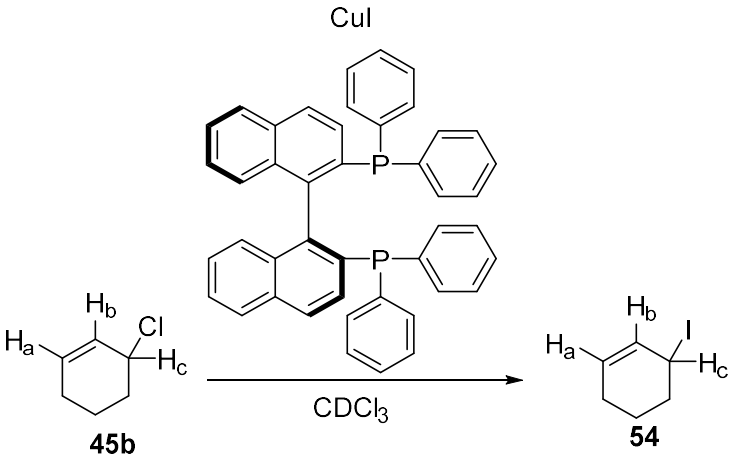

Summary of EXSY Exchanges

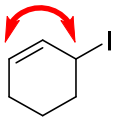

2D EXSY (gradient NOE t_{mix}= 800 ms)

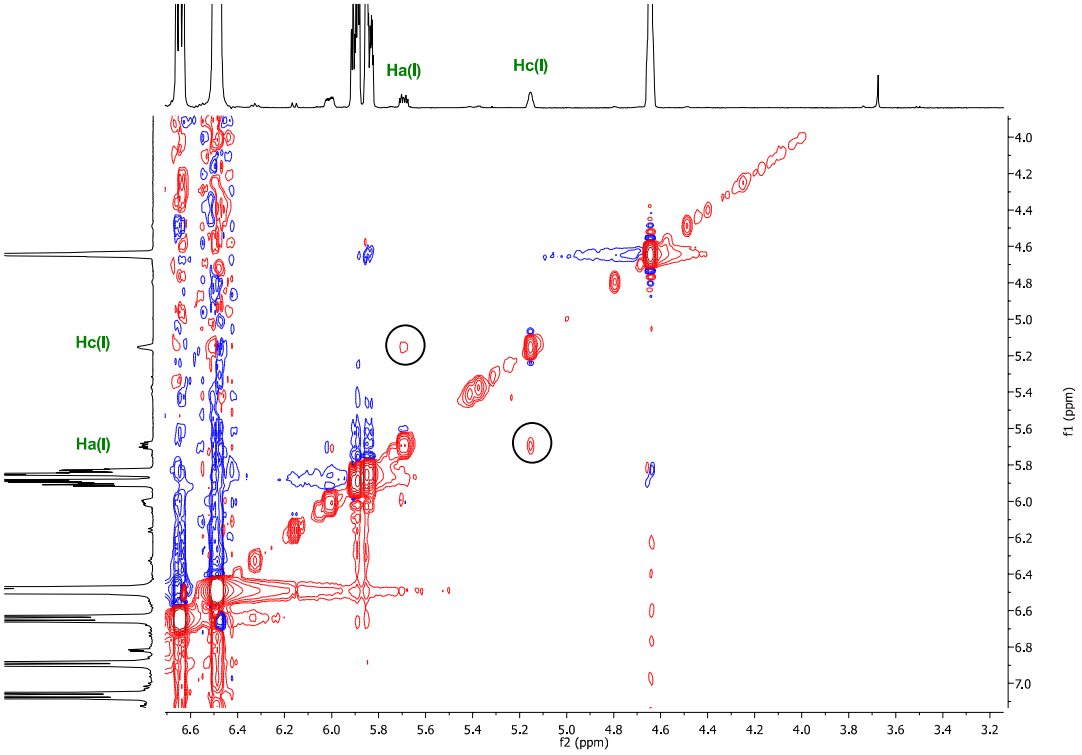

*3-Chlorocyclohex-1-ene **45b** and CuI-PPh$_3$*

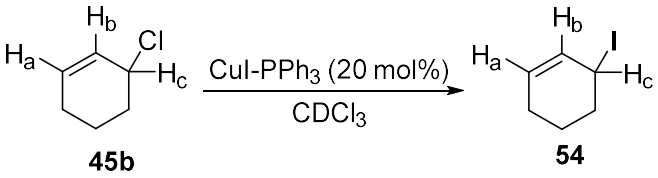

45b **54**

Summary of EXSY Exchanges

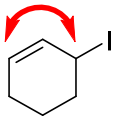

2D EXSY (gradient NOE t_{mix}= 800 ms)

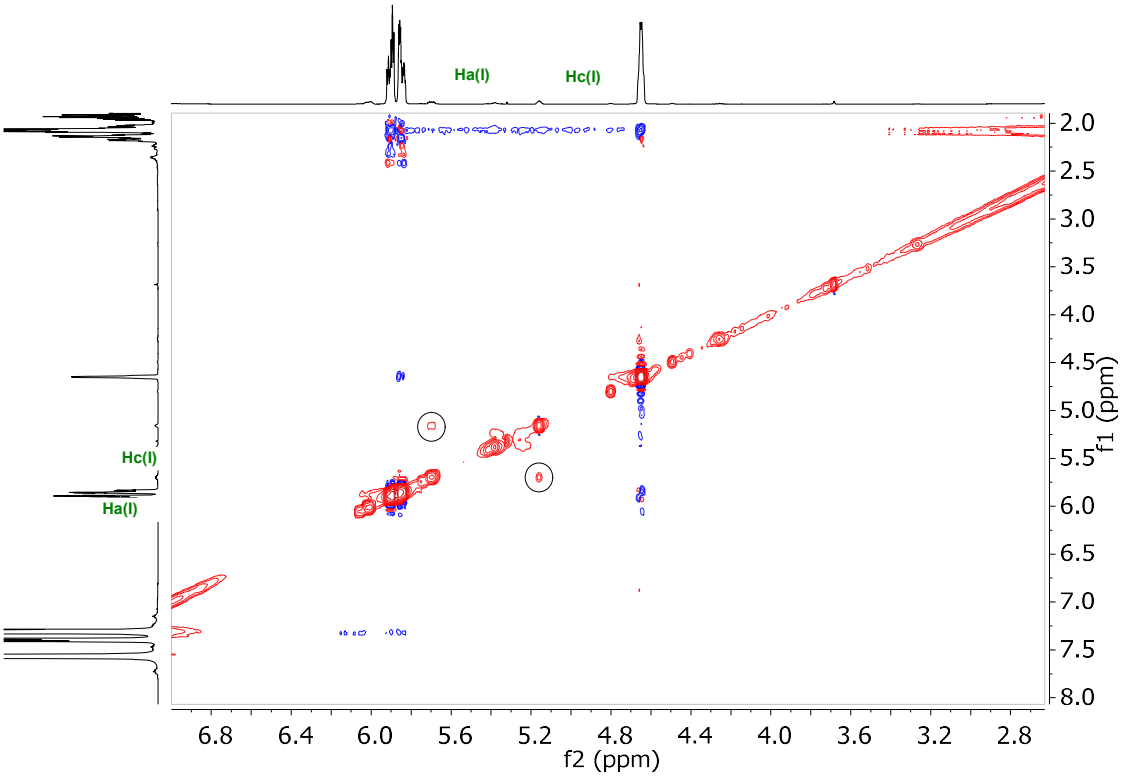

*3-Chlorocyclohex-1-ene **45b** and CuI-SIMes-leucinol*

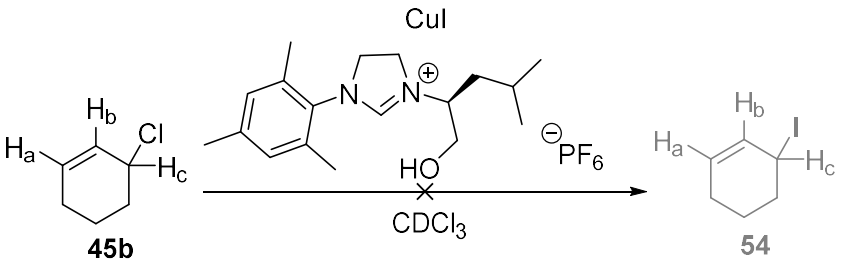

^{1}H NMR

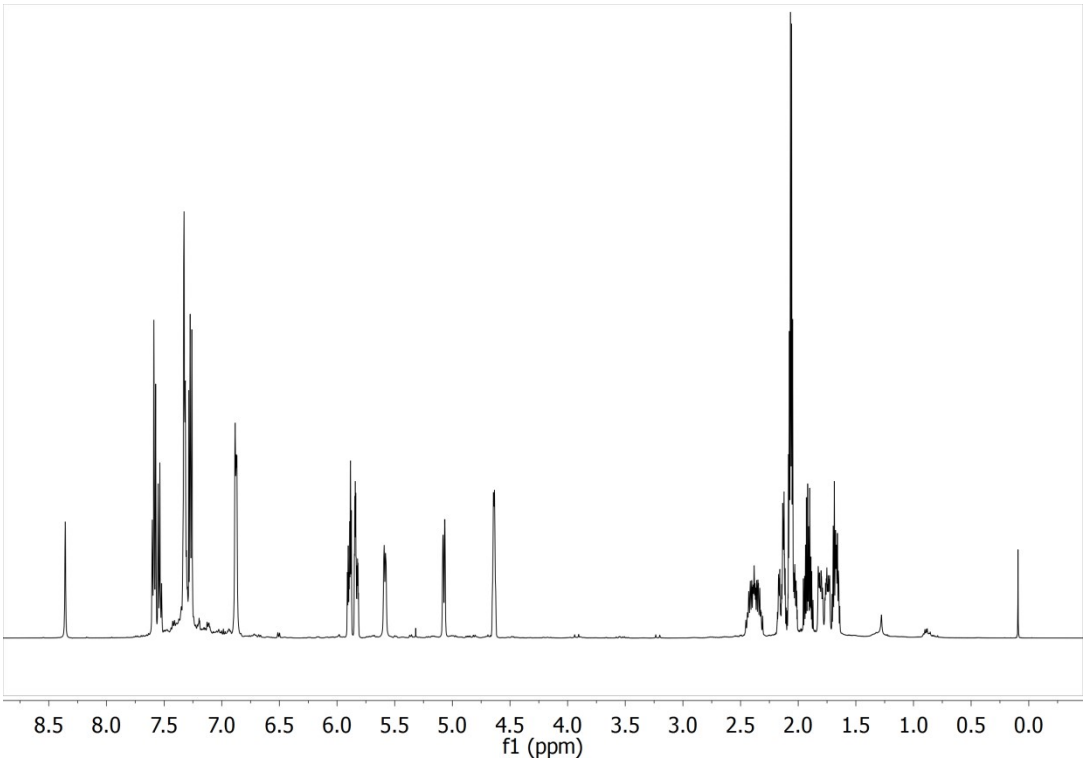

Summary of EXSY Exchanges

(none)

2D EXSY (gradient NOE t_{mix}= 800 ms)

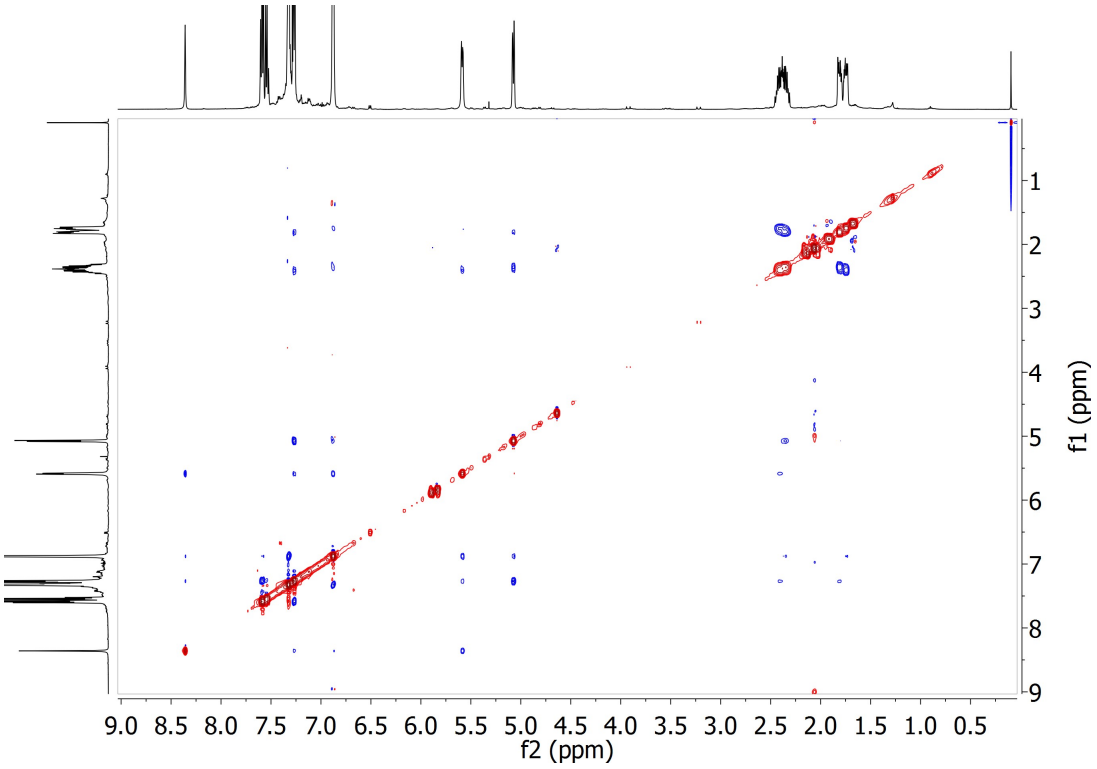

*3-Chlorocyclohex-1-ene **45b** and CuI·DMS*

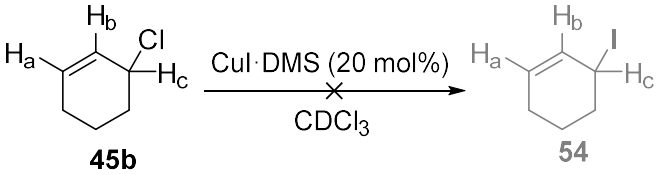

Traces of iodide

Summary of EXSY Exchanges

(none)

2D EXSY (gradient NOE t_{mix}= 800 ms)

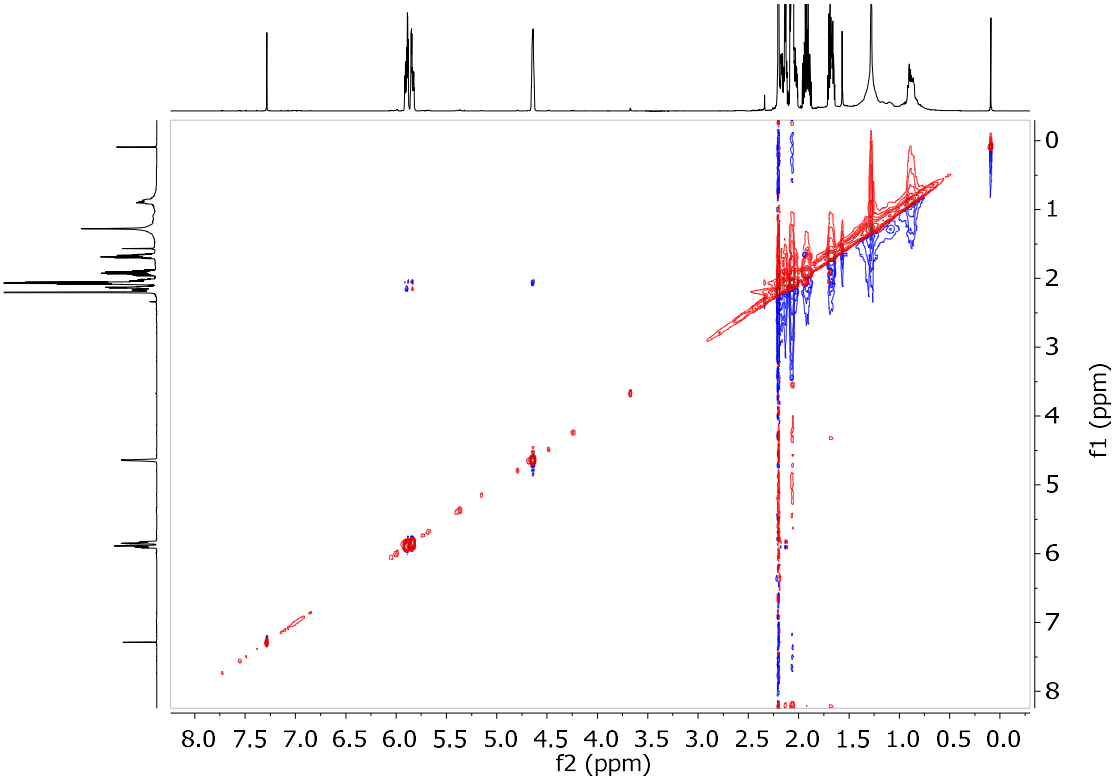

3-Chlorocyclohex-1-ene ***45b*** and CuI

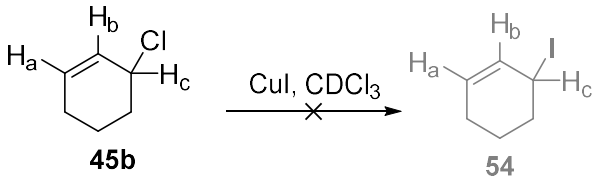

45b **54**

^{1}H NMR

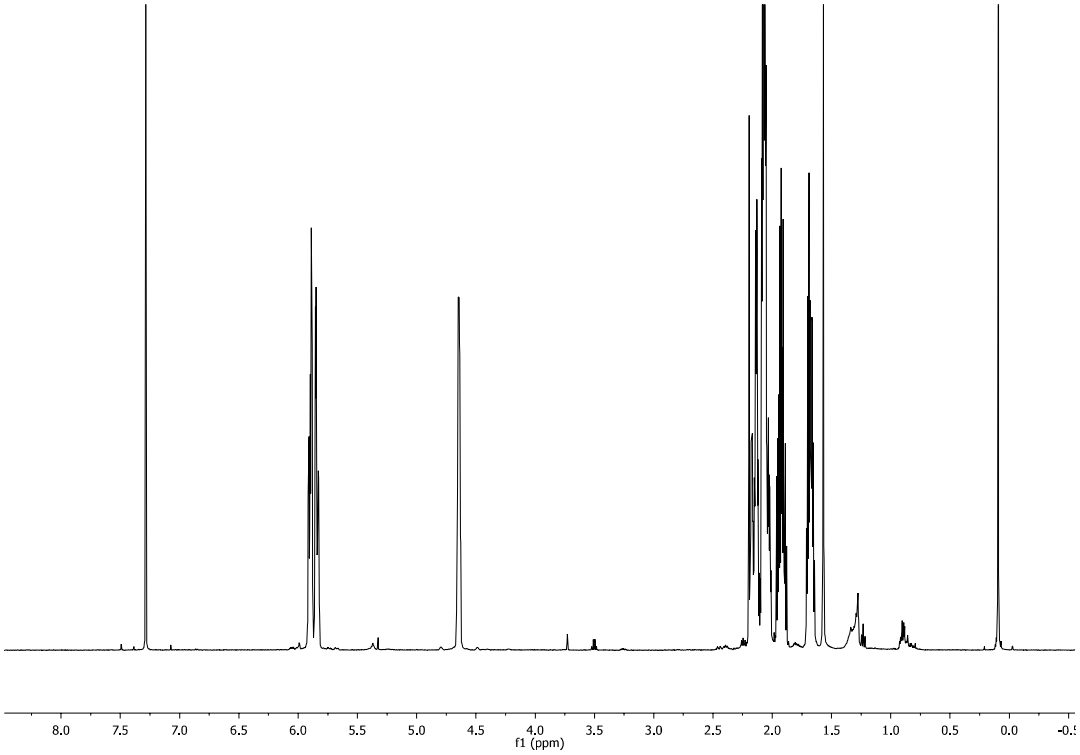

Summary of EXSY Exchanges

(None)

2D EXSY (gradient NOE t_{mix}= 800 ms)

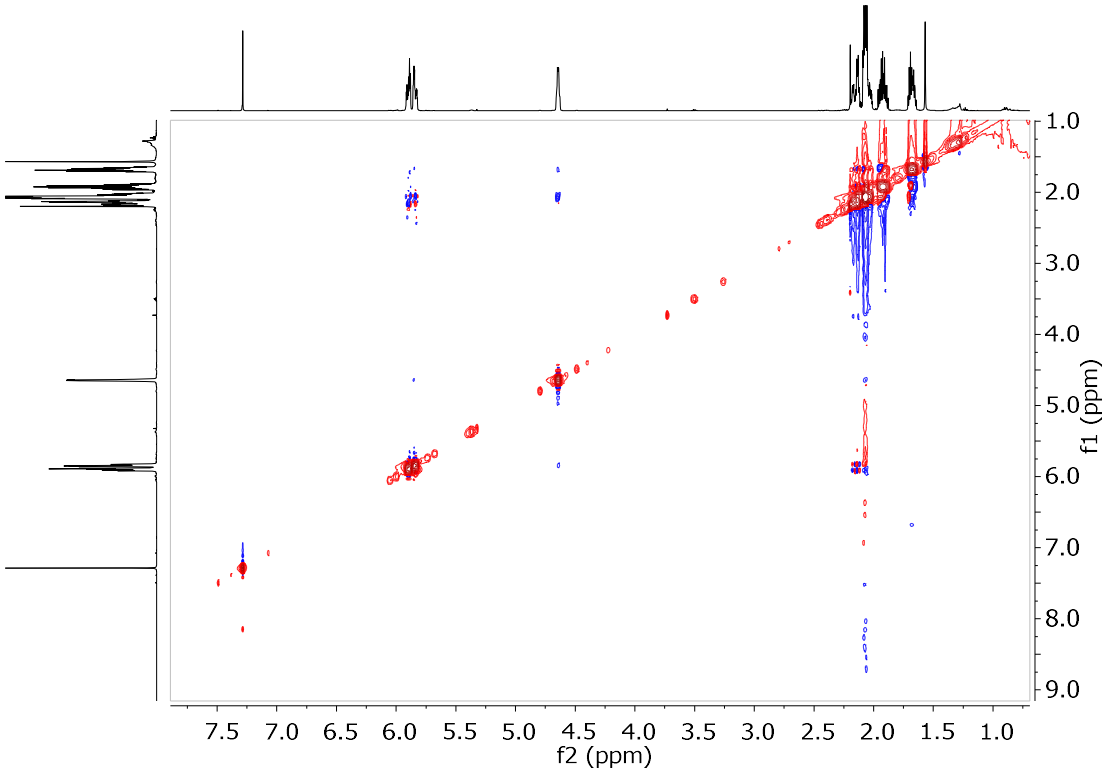

*3-Chlorocyclohex-1-ene **45b** and TBAI*

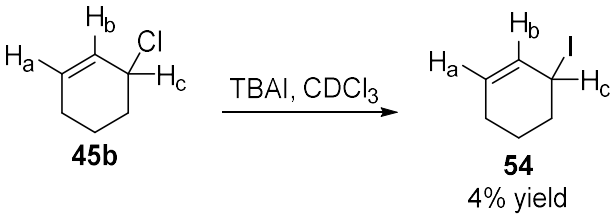

Summary of EXSY Exchanges

(None)

2D EXSY (gradient NOE t_{mix}= 800 ms)

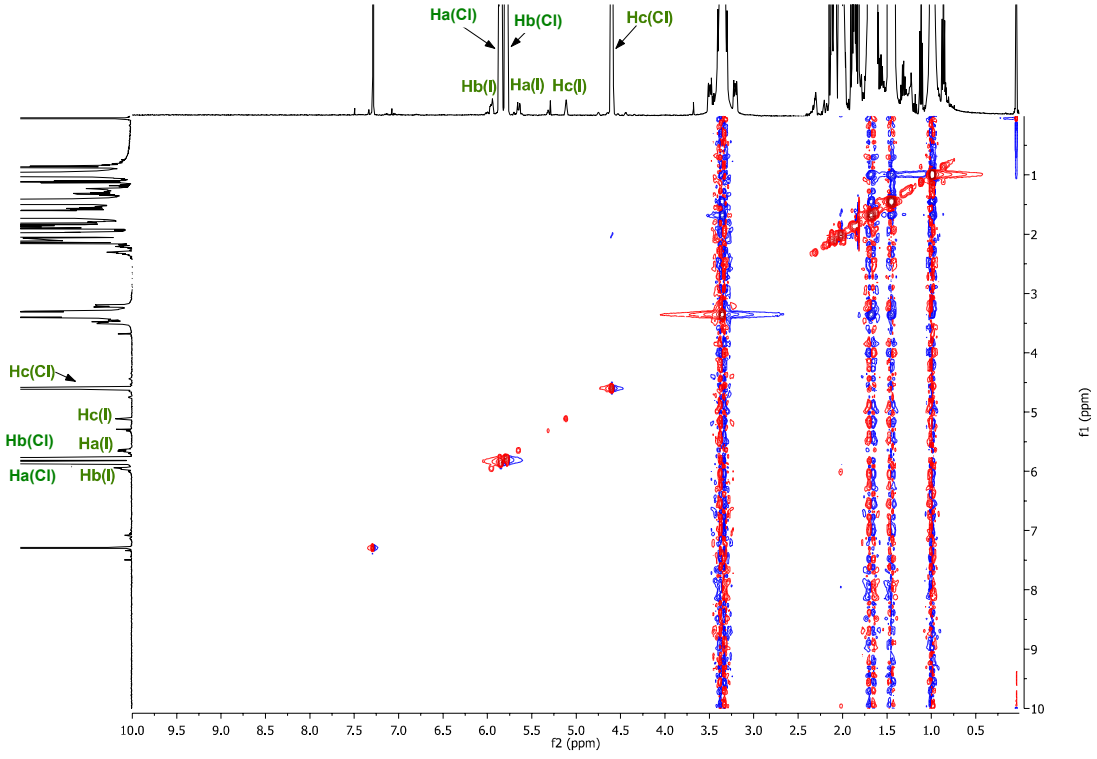

*3-Chlorocyclohex-1-ene **45b** and TMSI*

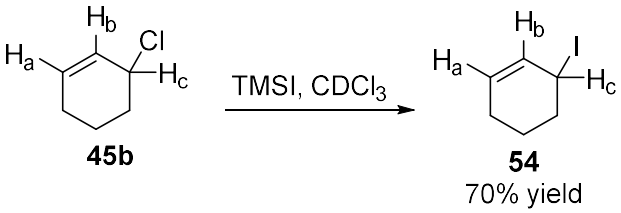

Summary of EXSY Exchanges

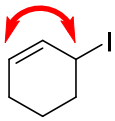

2D EXSY (gradient NOE t_{mix}= 800 ms)

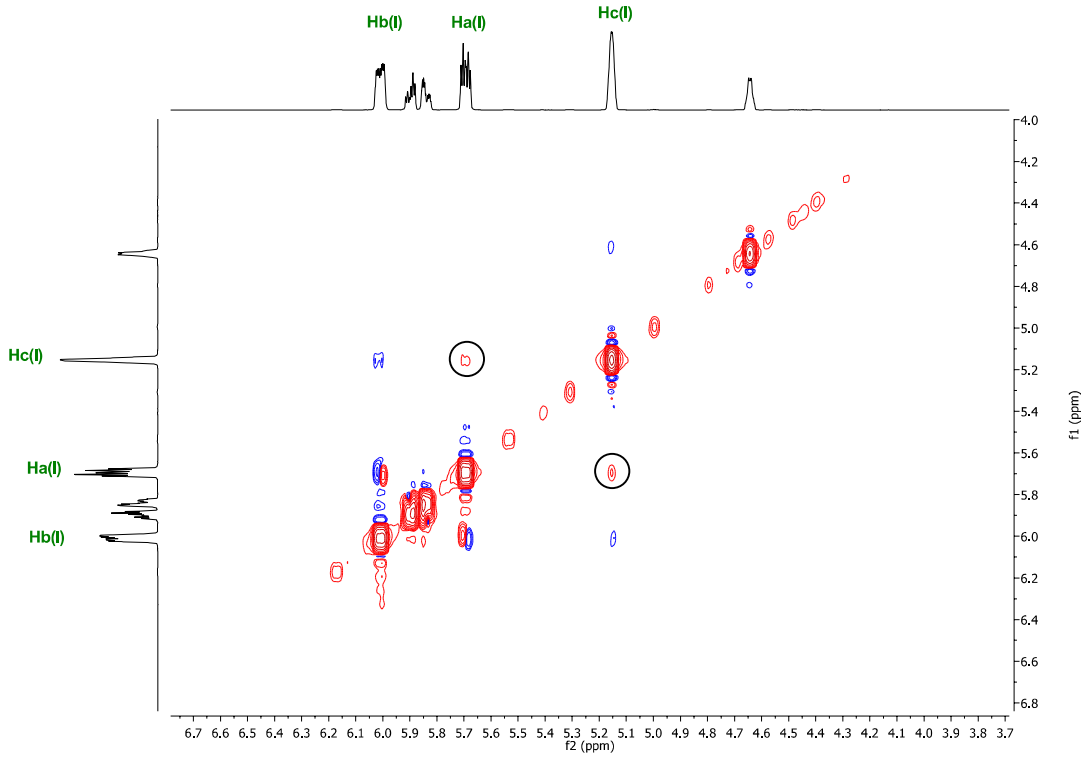

*3-Chlorocyclohex-1-ene **45b** and CuI-**A** complex in benzene-d_6*

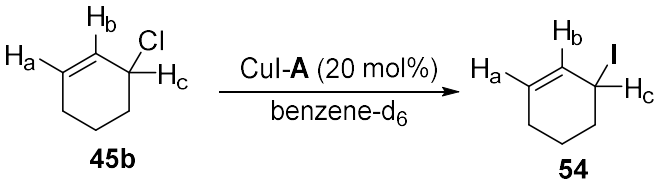

Summary of EXSY Exchanges

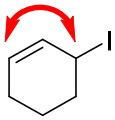

2D EXSY (gradient NOE t_{mix}= 800 ms)

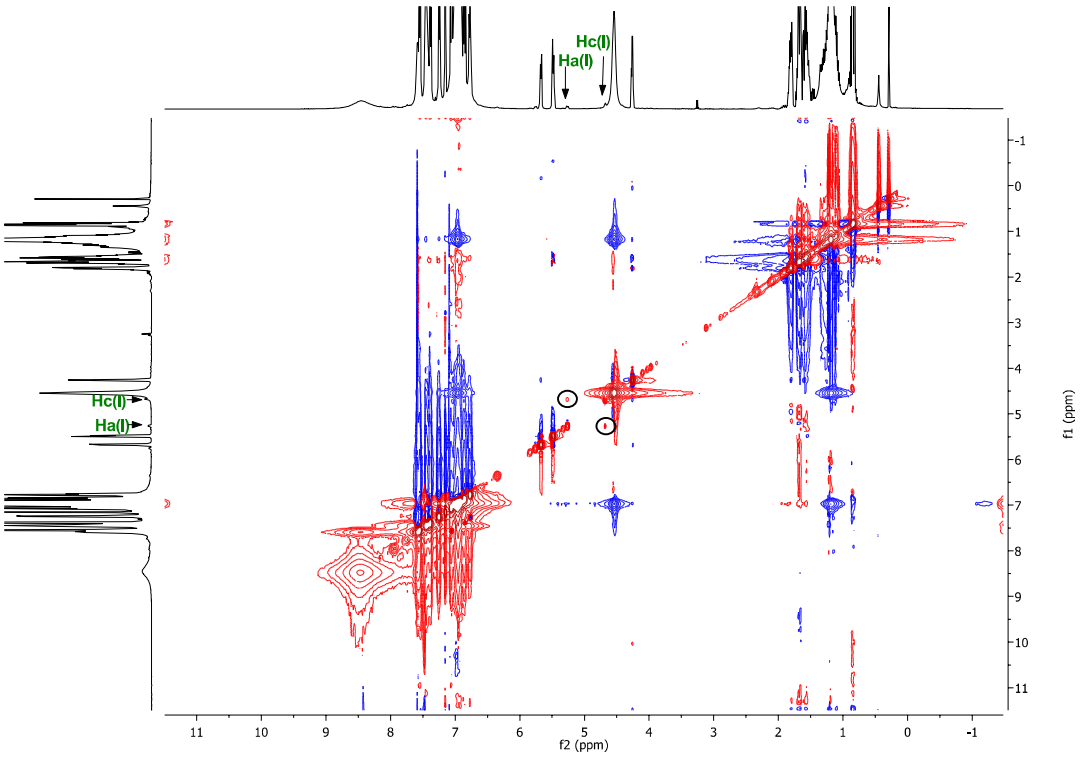

*3-Chlorocyclohex-1-ene **45b** and CuI-**A** complex in THF-d_8*

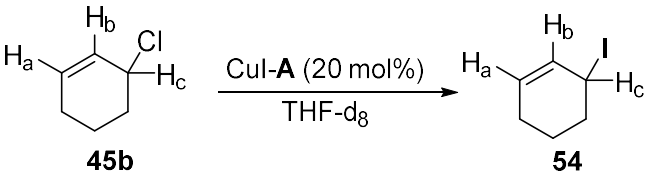

45b **54**

Summary of EXSY Exchanges

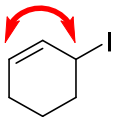

2D EXSY (gradient NOE t_{mix}= 800 ms)

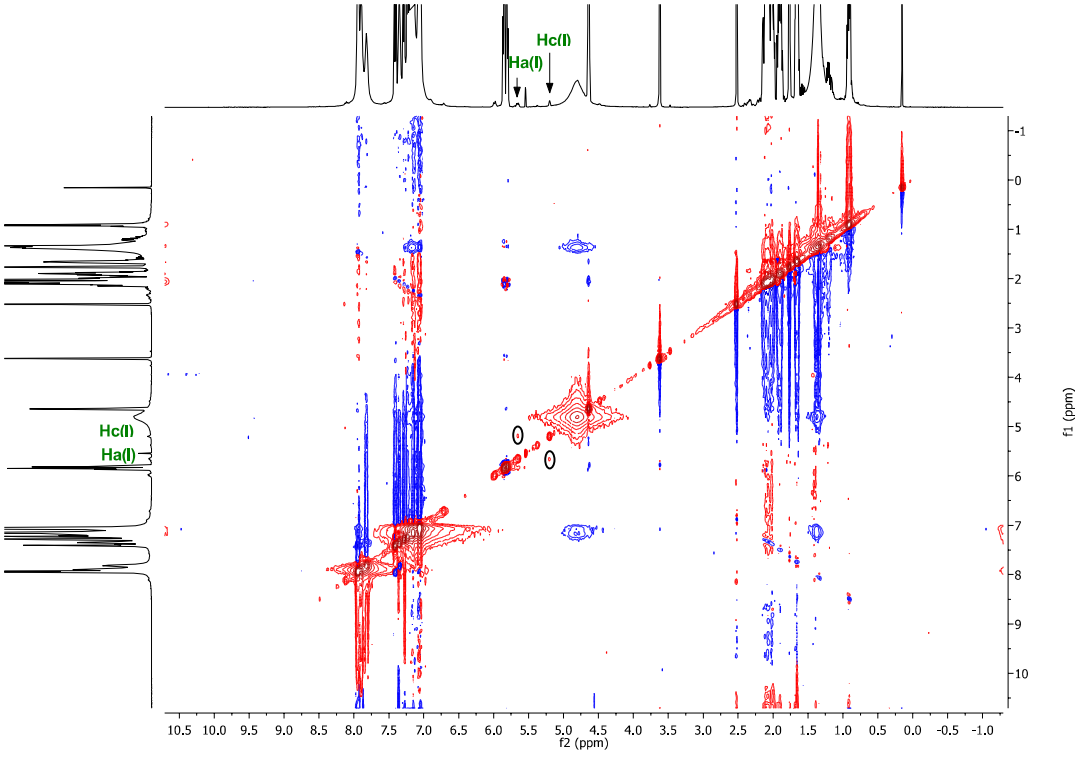

*3-Chlorocyclohex-1-ene **45b** and CuI-**A** complex in CD_3CN*

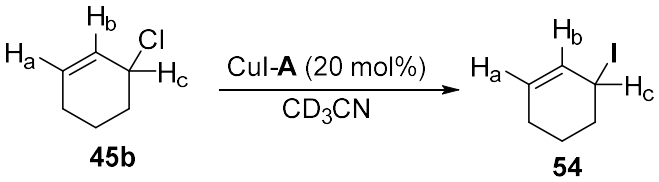

Summary of EXSY Exchanges

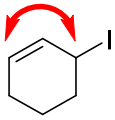

2D EXSY (gradient NOE t_{mix}= 800 ms)

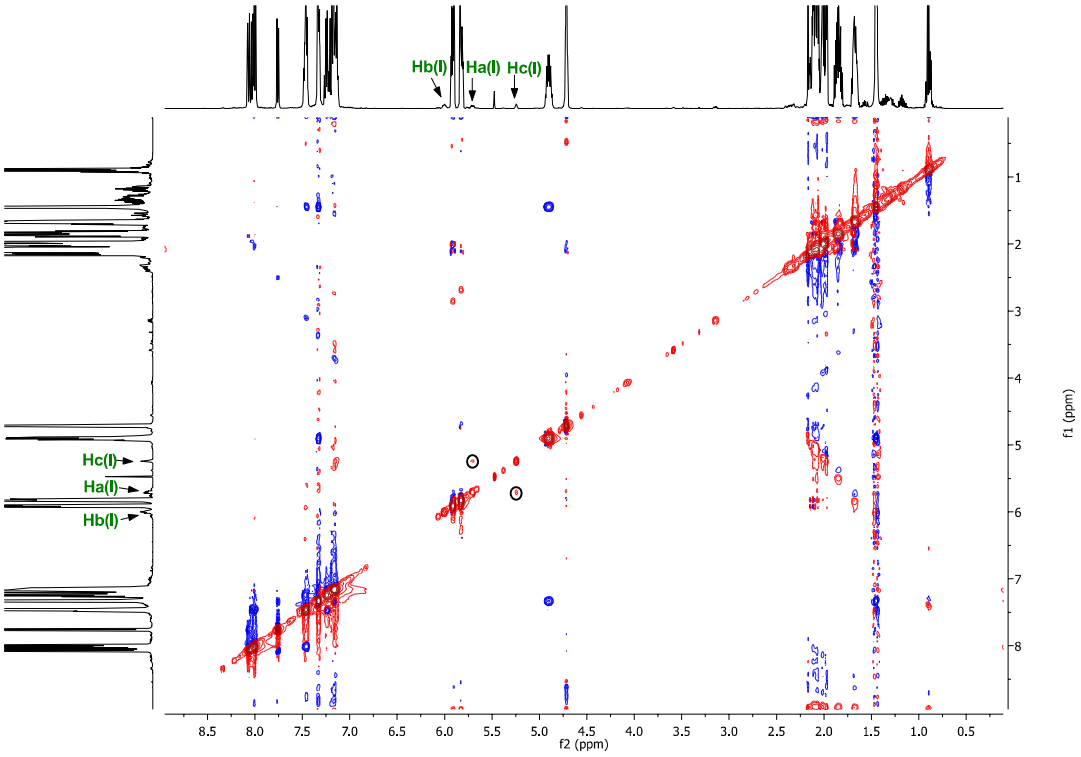

*3-Chlorocyclohex-1-ene **45b** and CuCl-**A***

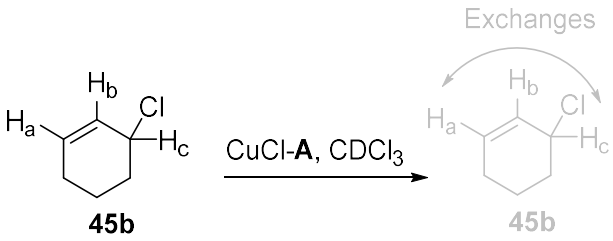

In a flame-dried flask, protected from light, under an argon atmosphere, CuCl (3.8 mg, 40 μmol, 20 mol%) and (*S,S,S*)-**A** (21.6 mg, 40.0 μmol, 20.0 mol%) were dissolved in $CDCl_3$ (0.8 mL) and allowed to stir for 1 h at room temperature. The solution was transferred via syringe to a flame-dried NMR tube under argon atmosphere equipped with a septa. A preliminary ^1H NMR was run with locking and shimming. Then 3-chlorocyclohex-1-ene **45b** (24 μL, 0.20 mmol, 1.0 eq) was added dropwise via a microsyringe to the NMR tube and shaken vigorously, further analysis were carried out without re-locking and shimming.

Summary of EXSY Exchanges

(none)

2D EXSY (gradient NOE t_{mix}= 800 ms)

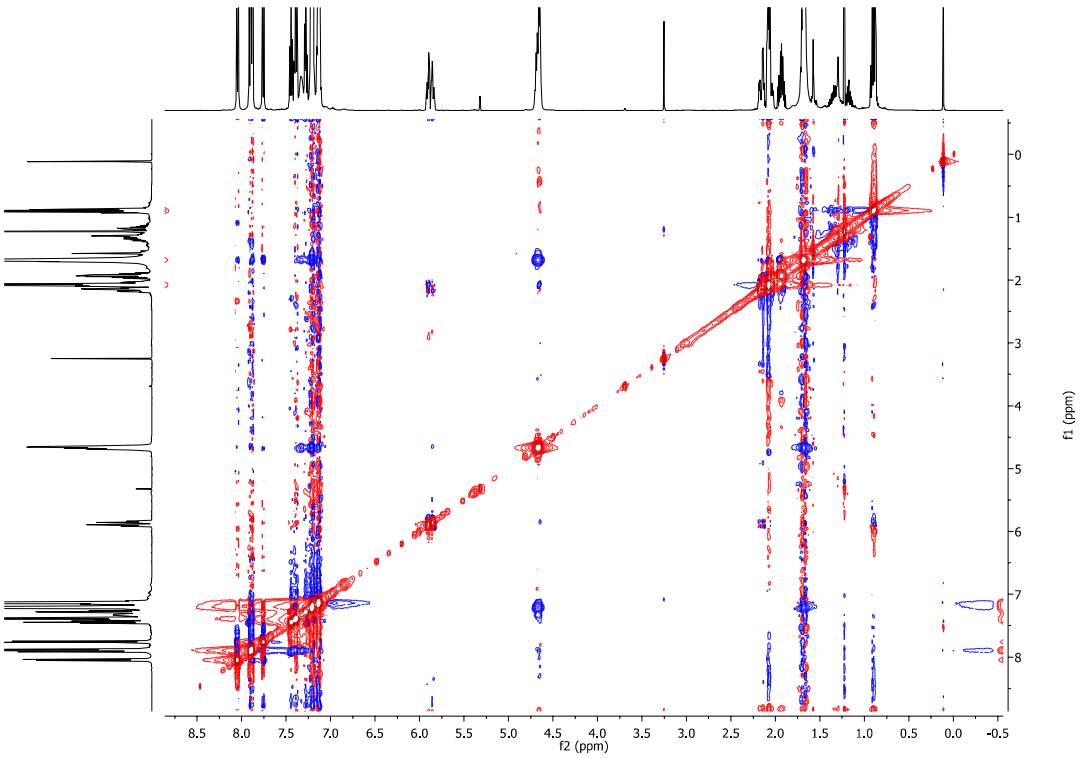

vi) *Rate of isomerization rate of allyl iodide **54***

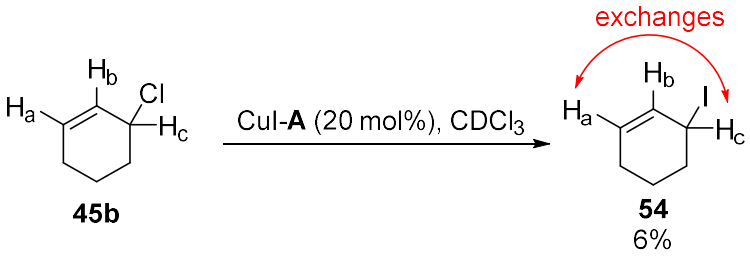

The rate of allyliodide exchange was determined through three different magnetisation transfer experiments recorded at 298K: 1D exchange

spectroscopy (1D EXSY), selective inversion transfer, and spin saturation transfer difference (SSTD).

Preparation of sample

In a flame-dried flask, protected from light, under an argon atmosphere, CuI (7.7 mg, 40 μmol, 20 mol%) and (*S, S, S*)-**A** (21.6 mg, 40.0 μmol, 20.0 mol%) were dissolved in $CDCl_3$ (0.8 mL) and allowed to stir for 1 h at room temperature. The cloudy white solution containing the Cu-complex was transferred via syringe to a flame-dried NMR tube under argon atmosphere equipped with a septum. Then 3-chlorocyclohex-1-ene **45b** (24 μL, 0.20 mmol, 1.0 eq) was added dropwise via a microsyringe to the NMR tube and shaken vigorously.

T_1 measurements

Longitudinal relaxation times constants (T_1s) were measured for protons Ha, Hb and Hc for compounds **45b** and **54** in the same sample using the (non-selective) inversion recovery sequence. Both systems exhibited strikingly long T_1 values, which were comparable those determined for allyl iodide **54** by the exchange experiments presented below. We ascribe these long values to the use of argon degassing and lack of dissolved paramagnetic O_2 in the samples under study.

	T_1 time constant /s		
^{1}H signal	Ha	Hb	Hc
Allylchloride **45b**	20.3	25.1	18.9
Allyliodide **54**	18.0	26.7	15.9

1D EXSY[300,301]

Spectra were collected with selective inversion of the target resonance (Hc) using a single pulsed field gradient spin-echo incorporating an 80 ms Gaussian inversion pulse. Exchange mixing times ranged from 10 ms to 3 s with either 1 or 2 non-selective 180° inversion pulses applied during this time.

Exchange peak intensities were plotted as normalised values *versus* mixing times and initial slopes used to determine the exchange rate constant. Normalisation to account for longitudinal relaxation was achieved either by plotting the ratio of exchange peak to selected peak intensities at each mixing time [$Ha_{(t)}/Hc_{(t)}$] versus time or by scaling the sum of the intensities of the selected and the exchange peaks at time t [$Ha_{(t)}$ + $Hc_{(t)}$] to match that of the selected peak intensity at zero mixing time (obtained by extrapolation) [$Hc_{(t=0)}$], and plotting this scaled Ha intensity [$Ha_{(t)}$*($Hc_{(t=0)}$/($Ha_{(t)}$+ $Hc_{(t)}$)] versus time. These two approaches delivered identical exchange rate constants of 0.108 s^{-1}at 298 K.

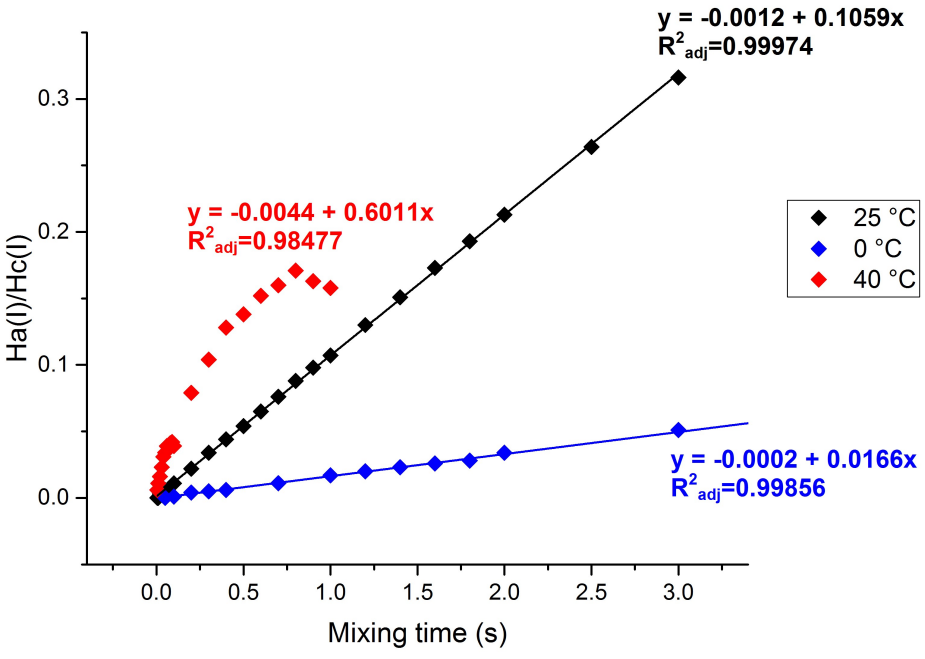

1D Selective Inversion Transfer[232-234,237]

Selective inversion of target resonance (Hc) was achieved using a 90-τ-90-τ_m-90-acq sequence in which Hc was placed on-resonance and the delay τ set to equal 1/(2δ) where δ is the frequency separation (in Hz) between resonances Hc and Ha (270 Hz). The result is to fully invert magnetisation of Hc (placing it along –z) but return that of Ha to +z longitudinal magnetisation. Magnetisation transfer through exchange then occurs during the mixing period τ_m prior to sampling with the final 90° pulse. Mixing times from 1 ms to 80 s were employed to map the complete exchange and relaxation processes, with a recovery delay between transients of 80 s. Peak intensities were fitted for the selective inversion recovery and exchange processes using the CIFIT program[237]. This yielded a rate constant of 0.104 s^{-1} at 298 K and selective T_1 values of 27 s (Ha) and 16 s (Hc).

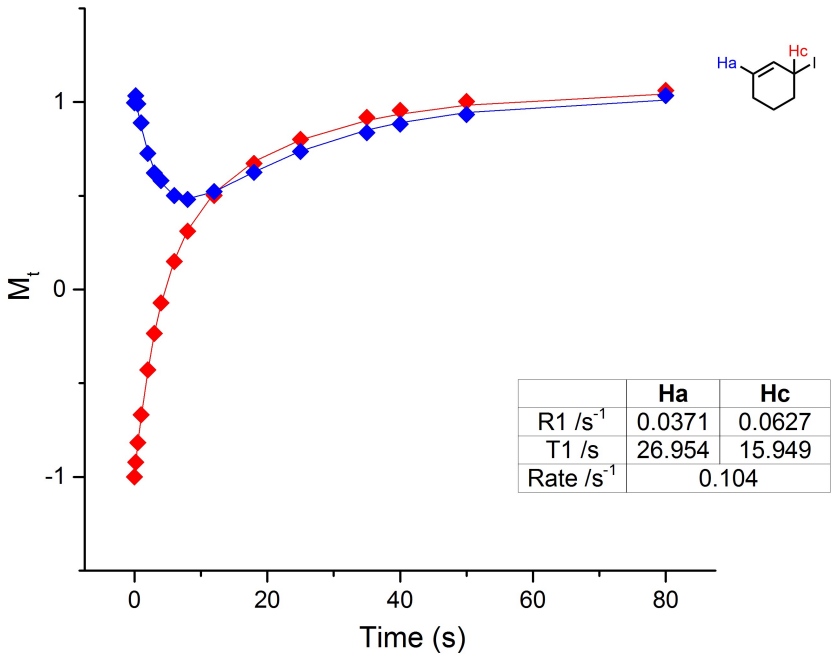

Spin saturation transfer difference[239]

Spin saturation build-up profiles were obtained by pre-saturating the resonance of Hc and monitoring the intensity change on Ha in the difference spectrum obtained by subtraction of the off-resonance control. Pre-saturation was achieved using a train of selective 90° Gaussian pulses with saturation times ranging from 0.5 s to 80 s, total recovery delays of 100s, with 8 transients recorded per spectrum using the *stddiff* pulse program (Bruker). The initial slope of the SSTD build-up profile provides the required exchange rate constant. This slope was obtained by fitting the profile to the expression:

$$\eta_{SSTD}(t) = A(1- \exp(-Bt)$$

with the initial slope being the product A.B and the maximum SSTD enhancement at long saturation times is A. Fitting was achieved using the *Boxlucas1* expression in Origin® 2015 to derive terms A (0.651) and B (0.123) which yielded a rate constant of 0.080 s^{-1} at 298K and a T_1 for Ha of 25 s.

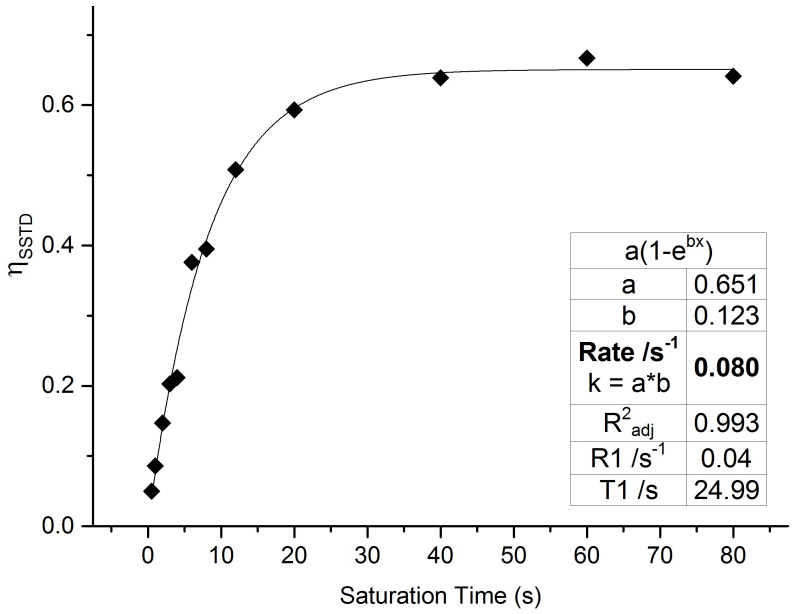

3) Diffusion Experiments

For each diffusion experiment, a preliminary ^{1}H NMR was run with locking and shimming. The delta parameters (diffusion delay Δ and diffusion gradient length δ) were determined using the dstebpgp3s DOSY pulse sequences developed by Muller[243,244] which uses convection compensation. Then the 2D DOSY experiment was run with the optimised parameters. Each DOSY was run in triplicate. The average and standard error of two aromatics signals and the CH-N benzylic signal of the ligand in each DOSY was calculated.

i) ***A***

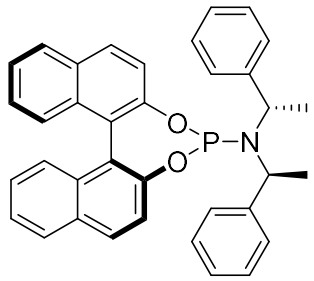

(*S, S, S*)-**A** (21.6 mg, 40.0 μmol, 10.0 mol%) was dissolved in $CDCl_3$ (0.8 mL). The clear solution was transferred via syringe to a flame-dried NMR tube under argon atmosphere equipped with a septa. After determining the optimised parameters, the DOSY experiment was ran (Δ=100 ms, δ=2000 μs, 16 pts, 32 scans, 2-98%).

*ii) CuI-****A***

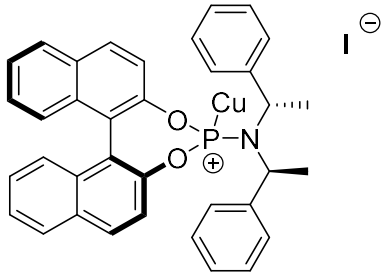

In a flame-dried flask, protected from light, under an argon atmosphere, CuI (7.7 mg, 40 μmol, 10 mol%) and (*S, S, S*)-**A** (21.6 mg, 40.0 μmol, 10.0 mol%) were dissolved in $CDCl_3$ (0.8 mL) and allowed to stir for 1 h at room temperature. The resulting mixture was transferred via syringe to a flame-dried NMR tube under

argon atmosphere equipped with a septa and vigorously shaken. After determining the optimised parameters, the DOSY experiment was ran (Δ=130 ms, δ=2000 μs, 16 pts, 64 scans, 2-95%). In a flame dried flask, ethylene (1 atm) was bubbled through a solution of Cp_2ZrHCl (201 mg, 0.80 mmol, 2.0 eq) in CD_2Cl_2 (0.5 mL) for 30 s and then stirred at room temperature under ethylene atmosphere until the solution went clear (15-20 min). The clear yellow hydrozirconation solution was transferred via syringe to the NMR tube under argon atmosphere and vigorously shaken. After determining the optimised parameters, the DOSY experiment was ran (Δ=130 ms, δ=2000 μs, 16 pts, 64 scans, 2-90%).

*iii) CuCl-**A***

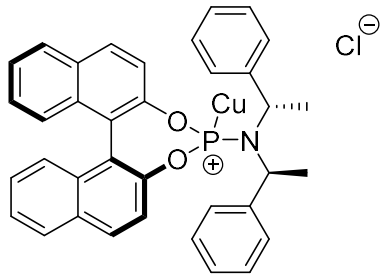

In a flame-dried flask, protected from light, under an argon atmosphere, CuCl (3.8 mg, 40 μmol, 10 mol%) and (*S, S, S*)-**A** (21.6 mg, 40.0 μmol, 10.0 mol%) were dissolved in $CDCl_3$ (0.8 mL) and allowed to stir for 1 h at room temperature. The resulting mixture was transferred via syringe to a flame-dried NMR tube under argon atmosphere equipped with a septa and vigorously shaken. After

determining the optimised parameters, the DOSY experiment was ran (Δ=120 ms, δ=2000 μs, 16 pts, 64 scans, 2-98%).

*iv) CuI-**A** and CuCl-**A***

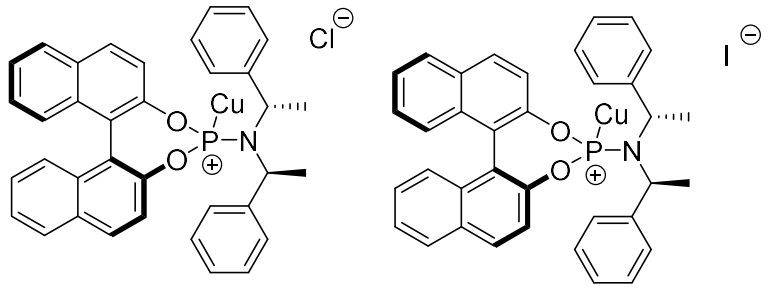

In a flame-dried flask, protected from light, under an argon atmosphere, CuI (3.9 mg, 20 μmol, 5.0 mol%), CuCl (1.9 mg, 20 μmol, 5.0 mol%) and (*S, S, S*)-**A** (21.6 mg, 40.0 μmol, 10.0 mol%) were dissolved in $CDCl_3$ (0.8 mL) and allowed to stir for 1 h at room temperature. After determining the optimised parameters, the DOSY experiment was ran (Δ=120 ms, δ=2000 μs, 16 pts, 64 scans, 2-98%).

*v) CuOTf-**A***

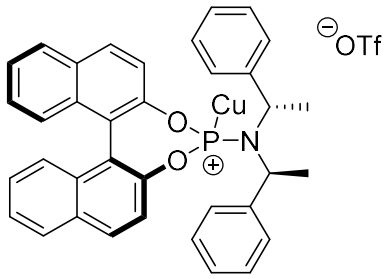

In a flame-dried flask, protected from light, under an argon atmosphere, CuCl (3.8 mg, 40 μmol, 10 mol%) and (*S, S, S*)-**A** (21.6 mg, 40.0 μmol, 10.0 mol%) were dissolved in $CDCl_3$ (0.8 mL) and allowed to stir for 1 h at room temperature. Then AgOTf (11.3 mg, 44.0 μmol, 11.0 mol%) was added to the Cu-complex and stirred for 15 min before filtering to a flame-dried NMR tube under argon atmosphere equipped with a septa. After determining the optimised parameters, the DOSY experiment was ran (Δ=100 ms, δ=2000 μs, 16 pts, 16 scans, 2-90%). In a flame dried flask, ethylene (1 atm) was bubbled through a solution of Cp_2ZrHCl (210 mg, 0.80 mmol, 2.0 eq) in CD_2Cl_2 (0.5 mL) for 30 s and then stirred at room temperature under ethylene atmosphere until the solution went clear (15-20 min). The clear yellow hydrozirconation solution was transferred via syringe to the NMR tube under argon atmosphere and vigorously shaken. After determining the optimised parameters, the DOSY experiment was ran (Δ=100 ms, δ=2000 μs, 16 pts, 16 scans, 2-90%).

4) Kinetic studies

*i) Kinetic using CuI-**A***

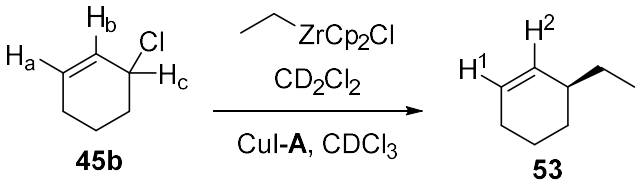

In a flame-dried flask, protected from light, under an argon atmosphere, CuI (7.7 mg, 40 μmol, 10 mol%) and (*S, S, S*)-**A** (21.6 mg, 40.0 μmol, 10.0 mol%) were dissolved in $CDCl_3$ (0.8 mL) and allowed to stir for 1 h at room temperature. In another flask, ethylene (1 atm) was bubbled through a solution of Cp_2ZrHCl (210 mg, 0.80 mmol, 2.0 eq) in CD_2Cl_2 (0.5 mL) for 30 s and then stirred at room temperature under ethylene atmosphere until the solution went clear (15-20 min). The cloudy white solution containing the Cu-complex was transferred via syringe to a flame-dried NMR tube under argon atmosphere equipped with a septa. The clear yellow hydrozirconation solution was transferred via syringe to the NMR tube under argon atmosphere and vigorously shaken. A preliminary ^1H NMR was run with locking and shimming. Then 3-chlorocyclohex-1-ene **45b** (47 μL, 0.40 mmol, 1.0 eq) was added dropwise via a microsyringe to the NMR tube and shaken vigorously, the kinetic was run without further locking and shimming.

^{1}H NMR Kinetics and modelling

First model

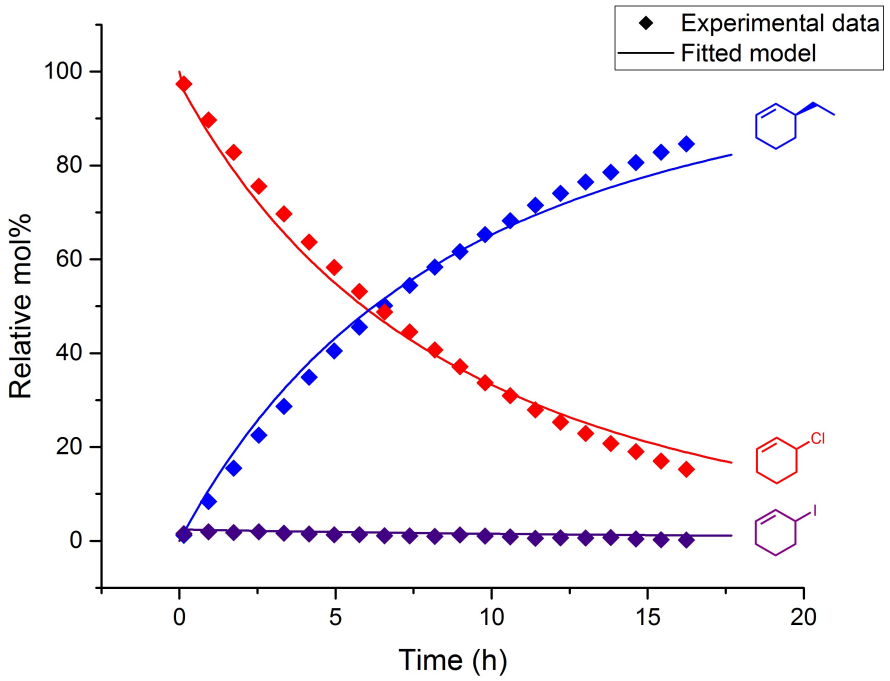

CuI-**A**+**45b**+$Cp_2ZrClEt$ → CuICl-**A**+**53** (k_I = 3.5x10^{-5} mol%.min^{-1}) (5.5)
CuI-**A**+**45b** → CuCl-**A**+**54** ($k_{allyliodide}$= 0.0080 mol%.min^{-1}) (5.6)
CuCl-**A**+**54** → CuI-**A**+**45b** ($k_{allylchloride}$= 0.029 mol%.min^{-1}) (5.7)

Residuals

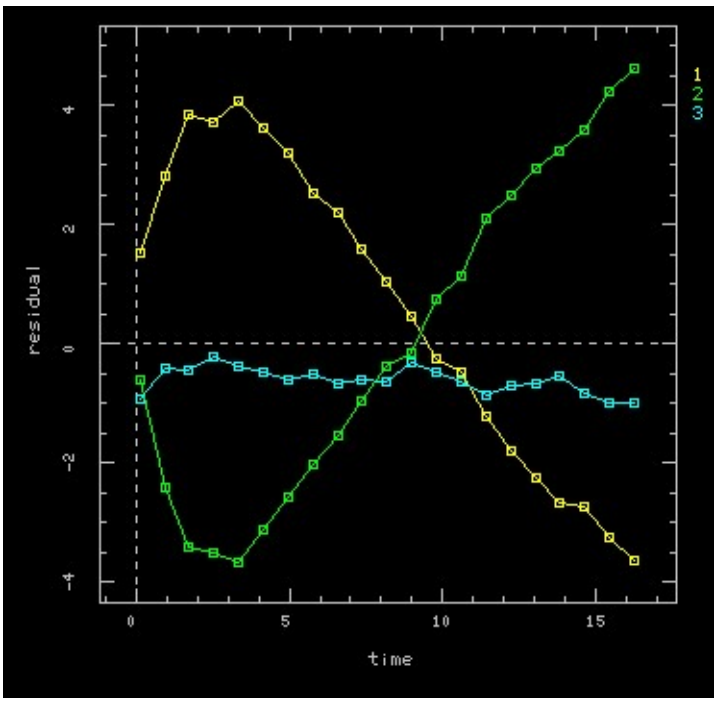

Second model

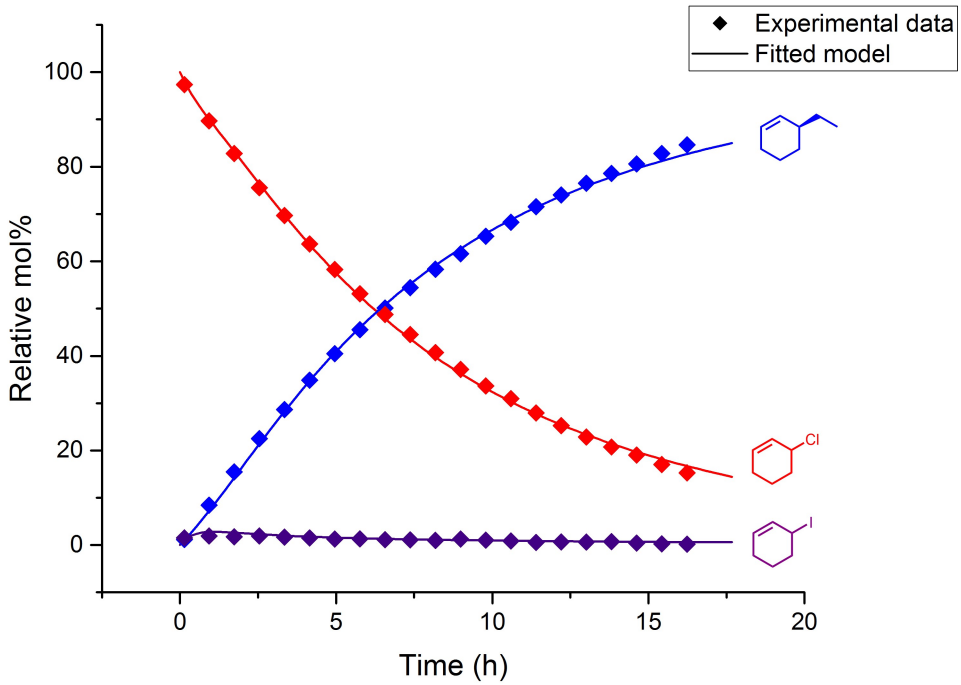

CuI-**A**+**45b**+$Cp_2ZrClEt$ → CuICl-**A**+**53**	(k_I = 3.5x10^{-5} mol%.min^{-1}) (5.8)
CuICl-**A**+**45b**+$Cp_2ZrClEt$ → CuICl-**A**+**53**+Cl	(k_{ICl}= 9.9x10^{-5} mol%.min^{-1}) (5.9)
CuI-**A**+**45b** → CuCl-**A**+**54**	($k_{allyliodide}$= 0.0080 mol%.min^{-1}) (5.10)
CuCl-**A**+**54** → CuI-**A**+**45b**	($k_{allylchloride}$= 0.029 mol%.min^{-1}) (5.11)

Residuals

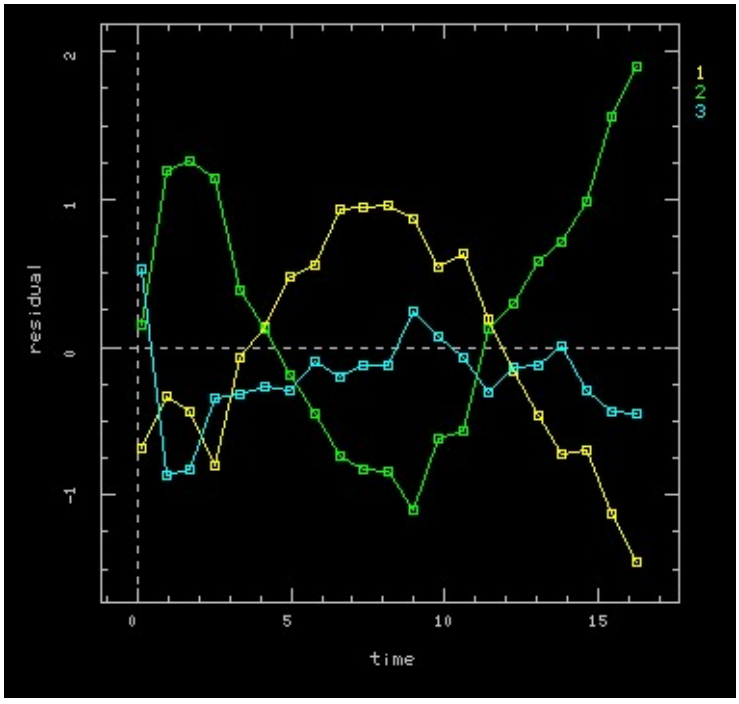

^{1}H NMR of Cu-Zr interactions when using CuI

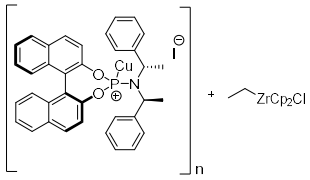

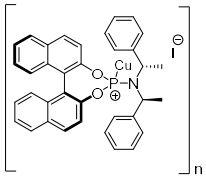

^{31}P NMR Kinetics

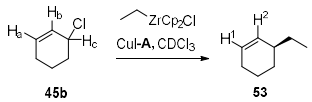

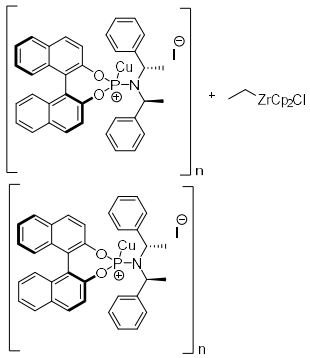

*ii) Kinetic using CuCl-**A***

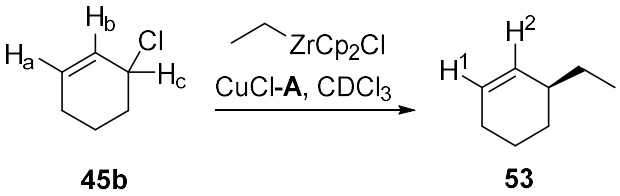

45b **53**

In a flame-dried flask, protected from light, under an argon atmosphere, CuCl (3.8 mg, 40 μmol, 10 mol%) and (*S, S, S*)-**A** (21.6 mg, 40.0 μmol, 10.0 mol%) were dissolved in $CDCl_3$ (0.8 mL) and allowed to stir for 1 h at room temperature. In another flask, ethylene (1 atm) was bubbled through a solution of Cp_2ZrHCl (210 mg, 0.80 mmol, 2.0 eq) in CD_2Cl_2 (0.5 mL) for 30 s and then stirred at room temperature under ethylene atmosphere until the solution went clear (15-20 min). The cloudy white solution containing the Cu-complex was transferred via syringe to a flame-dried NMR tube under argon atmosphere equipped with a septa. The clear yellow hydrozirconation solution was transferred via syringe to the NMR tube under argon atmosphere and vigorously shaken. A preliminary ^1H NMR was run with locking and shimming. Then 3-chlorocyclohex-1-ene **45b** (47 μL, 0.40 mmol, 1.0 eq) was added dropwise via a microsyringe to the NMR tube and shaken vigorously, the kinetic was run without further locking and shimming.

^{1}H NMR Kinetics and modelling

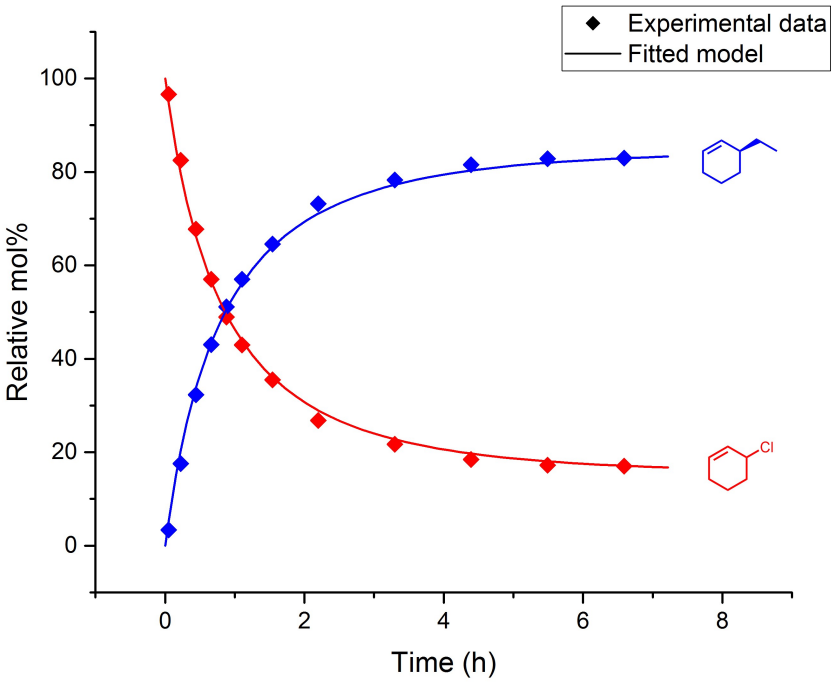

CuCl-**A** + **45b** → CuCl-**A** + **53** (k_{Cl}=5.9x10^{-4} mol%.min^{-1}) (5.3)
CuCl-**A** → CuCl-**A**$_{decomposed}$ (k_{dec2} = 0.46 mol%.min^{-1}) (5.4)

Residuals

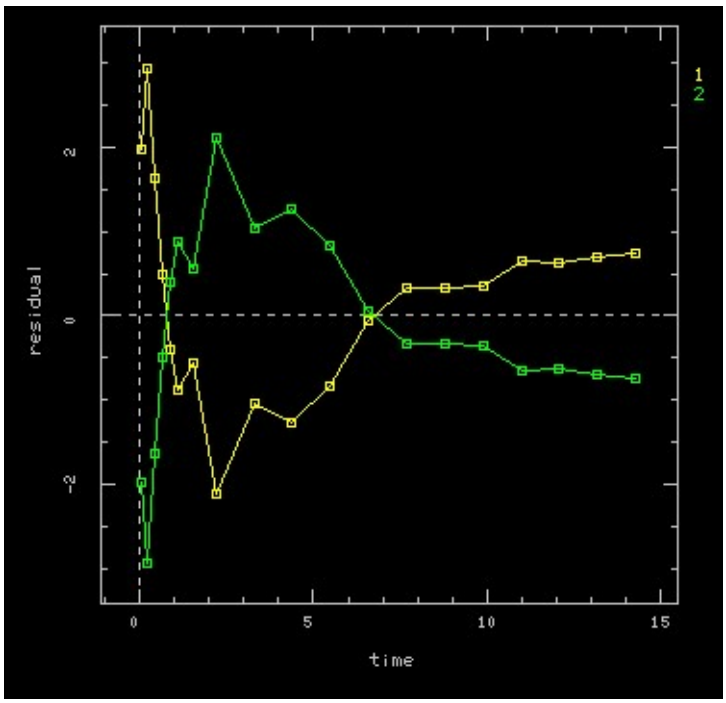

^{1}H NMR of Cu-Zr interactions when using CuCl

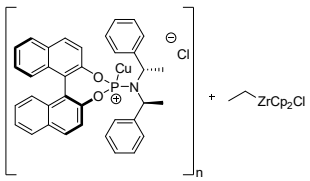

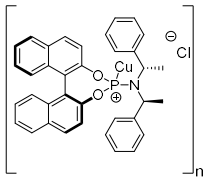

^{31}P NMR Kinetics

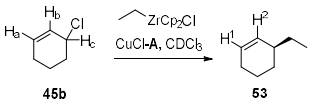

45b 53

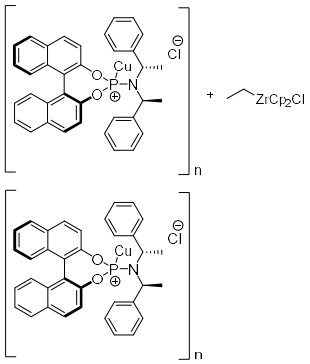

*iii) Kinetic using CuOTf-**A***

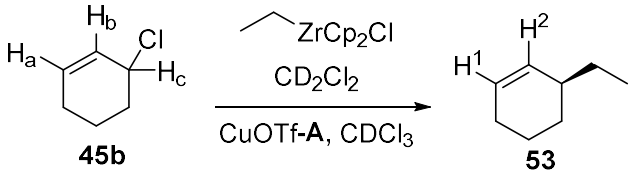

In a flame-dried flask, protected from light, under an argon atmosphere, CuCl (3.8 mg, 40 μmol, 10 mol%) and (*S, S, S*)-**A** (21.6 mg, 40.0 μmol, 10.0 mol%) were dissolved in $CDCl_3$ (0.8 mL) and allowed to stir for 1 h at room temperature. Then AgOTf (11.3 mg, 44.0 μmol, 11.0 mol%) was added to the Cu-complex and stirred for 15 min before filtering to a flame-dried NMR tube under argon atmosphere equipped with a septa. In another flask, ethylene (1 atm) was bubbled through a solution of Cp_2ZrHCl (210 mg, 0.80 mmol, 2.0 eq) in CD_2Cl_2 (0.5 mL) for 30 s and then stirred at room temperature under ethylene atmosphere until the solution went clear (15-20 min). The clear yellow hydrozirconation solution was transferred via syringe to the NMR tube under argon atmosphere and vigorously shaken. A preliminary ^1H NMR was run with locking and shimming. Then 3-chlorocyclohex-1-ene **45b** (47 μL, 0.40 mmol, 1.0 eq) was added dropwise via a microsyringe to the NMR tube and shaken vigorously, the kinetic was run without further locking and shimming.

^{1}H NMR Kinetics and modelling

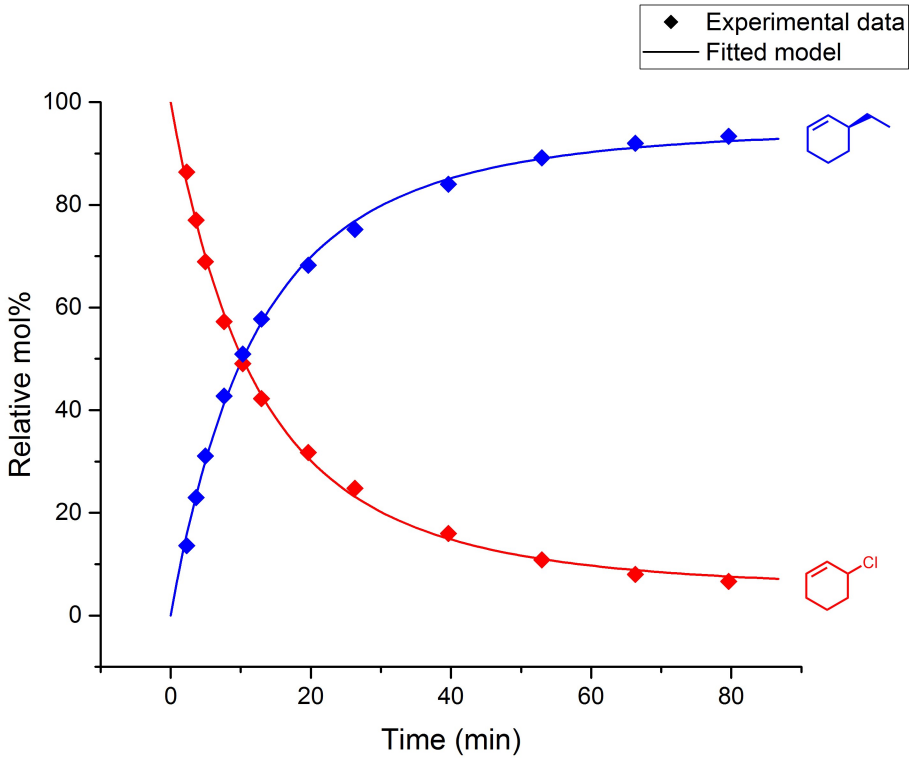

CuOTf-**A**+**45b** → CuOTf-**A**+**53** (k_{OTf} = 7.7x10^{-3} mol%.min^{-1}) (5.1)
CuOTf-**A** → CuOTf-**A**$_{decomposed}$ (k_{dec1} = 0.026 mol%.min^{-1}) (5.2)

Residuals

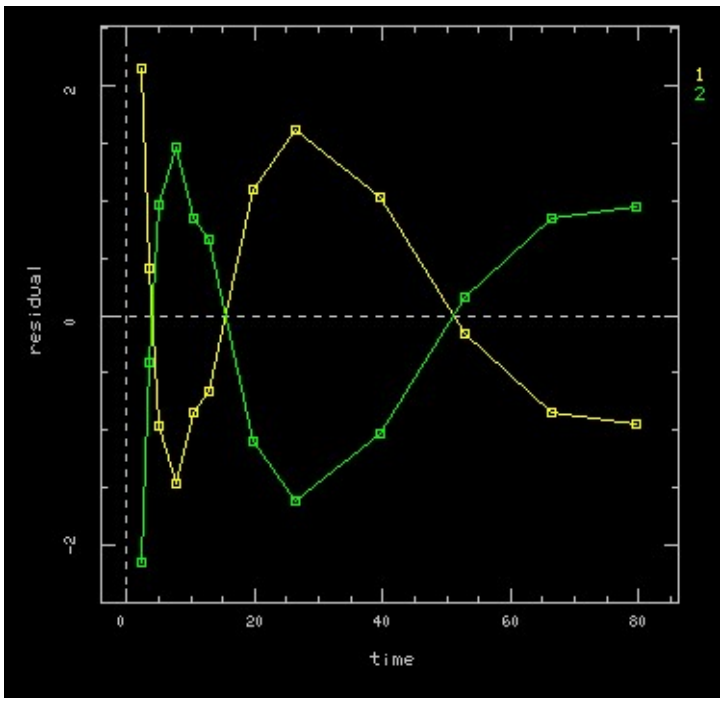

^{1}H NMR of Cu-Zr interactions when using CuOTf

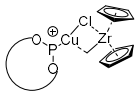

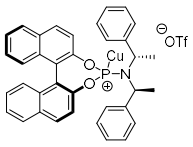

^{31}P NMR Kinetics

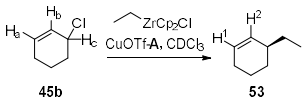

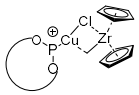

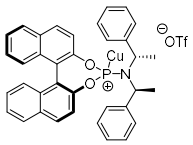

VIII. EXPERIMENTALS CHAPTER 6

1) Starting materials

Cyclohex-2-en-1-yl diethyl phosphate ***57***

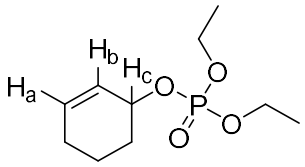

57

In analogy to a published procedure by Jackson[302], diethylchlrophosphate (7.0 mL, 48 mmol, 1.2 eq) was added to a solution of 2-cyclohexen-1-ol (4.0 mL, 41 mmol, 1.0 eq) and pyridine (16.4 mL, 203 mmol, 5.00 eq) in CH_2Cl_2 (100 mL) at 0 °C. After stirring overnight, the resulting solution was concentrated under reduced pressure, quenched with H_2O (10 mL) and washed with CH_2Cl_2 (3 x 10 mL). The combined organic layers were washed with brine (sat., 20 mL), dried over $MgSO_4$, filtered and concentrated under reduced pressure to afford the crude product. Purification by flash column chromatography (SiO_2, 30→100% Et_2O in pentane) yielded cyclohex-2-en-1-yl diethyl phosphate **57** (2.58 g, 11.8 mmol, 29% yield) as a colourless oil. **^{1}H NMR** (500 MHz, CD_2Cl_2) δ_H/ppm 5.94 (ddd, *J*=3.7, 4.2, 10.1 Hz, 1H, H*a*), 5.79-5.73 (m, 1H, H*b*), 4.84-4.77 (br m, 1H, H*c*), 4.05 (app quint., 4H, P(OC**H$_2$**-CH_3)$_2$), 2.12-2.02 (m, 1H, C**H$_2$**), 2.02-1.96 (m, 4H, C**H$_2$**), 1.66-1.55 (m, 1H, C**H$_2$**), 1.30 (t, *J*=7.1 Hz, 6H, C**H$_3$**); **^{13}C NMR** (125 MHz, CD_2Cl_2) δ_C/ppm 133.0 (**C**H=CH-CH), 126.7 (d, *J*=4.6 Hz, CH=**C**H-CH), 72.4 (d, *J*=6.3 Hz, CH=CH-**C**H), 63.4 (dd, *J*=5.8, 1.8 Hz, P(O**C**H$_2$-CH_3)$_2$), 30.3 (d,

J=4.6 Hz, **C**H$_2$), 25.2 (**C**H$_2$), 18.9 (**C**H$_2$), 16.3 (d, *J*=7.2 Hz, P(OCH$_2$-**C**H$_3$)$_2$); **^{31}P NMR** (202 MHz, CD_2Cl_2) δ_P/ppm -1.46 (s, 1P); **HRMS** (ESI) *m*/z calcd for $C_{10}H_{19}O_4NaP$ $[M+Na]^+$:257.09132, found: 257.09117; **IR (neat)** ν_{max}/cm^{-1} 2983, 2936, 1267, 970, 894, 817, 727. The spectral data was in accordance with literature[302].

^{1}H NMR (500 MHz, $CDCl_3$) δ_H/ppm 5.99-5.82 (m, 1H, H*a*), 5.84-5.77 (m, 1H, H*b*), 4.89 (br s, 1H, H*c*), 4.12 (2 x q, *J*= 7.2 Hz, 4H, P(OC**H$_2$**-CH$_3$)$_2$), 2.15-2.05 (m, 1H, C**H$_2$**), 2.05–1.84 (m, 4H, C**H$_2$**), 1.84-1.72 (m, 1H, C**H$_2$**), 1.36 (t, *J*=7.2 Hz, 6H, 2 x C**H$_3$**); **^{13}C NMR** (125 MHz, $CDCl_3$) δ_C/ppm 132.7 (**C**H=CH-CH), 126.3 (d, *J*=4.9 Hz, CH=**C**H-CH), 72.1 (d, *J*=5.8 Hz, CH=CH-**C**H), 63.5 (dd, *J*=5.6, 2.8 Hz, P(O**C**H$_2$-CH$_3$)$_2$), 29.9 (d, *J*=3.9 Hz, **C**H$_2$), 24.8 (**C**H$_2$), 18.5 (**C**H$_2$), 16.1 (d, *J*=6.8 Hz, P(OCH$_2$-**C**H$_3$)$_2$); **^{31}P NMR** (202 MHz, $CDCl_3$) δ_P/ppm -1.26 (s, 1P).

*Dynamics of cyclohex-2-en-1-yl diethyl phosphate **57***

Summary of EXSY Exchanges

(none)

2D EXSY (gradient NOE t_{mix}=800 ms)

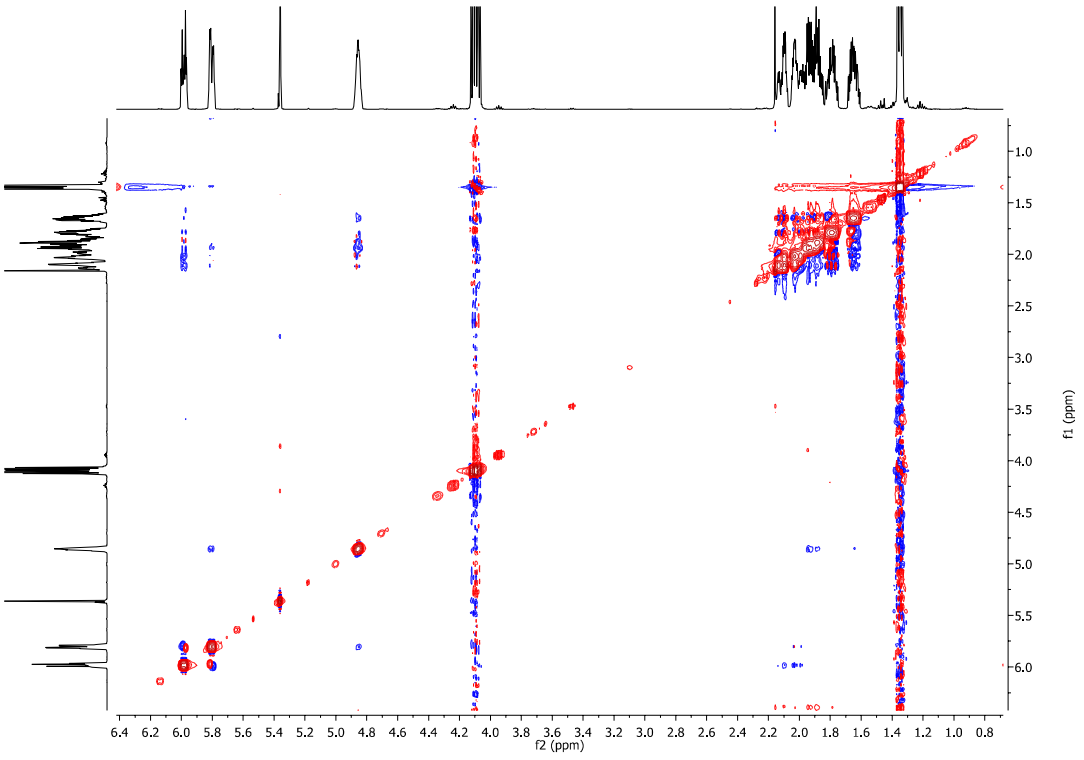

Cyclohex-2-en-1-yl-1-d diethyl phosphate (82% D) ***58***

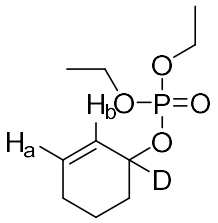

58

In analogy to a published procedure by Baldwin[303], in a flame-dried flask under argon atmosphere, $NaBD_4$ (867 mg, 20.7 mmol, 1.00 eq) was added portion-wise to a solution of 2-cyclohexenone (2.00 mL, 20.7 mmol, 1.00 eq) and $CeCl_3.7H_2O$ (7.7 g, 21 mmol, 1.0 eq) in MeOH (10 mL) at room temperature. After stirring at room temperature for 3 h, the resulting solution was quenched with ice (10 mL) and let to warm up at room temperature. The resulting suspension was washed extracted with Et_2O (3 x 20 mL). The combined organic layers were washed with brine (sat., 50 mL), dried over $MgSO_4$, filtered over Celite® and concentrated under reduced pressure to afford 1-deuteriocyclohex-2-en-1-ol (1.42 g, 14.3 mmol, 69%) as a colourless oil. **^{1}H NMR** (500 MHz, CD_2Cl_2) δ_H/ppm 5.84 (ddd, *J*= 10.1, 4.1, 3.7 Hz, 1H, H*a*), 5.78-5.72 (m, 1H, H*b*), 4.24-4.15 (br. m, 0.2 H, H*c*), 2.10-2.81 (m, 3H, C**H$_2$**), 1.81-1.67 (m, 1H, C**H$_2$**), 1.67-1.53 (m, 2H, C**H$_2$**), 1.48 (br. s, 1H, O**H**). The crude product was used as such in the subsequent step.

In analogy to a published procedure by Jackson[302], diethylchlrophosphate (2.5 mL, 17 mmol, 1.2 eq) was added to a solution of 1-deuteriocyclohex-2-en-1-ol (1.42 mg, 14.3 mmol, 1.00 eq) and pyridine (5.8 mL, 72 mmol, 5.0 eq) in CH_2Cl_2 (35 mL) at 0 °C. After stirring overnight, the resulting solution was concentrated under reduced pressure, quenched with H_2O (10 mL) and washed with CH_2Cl_2 (3

x 10 mL). The combined organic layers were washed with brine (sat., 20 mL), dried over $MgSO_4$, filtered and concentrated under reduced pressure to afford the crude product. Purification by flash column chromatography (SiO_2, 30->100% Et_2O in pentane) yielded cyclohex-2-en-1-yl-1-*d* diethyl phosphate **58** (1.61 g, 6.86 mmol, 48% yield, 82% D) as a colourless oil. **^{1}H NMR** (500 MHz, CD_2Cl_2) δ_H/ppm 5.87 (ddd, *J*= 10.0, 4.7, 3.7 Hz, 1H, H*a*), 5.68 (d, *J*= 10.2 Hz, 1H, H*b*), 4.78-4.70 (br. m, 0.2 H, H*c*), 4.03–3.93 (app. dquint., 4H, P(OC**H$_2$**-CH_3)$_2$), 2.06-1.95 (m, 1H, C**H$_2$**), 1.94-1.72 (m, 3H, C**H$_2$**), 1.72-1.62 (m, 1H, C**H$_2$**), 1.58-1.48 (m, 1H, C**H$_2$**), 1.23 (t, *J*=7.0 Hz, 6H, C**H$_3$**); **^{13}C NMR** (125 MHz, CD_2Cl_2) δ_C/ppm 132.7 (**C**H=CH-CH), 126.2 (d, *J*= 5.4 Hz, CH=**C**H-CH), 71.8 (d, *J*= 6.0 Hz, CH=CH-**C**H), 63.4 (dd, *J*= 6.4, 1.9 Hz, P(O**C**H_2-CH_3)$_2$), 29.7 (d, *J*=4.5 Hz, **C**H$_2$), 24.7 (**C**H$_2$), 18.5 (**C**H$_2$), 18.5, 15.9 (d, *J*=7.1 Hz, P(OCH_2-**C**H_3)$_2$); **^{31}P NMR** (202 MHz, CD_2Cl_2) δ_P/ppm -1.4 (s, 1P); **^{2}D NMR** (500 MHz, CH_2Cl_2) δ_D/ppm 4.80 (s, 1D); **HRMS** (ESI) *m*/z calcd for $C_{10}H_{18}DO_4NaP$ $[M+Na]^+$:258.09759, found: 258.09747; **IR (neat)** ν_{max}/cm^{-1} 2983, 2936, 1262, 1028, 967, 891.

(R)-N-isopropyl-2,3-dihydro-1H-inden-1-amine

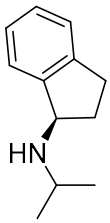

According to a modified procedure[9], acetone (0.32 mL, 4.3 mmol, 2.0 eq), was added to s stirring solution of (*R*)-2,3-dihydro-1*H*-inden-1-amine (0.28 mL, 2.2 mmol, 1.0 eq), in THF (10 mL) at room temperature. After 5 min, $NaB(OAc)_3H$ (910 mg 5.2 mmol, 2.4 eq) was added and the resulting suspension was stirred

for 48 h. Et_2O (15 mL) and $NaHCO_3$ (aq. sat., 10 mL) were added to the suspension and stirred for a further 30 min. The mixture was partitioned and washed with Et_2O (3 x 10 mL). The combined organic layers were dried over $MgSO_4$, filtered and concentrated under reduced pressure to afford the desired title amine (0.36 g, 1.5 mmol, 65%) as a yellow oil. The amine was used in the following step without further purification. **^{1}H NMR** (400 MHz, $CDCl_3$) δ_H/ppm 7.48-7.35 (m, 1H), 7.23 (dt, *J*= 9.5, 4.8 Hz, 3H), 4.36 (t, *J*= 6.7 Hz, 1H), 3.21-3.10 (m, 1H), 3.04 (ddd, *J*= 15.7, 8.6, 4.8 Hz, 1H), 2.82 (dt, *J*= 15.7, 7.6 Hz, 2H), 2.45 (dtd, *J*= 12.5, 7.6, 4.8 Hz, 1H), 1.93-1.81 (m, 1H), 1.27-1.12 (app. t, 6H). **^{13}C NMR** (100 MHz, $CDCl_3$) δ_C/ppm 144.8, 143.1, 127.0, 125.9, 124.3, 123.8, 60.0, 46.2, 33.8, 29.9, 23.0, 22.2. **HRMS** (ESI) *m*/z calcd for $C_{12}H_{18}N$ $[M+H]^+$:176.1428, found: 176.1434; **IR (neat)** ν_{max}/cm^{-1} 2946, 1378, 851, 753.

*(11bR)-N-((R)-2,3-dihydro-1H-inden-1-yl)-N-isopropyldinaphtho[2,1-d:1',2'-f][1,3,2]dioxaphosphepin-4-amine ((R,R)-**P**)*

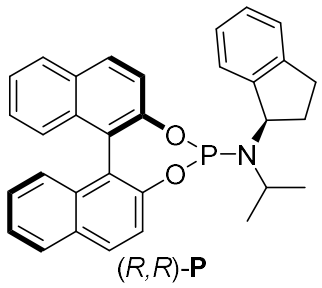

(*R*,*R*)-**P**

According to a modified procedure from Trost[293], triethylamine (0.72 mL, 4.0 mmol, 5.0 eq) was added dropwise to a solution of PCl_3 (0.10 mL, 0.80 mmol, 1.0 eq) in CH_2Cl_2 (2.5 mL) at 0 °C. The ice bath was removed and the solution left

to warm to room temperature before (*S*)-*N*-isopropyl-2,3-dihydro-1H-inden-1-amine (180 mg, 0.80 mmol, 1.0 eq) was added to the stirring solution. After 5 h, (*S*)-binaphthol (296 mg, 0.800 mmol, 1.00 eq) was added to the suspension and the subsequent mixture was left to stir overnight at room temperature. Then, the solution was filtered over a pad of silica and Celite® and rinsed with CH_2Cl_2 (15 mL). The resulting solution was concentrated under reduced pressure to afford a yellow residue. After flash column chromatography (Petrol: CH_2Cl_2: Et_3N; 74:25:1 SiO_2), the title ligand (*R,R*)-**P** (86 mg, 0.18 mmol, 17%) was obtained as a crystalline white foaming solid. **^{1}H NMR** (500 MHz, $CDCl_3$) δ_H/ppm 7.84 (d, *J*=8.7 Hz, 1H, Ar-**H**), 7.83-7.74 (m, 2H, Ar-**H**), 7.78 (d, *J*=6.5 Hz, 1H, Ar-**H**), 7.52 (d, *J*=7.7 Hz, 1H, Ar-**H**), 7.47 (d, *J*=8.7 Hz, 1H, Ar-**H**), 7.39 (d, *J*=8.9 Hz, 1H, Ar-**H**), 7.32-7.26 (m, 3H, Ar-**H**), 7.24-7.18 (m, 2H, Ar-**H**), 7.18-7.07 (m, 4H, Ar-**H**), 4.65 (dt, *J*=14.7, 8.1 Hz, 1H, N-C**H**-CH_2), 3.24 (dq, *J*=14.7, 6.9 Hz, 1H, N-C**H**-$(CH_3)_2$), 2.86 (ddd, *J*=15.8, 9.1, 1.7 Hz, 1H, C**H**$_2$), 2.65-2.56 (m, 1H, C**H**$_2$), 2.42-2.32 (m, 1H, C**H**$_2$), 2.11-1.99 (m, 1H, C**H**$_2$), 1.20 (d, *J*=6.8 Hz, 3H, C**H$_3$**), 1.11 (d, *J*=6.6 Hz, 3H, C**H$_3$**); **^{13}C NMR** (125 MHz, $CDCl_3$) δ_C/ppm 150.3 (d, *J*= 8.0 Hz, **Cq**-Ar), 150.0 (**Cq**-Ar), 144.6 (d, *J*=5.1 Hz, **Cq**-Ar), 143.1 (**Cq**-Ar), 132.8 (d, *J*= 1.5 Hz, **Cq**-Ar), 132.7 (**Cq**-Ar), 131.3 (**Cq**-Ar), 130.5 (**Cq**-Ar), 130.2 (**C**H-Ar), 129.5 (**C**H-Ar), 128.2 (**C**H-Ar), 128.2 (**C**H-Ar), 127.3 (**C**H-Ar), 127.1 (**C**H-Ar), 127.1 (**C**H-Ar), 126.4, (**C**H-Ar) 125.9 (**C**H-Ar), 125.8 (**C**H-Ar), 124.8 (**C**H-Ar), 124.6 (**C**H-Ar), 124.6, (**C**H-Ar) 124.3 (**C**H-Ar), 124.1 (d, *J*=5.4 Hz, **Cq**-Ar), 122.4 (**C**H-Ar), 122.4 (**C**H-Ar), 121.7 (d, *J*=2.7 Hz, **Cq**-Ar), 59.4 (d, *J*=17.6 Hz, N-**C**H-CH_2), 45.9 (d, *J*=7.4 Hz, N-**C**H-$(CH_3)_2$), 36.6 (**C**H_2), 30.1 (**C**H_2), 25.1 (d, *J*=5.4 Hz, **C**H_3), 23.9 (d, *J*=6.6 Hz, **C**H_3); **^{31}P NMR** (200 MHz, $CDCl_3$) δ_P/ppm 151.4 (s, 1P). **HRMS** (EI) *m*/z calcd for $C_{32}H_{28}NO_2P$

$[M]^+$:489.1858, found: 489.1865; **IR (neat)** ν_{max}/cm^{-1} 2969, 1590, 1232, 947, 790, 751. $\mathbf{[\alpha]_D^{25}}$ = +145.5 (c=0.8 in $CHCl_3$); **Mp** 238-242°C;

^{1}H NMR (500 MHz, CD_2Cl_2) δ_H/ppm 7.98 (d, *J*=9.2 Hz, 1H, Ar-**H**), 7.96-7.88 (m, 3H, Ar-**H**), 7.63 (d, *J*=7.6 Hz, 1H, Ar-**H**), 7.60 (d, *J*=8.8 Hz, 1H, Ar-**H**), 7.51 (d, *J*=8.8 Hz, 1H, Ar-**H**), 7.45-7.38 (m, 2H, Ar-**H**), 7.36 (d, *J*=8.4 Hz, 1H, Ar-**H**), 7.34-7.30 (m, 1H, Ar-**H**), 7.29-7.19 (m, 5H, Ar-**H**), 4.65 (dt, *J*= 16.1, 8.1 Hz, 1H, N-C**H**-CH_2), 3.22 (dq, *J*= 14.5, 6.7 Hz, 1H, N-C**H**-$(CH_3)_2$), 2.86 (ddd, *J*= 15.9, 9.1, 2.6 Hz, 1H, C**H**$_2$), 2.67-2.56 (m, 1H, C**H**$_2$), 2.42-2.31 (m, 1H, C**H**$_2$), 2.11–1.99 (m, 1H, C**H**$_2$), 1.28 (d, *J*=6.5 Hz, 3H, C**H$_3$**), 1.18 (d, *J*=6.3 Hz, 3H, C**H$_3$**); **^{13}C NMR** (125 MHz, CD_2Cl_2) δ_C/ppm 150.7 (d, *J*= 8.2 Hz, **Cq**-Ar), 150.5 (**Cq**-Ar), 145.2 (d, *J*=4.3 Hz, **Cq**-Ar), 143.6 (**Cq**-Ar), 133.1 (d, *J*= 1.8 Hz, **Cq**-Ar), 133.1 (**Cq**-Ar), 131.8 (**Cq**-Ar), 131.0 (**Cq**-Ar), 130.7 (**C**H-Ar), 130.0 (**C**H-Ar), 128.7 (**C**H-Ar), 128.7 (**C**H-Ar), 127.7 (**C**H-Ar), 127.3 (**C**H-Ar), 127.2 (**C**H-Ar), 126.8 (**C**H-Ar), 126.4 (**C**H-Ar), 126.3 (**C**H-Ar), 125.1 (**C**H-Ar), 125.1 (**C**H-Ar), 125.0 (**C**H-Ar), 124.8 (**C**H-Ar), 124.3 (d, *J*= 5.4 Hz, **Cq**-Ar), 122.7 (**C**H-Ar), 122.6 (d, *J*=1.6 Hz, **C**H-Ar), 122.0 (d, *J*=2.5 Hz, **Cq**-Ar), 59.6 (d, *J*=21.1 Hz, N-**C**H-CH_2), 46.4 (d, *J*=6.3 Hz, N-**C**H-$(CH_3)_2$), 37.2 (**C**H_2), 30.5 (**C**H_2), 25.0 (d, *J*=5.3 Hz, **C**H_3), 23.8 (d, *J*=5.3 Hz, **C**H_3); **^{31}P NMR** (200 MHz, CD_2Cl_2) δ_P/ppm 152.1 (s, 1P).

*CuI-**P***

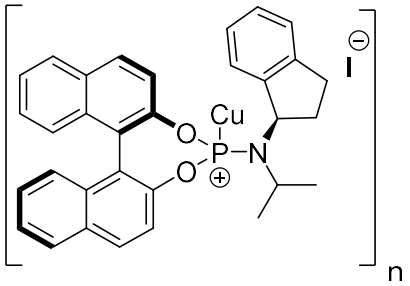

In a flame-dried flask, protected from light, under an argon atmosphere, CuI (7.6 mg, 40 μmol, 10 mol%) and (*R, R*)-**P** (19.6 mg, 40.0 μmol, 10.0 mol%) were dissolved in CH_2Cl_2 (0.8 mL) and CD_2Cl_2 (1 drop) and allowed to stir for 1 h at room temperature. The cloudy white solution containing the Cu-complex was transferred via syringe to a flame-dried NMR tube under argon atmosphere equipped with a septa. **^{1}H NMR** (500 MHz, CD_2Cl_2) δ_H/ppm 7.93-7.72 (m, 5H, Ar-**H**), 7.44 (br. d, *J*=8.1 Hz, 1H, Ar-**H**), 7.36 (d, *J*=7.7 Hz, 1H, Ar-**H**), 7.35-7.30 (m, 2H, Ar-**H**), 7.24 (d, *J*=8.1 Hz, 1H, Ar-**H**), 7.19-7.10 (m, 3H, Ar-**H**), 7.05 (br dd, *J*=8.6, 7.2 Hz, 1H, Ar-**H**), 6.86 (br dd, *J*=9.0, 6.3 Hz, 1H, Ar-**H**), 6.57 (br s, 1H, Ar-**H**), 4.63 (br s, 1H, N-C**H**-CH_2), 3.06 (br s, 1H, N-C**H**$(CH_3)_2$), 2.63 (br s, 1H, C**H$_2$**), 2.26 (br s, 1H, C**H$_2$**), 2.11 (br s, 1H, C**H$_2$**), 1.98 (br s, 1H, C**H$_2$**), 0.89 (br s, 6H, 2 x C**H$_3$**); **^{13}C NMR** (125 MHz, CD_2Cl_2) δ_C/ppm 149.5 (br. s, **Cq**-Ar), 149.0 (br. s, **Cq**-Ar), 143.3 (**Cq**-Ar), 142.8 (br, **Cq**-Ar), 133.0 (**Cq**-Ar), 132.9 (**Cq**-Ar), 132.1 (**Cq**-Ar), 131.4 (**Cq**-Ar), 130.9 (**C**H-Ar), 130.4 (**C**H-Ar), 128.9 (**C**H-Ar), 128.7 (**C**H-Ar), 128.0 (br, **C**H-Ar), 127.5 (**C**H-Ar), 127.2 (**C**H-Ar), 126.9 (br, **C**H-Ar), 126.6 (**C**H-Ar), 126.5 (**C**H-Ar), 125.5 (**C**H-Ar), 125.3 (**C**H-Ar), 125.2 (**C**H-Ar), 125.1 (**C**H-Ar), 123.8 (br. s, **Cq**-Ar), 123.5 (br. s, **Cq**-Ar), 122.2 (**C**H-Ar), 122.1 (**C**H-Ar), 60.9 (br,

N-**C**H-CH_2), 47.8 (N-**C**H(CH_3)$_2$), 35.4 (br, **C**H_2), 30.2 (**C**H_2), 24.9 (br, **C**H_3), 23.5 (**C**H_3); **^{31}P NMR** (200 MHz, CD_2Cl_2) δ_P/ppm 127.41 (br. s, 1P).

*CuCl-**P***

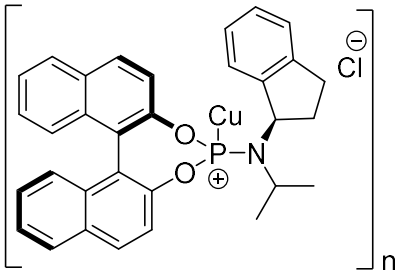

In a flame-dried flask, protected from light, under an argon atmosphere, CuCl (3.8 mg, 40 μmol, 10 mol%) and (*R, R*)-**P** (19.6 mg, 40.0 μmol, 10.0 mol%) were dissolved in CH_2Cl_2 (0.8 mL) and CD_2Cl_2 (1 drop) and allowed to stir for 1 h at room temperature. The cloudy white solution containing the Cu-complex was transferred via syringe to a flame-dried NMR tube under argon atmosphere equipped with a septa. **^{1}H NMR** (500 MHz, CD_2Cl_2) δ_H/ppm 7.93 (d, *J*=8.4 Hz, 1H, Ar-**H**), 7.83 (d, *J*=9.0 Hz, 1H, Ar-**H**), 7.80 (d, *J*=8.4 Hz, 2H, Ar-**H**), 7.67 (d, *J*=9.0 Hz, 1H, Ar-**H**), 7.43-7.30 (m, 4H, Ar-**H**), 7.26 (d, *J*=9.0 Hz, 1H, Ar-**H**), 7.20-7.07 (m, 4H, Ar-**H**), 6.96 (dd, *J*=8.4, 7.2 Hz, 1H, Ar-**H**), 6.72 (br d, *J*=6.0 Hz, 1H, Ar-**H**), 4.67-4.56 (m, 1H, N-C**H**-CH_2), 3.03 (br s, 1H, N-C**H**(CH_3)$_2$), 2.77-2.61 (m, 1H, C**H$_2$**), 2.42-2.29 (m, 1H, C**H$_2$**), 2.19 (br s, 1H, C**H$_2$**), 2.01 (br s, 1H, C**H$_2$**), 0.97 (d, *J*=6.8 Hz, 3H, C**H$_3$**), 0.90 (br s, 3H, C**H$_3$**); **^{13}C NMR** (125 MHz, CD_2Cl_2) δ_C/ppm 149.4 (d, *J*=11.7 Hz, **Cq**-Ar), 149.1 (**Cq**-Ar), 143.6 (**Cq**-Ar), 142.9 (br s., **Cq**-Ar), 132.9 (**Cq**-Ar), 132.9 (**Cq**-Ar), 132.2 (**Cq**-Ar), 131.4 (**Cq**-Ar), 131.2 (**C**H-Ar), 130.4 (**C**H-Ar), 128.8 (**C**H-Ar),

128.7 (**C**H-Ar), 128.1 (**C**H-Ar), 127.4 (**C**H-Ar), 127.2 (**C**H-Ar), 126.9 (br. s, **C**H-Ar), 126.6 (**C**H-Ar), 126.5 (**C**H-Ar), 125.5 (**C**H-Ar), 125.4 (**C**H-Ar), 125.3 (d, *J*=2.7 Hz, **C**H-Ar), 124.9 (**Cq**-Ar), 123.7 (br. **C**H-Ar), 123.2 (br. **C**H-Ar), 122.0 (**C**H-Ar), 121.9 (**Cq**-Ar), 61.0 (br. s, N-**C**H-CH_2), 47.6 (br. d, *J*=5.5 Hz, N-**C**H$(CH_3)_2$), 35.6 (br s., **C**H_2), 30.1 (**C**H_2), 25.0 (**C**H_3), 23.7 (**C**H_3); **^{31}P NMR** (200 MHz, CD_2Cl_2) δ_P/ppm 128.1 (br. s, 1P).

2) Kinetics

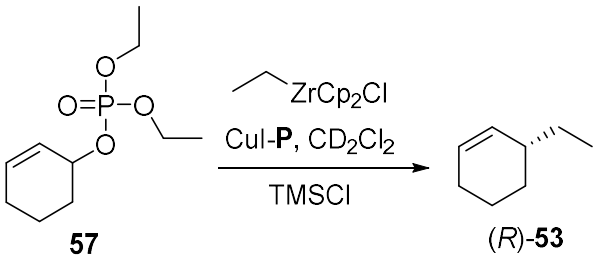

In a flame-dried flask, protected from light, under an argon atmosphere, CuI (7.7 mg, 40 μmol, 10 mol%) and (*R, R*)-**P** (19.6 mg, 40.0 μmol, 10.0 mol%) were dissolved in CD_2Cl_2 (0.8 mL) and allowed to stir for 1 h at room temperature. In another flask, ethylene (1 atm) was bubbled through a solution of Cp_2ZrHCl (210 mg, 0.80 mmol, 2.0 eq) in CD_2Cl_2 (0.5 mL) for 30 s and then stirred at room temperature under ethylene atmosphere until the solution went clear (15-20 min). The cloudy white solution containing the Cu-complex was transferred via syringe to a flame-dried NMR tube under argon atmosphere equipped with a septa. The clear yellow hydrozirconation solution was transferred via syringe to the NMR tube under argon atmosphere and vigorously shaken. A preliminary ^{1}H NMR was run with locking and shimming. Then cyclohex-2-en-1-yl diethyl

phosphate **57** (74 µL, 0.40 mmol, 1.0 eq) was added dropwise via a microsyringe to the NMR tube and shaken vigorously, then TMSCl (50 µL, 0.40 mmol, 1.0 eq) was added via a microsyringe to the NMR tube and shaken vigorously. The kinetic was run without further locking and shimming.

^{1}H NMR Kinetics and modelling

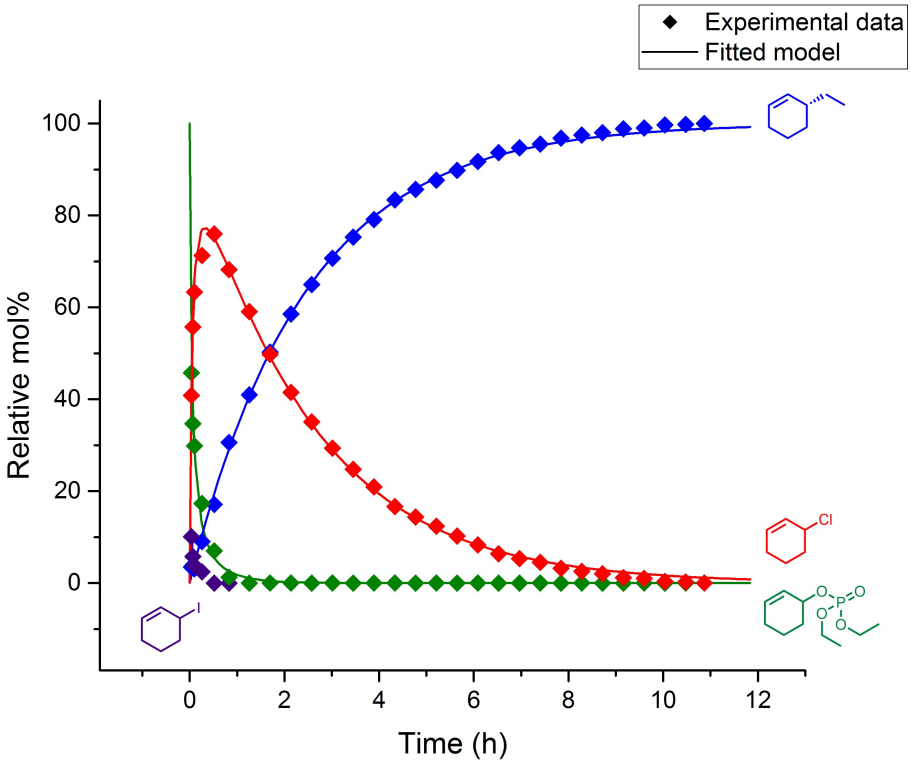

45b + CuI-**P** → **53** + CuI-**P** + Cl^- (k_1 = 0.0421 mol%.min^{-1}) (6.1)
57 + CuI-**P** → **53** + CuI-**P** (k_2 = 0.023 mol%.min^{-1}) (6.2)
57 + TMSCl → **45b** (k_{TMSCl} = 0.212 mol%.min^{-1}) (6.3)
57 + Cl^- → **45b** (k_{Cl} = 0.05 mol%.min^{-1}) (6.4)

Residuals

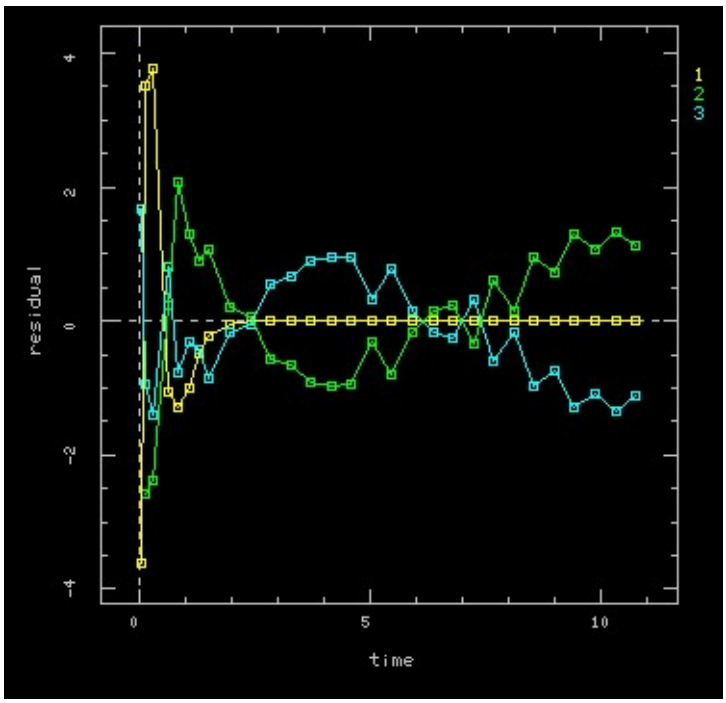

^{31}P NMR Kinetics

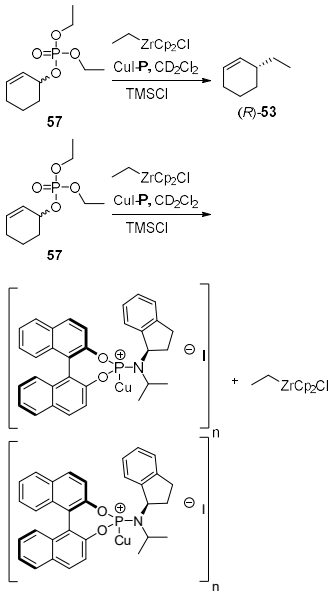

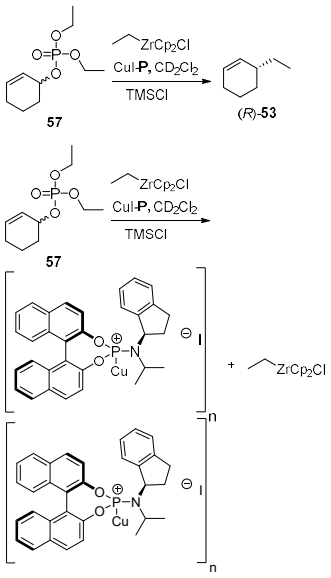

Dynamics during kinetics

Summary of EXSY Exchanges

(none)

2D EXSY (gradient NOE t_{mix}=800 ms)

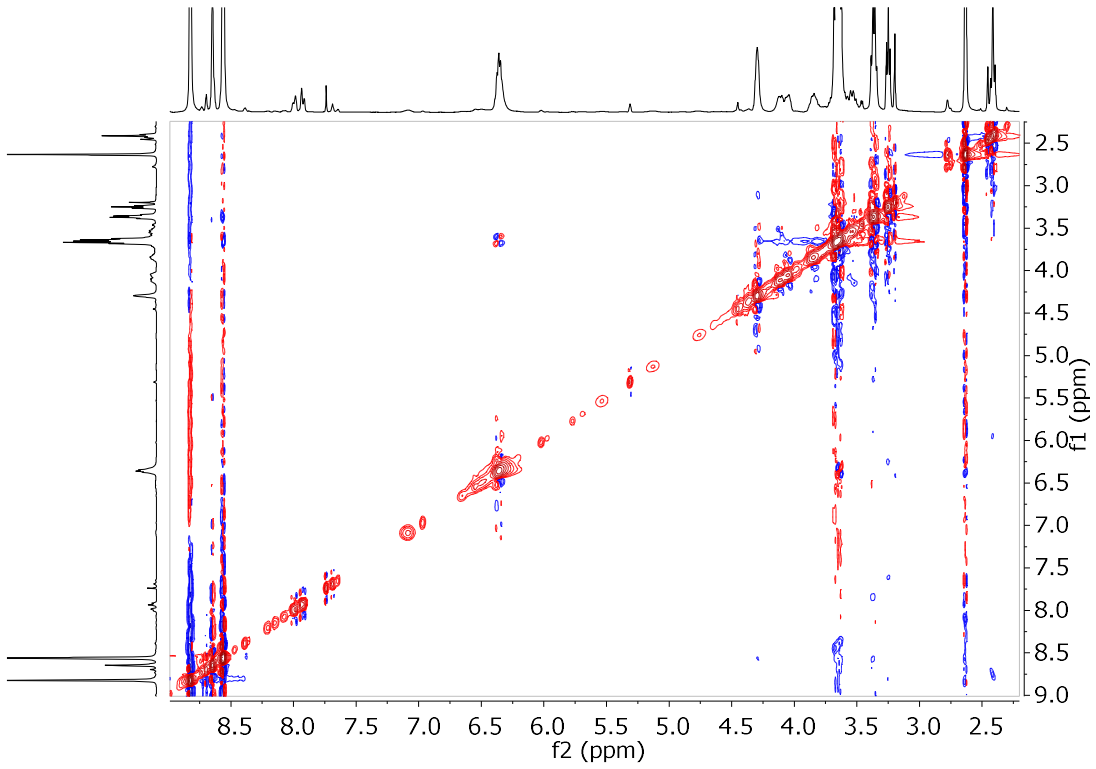

3) Interactions

*Allylphosphate **57** + TMSCl*

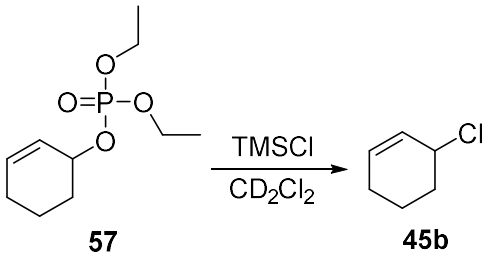

Cyclohex-2-en-1-yl diethyl phosphate **57** (74 µL, 0.40 mmol, 1.0 eq) was added via a microsyringe to a flame-dried NMR tube under argon atmosphere equipped with a septa and dissolved in CD_2Cl_2. A preliminary ^1H NMR was run with locking and shimming. Then TMSCl (50 µL, 0.40 mmol, 1.0 eq) was added via a microsyringe to the NMR tube and shaken vigorously and the kinetic was run without further locking and shimming.

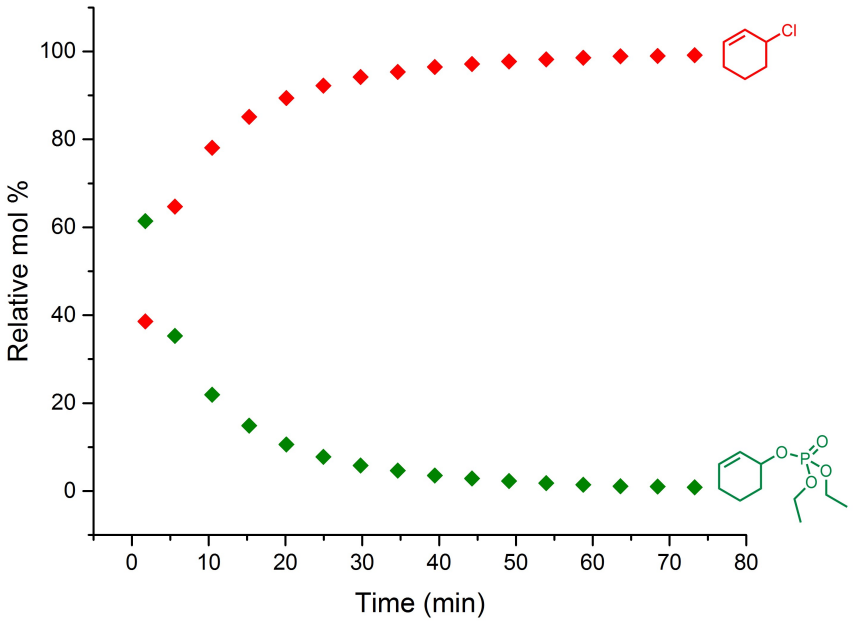

^{31}P NMR

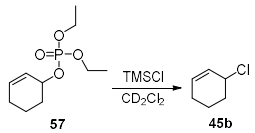

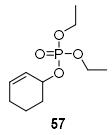

*CuI-**P**+Allylphosphate **57***

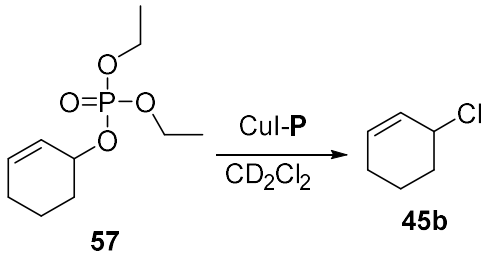

In a flame-dried flask, protected from light, under an argon atmosphere, CuI (7.7 mg, 40 μmol, 10 mol%) and (*R, R*)-**P** (19.6 mg, 40.0 μmol, 10.0 mol%) were dissolved in CD_2Cl_2 (0.8 mL) and allowed to stir for 1 h at room temperature. The cloudy white solution containing the Cu-complex was transferred via syringe to a flame-dried NMR tube under argon atmosphere equipped with a septa. A

preliminary ^{1}H NMR was run with locking and shimming. Then cyclohex-2-en-1-yl diethyl phosphate **57** (74 µL, 0.40 mmol, 1.0 eq) was added dropwise via a microsyringe to the NMR tube and shaken vigorously. The kinetic was run without locking and shimming.

^{1}H NMR

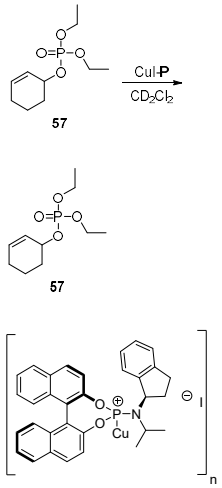

^{31}P NMR

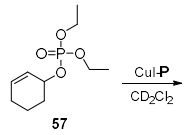

57

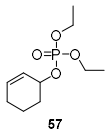

57

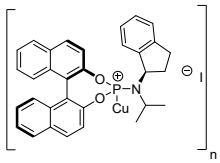

*Dynamics of Cyclohex-2-en-1-yl diethyl phosphate **57**+CuI-**P***

Summary of EXSY Exchanges

(none)

2D EXSY (gradient NOE t_{mix}=800 ms)

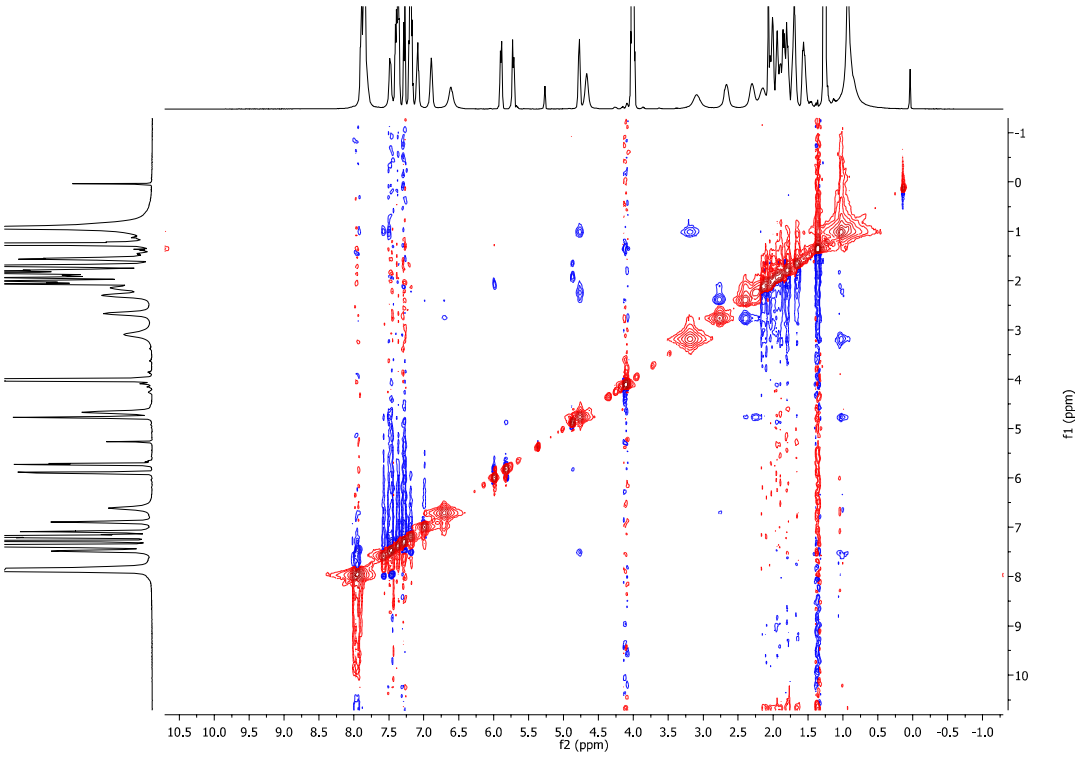

*CuI-**P** + Allylphosphate **57** + TMSCl*

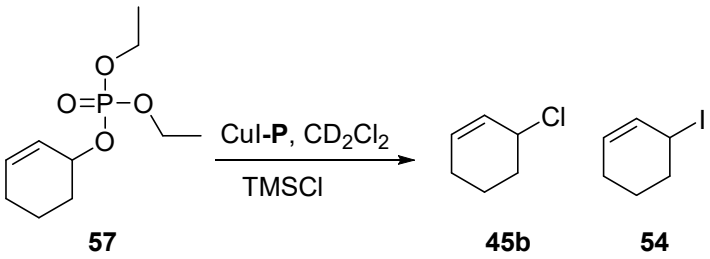

In a flame-dried flask, protected from light, under an argon atmosphere, CuI (7.7 mg, 40 μmol, 10 mol%) and *(R,R)*-**P** (19.6 mg, 40.0 μmol, 10.0 mol%) were dissolved in CD_2Cl_2 (0.8 mL) and allowed to stir for 1 h at room temperature. The cloudy white solution containing the Cu-complex was transferred via syringe to a flame-dried NMR tube under argon atmosphere equipped with a septa. A preliminary ^1H NMR was run with locking and shimming. Then cyclohex-2-en-1-

yl diethyl phosphate **57** (74 µL, 0.40 mmol, 1.0 eq) was added dropwise via a microsyringe to the NMR tube and shaken vigorously. A short ^{1}H NMR kinetic was run (20 min) without locking and shimming. Then TMSCl (50 µL, 0.40 mmol, 1.0 eq) was added via a microsyringe to the NMR tube and shaken vigorously. The kinetic was run without locking and shimming.

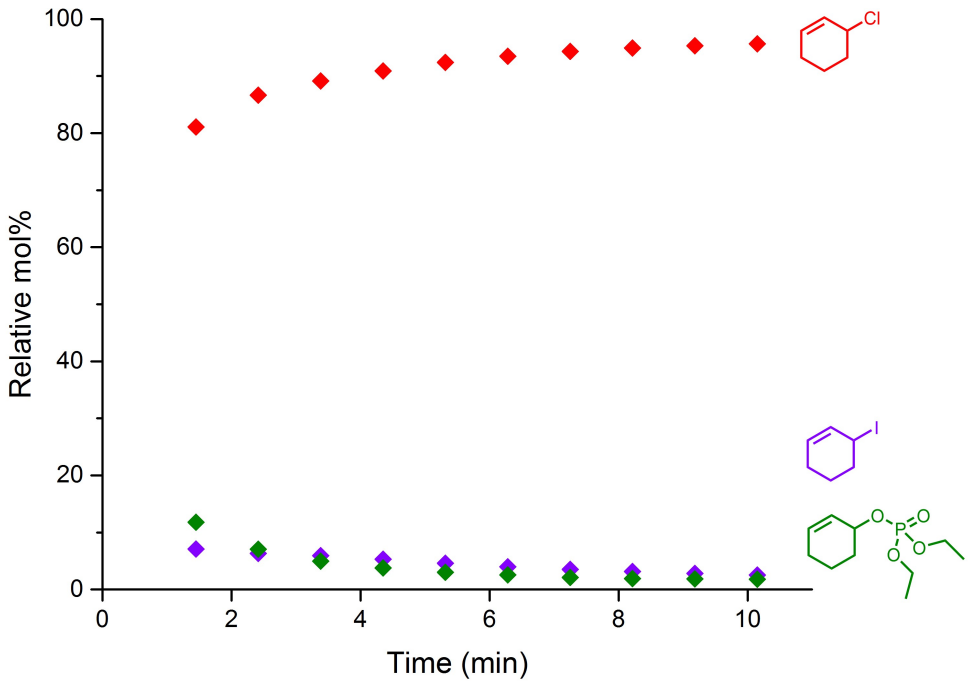

^{1}H NMR

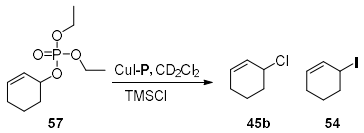

57 45b 54

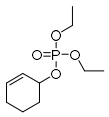

57

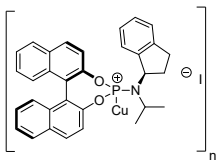

^{31}P NMR

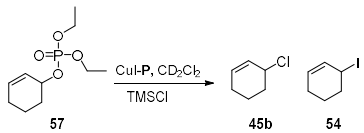

57 45b 54

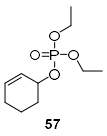

57

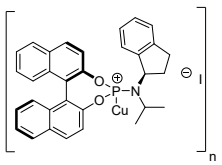

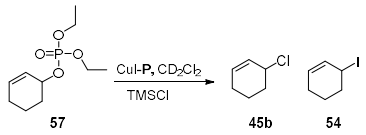

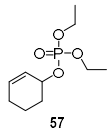

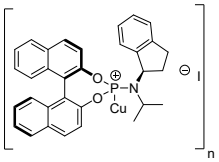

*Dynamics of cyclohex-2-en-1-yl diethyl phosphate **57** +CuI-**P**+TMSCl*

Summary of EXSY Exchanges

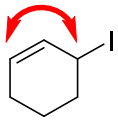

2D EXSY (gradient NOE t_{mix}=800 ms)

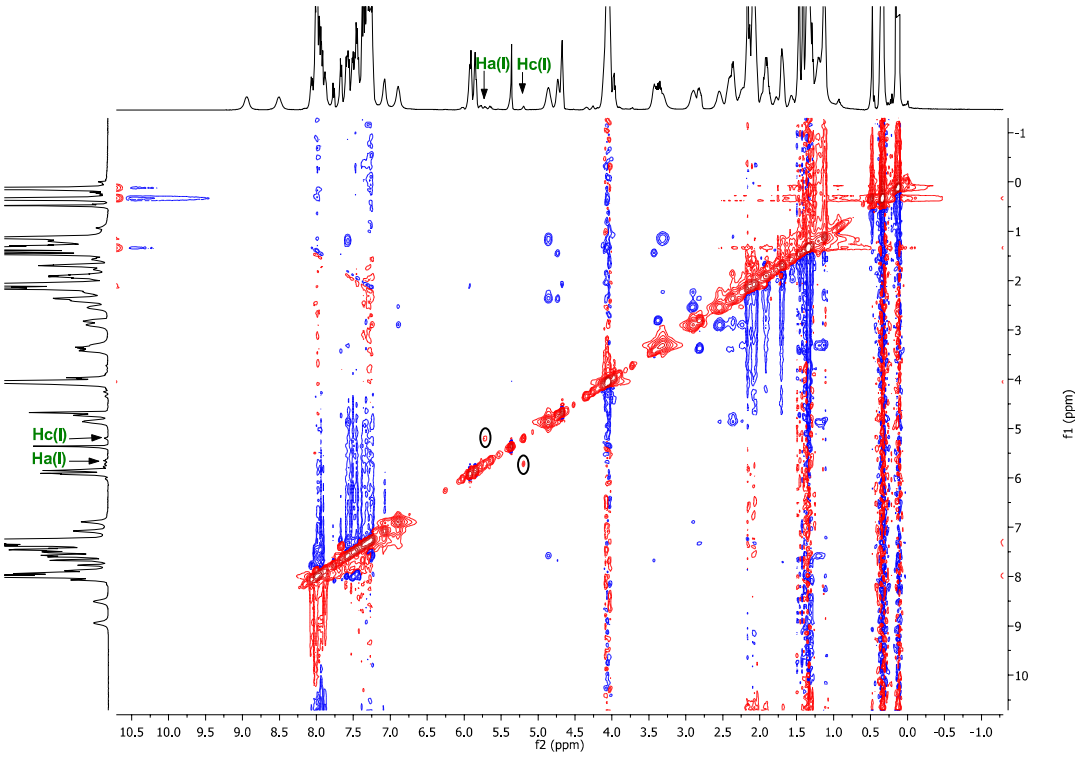

*$Cp_2ZrEtCl$ + Allylphosphate **57** + TMSCl*

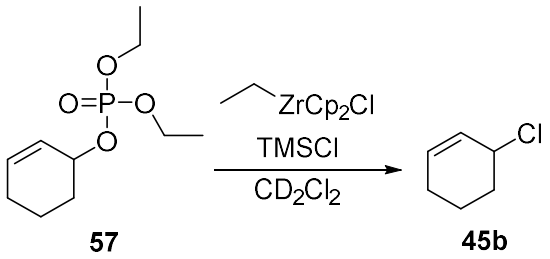

In a flame-dried flask, protected from light, ethylene (1 atm) was bubbled through a solution of Cp_2ZrHCl (210 mg, 0.80 mmol, 2.0 eq) in CD_2Cl_2 (0.5 mL) for 30 s and then stirred at room temperature under ethylene atmosphere until the solution went clear (15-20 min). The clear yellow hydrozirconation solution was transferred via syringe to a flame-dried NMR tube under argon atmosphere equipped with a septa. CD_2Cl_2 (0.8 mL) was added to the NMR tube. A

preliminary ^{1}H NMR was run with locking and shimming. Then cyclohex-2-en-1-yl diethyl phosphate **57** (74 µL, 0.40 mmol, 1.0 eq) was added dropwise via a microsyringe to the NMR tube and shaken vigorously. A short ^{1}H NMR kinetic was run (20 min) without locking and shimming. Then TMSCl (50 µL, 0.40 mmol, 1.0 eq) was added via a microsyringe to the NMR tube and shaken vigorously. The kinetic was run without locking and shimming.

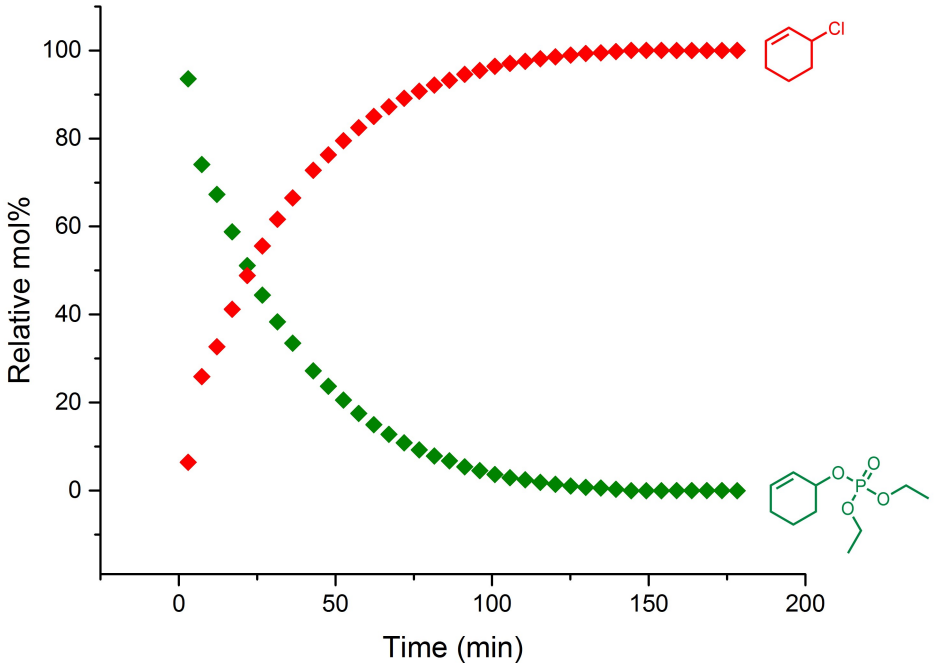

^{1}H NMR

^{31}P NMR

$Cp_2ZrEtCl$+TMSCl

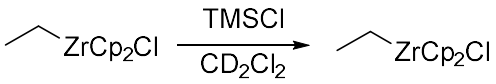

In a flame-dried flask, protected from light, ethylene (1 atm) was bubbled through a solution of Cp_2ZrHCl (210 mg, 0.80 mmol, 2.0 eq) in CD_2Cl_2 (0.5 mL) for 30 s and then stirred at room temperature under ethylene atmosphere until the solution went clear (15-20 min). The clear yellow hydrozirconation solution was transferred via syringe to a flame-dried NMR tube under argon atmosphere equipped with a septa. CD_2Cl_2 (0.8 mL) was added to the NMR tube. A preliminary ^1H NMR was run with locking and shimming. Then TMSCl (50 µL, 0.40 mmol, 1.0 eq) was added via a microsyringe to the NMR tube and shaken vigorously. The kinetic was run without further locking and shimming.

^1H NMR

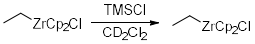



*CuI-**P**+TMSCl*

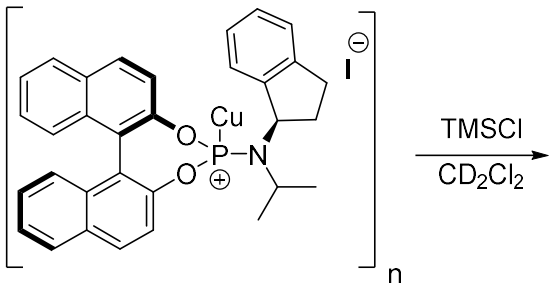

In a flame-dried flask, protected from light, under an argon atmosphere, CuI (7.7 mg, 40 μmol, 10 mol%) and *(R,R)*-**P** (19.6 mg, 40.0 μmol, 10.0 mol%) were dissolved in CD_2Cl_2 (0.8 mL) and allowed to stir for 1 h at room temperature. The cloudy white solution containing the Cu-complex was transferred via syringe to a flame-dried NMR tube under argon atmosphere equipped with a septa. A preliminary ^1H NMR was run with locking and shimming. Then TMSCl (50 μL, 0.40 mmol, 1.0 eq) was added via a microsyringe to the NMR tube and shaken vigorously. The kinetic was run without further locking and shimming.

^{1}H NMR

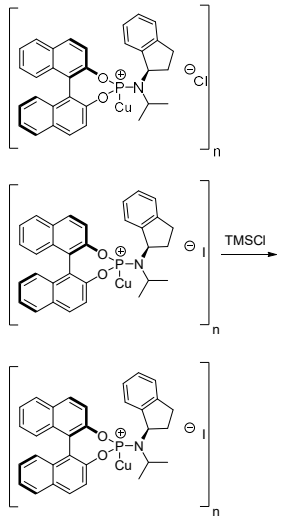

^{31}P NMR

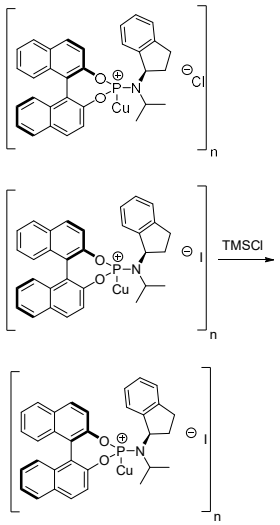

4) Kinetics without TMSCl

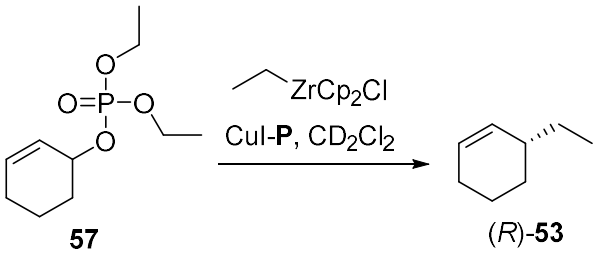

In a flame-dried flask, protected from light, under an argon atmosphere, CuI (7.7 mg, 40 μmol, 10 mol%) and (*R, R*)-**P** (19.6 mg, 40.0 μmol, 10.0 mol%) were dissolved in CD_2Cl_2 (0.8 mL) and allowed to stir for 1 h at room temperature. In another flask, ethylene (1 atm) was bubbled through a solution of Cp_2ZrHCl (210 mg, 0.80 mmol, 2.0 eq) in CD_2Cl_2 (0.5 mL) for 30 s and then stirred at room temperature under ethylene atmosphere until the solution went clear (15-20 min). The cloudy white solution containing the Cu-complex was transferred via syringe to a flame-dried NMR tube under argon atmosphere equipped with a septa. The clear yellow hydrozirconation solution was transferred via syringe to the NMR tube under argon atmosphere and vigorously shaken. A preliminary ^1H NMR was run with locking and shimming. Then cyclohex-2-en-1-yl diethyl phosphate **57** (74 μL, 0.40 mmol, 1.0 eq) was added dropwise via a microsyringe to the NMR tube and shaken vigorously. The kinetic was run without further locking and shimming.

^{1}H NMR Kinetics and modelling

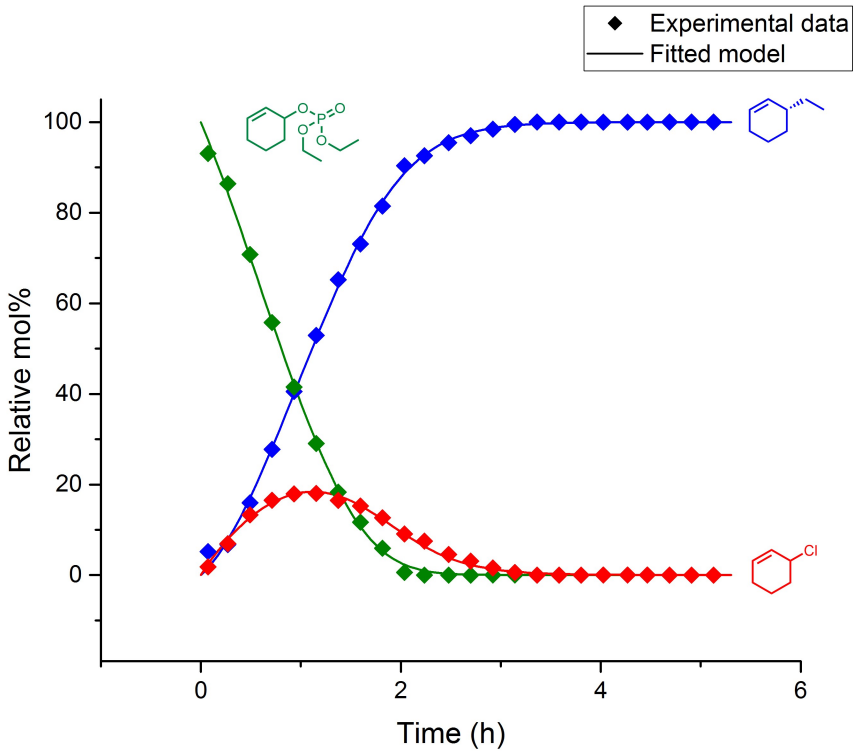

45b + CuI-**P** → **53** + CuI-**P** + Cl^- (k_1 = 0.26 mol%.min^{-1}) (6.5)
57 + CuI-**P** → **53** + CuI-**P** (k_2 = 0.019 mol%.min^{-1}) (6.6)
57 + Cl source → **45b** (k_{Cl1} = 0.0018 mol%.min^{-1}) (6.7)
57 + Cl^- →**45b** (k_{Cl2} = 0.18 mol%.min^{-1}) (6.8)

Residuals

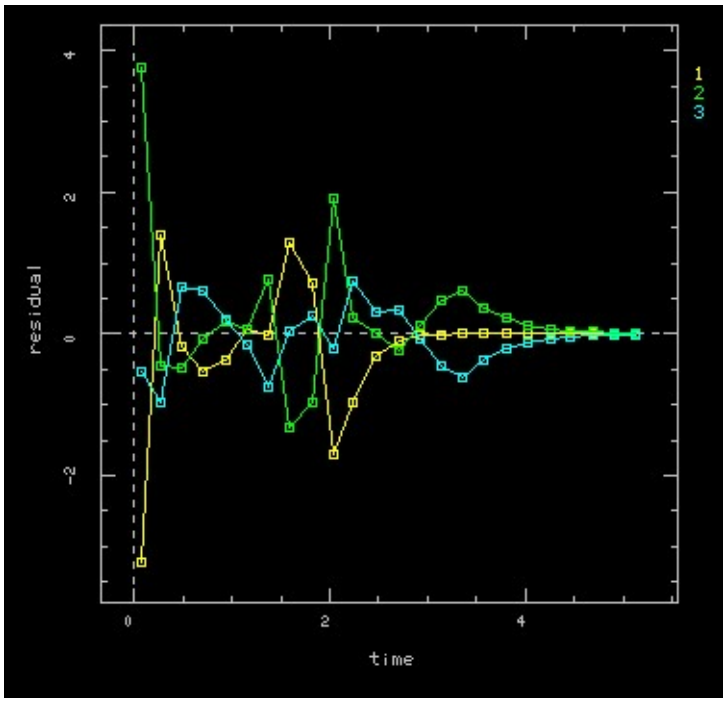

^{31}P NMR

Dynamics during kinetics

Summary of EXSY Exchanges

(none)

2D EXSY (gradient NOE t_{mix}=800 ms)

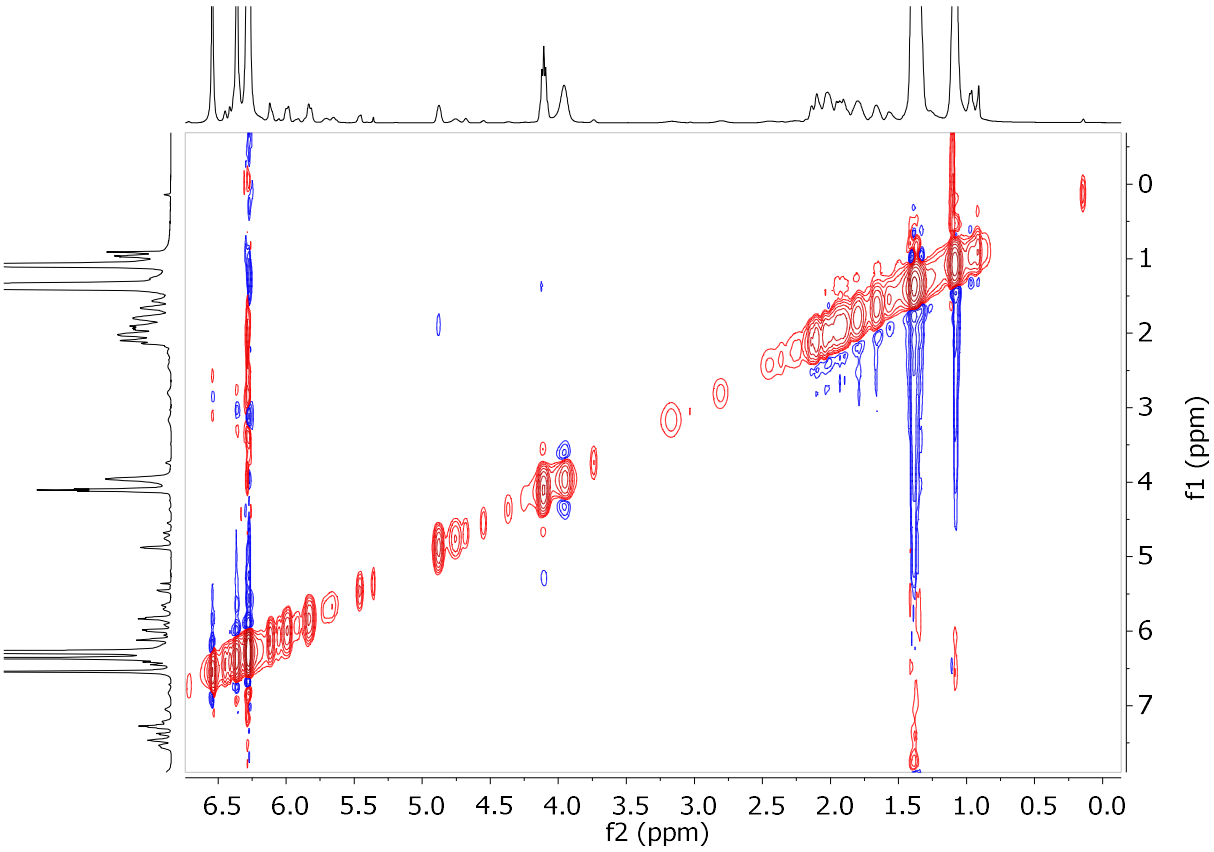

5) Deuterium Studies

Kinetics

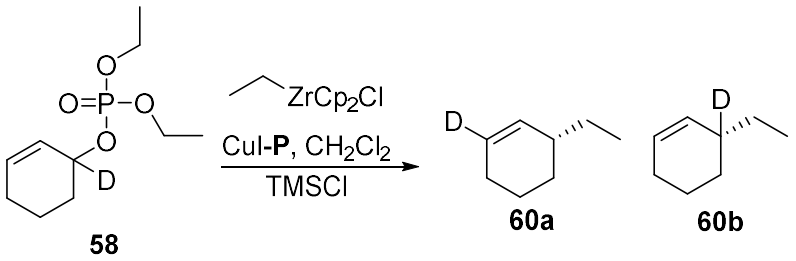

58 **60a** **60b**

In a flame-dried flask, protected from light, under an argon atmosphere, CuI (7.7 mg, 40 μmol, 10 mol%) and *(R,R)*-**P** (19.6 mg, 40.0 μmol, 10.0 mol%) were dissolved in CH_2Cl_2 (0.8 mL) and CD_2Cl_2 (1 drop) and allowed to stir for 1 h at room temperature. In another flask, ethylene (1 atm) was bubbled through a solution of Cp_2ZrHCl (210 mg, 0.80 mmol, 2.0 eq) in CD_2Cl_2 (0.5 mL) for 30 s and then stirred at room temperature under ethylene atmosphere until the solution went clear (15-20 min). The cloudy white solution containing the Cu-complex was transferred via syringe to a flame-dried NMR tube under argon atmosphere equipped with a septa. The clear yellow hydrozirconation solution was transferred via syringe to the NMR tube under argon atmosphere and vigorously shaken. A preliminary ^2H NMR was run. Then cyclohex-2-en-1-yl-1-*d* diethyl phosphate **58** (75 μL, 0.40 mmol, 1.0 eq) was added dropwise via a microsyringe to the NMR tube and shaken vigorously, then TMSCl (50 μL, 0.40 mmol, 1.0 eq) was added via a microsyringe to the NMR tube and shaken vigorously.

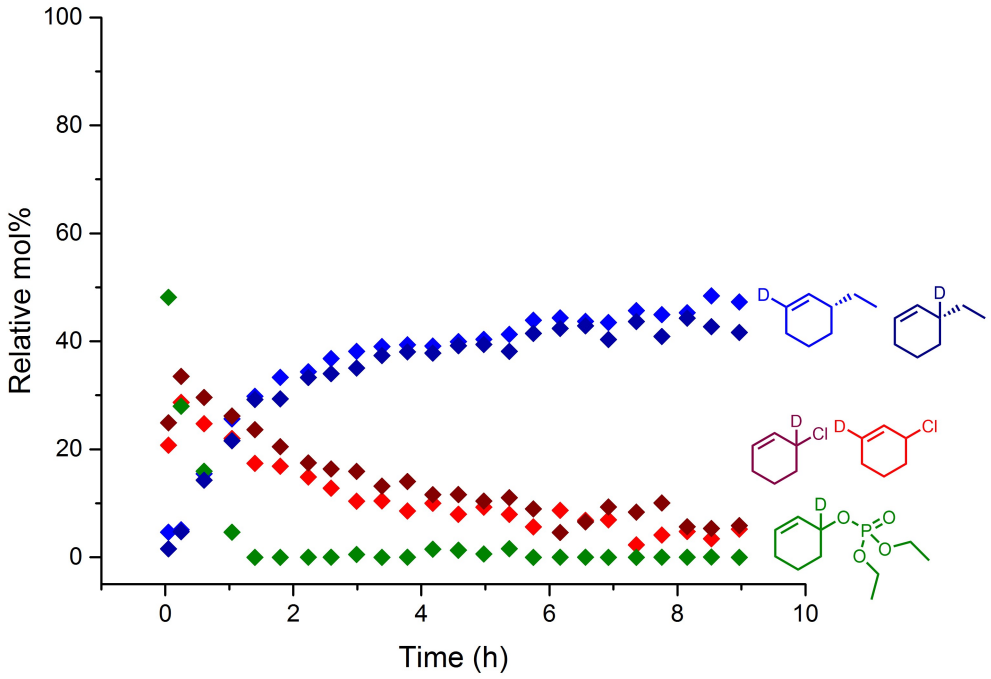

Kinetic without TMSCl

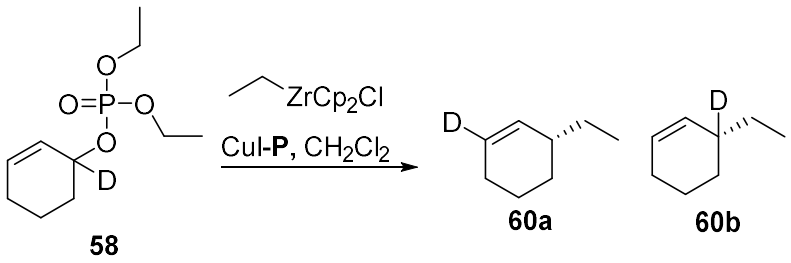

In a flame-dried flask, protected from light, under an argon atmosphere, CuI (7.7 mg, 40 μmol, 10 mol%) and *(R,R)*-**P** (19.6 mg, 40.0 μmol, 10.0 mol%) were dissolved in CH_2Cl_2 (0.8 mL) and CD_2Cl_2 (1 drop) and allowed to stir for 1 h at room temperature. In another flask, ethylene (1 atm) was bubbled through a solution of Cp_2ZrHCl (210 mg, 0.80 mmol, 2.0 eq) in CD_2Cl_2 (0.5 mL) for 30 s and then stirred at room temperature under ethylene atmosphere until the solution went clear (15-20 min). The cloudy white solution containing the Cu-complex

was transferred via syringe to a flame-dried NMR tube under argon atmosphere equipped with a septa. The clear yellow hydrozirconation solution was transferred via syringe to the NMR tube under argon atmosphere and vigorously shaken. A preliminary ^{2}H NMR was run. Then cyclohex-2-en-1-yl-1-*d* diethyl phosphate **58** (75 µL, 0.40 mmol, 1.0 eq) was added dropwise via a microsyringe to the NMR tube and shaken vigorously.

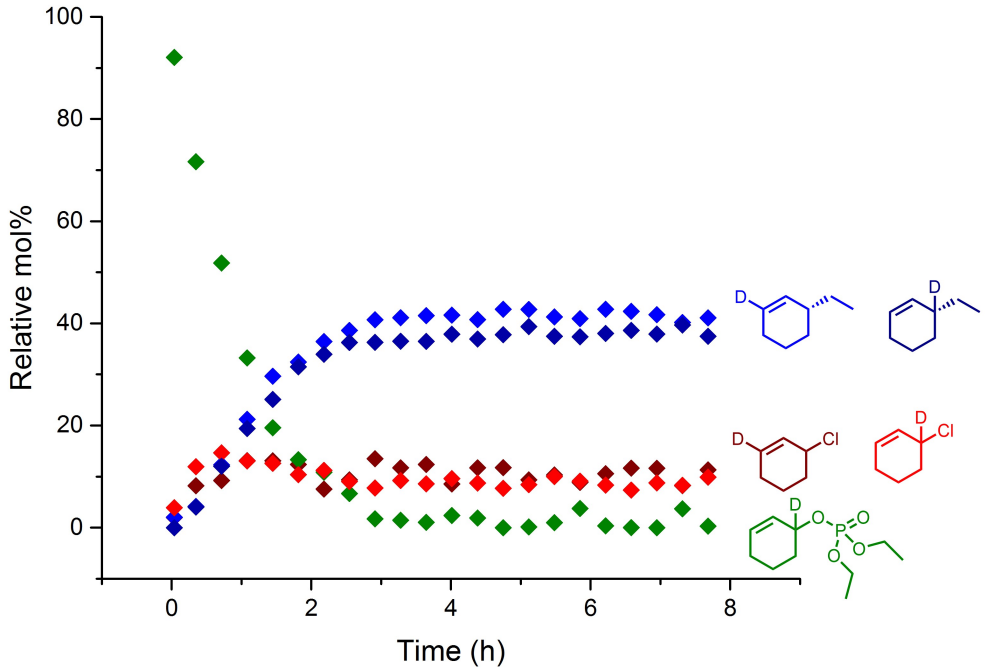

*Deuterated-Allylphosphate **58** +TMSCl*

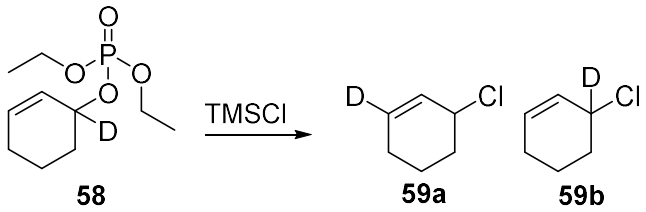

Cyclohex-2-en-1-yl-1-*d* diethyl phosphate **58** (75 µL, 0.40 mmol, 1.0 eq) was added via a microsyringe to a flame-dried NMR tube under argon atmosphere equipped with a septa and dissolved in CH_2Cl_2 (0.8 mL) and CD_2Cl_2 (1 drop) A preliminary ^2H NMR was run. Then TMSCl (50 µL, 0.40 mmol, 1.0 eq) was added via a microsyringe to the NMR tube and shaken vigorously.

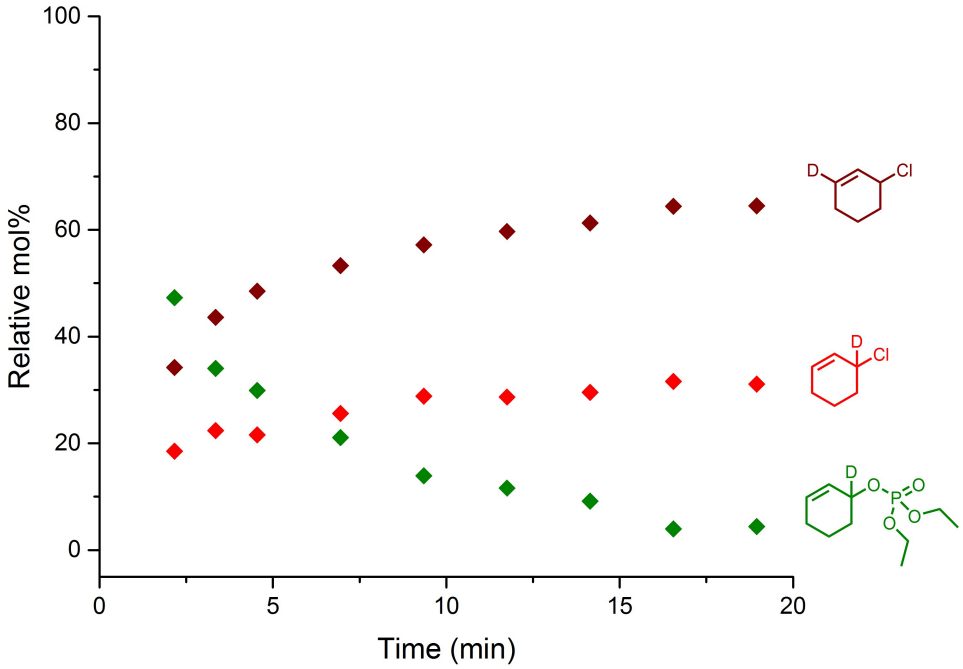

*Deuterated-Allylphosphate **58** +$Cp_2ZrCl(Et)$+TMSCl*

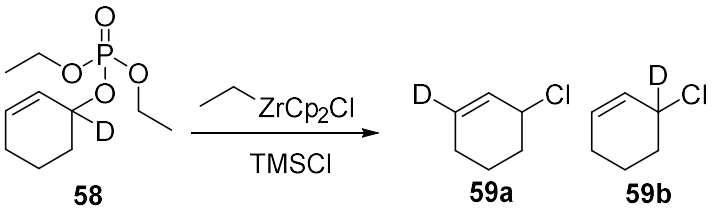

In a flame-dried flask, protected from light, ethylene (1 atm) was bubbled through a solution of Cp_2ZrHCl (210 mg, 0.80 mmol, 2.0 eq) in CH_2Cl_2 (0.5 mL) and CD_2Cl_2 (1 drop) for 30 s and then stirred at room temperature under ethylene atmosphere until the solution went clear (15-20 min). The clear yellow hydrozirconation solution was transferred via syringe to a flame-dried NMR tube under argon atmosphere equipped with a septa. CH_2Cl_2 (0.8 mL) was added to the NMR tube. A preliminary ^2H NMR was run. Then cyclohex-2-en-1-yl-1-*d* diethyl phosphate **58** (75 µL, 0.40 mmol, 1.0 eq) was added dropwise via a microsyringe to the NMR tube and shaken vigorously. A short ^2H NMR kinetic was run (20 min). Then TMSCl (50 µL, 0.40 mmol, 1.0 eq) was added via a microsyringe to the NMR tube and shaken vigorously.

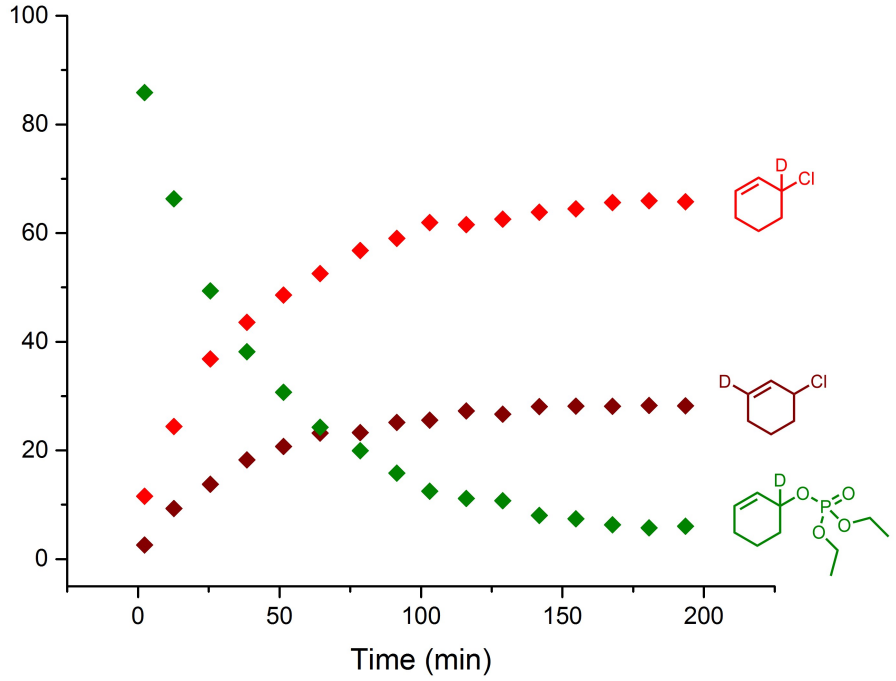

*Deuterated-Allylphosphate **58** +CuI-**P** +TMSCl*

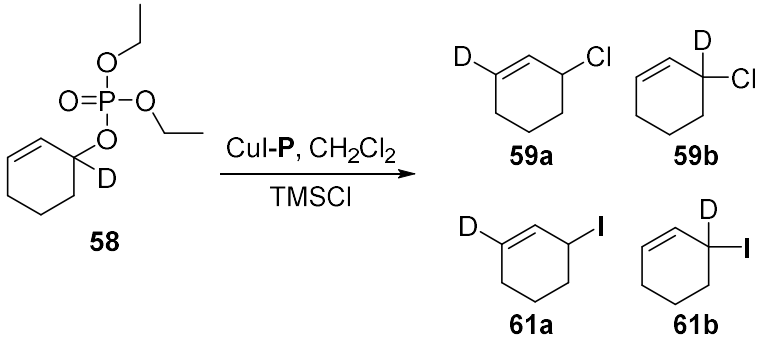

In a flame-dried flask, protected from light, under an argon atmosphere, CuI (7.7 mg, 40 µmol, 10 mol%) and *(R,R)*-**P** (19.6 mg, 40.0 µmol, 10.0 mol%) were dissolved in CH_2Cl_2 (0.8 mL) and CD_2Cl_2 (1 drop) and allowed to stir for 1 h at room temperature. The cloudy white solution containing the Cu-complex was transferred via syringe to a flame-dried NMR tube under argon atmosphere

equipped with a septa. A preliminary ^{2}H NMR was run. Then cyclohex-2-en-1-yl-1-*d* diethyl phosphate **58** (75 µL, 0.40 mmol, 1.0 eq) was added dropwise via a microsyringe to the NMR tube and shaken vigorously. A short ^{2}H NMR kinetic was run (20 min). Then TMSCl (50 µL, 0.40 mmol, 1.0 eq) was added via a microsyringe to the NMR tube and shaken vigorously.

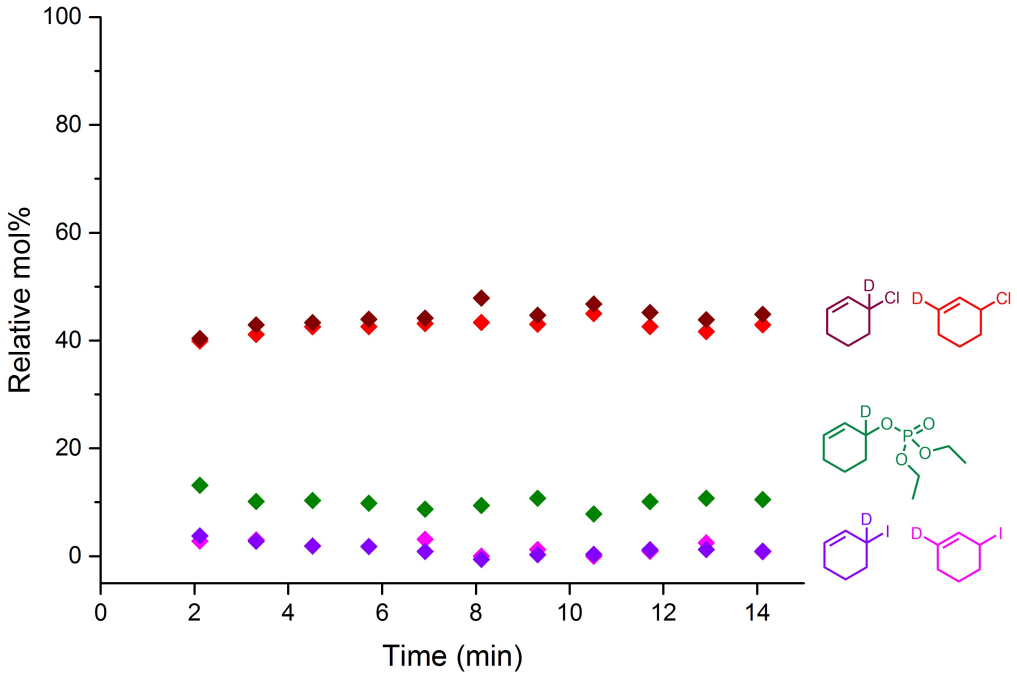

IX. EXPERIMENTALS CHAPTER 7

1) Starting materials

*1-(allyloxy)pent-4-en-2-ol (**80**)*

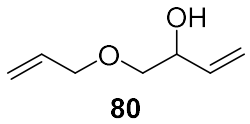

80

In analogy to a published procedure[299], prop-2-en-1-ol (3.4 mL, 50 mmol, 2.0 eq) was added to a solution of butadiene monoxide (2.0 mL, 25 mmol, 1.0 eq) in DMF (50 mL). Sodium hydride (2.0 g, 60% w/w in mineral oil, 50 mmol, 2.0 eq) was added in 1 g portions at 0 °C The resulting mixture was stirred for an additional 30 min at 0 °C and then overnight at 50 °C. The reaction mixture was quenched at 0 °C with HCl (aq.) (100 mL, 1 M) and stirred for 1 h to cool down. The resulting orange aqueous layer was extracted with ether (3 x 50 mL). The combined organic layers were washed with LiCl (10 % w/w, 100 mL), brine (100 mL), dried over $MgSO_4$, filtered and concentrated under reduced pressure to afford the crude product as a yellow oil. Purification by flash column chromatography (SiO_2, 30% Et_2O in pentane) yielded the title product **80** (2.1 g, 16 mmol, 66%) as a yellow oil. **^{1}H NMR** (400 MHz, $CDCl_3$) δ_H/ppm 5.97-5.78 (m, 2H, C**H**=CH_2), 5.36 (d, 17.0 Hz, 1H, CH=C**H**$_2$), 5.28 (d, 17.0 Hz, 1H, CH=C**H**$_2$), 5.20 (d, 10.9 Hz, 2H, CH=C**H**$_2$), 4.32 (br. s, 1H, C**H**-OH), 4.04 (d, 5.8 Hz, 2H, C**H$_2$**-O), 3.51 (dd, 9.6, 3.3 Hz, 1H, C**H$_2$**-O), 3.33 (dd, 9.8, 8.2 Hz, 1H, C**H$_2$**), 2.44 (br s, 1H, O**H**); **^{13}C NMR** (100 MHz, $CDCl_3$) δ_C/ppm 136.7 (**C**H=CH_2), 134.5 (**C**H=CH_2), 117.6

(CH=**C**H_2), 116.6 (CH=**C**H_2), 74.0 (**C**H-O), 72.4 (**C**H_2-O), 71.6 (**C**H_2-O); **HRMS** (ESI) *m*/z calcd for $C_7H_{12}O_2Na$ $[M+Na]^+$: 151.07295, found: 151.07286; **IR (neat)** ν_{max}/cm^{-1} 3422, 2924, 2857, 2360, 1424, 1104, 992, 927. Spectral data was in accordance with literature[299].

*3,6-dihydro-2H-pyran-3-ol (**81**)*

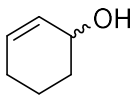

81

In analogy to a published procedure[299], Grubbs catalyst 1st generation (310 mg, 0.37 mmol, 0.020 eq) was added to a solution of 1-(allyloxy)pent-4-en-2-ol **80** (2.0 g, 16 mmol, 1.0 eq) in CH_2Cl_2 (150 mL) at room temperature and stirred overnight. The resulting reaction mixture was concentrated under reduced pressure to obtain the crude product as a brown oil. Purification by flash column chromatography (SiO_2, 50→100% Et_2O in pentane) yielded the title product **81** (1.4 g, 14 mmol, 92%) as a brown oil. **^{1}H NMR** (400 MHz, $CDCl_3$) δ_H/ppm 6.05-5.98 (m, 1H, C**H**=CH), 6.05-5.98 (m, 1H, C**H**=CH), 4.19 (ddt, *J*=16.8, 2.9, 1.4 Hz, 1H, C**H$_2$**-O), 4.09 (ddd, *J*= 17.0, 4.6, 2.1 Hz, 1H, C**H$_2$**-O), 4.04-3.97 (m, 1H, C**H**-O), 3.88 (ddd, *J*=11.7, 3.0, 1.0 Hz, 1H, C**H$_2$**-O), 3.77 (dd, *J*= 11.7, 3.0 Hz, 1H, C**H$_2$**-O), 1.99 (d, *J*= 11.9 Hz, 1H, O**H**); **^{13}C NMR** (100 MHz, $CDCl_3$) δ_C/ppm 130.0 (**C**H=CH), 126.7 (**C**H=CH), 70.8 (**C**H_2-O), 65.4 (**C**H_2-O), 62.7 (**C**H-O); **HRMS** (ESI) *m*/z calcd for $C_5H_8O_2Na$ $[M+Na]^+$: 123.04165, found: 123.04143. **IR (neat)** ν_{max}/cm^{-1} 3381, 2846, 1226, 1086, 1064, 1014, 937, 835, 817, 695. Spectral data was in accordance with literature[299].

*3-chloro-3,6-dihydro-2H-pyran (**62a**)*

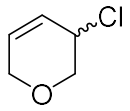

62a

Based on a modified procedure [299], PCl_3 (1.6 mL, 19 mmol, 0.37 eq) was added dropwise to a mixture of 3,6-dihydro-2*H*-pyran-3-ol **81** (5.0 g, 50 mmol, 1.0 eq) and pyridine (0.40 mL, 5.0 mmol, 0.10 eq) at 0 °C. After stirring for 30 min at 0 °C, the reaction mixture was allowed to warm up to room temperature and stirred overnight. The non-viscous organic layer of the resulting solution was removed by pipette and the bottom layer was rinsed with pentane (3 x 1 mL). The resulting organic solution was concentrated under reduced pressure and purified by Kugelrohr distillation (20 mbar, 100 °C) to afford the title product **62a** (4.1 g, 35 mmol, 69%) as a very pale yellow solution. **^{1}H NMR** (400 MHz, $CDCl_3$) δ_H/ppm 5.97-5.88 (m, 2H, C**H**=C**H**), 4.52-4.45 (m, 1H, C**H**=Cl), 4.23 (ddd, *J*= 16.8, 3.8, 2.2 Hz, 1H, C**H$_2$**), 4.12 (ddd, *J*= 16.8, 3.8, 1.9 Hz, 1H, C**H$_2$**), 4.04 (dd, *J*= 12.1, 4.0 Hz, 1H, C**H$_2$**), 3.84 (dd, *J*= 12.1, 5.0 Hz, 1H, C**H$_2$**); **^{13}C NMR** (100 MHz, $CDCl_3$) δ_C/ppm 129.8 (**C**H=CH), 126.0 (**C**H=CH), 70.1 (**C**H_2), 65.1 (**C**H_2), 51.0 (**C**H-Cl); **HRMS** (EI/FI) *m*/z calcd for C_5H_7OCl $[M]^+$:118.0185, found:118.0185; **IR (neat)** ν_{max}/cm^{-1} 2833, 1289, 1114, 1094, 997, 829, 735. Spectral data was in accordance with literature[299].

^{1}H NMR (500 MHz, CD_2Cl_2) δ_H/ppm 6.01-5.95 (m, 2H, C**H**=C**H**), 4.55-4.50 (m, 1H, C**H**-Cl), 4.24 (d, *J*= 16.3 Hz, 1H, C**H$_2$**-O), 4.15 (dd, *J*= 17.2, 2.5 Hz, 1H, C**H$_2$**-O), 4.06

(dd, *J*= 12.0, 3.9 Hz, 1H, C**H$_2$**-O), 3.87 (dd, *J*= 12.0, 4.6 Hz, 1H, C**H$_2$**-O); **^{13}C NMR** (125 MHz, CD_2Cl_2) δ_C/ppm 130.1 (**C**H=CH), 125.7 (**C**H=CH), 70.0 (**C**H_2-O), 65.0 (**C**H_2-O), 51.4 (**C**H-Cl).

*3-bromo-3,6-dihydro-2H-pyran (**62b**)*

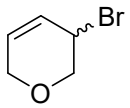

62b

In analogy to the 3-chloro-3,6-dihydro-2*H*-pyran **62a** procedure, PBr_3 (0.18 mL, 1.9 mmol, 0.37 eq) was added dropwise to a mixture of 3,6-dihydro-2*H*-pyran-3-ol **81** (0.50 g, 5.0 mmol, 0.98 eq) and pyridine (41 μL, 0.50 mmol, 0.10 eq) at 0 °C. After stirring for 30 min at 0 °C, the reaction mixture was allowed to warm up to room temperature and stirred overnight. The non-viscous organic layer of the resulting solution was removed by pipette and the bottom layer was rinsed with pentane (3 x 1 mL). The resulting organic solution was concentrated under reduced pressure and purified by Kugelrohr distillation (57 mbar, 140 °C) to afford the title product **62b** (296 mg, 1.81 mmol, 36%) as an orange oil. **^{1}H NMR** (400 MHz, $CDCl_3$) δ_H/ppm 6.07-6.00 (m, 1H, C**H**=CH), 5.90-5.83 (m, 1H, C**H**=CH), 4.63 (br s, 1H, C**H**-Br), 4.31 (ddd, 17.3, 4.4, 2.2 Hz, 1H, C**H$_2$**-O), 4.20 (ddd, 17.3, 4.6, 2.4 Hz, 1H, C**H$_2$**-O), 4.07 (dd, 12.2, 3.9, 1H, C**H$_2$**-O), 3.98 (dd, 12.2, 4.6, 1H, C**H$_2$**-O); **^{13}C NMR** (100 MHz, $CDCl_3$) δ_C/ppm 129.6 (**C**H=CH), 126.7 (**C**H=CH), 70.3 (**C**H_2-O), 65.1 (**C**H_2-O), 43.0 (**C**H-Br); **HRMS**

(EI/FI) *m*/z calcd for C_5H_7OBr $[M]^+$: 161.9680, found: 161.9685; **IR (neat)** ν_{max}/cm^{-1} 2867, 1307, 1156, 987, 795, 624.

*3,6-dihydro-2H-pyran-3-yl acetate (**62c**)*

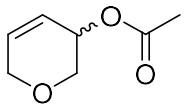

62c

According to a modified procedure[304], 6-dihydro-2*H*-pyran-3-ol **81** (0.20 g, 2.0 mmol, 1.0 eq) was dissolved in Et_2O (2.0 mL). Pyridine (0.20 mL, 3.0 mmol, 1.5 eq), DMAP (243 mg, 2.00 mmol, 1.00 eq) and then acetic anhydride (0.38 mL, 4.0 mmol, 2.0 eq) were added dropwise to the stirring yellow solution. The reaction mixture was stirred overnight. The reaction was diluted in Et_2O (10 mL) and quenched with H_2O (2 x 15 mL). The mixture was partitioned and the aqueous phase was extracted with Et_2O (3 x 10 mL). The combined organic extracts were washed with brine (20 mL), dried over $MgSO_4$, filtered and concentrated under reduced pressure. Purification by flash column chromatography (SiO_2, 20% Et_2O in pentane) yielded the title product **62c** (106 mg, 0.746 mmol, 37%) as a yellow oil. **^{1}H NMR** (400 MHz, $CDCl_3$) δ_H/ppm 6.10-6.04 (m, 1H, C**H**=CH), 5.96-5.89 (m, 1H, C**H**=CH), 5.11-5.06 (m, 1H, C**H**-O), 4.22 (d, 16.9 Hz, 1H, C**H$_2$**-O), 4.08 (ddd, 16.9, 5.4, 2.2 Hz, 1H, C**H$_2$**-O), 3.92 (dd, 12.5, 2.5 Hz, 1H, C**H$_2$**-O), 3.80 (dd, 12.5, 3.4 Hz, 1H, C**H$_2$**-O), 2.09 (s, 3H, C**H$_3$**); **^{13}C NMR** (100 MHz, $CDCl_3$) δ_C/ppm 170.8 (**C**=O), 132.2 (**C**H=CH), 122.5 (**C**H=CH), 67.7 (**C**H_2-O), 65.0 (**C**H_2-O), 64.8 (**C**H-O), 21.2 (**C**H_3); **HRMS** (ESI) *m*/z calcd for

$C_7H_{10}O_3Na$ $[M+Na]^+$: 165.05222, found: 165.05219; **IR (neat)** ν_{max}/cm^{-1} 1727, 1371, 1227, 1188, 1097, 1063, 1020, 896, 846. Spectral data is in accordance with literature[305].

*3,6-dihydro-2H-pyran-3-yl diethyl phosphate (**62d**)*

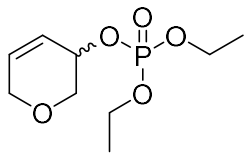

62d

According to a modified procedure[306], diethylchlorophosphate (2.4 mL, 17 mmol, 1.0 eq) was added dropwise to a mixture of 6-dihydro-2*H*-pyran-3-ol **81** (1.6 g, 16 mmol, 1.0 eq) and pyridine (6.7 mL, 83 mmol, 5.2 eq) in CH_2Cl_2 (15 mL) at 0 °C. After stirring for 10 min at 0 °C, DMAP (0.39 g, 0.32 mmol, 0.020 eq) was added to the reaction mixture. The reaction mixture was allowed to warm up to room temperature and stirred overnight. The reaction was diluted in CH_2Cl_2 (10 mL) and quenched with H_2O (2 x 15 mL). The mixture was partitioned and the aqueous phase was extracted with CH_2Cl_2 (3 x 10 mL). The combined organic extracts were washed with brine (20 mL), dried over $MgSO_4$, filtered and concentrated under reduced pressure. Purification by flash column chromatography (SiO_2, 100% Et_2O and then 10% MeOH in $CHCl_3$) yielded the title product **62d** (3.4 mg, 14 mmol, 90%) as a yellow oil. **^{1}H NMR** (400 MHz, $CDCl_3$) δ_H/ppm 6.07-6.02 (m, 1H, C**H**=CH-CH), 6.01-5.95 (m, 1H, CH=C**H**-CH), 4.87-4.71 (br. m, 1H, C**H**-OP), 4.30-4.21 (m, 1H, C**H**$_2$), 4.20-4.07 (m, 5H, C**H**$_2$), 3.95 (dd, 12.5, 3.4 Hz, 1H, C**H$_2$**), 3.85 (dd, 12.1, 3.6 Hz, 1H, C**H$_2$**), 1.34 (ddt, 7.2, 1.3,

1.2 Hz, 6H, 2 x C**H**$_3$); **^{13}C NMR** (100 MHz, $CDCl_3$) δ_C/ppm 131.9 (**C**H=CH-CH), 123.6 (d, *J*= 4.8 Hz, CH=**C**H-CH), 68.5 (d, *J*= 5.6 Hz, **C**H$_2$), 68.2 (d, *J*= 5.6 Hz, **C**H-OP), 65.1 (**C**H$_2$), 64.0 (d, *J*= 6.3 Hz, **C**H$_2$), 16.2 (d, *J*= 7.3 Hz, **C**H$_3$); **^{31}P NMR** (200 MHz, $CDCl_3$) δ_p/ppm -0.00 (s, 1P); **HRMS** (ESI) *m*/z calcd for $C_9H_{18}O_5P$ $[M]^+$: 237.08864, found: 237.08840; **IR (neat)** ν_{max}/cm^{-1} 2984, 1262, 1006, 974, 800.

^{1}H NMR (500 MHz CD_2Cl_2) δ_H/ppm 5.97 (dt, *J*= 10.3, 2.7 Hz, 1H, C**H**=CH-CH), 5.87 (ddd, *J*=10.4, 4.5, 2.2 Hz, 1H, CH=C**H**-CH), 4.59 (dt, *J*= 6.9, 3.5 Hz, 1H, C**H-**OP), 4.08 (d, *J*= 17.1 Hz, 1H, O-C**H**$_2$), 4.08–3.98 (m, 5H, O-C**H**$_2$), 3.81 (dd, *J*= 12.2, 3.5 Hz, 1H, O-C**H**$_2$), 3.74 (dd, *J*= 12.3, 3.4 Hz, 1H, O- C**H**$_2$), 1.24 (t, *J*= 7.1 Hz, 6H, 2 x C**H$_3$**); **^{13}C NMR** (125 MHz, CD_2Cl_2) δ_C/ppm 131.9 (**C**H=CH-CH), 123.3 (d, *J*= 4.6 Hz, CH=**C**H-CH), 68.3 (d, *J*= 5.3 Hz, O-**C**H$_2$), 68.1 (d, *J*= 5.3 Hz, **C**H-OP), 64.9 (O-**C**H$_2$), 63.8 (d, *J*=1.7 Hz, O-**C**H$_2$), 63.7 (O-**C**H$_2$), 15.9 (d, *J*= 7.2 Hz, **C**H$_3$); **^{31}P NMR** (202 MHz, CD_2Cl_2) δ_P/ppm -1.46 (s, 1P).

*Bis(2-methoxyphenyl)methanol (**82**)*

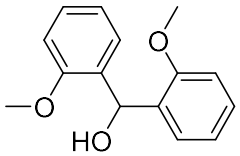

82

According to a modified procedure from Diederich[307], THF (30 mL) was added to immerse magnesium turnings (1.1 g, 39 mmol, 1.1 eq). The reaction was heated at 40°C and I_2 (1 crystal) was added to the solution. After 10 minute, 1-bromo-2-methoxybenzene (4.8 mL, 48 mmol, 1.3 eq) in THF (15 mL) was

added slowly to the reaction mixture. The reaction mixture was refluxed for 4 h. Upon cooling at room temperature, 2-methoxybenzaldehyde (4.4 mL, 37 mmol, 1.0 eq) was added dropwise to the reaction mixture and stirred for 18 h. H_20 (40 mL), HCl (25 mL, 2 M) and Et_2O (40 mL) were added successfully to the reaction mixture which was stirred at room temperature for 20 min. The mixture was partitioned between the aqueous and organic layers and the aqueous phase extracted with Et_2O (3 × 50 mL). The combined organic phase was dried over $MgSO_4$, filtered and concentrated under reduced pressure to give the title product **82** (8.5 g, 35 mmol, 94%) as a white solid. The product was used as such without further purification. **^{1}H NMR** (400 MHz, $CDCl_3$) δ_H/ppm 7.27 - 7.31 (m, 2 H), 7.23 - 7.27 (m, 2 H), 6.95 (td, *J*=7.5, 0.9 Hz, 2H), 6.91 (d, *J*=8.3 Hz, 2H), 6.37 (d, *J*=5.4 Hz, 1H), 3.84 (s, 6 H), 3.57 (dd, *J*=5.1, 0.7 Hz, 1H); **^{13}C NMR** (100 MHz, $CDCl_3$) δ_C/ppm 156.8 (2C), 130.9 (2C), 128.4 (2C), 127.8 (2C), 120.5 (2C), 110.4 (2C), 67.4, 55.4 (2C); **HRMS** (ESI) *m/z* calcd for $C_{15}H_{16}NaO_3$ $[M+Na]^+$: 267.0992, found: 267.0999; **IR** (ν_{max} /cm^{-1}): 2970, 1759, 1342, 1204. Spectral data was in accordance with literature[307].

*Bis(2-methoxyphenyl)methanone (**83**)*

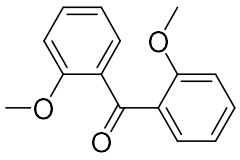

83

According to a modified procedure from Diederich[307], MnO_2 (7.6 g, 88 mmol, 5.0 eq) was added to a stirring solution of bis(2-

methoxyphenyl)methanol **82** (4.2 g, 17 mmol, 1.0 eq) in CD_2Cl_2 (50 mL) at room temperature. The solution was stirred for 18 h. MnO_2 (7.6 g, 88 mmol, 5.0 eq) was added to the reaction mixture and the reaction mixture was stirred for another 24 h. The reaction mixture was then filtered over Celite® and concentrated under reduced pressure to give the desired title product **83** (3.3 g, 14 mmol, 79%) as a colourless solid. The product was used as such without further purification. **^{1}H NMR** (400 MHz, $CDCl_3$) δ_H/ppm 7.52 (dd, *J*=7.6, 1.7 Hz, 2H), 7.44 (ddd, *J*=8.3, 7.4, 2.0 Hz, 2H), 6.99 (td, *J*=7.5, 0.7 Hz, 2H), 6.92 (d, *J*=8.3 Hz, 2H), 3.67 (s, 6H); **^{13}C NMR** (100 MHz, $CDCl_3$) δ_C/ppm 195.3, 158.2 (2C), 132.5 (2C), 130.3 (2C), 130.2 (2C), 120.3 (2C), 111.4 (2C), 55.6 (2C); **HRMS** (ESI) *m/z* calcd for $C_{15}H_{14}NaO$ $[M+Na]^+$: 265.0835, found: 265.0836; **IR** (ν_{max} /cm^{-1}): 2970, 1730, 1597, 1369, 1250, 1023, 751. Spectral data was in accordance with literature[307].

*N-(bis(2-methoxyphenyl)methyl)propan-2-amine (**84**)*

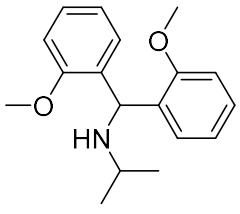

84

According to a modified procedure from Gilbert[308], $TiCl_4$ (15 mL, 15 mmol, 1.1 eq, 1 M solution in CD_2Cl_2) was added slowly to an ice-bathed solution of bis(2-methoxyphenyl)methanone **83** (3.33 g, 13.8 mmol, 1.00 eq) in CD_2Cl_2 (40 mL). The solution was stirred for 10 min at room temperature and then a

solution of isopropylamine (3.5 mL, 41 mmol, 3.0 eq) in THF (20 mL, 2.0 M solution) was added dropwise to the reaction mixture. The reaction flask was stirred for 6 h. A solution of $NaB(CN)H_3$ (4.3 g, 69 mmol, 5.0 eq) in THF (68 mL, 1.0 M solution) was added slowly to the reaction mixture. MeOH (24 mL) was added slowly to the reaction mixture. The reaction mixture was stirred at room temperature for 18 h. NaOH (50 mL, 2 M aq. solution) was added slowly and the reaction mixture was stirred for 30 min. The reaction mixture was filtered on Celite® and washed with Et_2O (70 mL). Then, $NaHCO_3$ (aq. sat., 50 mL) was added to the suspension. The mixture was partitioned and the aqueous phase extracted with Et_2O (3 × 50 mL). The combined organic phase was dried over $MgSO_4$, filtered and concentrated under reduced pressure to give an oil. Et_2O (50 mL) were added to the crude mixture. Concentrated HCl (~5 mL, 37% w/v solution) was added. The mixture was left and crystals formed after 5 min. The mixture was partitioned and the organic phase extracted with HCl (aq. 2.0 M, 3 × 30 mL). Then CH_2Cl_2 (20 mL) was added to the combined aqueous phases and NaOH (aq. saturated with brine solution, 25%) was added till the mixture became basic (pH ~14). The mixture was partitioned and the aqueous phase extracted with CH_2Cl_2 (3 × 50 mL). The combined organic phase was dried ($MgSO_4$), filtered and concentrated under reduced pressure to afford the desired pure title amine **84** (2.1 g, 7.4 mmol, 54%). **^{1}H NMR** (400 MHz, $CDCl_3$) δ_H/ppm 7.37 (d, *J*=7.3 Hz, 2H), 7.20 (td, *J*=7.7, 1.5 Hz, 2H), 6.93 (t, *J*=7.5 Hz, 2H), 6.85 (d, *J*=8.3 Hz, 2H), 5.63 (s, 1 H), 3.80 (s, 6H), 2.76 (spt, *J*=6.2 Hz, 1H), 1.86-2.25 (m, 1H), 1.12 (d, *J*=6.1 Hz, 6H); **^{13}C NMR** (100 MHz, $CDCl_3$) δ_C/ppm 157.2 (2C), 131.8 (2C), 128.5 (2C), 127.4 (2C), 120.3 (2C), 110.7 (2C), 55.4 (2C), 52.5, 46.2, 23.1 (2C); **HRMS** (ESI) *m/z*

calcd for $C_{18}H_{24}NO_2[M+H]^+$: 286.1802, found: 286.1804; **IR** ν_{max} /cm^{-1} 2950, 1771, 1709, 1598, 1380, 1351, 1229.

*(R)-N-(bis(2-methoxyphenyl)methyl)-N-isopropyldinaphtho[2,1-d:1',2'-f][1,3,2]dioxaphosphepin-4-amine ((R)-**W**)*

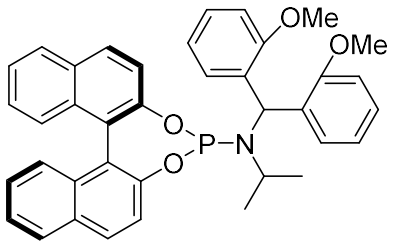

W

According to a modified procedure from Trost[191], triethylamine (5.1 mL, 37 mmol, 5.0 eq) was added dropwise to a solution of PCl_3 (0.64 mL, 7.4 mmol, 1.0 eq) at 0 °C in CH_2Cl_2 (50 mL). The ice bath was removed and the solution left to warm to room temperature before N-(bis(3-methoxyphenyl)methyl)propan-2-amine **84** (2.1 g, 7.4 mmol, 1.0 eq) was added to the stirring solution. (*R*)-Binaphthol (2.1 g, 7.4 mmol, 1.0 eq) was added to the suspension after 5 h and the subsequent mixture was left stirring overnight. The solution was then filtered over a small SiO_2 (3 mm) and Celite® (1.5 mm) pad and washed with CH_2Cl_2. The resulting reaction mixture was concentrated under reduced pressure. Flash column chromatography of the yellow residue (80:19:1; Petrol/CH_2Cl_2/ Et_3N; SiO_2) gave the title phosphoramidite ligand (*R*)-**W** (4.2 g, 7.0 mmol, 95%) as a white solid. **^{1}H NMR** (500 MHz, CD_2Cl_2) δ_H/ppm 7.95–7.69 (m, 4H, C**H**-Ar), 7.46–7.35 (m, 2H, C**H**-Ar), 7.35–7.28 (m, 3H, C**H**-Ar), 7.28–7.04

(m, 7H, C**H**-Ar), 6.96–6.78 (m, 4H, C**H**-Ar), 6.29 (d, *J*= 16.4 Hz, 1H, N-C**H**(*o*OMe-Ph)$_2$), 3.83 (s, 3H, OC**H$_3$**), 3.76 (s, 3H, OC**H$_3$**), 3.45-3.33 (m, 1H, N-C**H**), 0.85 (d, *J*= 6.7 Hz, 3H, CH(C**H$_3$**)$_2$), 0.76 (d, *J*= 6.7 Hz, 3H, CH(C**H$_3$**)$_2$). **^{13}C NMR** (125 MHz, CD2Cl$_2$) δ_C/ppm 156.7 (d, *J*=1.4 Hz, **Cq**-Ar), 156.5 (**Cq**-Ar), 150.8 (d, *J*=6.7 Hz, **Cq**-Ar), 150.1 (**Cq**-Ar), 132.7 (**Cq**-Ar), 132.6 (**Cq**-Ar), 131.5 (d, *J*=7.5 Hz, **Cq**-Ar), 131.3 (**Cq**-Ar), 131.1 (d, *J*=6.7 Hz, **Cq**-Ar), 130.6 (d, *J*=5.0 Hz, **C**H-Ar), 130.5 (**Cq**-Ar), 130.4 (d, *J*=5.7 Hz, **C**H-Ar), 130.1 (**C**H-Ar), 129.4 (**C**H-Ar), 128.3 (**C**H-Ar), 128.2 (d, *J*= 3.7 Hz, **C**H-Ar), 126.8 (**C**H-Ar), 125.9 (**C**H-Ar), 125.8 (**C**H-Ar), 124.6 (**C**H-Ar), 124.2 (**C**H-Ar), 124.0 (d, *J*=5.3 Hz, **Cq**-Ar), 122.4 (**C**H-Ar), 122.3 (d, *J*= 1.8 Hz, **C**H-Ar), 121.4 (d, *J*= 2.3 Hz, **Cq**-Ar), 119.8 (d, *J*= 1.8 Hz, **C**H-Ar), 110.6 (**C**H-Ar), 55.3 (O**C**H$_3$), 55.3 (O**C**H$_3$), 48.9 (N-**C**H(*o*OMe-Ph)$_2$), 47.3 (d, *J*= 5.5 Hz, **C**H(CH$_3$)$_2$), 22.6, ((CH(**C**H$_3$)$_2$) 21.7 (CH(**C**H$_3$)$_2$).**^{31}P NMR** (202 MHz CD$_2$Cl$_2$) δ_P/ppm 148.8 (1P); **HMRS** (EI) *m*/*z* calcd for $C_{36}H_{30}NO_2P$ $[M]^+$: 599.2225, found: 599.2231; **IR** (neat) ν_{max}/cm^{-1} 2972, 1589, 1463, 1232, 1053, 948, 751, 695; **$[\alpha]_D^{25}$** = −89.7 (*c* 2.00, $CHCl_3$); **Mp** 134-137 °C.

*$CuClO_4$-**W***

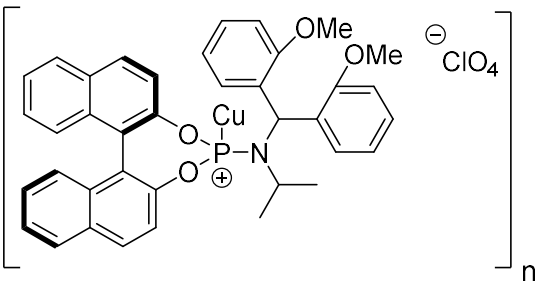

In a flame-dried flask under inert atmosphere, CuCl (1.9 mg, 20 μmol, 10 mol%) and (*R*)-**W** (12.0 mg, 20.0 μmol, 10.0 mol%) were dissolved in CD_2Cl_2 (1.0 mL) and stirred for 1 h at room temperature. $AgClO_4$ (4.6 mg, 22 μmol, 0.11 eq ***Perchlorates are explosive and should be handled with caution***) was added to the freshly formed Cu-ligand complex solution and stirred for 15 min. The resulting catalyst complex mixture was filtered into a flamed dried NMR tube adapted with an NMR septa and parafilmed. **^{1}H NMR** (500 MHz, CD_2Cl_2) δ_H/ppm 7.98 (d, *J*=9.0 Hz, 1H, C**H**-Ar), 7.94 (d, *J*=9.3 Hz, 1H, C**H**-Ar), 7.88 (d, *J*=8.2 Hz, 1H, C**H**-Ar), 7.85 (d, *J*=8.2 Hz, 1H, C**H**-Ar), 7.51 (d, *J*=8.2 Hz, 1H, C**H**-Ar), 7.47-7.18 (m, 9H, C**H**-Ar), 7.14 (d, *J*=3.6 Hz, 2H, C**H**-Ar), 7.02-6.85 (m, 4H, C**H**-Ar), 6.29 (d, *J*=18.8 Hz, 1H, N-C**H**(*o*OMe-Ph)$_2$), 3.89 (s, 3H, OC**H$_3$**), 3.79 (s, 3H, OC**H$_3$**), 3.40 (br. s, 0.5 H, N-C**H**(m)), 3.33 (h, *J*=6.1 Hz, 1H, N-C**H**), 0.96 (br. s, 3H, CH(C**H$_3$**)$_2$), 0.75 (br. s, 3H, CH(C**H$_3$**)$_2$); **^{13}C NMR** (125 MHz, CD_2Cl_2) δ_C/ppm 156.6 (**Cq**-Ar), 156.3 (**Cq**-Ar), 148.8 (**Cq**-Ar), 148.7 (**Cq**-Ar), 148.2 (d, *J*=3.6 Hz, **Cq**-Ar), 133.1 (**Cq**-Ar), 132.6 (**Cq**-Ar), 132.5 (**Cq**-Ar), 132.1 (**Cq**-Ar), 131.6 (**C**H-Ar), 131.4 (**Cq**-Ar), 130.6 (**C**H-Ar), 129.9 (**C**H-Ar), 129.8 (**C**H-Ar), 128.7 (**C**H-Ar), 128.6 (**C**H-Ar), 128.3 (br. d, *J*=7.3 Hz, **Cq**-Ar), 127.2 (**C**H-Ar), 127.0 (**C**H-Ar), 126.7 (**C**H-Ar),

126.6 (**C**H-Ar), 125.6 (**C**H-Ar), 125.5 (**C**H-Ar), 123.1 (d, *J*=4.2 Hz, **Cq**-Ar), 121.8 (**C**H-Ar), 121.7 (**C**H-Ar), 121.5 (d, *J*=1.7 Hz, **C**H-Ar), 121.4 (**C**H-Ar), 121.0 (**C**H-Ar), 120.8 (br. s, **C**H-Ar), 112.4 (**C**H-Ar), 112.0 (**C**H-Ar), 55.7 (O**C**H_3), 55.6 (O**C**H_3), 50.6 (br. s, **C**H(CH_3)$_2$), 49.5 (d, *J*=5.6 Hz, N-**C**H(*o*OMe-Ph)$_2$), 22.5 ((CH(**C**H_3)$_2$), 21.2 ((CH(**C**H_3)$_2$); **^{31}P NMR** (202 MHz, CD_2Cl_2) δ_P/ppm 128.3 (br. s, 0.1P), 119.8 (br. s, 1P).

*(S)-N-isopropyl-2,3-dihydro-1H-inden-1-amine (**85**)*

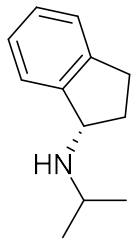

85

According to a modified procedure from Davies and coworkers,[291] acetone (0.32, 4.3 mmol, 2.0 eq) was added to a stirring solution of (*S*)-2,3-dihydro-1H-inden-1-amine (0.28 mL, 2.2 mmol, 1.0 eq) in THF (10 mL) at room temperature. After 5 min, NaB(OAc)$_3$H (912 mg, 5.16 mmol, 2.40 eq) was added into the reaction mixture at room temperature and the resulting suspension was stirred for 48 h. Et_2O (15 mL) and $NaHCO_3$ (aq. sat., *ca* 10 mL) were added to the suspension and stirring was continued for 30 min. The mixture was partitioned between the aqueous and Et_2O layers and the aqueous phase extracted with Et_2O (3 × 10 mL). The combined organic phase was dried ($MgSO_4$), filtered and concentrated under reduced pressure to afford the desired title amine **85** (0.36 g, 1.5 mmol, 65%) as a yellow oil. The amine was used without further

purification. **^{1}H NMR** (400 MHz, $CDCl_3$) δ_H/ppm 7.35-7.48 (m, 1 H), 7.23 (dt, *J*= 9.5, 4.8 Hz, 3 H), 4.36 (t, *J*= 6.7 Hz, 1 H), 3.10-3.21 (m, 1 H), 3.04 (ddd, *J*= 15.7, 8.6, 4.8 Hz, 1 H), 2.82 (dt, *J*= 15.7, 7.6 Hz, 2 H), 2.45 (dtd, *J*= 12.5, 7.6, 7.6, 4.8 Hz, 1 H), 1.81-1.93 (m, 1 H), 1.12-1.27 (app. t, 6H); **^{13}C NMR** (100 MHz, $CDCl_3$) δ_C/ppm 144.8, 143.1, 127.0, 125.9, 124.3, 123.8, 60.0, 46.2, 33.8, 29.9, 23.0, 22.2; **HRMS** (ESI) *m/z* calcd for $C_{12}H_{18}N$ $[M+H]^+$: 176.1428, found: 176.1434; **IR** (ν_{max}/cm^{-1}) 2946, 1378, 851, 753.

*(11bS)-N-((S)-2,3-dihydro-1H-inden-1-yl)-N-isopropyldinaphtho[2,1-d:1',2'-f][1,3,2]dioxaphosphepin-4-amine ((S,S)-**P**)*

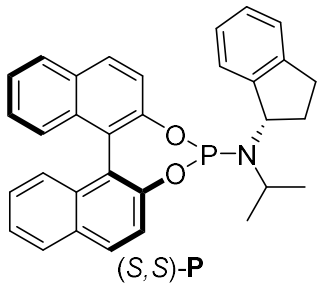

(*S*,*S*)-**P**

According to a modified procedure from Trost[293], triethylamine (0.72 mL, 4.0 mmol, 5.0 eq) was added dropwise to a solution of PCl_3 (0.10 mL, 0.80 mmol, 1.0 eq) in CH_2Cl_2 (2.5 mL) at 0 °C. The ice bath was removed and the solution left to warm to room temperature before (*S*)-*N*-isopropyl-2,3-dihydro-1H-inden-1-amine **85** (180 mg, 0.800 mmol, 1.00 eq) was added to the stirring solution. After 5 h, (*S*)-binaphthol (296 mg, 0.800 mmol, 1.00 eq) was added to the suspension and the subsequent mixture was left to stir overnight at room temperature. Then, the solution was filtered over a pad of silica and Celite® and rinsed with

CH_2Cl_2 (15 mL). The resulting solution was concentrated under reduced pressure to afford a yellow residue. After flash column chromatography (Petrol: CH_2Cl_2: Et_3N; 74:25:1 SiO_2), the title ligand (*S,S*)-**P** (86 mg, 0.18 mmol, 17%) was obtained as a crystalline white foaming solid. **^{1}H NMR** (500 MHz, $CDCl_3$) δ_H/ppm 7.84 (d, *J*=8.7 Hz, 1H, Ar-**H**), 7.83-7.74 (m, 2H, Ar-**H**), 7.78 (d, *J*=6.5 Hz, 1H, Ar-**H**), 7.52 (d, *J*=7.7 Hz, 1H, Ar-**H**), 7.47 (d, *J*=8.7 Hz, 1H, Ar-**H**), 7.39 (d, *J*=8.9 Hz, 1H, Ar-**H**), 7.32-7.26 (m, 3H, Ar-**H**), 7.24-7.18 (m, 2H, Ar-**H**), 7.18-7.07 (m, 4H, Ar-**H**), 4.65 (dt, *J*=14.7, 8.1 Hz, 1H, N-C**H**-CH_2), 3.24 (dq, *J*=14.7, 6.9 Hz, 1H, N-C**H**-$(CH_3)_2$), 2.86 (ddd, *J*=15.8, 9.1, 1.7 Hz, 1H, C**H**$_2$), 2.65-2.56 (m, 1H, C**H**$_2$), 2.42-2.32 (m, 1H, C**H**$_2$), 2.11-1.99 (m, 1H, C**H**$_2$), 1.20 (d, *J*=6.8 Hz, 3H, C**H$_3$**), 1.11 (d, *J*=6.6 Hz, 3H, C**H$_3$**); **^{13}C NMR** (125 MHz, $CDCl_3$) δ_C/ppm 150.3 (d, *J*= 8.0 Hz, **Cq**-Ar), 150.0 (**Cq**-Ar), 144.6 (d, *J*=5.1 Hz, **Cq**-Ar), 143.1 (**Cq**-Ar), 132.8 (d, *J*= 1.5 Hz, **Cq**-Ar), 132.7 (**Cq**-Ar), 131.3 (**Cq**-Ar), 130.5 (**Cq**-Ar), 130.2 (**C**H-Ar), 129.5 (**C**H-Ar), 128.2 (**C**H-Ar), 128.2 (**C**H-Ar), 127.3 (**C**H-Ar), 127.1 (**C**H-Ar), 127.1 (**C**H-Ar), 126.4, (**C**H-Ar) 125.9 (**C**H-Ar), 125.8 (**C**H-Ar), 124.8 (**C**H-Ar), 124.6 (**C**H-Ar), 124.6, (**C**H-Ar) 124.3 (**C**H-Ar), 124.1 (d, *J*=5.4 Hz, **Cq**-Ar), 122.4 (**C**H-Ar), 122.4 (**C**H-Ar), 121.7 (d, *J*=2.7 Hz, **Cq**-Ar), 59.4 (d, *J*=17.6 Hz, N-**C**H-CH_2), 45.9 (d, *J*=7.4 Hz, N-**C**H-$(CH_3)_2$), 36.6 (**C**H_2), 30.1 (**C**H_2), 25.1 (d, *J*=5.4 Hz, **C**H_3), 23.9 (d, *J*=6.6 Hz, **C**H_3); **^{31}P NMR** (200 MHz, $CDCl_3$) δ_P/ppm 151.4 (s, 1P); **HRMS** (EI) *m*/z calcd for $C_{32}H_{28}NO_2P$ $[M]^+$:489.1858, found: 489.1865; **IR (neat)** ν_{max}/cm^{-1} 2969, 1590, 1232, 947, 790, 751; **$[\alpha]_D^{25}$** = +145.5 (c=0.8 in $CHCl_3$); **Mp** 238-242°C.

^{1}H NMR (500 MHz, CD_2Cl_2) δ_H/ppm 7.98 (d, *J*=9.2 Hz, 1H, Ar-**H**), 7.96-7.88 (m, 3H, Ar-**H**), 7.63 (d, *J*=7.6 Hz, 1H, Ar-**H**), 7.60 (d, *J*=8.8 Hz, 1H, Ar-**H**), 7.51 (d, *J*=8.8 Hz, 1H, Ar-**H**), 7.45-7.38 (m, 2H, Ar-**H**), 7.36 (d, *J*=8.4 Hz, 1H, Ar-**H**), 7.34-

7.30 (m, 1H, Ar-**H**), 7.29-7.19 (m, 5H, Ar-**H**), 4.65 (dt, *J*= 16.1, 8.1 Hz, 1H, N-C**H**-CH_2), 3.22 (dq, *J*= 14.5, 6.7 Hz, 1H, N-C**H**-$(CH_3)_2$), 2.86 (ddd, *J*= 15.9, 9.1, 2.6 Hz, 1H, C**H**$_2$), 2.67-2.56 (m, 1H, C**H**$_2$), 2.42-2.31 (m, 1H, C**H**$_2$), 2.11–1.99 (m, 1H, C**H**$_2$), 1.28 (d, *J*=6.5 Hz, 3H, C**H**$_3$), 1.18 (d, *J*=6.3 Hz, 3H, C**H**$_3$); **^{13}C NMR** (125 MHz, CD_2Cl_2) δ_C/ppm 150.7 (d, *J*= 8.2 Hz, **Cq**-Ar), 150.5 (**Cq**-Ar), 145.2 (d, *J*=4.3 Hz, **Cq**-Ar), 143.6 (**Cq**-Ar), 133.1 (d, *J*= 1.8 Hz, **Cq**-Ar), 133.1 (**Cq**-Ar), 131.8 (**Cq**-Ar), 131.0 (**Cq**-Ar), 130.7 (**C**H-Ar), 130.0 (**C**H-Ar), 128.7 (**C**H-Ar), 128.7 (**C**H-Ar), 127.7 (**C**H-Ar), 127.3 (**C**H-Ar), 127.2 (**C**H-Ar), 126.8 (**C**H-Ar), 126.4 (**C**H-Ar), 126.3 (**C**H-Ar), 125.1 (**C**H-Ar), 125.1 (**C**H-Ar), 125.0 (**C**H-Ar), 124.8 (**C**H-Ar), 124.3 (d, *J*= 5.4 Hz, **Cq**-Ar), 122.7 (**C**H-Ar), 122.6 (d, *J*=1.6 Hz, **C**H-Ar), 122.0 (d, *J*=2.5 Hz, **Cq**-Ar), 59.6 (d, *J*=21.1 Hz, N-**C**H-CH_2), 46.4 (d, *J*=6.3 Hz, N-**C**H-$(CH_3)_2$), 37.2 (**C**H_2), 30.5 (**C**H_2), 25.0 (d, *J*=5.3 Hz, **C**H_3), 23.8 (d, *J*=5.3 Hz, **C**H_3); **^{31}P NMR** (200 MHz, CD_2Cl_2) δ_P/ppm 152.1 (s, 1P).

*CuOTf-**P***

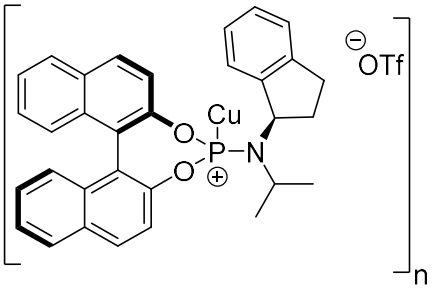

In a flame-dried flask under inert atmosphere, CuCl (1.9 mg, 20 μmol, 10 mol%) and (*S,S*)-**P** (12.0 mg, 20.0 μmol, 10.0 mol%) were dissolved in CD_2Cl_2 (1.0 mL) and stirred for 1 h at room temperature. AgOTf (5.7 mg, 22.0 μmol,

11.0 mol%) was added to the freshly formed Cu-ligand complex solution and stirred for 15 min. The resulting catalyst complex mixture was filtered into a flamed dried NMR tube adapted with an NMR septa and parafilmed. **^{1}H NMR** (500 MHz, CD_2Cl_2) δ_H/ppm 7.97(d, *J*= 8.8 Hz, 1H, Ar-**H**), 7.93 (d, *J*= 8.8 Hz, 1H, Ar-**H**), 7.90 (d, *J*= 8.2 Hz, 1H, Ar-**H**), 7.83 (d, *J*= 8.2 Hz, 1H, Ar-**H**), 7.54 (d, *J*= 8.3 Hz, 1H, Ar-**H**), 7.50–7.43 (m, 2H, Ar-**H**), 7.41 (dd, *J*= 8.2, 7.6 Hz, 1H, Ar-**H**), 7.38–7.33 (m, 1H, Ar-**H**), 7.31-7.19 (m, 5H, Ar-**H**), 7.18-7.14 (m, 2H, Ar-**H**), 4.83 (dt, *J*= 23.9, 8.5 Hz, 1H, N-C**H**-CH_2), 3.40 (sep., *J*= 6.6 Hz, 1H, N-C**H**-$(CH_3)_2$), 3.20 (dd, *J*= 16.2, 9.4 Hz, 1H, C**H**$_2$), 2.84–2.66 (m, 2H, C**H**$_2$), 2.35-2.21 (m, 1H, C**H**$_2$), 1.23 (d, *J*= 6.6 Hz, 3H, C**H$_3$**), 1.04 (d, *J*= 6.6 Hz, 3H, C**H$_3$**); **^{13}C NMR** (125 MHz, CD_2Cl_2) δ_C/ppm 148.5 (**Cq**-Ar), 148.4 (**Cq**-Ar), 147.9 (d, *J*=4.6 Hz, **Cq**-Ar), 143.6 (**Cq**-Ar), 142.4 (d, *J*=10.9 Hz, **Cq**-Ar), 132.6 (**Cq**-Ar), 132.5 (**Cq**-Ar), 132.2 (**Cq**-Ar), 131.8 (**C**H-Ar), 131.5 (**Cq**-Ar), 130.8 (**C**H-Ar), 128.8 (**C**H-Ar), 128.7 (**C**H-Ar), 128.5 (**C**H-Ar), 127.8 (**C**H-Ar), 127.2 (**C**H-Ar), 126.8 (**C**H-Ar), 126.8 (**C**H-Ar), 126.8 (**C**H-Ar), 126.6 (**C**H-Ar), 125.7 (**C**H-Ar), 125.7 (**C**H-Ar), 124.1 (d, *J*=2.7 Hz, **C**H-Ar), 123.2 (d, *J*=3.7 Hz, **Cq**-Ar), 121.3 (**C**H-Ar), 120.6 (**C**H-Ar), 59.1 (d, *J*= 25.1 Hz, N-**C**H-CH_2), 47.9 (d, *J*=4.6 Hz, N-**C**H-$(CH_3)_2$), 39.5 (br. s, **C**H_2), 30.3 (**C**H_2), 23.3 (**C**H_3), 21.9 (**C**H_3); **^{31}P NMR** (202 MHz, CD_2Cl_2) δ_P/ppm 122.0 (br. s, 1P); **^{19}F NMR** (470 MHz, CD_2Cl_2) δ_F/ppm -77.8 (s, 1F).

2) General Procedures

*Procedures of enantioenriched products from **62a***

In a flame-dried flask under inert atmosphere, Cp_2ZrHCl (2.0 eq) was added to a solution of alkene (2.5 eq) in CH_2Cl_2 under an argon atmosphere and stirred

vigorously until a clear yellow solution was obtained (20-40 min). Simultaneously, in another flask under inert atmosphere, CuCl (10 mol%) and (*R*)-**W** (10.0 mol%) were dissolved in CH_2Cl_2 (0.2 M) and stirred for 1 h at room temperature. $AgClO_4$ (0.11 eq ***Perchlorates are explosive and should be handled with caution***) was added to the freshly formed Cu-ligand complex solution and stirred for 15 min. The resulting catalyst complex mixture was filtered into the freshly prepared alkylzirconocene species. After 10 min, 3-chloro-3,6-dihydro-2*H*-pyran **62a** (1.0 eq) was added dropwise via a microsyringe to the resulting black solution followed by the dropwise addition of $B(OiPr)_3$ (1.0 eq). The reaction mixture was stirred overnight. The reaction mixture was diluted with Et_2O (2 mL) and quenched with NH_4Cl (3 mL, 1 M). The mixture was partitioned and the aqueous phase was extracted with Et_2O (3 x 10 mL). The combined organic extracts were washed with $NaHCO_3$ (aq., sat., 30 mL), dried over $MgSO_4$, filtered and concentrated under reduced pressure. Purification by flash column chromatography (Et_2O 0→2% in pentane; SiO_2) yielded the enantioenriched products.

*Procedures of enantioenriched products from **62d***

In a flame-dried flask under inert atmosphere, Cp_2ZrHCl (2.0 eq) was added to a solution of alkene (2.5 eq) in CH_2Cl_2 under an argon atmosphere and stirred vigorously until a clear yellow solution was obtained (20-40 min). Simultaneously, in another flask under inert atmosphere, CuCl (10 mol%) and (*S, S*)-**P** (10.0 mol%) were dissolved in CH_2Cl_2 (0.2 M) and stirred for 1 h at room temperature. AgOTf (0.11 eq) was added to the freshly formed Cu-ligand complex solution and stirred for 15 min. The resulting catalyst complex mixture

was filtered into the freshly prepared alkylzirconocene species. After 10 min, 3,6-dihydro-2*H*-pyran-3-yl diethyl phosphate **62d** (1.0 eq) was added dropwise via a microsyringe to the resulting black solution and stirred overnight. The reaction mixture was diluted with Et_2O (2 mL) and quenched with NH_4Cl (3 mL, 1 M). The mixture was partitioned and the aqueous phase was extracted with Et_2O (3 x 10 mL). The combined organic extracts were washed with $NaHCO_3$ (aq., sat., 30 mL), dried over $MgSO_4$, filtered and concentrated under reduced pressure. Purification by flash column chromatography (SiO_2, Et_2O 0→2% in pentane) yielded the enantioenriched products.

*Procedures of racemic products from **62a***

In a flame-dried flask under inert atmosphere, Cp_2ZrHCl (2.0 eq) was added to a solution of alkene (2.5 eq) in CH_2Cl_2 under an argon atmosphere and stirred vigorously until a clear yellow solution was obtained (20-40 min). Simultaneously, in another flask under inert atmosphere, CuCl (10 mol%) and (*S, S, S*)-**A** (5.0 mol) and (*R, R, R*)-**A** (5.0 mol) were dissolved in CH_2Cl_2 (0.2 M) and stirred for 1 h at room temperature. $AgClO_4$ (0.11 eq ***Perchlorates are explosive and should be handled with caution***) was added to the freshly formed Cu-ligand complex solution and stirred for 15 min. The resulting catalyst complex mixture was filtered into the freshly prepared alkylzirconocene species. After 10 min, 3-chloro-3,6-dihydro-2*H*-pyran **62a** (1.0 eq) was added dropwise via a microsyringe to the resulting black solution followed by the dropwise addition of $B(O\textit{i}Pr)_3$ (1.0 eq). The reaction mixture was stirred overnight. The reaction mixture was diluted with Et_2O (2 mL) and quenched with NH_4Cl (3 mL, 1 M). The mixture was partitioned and the aqueous phase was extracted with Et_2O (3 x

10 mL). The combined organic extracts were washed with $NaHCO_3$ (aq., sat., 30 mL), dried over $MgSO_4$, filtered and concentrated under reduced pressure. Purification by flash column chromatography (SiO_2, Et_2O 0→2% in pentane) yielded the racemic products.

*Procedures of racemic products from **62d***

In a flame-dried flask under inert atmosphere, Cp_2ZrHCl (210 mg, 0.80 mmol, 2.0 eq) was added to a solution of alkene (1.0 mmol, 2.5 eq) in CH_2Cl_2 (0.40 mL) under an argon atmosphere and stirred vigorously until a clear yellow solution was obtained (20-40 min). The hydrozirconated mixture was dissolved in CH_2Cl_2 (2.0 mL) and then CuBr·DMS (82 mg, 0.40 mmol, 1.0 eq) was added. After 10 min, 3,6-dihydro-2*H*-pyran-3-yl diethyl phosphate **62d** (94.5 mg, 0.400 mmol, 1.00 eq) was added dropwise via a microsyringe to the resulting black solution and stirred overnight. The reaction mixture was diluted with Et_2O (2 mL) and quenched with NH_4Cl (3 mL, 1 M). The mixture was partitioned and the aqueous phase was extracted with Et_2O (3 x 10 mL). The combined organic extracts were washed with $NaHCO_3$ (aq., sat., 30 mL), dried over $MgSO_4$, filtered and concentrated under reduced pressure. Purification by flash column chromatography (SiO_2, Et_2O 0→2% in pentane) yielded the racemic products.

Derivatisation of products to the corresponding epoxides for GC analysis

In a flame-dried flask, the isolated product **63** (1.0 eq) was dissolved in CH_2Cl_2 (0.07 M) under an argon atmosphere. *m*-CPBA (2.0 eq) and Na_2HPO_4 (3.0 eq) were added at room temperature and the reaction mixture was stirred arbitrarily for 3 h before being diluted and quenched by addition of Et_2O (10 mL)

and an aqueous solution of saturated $Na_2S_2O_3$ (10 mL). The organic layer was washed with NaOH (1 M aq., 3× 5mL), dried over mg_2SO_4, filtered and concentrated under vacuum. The crude mixture of diastereomeric epoxides was directly analysed by GC chromatography using a chiral non-racemic stationary phase.

3) Specific Procedures

*3-(4-phenylbutyl)-3,6-dihydro-2H-pyran (**63a**)*

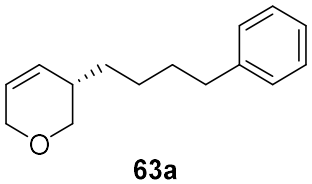

63a

Procedures from 62a

In a flame-dried flask under inert atmosphere, Cp_2ZrHCl (310 mg, 1.2 mmol, 2.0 eq) was added to a solution of 4-phenyl-1-butene **16** (0.23 mL, 1.5 mmol 2.5 eq) in CH_2Cl_2 (0.6 mL) under an argon atmosphere and stirred vigorously until a clear yellow solution was obtained (20-40 min). Simultaneously, in another flask under inert atmosphere, CuCl (5.7 mg, 0.06 mmol, 10 mol%) and (*R*)-**W** (36.0 mg, 60.0 μmol, 10.0 mol%) were dissolved in CH_2Cl_2 (3.0 mL) and stirred for 1 h at room temperature. $AgClO_4$ (13.8 mg, 66.0 μmol, 11.0 mol% ***Perchlorates are explosive and should be handled with caution***) was added to the freshly formed Cu-ligand complex solution and stirred for 15 min. The resulting catalyst complex mixture was

filtered into the freshly prepared alkylzirconocene species. After 10 min, 3-chloro-3,6-dihydro-2*H*-pyran **62a** (71 mg, 0.60 mmol, 1.0 eq) was added dropwise via a microsyringe to the resulting black solution followed by the dropwise addition of $B(OiPr)_3$ (0.14 mL, 0.60 mmol, 1.0 eq). The reaction mixture was stirred overnight. The reaction mixture was diluted with Et_2O (2 mL) and quenched with NH_4Cl (3 mL, 1 M). The mixture was partitioned and the aqueous phase was extracted with Et_2O (3 x 10 mL). The combined organic extracts were washed with $NaHCO_3$ (aq., sat., 30 mL), dried over $MgSO_4$, filtered and concentrated under reduced pressure. Purification by flash column chromatography (SiO_2, 0→2% Et_2O in pentane) yielded the title (*S*)-**63a** (30 mg, 0.14 mmol, 25% yield, 100% conversion, 83% ee) as a colourless oil.

Procedures from 62d

In a flame-dried flask under inert atmosphere, Cp_2ZrHCl (310 mg, 1.2 mmol, 2.0 eq) was added to a solution of 4-phenyl-1-butene **16** (0.23 mL, 1.5 mmol, 2.5 eq) in CH_2Cl_2 (0.6 mL) under an argon atmosphere and stirred vigorously until a clear yellow solution was obtained (20-40 min). Simultaneously, in another flask under inert atmosphere, CuCl (5.7 mg, 0.06 mmol, 10 mol%) and (*S, S*)-**P** (29.7 mg, 60.0 μmol, 10.0 mol%) were dissolved in CH_2Cl_2 (3.0 mL) and stirred for 1 h at room temperature. AgOTf (17.1 mg, 66.0 μmol, 11.0 mol%) was added to the freshly formed Cu-ligand complex solution and stirred for 15 min. The resulting catalyst complex mixture was filtered into the freshly prepared alkylzirconocene species. After 10 min, 3,6-dihydro-2*H*-pyran-3-yl diethyl phosphate **62d** (142 mg, 0.600 mmol, 1.00 eq)

was added dropwise via a microsyringe to the resulting black solution and stirred overnight. The reaction mixture was diluted with Et_2O (2 mL) and quenched with NH_4Cl (3 mL, 1 M). The mixture was partitioned and the aqueous phase was extracted with Et_2O (3 x 10 mL). The combined organic extracts were washed with $NaHCO_3$ (aq., sat., 30 mL), dried over $MgSO_4$, filtered and concentrated under reduced pressure. Purification by flash column chromatography (SiO_2, Et_2O 0→2% in pentane) yielded the title (*R*)-**63a** (23 mg, 0.10 mmol, 17% yield, 31% conversion, 83% ee) as a colourless oil. **^{1}H NMR** (400 MHz, $CDCl_3$) δ_H/ppm 7.36-7.30 (m, 2H, C**H**-Ar), 7.26-7.21 (m, 3H, C**H**-Ar), 5.82 (ddd, *J*= 10.4, 4.7, 2.2 Hz, 1H, C**H**=CH), 5.75 (ddd, *J*= 10.1, 4.2, 2.2 Hz, 1H, C**H**=CH), 4.17-4.13 (m, 2H, C**H$_2$**-O), 3.90 (dd, *J*= 10.9, 4.7 Hz, 1H, C**H$_2$**-O), 3.45 (dd, *J*= 11.1, 6.7 Hz, 1H, C**H$_2$**-O), 2.67 (t, *J*= 7.7 Hz, 2H, C**H$_2$**-Ph), 2.28-2.17 (m, 1H, C**H**-CH_2), 1.73-1.62 (m, 2H, C**H$_2$**), 1.46-1.35 (m, 4H, C**H$_2$**); **^{13}C NMR** (100 MHz, $CDCl_3$) δ_C/ppm 142.6 (**Cq-**Ar), 129.3 (**C**H=CH), 128.4 (**C**H-Ar), 128.3 (**C**H-Ar), 125.8 (**C**H=CH), 125.7 (**C**H-Ar), 69.3 (**C**H_2-O), 65.6 (**C**H_2-O), 35.9 (**C**H_2), 34.6 (**C**H), 32.4 (**C**H_2), 31.7 (**C**H_2), 26.5 (**C**H_2); **HRMS** (CI GCMS) *m*/z calcd for $C_{15}H_{20}O$ $[M+H]^+$: 217.1587, found: 217.1586; **IR (neat)** ν_{max}/cm^{-1} 3027, 2929, 2856, 1496, 1454, 1117, 1087, 746, 699; **$[\alpha]_D^{25}$** = -46.3° (c= 1.0 in $CHCl_3$, 80% ee). (From phosphate)

The enantiomeric excess of 83% was determined by HPLC [Chiralpak® IB; hexane:*i*PrOH 99.2:0.8; 1.0 mL.min^{-1}, λ= 210 nm, t_R = 5.67 min (minor enantiomer), t_R = 6.07 min (major enantiomer)].

From allylphosphate **62d** (83% ee of (*R*)-**63a**)

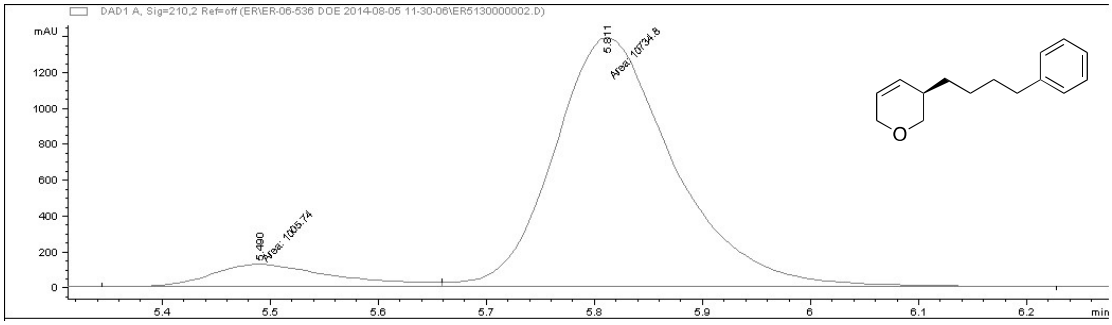

From allylchloride **62a** (83% ee for (*S*)-**63a**)

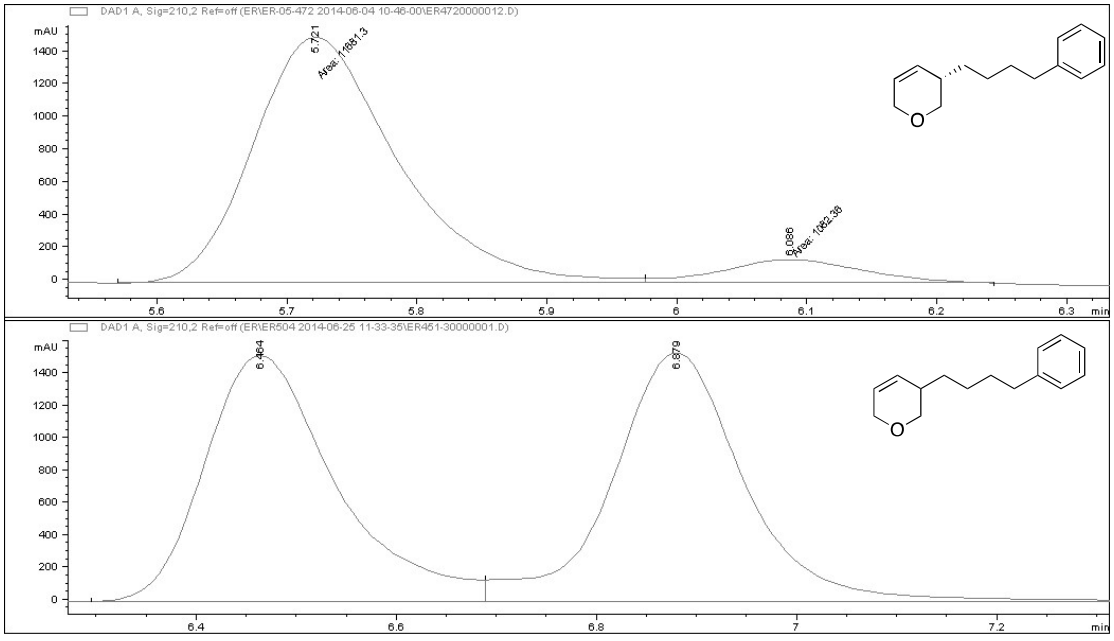

*(S)-3-(3-(4-(trifluoromethyl)phenyl)propyl)-3,6-dihydro-2H-pyran (**63b**)*

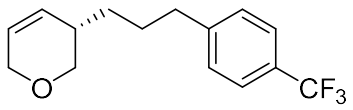

63b

In a flame-dried flask under inert atmosphere, Cp_2ZrHCl (310 mg, 1.2 mmol, 2.0 eq) was added to a solution of 1-allyl-4-(trifluoromethyl)benzene (0.25 mL, 1.5 mmol 2.5 eq) in CH_2Cl_2 (0.6 mL) under an argon atmosphere and stirred vigorously until a clear yellow solution was obtained (20-40 min). Simultaneously, in another flask under inert atmosphere, CuCl (5.7 mg, 60 μmol, 10 mol%) and (*R*)-**W** (36.0 mg, 60.0 μmol, 10.0 mol%) were dissolved in CH_2Cl_2 (3.0 mL) and stirred for 1 h at room temperature. $AgClO_4$ (13.8 mg, 66.0 μmol, 11.0 mol% ***Perchlorates are explosive and should be handled with caution***) was added to the freshly formed Cu-ligand complex solution and stirred for 15 min. The resulting catalyst complex mixture was filtered into the freshly prepared alkylzirconocene species. After 10 min, 3-chloro-3,6-dihydro-2*H*-pyran **62a** (71 mg, 0.60 mmol, 1.0 eq) was added dropwise via a microsyringe to the resulting black solution followed by the dropwise addition of $B(OiPr)_3$ (0.14 mL, 0.60 mmol, 1.0 eq). The reaction mixture was stirred overnight. The reaction mixture was diluted with Et_2O (2 mL) and quenched with NH_4Cl (3 mL, 1 M). The mixture was partitioned and the aqueous phase was extracted with Et_2O (3 x 10 mL). The combined organic extracts were washed with $NaHCO_3$ (aq., sat., 30 mL), dried over $MgSO_4$, filtered and concentrated under reduced pressure. Purification by flash column chromatography (SiO_2, Et_2O 0→2% in pentane)

yielded the title product **63b** (29 mg, 0.11 mmol, 18% yield, 75% ee) as a colourless oil. **^{1}H NMR** (400 MHz, $CDCl_3$) δ_H/ppm 7.54 (d, *J*= 8.3 Hz, 2H, C**H**-Ar), 7.29 (d, *J*= 7.9 Hz, 2H, C**H**-Ar), 5.82-5.69 (m, 2H, C**H**=C**H**), 4.16-4.05 (m, 2H, C**H$_2$**-O), 3.86 (dd, *J*= 11.4, 4.8 Hz, 1H, C**H$_2$**-O), 3.43 (dd, *J*= 11.4, 6.5Hz, 1H, C**H$_2$**-O), 2.68 (t, *J*= 7.6 Hz, 2H, C**H$_2$**-Ph), 2.27-2.17 (m, 1H, C**H**), 1.76-1.65 (m, 2H, C**H$_2$**), 1.45-1.35 (m, 2H, C**H$_2$**); **^{13}C NMR** (100 MHz, $CDCl_3$) δ_C/ppm 146.4 (**Cq-**Ar), 128.8 (**C**H=CH), 128.7 (**C**H-Ar), 126.2 (**C**H=CH), 125.3 (q, *J*=3.8 Hz, **C**H-Ar), 69.1 (**C**H_2-O), 65.6 (**C**H_2-O), 35.9 (**C**H_2), 34.5 (**C**H), 32.1 (**C**H_2), 28.4 (**C**H_2); **^{19}F NMR** (377 MHz, $CDCl_3$) δ_F/ppm -62.28 (s, 1F); **HRMS** (EI/FI) *m*/z calcd for $C_{15}H_{17}OF_3$ $[M]^+$:270.1231, found:270.1232; **IR (neat)** ν_{max}/cm^{-1} 2933, 1326, 1164, 1122, 1068, 1019, 908, 733; **$[\alpha]_D^{25}$** = +30.6° (c=0.8 in $CHCl_3$, 75% ee).

GC analysis of the crude mixture of epoxides derived from **63b** indicated an enantiomeric excess of 75% (Hydrodex 6-TBDM, 60-170 °C at 1 ˚C/min, 170 ˚C for 100 min, 10 psi); major enantiomer t_R= 135.5, 149.8 min; minor enantiomer t_R = 133.4, 164.8 min.

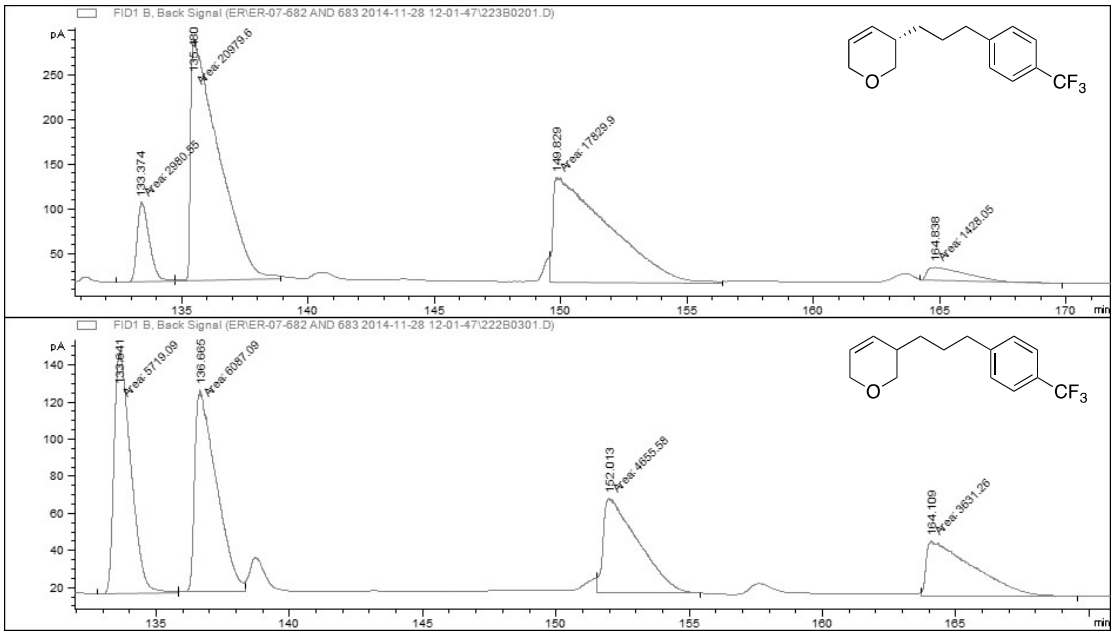

*(S)-3-(6-chlorohexyl)-3,6-dihydro-2H-pyran (**63c**)*

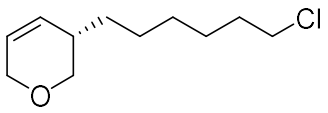

63c

In a flame-dried flask under inert atmosphere, Cp_2ZrHCl (310 mg, 1.2 mmol, 2.0 eq) was added to a solution of 6-chlorohex-1-ene (0.20 mL, 1.5 mmol 2.5 eq) in CH_2Cl_2 (0.6 mL) under an argon atmosphere and stirred vigorously until a clear yellow solution was obtained (20-40 min). Simultaneously, in another flask under inert atmosphere, CuCl (5.7 mg, 60 μmol, 10 mol%) and (*R*)-**W** (36.0 mg, 60.0 μmol, 10.0 mol%) were dissolved in CH_2Cl_2 (3.0 mL) and stirred for 1 h at room temperature. $AgClO_4$ (13.8 mg, 66.0 μmol, 0.11 eq ***Perchlorates are explosive and should be handled with caution***) was added to the freshly formed Cu-ligand complex solution and stirred for 15 min. The resulting catalyst complex mixture was filtered into the freshly prepared alkylzirconocene species. After 10 min, 3-chloro-3,6-dihydro-2*H*-pyran **62a** (71 mg, 0.60 mmol, 1.0 eq) was added dropwise via a microsyringe to the resulting black solution followed by the dropwise addition of $B(OiPr)_3$ (0.14 mL, 0.60 mmol, 1.0 eq). The reaction mixture was stirred overnight. The reaction mixture was diluted with Et_2O (2 mL) and quenched with NH_4Cl (3 mL, 1 M). The mixture was partitioned and the aqueous phase was extracted with Et_2O (3 x 10 mL). The combined organic extracts were washed with $NaHCO_3$ (aq., sat., 30 mL), dried over $MgSO_4$, filtered and concentrated under reduced pressure. Purification by flash column chromatography (SiO_2, Et_2O 0→2% in pentane)

yielded the title product **63c** (41 mg, 0.20 mmol, 33% yield, 77% ee) as a colourless oil. **^{1}H NMR** (400 MHz, $CDCl_3$) δ_H/ppm 5.80-5.73 (m, 1H, C**H**=CH), 5.73-5.67 (m, 1H, C**H**=CH), 4.16-4.05 (m, 2H, C**H**$_2$-O), 3.87 (dd, *J*= 10.9, 6.6 Hz, 1H, C**H**$_2$-O), 3.54 (t, *J*= 6.8 Hz, 2H, C**H**$_2$-Cl), 3.41 (dd, *J*= 11.1, 4.9 Hz, 1H, C**H**$_2$-O), 2.24-2.15 (m, 1H, C**H**), 1.78 (tt, *J*= 14.8, 6.9 Hz, 2H, C**H**$_2$), 1.50-1.40 (m, 2H, C**H**$_2$), 1.39-1.30 (m, 6H, C**H**$_2$); **^{13}C NMR** (100 MHz, $CDCl_3$) δ_C/ppm 129.2 (**C**H=CH), 125.8 (**C**H=CH), 69.3 (**C**H$_2$-O), 65.6 (**C**H$_2$-O), 45.1 (**C**H$_2$-Cl), 34.6 (**C**H), 32.6 (**C**H$_2$), 32.4 (**C**H$_2$), 29.1 (**C**H$_2$), 26.8 (**C**H$_2$), 26.7 (**C**H$_2$); **HRMS** (ESI) *m*/z calcd for $C_{11}H_{19}OClNa$ $[M+Na]^+$:225.10166, found:225.10132; **IR (neat)** ν_{max}/cm^{-1} 2928, 2855, 1458, 1142, 1088; **$[\alpha]_D^{25}$** = +46.6° (c=1.1 in $CDCl_3$, 77% ee).

GC analysis of the crude mixture of epoxides derived from **63c** indicated an enantiomeric excess of 77% (Hydrodex 6-TBDM, 60-170 °C at 1 ˚C/min, 170 ˚C for 70 min, 10 psi); major enantiomer t_R= 114.8, 122.9 min; minor enantiomer t_R = 115.9, 126.2 min.

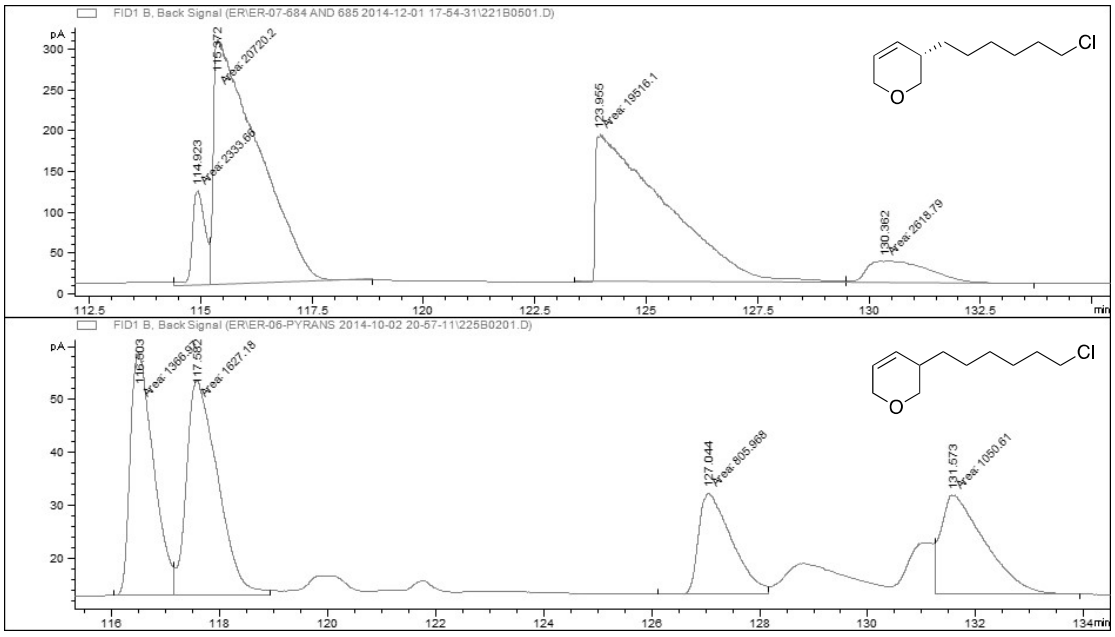

*(S)-3-(2-cyclohexylethyl)-3,6-dihydro-2H-pyran (**63d**)*

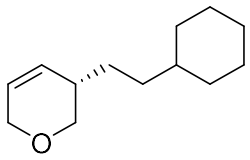

63d

In a flame-dried flask under inert atmosphere, Cp_2ZrHCl (310 mg, 1.2 mmol, 2.0 eq) was added to a solution of vinylcyclohexane (0.21 mL, 1.5 mmol 2.5 eq) in CH_2Cl_2 (0.6 mL) under an argon atmosphere and stirred vigorously until a clear yellow solution was obtained (20-40 min). Simultaneously, in another flask under inert atmosphere, CuCl (5.7 mg, 60 μmol, 10 mol%) and (*R*)-**W** (36.0 mg, 60.0 μmol, 10.0 mol%) were dissolved in CH_2Cl_2 (3.0 mL) and stirred for 1 h at room temperature. $AgClO_4$ (13.8 mg, 66.0 μmol, 11.0 mol% ***Perchlorates are explosive and should be handled with caution***) was added to the freshly formed Cu-ligand complex solution and stirred for 15 min. The resulting catalyst complex mixture was filtered into the freshly prepared alkylzirconocene species. After 10 min, 3-chloro-3,6-dihydro-2*H*-pyran **62a** (71 mg, 0.60 mmol, 1.0 eq) was added dropwise via a microsyringe to the resulting black solution followed by the dropwise addition of $B(OiPr)_3$ (0.14 mL, 0.60 mmol, 1.0 eq). The reaction mixture was stirred overnight. The reaction mixture was diluted with Et_2O (2 mL) and quenched with NH_4Cl (3 mL, 1 M). The mixture was partitioned and the aqueous phase was extracted with Et_2O (3 x 10 mL). The combined organic extracts were washed with $NaHCO_3$ (aq., sat., 30 mL), dried over $MgSO_4$, filtered and concentrated under reduced pressure. Purification by flash column chromatography (SiO_2, Et_2O 0→2% in pentane)

yielded the title product **63d** (24 mg, 0.12 mmol, 20% yield, 88% ee) as a colourless oil. **^{1}H NMR** (400 MHz, $CDCl_3$) δ_H/ppm 5.71 (ddd, *J*= 10.3, 5.5 Hz, 2.3 Hz, 1H, C**H**=CH), 5.62 (ddd, *J*= 10.3, 5.2 Hz, 2.2 Hz, 1H, C**H**=CH), 4.04-4.00 (m, 2H, C**H**$_2$-O), 3.79 (ddd, *J*= 11.0, 4.8, 0.4 Hz, 1H, C**H**$_2$-O), 3.31 (dd, *J*= 11.3, 6.9 Hz, 1H, C**H**$_2$-O), 2.14-2.03 (m, 1H, C**H**) 1.69-1.52 (m, 4H, C**H**$_2$), 1.31-1.06 (m, 9H, C**H**$_2$ and C**H**), 0.88-0.73 (m, 2H, C**H**$_2$); **^{13}C NMR** (100 MHz, $CDCl_3$) δ_C/ppm 129.4 (**C**H=CH), 125.7 (**C**H=CH), 69.4 (C**H**$_2$-O), 65.6 (C**H**$_2$-O), 37.9 (**C**H), 34.9 (**C**H), 34.5 (**C**H_2), 33.4 (**C**H_2), 29.8 (**C**H_2), 26.7 (**C**H_2), 26.4 (**C**H_2); **HRMS** (CI GCMS) *m*/z calcd for $[M]^+$: 194.1671, found: 194.1668; **IR (neat)** ν_{max}/cm^{-1} 3029, 2919, 2850, 1448, 1224, 1089, 886, 701, 686; **$[\alpha]_D^{25}$** = +55.6° (c= 1.1 in $CHCl_3$, 88% ee).

GC analysis of the crude mixture of epoxides derived from **63d** indicated an enantiomeric excess of 88% (Hydrodex 6-TBDM, 60-165 °C at 1 ˚C/min, 165 ˚C for 70 min, 10 psi); major enantiomer t_R= 100.8, 105.2 min; minor enantiomer t_R = 100.2, 109.1 min.

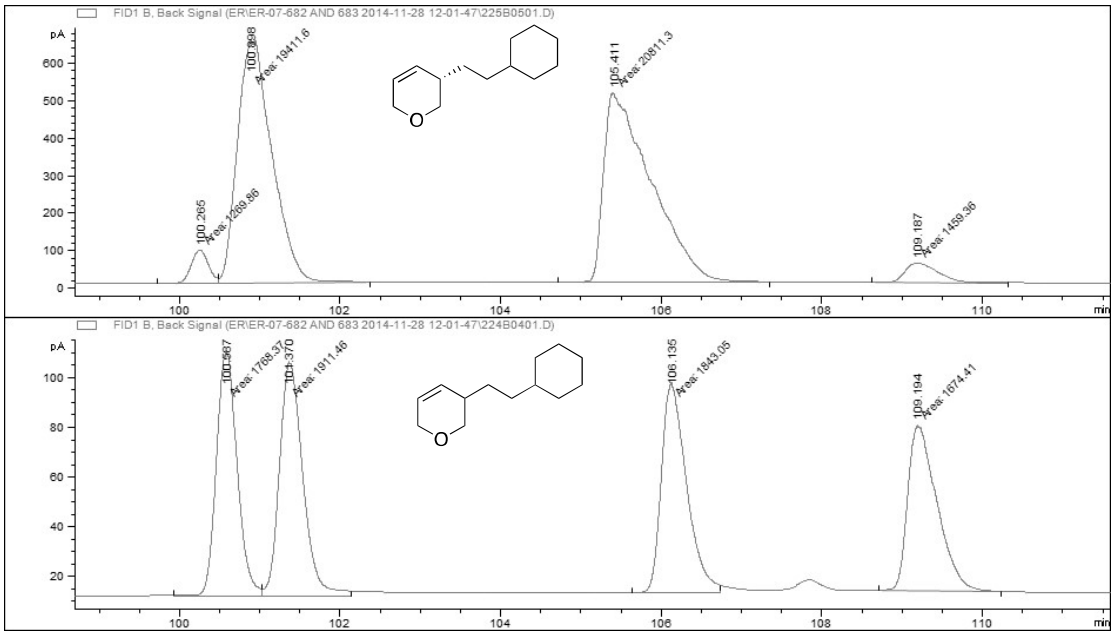

*(S)-(3-(3,6-dihydro-2H-pyran-3-yl)propyl)trimethylsilane (**63e**)*

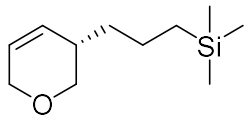

63e

In a flame-dried flask under inert atmosphere, Cp_2ZrHCl (410 mg, 1.6 mmol, 2.0 eq) was added to a solution of allyltrimethylsilane (0.32 mL, 2.0 mmol 2.5 eq) in CH_2Cl_2 (0.8 mL) under an argon atmosphere and stirred vigorously until a clear yellow solution was obtained (20-40 min). Simultaneously, in another flask under inert atmosphere, CuCl (7.6 mg, 80 μmol, 10 mol%) and (*R*)-**W** (48.0 mg, 80.0 μmol, 10.0 mol%) were dissolved in CH_2Cl_2 (4.0 mL) and stirred for 1 h at room temperature. $AgClO_4$ (18.2 mg, 88.0 μmol, 11.0 mol% ***Perchlorates are explosive and should be handled with caution***) was added to the freshly formed Cu-ligand complex solution and stirred for 15 min. The resulting catalyst complex mixture was filtered into the freshly prepared alkylzirconocene species. After 10 min, 3-chloro-3,6-dihydro-2*H*-pyran **62a** (95 mg, 0.80 mmol, 1.0 eq) was added dropwise via a microsyringe to the resulting black solution followed by the dropwise addition of $B(OiPr)_3$ (0.18 mL, 0.80 mmol, 1.0 eq). The reaction mixture was stirred overnight. The reaction mixture was diluted with Et_2O (2 mL) and quenched with NH_4Cl (3 mL, 1 M). The mixture was partitioned and the aqueous phase was extracted with Et_2O (3 x 10 mL). The combined organic extracts were washed with $NaHCO_3$ (aq., sat., 30 mL), dried over $MgSO_4$, filtered and concentrated under reduced pressure. Purification by flash column chromatography (SiO_2, Et_2O 0→2% in pentane)

yielded the title product **63e** (13 mg, 66 μmol, 8% yield, 93% ee) as a volatile colourless oil. **^{1}H NMR** (400 MHz, $CDCl_3$) δ_H/ppm 5.77(ddd, *J*= 10.3, 4.5, 2.1 Hz, 1H, C**H**=CH), 5.69 (ddd, *J*= 10.3, 4.5, 2.2 Hz, 1H, C**H**=CH), 4.13-4.08 (m, 2H, C**H**$_2$-O), 3.86 (dd, *J*= 10.9, 4.8 Hz, 1H, C**H**$_2$-O), 3.39 (dd, *J*= 10.9, 6.9 Hz, 1H, C**H**$_2$-O), 2.26-2.18 (br. m, 1H, C**H**), 1.38-1.32 (m, 4H, C**H**$_2$), 0.53-0.45 (m, 2H, C**H**$_2$), -0.02 (s, 9H, C**H**$_3$); **^{13}C NMR** (100 MHz, $CDCl_3$) δ_C/ppm 129.5 (**C**H=CH), 125.8 (**C**H=CH), 69.4 (**C**H$_2$-O), 65.8 (**C**H$_2$-O), 36.5 (**C**H$_2$), 34.5 (**C**H), 21.3 (**C**H$_2$), 17.0 (**C**H$_2$), -1.5 (**C**H$_3$); **HRMS** (EI/FI) *m*/z calcd for $C_{11}H_{22}OSi$ $[M]^+$: 198.1440, found: 198.1446; **IR (neat)** ν_{max}/cm^{-1}2953, 2920, 2856, 1248, 1109, 1089, 861, 836; **$[\alpha]_D^{25}$** = +33.3° (c=1.0 in $CDCl_3$, 93% ee).

GC analysis of the crude mixture of epoxides derived from **63e** indicated an enantiomeric excess of 93% (Hydrodex 6-TBDM, 60-170 °C at 1 ˚C/min, 170 ˚C for 50 min, 10 psi); major enantiomer t_R= 76.6, 81.6 min; minor enantiomer t_R = 75.7, 86.2 min.

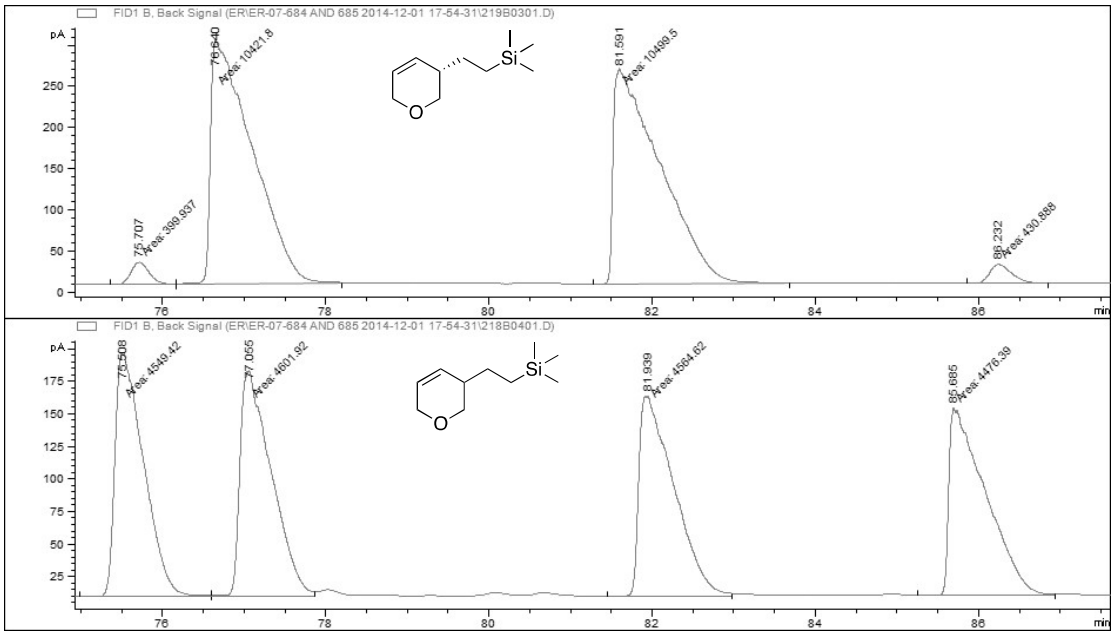

iv) Side-product

*3,3',6,6'-tetrahydro-2H,2'H-3,3'-bipyran (**64**)*

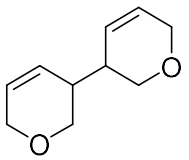

64

In a flame-dried flask under inert atmosphere, Cp_2ZrHCl (310 mg, 1.2 mmol, 2.0 eq) was added to a solution of 4-phenyl-1-butene **16** (0.23 mL, 1.5 mmol 2.5 eq) in CH_2Cl_2 (0.6 mL) under an argon atmosphere and stirred vigorously until a clear yellow solution was obtained (20-40 min). Simultaneously, in another flask under inert atmosphere, CuCl (5.7 mg, 60 μmol, 10 mol%) and (*R*)-**W** (36.0 mg, 60.0 μmol, 10.0 mol%) were dissolved in CH_2Cl_2 (3.0 mL) and stirred for 1 h at room temperature. $AgClO_4$ (13.8 mg, 66.0 μmol, 11.0 mol% ***Perchlorates are explosive and should be handled with caution***) was added to the freshly formed Cu-ligand complex solution and stirred for 15 min. The resulting catalyst complex mixture was filtered into the freshly prepared alkylzirconocene species. After 10 min, 3-chloro-3,6-dihydro-2*H*-pyran **62a** (71 mg, 0.60 mmol, 1.0 eq) was added dropwise via a microsyringe to the resulting black solution followed by the dropwise addition of $B(O\textit{i}Pr)_3$ (0.14 mL, 0.60 mmol, 1.0 eq). The reaction mixture was stirred overnight. The reaction mixture was diluted with Et_2O (2 mL) and quenched with NH_4Cl (3 mL, 1 M). The mixture was partitioned and the aqueous phase was extracted with Et_2O (3 x

10 mL). The combined organic extracts were washed with $NaHCO_3$ (aq., sat., 30 mL), dried over $MgSO_4$, filtered and concentrated under reduced pressure. Purification by flash column chromatography (SiO_2, Et_2O 0→2% in pentane) yielded the enantioenriched product **63a** (30.2 mg, 0.14 mmol, 23%) as a colourless oil and (SiO_2, Et_2O 20% in pentane) the title dimer side-product **64** (30 mg, 0.36 mmol, 60% yield) as a yellow oil. **^{1}H NMR** (400 MHz, $CDCl_3$) δ_H/ppm 5.84-5.75 (m, 4H, C**H**=C**H**), 4.12-4.06 (m, 4H, C**H**$_2$-O), 3.84 (dd, *J*= 11.5, 4.3 Hz, 1H, C**H**$_2$-O), 3.75 (dd, *J*= 11.5, 4.4 Hz, 1H, C**H**$_2$-O), 3.68 (dd, *J*= 11.2, 4.7 Hz, 1H, C**H**$_2$-O), 3.64 (dd, *J*= 11.5, 5.6 Hz, 1H, C**H**$_2$-O), 2.35-2.25 (m, 2H, C**H**); **^{13}C NMR** (100 MHz, $CDCl_3$) δ_C/ppm 127.7 (2C, **C**H=**C**H), 127.3 (**C**H=CH), 126.8 (**C**H=CH), 67.4, (**C**H$_2$-O) 67.0 (**C**H$_2$-O), 66.2 (**C**H$_2$-O), 65.8 (**C**H$_2$-O), 37.5 (**C**H), 37.2 (**C**H); **HRMS** (ESI) *m*/z calcd for $C_{10}H_{15}O_2$ $[M+H]^+$: 167.10666, found: 167.10675; **IR (neat)** ν_{max}/cm^{-1} 3031, 2963, 2929, 2855, 2820, 1087, 1047, 1017; **$[\alpha]_D^{25}$** = -1.8° (c= 1.0 in $CHCl_3$).

^{1}H NMR (500 MHz, CD_2Cl_2) δ_H/ppm 5.84 (d, *J*= 6.9 Hz, 4H, C**H**=C**H**), 4.11–4.06 (m, 4H, C**H$_2$**-O), 3.87 (dd, *J*= 11.2, 4.3 Hz, 1H, C**H$_2$**-O), 3.78 (dd, *J*= 11.2, 4.3 Hz, 1H, C**H$_2$**-O), 3.67 (ddd, *J*= 18.2, 11.3, 5.4 Hz, 2H, C**H$_2$**-O), 2.36–2.26 (m, 2H, C**H**-C**H**); **^{13}C NMR** (125 MHz, CD_2Cl_2) δ_C/ppm 127.5 (2C, **C**H=**C**H), 126.9 (**C**H=CH), 126.5 (**C**H=CH), 67.0 (**C**H$_2$-O), 66.6 (**C**H$_2$-O), 65.4 (**C**H$_2$-O), 65.4 (**C**H$_2$-O), 37.2 (**C**H-CH), 37.0 (**C**H-CH).

Racemic synthesis of 3,3',6,6'-tetrahydro-2H,2'H-3,3'-bipyran 64

In a flame-dried flask under inert atmosphere, Cp_2ZrHCl (210 mg, 0.80 mmol, 2.0 eq) was added to a solution of 4-phenyl-1-butene **16** (0.15 mL, 1.0 mmol, 2.5 eq) in CH_2Cl_2 (0.4 mL) under an argon atmosphere and stirred

vigorously until a clear yellow solution was obtained (20-40 min). Simultaneously, in another flask under inert atmosphere, CuCl (47 mg, 40 μmol, 10 mol%) and (*S, S, S*)-**A** (10.8 mg, 20.0 μmol, 5.00 mol%) and (*R, R, R*)-**A** (10.8 mg, 20.0 μmol, 5.00 mol%) were dissolved in CH_2Cl_2 (2.0 mL) and stirred for 1 h at room temperature. $AgClO_4$ (9.1 mg, 44 μmol, 0.11 eq ***Perchlorates are explosive and should be handled with caution***) was added to the freshly formed Cu-ligand complex solution and stirred for 15 min. The resulting catalyst complex mixture was filtered into the freshly prepared alkylzirconocene species. After 10 min, 3-chloro-3,6-dihydro-2*H*-pyran **62a** (47 mg, 0.40 mmol, 1.0 eq) was added dropwise via a microsyringe to the resulting black solution followed by the dropwise addition of $B(O\textit{i}Pr)_3$ (92 μL, 0.40 mmol, 1.0 eq). The reaction mixture was stirred overnight. The reaction mixture was diluted with Et_2O (2 mL) and quenched with NH_4Cl (3 mL, 1 M). The mixture was partitioned and the aqueous phase was extracted with Et_2O (3 x 10 mL). The combined organic extracts were washed with $NaHCO_3$ (aq., sat., 30 mL), dried over $MgSO_4$, filtered and concentrated under reduced pressure. Purification by flash column chromatography (SiO_2, Et_2O 20% in pentane) yielded the racemic title product **64**.

4) Mechanistic experiments

*3-chloro-3,6-dihydro-2H-pyran (**62a**)*

Kinetic NMR

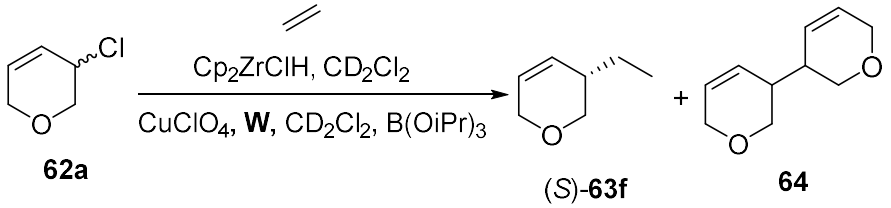

In a flame-dried flask under inert atmosphere, ethylene (1 atm) was bubble through a solution of Cp_2ZrHCl (100 mg, 0.40 mmol, 2.0 eq) in CD_2Cl_2 (0.4 mL) under an argon atmosphere and stirred vigorously until a clear yellow solution was obtained (15 min). Simultaneously, in another flask under inert atmosphere, CuCl (1.9 mg, 20 μmol, 10 mol%) and (*R*)-**W** (12.0 mg, 20.0 μmol, 10.0 mol%) were dissolved in CD_2Cl_2 (1.0 mL) and stirred for 1 h at room temperature. $AgClO_4$ (4.6 mg, 22 μmol, 0.11 eq ***Perchlorates are explosive and should be handled with caution***) was added to the freshly formed Cu-ligand complex solution and stirred for 15 min. The resulting catalyst complex mixture was filtered into a flamed dried NMR tube adapted with an NMR septa and parafilmed. Then the freshly prepared alkylzirconocene species was added to the NMR tube and the tube was thoroughly shaken to obtain a black solution. A preliminary ^1H NMR was run with locking and shimming. 3-chloro-3,6-dihydro-2*H*-pyran **62a** (24 mg, 0.20 mmol, 1.0 eq) was added via a microsyringe to the NMR tube followed by $B(OiPr)_3$ (46 μL, 0.20 mmol, 1.0 eq). The reaction mixture

was shaken vigorously (upside-down mixing) between additions and NMRs were recorded at regular intervals without further locking and shimming.

^{1}H NMR kinetic

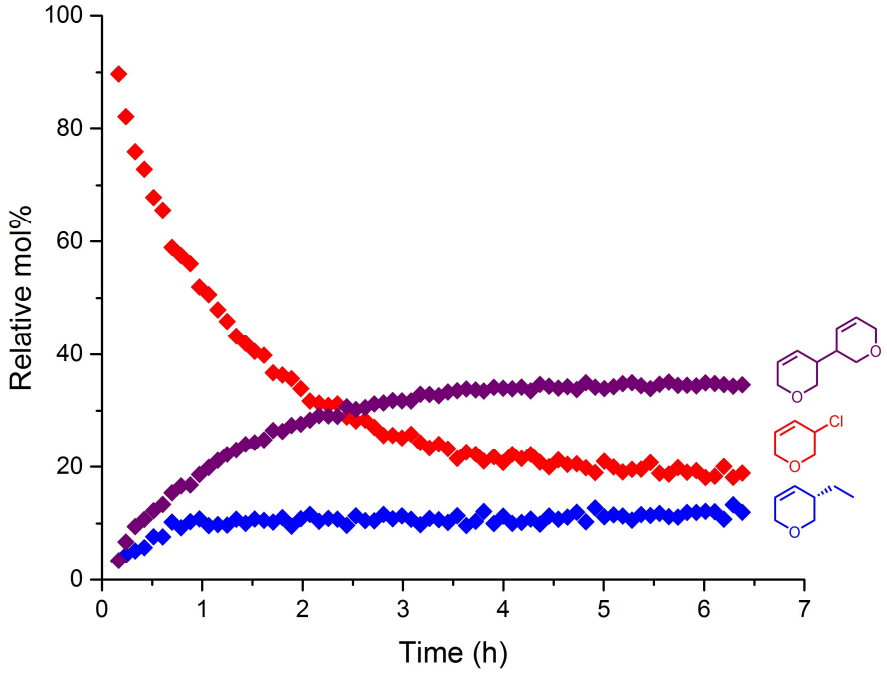

^{31}P NMR Kinetics

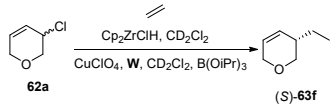

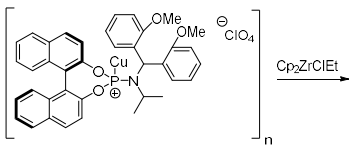

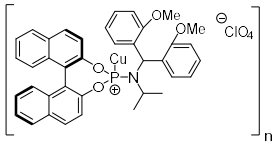

Kinetic ee

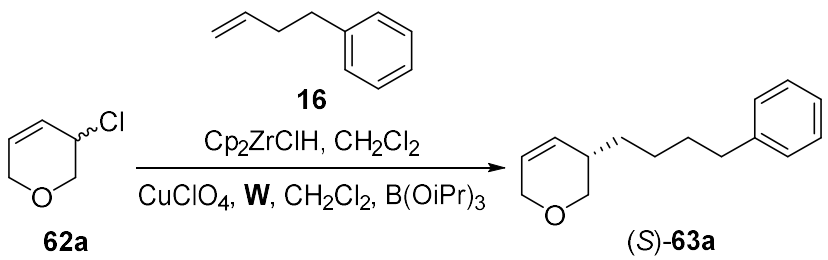

In a flame-dried flask under inert atmosphere, Cp_2ZrHCl (310 mg, 1.2 mmol, 2.0 eq) was added to a solution of 4-phenyl-1-butene **16** (0.23 mL, 1.5 mmol 2.5 eq) in CH_2Cl_2 (0.6 mL) under an argon atmosphere and stirred vigorously until a clear yellow solution was obtained (20-40 min). Simultaneously, in another flask under inert atmosphere, CuCl (5.7 mg, 60 μmol, 10 mol%) and (*R*)-**W** (36.0 mg, 60.0 μmol, 10.0 mol%) were dissolved in CH_2Cl_2 (3.0 mL) and stirred for 1 h at room temperature. $AgClO_4$ (13.8 mg, 66.0 μmol, 11.0 mol% ***Perchlorates are explosive and should be handled with caution***) was added to the freshly formed Cu-ligand complex solution and stirred for 15 min. The resulting catalyst complex mixture was filtered into the freshly prepared alkylzirconocene species. After 10 min, 3-chloro-3,6-dihydro-2*H*-pyran **62a** (71 mg, 0.60 mmol, 1.0 eq) was added dropwise via a microsyringe to the resulting black solution followed by the dropwise addition of $B(OiPr)_3$ (0.14 mL, 0.60 mmol, 1.0 eq). The reaction mixture was stirred overnight. Aliquots were taken regularly and analysed by HPLC and GC to obtain the ee of product (*S*)-**63a** and starting material **62a**.

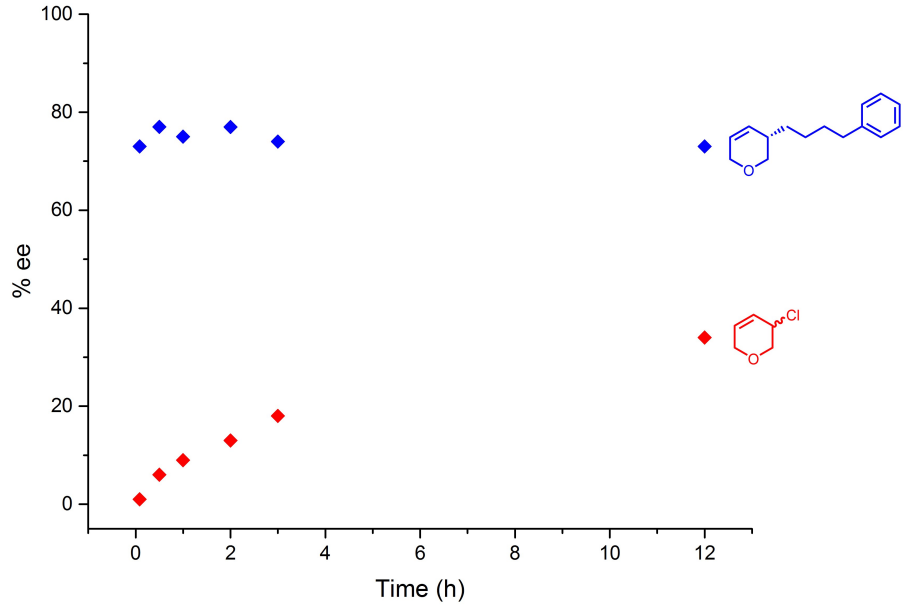

GC traces of 62a

The enantiomeric excess of 3-chloro-3,6-dihydro-2*H*-pyran **62a** was determined by GC [Hydrodex 6-TBDM, 60-120 °C at 1 °C/min, 10 psi, injector temperature 250 °C, detector temperature 300 °C; t_R= 34.8 min (major enantiomer), t_R = 39.0 min (minor enantiomer)].

5 min

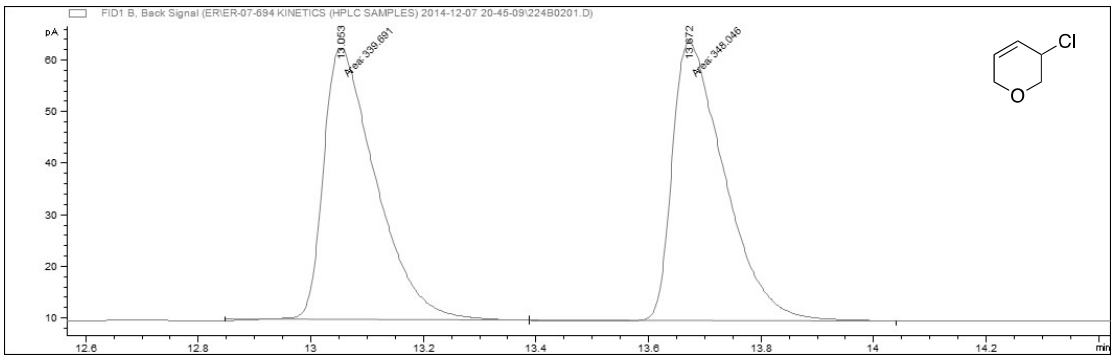

30 min

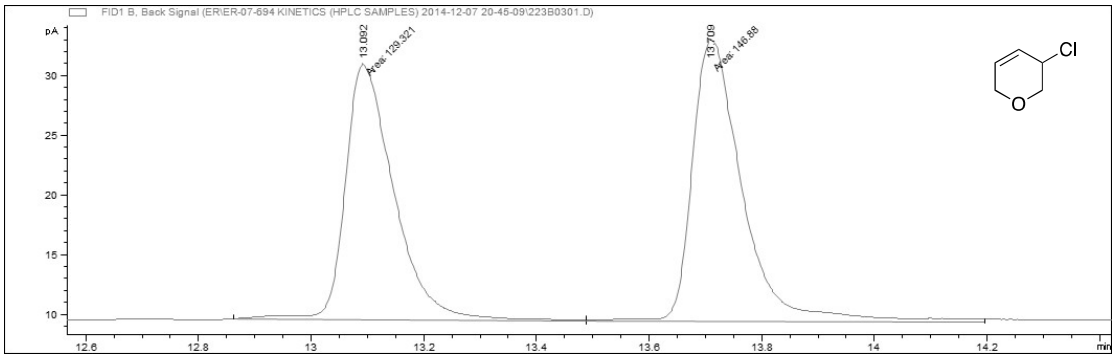

1 h

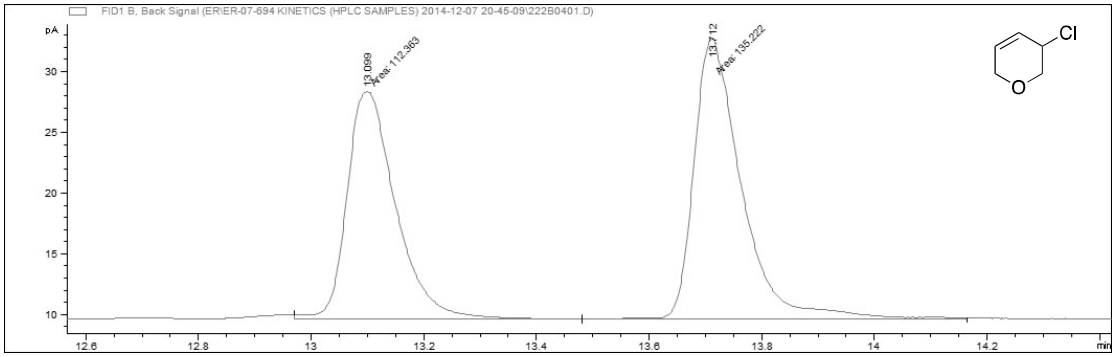

2 h

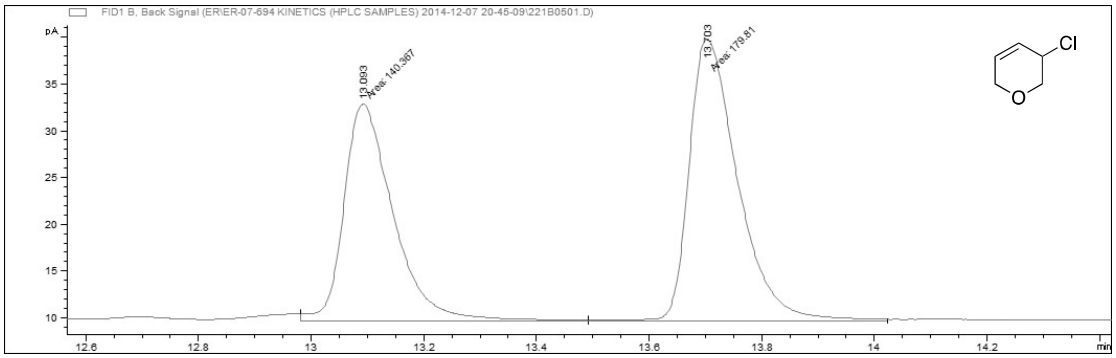

3 h

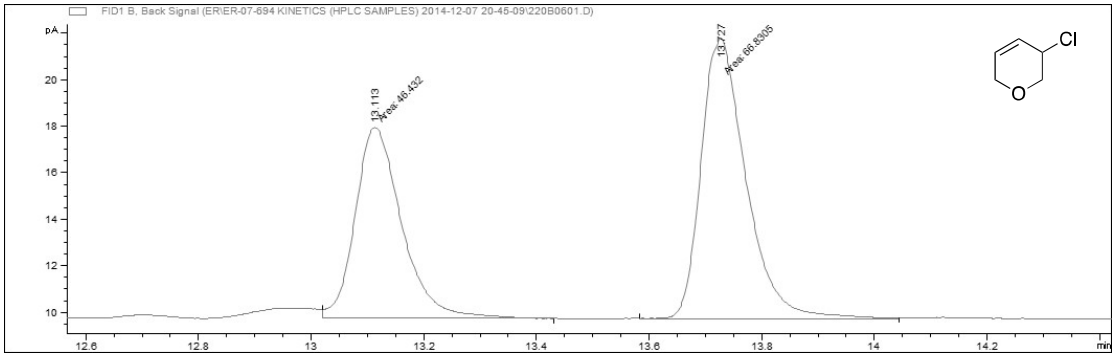

Overnight

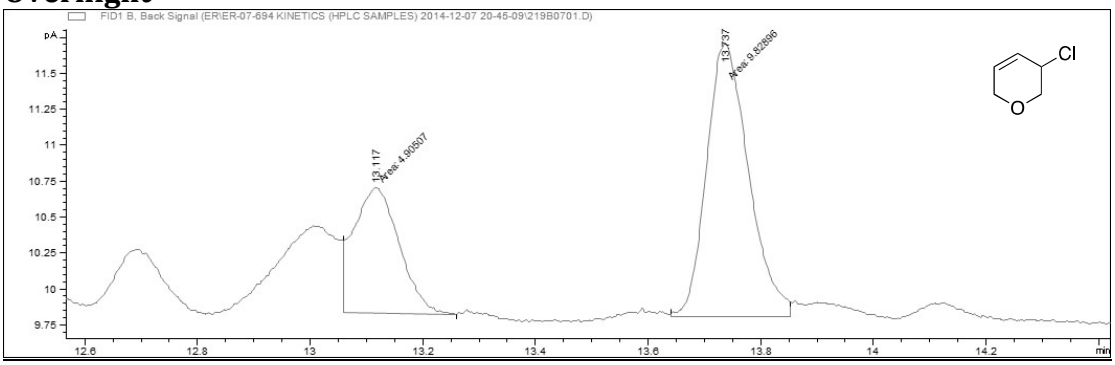

Racemic

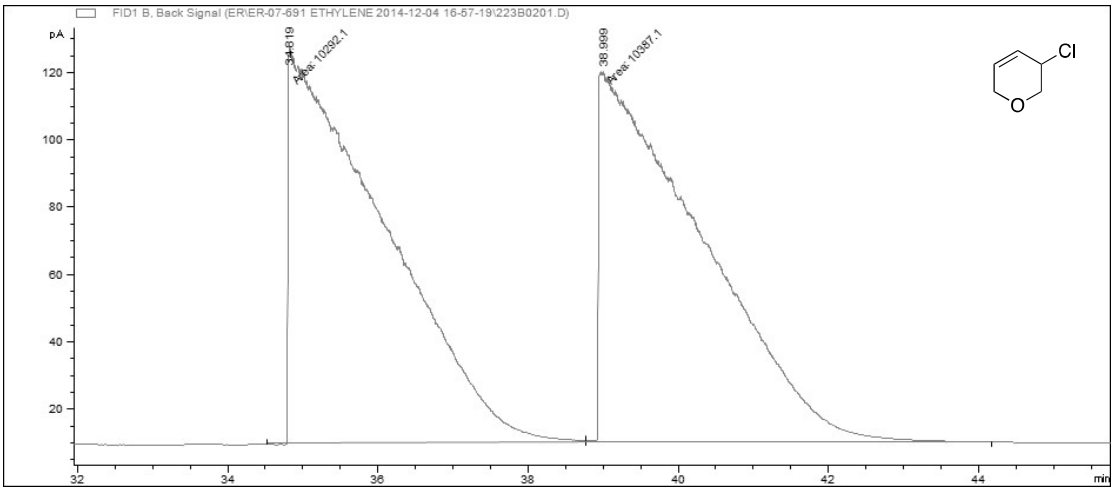

HPLC traces of 63a

The enantiomeric excess of the product **63a** was determined by HPLC [Chiralpak® IB; hexane:*i*PrOH 99.2:0.8; 1.0 mL.min^{-1}, λ= 210 nm, t_R **=** 5.67 min (minor enantiomer), t_R = 6.07 min (major enantiomer)].

5 min

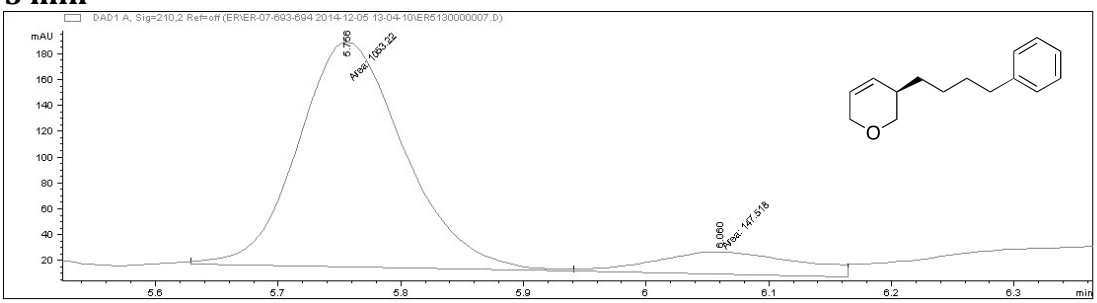

30 min

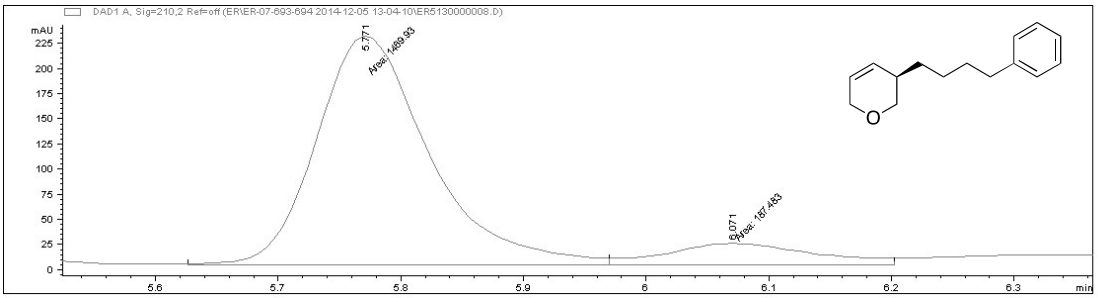

2 h

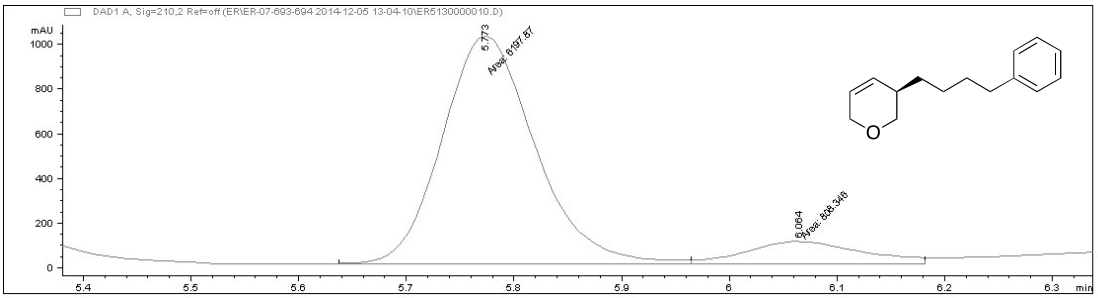

3 h

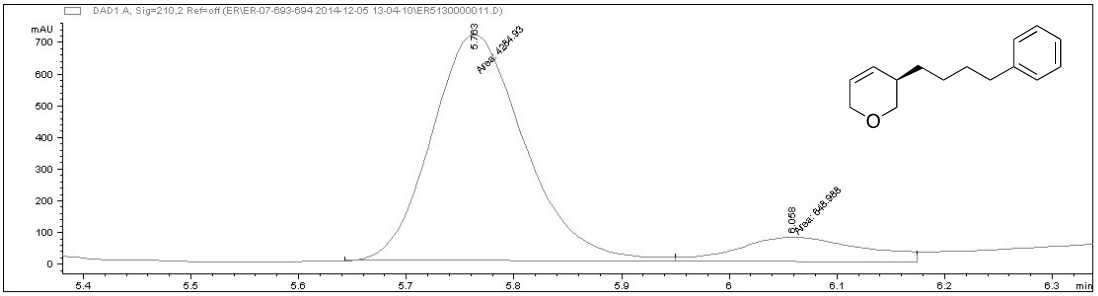

Overnight

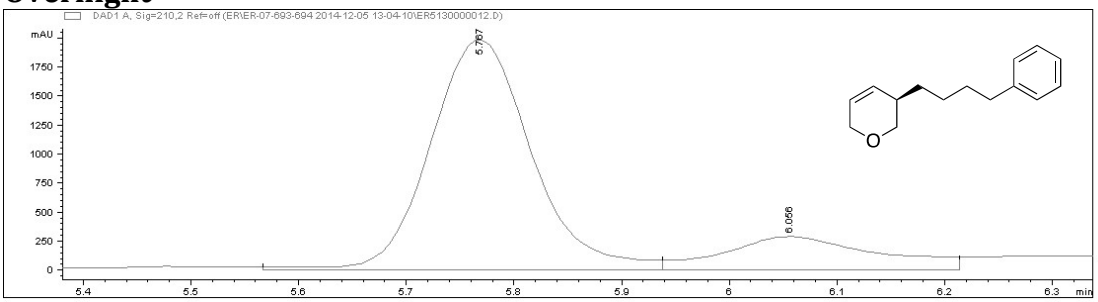

Racemic

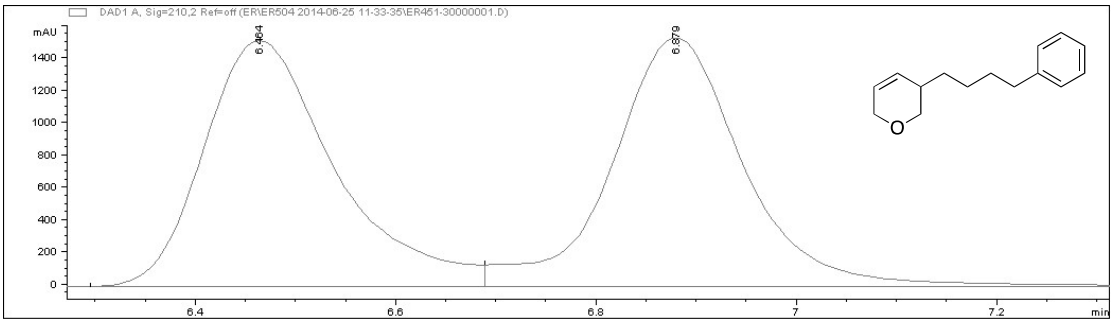

*3,6-dihydro-2H-pyran-3-yl diethyl phosphate (**62d**)*

Kinetic NMR

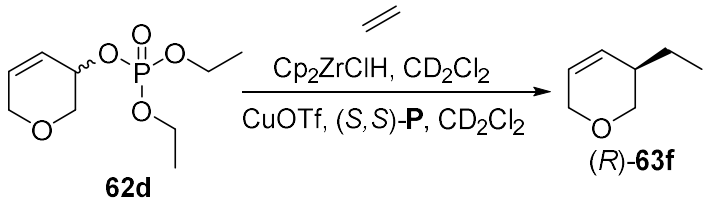

In a flame-dried flask under inert atmosphere, ethylene (1 atm) was bubble through a solution of Cp_2ZrHCl (100 mg, 0.40 mmol, 2.0 eq) in CD_2Cl_2 (0.4 mL) under an argon atmosphere and stirred vigorously until a clear yellow solution was obtained (15 min). Simultaneously, in another flask under inert atmosphere, CuCl (1.9 mg, 20 μmol, 10 mol%) and (*S, S*)-**P** (9.9 mg, 20 μmol, 10.0 mol%) were dissolved in CD_2Cl_2 (1.0 mL) and stirred for 1 h at room temperature. AgOTf (5.7 mg, 22 μmol, 0.11 eq) was added to the freshly formed Cu-ligand complex solution and stirred for 15 min. The resulting catalyst complex mixture was filtered into a flamed dried NMR tube adapted with an NMR septa. Then the freshly prepared alkylzirconocene species was added to the NMR tube and the tube was thoroughly shaken to obtain a black solution. A preliminary ^1H NMR was run with locking and shimming. 3,6-dihydro-2*H*-pyran-3-yl diethyl phosphate **62d** (27 μL, 0.20 mmol, 1.0 eq) was added via a microsyringe to the NMR tube. The reaction mixture was shaken vigorously (upside-down mixing) and NMRs were recorded at regular intervals without further locking and shimming.

^{1}H NMR kinetic

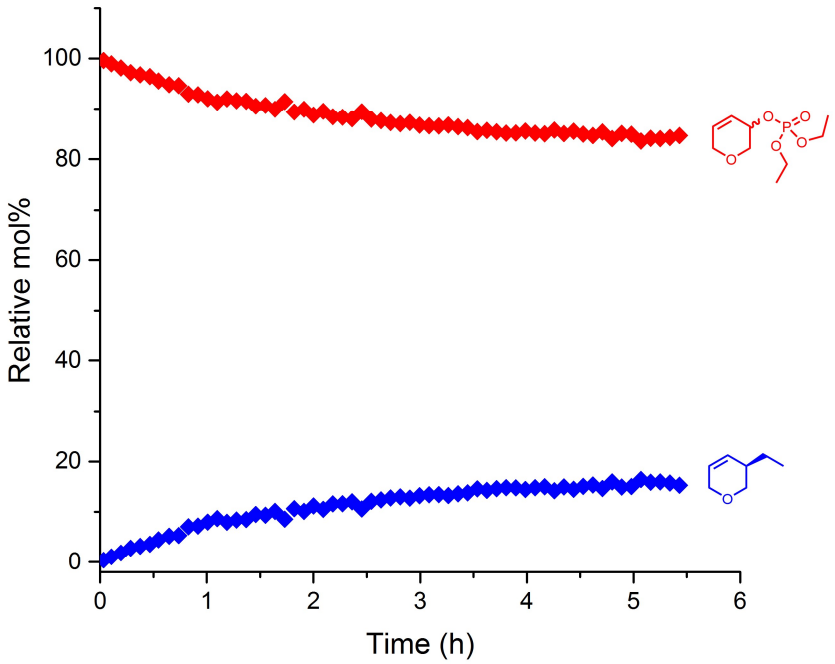

^{31}P NMR

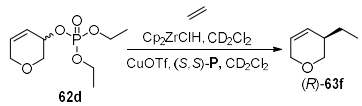

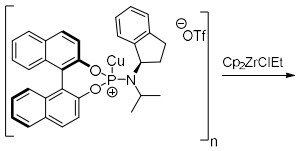

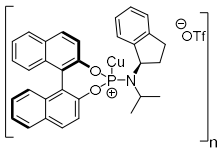

Kinetic ee

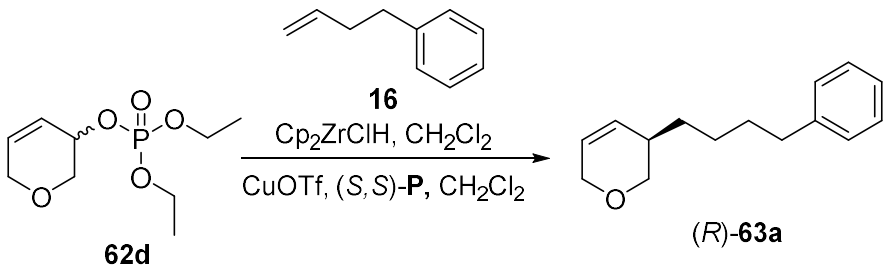

In a flame-dried flask under inert atmosphere, Cp_2ZrHCl (310 mg, 1.20 mmol, 2.0 eq) was added to a solution of 4-phenyl-1-butene **16** (0.23 mL, 1.5 mmol, 2.5 eq) in CH_2Cl_2 (0.6 mL) under an argon atmosphere and stirred vigorously until a clear yellow solution was obtained (20-40 min). Simultaneously, in another flask under inert atmosphere, CuCl (5.7 mg, 60 μmol,

10 mol%) and (*S, S*)-**A** (29.7 mg, 60.0 μmol, 10.0 mol%) were dissolved in CH_2Cl_2 (3.0 mL) and stirred for 1 h at room temperature. AgOTf (17.1 mg, 66.0 μmol, 11.0 mol%) was added to the freshly formed Cu-ligand complex solution and stirred for 15 min. The resulting catalyst complex mixture was filtered into the freshly prepared alkylzirconocene species. After 10 min, 3,6-dihydro-2*H*-pyran-3-yl diethyl phosphate **62d** (140 mg, 0.60 mmol, 1.0 eq) was added dropwise via a microsyringe to the resulting black solution and stirred overnight. Aliquots were taken regularly and analysed by HPLC to obtain the ee of product (*R*)-**63a**.

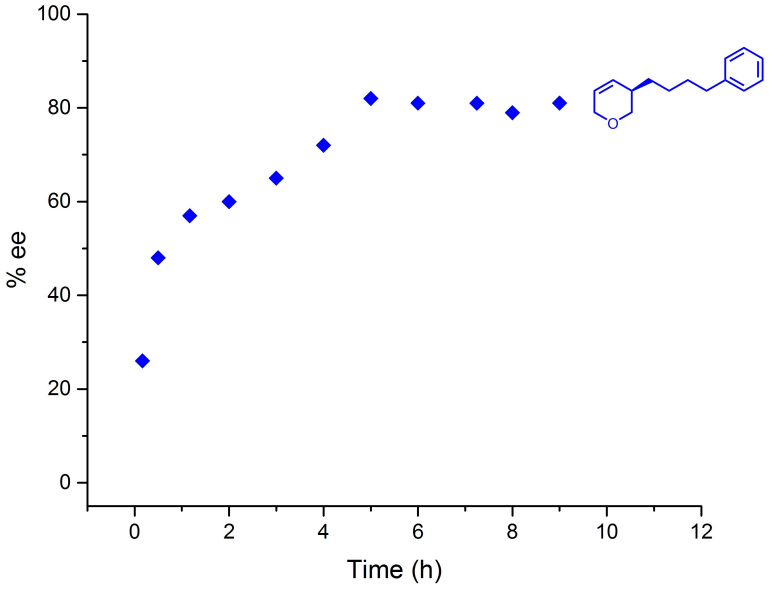

HPLC traces of 63a

The enantiomeric excess of the product was determined by HPLC [Chiralpak® IB; hexane:*i*PrOH 99.2:0.8; 1.0 mL.min^{-1}, λ= 210 nm, t_R = 5.67 min (minor enantiomer), t_R = 6.07 min (major enantiomer)].

10 min

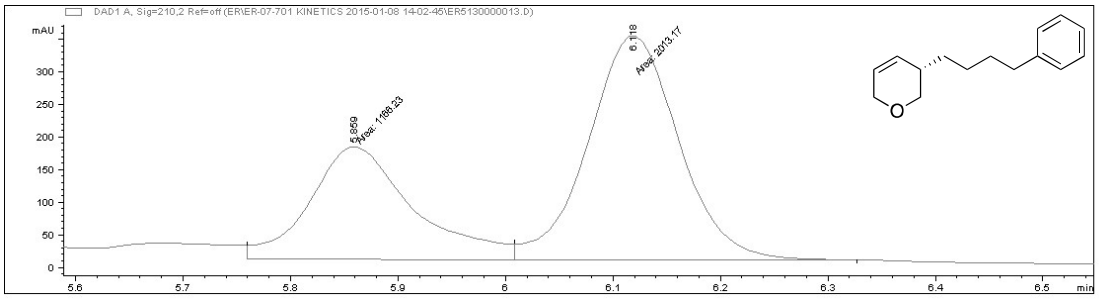

30 min

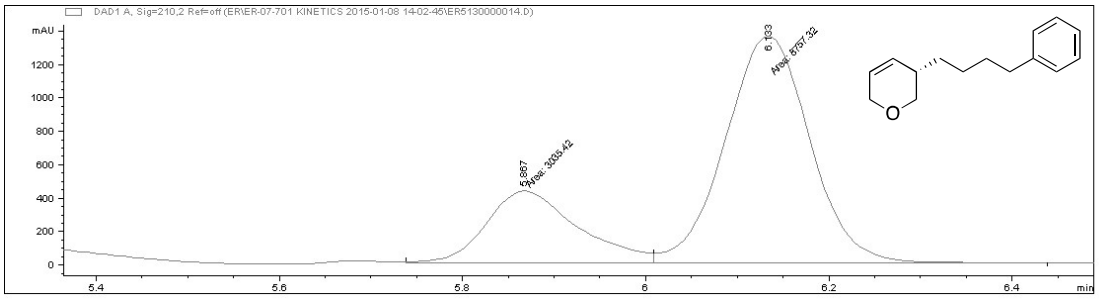

1.2 h

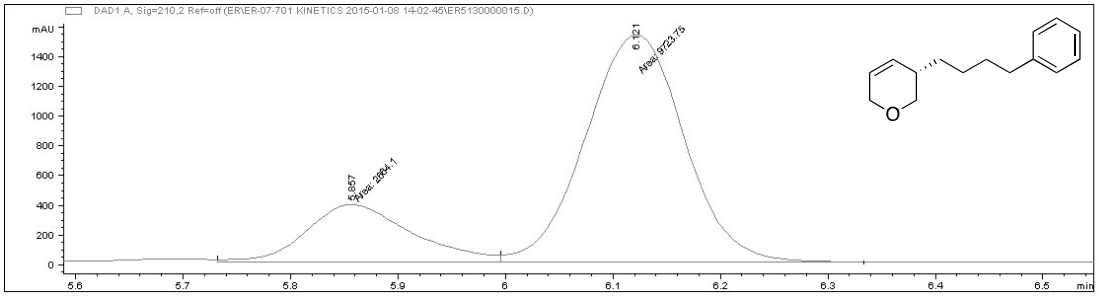

2 h

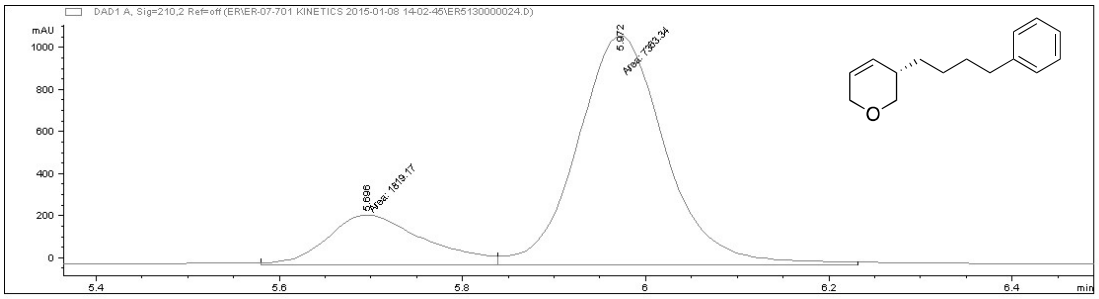

3 h

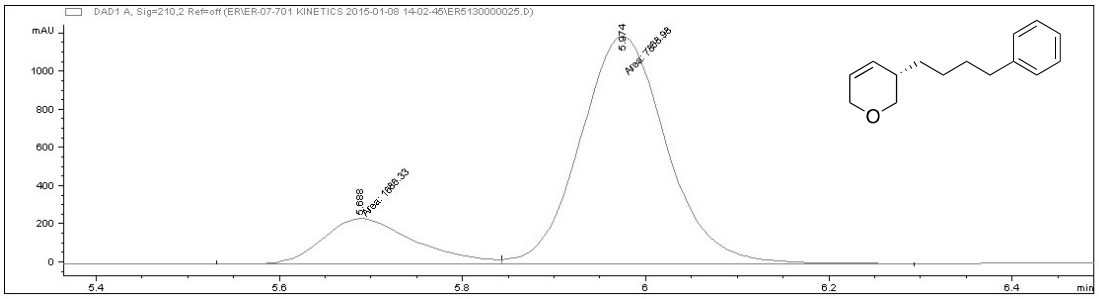

5 h

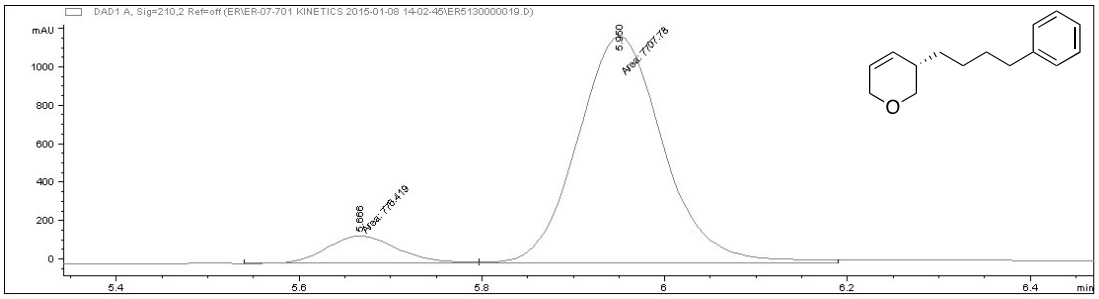
DAD1 A, Sig=210,2 Ref=off (ER\ER-07-701 KINETICS 2015-01-08 14-02-45\ER5130000019.D)
mAU
5.960
Area: 7707.78
5.666
Area: 776.419
min

6 h

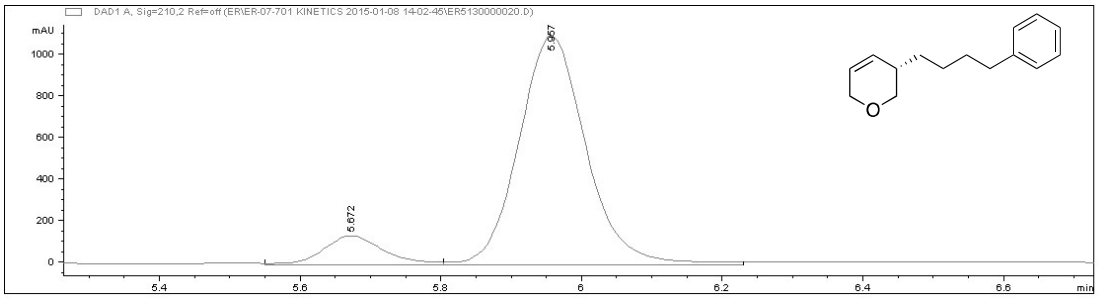
DAD1 A, Sig=210,2 Ref=off (ER\ER-07-701 KINETICS 2015-01-08 14-02-45\ER5130000020.D)
mAU
5.967
5.672
min

7 h

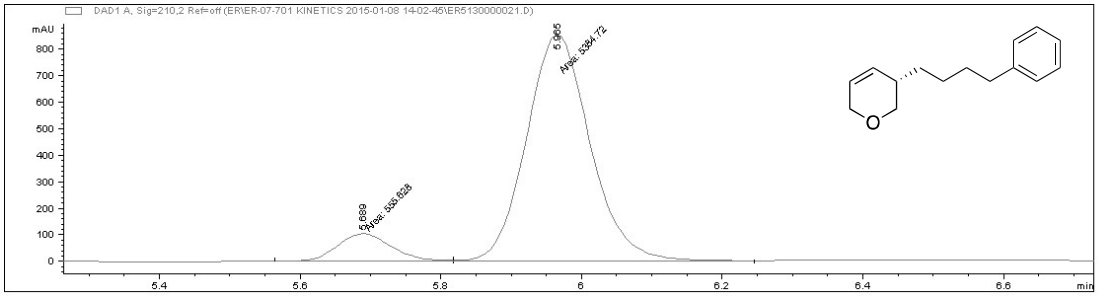
DAD1 A, Sig=210,2 Ref=off (ER\ER-07-701 KINETICS 2015-01-08 14-02-45\ER5130000021.D)
mAU
5.965
Area: 5364.72
5.689
Area: 555.828
min

8 h

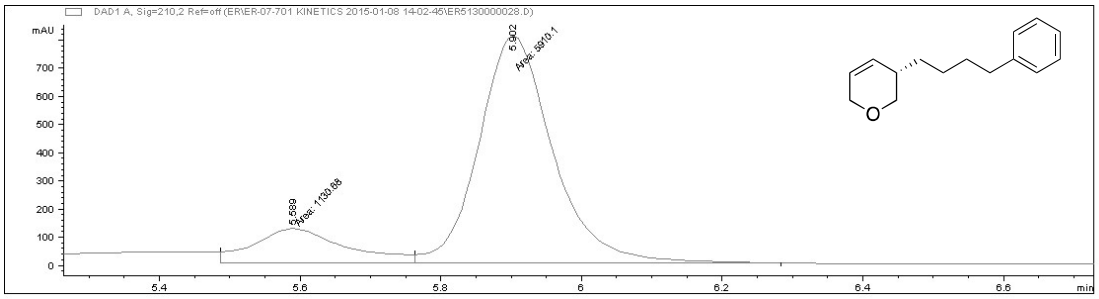
DAD1 A, Sig=210,2 Ref=off (ER\ER-07-701 KINETICS 2015-01-08 14-02-45\ER5130000028.D)
mAU
5.902
Area: 5010.1
5.689
Area: 1130.88
min

9 h

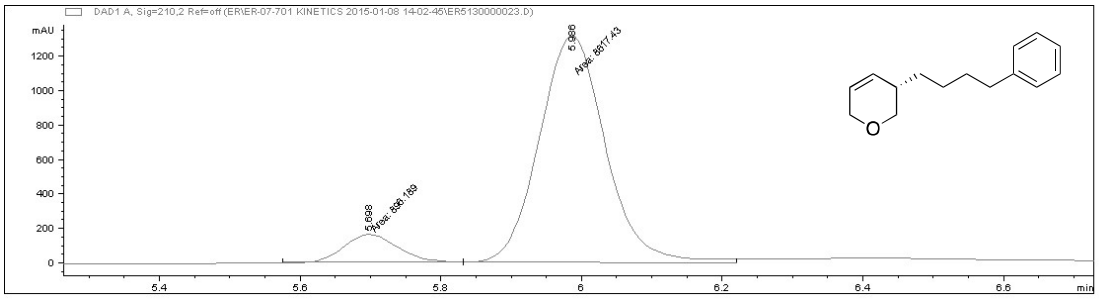
DAD1 A, Sig=210,2 Ref=off (ER\ER-07-701 KINETICS 2015-01-08 14-02-45\ER5130000023.D)
mAU
5.966
Area: 8817.43
5.698
Area: 656.169
min

Racemic

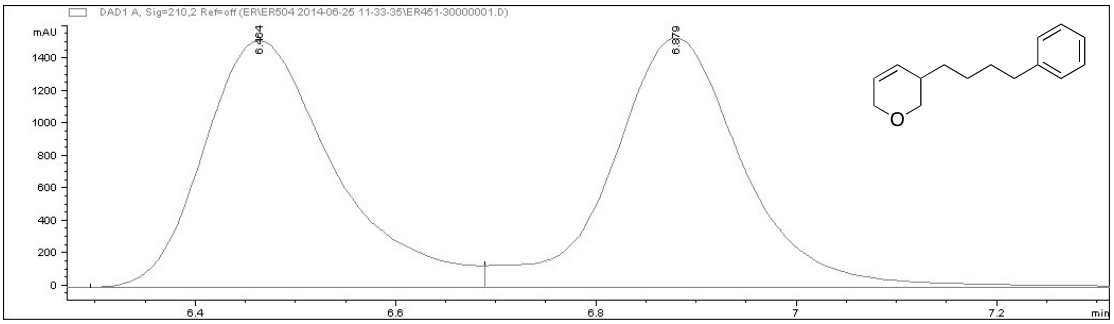

X. EXPERIMENTALS CHAPTER 8

1) Starting Materials

*Cyclohexenone (**4**)*

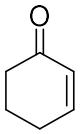

4

^{1}H NMR (500 MHz, CD_2Cl_2) δ_H/ppm 7.02 (dt, *J*= 10.1, 4.1 Hz, 1H, C**H**=CH-C=O), 5.98 (dt, *J*=10.1, 2.1 Hz, 1H, CH=C**H**-C=O), 2.45–2.39 (m, 2H, O=C-C**H$_2$**), 2.39-2.33 (m, 2H, CH=CH-C**H$_2$**), 2.08–1.99 (m, 2H, CH_2-C**H$_2$**-CH_2). **^{13}C NMR** (125 MHz, CD_2Cl_2) δ_C/ppm 199.1 (**C**=O), 150.6 (**C**H=CH-C=O), 129.6 (CH=**C**H-C=O), 38.1 (O=C-**C**H_2), 25.7 (CH=CH-**C**H_2), 22.8 (CH_2-**C**H_2-CH_2).

*3-methylcyclohexan-1-one (**65a**)*

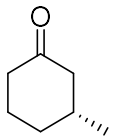

65a

In a flame-dried flask, under argon atmosphere, CuCl (3.8 mg, 40 μmol, 10 mol%) and (*S,S,S*)-**A** (21.6 mg, 40.0 μmol, 10.0 mol%) were dissolved in anhydrous Et_2O (2.0 mL) under an argon atmosphere and allowed to stir for 1 h at room temperature. In a separate flame-dried flask, under argon atmosphere, CH_2Cl_2 (0.4 mL) was added to $Cp_2ZrMeCl$ (174 mg, 0.640 mmol, 1.60 eq) at room temperature under an argon atmosphere. Then AgOTf (11.3 mg, 44.0 μmol, 11.0 mol%) was added to the Cu-Complex solution and the suspension was stirred for another 15 min protected from light before filtering using a syringe filter to the $Cp_2ZrMeCl$ suspension. The resulting dark-brown to black mixture was stirred for an additional 10 min before the cyclohex-2-en-1-one **4** (39 μL, 0.40 mmol, 1.0 eq) and then TMSCl (0.25 mL, 2.0 mmol, 5.0 eq) were added dropwise. The reaction mixture was let to stir overnight before the reaction was quenched by NH_4Cl (1.5 mL, 1 M, aq.) and washed with Et_2O (3 mL). The combined organic extracts were washed with $NaHCO_3$ (aq. sat. 30 mL), dried over $MgSO_4$, filtered and concentrated under reduced pressure. Purification by flash column chromatography (SiO_2, Et_2O 25% in pentane) yielded the title product **65a** (9.5 mg, 80 μmol, 21%, 91% *ee*) as a clear oil. **^{1}H NMR** (500 MHz, CD_2Cl_2) $\delta_{H/ppm}$ 2.39–2.19 (m, 3H, C**H$_2$**), 2.10–1.97 (m, 2H, C**H$_2$**), 1.97–1.82 (m, 2H, C**H$_2$**, C**H**-CH_3), 1.73-1.61 (m, 1H, C**H**$_2$), 1.42–1.30 (m, 1H, C**H**$_2$), 1.04 (d, *J*= 6.4 Hz,

3H, C**H₃**). **^{13}C NMR** (125 MHz, CD_2Cl_2) $\delta_{C/ppm}$ 211.1 (**C**=O), 49.9 (**C**H_2), 41.0 (**C**H_2), 34.2 (**C**H-CH_3), 33.3 (**C**H_2), 25.3 (**C**H_2), 21.8 (**C**H_3). **IR (neat)** ν_{max}/cm^{-1} 2951, 2926, 2867, 1710, 1456; **LRMS** (ESI) *m*/z 247.1 ([2M+Na] $^+$, 100%), 135.0 ([M+Na]$^+$, 15%); **$[\alpha]_D^{25}$** = +9.9° (c = 0.8, in $CHCl_3$, 91% ee). Spectral data was identical to authentic sample (commercially available) and absolute configuration was assigned by comparison to literature optical rotation[309].

The enantiomeric excess of 91% ee was determined by chiral GC [β-DEX 325 (Supelco); 60 ° for 10 min, 1 °C/min to 120 °C] t_R = 31.92 min (major, (*R*)-isomer), t_R = 32.54 min (minor, (*S*)-isomer).

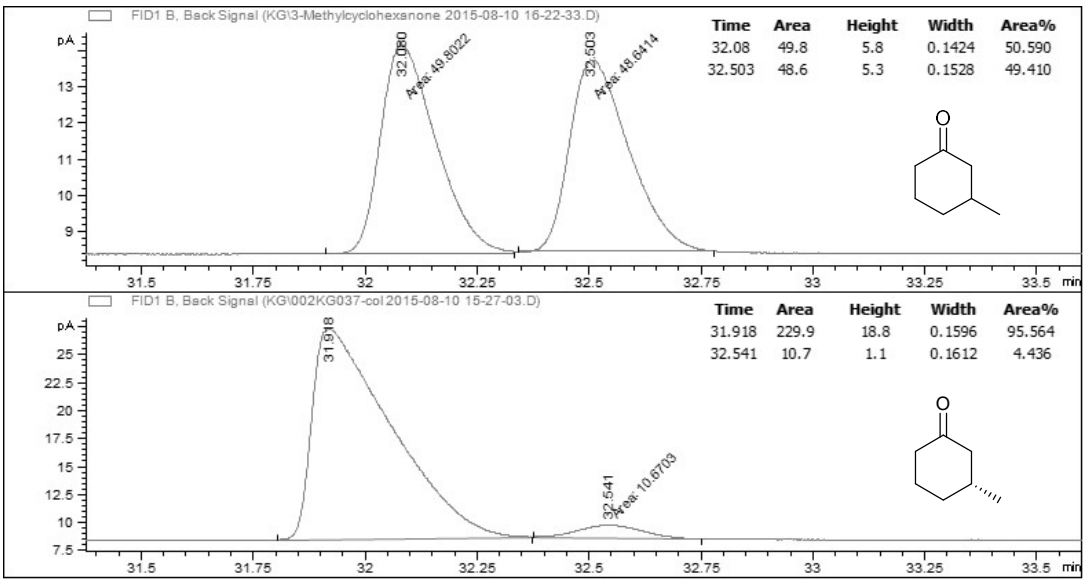

*4,4-dimethylcyclohexenone (**11**)*

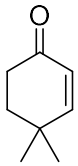

11

^{1}H NMR (500 MHz, CD_2Cl_2) δ_H/ppm 6.69 (dt, *J*= 10.1 Hz, 1H, CH=C**H**-C=O), 5.81 (d, *J*= 10.1 Hz, 1H, C**H**=CH-C=O), 2.45 (t, *J*= 6.6 Hz, 2H, **C**H_2-C$(CH_3)_2$), 1.89 (t, *J*= 7.0 Hz, 2H, C**H$_2$**-C=O), 1.19 (s, 6H, C(C**H$_3$**)$_2$). **^{13}C NMR** (125 MHz, CD_2Cl_2) δ_C/ppm 199.0 (**C**=O), 159.6 (CH=**C**H-C=O), 126.6 (**C**H=CH-C=O), 36.1 (**C**H_2-C=O), 34.4 (**C**H_2-C$(CH_3)_2$), 32.7 (**C**$(CH_3)_2$), 27.4 (C(**C**$H_3)_2$).

*3,4,4-trimethylcyclohexan-1-one (**66a**)*

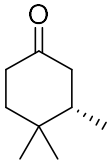

66a

In a flame-dried flask, under argon atmosphere, CuCl (3.8 mg, 40 μmol, 10 mol%) and (*S,S,S*)-**A** (21.6 mg, 40.0 μmol, 10.0 mol%) were dissolved in anhydrous Et_2O (2.0 mL) under an argon atmosphere and allowed to stir for 1 h at room temperature. In a separate flame-dried flask, under argon atmosphere, CH_2Cl_2 (0.4 mL) was added to $Cp_2ZrMeCl$ (174 mg, 0.640 mmol, 1.60 eq) at room temperature under an argon atmosphere. Then AgOTf (11.3 mg, 44.0 μmol,

11.0 mol%) was added to the Cu-Complex solution and the suspension was stirred for another 15 min protected from light before filtering using a syringe filter to the $Cp_2ZrMeCl$ suspension. The resulting dark-brown to black mixture was stirred for an additional 10 min before the 4,4-dimethylcyclohex-2-en-1-one **11** (39 µL, 0.40 mmol, 1.0 eq) and then TMSCl (0.25 mL, 2.0 mmol, 5.0 eq) were added dropwise. The reaction mixture was let to stir overnight before the reaction was quenched by NH_4Cl (1.5 mL, 1 M, aq.) and washed with Et_2O (3 mL). The combined organic extracts were washed with $NaHCO_3$ (aq. sat. 30 mL), dried over $MgSO_4$, filtered and concentrated under reduced pressure. Purification by flash column chromatography (SiO_2, Et_2O 25% in pentane) yielded the title product **66a** (15 mg, 0.11 mmol, 27%, 87% *ee*) as a clear oil. **^{1}H NMR** (500 MHz, CD_2Cl_2) $\delta_{H/ppm}$ 2.34–2.23 (m, 1H, C**H**$_2$), 2.18–2.07 (m, 2H, C**H**$_2$), 2.09–1.99 (m, 1H, C**H**$_2$), 1.68–1.56 (m, 2H, C**H**$_2$, C**H**-CH_3), 1.48 (td, *J*= 13.2, 4.9 Hz, 1H, C**H**$_2$), 0.93 (s, 3H, C(C**H$_3$**)$_2$), 0.90 (s, 3H, C(C**H$_3$**)$_2$), 0.81 (d, *J*= 6.8 Hz, 3H, CH-C**H$_3$**). **^{13}C NMR** (125 MHz, CD_2Cl_2) $\delta_{C/ppm}$ 211.3 (**C**=O), 46.0 (**C**H_2), 41.6 (**C**H-CH_3), 40.0 (**C**H_2), 38.4 (**C**H_2), 32.5 (**C**$(CH_3)_2$), 28.4 (C(**C**$H_3)_2$), 18.7 (C(**C**$H_3)_2$), 16.2 (CH-**C**H_3); **IR (neat)** ν_{max}/cm^{-1} 2960, 2926, 2872, 1715, 1418; **HRMS** (ESI) *m*/z calcd for $C_9H_{16}ONa$ $[M+Na]^+$: 163.1093, found: 163.1094; **$[\alpha]_D^{25}$** = -31.2° (c = 0.25, in $CHCl_3$, 87% ee). Spectral data was in accordance with literature and the absolute configuration was assigned by comparison to literature optical rotation[310].

The enantiomeric excess of 87% ee was determined by chiral GC [β-DEX 325 (Supelco); 60 °C for 10 min, 1 °C/min to 110 °C] t_R = 50.46 min (major, (*S*)-isomer), t_R = 51.24 min (minor, (*R*)-isomer).

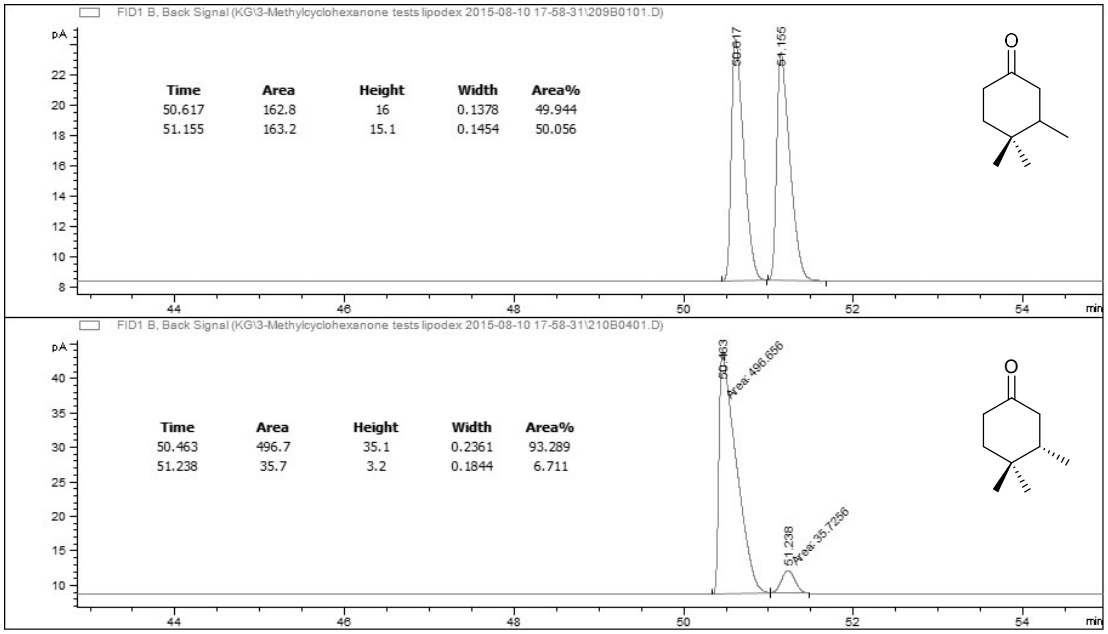

*4,4-diphenylcyclohexenone (**67**)*

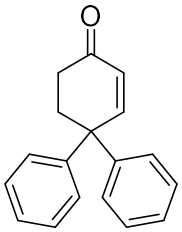

67

^{1}H NMR (500 MHz, CD_2Cl_2) $\delta_{H/ppm}$ 7.41–7.35 (m, 5H, Ar-**H**, C**H**=CH-CH_2), 7.32-7.27 (m, 6H, Ar-**H**), 6.21 (d, *J*=10.4 Hz, 1H, CH=C**H**-CH_2), 2.74 (dt, *J*=6.5, 0.6 Hz, 2H, C**H$_2$**), 2.41 (t, *J*=6.5 Hz, 2H, C**H$_2$**). **^{13}C NMR** (125 MHz, CD_2Cl_2) $\delta_{C/ppm}$ 198.3 (**C**=O), 155.9 (**C**H=CH-CH_2), 145.7 (**Cq**-Ar), 129.0 (CH=**C**H-CH_2), 128.5 (**C**H-Ar), 127.6 (**C**H-Ar), 126.7 (**C**H-Ar), 49.2 (**Cq**-Ph_2), 35.8 (**C**H_2), 34.9 (**C**H_2).

*3-methyl-4,4-diphenylcyclohexan-1-one (**68**)*

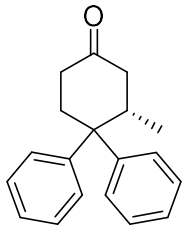

68a

In a flame-dried flask, under argon atmosphere, CuCl (3.8 mg, 40 μmol, 10 mol%) and (*S,S,S*)-**A** (21.6 mg, 40.0 μmol, 10.0 mol%) were dissolved in anhydrous Et_2O (2.0 mL) under an argon atmosphere and allowed to stir for 1 h at room temperature. In a separate flame-dried flask, under argon atmosphere, CH_2Cl_2 (0.4 mL) was added to $Cp_2ZrMeCl$ (174 mg, 0.640 mmol, 1.60 eq) at room temperature under an argon atmosphere. Then AgOTf (11.3 mg, 44.0 μmol, 11.0 mol%) was added to the Cu-Complex solution and the suspension was stirred for another 15 min protected from light before filtering using a syringe filter to the $Cp_2ZrMeCl$ suspension. The resulting dark-brown to black mixture was stirred for an additional 10 min before the 4,4-diphenylcyclohexenone **67** (39 μL, 0.40 mmol, 1.0 eq) and then TMSCl (0.25 mL, 2.0 mmol, 5.0 eq) were added dropwise. The reaction mixture was let to stir overnight before the reaction was quenched by NH_4Cl (1.5 mL, 1 M, aq.) and washed with Et_2O (3 mL). The combined organic extracts were washed with $NaHCO_3$ (aq. sat. 30 mL), dried over $MgSO_4$, filtered and concentrated under reduced pressure. Purification by flash column chromatography (SiO_2, Et_2O 25% in pentane) yielded the title product **68a** (86 mg, 0.33 mmol, 82%, 92% ee) as a clear oil. **^{1}H NMR** (500 MHz, CD_2Cl_2) $\delta_{H/ppm}$ 7.51–7.44 (m, 2H, Ar-**H**), 7.33–7.25 (m, 2H, Ar-**H**), 7.20–7.10 (m,

5H, Ar-**H**), 7.07-7.00 (m, 1H, Ar-**H**), 3.35-3.25 (m, 1H, C**H**), 2.90–2.77 (m, 2H, C**H**$_2$), 2.66–2.52 (m, 1H, C**H**$_2$), 2.33–2.09 (m, 3H, C**H**$_2$), 0.71 (dd, J= 7.0, 0.7 Hz, 3H, C**H**$_3$). **^{13}C NMR** (125 MHz, CD_2Cl_2) $\delta_{C/ppm}$ 210.9 (**C**=O), 147.6 (**Cq**-Ar), 145.6 (**Cq**-Ar), 129.3 (**C**H-Ar), 128.7 (**C**H-Ar), 127.2 (**C**H-Ar), 126.8 (**C**H-Ar), 126.6 (**C**H-Ar), 126.1 (**C**H-Ar), 48.6 (**Cq**-Ph$_2$), 45.9 (**C**H$_2$), 38.8 (**C**H$_2$), 37.9 (**C**H), 29.26(**C**H$_2$), 16.8 (**C**H$_3$). **IR (neat)** ν_{max}/cm^{-1} 2956, 1708, 1495, 1446, 1186, 698; **HRMS** (ESI) m/z calcd for $C_{19}H_{21}O$ $[M+H]^+$: 265.1587, found: 265.1587; **$[\alpha]_D^{25}$** = +195.1° (c = 1.0, in $CHCl_3$, 92% ee).

The enantiomeric excess of 92% ee was determined by non-racemic chiral HPLC [Chiralpak® IC: hexane/isopropanol 98:2; 1.0 mL/min; λ = 210 nm] t_R = 23.70 min (major, (*S*)-isomer), t_R = 26.21 min (minor, (*R*)-isomer).

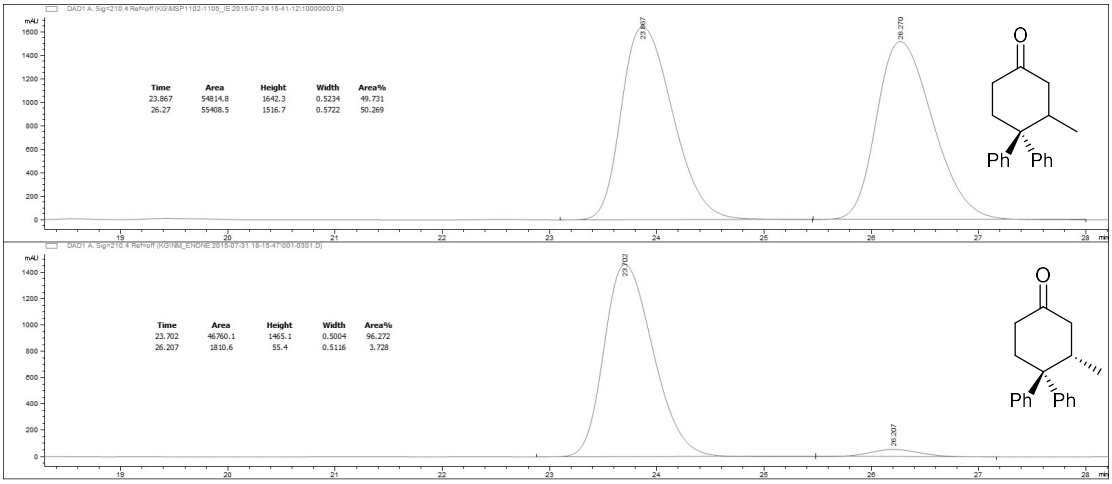

*CuOTf-**A** in CD_2Cl_2*

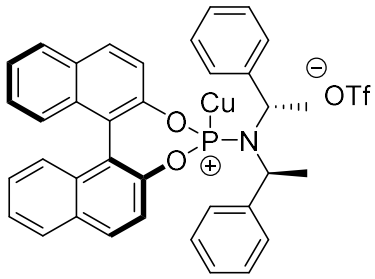

In a flame-dried flask, protected from light, under an argon atmosphere, CuCl (3.8 mg, 40 μmol, 1.0 eq) and (*S, S, S*)-**A** (21.6 mg, 40.0 μmol, 1.00 eq) were dissolved in CD_2Cl_2 (1.0 mL) and allowed to stir for 1 h at room temperature. Then the Cu-Complex solution was transferred to a flame-dried NMR tube under argon atmosphere equipped with a septa. **^{1}H NMR** (500 MHz, CD_2Cl_2) $\delta_{H/ppm}$ 8.10 (d, *J*=9.1 Hz, 1H), 8.04-7.89 (m, 3H), 7.65 (d, *J*=8.6 Hz, 2H), 7.55-7.39 (m, 9H), 7.38-7.14 (m, 6H), 7.07-6.58 (m, 1H), 4.60 (q, *J*=8.2 Hz, 2H, C**H**), 1.84 (d, *J*=6.8 Hz, 6H, C**H$_3$**). **^{13}C NMR** (101 MHz, CD_2Cl_2) $\delta_{C/ppm}$ 148.8 (br. s, **Cq**-Ar), 147.8 (**Cq**-Ar), 140.8 (**Cq**-Ar), 132.6 (**Cq**-Ar), 132.4 (**Cq**-Ar), 132.0 (br. s, **Cq**-Ar), 131.9 (br. s, **C**H-Ar), 131.1 (**Cq**-Ar), 130.7 (br. s, **C**H-Ar), 129.1 (br. s, **C**H-Ar), 128.6 (br. s, **C**H-Ar), 128.2 (**C**H-Ar), 128.1 (br. s, **C**H-Ar), 127.4 (br. s, **C**H-Ar), 127.2 (**C**H-Ar), 126.7 (**C**H-Ar), 126.6 (**C**H-Ar), 126.4 (**C**H-Ar), 125.5 (br. s, **C**H-Ar), 125.4 (**C**H-Ar), 123.2 (**Cq**-Ar), 121.7 (**C**H-Ar), 121.5 (**Cq**-Ar), 120.9 (br. s, **C**H-Ar), 118.3 (**Cq**-Ar), 54.0 (**C**H-N), 21.6 (br. s, **C**H_3). **^{31}P NMR** (202 MHz, CD_2Cl_2) δ_P/ppm 132.6 (br. d, *J*=95.1 Hz, 0.02P), 131.0 (br. d, *J*=58.1 Hz, 0.02P), 126.9 (br. d, *J*= 58.1 Hz, 0.05P), 123.9 (br. s, 0.15P), 122.5 (br. s, 1P)**. ^{19}F NMR** (470 MHz, CD_2Cl_2) δ_F/ppm −78.1 (1F).

$Cp_2ZrMeCl$



^{1}H NMR (500 MHz, CD_2Cl_2) $\delta_{H/ppm}$ 6.35 (s, 3H, Cp), 6.29 (s, 3H, Cp), 0.33 (s, 3H, C**H$_3$**). **^{13}C NMR** (125 MHz, CD_2Cl_2) $\delta_{C/ppm}$ 114.4 (**C**H-Cp), 113.0 (**C**H-Cp), 32.1 (**C**H_3).

2) Interactions

*Enone **67** + $Cp_2ZrMeCl$ + TMSCl*

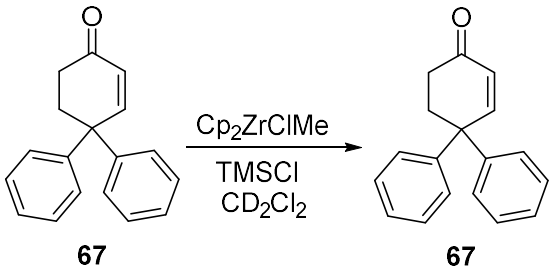

$Cp_2ZrMeCl$ (87 mg, 0.32 mmol, 1.6 eq) was added to a flame-dried NMR tube equipped with a septa under argon atmosphere and covered with CD_2Cl_2 (1.0 mL). A preliminary ^{1}H NMR was run with locking and shimming. Then 4,4-diphenylcyclohexenone **67** (50 mg, 0.20 mmol, 1.0 eq) dissolved in CD_2Cl_2 (0.1 mL) was added dropwise to the NMR tube and shaken vigorously, the kinetic was run without further locking and shimming. TMSCl (0.13 mL, 1.0 mmol,

5.0 eq) was then added dropwise to the NMR tube and shaken vigorously, the kinetic was run without further locking and shimming.

^{1}H NMR

*Enone **67** + TMSCl*

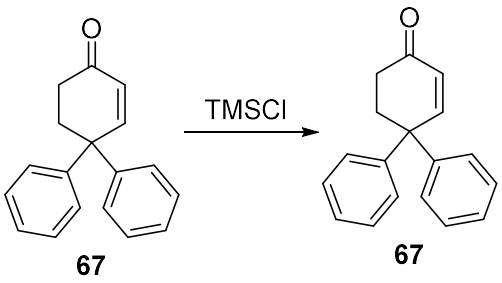

In a flame-dried NMR tube under argon atmosphere equipped with a septa 4,4-diphenylcyclohexenone **67** (24.8 mg, 0.100 mmol, 1.00 eq) was dissolved in CD_2Cl_2 (0.6 mL). A preliminary ^{1}H NMR was run with locking and shimming.

Then TMSCl (63 µL, 0.50 mmol, 5.0 eq) was added dropwise to the NMR tube and shaken vigorously, the kinetic was run without further locking and shimming.

^{1}H NMR

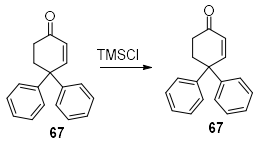

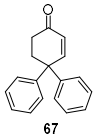

$Cp_2ZrMeCl$ +TMSCl

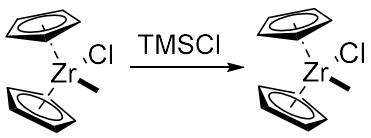

$Cp_2ZrMeCl$ (87 mg, 0.32 mmol, 1.6 eq) was added to a flame-dried NMR tube under argon atmosphere equipped with a septa and covered with CD_2Cl_2 (1.0 mL). TMSCl (50 µL, 0.40 mmol, 2.0 eq) was then added dropwise to the NMR tube and shaken vigorously.

^{1}H NMR

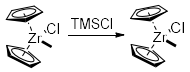



*CuOTf-**A** + TMSCl*

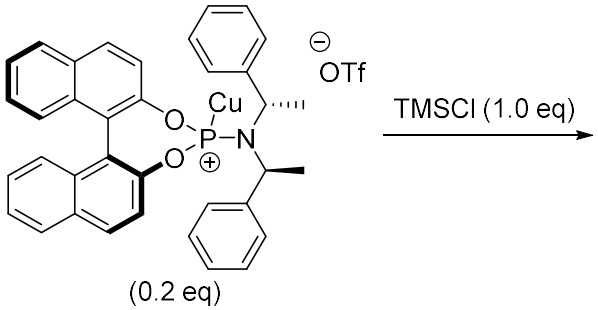

In a flame-dried flask, protected from light, under an argon atmosphere, CuCl (3.8 mg, 40 μmol, 1.0 eq) and (*S, S, S*)-**A** (21.6 mg, 40.0 μmol, 1.00 eq) were dissolved in Et_2O (1.0 mL) and allowed to stir for 1 h at room temperature. Then AgOTf (11.3 mg, 44.0 μmol, 1.10 eq) was added to the clear Cu-complex solution. After 15 min stirring, the brown solution was filtered to a flame-dried NMR tube

under argon atmosphere equipped with a septa and shaken vigorously. TMSCl (10 μL, 80 μmol, 2.0 eq) was then added dropwise to the NMR tube and shaken vigorously.

^{1}H NMR

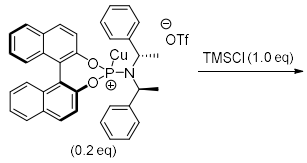

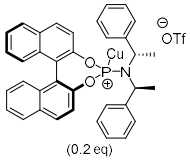

^{31}P NMR

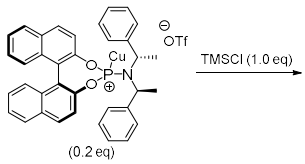

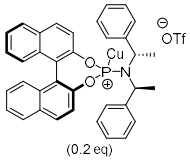

^{19}F NMR

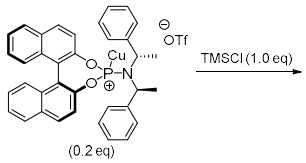

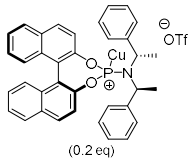

*Enone **67** + CuOTf-**A** (1:1)*

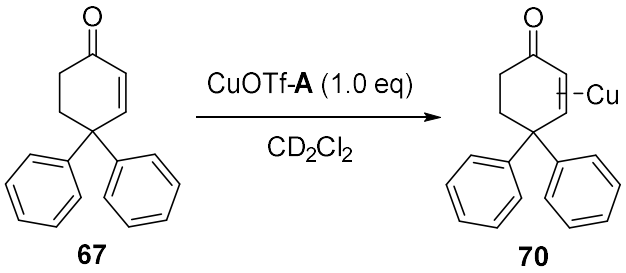

In a flame-dried flask, protected from light, under an argon atmosphere, CuCl (3.8 mg, 40 μmol, 1.0 eq) and (*S, S, S*)-**A** (21.6 mg, 40.0 μmol, 1.00 eq) were dissolved in CD_2Cl_2 (1.0mL) and allowed to stir for 1 h at room temperature. Then AgOTf (11.3 mg, 44.0 μmol, 1.10 eq) was added to the clear Cu-complex solution. After 15 min stirring, the brown solution was filtered to a flame-dried NMR tube under argon atmosphere equipped with a septa and shaken vigorously. A preliminary ^{1}H NMR was run with locking and shimming. Then 4,4-diphenylcyclohexenone **67** (10 mg, 40 μmol, 1.0 eq) dissolved in CD_2Cl_2 (0.1 mL)

was added dropwise to the NMR tube and shaken vigorously, the kinetic was run without further locking and shimming.

^{1}H NMR

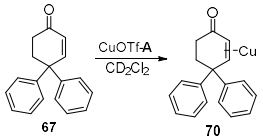

67 70

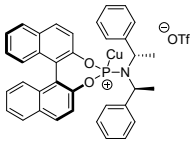

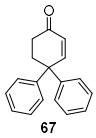

67

^{13}C NMR

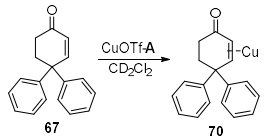

67 70

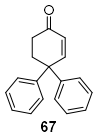

67

^{31}P NMR

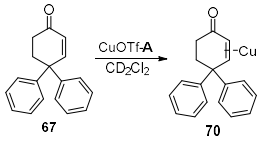

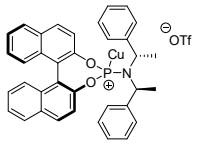

*Enone **67** + CuOTf-**A** (1:0.2)*

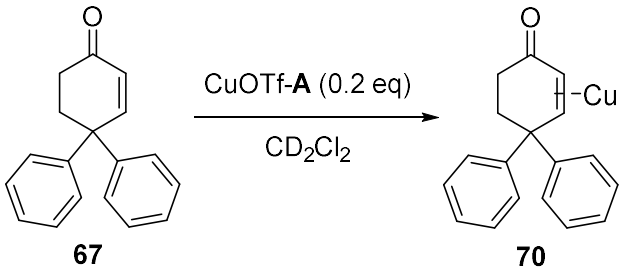

In a flame-dried flask, protected from light, under an argon atmosphere, CuCl (3.8 mg, 40 μmol, 20 mol%) and (*S, S, S*)-**A** (21.6 mg, 40.0 μmol, 20 mol%) were dissolved in CD_2Cl_2 (1.0 mL) and allowed to stir for 1 h at room temperature. Then AgOTf (11.3 mg, 44.0 μmol, 22.0 mol%) was added to the clear Cu-complex solution. After 15 min stirring, the brown solution was filtered to a flame-dried NMR tube under argon atmosphere equipped with a septa and shaken vigorously. A preliminary ^{1}H NMR was run with locking and shimming.

Then 4,4-diphenylcyclohexenone **67** (50 mg, 0.20 mmol, 1.0 eq) dissolved in CD_2Cl_2 (0.1 mL) was added dropwise to the NMR tube and shaken vigorously, the kinetic was run without further locking and shimming.

^{1}H NMR

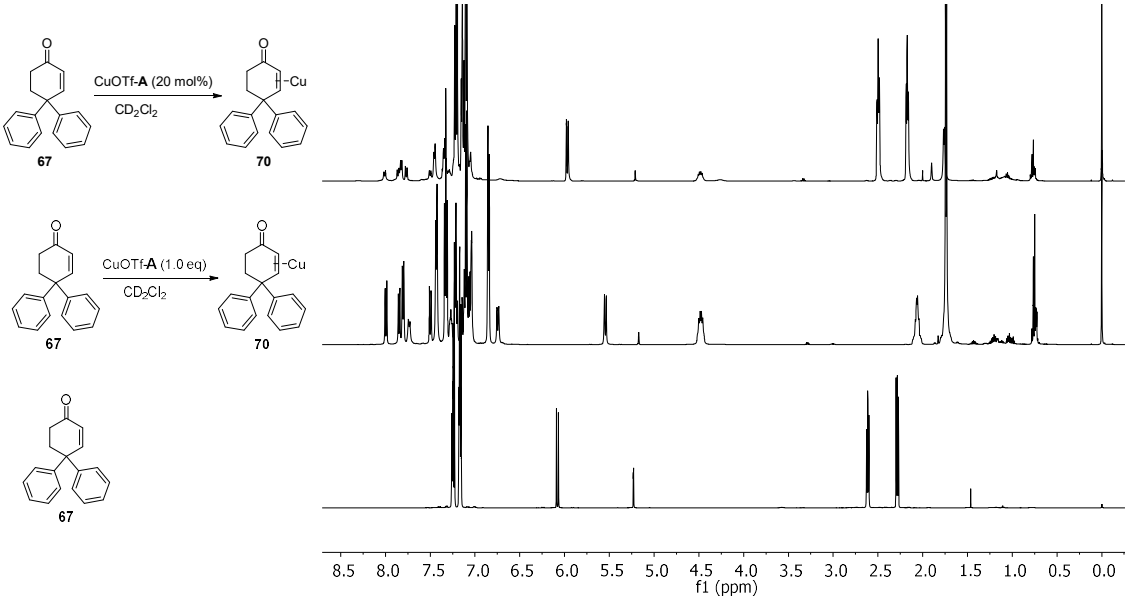

^{13}C NMR

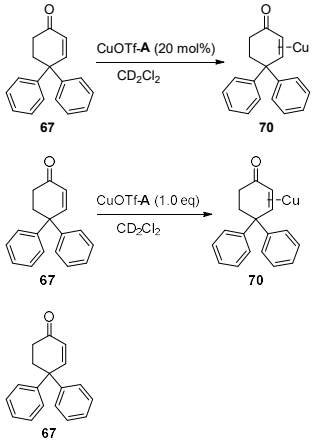

*Enone **67** + CuOTf-**A** (1:0.2) then $Cp_2ZrMeCl$*

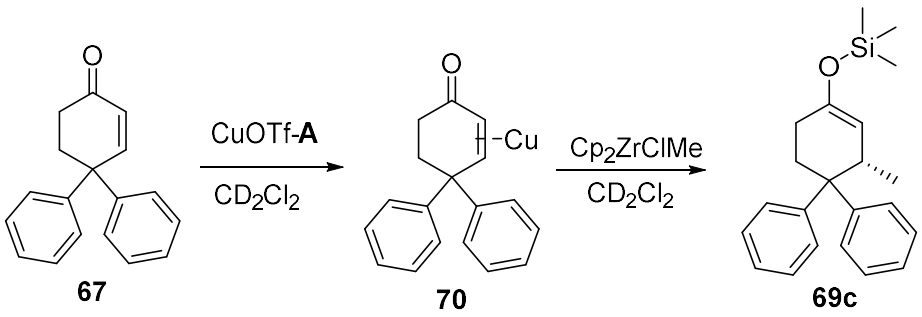

In a flame-dried flask, protected from light, under an argon atmosphere, CuCl (3.8 mg, 40 μmol, 20 mol%) and (*S, S, S*)-**A** (21.6 mg, 40.0 μmol, 20.0 mol%) were dissolved in CD_2Cl_2 (1.0 mL) and allowed to stir for 1 h at room temperature. Then AgOTf (11.3 mg, 44.0 μmol, 22.0 mol%) was added to the clear Cu-complex solution. After 15 min stirring, the brown solution was filtered to a flame-dried NMR tube under argon atmosphere equipped with a septa. 4,4-diphenylcyclohexenone **67** (49.6 mg, 0.200 mmol, 1.00 eq) dissolved in CD_2Cl_2 (0.1 mL) was added dropwise to the NMR tube and shaken vigorously. A preliminary ^1H NMR was run with locking and shimming. In a flame-dried flask, protected from light, under an argon atmosphere, $Cp_2ZrMeCl$ (87 mg, 0.32 mmol, 1.6 eq) was covered with CD_2Cl_2 (0.3 mL) and stirred for 15 min. The $Cp_2ZrMeCl$ solution was then added to the NMR tube and shaken vigorously, the kinetic was run without further locking and shimming.

^{1}H NMR

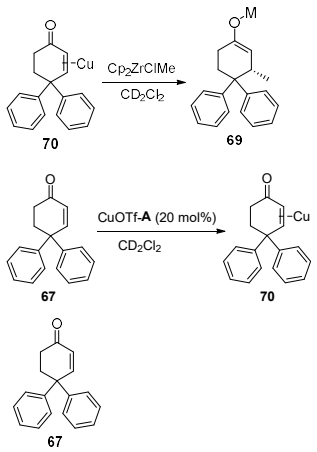

*Enone **67** + CuOTf-**A** +TMSCl*

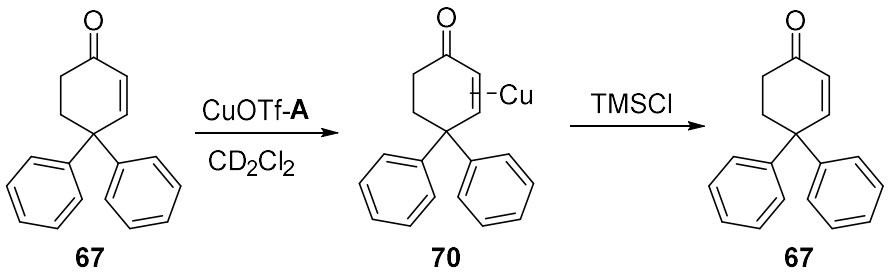

In a flame-dried flask, protected from light, under an argon atmosphere, CuCl (3.8 mg, 40 μmol, 1.0 eq) and (*S, S, S*)-**A** (21.6 mg, 40.0 μmol, 1.00 eq) were dissolved in CD_2Cl_2 (1.0 mL) and allowed to stir for 1 h at room temperature. Then AgOTf (11.3 mg, 44.0 μmol, 1.10 eq) was added to the clear Cu-complex solution. After 15 min stirring, the brown solution was filtered to a flame-dried NMR tube under argon atmosphere equipped with a septa and shaken vigorously. A preliminary ^{1}H NMR was run with locking and shimming. Then 4,4-diphenylcyclohexenone **67** (50 mg, 0.20 mmol, 1.0 eq) dissolved in CD_2Cl_2

(0.1 mL) was added dropwise to the NMR tube and shaken vigorously, the kinetic was run without further locking and shimming. TMSCl (0.13 mL, 1.0 mmol, 50 eq) was then added dropwise to the NMR tube and shaken vigorously. The kinetic was run without further locking and shimming.

^{1}H NMR

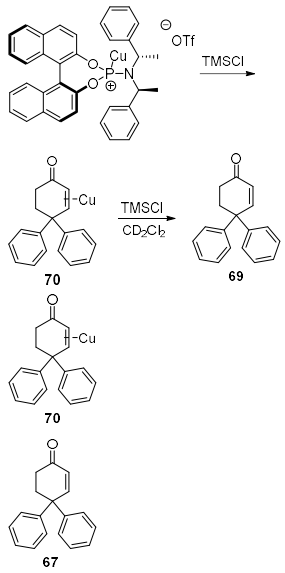

^{31}P NMR

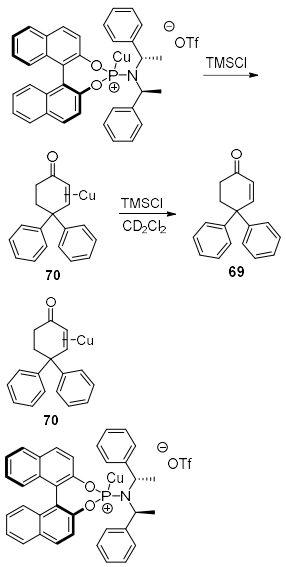

*CuOTf-**A** (0.2 eq) + $Cp_2ZrMeCl$ (1.6 eq)*

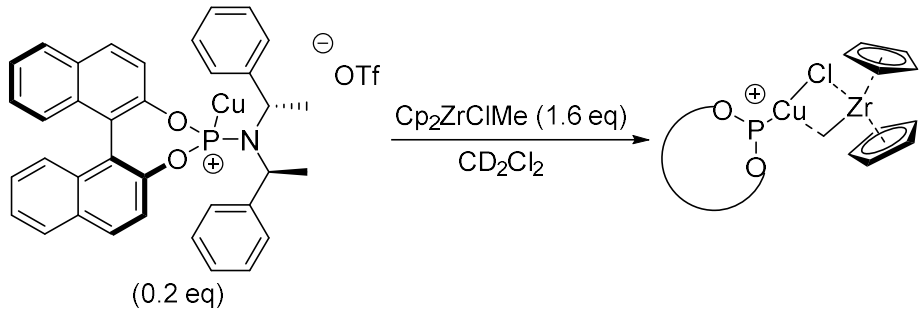

In a flame-dried flask, protected from light, under an argon atmosphere, CuCl (3.8 mg, 40 μmol, 20 mol%) and (*S, S, S*)-**A** (21.6 mg, 40.0 μmol, 20.0 mol%) were dissolved in CD_2Cl_2 (1.0 mL) and allowed to stir for 1 h at room temperature. $Cp_2ZrMeCl$ (87 mg, 0.32 mmol, 1.6 eq) was added to a flame-dried NMR tube under argon atmosphere equipped with a septa and covered with CD_2Cl_2 (0.2 mL). Then AgOTf (11.3 mg, 44.0 μmol, 22.0 mol%) was added to the

clear Cu-complex solution. After 15 min stirring, the brown solution was filtered to the NMR tube and shaken vigorously.

^{1}H NMR

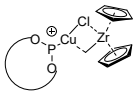

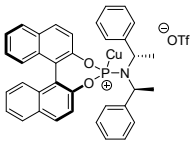

^{31}P NMR

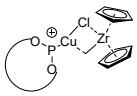

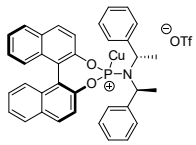

*CuOTf-**A** (1.0 eq) + $Cp_2ZrMeCl$ (2.0 eq)*

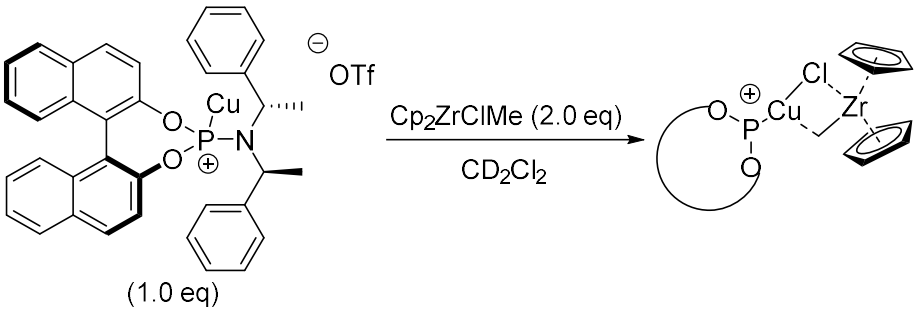

In a flame-dried flask, protected from light, under an argon atmosphere, CuCl (3.8 mg, 40 μmol, 1.0 eq) and (*S, S, S*)-**A** (21.6 mg, 40.0 μmol, 1.00 eq) were dissolved in CD_2Cl_2 (1.0mL) and allowed to stir for 1 h at room temperature. $Cp_2ZrMeCl$ (21.8 mg, 80.0 μmol, 2.00 eq) was added to a flame-dried NMR tube under argon atmosphere equipped with a septa and covered with CD_2Cl_2 (0.2 mL). Then AgOTf (11.3 mg, 44.0 μmol, 1.10 eq) was added to the clear Cu-complex solution. After 15 min stirring, the brown solution was filtered to the NMR tube and shaken vigorously.

^{1}H NMR

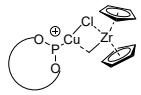



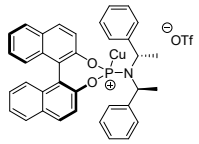

^{13}C NMR

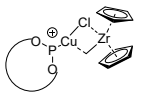



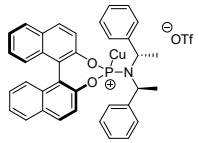

HSQC

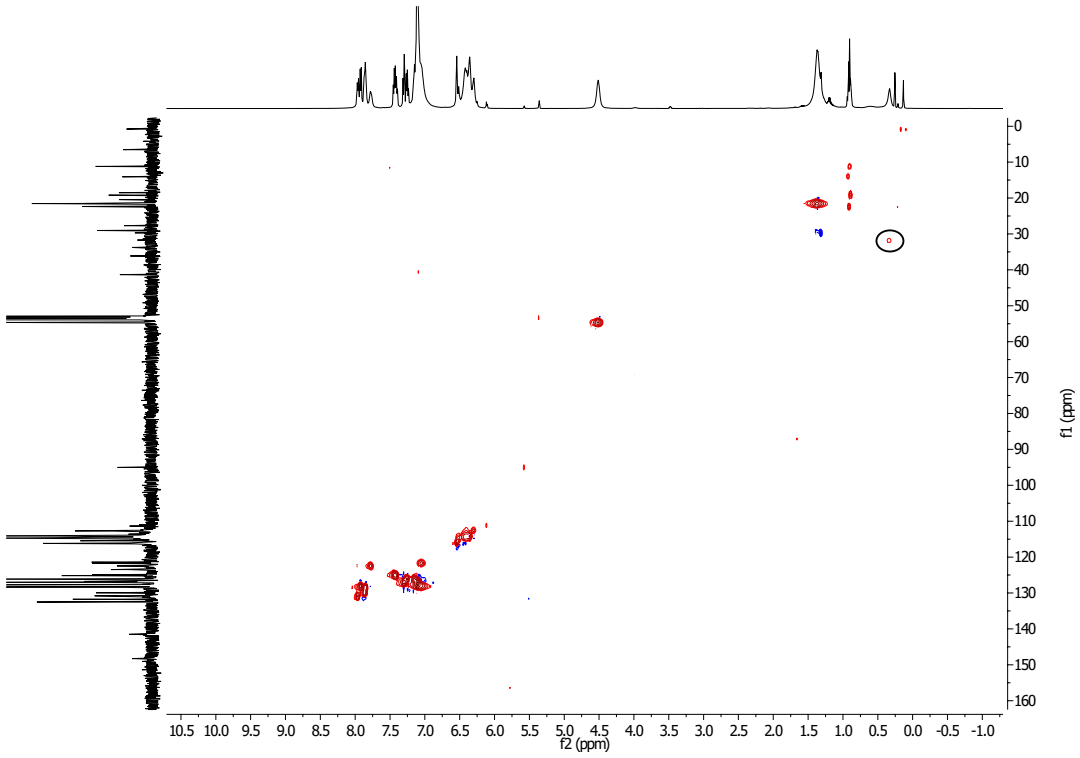

^{31}P NMR

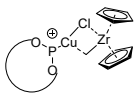

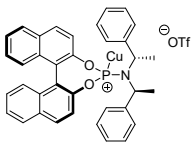

*CuOTf-**A** (0.2 eq) + $Cp_2ZrMeCl$ (1.6 eq) + TMSCl (1.0 eq)*

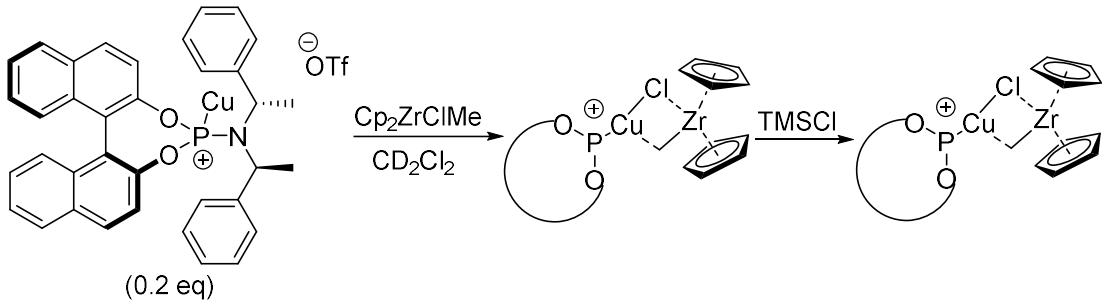

In a flame-dried flask, protected from light, under an argon atmosphere, CuCl (3.8 mg, 40 μmol, 0.2 eq) and (*S, S, S*)-**A** (21.6 mg, 40.0 μmol, 20.0 mol%) were dissolved in CD_2Cl_2 (1.0 mL) and allowed to stir for 1 h at room temperature. $Cp_2ZrMeCl$ (87 mg, 0.32 mmol, 1.6 eq) was added to a flame-dried NMR tube under argon atmosphere equipped with a septa and covered with CD_2Cl_2 (0.2 mL). Then AgOTf (11.3 mg, 44.0 μmol, 22.0 mol%) was added to the clear Cu-complex solution. After 15 min stirring, the brown solution was filtered to the NMR tube and shaken vigorously. A preliminary ^1H NMR was run with locking and shimming. TMSCl (50 μL, 0.40 mmol, 2.0 eq) was then added dropwise to the NMR tube and shaken vigorously, the kinetic was run without further locking and shimming.

^{1}H NMR

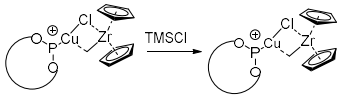

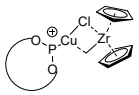

^{31}P NMR

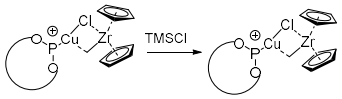

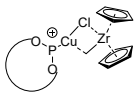

*CuOTf-**A** (0.2 eq) + $Cp_2ZrMeCl$ (1.6 eq) in Et_2O*

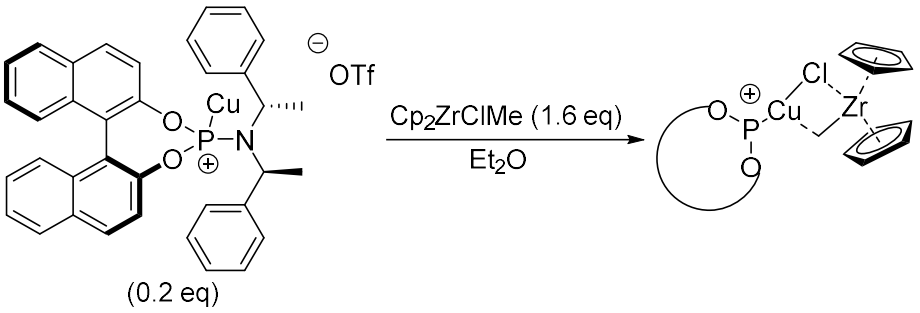

In a flame-dried flask, protected from light, under an argon atmosphere, CuCl (3.8 mg, 40 μmol, 20 mol%) and (*S, S, S*)-**A** (21.6 mg, 40.0 μmol, 20.0 mol%) were dissolved in Et_2O (1.0 mL) and allowed to stir for 1 h at room temperature. $Cp_2ZrMeCl$ (87 mg, 0.32 mmol, 1.6 eq) was added to a flame-dried NMR tube under argon atmosphere equipped with a septa and covered with CD_2Cl_2 (0.2 mL). Then AgOTf (11.3 mg, 44.0 μmol, 22.0 mol%) was added to the clear Cu-complex solution. After 15 min stirring, the brown solution was filtered to the NMR tube and shaken vigorously.

^{31}P NMR

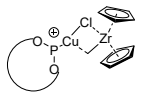

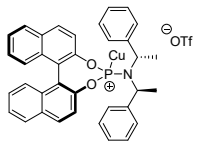

Kinetics

Kinetic in CD_2Cl_2 without TMSCl

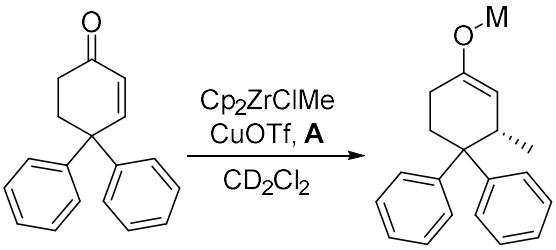

In a flame-dried flask, protected from light, under an argon atmosphere, CuCl (3.8 mg, 40 μmol, 20 mol%) and (*S, S, S*)-**A** (21.6 mg, 40.0 μmol, 20.0 mol%) were dissolved in CD_2Cl_2 (1.0 mL) and allowed to stir for 1 h at room temperature. $Cp_2ZrMeCl$ (87 mg, 0.32 mmol, 1.6 eq) was added to a flame-dried NMR tube under argon atmosphere equipped with a septa and covered with

CD_2Cl_2 (0.2 mL). Then AgOTf (11.3 mg, 44.0 μmol, 22.0 mol%) was added to the clear Cu-complex solution. After 15 min stirring, the brown solution was filtered to the NMR tube and shaken vigorously. A preliminary ^1H NMR was run with locking and shimming. Then 4,4-diphenylcyclohexenone **67** (49.6 mg, 0.200 mmol, 1.00 eq) dissolved in CD_2Cl_2 (0.1 mL) was added dropwise to the NMR tube and shaken vigorously, the kinetic was run without further locking and shimming.

^1H NMR

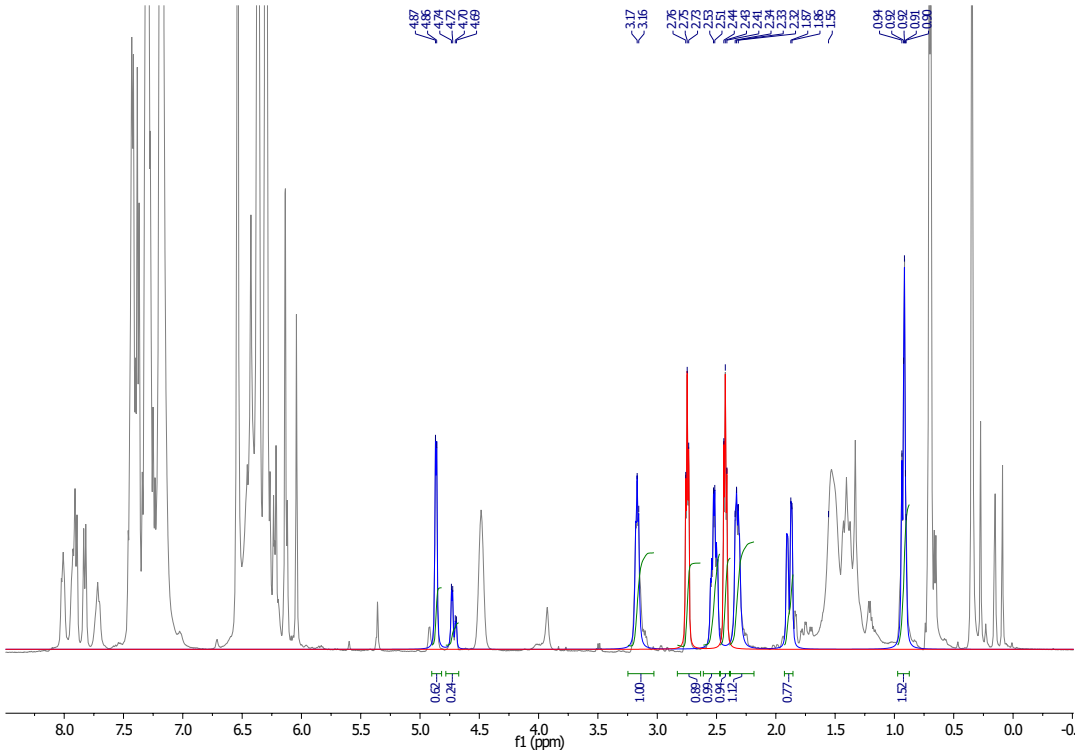

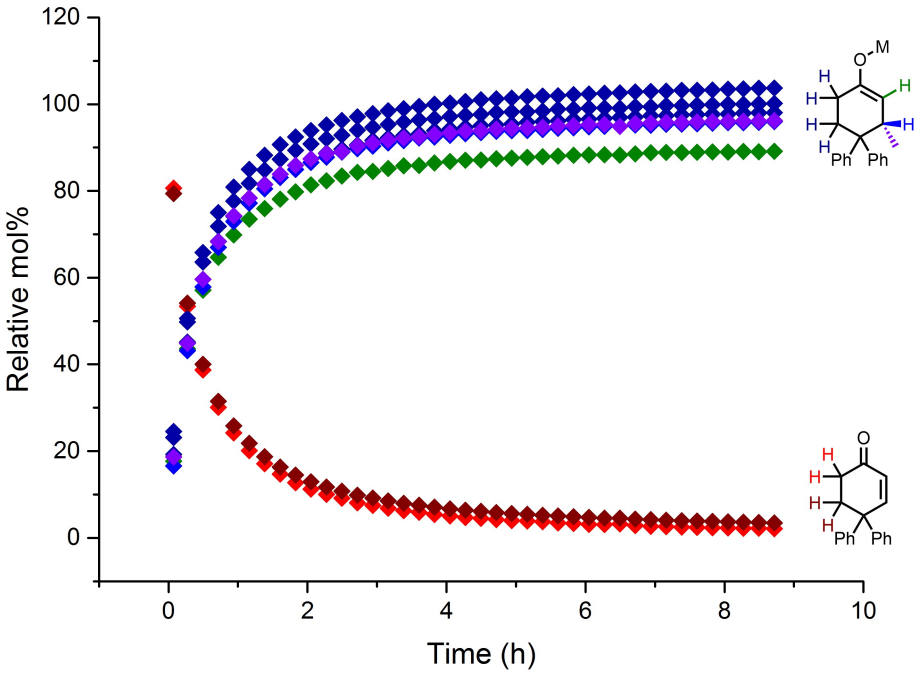
Relative mol%
Time (h)
0
20
40
60
80
100
120
0
2
4
6
8
10
O
M
H
Ph
Ph

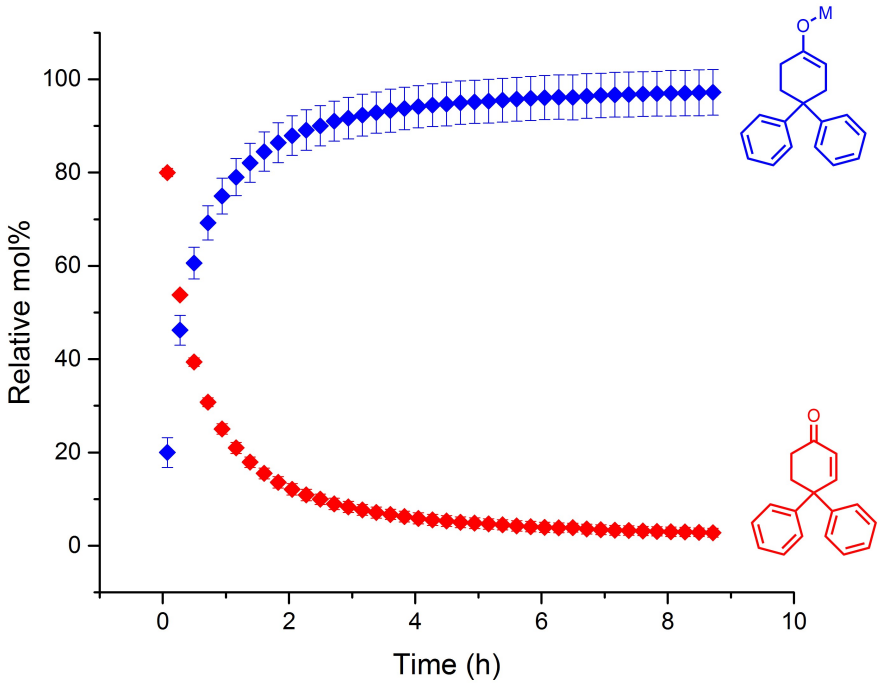
Relative mol%
Time (h)
0
20
40
60
80
100
0
2
4
6
8
10
O
M

^{31}P NMR

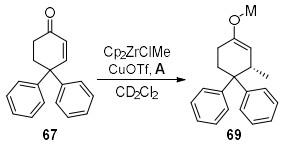

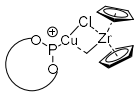

*In situ characterisation of the zirconium enolate **69a** and cupper enolate **69b** (0.7:0.2 ratio)*

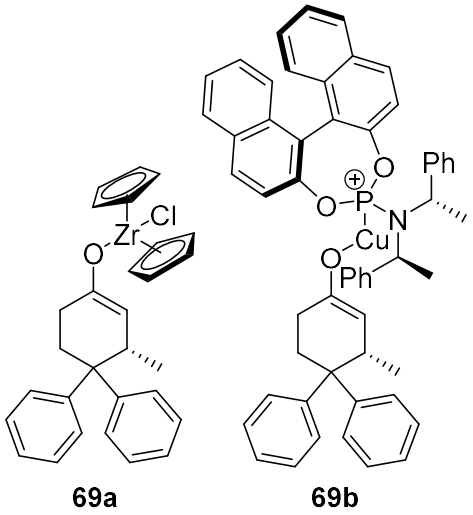

^{1}H NMR (500 MHz, CD_2Cl_2) $\delta_{H/ppm}$ 7.46-7.40 (m, 2H, Ar-**H**), 7.23-7.13 (m, 8H, Ar-**H**), 4.86 (d, *J*= 5.2 Hz, 0.7H, C**H**-COZr), 4.73 (d, *J*= 5.4 Hz, 0.2H, C**H**-COCu), 3.24-3.10 (m, 1H, C**H**-CH_3), 2.60-2.46 (m, 1H, C**H**$_2$), 2.39-2.27 (m, 1H, C**H**$_2$), 1.89 (dd, *J*=17.2, 4.1 Hz, 1H, C**H**$_2$), 1.48-1.35 (m, 1H, C**H**$_2$), 0.74-0.68 (m, 3H, C**H**$_3$).

COSY

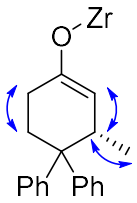

NOESY- to determine Ar-H

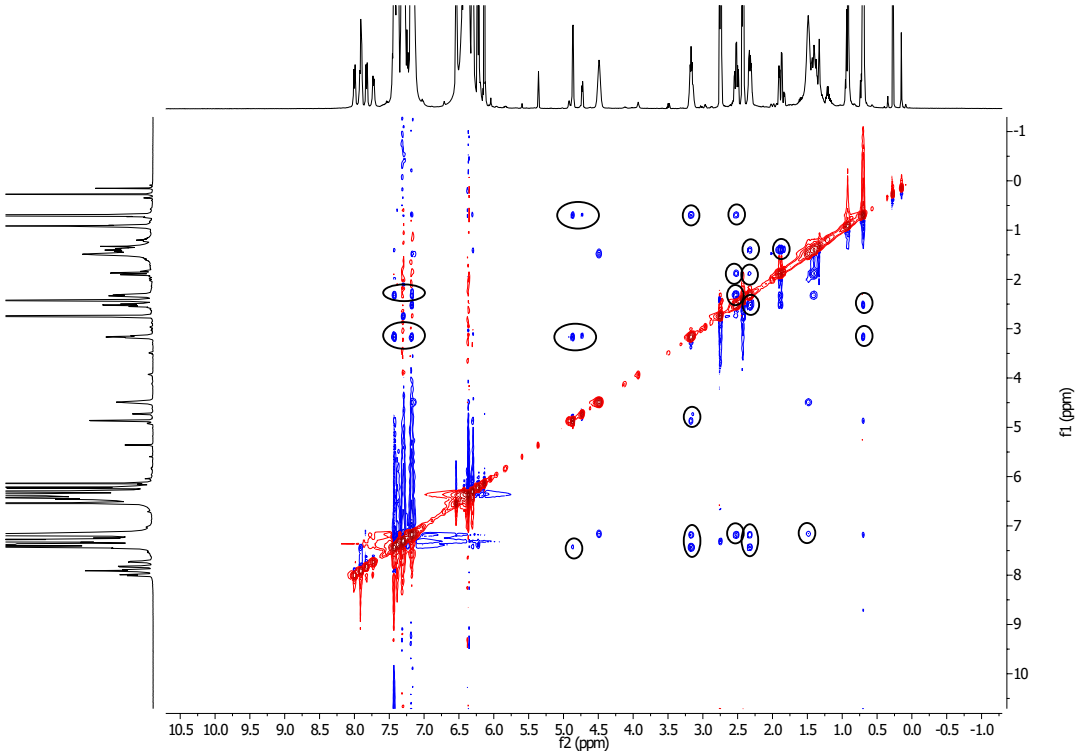

HSQC – to determine ^{13}C shifts

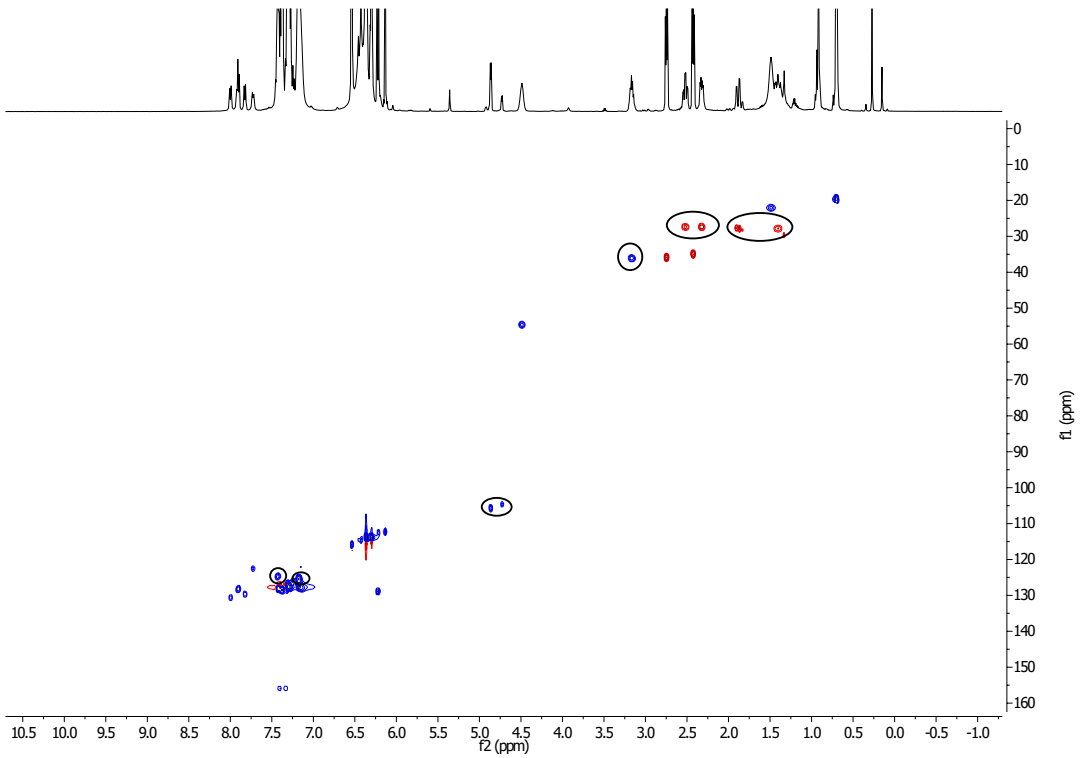

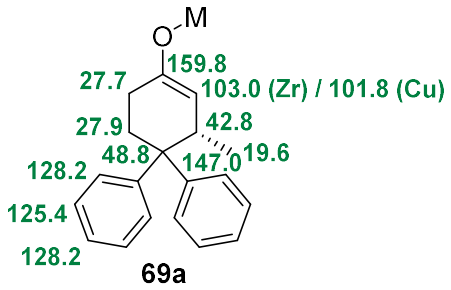

69a

^{13}C NMR (125 MHz, CD_2Cl_2) 159.8 (CH=**Cq**-O), 147.0 (Ar-**Cq**), 128.2 (2 x Ar-**C**H), 125.4 (Ar-**C**H), 103.0 (**C**H-COZr), 101.8 (**C**H-COCu), 48.8 (**Cq**-Ph_2), 42.8 (**C**H-CH_3), 27.9 (**C**H_2), 27.7 (**C**H_2), 19.6 (**C**H_3).

Effect of H_2O (1.0 eq)

Kinetic in CD_2Cl_2 with TMSCl

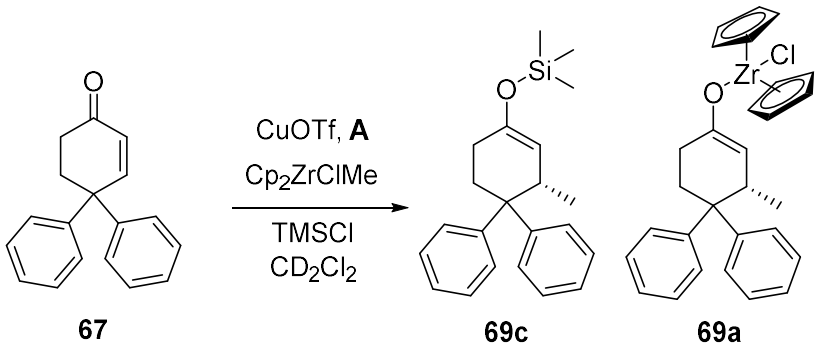

67 **69c** **69a**

In a flame-dried flask, protected from light, under an argon atmosphere, CuCl (3.8 mg, 40 μmol, 20 mol%) and (*S, S, S*)-**A** (21.6 mg, 40.0 μmol, 20.0 mol%) were dissolved in CD_2Cl_2 (1.0 mL) and allowed to stir for 1 h at room temperature. $Cp_2ZrMeCl$ (87 mg, 0.32 mmol, 1.6 eq) was added to a flame-dried NMR tube under argon atmosphere equipped with a septa and covered with CD_2Cl_2 (0.2 mL). Then AgOTf (11.3 mg, 44.0 μmol, 22.0 mol%) was added to the clear Cu-complex solution. After 15 min stirring, the brown solution was filtered to the NMR tube and shaken vigorously. A preliminary ^1H NMR was run with locking and shimming. Then 4,4-diphenylcyclohexenone **67** (49.6 mg, 0.200 mmol, 1.00 eq) dissolved in CD_2Cl_2 (0.1 mL) was added dropwise to the NMR tube and shaken vigorously. TMSCl (0.13 mL, 1.0 mmol, 5.0 eq) was added dropwise to the NMR tube and shaken vigorously. The kinetic was run without further locking and shimming.

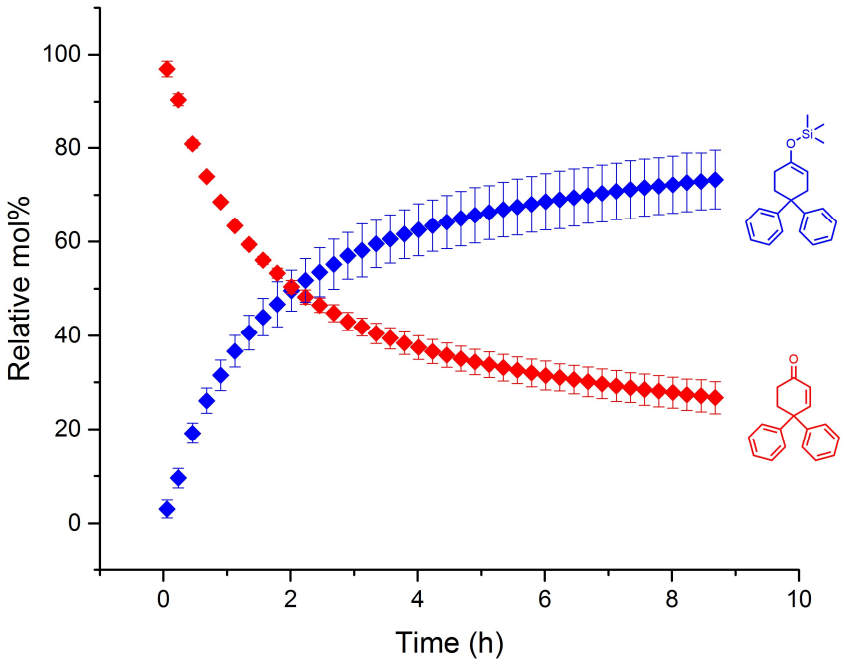
Relative mol%
Time (h)
0
20
40
60
80
100
0
2
4
6
8
10

^{31}P NMR

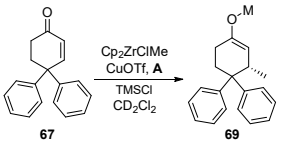
Cp2ZrClMe
CuOTf, A
TMSCl
CD2Cl2
67
69

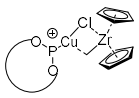

In situ characterisation of the TMS enolate

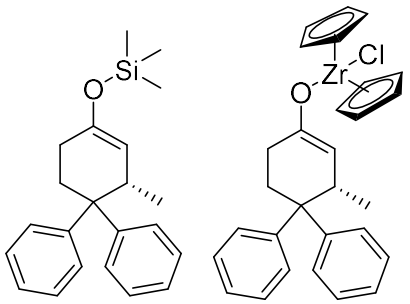

69c **69a**

^{1}H NMR (500 MHz, CD_2Cl_2) 7.33 (m, 4H, Ar-**H**), 7.16 (m, 6H, Ar-**H**), 5.20-5.15 (m, 0.8H, C**H**-COSi), 4.87 (d, *J*=5.4 Hz, 0.04H, C**H**-COZr), 3.13-3.05 (m, 1H, C**H**-CH_3), 2.52 (ddd, *J*=13.1, 12.5, 5.3 Hz, 1H, C**H**$_2$), 2.28 (dd, *J*=13.1, 4.5 Hz, 1H, C**H**$_2$), 1.96 (dd, *J*=17.1, 4.8 Hz, 1H, C**H**$_2$), 1.50-1.40 (m, 1H, C**H**$_2$), 0.97 (d, *J*=6.7 Hz, 3H, C**H**$_3$), 0.14 (d, *J*= 8.3 Hz, 9H, Si(C**H**$_3$)$_3$).

COSY

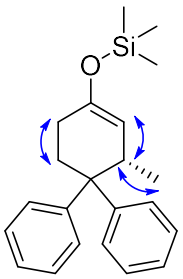

NOESY - to determine Ar-H

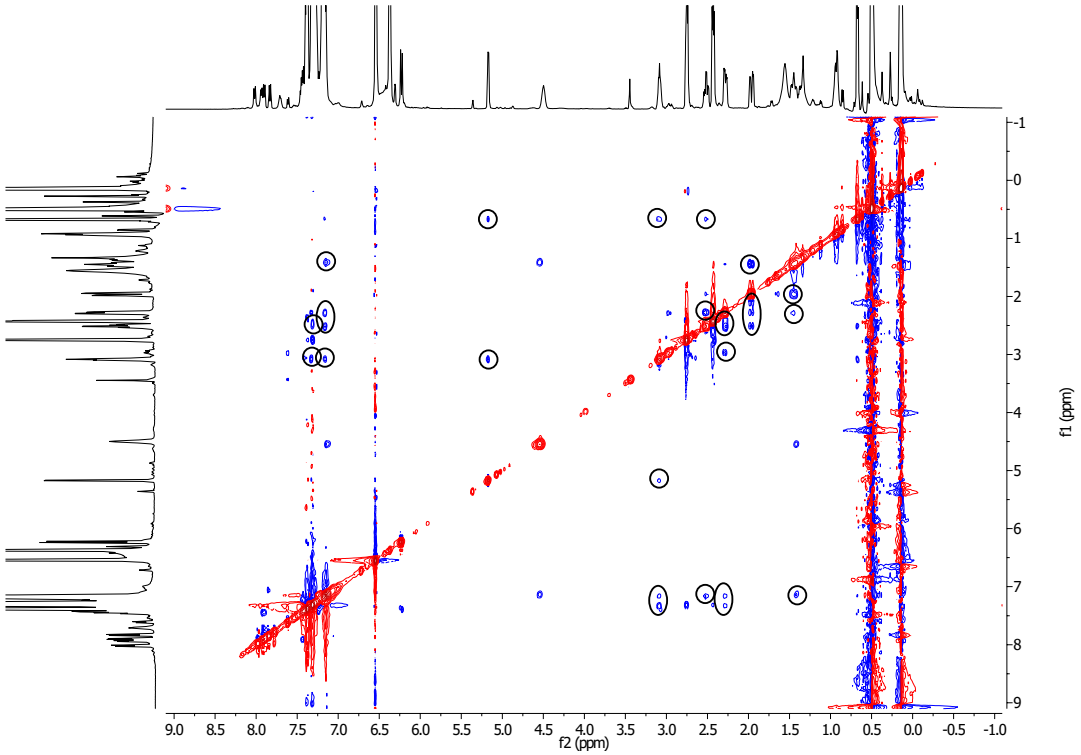

HSQC

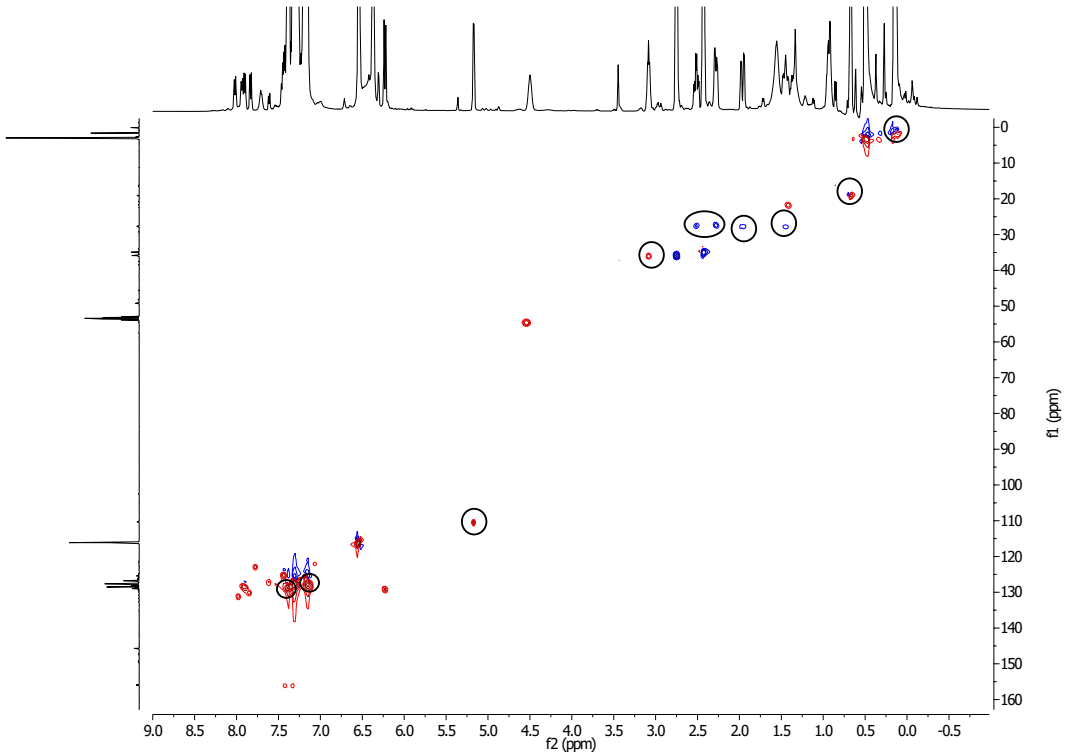

Determined by HSQC:

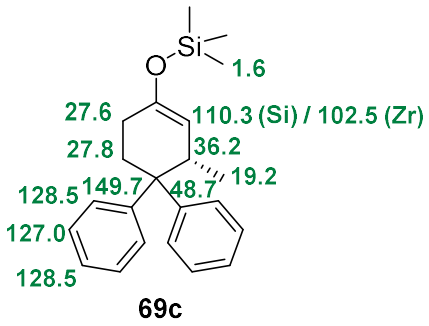

69c

^{13}C NMR (125 MHz, CD_2Cl_2) 149.7 (Ar-**Cq**), 128.5 (2 x Ar-**C**H), 127.0 (Ar-**C**H), 110.3 (**C**H-COSi), 102.5 (**C**H-COZr), 48.7 (**Cq**-Ph_2), 36.2 (**C**H-CH_3), 27.8 (**C**H_2), 27.6 (**C**H_2), 19.2 (**C**H_3), 1.6 ($Si(CH_3)_3$).

Effect of H_2O (1.0 eq)

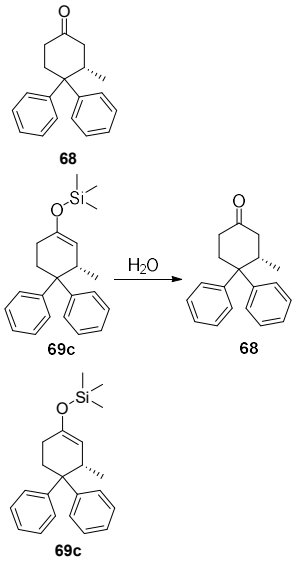

REFERENCES

(1) Harutyunyan, S. R.; den Hartog, T.; Geurts, K.; Minnaard, A. J.; Feringa, B. L. *Chem. Rev.* **2008**, *108*, 2824.

(2) Alexakis, A.; Krause, N.; Woodward, S. *Copper-Catalyzed Asymmetric Synthesis*; Wiley-VCH: Weinheim, **2014**.

(3) Rideau, E.; Masing, F.; Fletcher, S. P. *Synthesis* **2015**, *47*, 2217.

(4) You, H.; Rideau, E.; Sidera, M.; Fletcher, S. P. *Nature* **2015**, *517*, 351.

(5) Rideau, E.; Fletcher, S. P. *Beilstein J. Org. Chem.* **2015**, *11*, 2435.

(6) Fletcher, S. P. *Nat. Chem.* **2009**, *1*, 692.

(7) Alexakis, A.; Backvall, J. E.; Krause, N.; Pamies, O.; Dieguez, M. *Chem. Rev.* **2008**, *108*, 2796.

(8) Hanessian, S. *Total Synthesis of Natural Producs, the "Chiron" Approach*; Pergamon Press: Oxford [Oxfordshire], **1983**.

(9) Nguyen, L. A.; He, H.; Pham-Huy, C. *Int. J. Biomed. Sci.* **2006**, *2*, 85.

(10) Kaspereit, M.; Swernath, S.; Kienle, A. *Org. Process. Res. Dev.* **2012**, *16*, 353.

(11) Cooper, T. W. J.; Campbell, I. B.; Macdonald, S. J. F. *Angew. Chem. Int. Ed.* **2010**, *49*, 8082.

(12) Rossiter, B. E.; Swingle, N. M. *Chem. Rev.* **1992**, *92*, 771.

(13) Ager, D. J.; Prakash, I.; Schaad, D. R. *Chem. Rev.* **1996**, *96*, 835.

(14) Seebach, D.; Beck, A. K.; Heckel, A. *Angew. Chem. Int. Ed.* **2001**, *40*, 92.

(15) Gnas, Y.; Glorius, F. *Synthesis* **2006**, 1899.

(16) Meggers, E. *Chem. Eur. J.* **2010**, *16*, 752.

(17) Davies, S. G.; Fletcher, A. M.; Roberts, P. M.; Shah, R. S.; Thompson, A. L.; Thomson, J. E. *Org. Lett.* **2014**, *16*, 1354.

(18) Blaser, H. U. *Chem. Rev.* **1992**, *92*, 935.

(19) Taylor, R. J. K. *Organocopper reagents: a practical approach*; Oxford University Press, **1994**.

(20) Krause, N. *Modern Organocopper Chemistry*; Wiley-VCH, **2002**.

(21) Hanessian, S.; Giroux, S.; Mascitti, V. *Synthesis* **2006**, 1057.

(22) Jorgensen, L.; McKerrall, S. J.; Kuttruff, C. A.; Ungeheuer, F.; Felding, J.; Baran, P. S. *Science* **2013**, *341*, 878.

(23) Krause, N.; Gerold, A. *Angew. Chem. Int. Ed.* **1997**, *36*, 187.

(24) Karlstrom, A. S. E.; Huerta, F. F.; Meuzelaar, G. J.; Backvall, J. E. *Synlett* **2001**, 923.

(25) Noyori, R. *Asymmetric catalysis in organic synthesis*; Wiley, **1994**.

(26) Jacobsen, E. N.; Pfaltz, A.; Yamamoto, H. *Comprehensive Asymmetric Catalysis: Supplement 1*; Springer Berlin Heidelberg, **2003**.

(27) Ojima, I. *Catalytic Asymmetric Synthesis*; Wiley, **2013**.

(28) Dalko, P. I.; Moisan, L. *Angew. Chem. Int. Ed.* **2001**, *40*, 3726.

(29) Dalko, P. I.; Moisan, L. *Angew. Chem. Int. Ed.* **2004**, *43*, 5138.

(30) Mager, I.; Zeitler, K. *Org. Lett.* **2010**, *12*, 1480.

(31) Fox, M. A.; Whitesell, J. K. *Organic Chemistry*; Jones and Bartlett Publishers, **2004**.

(32) Roughley, S. D.; Jordan, A. M. *J. Med. Chem.* **2011**, *54*, 3451.

(33) Krause, N.; Hoffmann-Roder, A. *Synthesis* **2001**, 171.

(34) Christoffers, J.; Koripelly, G.; Rosiak, A.; Rossle, M. *Synthesis* **2007**, 1279.

(35) Christmann, M.; Bräse, S. *Asymmetric Synthesis: The Essentials*; Wiley, **2008**.

(36) Roth, P. M. C. *Phosphoramidite ligand design for the enantioselective conjugate addition of alkylzirconium reagents to enones*; PhD Thesis: University of Oxford, **2014**.

(37) Yoshikai, N.; Nakamura, E. *Chem. Rev.* **2012**, *112*, 2339.

(38) Jerphagnon, T.; Pizzuti, M.; Minnaard, A.; Feringa, B. *Chem. Soc. Rev.* **2009**, *38*, 1039.

(39) Hayashi, T.; Yamasaki, K. *Chem. Rev.* **2003**, *103*, 2829.

(40) Muller, D.; Alexakis, A. *Chem. Commun.* **2012**, *48*, 12037.

(41) Doyle, M. P. *Advances in Catalytic Processes*; Elsevier Science & Technology Books, **1997**.

(42) Trost, B. M. *Chem. Pharm. Bull.* **2002**, *50*, 1.

(43) Trost, B. M.; Crawley, M. L. *Chem. Rev.* **2003**, *103*, 2921.

(44) Yorimitsu, H.; Oshima, K. *Angew. Chem. Int. Ed.* **2005**, *44*, 4435.

(45) Alexakis, A.; Malan, C.; Lea, L.; Tissot-Croset, K.; Polet, D.; Falciola, C. *Chimia* **2006**, *60*, 124.

(46) Evans, P. A.; Robinson, J. E. *Org. Lett.* **1999**, *1*, 1929.

(47) Trnka, T. M.; Grubbs, R. H. *Acc. Chem. Res.* **2001**, *34*, 18.

(48) Giacomina, F.; Alexakis, A. *Eur. J. Org. Chem.* **2013**, *2013*, 6710.

(49) Persson, E. S. M.; Vanklaveren, M.; Grove, D. M.; Backvall, J. E.; Vankoten, G. *Chem. Eur. J.* **1995**, *1*, 351.

(50) Vanklaveren, M.; Persson, E. S. M.; Delvillar, A.; Grove, D. M.; Backvall, J. E.; Vankoten, G. *Tetrahedron Lett.* **1995**, *36*, 3059.

(51) Tissot-Croset, K.; Polet, D.; Alexakis, A. *Angew. Chem. Int. Ed.* **2004**, *43*, 2426.

(52) Lopez, F.; van Zijl, A. W.; Minnaard, A. J.; Feringa, B. L. *Chem. Commun.* **2006**, 409.

(53) van Zijl, A. W.; Szymanski, W.; Lopez, F.; Minnaard, A. J.; Feringa, B. L. *J. Org. Chem.* **2008**, *73*, 6994.

(54) Selim, K. B.; Yamada, K.; Tomioka, K. *Chem. Commun.* **2008**, 5140.

(55) Jerphagnon, T.; Pizzuti, M. G.; Minnaard, A. J.; Feringa, B. L. *Chem. Soc. Rev.* **2009**, *38*, 1039.

(56) deVries, A. H. M.; Meetsma, A.; Feringa, B. L. *Angew. Chem. Int. Ed.* **1996**, *35*, 2374.

(57) Krause, N. *Angew. Chem. Int. Ed.* **1998**, *37*, 283.

(58) Feringa, B. L. *Acc. Chem. Res.* **2000**, *33*, 346.

(59) Knochel, P.; Dohle, W.; Gommermann, N.; Kneisel, F. F.; Kopp, F.; Korn, T.; Sapountzis, I.; Vu, V. A. *Angew. Chem. Int. Ed.* **2003**, *42*, 4302.

(60) van Zijl, A. W.; Arnold, L. A.; Minnaard, A. J.; Feringa, B. L. *Adv. Synth. Catal.* **2004**, *346*, 413.

(61) Feringa, B. L.; Pineschi, M.; Arnold, L. A.; Imbos, R.; de Vries, A. H. M. *Angew. Chem. Int. Ed.* **1997**, *36*, 2620.

(62) Lee, Y.; Akiyama, K.; Gillingham, D. G.; Brown, M. K.; Hoveyda, A. H. *J. Am. Chem. Soc.* **2008**, *130*, 446.

(63) Akiyama, K.; Gao, F.; Hoveyda, A. H. *Angew. Chem. Int. Ed.* **2010**, *49*, 419.

(64) Gao, F.; Lee, Y.; Mandai, K.; Hoveyda, A. H. *Angew. Chem. Int. Ed.* **2010**, *49*, 8370.

(65) Gao, F.; McGrath, K. P.; Lee, Y.; Hoveyda, A. H. *J. Am. Chem. Soc.* **2010**, *132*, 14315.

(66) Dabrowski, J. A.; Gao, F.; Hoveyda, A. H. *J. Am. Chem. Soc.* **2011**, *133*, 4778.

(67) Maksymowicz, R. M.; Bissette, A. J.; Fletcher, S. P. *Chem. Eur. J.* **2015**, *21*, 5668–5678.

(68) Connon, S. J. *Angew. Chem. Int. Ed.* **2006**, *45*, 3909.

(69) Hamilton, G. L.; Kang, E. J.; Mba, M.; Toste, F. D. *Science* **2007**, *317*, 496.

(70) Mahlau, M.; List, B. *Isr. J. Chem.* **2012**, *52*, 630.

(71) Feringa, B. L.; Badorrey, R.; Pena, D.; Harutyunyan, S. R.; Minnaard, A. J. *Proc. Natl. Acad. Sci. USA.* **2004**, *101*, 5834.

(72) Martin, D.; Kehrli, S.; d'Augustin, M.; Clavier, H.; Mauduit, M.; Alexakis, A. *J. Am. Chem. Soc.* **2006**, *128*, 8416.

(73) Luchaco-Cullis, C. A.; Mizutani, H.; Murphy, K. E.; Hoveyda, A. H. *Angew. Chem. Int. Ed.* **2001**, *40*, 1456.

(74) Cesati, R. R.; de Armas, J.; Hoveyda, A. H. *J. Am. Chem. Soc.* **2004**, *126*, 96.

(75) Dijk, E. W.; Panella, L.; Pinho, P.; Naasz, R.; Meetsma, A.; Minnaard, A. J.; Feringa, B. L. *Tetrahedron* **2004**, *60*, 9687.

(76) Brown, M. K.; Degrado, S. J.; Hoveyda, A. H. *Angew. Chem. Int. Ed.* **2005**, *44*, 5306.

(77) Brown, M. K.; Hoveyda, A. H. *J. Am. Chem. Soc.* **2008**, *130*, 12904.

(78) Mao, B.; Geurts, K.; Fananas-Mastral, M.; van Zijl, A. W.; Fletcher, S. P.; Minnaard, A. J.; Feringa, B. L. *Org. Lett.* **2011**, *13*, 948.

(79) Mendoza, A.; Ishihara, Y.; Baran, P. S. *Nat. Chem.* **2012**, *4*, 21.

(80) Alexakis, A.; Benhaim, C.; Fournioux, X.; van den Heuvel, A.; Leveque, J. M.; March, S.; Rosset, S. *Synlett* **1999**, 1811.

(81) Scafato, P.; Labano, S.; Cunsolo, G.; Rosini, C. *Tetrahedron Asymmetry* **2003**, *14*, 3873.

(82) Scafato, P.; Superchi, S.; Rosini, C. *Arkivoc* **2008**, 116.

(83) Fuchs, N.; d'Augustin, M.; Humam, M.; Alexakis, A.; Taras, R.; Gladiali, S. *Tetrahedron Asymmetry* **2005**, *16*, 3143.

(84) Howell, G. P. *Org. Process. Res. Dev.* **2012**, *16*, 1258.

(85) Maksymowicz, R.; Roth, P.; Fletcher, S. *Nat. Chem.* **2012**, *4*, 649.

(86) Sidera, M.; Roth, P.; Maksymowicz, R.; Fletcher, S. *Angew. Chem. Int. Ed.* **2013**, *52*, 7995.

(87) Maciver, E. E.; Maksymowicz, R. M.; Wilkinson, N.; Roth, P. M. C.; Fletcher, S. P. *Org. Lett.* **2014**, *16*, 3288.

(88) Roth, P. M. C.; Fletcher, S. P. *Org. Lett.* **2015**, *17*, 912.

(89) Maksymowicz, R.; Roth, P.; Thompson, A.; Fletcher, S. *Chem. Commun.* **2013**, *49*, 4211.

(90) Caprioglio, D.; Fletcher, S. P. *Chem. Commun.* **2015**, *51*, 14866.

(91) Gschwind, R. M. *Chem. Rev.* **2008**, *108*, 3029.

(92) Shi, W. J.; Wang, L. X.; Fu, Y.; Zhu, S. F.; Zhou, Q. L. *Tetrahedron Asymmetry* **2003**, *14*, 3867.

(93) Bertz, S. H.; Cope, S.; Murphy, M.; Ogle, C. A.; Taylor, B. J. *J. Am. Chem. Soc.* **2007**, *129*, 7208.

(94) Gartner, T.; Henze, W.; Gschwind, R. M. *J. Am. Chem. Soc.* **2007**, *129*, 11362.

(95) Bartholomew, E. R.; Bertz, S. H.; Cope, S.; Dorton, D. C.; Murphy, M.; Ogle, C. A. *Chem. Commun.* **2008**, 1176.

(96) Bartholomew, E. R.; Bertz, S. H.; Cope, S.; Murphy, M.; Ogle, C. A. *J. Am. Chem. Soc.* **2008**, *130*, 11244.

(97) Bindra, J. S.; Bindra, R. *Prostaglandin synthesis*; Academic Press, **1977**.

(98) Sorokin, A. *Glomerulonephritis and Cellular Regulation of Prostaglandin Synthesis*; INTECH Open Access Publisher, **2011**.

(99) Coulthard, G.; Erb, W.; Aggarwal, V. K. In *Nature* **2012**; Vol. 489, p 278.

(100) North, T. E.; Goessling, W.; Walkley, C. R.; Lengerke, C.; Kopani, K. R.; Lord, A. M.; Weber, G. J.; Bowman, T. V.; Jang, I. H.; Grosser, T.; Fitzgerald, G. A.; Daley, G. Q.; Orkin, S. H.; Zon, L. I. *Nature* **2007**, *447*, 1007.

(101) Hoggatt, J.; Mohammad, K. S.; Singh, P.; Hoggatt, A. F.; Chitteti, B. R.; Speth, J. M.; Hu, P.; Poteat, B. A.; Stilger, K. N.; Ferraro, F.; Silberstein, L.; Wong, F. K.; Farag, S. S.; Czader, M.; Milne, G. L.; Breyer, R. M.; Serezani, C. H.; Scadden, D. T.; Guise, T. A.; Srour, E. F.; Pelus, L. M. *Nature* **2013**, *495*, 365.

(102) Nicolaou, K. C.; Sorensen, E. J. *Classics in Total Synthesis: Targets, Strategies, Methods*; Wiley, **1996**.

(103) Rouzer, C. A.; Marnett, L. J. *Chem. Rev.* **2003**, *103*, 2239.

(104) Das, S.; Chandrasekhar, S.; Yadav, J. S.; Gree, R. *Chem. Rev.* **2007**, *107*, 3286.

(105) Prevost, S.; Thai, K.; Schutzenmeister, N.; Coulthard, G.; Erb, W.; Aggarwal, V. K. *Org Lett* **2015**, *17*, 504.

(106) Collins, P. W.; Djuric, S. W. *Chem. Rev.* **1993**, *93*, 1533.

(107) Gamaniel, K.; Wuorela, H.; Vapaatalo, H. *Prostaglandins Leukot. Essent. Fatty Acids* **1989**, *35*, 63.

(108) Lacy, B. E.; Levy, L. C. *Clin. Interv. Aging* **2008**, *3*, 357.

(109) Chan, W. W.; Mashimo, H. *J. Neurogastroenterol. Motil.* **2013**, *19*, 312.

(110) Corey, E. J.; Weinshenker, N. M.; Schaaf, T. K.; Huber, W. *J. Am. Chem. Soc.* **1969**, *91*, 5675.

(111) Evans, D. A.; Lectka, T.; Miller, S. J. *Tetrahedron Lett.* **1993**, *34*, 7027.

(112) Evans, D. A.; Miller, S. J.; Lectka, T. *J. Am. Chem. Soc.* **1993**, *115*, 6460.

(113) Ahrendt, K. A.; Borths, C. J.; MacMillan, D. W. C. *J. Am. Chem. Soc.* **2000**, *122*, 4243.

(114) Corey, E. J. *Angew. Chem. Int. Ed.* **2002**, *41*, 1650.

(115) Ryu, D. H.; Corey, E. J. *J. Am. Chem. Soc.* **2003**, *125*, 6388.

(116) Schaefer, B. *Natural Products in the Chemical Industry*; Springer Berlin Heidelberg, **2015**.

(117) Stork, G.; Isobe, M. *J. Am. Chem. Soc.* **1975**, *97*, 6260.

(118) Stork, G.; Isobe, M. *J. Am. Chem. Soc.* **1975**, *97*, 4745.

(119) Suzuki, M.; Kawagishi, T.; Noyori, R. *Tetrahedron Lett.* **1982**, *23*, 5563.

(120) Suzuki, M.; Kawagishi, T.; Suzuki, T.; Noyori, R. *Tetrahedron Lett.* **1982**, *23*, 4057.

(121) Noyori, R.; Suzuki, M. *Angew. Chem. Int. Ed.* **1984**, *23*, 847.

(122) Suzuki, M.; Yanagisawa, A.; Noyori, R. *J. Am. Chem. Soc.* **1985**, *107*, 3348.

(123) Toure, B. B.; Hall, D. G. *Chem. Rev.* **2009**, *109*, 4439.

(124) Aggarwal, V. K.; Coulthard, M. G.; Erb, W. *WO/2013/186550 PCT/GB2013/051532*; University of Bristol, **2013**.

(125) Hart, D. W.; Blackburn, T. F.; Schwartz, J. *J. Am. Chem. Soc.* **1975**, *97*, 679.

(126) Schwartz, J.; Labinger, J. A. *Angew. Chem. Int. Ed.* **1976**, *15*, 333.

(127) Schwartz, J.; Loots, M. J.; Kosugi, H. *J. Am. Chem. Soc.* **1980**, *102*, 1333.

(128) Coffen, D. L.; Manchand, P. S.; Truesdale, L. K. *EP0153689 (A2) - Prostaglandin intermediates.*; F. Hoffmann-La Roche & Co., **1986**.

(129) Oi, S.; Sato, T.; Inoue, Y. *Tetrahedron Lett.* **2004**, *45*, 5051.

(130) Nicolaou, K.; Tang, W.; Dagneau, P.; Faraoni, R. *Angew. Chem. Int. Ed.* **2005**, *44*, 3874.

(131) Corey, E. J.; Boaz, N. W. *Tetrahedron Lett.* **1985**, *26*, 6015.

(132) Corey, E. J.; Boaz, N. W. *Tetrahedron Lett.* **1985**, *26*, 6019.

(133) Alexakis, A.; Berlan, J.; Besace, Y. *Tetrahedron Lett.* **1986**, *27*, 1047.

(134) Nakamura, E.; Matsuzawa, S.; Horiguchi, Y.; Kuwajima, I. *Tetrahedron Lett.* **1986**, *27*, 4029.

(135) Corey, E. J.; Hannon, F. J.; Boaz, N. W. *Tetrahedron* **1989**, *45*, 545.

(136) Alexakis, A.; Sedrani, R.; Mangeney, P. *Tetrahedron Lett.* **1990**, *31*, 345.

(137) Lipshutz, B. H.; Dimock, S. H.; James, B. *J. Am. Chem. Soc.* **1993**, *115*, 9283.

(138) Sidera, M.; Fletcher, S. P. *Chem. Commun.* **2015**, *51*, 5044.

(139) Sidera, M.; Fletcher, S. P. *Nat. Chem.* **2015**, *7*, 935.

(140) Rideau, E.; Masing, F.; Fletcher, S. P. *Synthesis* **2015**, *47*, 2217.

(141) Yamamoto, H.; Zhou, F. *Synfacts* **2015**; *11*(11), 1163.

(142) Sidera, M.; Roth, P. M. C.; Maksymowicz, R. M.; Fletcher, S. P. *Angew. Chem. Int. Ed.* **2013**, *52*, 7995.

(143) Kanai, M.; Nakagawa, Y.; Tomioka, K. *Tetrahedron* **1999**, *55*, 3843.

(144) Hawner, C.; Alexakis, A. *Chem. Commun.* **2010**, *46*, 7295.

(145) Degrado, S. J.; Mizutani, H.; Hoveyda, A. H. *J. Am. Chem. Soc.* **2001**, *123*, 755.

(146) Sunazuka, T.; Hirose, T.; Shirahata, T.; Harigaya, Y.; Hayashi, M.; Komiyama, K.; Omura, S.; Smith, A. B. *J. Am. Chem. Soc.* **2000**, *122*, 2122.

(147) Arnold, L. A.; Naasz, R.; Minnaard, A. J.; Feringa, B. L. *J. Am. Chem. Soc.* **2001**, *123*, 5841.

(148) Jansen, D. J.; Shenvi, R. A. *J. Am. Chem. Soc.* **2013**, *135*, 1209.

(149) Arnold, L. A.; Naasz, R.; Minnaard, A. J.; Feringa, B. L. *J. Org. Chem.* **2002**, *67*, 7244.

(150) Stjernschantz, J. W.; Resul, B. *US 5296504 A - Prostaglandin derivatives for the treatment of glaucoma or ocular hypertension.*; Kabi Pharmacia, **1994**.

(151) Stjernschantz, J. W.; Resul, B. *EP0364417B9 - Prostaglandin derivatives for the treatment of glaucoma or ocular hypertension.*; Pharmacia AB, **2004**.

(152) *WHO Model List of Essential Medicines 19th List (April 2015)*; World Health Organisation, **2015**.

(153) Martynow, J. G.; Jozwik, J.; Szelejewski, W.; Achmatowicz, O.; Kutner, A.; Wisniewski, K.; Winiarski, J.; Zegrocka-Stendel, O.; Golebiewski, P. *Eur. J. Org. Chem.* **2007**, 689.

(154) Mariani, E.; Montorsi, M.; Andriolo, E.; Bandini, M.; Contento, M.; Tolomelli, A. *EP2495235 - Process for the synthesis of prostaglandins and intermediates thereof.*; Newchem S.p.A. **2012**.

(155) Zanoni, G.; D'Alfonso, A.; Porta, A.; Feliciani, L.; Nolan, S. P.; Vidari, G. *Tetrahedron* **2010**, *66*, 7472.

(156) Xiu, Z. M.; Wang, L. C.; Huang, M. Y.; Zhang, P.; Guo, Y. M.; Zhang, W. Q.; Wang, L. P. *Chin. J. Org. Chem.* **2014**, *34*, 1786.

(157) Vijendhar, K.; Srinivas, B.; Boodida, S. *J. Chem. Sci.* **2015**, *127*, 2023.

(158) North, T. E.; Goessling, W.; Kopani, K. R.; Mayhall, E.; Jang, I. H.; Lengerke, C.; Burns, C. E.; Lord, A.; Grosser, T.; FitzGerald, G. A.; Daley, G. Q.; Zon, L. I. *Blood Cells Mol. Dis.* **2007**, *38*, 191.

(159) Thomson, J. A.; Itskovitz-Eldor, J.; Shapiro, S. S.; Waknitz, M. A.; Swiergiel, J. J.; Marshall, V. S.; Jones, J. M. *Science* **1998**, *282*, 1145.

(160) Hochedlinger, K.; Jaenisch, R. *Nature* **2006**, *441*, 1061.

(161) Robinton, D. A.; Daley, G. Q. *Nature* **2012**, *481*, 295.

(162) Davies, S. G.; Kennewell, P. D.; Russell, A. J.; Seden, P. T.; Westwood, R.; Wynne, G. M. *J. Med. Chem.* **2015**, *58*, 2863.

(163) Greenwood, N. N.; Earnshaw, A. *Chemistry of the Elements*; Elsevier Science, **2012**.

(164) Calvo, B. C.; Madduri, A. V. R.; Harutyunyan, S. R.; Minnaard, A. J. *Adv. Synth. Catal.* **2014**, *356*, 2061.

(165) Westmeier, J.; Pfaff, C.; Siewert, J.; von Zezschwitz, P. *Adv. Synth. Catal.* **2013**, *355*, 2651.

(166) Nicolaou, K. C.; Heretsch, P.; ElMarrouni, A.; Hale, C. R. H.; Pulukuri, K. K.; Kudva, A. K.; Narayan, V.; Prabhu, K. S. *Angew. Chem. Int. Ed.* **2014**, *53*, 10443.

(167) Nicolaou, K. C.; Heretsch, P.; Hale, C. R. H.; El, G. A. E. M.; Pulikuri, K. K.; Yu, R.; Grove, C. *WO 2015048268 A1 - Synthesis of delta 12-pgj3 and related compounds.*; William Marsh Rice University, **2015**.

(168) Ibrahem, I.; Cordova, A. *Angew. Chem. Int. Ed.* **2006**, *45*, 1952.

(169) Bystrom, S. E.; Larsson, E. M.; Akermark, B. *J. Org. Chem.* **1990**, *55*, 5674.

(170) Akermark, B.; Larsson, E. M.; Oslob, J. D. *J. Org. Chem.* **1994**, *59*, 5729.

(171) Yu, J. Q.; Corey, E. J. *J. Am. Chem. Soc.* **2003**, *125*, 3232.

(172) Catino, A. J.; Forslund, R. E.; Doyle, M. P. *J. Am. Chem. Soc.* **2004**, *126*, 13622.

(173) Shing, T. K. M.; Yeung, Y. Y.; Su, P. L. *Org. Lett.* **2006**, *8*, 3149.

(174) Li, Y. C.; Lee, T. B.; Wang, T. Y.; Gamble, A. V.; Gorden, A. E. V. *J. Org. Chem.* **2012**, *77*, 4628.

(175) Nakamura, A.; Nakada, M. *Synthesis* **2013**, *45*, 1421.

(176) Rosen, B. R.; Werner, E. W.; O'Brien, A. G.; Baran, P. S. *J. Am. Chem. Soc.* **2014**, *136*, 5571.

(177) Jin, Y. H.; Yeh, C. H.; Kuttruff, C. A.; Jorgensen, L.; Dunstl, G.; Felding, J.; Natarajan, S. R.; Baran, P. S. *Angew. Chem. Int. Ed.* **2015**, *54*, 14044.

(178) Mann, S. E.; Benhamou, L.; Sheppard, T. D. *Synthesis* **2015**, *47*, 3079.

(179) Kende, A. S.; Johnson, S.; Sanfilippo, P.; Hodges, J. C.; Jungheim, L. N. *J. Am. Chem. Soc.* **1986**, *108*, 3513.

(180) Nicolaou, K. C.; Nantermet, P. G.; Ueno, H.; Guy, R. K.; Couladouros, E. A.; Sorensen, E. J. *J. Am. Chem. Soc.* **1995**, *117*, 624.

(181) Wilde, N. C.; Isomura, M.; Mendoza, A.; Baran, P. S. *J. Am. Chem. Soc.* **2014**, *136*, 4909.

(182) Umbreit, M. A.; Sharpless, K. B. *J. Am. Chem. Soc.* **1977**, *99*, 5526.

(183) Chen, J. S.; Abeykoon, G. A. *Org. Lett.* **2015**, *17*, 6050.

(184) van der Klink, J. J.; Brom, H. B. *Prog. Nucl. Mag. Res. Sp.* **2000**, *36*, 89.

(185) Martins, J. C.; Biesemans, M.; Willem, R. *Prog. Nucl. Mag. Res. Sp.* **2000**, *36*, 271.

(186) Still, B. M.; Kumar, P. G.; Aldrich-Wright, J. R.; Price, W. S. *Chem. Soc. Rev.* **2007**, *36*, 665.

(187) von Rekowski, F.; Gschwind, R. M. *Organometallics* **2014**, *33*, 6259.

(188) von Rekowski, F.; Koch, C.; Gschwind, R. M. *J. Am. Chem. Soc.* **2014**, *136*, 11389.

(189) Harutyunyan, S. R.; Lopez, F.; Browne, W. R.; Correa, A.; Pena, D.; Badorrey, R.; Meetsma, A.; Minnaard, A. J.; Feringa, B. L. *J. Am. Chem. Soc.* **2006**, *128*, 9103.

(190) Jacobsen, E. N.; Pfaltz, A.; Yamamoto, H.; Eds. *Comprehensive Asymmetric Catalysis: Suppl. 2*; Springer-Verlag: Berlin, **2004**.

(191) Trost, B. M. *Proc. Natl. Acad. Sci. USA.* **2004**, *101*, 5348.

(192) Eliel, E. L.; Wilen, S. H. *Stereochemistry of Organic Compounds*; Wiley: New York, **1994**.

(193) Trost, B. M.; VanVranken, D. L. *Chem. Rev.* **1996**, *96*, 395.

(194) Helmchen, G.; Dahnz, A.; Dubon, P.; Schelwies, M.; Weihofen, R. *Chem. Commun.* **2007**, 675.

(195) Lu, Z.; Ma, S. *Angew. Chem. Int. Ed.* **2008**, *47*, 258.

(196) Geurts, K.; Fletcher, S. P.; van Zijl, A. W.; Minnaard, A. J.; Feringa, B. L. *Pure Appl. Chem.* **2008**, *80*, 1025.

(197) Hartwig, J. F.; Stanley, L. M. *Acc. Chem. Res.* **2010**, *43*, 1461.

(198) Basle, O.; Denicourt-Nowicki, A.; Crevisy, C.; Mauduit, M. In *Copper-Catalyzed Asymmetric Synthesis*; Alexakis, A., Krause, N., Woodward, S., Eds.; Wiley-VCH: Weinheim, **2014**, p 85.

(199) Trost, B. M.; Bunt, R. C. *J. Am. Chem. Soc.* **1994**, *116*, 4089.

(200) Vedejs, E.; Jure, M. *Angew. Chem. Int. Ed.* **2005**, *44*, 3974.

(201) Trost, B. M.; Fandrick, D. R. *Aldrichimica Acta* **2007**, *40*, 59.

(202) Pfaltz, A.; Lautens, M. In *Comprehensive Asymmetric Catalysis II*; Jacobsen, E. N., Pfaltz, A., Yamamoto, H., Eds.; Springer-Verlag: Berlin, **1999**; Vol. 2, p 833.

(203) Trost, B. M.; Thaisrivongs, D. A. *J. Am. Chem. Soc.* **2008**, *130*, 14092.

(204) Sha, S. C.; Zhang, J. D.; Carroll, P. J.; Walsh, P. J. *J. Am. Chem. Soc.* **2013**, *135*, 17602.

(205) Misale, A.; Niyomchon, S.; Luparia, M.; Maulide, N. *Angew. Chem. Int. Ed.* **2014**, *53*, 7068.

(206) Kimura, M.; Yamazaki, T.; Kitazume, T.; Kubota, T. *Org. Lett.* **2004**, *6*, 4651.

(207) Breit, B.; Breuninger, D. *Synthesis* **2005**, 147.

(208) Piarulli, U.; Daubos, P.; Claverie, C.; Roux, M.; Gennari, C. *Angew. Chem. Int. Ed.* **2003**, *42*, 234.

(209) Teichert, J. F.; Zhang, S. Y.; van Zijl, A. W.; Slaa, J. W.; Minnaard, A. J.; Feringa, B. L. *Org. Lett.* **2010**, *12*, 4658.

(210) Langlois, J. B.; Alexakis, A. In *Transition Metal Catalyzed Enantioselective Allylic Substitution in Organic Synthesis*; Kazmaier, U., Ed.; Springer-Verlag Berlin: Berlin, **2012**; Vol. 38, p 235.

(211) Norinder, J.; Bäckvall, J. E. *Chem. Eur. J.* **2007**, *13*, 4094.

(212) Langlois, J. B.; Alexakis, A. *Chem. Commun.* **2009**, 3868.

(213) Langlois, J. B.; Emery, D.; Mareda, J.; Alexakis, A. *Chem. Sci.* **2012**, *3*, 1062.

(214) Breit, B.; Demel, P.; Studte, C. *Angew. Chem. Int. Ed.* **2004**, *43*, 3786.

(215) Ito, H.; Kunii, S.; Sawamura, M. *Nat. Chem.* **2010**, *2*, 972.

(216) a) Gao, Y.; Hanson, R. M.; Klunder, J. M.; Ko, S. Y.; Masamune, H.; Sharpless, K. B. *J. Am. Chem. Soc.* **1987**, *109*, 5765. b) Tokunaga, M.; Larrow, J. F.; Kakiuchi, F.; Jacobsen, E. N. *Science* **1997**, *277*, 936.

(217) Huerta, F. F.; Minidis, A. B. E.; Bäckvall, J. E. *Chem. Soc. Rev.* **2001**, *30*, 321.

(218) Faber, K. *Chem. Eur. J.* **2001**, *7*, 5004.

(219) Mohr, J. T.; Ebner, D. C.; Stoltz, B. M. *Org. Biomol. Chem.* **2007**, *5*, 3571.

(220) Noyori, R.; Tokunaga, M.; Kitamura, M. *B. Chem. Soc. Jpn* **1995**, *68*, 36.

(221) Huerta, F. F.; Minidis, A. B. E.; Backvall, J. E. *Chem. Soc. Rev.* **2001**, *30*, 321.

(222) Pellissier, H. *Tetrahedron* **2008**, *64*, 1563.

(223) Sturmer, R. *Angew. Chem. Int. Ed.* **1997**, *36*, 1173.

(224) Norinder, J.; Bogar, K.; Kanupp, L.; Backvall, J. E. *Org. Lett.* **2007**, *9*, 5095.

(225) Norinder, J.; Backvall, J. E. *Chem. Eur. J.* **2007**, *13*, 4094.

(226) Zhang, H.; Gschwind, R. M. *Angew. Chem. Int. Ed.* **2006**, *45*, 6391.

(227) Hammond, G. S.; Warkentin, J. *J. Am. Chem. Soc.* **1961**, *83*, 2554.

(228) Langlois, J. B.; Alexakis, A. *Adv. Synth. Catal.* **2010**, *352*, 447.

(229) Streitwieser, A.; Jayasree, E. G.; Hasanayn, F.; Leung, S. S. *J. Org. Chem.* **2008**, *73*, 9426.

(230) Zhang, H.; Gschwind, R. M. *Chem. Eur. J.* **2007**, *13*, 6691.

(231) Neuhaus, D.; Williamson, M. P. *The Nuclear Overhauser Effect in Structural and Conformational Analysis*; VCH, **1989**.

(232) Bain, A. D. *Prog. Nucl. Mag. Res. Sp.* **2003**, *43*, 63.

(233) Bain, A. D. *Annu. Rep. NMR Spectrosc.* **2008**, *63*, 23.

(234) Claridge, T. D. W. *High-Resolution NMR Techniques in Organic Chemistry*; Elsevier Science, 3rd Edition, **2016**.

(235) Butts, C. P.; Jones, C. R.; Towers, E. C.; Flynn, J. L.; Appleby, L.; Barron, N. J. *Org. Biomol. Chem.* **2011**, *9*, 177.

(236) Sippl, S. P.; White, P. B.; Fry, C. G.; Volk, S. E.; Ye, L.; Schenck, H. L. *Magn. Reson. Chem.* **2016**, *54*, 46.

(237) Bain, A. D.; Cramer, J. A. *J. Magn. Reson.* **1996**, *118*, 21.

(238) Kwan, E. *Chemical Exchange*; PhD Thesis: Harvard University, **2012**.

(239) Quiros, M. T.; Angulo, J.; Munoz, M. P. *Chem. Commun.* **2015**, *51*, 10222.

(240) Zhang, H.; Kerssebaum, R.; Gschwind, R. M. *Magn. Reson. Chem.* **2009**, *47*, 568.

(241) Schober, K.; Hartmann, E.; Zhang, H.; Gschwind, R. M. *Angew. Chem. Int. Ed.* **2010**, *49*, 2794.

(242) Evans, R.; Deng, Z.; Rogerson, A. K.; McLachlan, A. S.; Richards, J. J.; Nilsson, M.; Morris, G. A. *Angew. Chem. Int. Ed.* **2013**, *52*, 3199.

(243) Jerschow, A.; Muller, N. *J. Magn. Reson.* **1997**, *125*, 372.

(244) Jerschow, A.; Muller, N. *J. Magn. Reson.* **1998**, *132*, 13.

(245) Maksymowicz, R. M.; Roth, P. M. C.; Fletcher, S. P. *Nat. Chem.* **2012**, *4*, 649.

(246) Girard, C.; Kagan, H. B. *Angew. Chem. Int. Ed.* **1998**, *37*, 2923.

(247) Kagan, H. B. *Adv. Synth. Catal.* **2001**, *343*, 227.

(248) Kagan, H. B. *Synlett* **2001**, 888.

(249) k rate constants were obtained by fitting of a binding model by non-linear least-squares regression using the DynaFit 4 software package: Kuzmič, P. *Anal. Biochem.* **1996**, *237*, 260.

(250) Fleet, G. W. J.; Gough, M. J. *Tetrahedron Lett.* **1982**, *23*, 4509.

(251) Ghosh, A. K.; Thompson, W. J.; Mckee, S. P.; Duong, T. T.; Lyle, T. A.; Chen, J. C.; Darke, P. L.; Zugay, J. A.; Emini, E. A.; Schleif, W. A.; Huff, J. R.; Anderson, P. S. *J. Med. Chem.* **1993**, *36*, 292.

(252) Alvarez-Manzaneda, E. J.; Chaboun, R.; Alvarez, E.; Cabrera, E.; Alvarez-Manzaneda, R.; Haidour, A.; Ramos, J. M. *Synlett* **2006**, 1829.

(253) Tollefson, E. J.; Erickson, L. W.; Jarvo, E. R. *J. Am. Chem. Soc.* **2015**, *137*, 9760.

(254) Morken, J. P.; Didiuk, M. T.; Visser, M. S.; Hoveyda, A. H. *J. Am. Chem. Soc.* **1994**, *116*, 3123.

(255) Fu, G. C.; Nguyen, S. T.; Grubbs, R. H. *J. Am. Chem. Soc.* **1993**, *115*, 9856.

(256) Clark, J. S. *Chem. Commun.* **2006**, 3571.

(257) Owen, M. R.; Luscombe, C.; Lai, L. W.; Godbert, S.; Crookes, D. L.; Emiabata-Smith, D. *Org. Process. Res. Dev.* **2001**, *5*, 308.

(258) Chen, J. J.; Nugent, T. C.; Lu, C. V.; Kondapally, S.; Giannousis, P.; Wang, Y.; Wilmot, J. T. *Org. Process Res. Dev.* **2003**, *7*, 313.

(259) Aggarwal, V. K.; Staubitz, A. C.; Owen, M. *Org. Process. Res. Dev.* **2006**, *10*, 64.

(260) Arnold, K.; Batsanov, A. S.; Davies, B.; Whiting, A. *Green Chem.* **2008**, *10*, 124.

(261) Denmark, S. E.; Butler, C. R. *J. Am. Chem. Soc.* **2008**, *130*, 3690.

(262) Penafiel, I.; Pastor, I. M.; Yus, M. *Eur. J. Org. Chem.* **2013**, 1479.

(263) Weissman, S. A.; Anderson, N. G. *Org. Process. Res. Dev.* **2014**. doi.org/10.1021/op500169m.

(264) Harper, K. C.; Sigman, M. S. *J. Org. Chem.* **2013**, *78*, 2813.

(265) Maougal, E.; Dalencon, S.; Pearson-Long, M. S. M.; Mathe-Allainmat, M.; Lebreton, J.; Legoupy, S. *Synthesis* **2014**, *46*, 3268.

(266) Lipshutz, B. H.; Kozlowski, J. A.; Breneman, C. M. *J. Am. Chem. Soc.* **1985**, *107*, 3197.

(267) Bertz, S. H.; Vellekoop, A. S.; Smith, R. A. J.; Snyder, J. P. *Organometallics* **1995**, *14*, 1213.

(268) Lipshutz, B. H.; James, B. *J. Org. Chem.* **1994**, *59*, 7585.

(269) Bertz, S. H.; Miao, G. B.; Eriksson, M. *Chem. Commun.* **1996**, 815.

(270) Garrec, K.; Fletcher, S. P. *Org. Lett.* **2016**, *18*, 3814.

(271) You, H. Z.; Rideau, E.; Sidera, M.; Fletcher, S. P. *Nature* **2015**, *517*, 351.

(272) Roth, P.; Ardkhean, R.; Curran, A.; Paton, R.; Fletcher, S. P. *Unpublished Work* **2016**.

(273) Evans, D. A.; Mcgee, L. R. *Tetrahedron Lett.* **1980**, *21*, 3975.

(274) Lipshutz, B. H.; Servesko, J. M.; Petersen, T. B.; Papa, P. P.; Lover, A. A. *Org. Lett.* **2004**, *6*, 1273.

(275) Simpson, J. H. *Organic Structure Determination Using 2-D NMR Spectroscopy: A Problem-based Approach*; Elsevier/AP, **2012**.

(276) Peelen, T. J.; Chi, Y. G.; English, E. P.; Gellman, S. H. *Org. Lett.* **2004**, *6*, 4411.

(277) Clayden, J.; Greeves, N.; Warren, S. *Organic Chemistry*; OUP Oxford, **2012**.

(278) Dempsey, D. F.; Girolami, G. S. *Organometallics* **1988**, *7*, 1208.

(279) Cosier, J.; Glazer, A. M. *J. Appl. Crystallogr.* **1986**, *19*, 105.

(280) *CrysAlisPro (Agilent Technologies)* Oxford, **2011**.

(281) Palatinus, L.; Chapuis, G. *J. Appl. Crystallogr.* **2007**, *40*, 786.

(282) Betteridge, P. W.; Carruthers, J. R.; Cooper, R. I.; Prout, K.; Watkin, D. J. *J. Appl. Crystallogr.* **2003**, *36*, 1487.

(283) Parois, P.; Cooper, R. I.; Thompson, A. L. *Chem. Cent.*, *in press*.

(284) Thompson, A. L.; Watkin, D. J. *J. Appl. Crystallogr.* **2011**, *44*, 1017.

(285) Cooper, R. I.; Thompson, A. L.; Watkin, D. J. *J. Appl. Crystallogr.* **2010**, *43*, 1100.

(286) S. L. Buchwald, S. J. L., R. B. Nielsen, B. T. Watson, and S. M. King. *Org. Synth.* **1993**, *71*, 77.

(287) Salomon, R. G.; Kochi, J. K. *J. Am. Chem. Soc.* **1973**, *95*, 3300.

(288) El-Batta, A.; Hage, T.; Plotkin, S.; Bergdahl, M. *Org. Lett.* **2004**, *6*, 107.

(289) El-Batta, A.; Bergdahl, M.; Miller, M. *Org. Synth.* **2007**, 192.

(290) Mannathan, S.; Cheng, C.-H. *Chem. Eur. J.* **2012**, *18*, 11771.

(291) Abdel-Magid, A. F.; Mehrman, S. J. *Org. Process. Res. Dev.* **2006**, *10*, 971.

(292) Kim, H.; Spivak, D. A. *J. Am. Chem. Soc.* **2003**, *125*, 11269.

(293) Trost, B. M.; Silverman, S. M.; Stambuli, J. P. *J. Am. Chem. Soc.* **2011**, *133*, 19483.

(294) Markees, D. G.; Burger, A. *J. Am. Chem. Soc.* **1949**, *71*, 2031.

(295) Kanbayashi, N.; Onitsuka, K. *Angew. Chem. Int. Ed.* **2011**, *50*, 5197.

(296) Moffett, R. B. *Org. Synth.* **1952**, *32*, 41.

(297) Maercker, A.; Geuss, R. *Chem. Ber-Recl.* **1973**, *106*, 773.

(298) Chapman, O. L.; Mattes, K. C.; Sheridan, R. S.; Klun, J. A. *J. Am. Chem. Soc.* **1978**, *100*, 4878.

(299) Katcher, M. H.; Doyle, A. G. *J. Am. Chem. Soc.* **2010**, *132*, 17402.

(300) Aski, S. N.; Takacs, Z.; Kowalewski, J. *Magn. Reson. Chem.* **2008**, *46*, 1135.

(301) Sippl, S. P.; White, P. B.; Fry, C. G.; Volk, S. E.; Ye, L.; Schenck, H. L. *Magn. Reson. Chem.* **2016**, *54*, 46.

(302) Carrillo-Marquez, T.; Caggiano, L.; Jackson, R. F.; Grabowska, U.; Rae, A.; Tozer, M. J. *Org Biomol Chem* **2005**, *3*, 4117.

(303) Baldwin, J. E.; Chapman, B. R. *J. Org. Chem.* **2005**, *70*, 377.

(304) Onishi, Y.; Nishimoto, Y.; Yasuda, M.; Baba, A. *Org. Lett.* **2011**, *13*, 2762.

(305) Grugel, H.; Minuth, T.; Boysen, M. M. K. *Synthesis* **2010**, 3248.

(306) Yasui, K.; Fugami, K.; Tanaka, S.; Tamaru, Y. *J. Org. Chem.* **1995**, *60*, 1365.

(307) Dharanipragada, R.; Ferguson, S. B.; Diederich, F. *J. Am. Chem. Soc.* **1988**, *110*, 1679.

(308) Hampton, S. E.; Baragana, B.; Schipani, A.; Bosch-Navarrete, C.; Alexander Musso-Buendia, J.; Recio, E.; Kaiser, M.; Whittingham, J. L.; Roberts, S. M.; Shevtsov, M.; Brannigan, J. A.; Kahnberg, P.; Brun, R.; Wilson, K. S.; Gonzalez-Pacanowska, D.; Johansson, N. G.; Gilbert, I. H. *ChemMedChem* **2011**, *6*.

(309) Sammet, K.; Gastl, C.; Baro, A.; Laschat, S.; Fischer, P.; Fettig, I. *Adv. Synth. Catal.* **2010**, *352*, 2281.

(310) Chapuis, C.; Brauchli, R.; Thommen, W. *Helv. Chim. Acta* **1993**, *76*, 535.